UNIVERSITÉ DE STRASBOURG

Ecole et Observatoire des Sciences de la Terre

THÈSE

Présentée à

L'UNIVERSITE de STRASBOURG

Pour obtenir

Le grade de Docteur
Discipline : Sciences de la Terre et de l'Univers
Spécialité : Géophysique

par
Mohamed Reda SBEINATI

Historical Seismology, Paleo-Archeoseismology and Seismic Hazard along the Dead Sea Fault in Syria

Sismicité Historique, Paleo-Archeosismologie et évaluation de l'aléa sismique le long de la faille du Levant en Syrie

Soutenue le **4 Juin 2010** à 14h 30 devant la commission d'examen :

Directeur de thèse	MEGHRAOUI Mustapha, *Université de Strasbourg, France*
Rapporteur interne	FRECHET Julien, *CNRS Strasbourg, France*
Rapporteur externe	BARAZANGI Muawia, *University Cornell, Ithaca, NY-USA*
Rapporteur externe	STUCCHI Massimiliano, *INGV Milano, Italie*
Examinateur	FINKBEINER Uwe, *University Tuebingen, Allemagne*
Examinateur	AL GHAZZI Riad, *Université de Syrie, Damas, Syrie*
Examinateur	GRANET Michel, *Université de Strasbourg, France*

Travail réalisé à l'Institut de Physique du Globe de Strasbourg – UMR 7516

Acknowledgments

I would like to start to thank my supervisor Mustapha Meghraoui who encouraged me to carry on and achieve this research; I appreciated his constant interest in the improvement of my liability in my research programme, and the chance he offered me to learn more about paleoseismology, geomorphology and active tectonics.

My sincere acknowledgements are also addressed to the members of the Jury for their acceptance in reviewing and judging my thesis manuscript.

I would like to express my sincere respect to Prof. Ibrahim Othman the director general of the Atomic Energy Commission of Syria (AECS) for his great support and constant interest in my research work under his patronage.

I owe many thanks to the University of Strasbourg and IPGS and especially to Prof. Jacques Hinderer (Head of IPGS) for supports, and Prof. Michel Cara and Prof. Luis Rivera for their valuable lectures during the Master courses. I am also grateful to all the administrative, secretary and technical staffs for their kindness during my numerous visits to the institute and for their help in making my stay productive with the access to the library and the high technical computing facilities.

My special thanks are here addressed to Francisco Gomez, Abdelnasser Darkal, Mohamad Daoud, Claudio Margotini and Salvador Paolini for the numerous scientific discussions and for attracting my attention to the different scientific issues that helped improving the presentation of my thesis manuscript. I will never forget the close colleagues of the active tectonics team to whom I owe my faithful gratitude for their help from my first day in Strasbourg until the printing of the last page and figure of this thesis; for this I am grateful to Tony Nemer, Samir Belabbes, Ziyadin Cakir, Yasser Mahmoud, Sophie Bertrand, and Sophie Lambotte, for their help in solving computer problems and many uncountable other things.

I also would like to express my deepest thanks to all heads of geology department of AECS (Damascus) who helped me in achieving my work during my PhD thesis preparation. I would like to start with Prof. Mikhail Mouty for his early encouragements and for my initiating research in historical and archeological seismology in Syria under his supervision; Prof. Ahmed Khaled Al-Maleh for his valuable support in facilitating the research work; the late Prof. Youssef Joubely, Prof. Souleiman Ramah, Prof. Ramez Nasser for facilitating my field missions. My special thanks are also addressed to Prof. Zouher Kattan for his constant support and scientific managing of my activities in the frame of this research.

I am thankful to my partners in the APAME Project, my best friend Hatham Al-Najjar for his valuable and effective participation in the project. My other best friend Miss Ghada Souleiman for her valuable remarks and sharing most of the archeoseismic field work activities, as well as Miss Evelin Samaan for her effective help in the archeological sounding in Apamea and Krak des Chevaliers sites.

I extend my thanks to Dr. Abdulrazzak Mouaz the ex-vice Minister of Culture for his efficient management of the APAME project in Syria; I include in my acknowledgements Dr. Bassam Jamous director general of the Directorate General of Antiquities and Museums (DGAM) as well as Dr. Tamam Fakush, the ex-general director of the DGAM for their effective supports in the APAME project activities.

I would like to thank my office partner Ryad Darawcheh and the colleagues of the geological department in the AECS, Youssef Radwan, Ihssan Layouss, Hassan Hassan for their valuable discussions and help during the different stages of this work, and Issa Al-Khudher, Bassam Ramadan, Rafik Shawish and Salim Zoulghina for their participation in the field work, Mr. Issmael Dozkangi for the administrative organisation of the project activities, and all the other colleagues in the department of geology.

I thank the many persons, local citizens and administrative staff for their hospitality and help during the field work in Deir Dahess, Al-Harif, Apamea, Krak des Chevaliers and in the many other sites.

This list will not be completed without great thanks to my Mother and Father *Dalal* and *Mohamed Diab*, also my life partners *Bassima* and my children *Zein, Leen and Hamzeh*; I own them a lot of continuous support.

Finally my deepest thank to everyone who read this thesis and may share with me any remarks that can improve this work.

Contents

Résumé de Thèse de Doctorat de Mohamed Reda SBEINATI

EOST - IPG Strasbourg

Titre : Sismicité historique, paléo-archéosismologie et évaluation de l'aléa sismique le long de la faille du Levant en Syrie

Ce travail de thèse a pour objectif d'étudier les séismes majeurs de la zone de faille du Levant (ou faille de la Mer Morte) en Syrie occidentale. La région du Moyen Orient est une des rares zones actives qui bénéficient d'un riche catalogue de sismicité historique (avec des séismes qui datent de plusieurs siècles avant JC). Plusieurs travaux sur l'activité sismique historique et contemporaine en Syrie et régions avoisinantes indiquent l'occurrence de forts séismes destructeurs notamment le long de la faille du Levant. Cependant, et malgré les importantes contributions à l'étude des caractéristiques de cette sismicité, une somme considérable de documents est restée inexploitée et un catalogue paramètrique nécessaire pour l'évaluation de l'aléa sismique restait à préparer.

La sismicité de la Syrie aurait pu être qualifiée de tout à fait modérée si on se limite à l'activité pendant les 2 derniers siècles. En effet, les évènements sismiques instrumentaux ($5 < Ms < 6$) se concentrent au nord à l'intersection de la faille du Levant avec la faille Est-Anatolienne. Plus au sud, une zone de lacune sismique apparaît entre la vallée (bassin en « pull-apart ») du Ghab et les monts du Liban (zone en transpression).

Les mécanismes focaux (CMT Harvard) des séismes récents indiquent des axes P de direction NNW-SSE liés à des failles décrochantes. Ces mécanismes illustrent la déformation active et la présence de failles décrochantes de direction Nord-Sud accompagnées de failles normales associées aux bassins en « pull-apart ». Les vitesses de déformation obtenues par la géodésie spatiale (GPS) varient de 5.6 to 7.5 mm/an en accord avec les récentes investigations paléosismiques et archéosismiques. En parallèle, d'autres questions sur le cycle sismique, la segmentation et la période de récurrence des forts séismes le long de la faille du Levant au nord du Liban restent posées.

Cette thèse traite des aspects de l'activité sismique à long terme le long de la faille du Levant et apporte quelques réponses sur le comportement des ces failles à travers les recherches que j'ai entrepris par des études de terrain couplées avec l'analyse des documents historiques. D'autre

part, ce travail a été effectué notamment dans le cadre du projet européen APAME (projet réalisé de mars 2003 à septembre 2006 et intitulé « *Archéo-Paleoseismology for the protection of cultural heritage in the Middle East* » (EC contract ICA-CT-2002-10024). En outre depuis 1999 et dans le cadre de mon activité professionnelle, j'ai également contribué au projet "*Seismic Data for Siting and Site-Revalidation of Nuclear Facility*" sous le patronage de l'Agence Internationale de l'Energie Atomique (IAEA, Vienne) pour l'étude de 181 évènements sismiques historiques (voir Chapitre IV).

Les problèmes de la sismicité épisodique en Syrie et les observations de terrain (faille et sites archéologiques) ont motivé mon intérêt à l'analyse de la sismicité historique, aux travaux de paléosismicité et d'archéosismicité, et à l'évaluation de l'aléa sismique dans la région.

Cette thèse s'organise suivant 5 chapitres principaux accompagnés d'un chapitre introductif, d'un chapitre de conclusions générales avec en annexe les articles publiés (ou en voie de publication) et rapports préparés dans le cadre de mes travaux de recherche.

Après le premier **chapitre I** Introduction qui présente essentiellement les motivations et le contexte de ce travail.

Le **chapitre II** intitulée « *Active faults and their relationships to earthquakes* » traite des aspects fondamentaux de la rupture sismique et des déformations de surface. Les méthodes et procédures d'étude des documents historiques dans le contexte des anciennes civilisations sont exposées en parallèle aux évaluations des intensités macrosismiques. Je présente également les principes et approches de la paléosismologie et de l'archéosismologie et l'intégration des données historiques et géologiques dans l'évaluation de l'aléa sismique.

Le **chapitre III** présente le contexte sismotectonique de la région libano-syrienne et du sud de la Turquie. J'analyse dans cette partie la géodynamique et les mécanismes au foyer et leur signification par rapport au domaine tectonique (bâti géologique, tectonique Mio-Pliocène et Quaternaire), du volcanisme, des caractéristiques de la lithosphère continentale et de la relation plaque Arabe et Afrique le long de la faille du Levant.

Le **chapitre IV** traite de la sismicité historique depuis 1365 avant JC à 1900 ; ce travail a fait l'objet d'une publication dans Annals of Geophysics :

Sbeinati M. R., R. Darawcheh and M. Mouty, (2005), The historical earthquakes of Syria: an analysis of large and moderate earthquakes from 1365 B.C. to 1900 A.D. ANNALS OF GEOPHYSICS 48, N. 3, June 2005, pp. 347-435.

Les sources originales ont été identifiées et étudiées pour la préparation d'un catalogue paramétrique unifié et homogène. J'ai étudié 181 séismes historiques et évalué les intensités macrosismiques de chaque localité liées aux évènements les plus significatifs en utilisant les méthodes et échelles standards (EMS-92, EMS-98) telle qu'employées en Italie, Russie, Royaume Uni et Iran. De nombreux documents en Arabe, Latin, Byzantin et Assyrien ont fait l'objet d'un examen détaillé pour l'identification de séismes historiques non mentionnés dans les travaux précédents. J'ai étudié en particulier les descriptions détaillées des effets liés aux séismes majeurs telles que rapportées dans les sources arabes. Ces effets comprennent les séismes précurseurs, les répliques, les ruptures en surface, la liquéfaction des sols, les glissements de terrain, les tsunamis, les feux et les dégâts des constructions. Un catalogue paramétrique de 36 séismes majeurs est préparé incluant les localisations épicentrales, les intensités maximum et minimum ($V \leq I_O \leq IX$) et les magnitudes estimées. Les calculs effectués pour ce catalogue indiquent des paramètres complétés pour des magnitudes $M_s > 6.5$ et constituent une contribution considérable pour une évaluation réaliste de l'aléa et du risque sismiques en Syrie.

Le **chapitre V** traite des travaux en archéosismologie et paléosismologie effectués sur des sites spécifiques favorables à l'étude du comportement à long terme des ruptures sismiques.

Auparavant, un inventaire des sites archéologiques affectés par des tremblements de terre est présenté. En Appendis une publication les résulta de l'investigation de 5 sites archéologiques

Sbeinati M. R., R. Darawcheh, and M. Mouty (1994). Field archeological evidences of seismic effects in Syria, in Materials of the CEC Project "Review of Historical Seismicity in Europe" – vol. 2., Albini P. and A. (edit.), CNR – Consiglio Nazionale delle Ricerche, Milano, Italy.

Après un rapport interne (*en Arabe*) présent l'introduction dédiée à la nomenclature et typologie des effets des séismes sur les constructions anciennes. J'ai pu décrire plus de 18 sites qui montrent des indices de destruction que j'attribue à des sollicitations sismiques. Les évidences de terrain montrent des décrochements latéraux de pierres de taille, des ruptures à travers les murs et pierres de taille, des basculements et torsions de constructions et effondrements d'édifices.

Sbeinati M. R., (1994), Evidences of Historical Earthquake Damages in some Archeological in Syria, *(Internal report in Arabic) Atomic Energy Commission of Syria*, Damascus, Syria.

An outre rapport présent l'étudiés des 13 sites archéologiques affectés par des tremblements de terre est situé le long de la faille du Levant et chaque site a livré un âge et un degré de destruction suivant la classification des intensités de l'échelle EMS-92 ou MSK-64.

Sbeinati M. R. and Darawcheh R., (1998). Archaeological Evidences of Earthquake Damage in Syria, research project "Seismic Data for Siting and Site-Revalidation of Nuclear Facility" (contract No. 6247/R3/RB), Atomic Energy Commission of Syria (AECS) and the International Atomic Energy Agency (IAEA), Damascus, Syria.

Etant donné mon implication dans les études de l'aqueduc faillé d'Al Harif, je présente les investigations détaillées des excavations, tranchées et analyse des carottes de travertins-tufa accumulés sur les parois de l'édifice Romain. Une publication est en révision:

Sbeinati et al., (2010), Timing of Earthquake Ruptures at the Al Harif Roman Aqueduct (Dead Sea fault, Syria) from Archeoseismology, Paleoseismology and Tufa Cores, submitted to Geological Society of America Bulletin, Special Issue on "Ancient Earthquake" (Accepted April 2010)

Ces études et analyses rendent compte directement des caractéristiques de la faille et du cycle sismique associé au cours des derniers 3000 ans.

Les ruptures cosismiques découvertes dans le « Krak des Chevaliers » est le deuxième exemple qui illustre la déformation sismique sur un site archéologique important (classée monument historique). La datation de l'effondrement des colonnes de l'Agora dans la ville archéologique Apamea (2 - 3eme siècle avant JC) livre des évidences sur l'occurrence de séismes majeurs anciens non répertoriés dans les catalogues. Les fouilles archéologiques sur la destruction d'un monastère byzantin à Deir Dahess rend compte de l'intensité du séisme historique de 526. L'ensemble de ces travaux a bénéficié de plus de 70 datations au C14 et m'a permis de complété le catalogue de sismicité pour la période antérieure à la civilisation byzantine.

L'intégration de la sismicité historique avec les données archéosismologiques et paléosismologiques pour l'évaluation de l'aléa sismique constitue la majeure partie du **chapitre VI**. Un traitement statistique de la sismicité historique et instrumentale suivant la loi Gutenberg-Richter nous livre la fréquence des séismes en fonction de la magnitude. Cette analyse est couplée par une détermination de la période de récurrence des séismes majeurs contrainte par les résultats des études archéosismologiques et paléosismologiques. Le couplage des approches déterministes et probabilistes est utilisé pour le calcul de l'aléa sismique. La possibilité de réaliser des cartes isoséistes pour des séismes historiques a rendu possible le calcul d'une loi d'atténuation pour la

Syrie occidentale. La prise en compte des caractéristiques des ruptures sismiques (initiation et terminaison en fonction de la géométrie des failles) m'a aidé au développement de modèles de mouvement et accélération des sols et à l'établissement de cartes d'iso-accélération. Ces cartes et la période de récurrence des forts séismes constituent un élément important dans le calcul de l'aléa sismique le long de la faille du Levant en Syrie.

En conclusion (**chapitre VII**), les travaux de cette thèse montrent essentiellement l'importance de l'approche multidisciplinaire dans l'étude des séismes historiques et ruptures sismiques associées. En effet, la combinaison des travaux sur les archives historiques avec les approches en sismologie, paléosismologie, archéosismologie et évaluation de l'aléa sismique a été nécessaire pour comprendre la répartition spatiale et temporelle de la sismicité le long de la faille du Levant. L'ensemble des sites historiques et archéologiques étudié a permis de mieux contraindre les effets des séismes sur les constructions et édifices et leur degré de destruction. L'établissement de cartes isoséistes pour des séismes historiques n'a été possible que grâce à la richesse des descriptions contenues dans les différentes archives. La segmentation de la faille (suivant les discontinuités géométriques), la répartition des destructions liées aux séismes historiques et les évidences des déplacements historiques et pré-historiques m'a permis d'établir la relation entre des ruptures cosismiques historiques et les caractéristiques des segments de faille. Plusieurs séismes auparavant décrits dans les sources historiques ont été identifiés dans les sites archéologiques et dans les tranchées paléosismolgoques. L'intégration des différents données et résultats à également permis une meilleure évaluation de l'aléa sismique en Syrie occidentale.

En suivant, je présente les différents travaux publiés ou en voie de publication dans des revues de rang A:

Publications:

Sbeinati M. R., R. Darawcheh, and M. Mouty (1994). Field archeological evidences of seismic effects in Syria, in Materials of the CEC Project "Review of Historical Seismicity in Europe" – vol. 2., Albini P. and A. (edit.), CNR – Consiglio Nazionale delle Ricerche, Milano, Italy. (in the Appendix section)

Darawcheh, R., **Sbeinati, M.R.**, Margottini, C., and Paolini, S., (2000), The 9 July 551 A.D. Beirut earthquake, eastern Mediterranean region: Journal of Earthquake Engineering, v. 4, p. 403–414, doi: 10.1142/S1363246900000229. (in the Appendix section)

Meghraoui, M., Gomez, F., **Sbeinati, R.**, Van der Woerd, J., Mouty, M., Darkal, A., Radwan, Y., Layyous, I., Najjar, H., M., Darawcheh, R., Hijazi, F., Al-Ghazzi, R., & Barazangi, M., (2003), Evidence for 830 years of seismic quiescence from paleoseismology, archeoseismology and historical seismicity along the Dead Sea fault in Syria, Earth. Planet. Sci. Letters 210, 35-52. (in the Appendix section)

Gomez, F., Meghraoui, M., Darkal, A., **Sbeinati, R.**, Darawcheh, R., Tabet, C., Khawlie, M., Charabe, M., Khair, K., and Barazangi, M., (2001), Coseismic displacements along the Serghaya Fault: an active branch of the Dead Sea Fault System in Syria and Lebanon, J. Geol. Soc. London 158, 405 – 408. (in the Appendix section)

Sbeinati M. R., R. Darawcheh and M. Mouty, (2005), The historical earthquakes of Syria: an analysis of large and moderate earthquakes from 1365 B.C. to 1900 A.D. ANNALS OF GEOPHYSICS 48, N. 3, June 2005, pp. 347-435. (in Chapter IV)

Alchalbi et al., and 15 authors (2009), Crustal deformation in northwestern Arabia from GPS measurements in Syria: Slow slip rate along the northern Dead Sea Fault, Geophys. J. Int. (2009), doi: 10.1111/j.1365-246X.2009.04431.x. (in the Appendix section)

Sbeinati et al., (2010), Timing of Earthquake Ruptures at the Al Harif Roman Aqueduct (Dead Sea fault, Syria) from Archeoseismology, Paleoseismology and Tufa Cores, submitted to Geological Society of America Bulletin, Special Issue on "Ancient Earthquake" (Accepted April 2010). (in Chapter V)

Summary of Ph.D Thesis of Mohamed Reda SBEINATI

EOST - IPG Strasbourg

Title : Historical Seismology, Paleo-Archeoseismology and seismic hazard along the Dead Sea Fault in Syria

The aim of this work is the study of major earthquakes along the Dead Sea Fault (DSF) in Syria. The Middle East region is among the few seismically active regions that have a rich and long historical seismicity catalogue with major events that date several centuries BC. Several previous works report the occurrence of large and destructive earthquakes (with M > 7) along the fault. Although a considerable work on their seismic characteristics has been achieved, the analysis of historical documents and field observations were, however, still needed in order to prepare a parametric catalogue of historical and instrumental earthquakes necessary for a realistic seismic hazard evaluation.

The seismicity of Syria can be qualified as moderate if we restrict the period of study to the last 2 centuries. The instrumental and historical seismicity during this period indicate magnitudes M ≤ 5.5 accompanied by a clear clustering of events along the Dead Sea Fault (DSF) and at the intersection with the East Anatolian Fault. However, a seismic gap appears clearly between the Ghab pull-apart basin and the Lebanese restraining bend.

A compilation of focal mechanisms (from Harvard CMT, Mednet and Salomon) indicates a NNW-SSE trending P axes along the DSF strike-slip fault. These mechanisms illustrate the stress distribution along the main active zones of western Syria with transpressive deformation and normal faulting in pull-apart basins. Slip rates range between 5.6 to 7.5 mm/yr. are estimated from geological, paleoseismological studies and in good agreement with results of GPS campaigns. In parallel, the return period of large earthquakes, related seismic cycle, fault segmentation and its long term behavior are the main issues to be addressed throughout our work.

The episodic seismicity of Syria (with the Missyaf seismic gap and quiescence period since the Middle Age) have increased my interest in the historical seismicity, paleoseismology and archeoseismology, and the seismic hazard assessment. In this work, the problem of long term seismic activity along the DSF is addressed from field investigations in archeoseismology, paleoseismology and the analysis of historical documents. This work benefited from the support of

the EC funded APAME Project [« *Archéo-Paleoseismology for the protection of cultural heritage in the Middle East* » (EC contract ICA-CT-2002-10024), from March 2003 to September 2006]. In parallel, I also benefited from the support of the project "*Seismic Data for Siting and Site-Revalidation of Nuclear Facility*" under the coordination of the International Atomic Energy Agency (IAEA, Vienne) for the study of 181 historical seismic events (see Chapter IV).

This thesis is organized into 5 main chapters accompanied by an introductory chapter I and a chapter VII of general conclusions with 2 appendixes for published articles in international journals and professional reports prepared in the frame of my scientific research program.

The introduction in **chapter I** shows the general tectonic and seismological context of the work, the main issues, motivations and structure of the work.

Chapter II titled « *Active faults and their relationships to earthquakes* » presents the fundamental aspects in active tectonic studies and the main concepts and theory of earthquake ruptures and surface faulting and deformation. The methods and approaches used to document the analysis of historical documents and its parametric component, and field investigations in archeoseismology and paleoseismology are presented with the integration of seismic parameters in the seismic hazard evaluation.

The active tectonics and seismotectonic context is presented in **chapter III** where the plate tectonics between Arabia, Africa-Sinai and Anatolia shows the regional geodynamics. The detailed fault mapping, geological and volcanic setting since the Miocene and the focal mechanism solutions provide some constraints on the lithospheric deformation along the plate boundary in western Syria.

The historical seismicity between 1365 BC and 1900 is documented in **chapter IV** through the extensive description of seismic events and their sources; this work is published in Annals of Geophysics:

Sbeinati M. R., R. Darawcheh and M. Mouty, (2005), The historical earthquakes of Syria: an analysis of large and moderate earthquakes from 1365 B.C. to 1900 A.D. *ANNALS OF GEOPHYSICS* 48, N. 3, June 2005, pp. 347-435. *See chapter IV*

The original sources have been studied in order to prepare a unified and homogeneous catalogue of 181 past events, with an estimate of macroseismic intensity using standard macroseismic scaling (EMS-92 and EMS-98) as already tested in Italy, Russia, United Kingdom and Iran. In a collaborative work with some colleagues, numerous historical documents in Arabic, Latin, Byzantine and Assyrian were studied for the identification of past earthquakes with some of them not mentioned in previous works. In particular, I have studied in detail the effects of major earthquakes in Arabic manuscripts. The study includes foreshocks and aftershocks, surface ruptures, soil liquefaction, landslides, tsunami, fires and building collapses. A parametric catalogue of 36 major earthquakes is prepared with their epicentral location, maximum and minimum intensities ($V \leq I_0 \leq IX$) and estimated magnitudes. Our calculation shows a completed parametric catalogue for $M_s > 6.5$ and contributes to a better estimate of the seismic hazard and risk in Syria.

Chapter V documents the field investigations in archeoseismology and paleoseismology along the DSF with a particular attention to some specific archeological sites that allow the study of seismic ruptures and their long term behaviour.

Previously, inventory studies of archeological sites that underwent earthquake damage were conducted, the study of 5 archeological sites presented in the **Appendix:**

Sbeinati M. R., R. Darawcheh, and M. Mouty (1994). Field archeological evidences of seismic effects in Syria, in Materials of the CEC Project "Review of Historical Seismicity in Europe" – vol. 2., Albini P. and A. (edit.), CNR – Consiglio Nazionale delle Ricerche, Milano, Italy.

Afterword; An internal report (*in Arabic*) presents an introduction on the nomenclature and typology of seismic effects on ancient buildings. In this report, I have described 18 archeological sites with clear earthquake-induced damage with field evidence of displaced key stones of aches in Roman buildings, cracks, ruptures, waving and rotation in stones of walls, and collapse of constructions.

Sbeinati M. R., (1994), Evidences of Historical Earthquake Damages in some Archeological in Syria, *(Internal report in Arabic) Atomic Energy Commission of Syria*, Damascus, Syria.

Another report covered 13 archeological sites distributed on the main active fault zones in Syria describes the types of historical earthquake damages with attribution to each site a degree of destruction following the classification given by EMS-92 or MSK-64 scales.

Sbeinati M. R. and Darawcheh R., (1998). Archaeological Evidences of Earthquake Damage in Syria, research project "Seismic Data for Siting and Site-Revalidation of Nuclear Facility" (contract No. 6247/R3/RB), Atomic Energy Commission of Syria (AECS) and the International Atomic Energy Agency (IAEA), Damascus, Syria.

The detailed archeoseismic work that I conducted for the study of the Al Harif aqueduct is presented throughout the excavations, trenching and analysis of Tufa deposits and collected cores. An article has been submitted for publication:

> **Sbeinati et al.**, (2010), Timing of Earthquake Ruptures at the Al Harif Roman Aqueduct (Dead Sea fault, Syria) from Archeoseismology, Paleoseismology and Tufa Cores, submitted to Geological Society of America Bulletin, Special Issue on "Ancient Earthquake" (accepted April 2010). *See Chapter V*

These studies and related analyses describe the faulting behavior and seismic cycle during the last 3000 years along the Missyaf segment of the DSF.

In parallel, I also conducted detailed works in 3 other different sites: The seismic ruptures discovered in the fortress « Krak des Chevaliers » (classified historical monument) immediately west of the DSF illustrate the seismic deformation associated with a moderate earthquake taking place between 1285 AD and 1295 AD. The collapse of main colonnades in the city of Apamea (II – III century BC) and a building collapse with deposited fire ashes indicate the occurrence of two major events in 420 – 570 AD and during the XII century. Archeological investigations at Deir Dahess show clear building collapses at different locations which can be dated around 526 AD and may be correlated to the 29 May 526 large earthquake that affected Saint Simon. The archeoseismic and paleoseismic investigations benefited from more than70 radiocarbon dating that help in the determination of past earthquakes during the pre-Islamic period.

The integration of data and results from the historical seismicity, archeoseismology and paleoseismology are prepared for the seismic hazard evaluation in **chapter VI**. A statistical analysis of seismicity catalogue (both instrumental and historical) following the Gutenberg-Richter relation provides the frequency of past events as a function of their magnitude. The analysis is coupled with the determination of recurrence time of large seismic events for different fault segments. The use of both deterministic and probabilistic approaches for the seismic hazard calculation allowed us to estimate peak ground acceleration and prepare maps for different scenarios of earthquake faulting. These maps and estimated return period of large earthquakes in zones of seismic gaps along the DSF constitute an important element for the seismic hazard and risk in Syria and surrounding regions.

The conclusion in **chapter VII** indicates the importance of multidisciplinary approaches in the study of past earthquakes. The combined studies of historical documents with field investigations in archeoseismology and paleoseismology provide with some insights on the physics of seismic ruptures and seismic damage to ancient buildings. The spatial and temporal distribution of large earthquakes observed from the historical catalogue is now constrained with physical observation of faulting episodes in excavations and trenching. Several past earthquakes described only in historical archives are now documented using archeoseismic and paleoseismic investigations and their seismic parameters listed in the parametric catalogue. The integration of different datasets with the seismic parameters of fault segments allows a better evaluation of the seismic hazard and risk in Syria.

I present in the following the titles of published articles prepared in the framework of my research during the thesis preparation.

Publications:

Sbeinati M. R., R. Darawcheh, and M. Mouty (1994). Field archeological evidences of seismic effects in Syria, in Materials of the CEC Project "*Review of Historical Seismicity in Europe*" – vol. 2., Albini P. and A. (edit.), CNR – Consiglio Nazionale delle Ricerche, Milano, Italy. (*in the Appendix section*)

Darawcheh, R., **Sbeinati, M.R.,** Margottini, C., and Paolini, S., (2000), The 9 July 551 A.D. Beirut earthquake, eastern Mediterranean region: *Journal of Earthquake Engineering*, v. 4, p. 403–414, doi: 10.1142/S1363246900000229. (*in the Appendix section*)

Meghraoui, M., Gomez, F., **Sbeinati, R.,** Van der Woerd, J., Mouty, M., Darkal, A., Radwan, Y., Layyous, I., Najjar, H., M., Darawcheh, R., Hijazi, F., Al-Ghazzi, R., & Barazangi, M., (2003), Evidence for 830 years of seismic quiescence from paleoseismology, archeoseismology and historical seismicity along the Dead Sea fault in Syria, *Earth. Planet. Sci. Letters* 210, 35-52. (*in the Appendix section*)

Gomez, F., Meghraoui, M., Darkal, A., **Sbeinati, R.,** Darawcheh, R., Tabet, C., Khawlie, M., Charabe, M., Khair, K., and Barazangi, M., (2001), Coseismic displacements along the Serghaya Fault: an active branch of the Dead Sea Fault System in Syria and Lebanon, *J. Geol. Soc. London* 158, 405 – 408. (*in the Appendix section*)

Sbeinati M. R., R. Darawcheh and M. Mouty, (2005), The historical earthquakes of Syria: an analysis of large and moderate earthquakes from 1365 B.C. to 1900 A.D. ANNALS OF GEOPHYSICS 48, N. 3, June 2005, pp. 347-435. (*in Chapter IV*)

Alchalbi et al., and 15 authors (2009), Crustal deformation in northwestern Arabia from GPS measurements in Syria: Slow slip rate along the northern Dead Sea Fault, *Geophys. J. Int.* (2009), doi: 10.1111/j.1365-246X.2009.04431.x. (*in the Appendix section*)

Sbeinati et al., (2010), Timing of Earthquake Ruptures at the Al Harif Roman Aqueduct (Dead Sea fault, Syria) from Archeoseismology, Paleoseismology and Tufa Cores, submitted to Geological Society of America Bulletin, Special Issue on "Ancient Earthquake" (Accepted April 2010). (*in Chapter V*)

ملخص أطروحة دكتوراه لـ محمد رضا سبيناتي

مدرسة رصد الاهتزازات الزلزالية والفلكية EOST – معهد فيزياء الأرض ستراسبورغ IPGS

جامعة ستراسبورغ

العنوان: الزلزالية التاريخة والزلزالية القديمة والآثارية والمخاطر الزلزالية على امتداد صدع البحر الميت في سوريا

يهدف هذا العمل إلى وضع تصور للمخاطر الزلزالية المحتملة في سوريا والتي مصدرها الجزء الشمالي لصدع البحر الميت من خلال دراسة الزلازل الكبيرة على امتداده عبر غرب سوريا ولبنان. إن منطقة الشرق الأوسط هي من المناطق القليلة في العالم ذات النشاط الزلزالي التي تتمتع بلائحة (كتالوغ) زلازل غنية وذات تغطية زمنية كبيرة لمعظم الحوادث الزلزالية ذات الدمار الكبير والتي تعود لحقبة ما قبل الميلاد. إن الأعمال السابقة التي تحدثت عن ظهور زلازل كبيرة ذات تأثير مدمر على امتداد الصدع بقدر (ماغنيتود) أكبر من سبعة درجات (M>7.0)، وعلى الرغم من إنجاز العديد من الأعمال ذات الأهمية في تحديد الخواص الزلزالية، و من أجل تحقيق تقدير واقعي للخطر الزلزالي، بقيت الحاجة المُلِحّة لتحليل الوثائق التاريخية والملاحظات الحقلية لإعداد كتالوغ لمُعامِلات (بارامترات) الزلازل التاريخية (مرحلة ما قبل ظهور أنظمة التسجيلات الآلية للزلازل أي قبل عام 1900 ميلادية) والآلية (أي مابعد ظهور التسجيلات الزلزالية بأجهزة المراقبة أي مابعد عام 1900 ميلادية).

يُصنَّف مستوى النشاط الزلزالي في سوريا ضمن المجال المتوسط، هذا فيما إذا حددنا الفترة الزمنية للدراسة بالقرنين الماضيين، حيث تشير معطيات الزلزالية الآلية والتاريخية خلال تلك الفترة لقيمة قدر أعظمي (M≤5.5) ولكنها من جهة أخرى تبدي تراتبية مكانية (spatial clustering) واضحة للحوادث الزلزالية على امتداد الصدع من خلال تركيز النشاط الزلزالي في منطقة التقاء صدع البحر الميت بصدع شرقي الأناضول من جهة، و من جهة أخرى تظهر وبشكل واضح الطفرة في غياب النشاط الزلزالي (seismic gap) في منطقتي انفتاح سهل الغاب ومصياف ونطاق ليّ الكبح اللبناني (صدع اليمونة).

تشير معطيات آلية البؤر الزلزالية (Focal mechanism) المحصول عليها من مركز(Harvard CMT) و بحسب كُلٍ من (Pondrelli et al., 2002) و (Salamon et al., 2003) إلى أن محاور الضغط P على امتداد صدع البحر الميت ذي الانزياح الجانبي بأنها ذات اتجاه عام شمال شمال – غرب و جنوب جنوب – شرق. تظهر آليات البؤر الزلزالية توزع الإجهادات على امتداد النطاقات النشطة الرئيسة في غرب سوريا مع التشوه التحويلي والتصدعات من نمط Normal faulting في أحواض الانفتاح pull-apart basins. يقدر معدل الإزاحة على امتداد صدع البحر الميت بحوالي من 5.6 إلى 7.5 ملم في العام وذلك بناءً على معطيات الدراسات الجيولوجية و الزلزالية القديمة وبتوافق مع نتائج حملات قياسات نظام التموضع العالمي GPS. وبالتوازي فإن الأهداف الرئيسة لهذا العمل تتمحور حول تحديد زمن تكرارية حوادث الزلازل الكبيرة المدمرة، و الدورة الزلزالية ذات الصلة، والمقاطع الصدعية وسلوكها طويل الأمد.

لقد زاد من اهتمامي في الزلزالية التاريخة، والقديمة، والآثارية هو العارض الزلزالي في سوريا والمتمثل بطفرة غياب النشاط الزلزالي الحديث على امتداد صدع مصياف وحقبة الهدوء الزلزالي الممتدة منذ القرون الوسطى. في هذا العمل تم عنونة مسألة النشاط الزلزالي طويل الأمد على امتداد صدع البحر الميت اعتماداً على التحريات الحقلية في مجال الزلزالية الآثارية والزلزالية القديمة بالإضافة إلى تحاليل الوثائق التاريخية. لقد تم إنجاز هذا العمل مستفيداً من الدعم المالي للهيئة الأوربية لمشروع APAME

(مشروع حماية الموروث الثقافي في الشرق الأوسط اعتماداً على معطيات الزلزالية الآثارية والقديم) رقم العقد (EC contract ICA-CT-2002-10024)، ابتداءً من آذار 2003 وحتى أيلول 2006، كذلك استفاد هذا العمل من دعم الوكالة الدولية للطاقة الذرية في فينا ضمن مشروع بحث بعنوان (استخدام المعطيات الزلزالية لاختيار مواقع وإعادة تقييم أهلية مواقع مقترحة لبناء منشآت تجهيزات نووية) لدراسة 181 حدث زلزالي تاريخي (انظر الفصل الرابع).

لقد نظمت هذه الأطروحة ضمن خمسة فصول رئيسة حيث وضع الفصل الأول كمدخل للعمل والفصل السابع كخلاصة عامة للعمل بالإضافة إلى قسم الملحقات تضمن خمسة ورقات علمية منشورة في كتب ومجلات علمية عالمية.

الفصل الأول (المقدمة): يعرض الوضع التكتوني والسيسمولوجي العام للعمل، الأهداف الرئيسة، الدوافع للقيام بهذا العمل وبنيته.

الفصل الثاني (الصدوع النشطة وعلاقتها بالزلازل): يعرض هذا الفصل التوجهات الأساسية لدراسات التكتونيك النشط والمفاهيم النظرية الرئيسة للتصدعات المرافقة للزلازل والتصدعات والتشوهات السطحية. كذلك الطرائق المستخدمة في تحليل الوثائق التاريخية وتحديد معاملات الزلازل التاريخية، أيضاً تم تقديم التحريات الحقلية في مجال الزلزالية الآثارية والقديمة ومكاملتها مع المعاملات الزلزالية الأخرى في مجال تقدير المخاطر الزلزالية.

الفصل الثالث (الوضع التكتوني النشط والسيسموتكتوني في منطقة الدراسة): عرض في هذا الفصل الوضع الجيوحركي المسيطر بين كلٍ من الصفائح التكتونية العربية والأفريقية-سيناء والأناضولية. أيضاً وضع خارطة دقيقة لصدع البحر الميت والوضع الجيولوجي والبركاني منذ عصر الميوسين ونتائج تحاليل آلية البؤر الزلزالية والتي تزودنا بشيءٍ من التأكيد على وضع التشوهات ضمن الطبقة الصخرية (ليثوسفير) على امتداد حدود الصفائح في غرب سوريا.

الفصل الرابع (الزلزالية التاريخية في سوريا والمناطق المجاورة): حيث عرضت مقالة علمية منشورة وثقت النشاط الزلزالي التاريخي للمنطقة خلال المرحلة الممتدة من 1365 قبل الميلاد وحتى 1900 ميلادية، من خلال الوصوفات التفصيلية للحوادث الزلزالية ومصادرها، نشرت هذه المقالة في مجلة حوليات الجيوفيزياء في إيطاليا (Annals of Geophysics) إعداد سبيناتي ودراوشة ومعطي:

Sbeinati M. R., R. Darawcheh and M. Mouty, (2005), The historical earthquakes of Syria: an analysis of large and moderate earthquakes from 1365 B.C. to 1900 A.D. *ANNALS OF GEOPHYSICS* 48, N. 3, June 2005, pp. 347-435.

تم في هذه المقالة دراسة وتحليل المصادر التاريخية الأصيلة ذات الصلة بهدف وضع لائحة متجانسة بالحوادث الزلزالية التاريخية والتي بلغ عددها 181 حدث زلزالي، وتقدير للشدات الزلزالية المترافقة بتطبيق سلم معياري لتقدير الشدة الزلزالية (EMS-92 و MSK-64) والذي سبق اختباره في كلٍ من إيطاليا والاتحاد السوفياتي السابق والمملكة المتحدة وإيران. وضمن بيئة من العمل المشترك بين الزملاء تم دراسة العديد من الوثائق التاريخية العربية واللاتينية والبيزنطية والسريانية بهدف تحديد الزلازل التاريخية التي لم يسبق التطرق إليها في مراجع علمية منشورة سابقاً، وبالتحديد فقد درستُ بالتفصيل تأثيرات الزلازل في المخطوطات العربية، وتم التطرق لدراسة الظواهر الأخرى المرافقة لها كالهزات السابقة واللاحقة لحدث زلزالي كبير، والتصدعات السطحية، تموه التربة، انزلاقات الأراضي، أمواج المد البحرية، النيران المتحرضة وانهيار المباني. وكانت النتيجة وضع لائحتين بالزلازل التاريخية: تضمنت الأولى معاملات (باراميترات) كاملة لـ 36 حدث زلزالي تاريخي (إحداثيات المركز السطحي، الشدة الزلزالية العظمى و الماغنيتود المقدر...إلخ) حيث كانت أعلى شدة زلزالية بين ($V \leq I_0 \leq IX$). أما اللائحة الثانية فشملت تقدير للشدات الزلزالية المترافقة مع 181 حدث زلزالي تاريخي. إن درجة كمالية اللائحة الأولى هي حتى عتبة $M_s > 6.5$ أي أنها شملت تحليل كامل الحوادث الزلزالية التاريخية لمنطقة الدراسة والتي أعلى من قيمة القدر المذكورة آنفاً، وهذا مما يساهم في تقدير أفضل لحالة الخطر الزلزالي في سوريا.

الفصل الخامس (الزلزالية القديمة و الآثارية): يوثق هذا الفصل أعمال التحريات في مجال الدراسات الزلزالية الآثارية والقديمة على امتداد صدع البحر الميت مع التركيز الخاص على بعض المواقع الأثرية التي سمحت لي في دراسة التصدعات المرافقة للزلازل القديمة وسلوكها على المدى الطويل.

لقد سبق هذه الدراسات التفصيلية أعمال مسح حقلية أولية لمواقع أثرية دُمِّرت بالزلازل نتج عنها ورقة علمية وتقريرين احترافيين. شملت الورقة العلمية دراسة خمسة مواقع أثرية وقد تضمنت في قسم الملحقات وهي:

Sbeinati M. R., R. Darawcheh, and M. Mouty (1994). Field archeological evidences of seismic effects in Syria, in Materials of the CEC Project "Review of Historical Seismicity in Europe" – vol. 2., Albini P. and A. (edit.), CNR – Consiglio Nazionale delle Ricerche, Milano, Italy.

بعد ذلك تم تقديم تقرير داخلي للهيئة (بالعربية) قدم فيه دراسة لثمانية عشر موقعاً أثرياً، تم التطرق فيه لأسماء المواقع وأنماط الدمار الزلزالي في الأبنية القديمة تمثلت بإزاحة أحجار القفل في أقواس الأبنية الرومانية والبيزنطية، والشقوق، والتمزقات، وتماوج ودوران أحجار البناء، ودمار المنشآت وهو:

شواهد دمار الزلازل التاريخية في بعض المواقع الأثرية في سوريا، إعداد محمد رضا سبيناتي (1994)، تقرير داخلي، هيئة الطاقة الذرية السورية، دمشق، سوريا.

Sbeinati M. R., (1994), Evidences of Historical Earthquake Damages in some Archeological in Syria, *(Internal report in Arabic) Atomic Energy Commission of Syria*, Damascus, Syria.

التقرير الثاني شمل دراسة ثلاثة عشر موقعاً أثرياً موزعة على امتداد الصدوع النشطة الرئيسة في سوريا، حيث فيه توصيف أنماط الدمار الزلزالي مع المساهمة في تحديد درجة الدمار اعتماداً على التصنيف المبين في سلمي قياس الشدة الزلزالية (EMS-92 أو MSK-64) وقد أُعِدَّ هذا التقرير كجزء من تقرير نهائي لمشروع بحث لصالح الوكالة الدولية للطاقة الذرية في فينا:

Sbeinati M. R. and Darawcheh R., (1998). Archaeological Evidences of Earthquake Damage in Syria, research project "Seismic Data for Siting and Site-Revalidation of Nuclear Facility" (contract No. 6247/R3/RB), Atomic Energy Commission of Syria (AECS) and the International Atomic Energy Agency (IAEA), Damascus, Syria.

أما أعمال الدراسات التفصيلية والكمية فقد تمثلت بدراسة لموقع قناة رومانية لجر المياه في موقع الحريف بالقرب من مدينة مصياف، وقد شملت الدراسة أعمال حفريات أثرية، وحفر خنادق وتحاليل لعينات مأخوذة من ترسبات الطف الكلسية الناتجة من تدفق ينبوع مياه في المنطقة، نشرتُ نتائج هذه الدراسة في ورقة علمية وقُبلت للنشر في نيسان 2010 وقد أدرجتها في الفصل الخامس من الأطروحة:

Sbeinati et al., (2010), Timing of Earthquake Ruptures at the Al Harif Roman Aqueduct (Dead Sea fault, Syria) from Archeoseismology, Paleoseismology and Tufa Cores, submitted to Geological Society of America Bulletin, Special Issue on "Ancient Earthquake" (accepted April 2010). **(***See Chapter V***)**

إن هذه الدراسات والتحاليل المرافقة وصفت السلوك التصدعي والدورة الزلزالية على مدى 3000 عام على امتداد مقطع صدع مصياف من الصدع الكلي وهو صدع البحر الميت.

على التوازي قمت بدراسات تفصيلية لثلاثة مواقع أثرية أخرى: ركزت الدراسة الأولى على التصدعات الزلزالية المكتشفة في قلعة الحصن والتي تقع مباشرة إلى الغرب من صدع البحر الميت وعرض للتشوهات الزلزالية المترافقة مع الزلازل المتوسطة الحجم التي حدثت خلال الفترة مابين 1285 و1295 ميلادية. الدراسة الثانية حول انهيار الأعمدة الرئيسة في مدينة أفاميا الأثرية (القرنين الثالث والثاني قبل الميلاد) وانهيار الأبنية مع الرماد الناتج عن النيران المرافقة، حيث بينت الدراسة وقوع حدثين زلزاليين مدمرين الأول خلال الفترة مابين 420 و 570 ميلادية والثاني خلال القرن الثاني عشر الميلادي. الدراسة الثالثة شملت تحريات زلزالية آثارية لموقع دير داحس في جبل باريشا، حيث بينت وجود شواهد دمار لعدد من الأبنية في عدة مواقع بتأثير زلازل 526 ميلادية وعلى الأرجح الزلزال الكبير الذي دمر دير سمعان في 29 أيار 526 ميلادية. لقد دعمت دراسات الزلزالية القديمة والآثارية بشكل واسع بنتائج تحاليل أكثر من 70 عينة لتحديد العمر المطلق بطريقة الكربون 14، حيث مكنت من تحديد الزلازل القديمة خلال عصور ما قبل عصر الإسلام.

الفصل السادس (المخاطر الزلزالية): بناءً على مكاملة نتائج دراسات الزلزالية القديمة والآثارية والتاريخية والآلية، تم إعداد لائحة متكاملة ومتجانسة للحوادث الزلزالية خلال الـ 3000 عام السابقة وطبق عليها تحاليل إحصائية، ثم تطبيق معادلة غوتنبرغ-ريختر لمعرفة تكرارية حدوث الزلازل بدلالة قيمة القدر (الماغنيتود)، لقد طبقت التحاليل من أجل حساب تكرارية الزلازل الكبيرة على كامل عدد المقاطع الصدعية، وباستخدام برنامج CRISIS-2008 تم حساب الخطر الزلزالي بطريقة هجينة بين الطريقتين التحديدية و الاحتمالية ومن ثم رسمت خرائط لقيم التسارعات الأرضية المقدرة من أجل عدة حواريات (سيناريو) للتصدعات الزلزالية. إن خرائط المخاطر الزلزالية و أزمنة التكرار المقدرة في نطاقات الثغرات الزلزالية على امتداد صدع البحر الميت تشكل عنصر هام في مجال دراسات المخاطر الزلزالية وكوارثها في سوريا والمناطق المجاورة.

الفصل السابع (الخلاصة): تشير الخلاصة إلى أهمية تطبيق نهج استخدام الطرائق المتعددة في دراسة الزلازل القديمة. إن عملية الجمع مابين الوثائق التاريخية وأعمال التحريات الحقلية في مجال الزلزالية القديمة والآثارية ومع تضمين مفاهيم فيزياء التصدعات الزلزالية والدمار الزلزالي في الأبنية الأثرية أصبح من الوضوح بمكان التوزع الزماني والمكاني للزلازل الكبيرة اعتماداً على الزلازل الملاحظة في لائحة (كتالوغ) الزلازل التاريخية وإضافة إلى القياسات الفيزيائية لمظاهر التصدعات المكتشفة في الخنادق المحفورة. الزلازل التاريخية التي ذكرت فقط في الأرشيف أصبحت الآن موثقة حقلياً من خلال تحريات الزلزالية الآثارية والقديمة والمعاملات الزلزالية المدرجة في لائحة الزلازل. إن مكاملة معطيات مختلف قواعد البيانات مع معاملات المقاطع الصدعية تسمح لنا في عمل تقدير أفضل للخطر الزلزالي في سوريا.

أقدم فيما يلي لائحة بعناوين أهم المقالات العلمية المنشورة التي شاركت فيها ضمن إطار بحثي خلال إعداد هذه الأطروحة:

Sbeinati M. R., R. Darawcheh, and M. Mouty (1994). Field archeological evidences of seismic effects in Syria, in Materials of the CEC Project "*Review of Historical Seismicity in Europe*" – vol. 2., Albini P. and A. (edit.), CNR – Consiglio Nazionale delle Ricerche, Milano, Italy. *(in the Appendix section في قسم الملحقات)*

Darawcheh, R., **Sbeinati, M.R.,** Margottini, C., and Paolini, S., (2000), The 9 July 551 A.D. Beirut earthquake, eastern Mediterranean region: *Journal of Earthquake Engineering*, v. 4, p. 403–414, doi: 10.1142/S1363246900000229. *(in the Appendix section في قسم الملحقات)*

Meghraoui, M., Gomez, F., **Sbeinati, R.,** Van der Woerd, J., Mouty, M., Darkal, A., Radwan, Y., Layyous, I., Najjar, H., M., Darawcheh, R., Hijazi, F., Al-Ghazzi, R., & Barazangi, M., (2003), Evidence for 830 years of seismic quiescence from paleoseismology, archeoseismology and historical seismicity along the Dead Sea fault in Syria, *Earth. Planet. Sci. Letters* 210, 35-52. *(in the Appendix section في قسم الملحقات)*

Gomez, F., Meghraoui, M., Darkal, A., **Sbeinati, R.,** Darawcheh, R., Tabet, C., Khawlie, M., Charabe, M., Khair, K., and Barazangi, M., (2001), Coseismic displacements along the Serghaya Fault: an active branch of the Dead Sea Fault System in Syria and Lebanon, *J. Geol. Soc. London* 158, 405 – 408. *(in the Appendix section في قسم الملحقات)*

Sbeinati M. R., R. Darawcheh and M. Mouty, (2005), The historical earthquakes of Syria: an analysis of large and moderate earthquakes from 1365 B.C. to 1900 A.D. ANNALS OF GEOPHYSICS 48, N. 3, June 2005, pp. 347-435. (*in Chapter IV في الفصل الرابع*)

Alchalbi et al., and 15 authors (2009), Crustal deformation in northwestern Arabia from GPS measurements in Syria: Slow slip rate along the northern Dead Sea Fault, *Geophys. J. Int.* (2009), doi: 10.1111/j.1365-246X.2009.04431.x. (*in the Appendix section في قسم الملحقات*)

Sbeinati et al., (2010), Timing of Earthquake Ruptures at the Al Harif Roman Aqueduct (Dead Sea fault, Syria) from Archeoseismology, Paleoseismology and Tufa Cores, submitted to Geological Society of America Bulletin, Special Issue on “Ancient Earthquake” (Accepted April 2010). (*in Chapter V في الفصل الخامس*)

List of Figures

Figure Captions of Chapter II

Figure Captions of Chapter III

Figure Captions of Chapter IV

Figure Captions of Chapter V

Figure Captions of GSA Paper in Chapter V

designed to bring fresh water from western ranges to Apamea and Shaizar. LRB is for Lebanese Restraining Bend.

Figure 4: a) Satellite view from Google Earth showing offset Al Harif Aqueduct (black arrow) along the DSF (white arrows); b) local geomorphologic framework of the aqueduct site as interpreted from Figure 4a indicating a shutter ridge (Mesozoic limestone east of the fault) and ~ 200 m of left-lateral offset. Blue arrow is for stream flow. See Figure 5 for the detailed aqueduct map and location of excavations and trenches.

Figure 5: Microtopographic survey (0.05 m contour lines) of the Al-Harif Aqueduct and related flat alluvial terrace. The aqueduct (thin blue crosses) shows a total 13.6 ±0.20 m of left-lateral slip along the fault zone (Meghraoui et al., 2003). Roman numbers indicate archeseismic excavations (in reddish and orange labeled I to IV) and letters indicate paleoseismic trenches (in grey and black labeled A, B, C and E). The dragged wall fragment is located between excavation IV and trench E and is marked by a dense cluster of survey points.

Figure 6: a) Schematic sketch of the aqueduct and locations of the selected cores BR3, 5 and 6; BR4 core sample consists in tufa accumulation at the location of the missing (broken) piece of the aqueduct wall near the fault. Mosaic of the archeological excavation I is detailed in Figure 8 b (see also location in Figure 5). b) Core section BR4 showing the limit between the wall stone and tufa deposits.

Figure 7: Schematic sections of the aqueduct western wall and related tufa deposits (B, C, D and E indicate earlier core sections of tufa deposits (Meghraoui et al., 2003). Tufa samples AQ-Tr B13 and AQ-Tr D5 (Table 1) are from cores B and D, respectively. The right and left vertical sections show the relative tufa thickness of the original built part (with *Opus caementum* and *quadratum* stones) and the rebuilt part, respectively. The plan view indicates the variation of tufa deposition and shows the cores distribution and related depths along the western wall of the aqueduct.

Figure 8: a) view of the fault zone from the western aqueduct wall, the dragged wall piece and eastern wall (string grid is 1 m x 1 m). Log of trench-excavation E is in Figure 7c; b) Mosaic of excavation I exhibits the main fallen wall (A and B) and dragged wall piece (C), scattered wall pieces and the fault zone; note also location of cement sample CS 1 to 4 (see text for explanation); c) Trench E (excavation I, north wall) exposes faulted sedimentary units below the archeological remains and wall fragment C visible in bottom of Figure 7 b; fz is for fault zone, sedimentary units are similar to those of trenches A, B and C (see also Figure 9) and dating characteristics are in Table 1.

Figure 9: Excavations II (a) and III (b) that expose the aqueduct wall foundation (see also Figure 5) and related sedimentary units e underneath. The difference in the size of stones (e.g., *Opus*

quadratum and *caementum*) between excavation II (a) and excavation III (b) implies a rebuilding phase of the latter wall.

Figure 10: Trench logs A, B and C north of the aqueduct site (see location in Figure 5). All trenches display the Dead Sea fault zone as a negative flower structure affecting all alluvial units below unit a. Calibrated C^{14} dating are in Table 1. Fault branches in trench C are labeled I to V (see text for explanation). The sedimentary units are very comparable and show 3 to 4 faulting events denoted W to Z (see text for explanation).

Figure 11**:** Synthetic description of cores with lithologic content and sample number for radiocarbon dating (see Table 1 and Figure 6 for core locations); I stands for major interruption. The very porous tufa indicates major interruptions in tufa growth (e.g., a major interruption of core growth in BR3 is visible at about 22 cm (Br 3-4 sample; see text for explanation). The correlation between major interruptions of tufa growth and faulting events in trenches and archeoseismic building constrains the timing of repeated earthquakes along the Missyaf segment of the Dead Sea Fault.

Figure 12: a) Calibrated dating of samples (with calibration curve INTCAL04 from Reimer et al. (2004) with 2σ age range and 94.5% probability) and sequential distribution from Oxcal program (see also Table 1; Bronk Ramsey C., 2001). The Bayesian distribution computes the time range of large earthquakes (events W, X, Y and Z) at the Al Harif Aqueduct according to faulting events, building and repair of walls, starts and interruptions of the tufa deposits (see text for explanation).

Figure 13: Correlation of results between paleoseismic trenching, archeoseismic excavations and tufa analysis. In paleoseismic trenching, the youngest age for event X is not constrained but it is, however, limited by event Y. In archeoseismic excavations, the period of first damage overlaps with that of the second damage due to poor age control. In tufa analysis, the onset and restart of Br3 and Br4 mark the damage episodes to the aqueduct; The growth of Br5 and Br6 shows interruptions [I] indicating the occurrence of major events. Except for the 29 June 1170, previous events have been unknown in the historical seismicity catalogue. The synthesis of large earthquake events results from the timing correlation between the faulting events, building repair and tufa interruptions (also summarized in Figure 12 and text). Although visible in trenches (faulting event X), archeoseismic excavations (first damage) and first interruption of tufa growth (in Br5 and Br6 cores), the AD 160 - 510 AD age of event X has a large bracket. In contrast, event Y is relatively well bracketed between AD 625 - 690 with the overlapped dating from trench results, the second damage of the aqueduct and the interruption and restart of Br3 and onset of Br4. The occurrence of the 1170

earthquake correlates well with event Z of trenches, the age of 3rd damage to the aqueduct, and the age of interruption of Br4, Br5 and Br6.

Figure 14: Schematic reconstruction (with final stage from Figure 5) of the AD 160 - 510, AD 625 - 690 and AD 1170 large earthquakes and related faulting of the Al Harif Aqueduct. Except for the AD 1170 earthquake (see historical catalogue of Sbeinati et al., 2005), the dating of earthquake events are from Figure 12. The white small section is the rebuilt wall after event X (see buried wall A and B in Figure 8 b); the subsequent grey piece corresponds to the rebuilt wall after event Y (see wall section C in Figure 8 b) which was damaged and dragged after event Z. The earlier aqueduct deformation (warping of the eastern wall near the fault rupture) may have recorded ~ 4.3 m of coseismic left-lateral slip well preserved during the subsequent fault movements.

Figure 15: Estimated fault-slip behavior and related slip rates (obtained from regression lines) from two scenarios of possible earthquake occurrence taking into account timing for paleo-earthquakes as in Figure 12 (with average X (AD 160 - 510) 375 ±175, average Y (AD 625-690) 640 ±32, Z (AD 1170) and two different timeframes for W (historical event of 1365 BC and . In both cases, the two regression lines indicate a minimum a maximum slip rate estimate. In parallel, we assume an average 4.3 m characteristic individual slip consistent with the cumulative 13.6 m measured on the aqueduct (Figure 5). a). If we assume a minimum age AD 962 for W (according to the dating in unit f, related rate of sedimentation and the interface between unit f and unit g in trench C) the slip rate ranges between 6.1 mm/yr and 6.3 mm/yr (dark regression line with 80% correlation coefficient) implying that a large seismic event is overdue. If we consider the historical catalogue and the BC 1365 earthquake sequence along the DSF for W (grey regression line with 78% correlation coefficient), the slip rate reduces to 4.9 – 5.5 mm/yr. The question mark indicates that for both scenarios a large earthquake is overdue along the Missyaf fault segment (according to the seismic gap and the 4.0 slip deficit). The temporal cluster of 3 large earthquakes in less than 1000 years suggests a Wallace model of fault behavior with periods of seismic quiescence reaching ~ 1700 years.

Figure Captions of Chapter V (continued)

Figure 17: location map of Krak des Chevaliers.

Figure 18: Draw by Baron Ray 1859. Facing SW direction (from Tlass, 1990).

Figure 19: General view of the castle from SW.

Figure 20: Space photo of Krak des Chevaliers showing its main structural elements, and the excavation site.

Figure 21: the construction stages of the Castle, the Mamluk bath and the fracture extension.

Figure Captions of Chapter VI

acceleration in cm/s^2. The maximum acceleration exceeds 0.6g situated along the Yammouneh, Serghaya, Missyaf, JES and Apamea faults with a minor increase of acceleration for the Afrin fault.

Figure 7a: Seismic hazard map obtained from the input data of Tables 1 and 2 for a Poissonian model and for a 0.5Hz frequency and 500 years of return period. Values correspond to acceleration in cm/s^2. The maximum acceleration exceeding 0.8g is concentrated in the Ghab area. Other high acceleration is along the Yammouneh, Serghaya, Missyaf and Afrin faults (see Figure 2 for fault segment names).

Figure 7b: Seismic hazard map obtained from the input data of Tables 1 and 2 for a Poissonian model and for a 0.5 Hz frequency and 1000 years of return period. Values correspond to acceleration in cm/s^2. The maximum acceleration exceeding 0.9g is concentrated along the JES, Apamea, Serghaya, Missyaf and Yammouneh fauls.

List of Tables

Table Captions of Chapter V

Table 1: Sample list and radiocarbon dating (AMS) at the Al Harif aqueduct site. All samples have been calibrated using the Oxcal program v3.5 (Bronk-Ramsey, 2001) and calibration curve INTCAL04 (Reimer et al., 2004) and adopted age ranges are equivalent to calibrated 2σ ranges (94.5%), in AD and BC. Trench and excavation units are marked in parenthesis from trenches A, B and C and excavations I, I-E, II and III. Location of cores B and D is in Figure 7.

Table 2: Detailed measurements presented here give proper insights regarding the quality (amount of carbon should be larger than 1 mg) of collected samples, the possibility of sample fraction (alkali residue, humic acids) enhances the dating accuracy. The 2σ-calibrations were performed using the OxCal 3.5 software (Bronk Ramsey, 2001) and the atmospheric data (INTCAL04) are from PJ Reimer et al. (2004). Level 1, Level 2, Level 3, Level 4.

Level 1: First level West the trench, beside the outcrop in the corner of the basement.

Level 2: Second level North the trench, directly above the channel cover, close to the door.

Level 3: Third level West the trench, same as the level of the channel cover.

Level 4: Forth level Center the trench, beneath the broken part of the channel & along the crack.

Table 3: Detailed measurements presented here give proper insights regarding the quality (amount of carbon should be larger than 1 mg) of collected samples, the possibility of sample fraction (alkali residue, humic acids) enhances the dating accuracy. The 2σ-calibrations were performed using the OxCal 3.5 software (Bronk Ramsey, 2001) and the atmospheric data (INTCAL04) are from PJ Reimer et al. (2004).

Table 4: Detailed measurements presented here give proper insights regarding the quality (amount of carbon should be larger than 1 mg) of collected samples, the possibility of sample fraction (alkali residue, humic acids) enhances the dating accuracy. The 2σ-calibrations were performed using the OxCal 3.5 software (Bronk Ramsey, 2001) and the atmospheric data (INTCAL04) are from PJ Reimer et al. (2004), sample marked by yellow are excluded because of in sufficient amount of Carbon content.

Table Captions of Chapter VI

Table 1 : Main input parameters of active faults for Poissonian Model. Fault zones are shown in Figure 2.

Table 2 : Main input parameters of active faults for Characteristic Model. Fault zones are shown in Figure 2.

CHAPTER I

INTRODUCTION

I INTRODUCTION

- <u>The scientific context.</u>

Syria has a long well recorded history of destructive earthquakes extending for more than three thousand years. These earthquakes caused thousands of casualties and injuries, severe destruction of the man-made buildings, accompanied by large tectonic deformation mostly along the Dead Sea Fault. One significant example is the 25th November 1759 earthquake that took place on the Serghaya fault, 35 km west and NW of Damascus. According to contemporaneous historical documents and eyewitnesses, this earthquake destroyed more than 80% of Damascus. The Damascene people stayed under tents for about three months until the next winter because of the threatens and fears from the aftershocks. The earthquake also caused a widespread devastating destruction that covered all SW Syria (Dahman, 1982). According to recent field measurement, the length of resulted surface rupture exceeded 30 km with ~ 2.0 m left lateral displacement suggesting an Mw ~7 (Gomez et al., 2003). This large seismic event was generated on a branch of the main N-S trending Dead Sea Transform Fault (DSF) which extends for about 1000 km from the Gulf of Aquaba in Jordan to the Amik Basin in Turkey. This event is symptomatic of the earthquake activity along the Dead Sea fault that has the potential to generate large and destructive earthquakes. Therefore, it is of utmost importance to characterize past rupture segments of the DSF, study its impact, understand its driving mechanism and reduce the associated seismic hazards and risks.

In this thesis, I have tried to shed light on the past earthquake activity of the northern part of the DSF that crosses mainly western Syria. This work program has been achieved by studying the active tectonics, paloseismology, archeoseismology, historical and instrumental seismicity of the DSF, and finally I used the outcome of the multidisciplinary researches to present my assumptions and models of the seismic hazards in Syria, through a collection of seismic hazards maps using probabilistic methods. During the preparation of this work, I benefited from the support of the Atomic Energy Commission of Syria (AECS), the APAME (European Community funded) contract No. project and the precious collaboration of the DGAM.

- <u>Lessons from other examples.</u>

Many worldwide examples of major continental fault structures can be compared to the DSF. The most studied faults with similar fault behavior to the DSF are the North Anatolian Fault (NAF) and the San Andreas Fault (SAF). The NAF is a major active with right-lateral displacement that crosses northern Anatolia. The fault extends for about 1600 km long plate boundary that slips at an average rate of 20–30 mm.yr-1 (McClusky et al., 2000). It has developed in the framework of the northward moving Arabian plate and the Hellenic subduction zone where the African lithosphere is subducting below the Aegean. It initiated westward from a junction with the East Anatolian Fault at the Karliova Triple Junction in eastern Turkey, across northern Turkey towards the west and into the Aegean Sea. It runs about 20 km south of Istanbul. During the twentieth century, the NAF has ruptured over 900 km of its length. A series of large earthquakes starting in 1939 near Erzincan in Eastern Anatolia propagated westward towards the Istanbul-Marmara region in northwestern Turkey that today represents a seismic gap western Turkey that today represents a seismic gap along a 100-km long segment below the Sea of Marmara. This segment did not rupture since 1766 and if locked may have accumulated a slip deficit of 4–5 m. It is believed of being capable of generating a M = 7.4 earthquake within the next decades (Hubert-Ferrari et al., 2000) and it could even rupture in a large Mw 7.6 single event (Le Pichon et al., 1999).

The San Andreas Fault dominates the tectonic pattern in California (USA). It extended for 1100 km long across land, right-lateral strike-slip continental transform fault by northwest trending. It forms the tectonic boundary between the Pacific Plate and the North American Plate. The fault is divided into three segments: **The southern segment** (known as the Mojave segment) begins near the Salton Sea at the northern terminus of the East Pacific Rise and runs northward before it begins a slow bend to the west. After crossing through Frazier Park, the fault begins to bend northward. This area is referred to as the "Big Bend" and is thought to be where the fault locks up in Southern California as the plates try to move past each other. This section of the fault has an earthquake-recurrence interval of roughly 140–160 years. Northwest of Frazier Park, the fault runs through the Carrizo Plain, a long, treeless plain within which much of the fault is plainly visible. The Elkhorn Scarp defines the fault trace along much of its length within the plain. **Central segment** of the San Andreas Fault runs in a northwestern direction from Parkfield to Hollister. While the southern section of the fault and the parts through Parkfield experience earthquakes, the rest of the central section of the fault exhibits a phenomenon called aseismic creep, where the fault slips slowly without causing earthquakes. **Northern segment** of the fault runs from Hollister, through the Santa Cruz Mountains, epicenter of the 1989 Loma Prieta earthquake, then on up the San Francisco Peninsula, terminating at the Mendocino Triple Junction. This segment is responsible about the earthquake of the 1906 San Francisco caused land offset over length of more than 400 km in California earthquake (Kasahara, 1981)

The major part of San Andreas Fault has a time period of 67 years since 1800 AD, the total length is 1240 km, the depth is 20 km and the slip rate is 6.6 cm per year (Brune, 1968).

- Main questions to address

The main issue of our research is to characterize the seismic parameters, fault segmentation, dimension, and slip-rate, the tectonic evolution, earthquake recurrence, the characteristic earthquake and focal mechanism. Process of the DSF in Syria. are defining its...etc.). The tectonic evolution of the Dead Sea Fault has been examined by many scholars along its length (McKenzie, 1970; Jackson and McKenzie, 1984; Chaimov, 1990; Brew, 2001; Rukieh, 2005). For details please refer to the Chapter II which is dealing with the seismotectonic setting. The slip rate estimation of the DSF is one of essential issues and It can be obtained using geomorphic studies, paleoseismic trenching and active deformation measurements. There are not so many scientific work and publications on the DSF in comparison with the publications on the SAF and the NAF. On the DSF in Syria, Meghraoui estimated 6.8 – 7.0 mm/yr left-lateral slip rate according to paleoseismological investigation along Missyaf segment (Meghraoui et al., 2003). However, GPS measurements of the active deformation along the DSF gives contradictory and variable slip rate results as 1.8 – 3.3 mm/y (Alchalabi, et al., 2009), 4.2 ± 0.3 mm/y (Gomez et al., 2007), 4.8 ± 0.3 mm/y (Reilinger et al., 2006), 4.7 ± 0.4 mm/y (Mahmud et al., 2005) and 6 ± 0.3 mm/y (McClusky et al., 2003); for details please refer to Chapter II. This example shows the variability of results for the same segment using deferent methods and block models, and by the same method but by different researchers. A comparable variation can be noticed on the San Andreas Fault where the earthquake recurrence interval is 21 ±4 yr (Bakun and McEvilly, 1984). Soil studies and paleoseismic trenching data suggest to Machette (1978) that the County Daumo Fault in New Mexico has a recurrence interval of 90000 yr. As pointed out by Wallace (1970) and Schwartz and Coppersmith (1984), the slip rate of a fault directly affects the recurrence rate. Finally, the paleoseismic trenching and the geomorphological investigations along the main fault structure and for each segment cover a few centuries of the earthquake activity. It can be extended to several thousands of years and provide a better slip rate evaluation for each segment, that do not fluctuate as we can see from the GPS measurements of active deformation .

Another issue is to take in consideration the available dating techniques of and bracketted age determination in the paleoseismic studies that often includes uncertainties and affect the accuracy of the earthquake timing and related slip rate value. The archeohistorical seismology combined with the instrumental seismicty offer a better constraint of the recurrence intervalof large seismic events and slip rate estimation because of the more precise dating even in the case of a short time window span (100 to 4000 yr).

Finally, I would like to point out the existence of seismic gaps along the main continental faults. As also observed from the comparison between the instrumental seismicity during the last century and the location of large historical earthquakes of the DSF, the seismic gap is obvious in along the Missyaf Fault during the last century and can be the site of a future large earthquake. This seismic gap needs to be better identified on both the short term and long term time window.

- Main methodologies and approaches (see also chapter II)

The strength of my work is based on the multidisciplinary effort as presented in the main chapters IV, V and VI of this thesis. Chapter II gives an overview of the methods I have choosen to apply in the frame of this thesis. The primary objective is to cover a long time-window (> 2000 years) for our paleoearthquake research and provide accurate dating of past earthquakes for the DSF segments in Syria (Missyaf and Ghab Faults). The ultimate goal is the use of the obtained results to develop seismic hazard maps with a realistic application for the public safety and to improve the construction engineering design in Syria.

- The thesis content and structure

The chapter II is dealing with the applied methodologies in order to analyze the nature of earthquake faulting and show a perspective for a realistic seismic hazard evaluation in Syria. Four different methodologies were applied in order to cover the whole spectrum of earthquake activity and the different time coverage using paleoseismology and archeoseismology, historical seismicity and the instrumental seismicity. The first method is dealing with the relation between the active faults and earthquakes. I have started from a fundamental level of definition of active faults and the types of fault rupture. Then I have explained the relation between earthquakes and surface ruptures, and their relationships with the elastic rebound theory. I have defined the four phases of the seismic cycles, the relation between the size of earthquakes and the fault parameters. Finally, I introduced the models of fault behavior including the issue of fault slip rate and seismic gap. The second approach is the paleoseismology. I start by defining the main issues of the paleoseismology. I explain the steps of how to define the active fault parameters with special concern on strike slip faults. I give some examples of applying paleoseismological method and the study of active strike slip faults in the world. I describe the different scales of investigations and the supporting tools. I emphasize the trenching techniques and how to identify paleoearthquakes in the recent sediments with the application of radiocarbon dating. Finally I present the importance of trench interpretation and the obtained parameters of paleo-earthquakes. The third method is dealing with the newly developed archeoseismology. I start with presenting the definition and applied techniques and mention the involved specialists that provide important conceptual views and results. I introduce the main types of destructions which are in direct relation with earthquake effects throughout examples. The fourth method is dealing with historical and instrumental seismicity. I start with showing the importance of the earthquake catalogue (historical and instrumental) and present a comparison between the applied steps in the study of historical and instrumental seismicity. The fifth approach is dealing with the seismic hazard analysis where I define the deterministic and the probabilistic approaches and then I explain the steps in applying the deterministic and probabilistic approaches. The chapter III is dealing with the seismotectonic setting of western Syria. I start with the description of the major tectonic structures in Syria. Then I present the main faults in Syria with special concern on the Dead Sea fault segments, and their geometrical complexities and fault branches. Then I show the historical and instrumental earthquake distribution. discuss the focal mechanism solutions and the latest results of the GPS measurements of the Syria region. In the end, I describe the crustal structure and plate tectonic deformation along the Dead Sea fault and the related seismogenic depth according to the depth of the instrumental seismicity.

The chapter IV is dealing with the historical seismicity of Syria. I present in this chapter the analysis of large and moderate earthquakes from 1365 BC to 1900 AD including the different types of textual sources of the catalogue. I also describe the steps of used method when preparing the earthquake catalogue. The resulted historical earthquakes are presented in four steps: i - The first one is a descriptive summary of 181 historical seismic events, and I define for each one the date, the seismic intensities at different localities, the different types of the compiled data and the descriptions of the seismic event. ii - The second step is the parametric catalogue of 36 seismic events; it contains the epicenter parameters, names of affected localities, the evaluated epicenter intensity and finally the estimated magnitude and depth of the seismic event. iii - The third step is a catalogue of the seismic intensities of some localities for the 181 seismic events with a thorough evaluation of their data completeness and quality. iv - The fourth step of presenting is a collection of isoseismal maps for most seismic events and a map of historical earthquake distribution of the parametric catalogue. I have ended the catalogue with the completeness test. I also add to the catalogue two appendixes. The first one is information about the authors and text cited in the catalogue. The second one is the different historical names of localities cited in the catalogue. This work has been published in Annals of geophysics, June 2005, entitled “The historical earthquakes of Syria: an analysis of large and moderate earthquakes from 1365 B.C. to 1900 A.D." by M. R. Sbeinati, R. Daraowcheh, and M. Mouty.

The chapter V is dealing with the archeoseismologiacl and paleoseismological investigations in Syria. I start in this chapter by introducing the framework of the field investigations in Syria and the location of the investigated sites. After this framework of research program, I present the paleo and archeo-seismological investigation in Al Harif Roman aqueduct, which crosses Missyaf fault and displays 13.6m left-lateral offset; this article is now accepted for publication in a special volume on "Ancient Earthquakes" of the Geological Society of America. Then I present the archeoseismological investigations in three archeological sites: Krak des Chevaliers, Apamea, and Deir Dahess. The four sites have been severely affected by past earthquakes generated by the Dead Sea Fault in Syria. For the Al Harif investigations, I start by the active faulting and the seismotectonic setting of the Missyaf segment. Then I present a site description, the aqueduct history with field measurements, the archeoseismology excavations and paleoseismic trenches. The analyses of the tufa accumulation on the aqueduct using 4 drilled cores are correlated with the archeoseismic excavations and paleoseismic trenches to strengthen the results and interpretation of the timing of earthquake faulting. The second work is dealing with the ruptures in the historical fortress of Krak des Chevaliers and the related archeoseismological investigations. I have started by presenting the history of the fortress. Then I describe the construction condition of the fortress, the historical earthquakes and the excavation work in the Mamluk bath showing the broken channel of the bathroom water disposal. In the end, I present the analysis of the damaged parts and the radiocarbon dating results in relation with historical earthquakes (and the estimated seismic intensities) that affected the fortress. The third work is dealing with the collapsed columns of the Apamea city and starts with a brief introduction about the historical account of Apamea. The main archeological features of Apamea are described together with the types of historical earthquake damages in the Agora and in the nearby house named "maison aux colonnes bilobées". I present the archeoseismological excavation work in both sites. and the C14 dating results with the age of historical earthquakes and their estimated intensities at the Apamea site. The fourth work is dealing with the collapse of monastery at Deir Dahess site. I start with a brief history of the region of Deir Dahess and a description of the main construction parts in the monastery complex. Here, I identified different features of destruction types in the tower, the church, the annex, and the domestic house followed by the archeoseismological excavation work at the annex, the domestic house, the tower. In the end I present the obtained results and the archeoseismic interpretation using the analysis of radiocarbon dating. The historical earthquakes that affected the sites are identified with their estimated seismic intensities. The chapter VI is dealing with the seismic hazards analysis. I start with a short introduction about the CRISES 2007 software. For this purpose, a new and complete set of earthquake database is prepared along with fault parameters, in order to calculate the probabilistic seismic hazards. After the identification of the main earthquake sources, I calculate the earthquake occurrence and define the properties of characteristic earthquakes. An attenuation models is chosen to proceed with calculations of the probabilistic seismic hazards for different cities in Syria using the time-independent (Poissonian) and time-dependent (renewal) processing. I calculate the probabilistic seismic hazards for different cities located along the Dead Sea Fault in Syria using the Characteristic Earthquake model. Different seismic hazard maps of Syria are generated for various intensities and return periods.

The chapter VII summarizes the main results with concluding remarks for a perspective work.

References

Atakan, K., Ojeda, A., Meghraoui, M., Barka, A., Erdik, M., & Bodare, A., (2002) Seismic Hazard in Istanbul Following the August 17, 1999 Izmit and November 12, 1999 Düzce Earthquakes, Bull. Seism. Soc. Amer., 92, 466-482.

Bakun, W. H., and T. V. McEvilly (1984). Recurrence models and the Parkfield California, earthquakes, J. Geophys. Res. 89, 305-3058.

Brew, G., M. Barazangi, A. K. Al-Maleh, T. Sawaf (2001). Tectonic and Geologic Evolution of Syria. GeoArabia, Vol. 6, No. 4, p. 573-616. Gulf PetroLink, Bahrain

Brune, J. N. (1968). Seismic moment, seismicity, and rate of slip along major fault zones, *J. Geophys. Res.*, 73, 777-84.

Chaimov, T., M. Barazangi, D. Al-Saad, T. Sawaf and A. Gebran (1990). Crustal shortening in the Palmyride fold belt, Syria, and implications for movement along the Dead Sea fault system. Tectonics, v. 9, no. 6, p. 1369–1386.

Dahman, M. A. (1982). Fi Rihab Dimashq (In Arabic), published by Dar Al-Fikr, Damascus.

Dresen, G., M. Bohnhoff, M. Aktar, and H. Eyidogan (2008). Drilling the North Anatolian Fault. Scientific drilling, No. 6, doi:10.2204/iodp.sd.6.10.2008.

Gomez, F., M. Meghraoui, A. N. Darkal, F. Hijazi, M. Mouty, Y. Suleiman, R. Sbeinati, R. Darawcheh, R. Al-Ghazzi, & M. Barazangi, 2003. Holocene faulting and earthquake recurrence along the Serghaya branch of the Dead Sea fault system in Syria and Lebanon, Geophysical Journal International, 153, p. 658-674.

Jackson, J. A., and D. P. McKenzie (1984). Active tectonics of the Alpine-Himalayan Belt between western Turkey and Pakistan, Geophys. J. R. Astr. Soc. 77, 185–246.

Hubert-Ferrari, A., Barka, A., Jacques, E., Nalbant, S.S., Meyer, B., Armijo, R., Tapponnier, P., and King, G.C.P., 2000. Seismic hazard in the Marmara Sea region following the 17 August 1999 Izmit earthquake. Nature, 404:269–273, doi:10.1038/35005054.

Kasahara K. (1981). Erthquake Mechnics, Cambredge University Press, USA.

Le Pichon, X., Şengör, A.M.C., and Taymaz, T., 1999. The Marmara fault and the future Istanbul earthquake. In Karaca, M., and Ural, D.N. (Eds.), ITU-IAHS International Conference on the Kocaeli earthquake 17 August 1999, Istanbul (Istanbul Technical University), 41–54.

Machett, M. N. (1978). Dating Quaternary faults in the southwestern United State by using buried calcic paleosols, J. Res. U.S. Geol. Surv. 6 (3), 369-381.

McClusky, S., Balassanian, S., Barka, A., Demir, C., Ergintav, S., Georgiev, I., Gurkan, O., Hamburger, M., Hust, K., Kahle, H., Kastens, K., Kekelidze, G., King, R., Kotzev, V., Lenk, O., Mahmoud, S., Mishin, A., Nadariya, M., Ouzounis, A., Paradissis, D., Peter, Y., Prilepin, M., Reilinger, R., Sanli, I., Seeger, H., Tealeb, A., Toksöz, M.N., and Veis, G., 2000. Global positioning system constraints on plate kinematics and dynamics in the eastern Mediterranean and Caucasus. J. Geophys. Res., 105:5695–5719, doi:10.1029/1999JB900351.

McKenzie, D. P. (1970). The plate tectonics of the Mediterranean region, Nature, 226, 239–241.

Rukieh, M., V.G. Trifonov, A.E. Dodonov, H. Minini, O. Ammara, T.P. Ivanova, T. Zaza, A. Yusef, M. Al-Shara, Y. Jobaili (2005). Journal of Geodynamics 40. p 235–256.

Schwartz, D. P., and K. J. Coppersmith (1984). Fault behehvior and characteristic earthquakes; Examples from the Wasatch and San Andreas Faults, J. Geophys. Res. 89, 5681-5698.

Wallace. R. E. (1970). Earthquake recurrence intervals on the San Andreas Fault, California, Geol. Soc. Am. Bull. 81, 2875-2890.

CHAPTER II

ACTIVE FAULTING AND RELATED EARTHQUAKE GENERATION

II - Active Faulting and Earthquake Generation

The definition of an active fault is mainly based on the following two elements: (1) the timing of most recent coseismic displacement that can be historical, Holocene, Quaternary or in the present seismotectonic regime, and (2) the potential or probability for future coseismic displacements in the present tectonic setting. Most of shallow earthquakes with magnitude Mw $\geq$ 5.5 are accompanied with surface ruptures (McCalpin, et al., 1996); these earthquakes have a tectonic origin and were generated after releasing the energy of the seismic strain along a fault. The sudden energy release along a fault implies that the earthquake must have involved an "elastic rebound" of previously stored elastic stress (Reid, 1910). Understanding the mechanical properties and long term behavior of a fault zone is fundamental in earthquake geology.

II - 1. Surface Rupture and Earthquakes

Generally, surface ruptures (fault) produce an offset parallel to a plane surface of maximum shear stress (σ_1, σ_2 and σ_3); a vertical fault geometry obeys a mode II rupture generation, and a fault with dip <90 (i.e., normal or reverse fault) which is bounded by *hangingwall* overlying the fault and a *footwall* beneath it, obeys a mode III rupture generation (Figures 1 a & b). The fault trace is visible at its intersection with the earth's surface and the fault slip is a vector measured on the fault rupture indicating the relative displacement of formerly adjacent points on opposite sides. The fault slip may be divided into strike-slip and dip-slip components, or horizontal and vertical components (heave and throw, respectively) (Yeats et al., 1997).

There are three major types of fault following the orientation of maximum stress vectors: Normal fault, Reverse fault and Strike-slip fault (e.g., the mid-Atlantic ocean spreading, the Himalaya subduction zone and the San Andreas fault, respectively). In the Eastern Mediterranean region normal faults such as the Amanos-Karasu fault (at the intersection between the East Anatolian Fault and the Dead Sea Fault), reverse faults in the Palmyrides folded zone (Jabal Abou-Zennar central Syria) and finally the strike-slip fault with a left lateral movement well illustrated by the Dead Sea fault that occupies the western part of Syria (Figure 2).

Figure 1a: Fault nomenclature for (a) normal fault, (b) oblique-slip normal fault. Band is a sedimentary bed offset by fault (modified from Yeats, 1997).

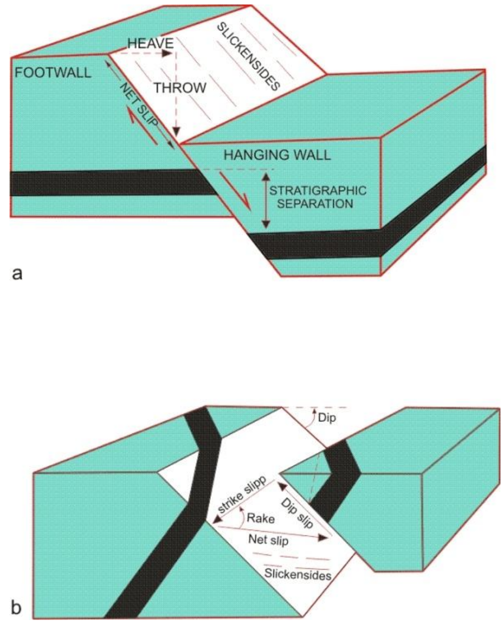

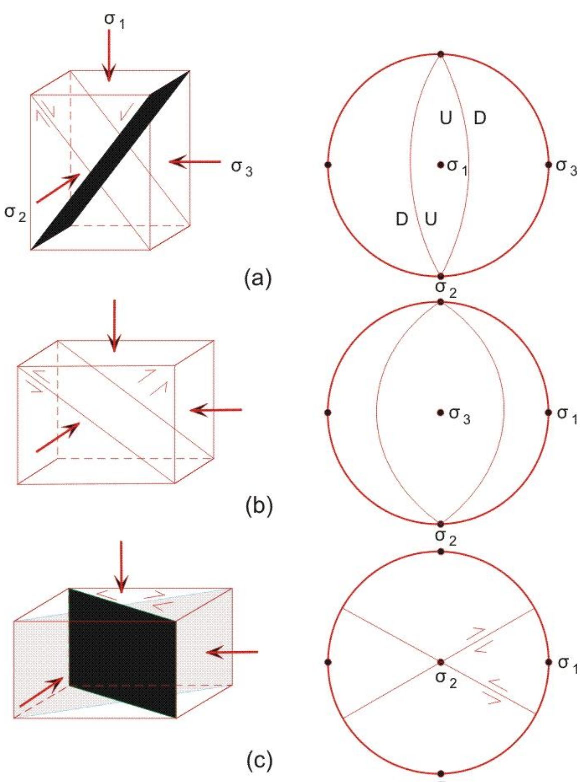

Figure 1b: orientation of conjugate fault planes (shaded) with respect to principal stress directions (σ_1, σ_2, σ_3) in isotropic rock for (a) normal faults, (b) reverse faults, (c) strike-slip faults. The faults are shown on left as block diagrams, and on the right in stereographic projection, to visualize the stereographic projection, imagine that you are looking at the inside of half sphere, its lower hemisphere concave downward into the page. The circle is the circumference of the sphere intersecting a horizontal plane. The lines are the intersection of planes that pass through the center of the sphere with the lower

hemisphere surface. Strike-slip faults dip=90^o and show as a straight line; normal and reverse faults dip<90^o and show as curved lines (modified from Yeats, 1997).

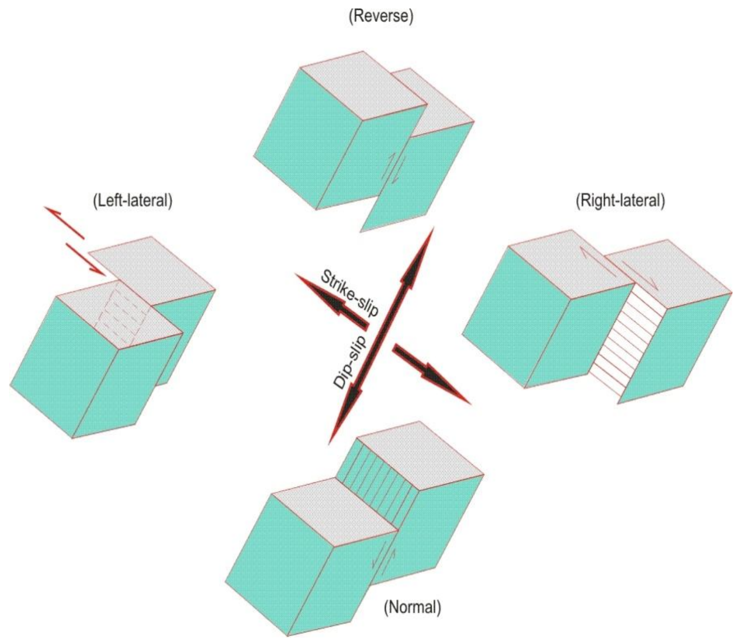

Figure 2:Basic models of fault slipping.

In the Reid (1910) physical concept on generating earthquakes by means of the elastic rebound theory, the mechanism of the 1906 San Francisco earthquake, results from a sudden relaxation of the elastic strain through rupture along the San Andreas Fault. The causative strains were accumulated over a long period of time and showed no motion of the fault blocks, which under normal conditions remains locked due to shear resistance and friction. The earthquake faulting is understood as a linear elastic system where the strain accumulation pattern was just opposite that of the strain release. Therefore, the net slip result of one earthquake cycle was a block offset of the fault with no net strain (Figure 3). Although the earth structure may be more complicated in earthquake mechanism as a pure elastic model, we conclude following Reid's theory that the recurrence of large earthquakes is periodic, or at least, in the modern phrase, time predictable. This concept of strain loading and relaxation oscillation known as the *seismic cycle* has critical implications for the seismic hazard assessment (Figure 4).

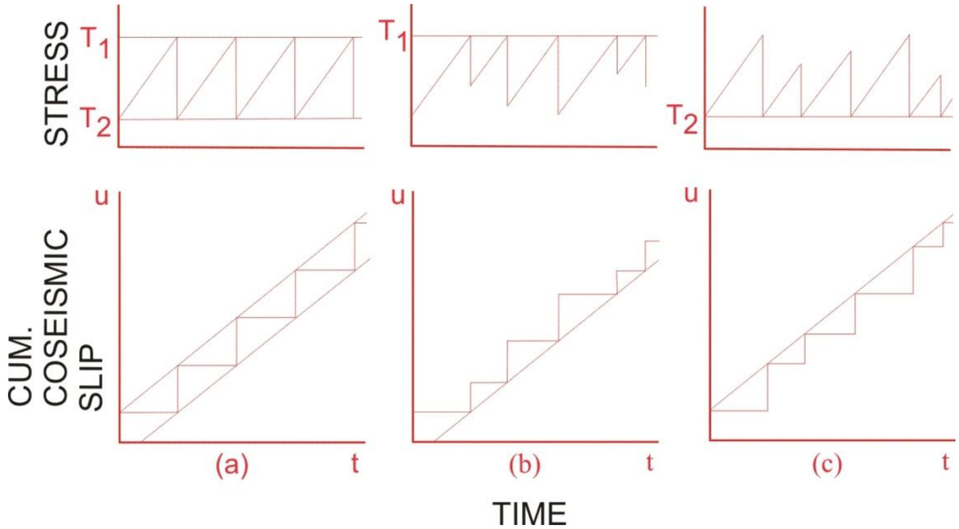

Figure 3: Simple earthquakes recurrence models: (a) Reid's perfectly periodic model; (b) time-predictable model; (c) size-predictable model (modified from Scholz, 1990).

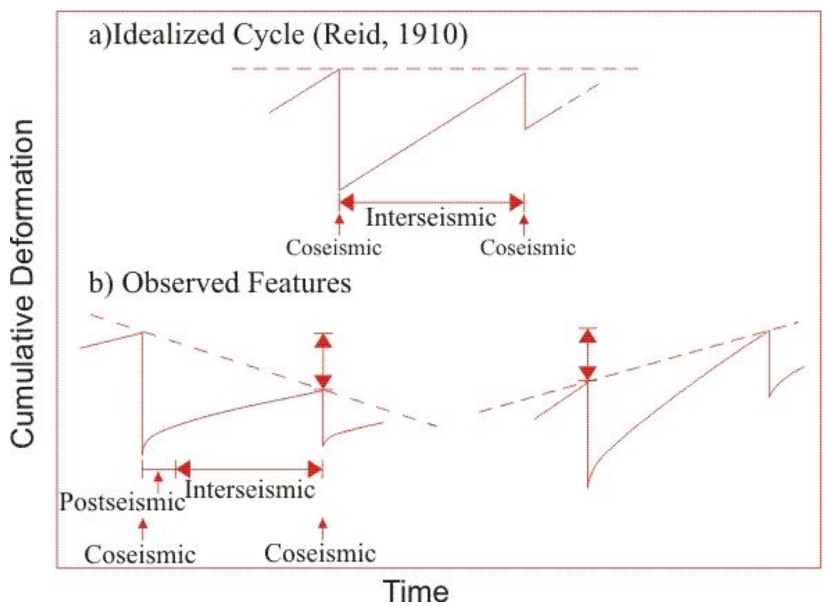

Figure 4: Simplified forms of the earthquake deformation cycle. Cumulative deformation (e.g., strain, tilt, displacement) is plotted as a function of time. Step offsets correspond to the occurrence times of major earthquakes. Dashed lines show level at which failure occurs; the level varies with the effects of long-term inelastic deformation (modified from Scholz, 1990).

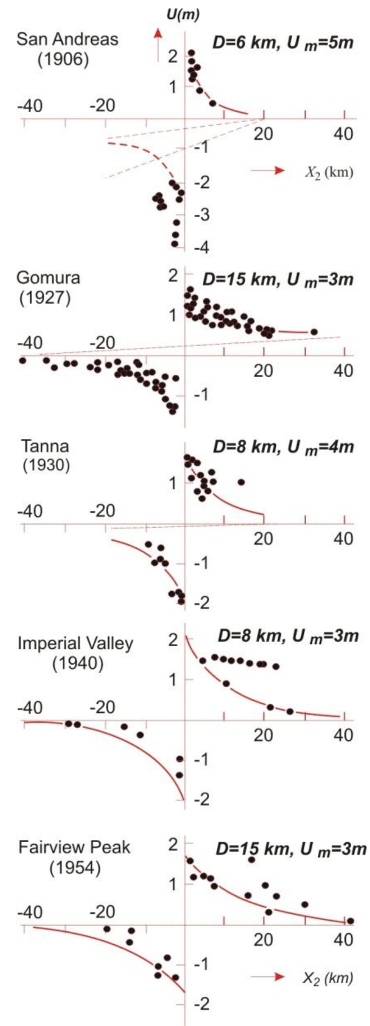

Figure 5: Surface displacements (parallel to the fault strike) associated with several representative strike-slip faults for comparison with the predictions of the vertical strike-slip model. Broken lines show corrections for the hypothetical strain accumulation during the period between pre- and post-earthquake surveys (modified from Kasahara, 1981).

The Seismic Cycle in the crustal deformation, the loading cycle is often divided in four phases: preseismic, coseismic, postseismic and interseismic. This fourfold structure has been assembled from geodetic observations and earthquake geology in many places; a typical seismic deformation fields for strike slip fault is shown in (Figure 5).

Following Reid's theory, this deformation is produced by the seismic strain release upon dynamic faulting. Since in our case this seismic strain is concentrated on the Dead Sea Fault, the simplified proposed physical model is to simulate a strike-slip fault and related seismic parameters. The vertical fault corresponds to an infinite long strip intersecting the surface of a semi-infinite elastic medium under uniform shear strain (Knopoff, 1958, Kasahara 1981). Following Knopoff (1958), we may take the coordinate axes x_i (i=1, 2, 3) to be as shown in (Figure 6) and let u_i denote the displacement in the x_i direction. Lamé's constants and the vertical extension of the fault (or half-width of the strip) are denoted by λ, μ and D, respectively.

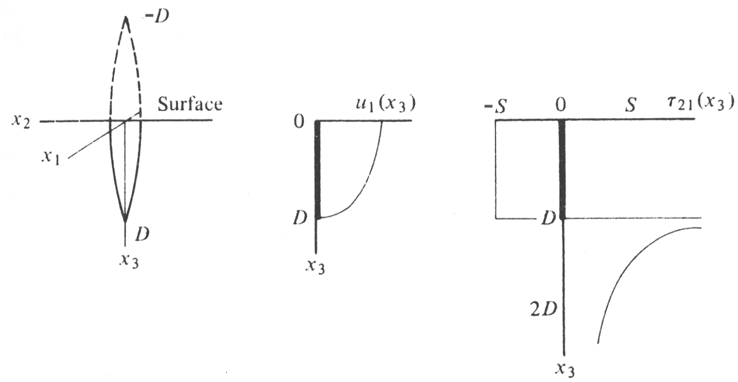

Figure 6: Knopoff's model applied to a vertical strike-slip fault intersecting the surface Displacement and stress as a function of depth are shown (modified from Kasahara, 1981).

Obviously, the displacement in the shear field of the simple model is parallel to the x_1 axis, hence $u_2 = u_3 = 0$ and the operation is $\partial/\partial x_1$. Therefore, the equations of the equilibrium along a fault rupture (rectangle) are:

$$(\lambda+\mu)(\partial/\partial\chi_i)\Delta+\mu\nabla^2 u_i = 0 \quad (i=1, 2, 3) \qquad \text{(II.1)}$$

Take the extremely simple form

$$\mu\left[(\partial^2/\partial\chi_2^2)+\left(\partial^2/\partial\chi_3^2\right)\right]u_1 = 0 \qquad \text{(II.2)}$$

where

$$\Delta = (\partial u_1/\partial\chi_1)+(\partial u_2/\partial\chi_2)+(\partial u_3/\partial\chi_3)$$

and

$$\nabla^2 = (\partial^2/\partial\chi_1^2)+(\partial^2/\partial\chi_2^2)+(\partial^2/\partial\chi_3^2)$$

The initial field of uniform shear strain, $\tau_{21}=S$, distributed along the fault may become $\tau_{21} = 0$ at all points on the strip (for $\chi_2=0$ and $|\chi_3|\leq D$). The most useful information for the interpretation of offsets that can be obtained from archeo/paleoseismological and geodetic data are field displacements on the earth's surface (i.e for $\chi_3 = 0$), which is given by

$$u_1(\chi_2)=u_m\left\{\left[(\chi_2/D)^2+1\right]^{1/2}-(\chi_2/D)\right\} \qquad \text{(II.3)}$$

Where u_m is half the maximum amplitude of offset U_m across the fault, which is related to the seismic moment and stress drop in the following way:

$$U_m = 2SD/\mu \qquad \text{(II.4)}$$

$$\Delta\sigma = S = \frac{1}{2}\left(U_m \mu / D\right) \tag{II.5}$$

Where $\Delta\sigma$ denotes the stress drop associated with faulting.

The figure 7 illustrates the relation (II.3); between surface displacement, u_1 and the dimentionless distance χ_2 / D, and Figure II-8; shows the displacement field about a strike-slip fault.

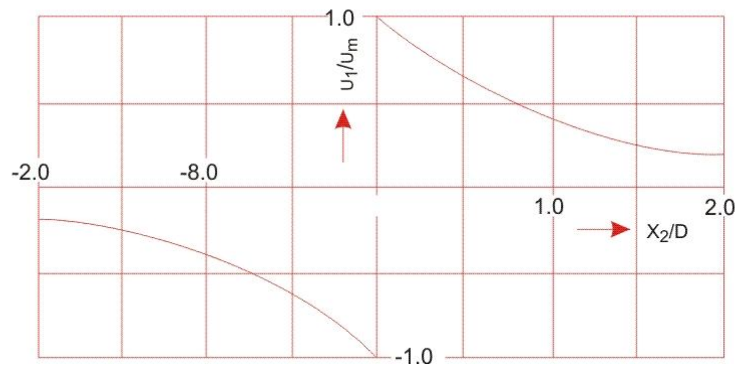

Figure 7: Surface displacement parallel to fault (u_1) as a function of distance from the fault; (x_2) for the vertical strike-slip fault model shown in the (Figure 8). in this figure, u_1 and x_2 are given in normalized units, taking u_m and D respectively as normalizations (modified from Kasahara, 1981).

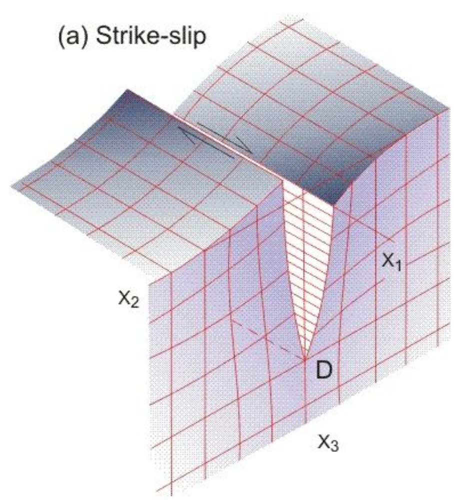

Figure 8: Displacement fields associated with vertical fault model for dip-slip (modified from Kasahara, 1981).

Another model for rupture generation was given by Star (1928), he proposed a two-dimensional elliptical crack in an infinite medium for dip-slip faults, the maximum occurred offset at the center of the crack, *D* and if $\lambda = \mu$ is given by:

$$U_m = 3/2(SD/\mu) \tag{II.6}$$

$$\Delta\sigma = S = \frac{2}{3}\left(U_m \mu / D\right) \tag{II.7}$$

These models of strike-slip and dip slip faults are similar to one another in their function forms, as can be seen from a comparison of (II.4) and (II.5) with (II.6) and (II.7).

The Earthquake Size: This is one of the most important factors in seismic-hazard analysis and it can be estimated using specific fault parameters. The traditional measurement of earthquake size is *magnitude*, which is a logarithmic scale based on the amplitude of specific seismic wave measured at particular frequency from the seismograms; the signal must be suitably corrected to distance and instrument response, therefore we have many types of magnitude (m_L, m_b, M_s, etc.). However, the more physically meaningful measurement of an earthquake size is given by the *seismic moment*

$$M_o = \mu S D \qquad \text{(II.8)}$$

Where M_o measured in *dyne.cm*, μ is the shear modulus, it estimated for the Earth's crust 3.3 10^{11} $dyne/cm^2$, S is the area of fault plane undergoing slip during the earthquake taken in cm^2 and D is the average displacement over the slip surface taken in *cm* (Aki, 1966). Hanks and Kanamori (1979) developed an empirical relation of moment magnitude (M_w) based on seismic moment, where:

$$M_w = 2/3 \log M_o - 10.7 \qquad \text{(II.9)}$$

The moment magnitude is related directly with the physical properties of the rupture and does not, by the definition, saturate.

The Gutenberg-Richter frequency relation and related recurrence relationship (Richter, 1958) has been defined for a large range of earthquake magnitude and completed earthquake catalogue, for a number of earthquakes that occur systematically, and comply with the relation:

$$\text{Log } N = a - bM \qquad \text{(II.10)}$$

N is the number of events (with a given magnitude or above) per unit of area per unit time, M is magnitude, and a and b are constants representing respectively, the overall level of seismicity and the ratio of small to large events for a region or for a fault segment.

The Fault Parameters**:** The earthquake magnitude can be correlated with coseismic rupture parameters such as the fault length, displacement and fault depth (Tocher, 1958; Chinnery, 1969); accordingly, paleoseismic and geologic studies of active faults focus on developing estimates of these parameters as seismic source characteristics (Schwartz and Coppersmith, 1984; Schwartz, 1988; Coppersmith, 1991). The empirical relationship between parameters presented by Wells and Coppersmith (1994) are based on the results of earthquake studies worldwide. Table 1 presents below only the regression formulas related to the strike-slip fault type (that are applicable to the Dead Sea Fault), and (Figure 9) illustrates the promotional relation between the size of earthquake (*Moment magnitude*) with the dimensions of the surface ruptures.

Equation	Magnitude range	Length/Area range (km/km^2)	Displacement range (m)
M = 5.02 + 1.19 log (SLR)	5.8-8.1	3.8-432	
M = 4.28 + 1.51 log (RLD)	4.8	1.5-350	
M = 3.92 + 1.03 log (RA)	4.8-7.9	3-5,184	
M = 6.78 + 0.98 log (MD)	5.8-8.1		0.03-14.6
M = 7.05 + 0.87 log (AD)	5.8-8.1		0.10-8.0

Table 1: Equations of moment magnitude and rupture length, rupture area, and displacement range (Wells & Coppersmith, 1993). SLR: surface rupture length (km), RLD: subsurface rupture length (km), RA: rupture area (km^2), MD: maximum displacement (m), AD: average displacement (m).

These empirical relations also point out the scaling factors between fault parameters (*U/L, W/L and U/W*).

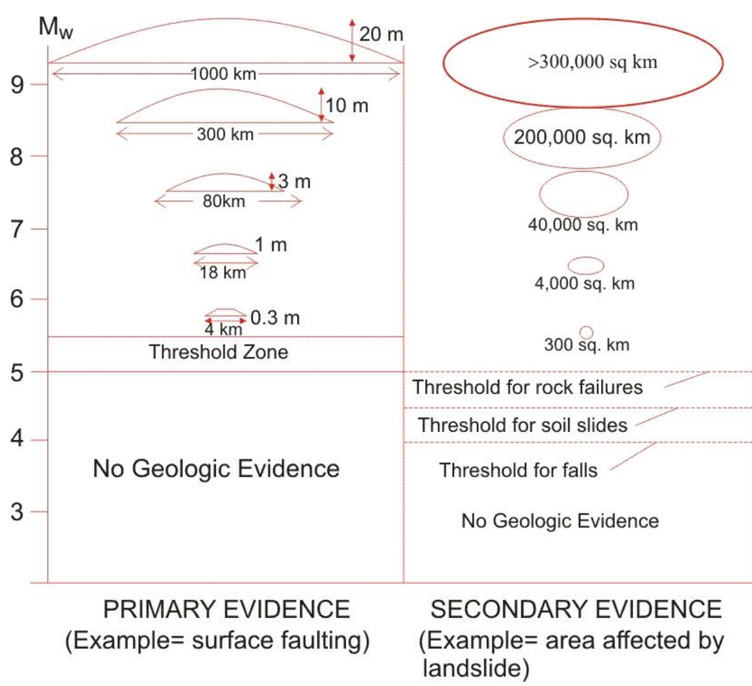

Figure 9: Schematic diagram showing the increase in size and extent of two types of paleoseismic evidence with increasing earthquake moment magnitude (M_w), based on measurements following historic earthquakes. The left side of the diagram shows the dimensions of surface faulting (primary evidence) observed in historic earthquakes of various magnitudes. Shaded areas schematically represent the dimensions of surface deformation but are not to scale. Values for lengths (beneath shaded areas) and maximum displacement (to right of the shaded areas). The threshold zone, showing the lower magnitude limit of surface faulting earthquakes. The right side of the diagram shows areas affected by coseismic landsliding

(secondary evidence); areas are not to scale. The largest area (>300,000 km2) is for M_w 9.2 1964 Alaskan earthquake from (McCalpin, 1996).

Faults are here subdivided into segments based on a variety of static geometric or geologic criteria. *The fault segment* is a portion of a fault defined by tectonic criteria (geometrical and structural complexities), and the segment boundaries are limited by at least two contiguous rupture zones (Wheeler, 1989). The following table presents the types of fault segments and the characteristic used to define them (Table 2).

Type of segment	Characteristics used to define the segment	Likelihood of being an earthquake segment
1. Earthquake	Historic rupture limits	By definition, 100%
2. Behavioral	1) Prehistoric rupture limits defined by multiple, well-dated paleoearthquakes.	High
	2) Segment bounded by changes in slip-rates, recurrence intervals, elapsed times, sense of displacement, creeping versus locked behavior, fault complexity.	Mod. 26%
3. Structural	Segment bounded by fault branches, or intersections with other faults, folds, or cross-structures.	Mod.-High 31%
4. Geologic	1) Bounded by Quaternary basins or volcanic fields. 2) Restricted by a single basement or rheologic terrain. 3) Bounded by geophysical anomalies. 4) Geomorphyic indicators such as range-front morphology, crest elevation.	Variable 39%
5. Geometric	Segments defined by changes in fault orientation, stopovers, separations, or gaps in faulting.	Low-Mod. 18%

Table 2: Types of fault segments and the characteristics used to define them (from McCalpin, 1996).

II - 2. Models of Fault Behaviour and Seismic Gaps:

Models of Fault Behaviour: they are characterized by the coseismic displacement at single location on a fault that may vary with time (temporal), and along the trace of the fault (spatial). Models of fault behaviour provide a useful conceptual framework that helps to interpret historic and paleoseismic data.

The *perfectly periodic model* conceived by Reid (1910) (Fig. II-3a) refers to earthquakes that occur when the stress reaches up to a given level (T1), the stress drop to a lower level (T2) and where the magnitude of each earthquake is identical; an additional assumption is the constant stress build up through the same period of time to obtain perfectly periodic earthquake recurrence. Based on the elastic rebound of uplifted marine terraces along the Japanese subduction zone, two other models are proposed by Nakata (1980) on this periodic model. The first one is the *time predictable* (Figure 3b), where an earthquake sequence occurs at a constant critical stress level (T1), but with a varying stress magnitude; the second one is the *slip predictable* (Figure 3c), which depends on the constant rate of displacement over time regardless of their size.

The observed coseismic slip variation along strike required the development of *one-dimensional* models into a second dimension along the fault rupture strike and get *two-dimensional* behaviour models. These observations were initially formulated based on strike-slip distribution in historic earthquakes, and were later expanded to include slip patterns for paleoearthquakes based on geomorphic offsets. Models of slip distribution can be classified into two broad groups, the *variable slip* models and the *uniform slip* models. The *variable slip* models predict that the slip rate along strike is constant, but the displacement per event at a point is variable. The earthquake size is hence variable, and rupture during individual seismic events is not limited to a fault segment. The *uniform slip* models have in common that displacement per event at a point on the fault is constant, but differ in that that slip rate along strike may be constant or variable. Three of the four uniform slip models (*characteristic earthquake*, *overlap*, and *coupled*) implicitly assume that fault segment boundaries are reasonably persistent. The following figures (Figure 10) and (Figure 11) draws the flowchart of the different types of fault segment behaviours and the types of pattern along strike-slip for different models of fault behaviour respectively. The *characteristic earthquake* model plays an essential role in the interpretation of the paleo and historical earthquakes data; it assumes that most strain is released in large earthquakes within a narrow, *characteristic magnitude* range (Schwartz and Coppersmith, 1984) and moderate earthquakes within a one magnitude range below the characteristic earthquake may be rare, if not entirely absent. Finally, a slip patch model (Sieh, 1996) takes into account the occurrence of moderate-sized earthquakes (with 5<M<7) where the recurrent coseismic slip distribution accommodates the slip deficit on fault sections left from previous characteristic earthquakes.

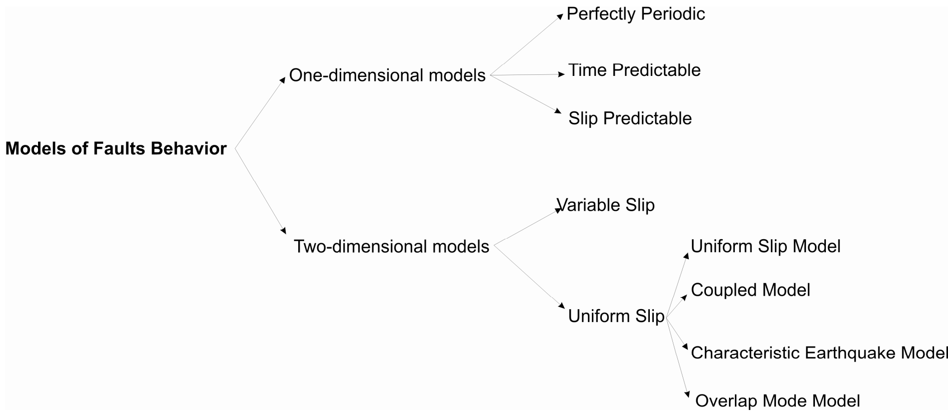

Figure 10: Flowchart illustrates the models of fault behaviour according to Nakata and shimazaki (1981), Schwartz and Coppersmith (1984) an Sieh (1996).

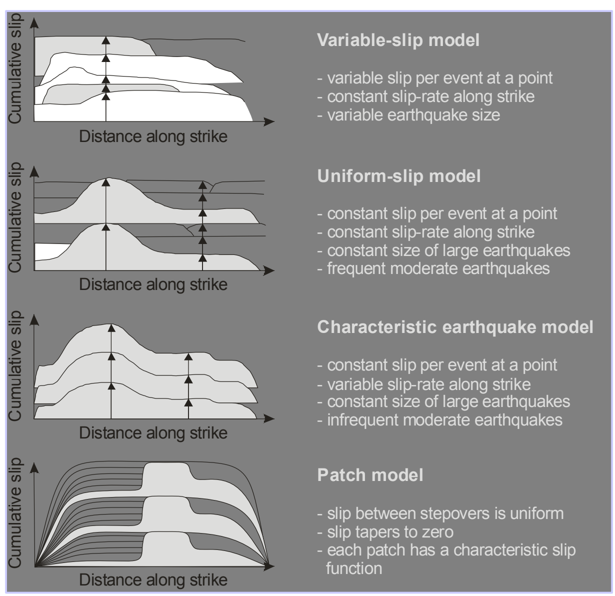

Figure 11: Models of fault behaviour (Schwartz and Coppersmith, 1984; Sieh, 1996)

From the above description and characterization of different types of the fault behaviour; we may conclude that the *seismic cycle* on a particular fault segment, or region, may cover a period of time that encompasses an episode of strain accumulation and its subsequent seismic release, see (Figure 4).

Fault Slip Rate: is the rate of displacement on a fault (in mm) averaged over a time period (years) that may involve several large earthquakes. The unit of measurement is mm/year that is simply calculated from the cumulative displacement of dated landforms or deposits; it can also be calculated from paleoseismic studies by dividing the measured displacement per event by the long term recurrence interval. The slip rate variability can be examined for certain types of faults, by the *ergotic substitution*, and apply those pattern to individual faults within short periods (McCalpin, 1996).

Seismic Gap: it corresponds to an area of active fault where there has been a below average level of seismic activity that is thought to be temporal. In other words, a seismic gap is a fault section or segment that has no seismic activity during a long period of time in comparison with the other sections of the same active fault (seismogenic zone). The gap and related slip deficit can be identified from a missing large earthquake after a long sequence of paleoearthquake. The positive evidence for the occurrence of a pre-historical (from paleoseismology) or historical large earthquake can be checked out from the negative evidence for fault creep.

II - 3. Paleoseismology

Paleoseismology is the study of prehistoric earthquakes [Solonenko, 1973; Wallace, 1981; in McCalpin], with the focus on their location, timing, size and recurrence interval of large events. The study of past earthquakes depends on interpreting geologic evidences of paleoearthquakes. Based on the instantaneous deformation of landforms and the young sediments during earthquakes (Allen, 1986), the paleoseismology identifies *coseismic* features and mostly uses 2D (dimensional) and 3D trench investigation across and parallel to active fault segments and in the recent sedimentation deposits..

Paleoseismology supplements historical and instrumental records (catalogues) of earthquakes by characterizing and dating large historic or prehistoric earthquakes (with magnitudes M > 6). This extension in time of earthquake catalogues for certain regions and/or fault segments plays an important role in estimating the long term behaviour, related slip rates and slip deficit, which are the essential parameter for seismic hazards assessment (McCalpin, 1996).

Paleoseismology has been applied on many active strike-slip faults worldwide since the early 1970's. The strike-slip faults that are typically associated with plate boundaries, such as the San Andreas Fault (North America/Pacific plates); the Dead Sea Fault (African/Arabian plates), the North Anatolian fault (Turkish/Eurasia plates), and the Eastern Anatolian fault (Turkish/Arabian plates) present a relatively high slip rate and short period of return for large earthquakes. The Dead Sea fault segments have been the site of paleoearthquake studies such as the Wadi Araba fault (Klinger et al., 2000; Neimi et al., 2001), the Jordan Valley fault (Al Isa et al, 1986; Marco et al., 1996; Ellenblum et al, 1998; Marco et al., 2005; Ferry et al., 2007), the Serghaya-Rachaya, Roum and Yammuneh faults (Lebanese restraining bend; Gomez et al., 2003 Daeron et al., 2007; Nemer and Meghraoui, 2006; Nemer et al., 2008), the Missyaf fault (Meghraoui et al., 2003), and in the northern fault end segment (Akyuz et al., 2006; Altunel et al., 2009).

The used techniques and the sequence of investigation in paleoseismology are mostly basic methods of geologic and tectonic investigations as typically applied to unconsolidated sediments by Quaternary geologists (McCalpin, 1996). The preferred sequence of paleoseismic investigations would progress from the *regional scale* (thousands of square of kilometres) using remote sensing, to *local scale* (few square of kilometres) using tectonic and geomorphic mapping, aerial photo, digital elevation model maps, Quaternary geologic map, to *site scale* (few hundreds to few square meters) using fault zone microtopography, fault scarp profiling, geophysical techniques (shallow seismic, ground-penetration radar GPR) trenching, and C14 dating (by accelerated mass spectrometry method AMS).

Trenching across faults is the major element of paleoseismic studies to optimize data of paleoearthquake displacement and paleoearthquake recurrence (Sieh et al., 1981). Trenching has many types and dimensions (*California-style trenches* and *Japanese style open-pit excavation, etc…*). Logging trench is an essential step; it must have the scale, identifying units of deposits and its contacts, soils, fault zones, and finally the location of taken samples for C14 dating. Photography is used in documenting walls of trenches and compiled with the log.

The interpretation of trench log that intervenes after dating the stratigraphic units helps to reconstructing and restoring stratigraphic units to their pre-deformation positions, and thus will identify the dates and number of paleo-earthquake events as well as the offsets in the spanned time.

II - 4. Archeoseismology

Archeoseismology is the study of the pre-instrumental seismicity period (prehistoric and historic earthquakes), based on faulted sites with coseismic slip and their seismic effects on man-made objects, buildings and monuments (Karcz and Kafri, 1978). The historic exploration of ancient earthquake's effects at archeological sites, archeoseismological investigations depends on multidisplinary work that may involve seismologist, geologist, historian, archaeologist, architect engineer and others. The collaboration of the multidisplinary group gives: i - a discrimination of cause of the archeological site destruction from other causes, ii - dating of different periods of civilization at the site, iii - types of destruction of the monuments (unified orientation of fallen structure elements, opening arches, waving and tilting of walls … etc.), iv - evaluating the degree of damage and estimation of seismic intensity of an ancient earthquake at a given site, v - the measurements of fault offset on buildings, vi – the modelling of seismic shaking using deterministic local acceleration with a comparison to the damage intensity.

The interpretation of archeoseismological data sometimes supports and very often extends the historical earthquake catalogue by providing field evidences on intensity distribution of historical earthquakes. Moreover, if the site is laying on an active fault segment, it plays an essential role with paleoseismology in defining the earthquake size and distribution of its damage area (Stiros, 1996; Marco, 1997)

In order to investigate further buried faulted buildings or vestiges and related damage, the archeoseismological technique is very often combined with shallow geophysical investigation methods such as Ground Penetrating Radar (GPR), micro gravity and magnetic measurements. In other cases, space and aerial photos of different scales and resolutions, with geological maps and dating techniques (C14 by AMS and others), and excavation and coring techniques.. etc.

Distinguishing coseismic from non-coseismic damage in ancient building structures need to be examined by cross evidences from different sources such as historical seismicity, seismogenic zone, local history. In some cases, field evidence of damage leaves no place to any debate about the seismic origin of damage.

Archeoseismic damage falls into five categories according to the dominant force type, as seen in the work of Sbeinati (1994) in many archeological sites in Syria along the Dead Sea

Fault, these aspects will be presented and discussed in Chapter V. First, ancient structures may have been cracked or displaced and separated due to surface faulting, as seen in the Al-Harif Roman aqueduct site of Missyaf Fault (Meghraoui, 2003). Second, waving walls and opening arches as a trace of surface waves such as in Samaan (San Simon) citadel, result from high signal amplitude with low frequency. Third, a unified orientation of fallen structure elements dominated in a site (columns, towers, long walls) as seen in the famous ancient city Apamea (Figure 12) resulted by effect of high horizontal ground acceleration. Fourth, opening the structure pieces as battles of flower and spread out of destruction such as in Kherbet Maez site, which can be resulted from site effect and the structure resonance phenomena. Fifth, the X shape crack in the walls and windows, resulted from shaking of structure as seen in modern structure.

Figure 12: General view of the Agora, at Apamea where the columns fallen down in a unified East West direction.

II - 5. Historical and Instrumental Seismicity

The earthquake catalogue forms the essential database for the seismic hazards study; it gives the geographical distribution of earthquake epicentres, location of possible active faults, depth of active layer, level of seismic activity of faults, aftershocks distribution along the fault, and the focal mechanism along the fault structures. The historical earthquake catalogue integrates the instrumental catalogue to have a wider time span extended to many centuries, and the earthquakes of high magnitudes which less frequent.

A comparison between the historical with the instrumental catalogues indicates several disadvantages: the first one has high variability in epicentre and magnitude determination, lesser level of completeness, and not always macroseismic data that allow us to estimate the epicentre parameters; the second one has shorten time coverage (100 year max.), limited coverage of high magnitude level but sometimes accurate magnitude and epicentral and hypocentral earthquake location, Figure 13; illustrates the comparison in steps between the *Macroseismic data* and *Instrumental data* procedures. (see Chapter III for further details on the seismicity of the study area).

Figure 13; illustrates the comparison in steps between the Macroseismic data and Instrumental data procedures (modifies from Stucchi, 1994).

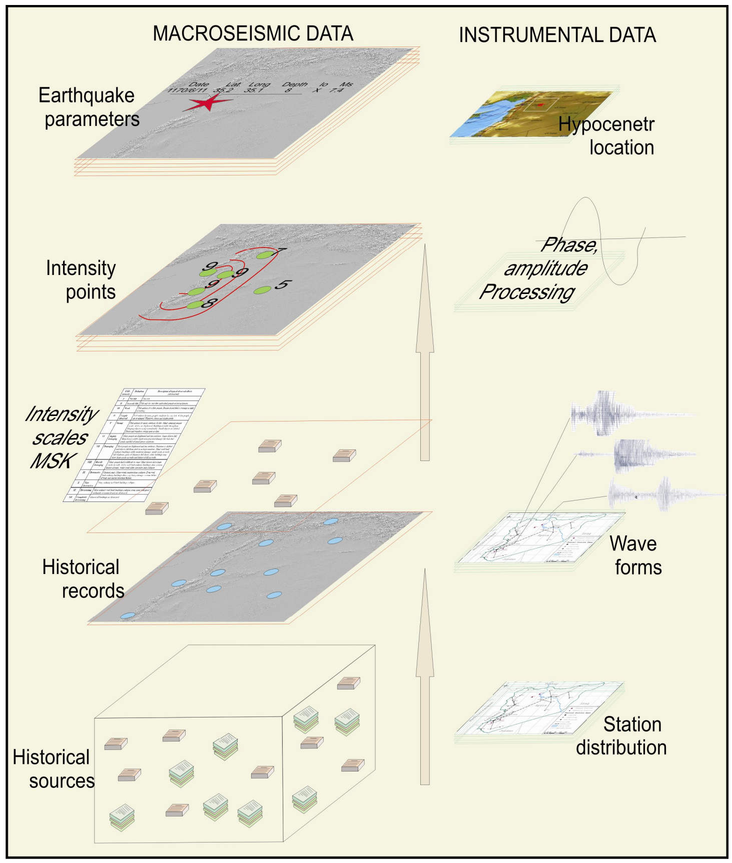

II - 6. The Seismic Hazard Analysis

The seismic hazard analysis consists of two parts: (1) characterizing the sources of earthquakes including the size and spatial location of earthquakes, (2) characterizing the effects (damage intensity) and ground motion of earthquake shaking from these sources at a particular location. The two fundamental approaches are probabilistic and deterministic. There are some very important differences between these two methods. In our work we combine the two approaches and apply the probabilistic method using CRISIS99 software.

6 - 1. The Deterministic Seismic Hazard Analysis

The deterministic analysis use discrete, single-valued events to arrive at scenario-like descriptions of earthquake hazard. This analysis required the specification of three basic elements; an earthquake source (fault Y), a controlling earthquake of specified size (Magnitude), and a mean of determination of the hazard which is the peak ground acceleration at the specific distance to the site.

The following basic steps in this process can be seen in (Figure 14) and briefly describe in the following: *Step 1*: Definition of the seismogenic sources within the tectonic and geologic framework; it can be points, lines, area, or volume. After the source definition, we take the nearest point from the various sources to the site which the hazard is to be estimated. *Step 2*: Estimate the maximum potential earthquake M_{max} for each source. *Step 3*: Determine an earthquake attenuation law that help in estimating the ground motion for an earthquake of a given magnitude at different distances by means of curve fitted to observed data. *Step 4*: Define the seismic hazard at the site as the direct output of step 3; usually, it corresponds to a specific peak ground acceleration, velocity and displacement or any other measure that describe the earthquake effect.

6 - 2. The Probabilistic Hazard Analysis

The probabilistic seismic hazard analysis allows the use of multi-valued or continuous events, models and scenarios. The used method was first defined by Cornell (1968) for most probabilistic seismic hazard analysis. The basic steps can be seen in Figure 15. The statistical analysis of the earthquake activity has been developed recently and evolved from a simple time-independent (Poisson) analysis to a time-dependant treatment of long term seismic activity. The basic probabilistic analysis initiates with the Gutenberg-Richter law (see also chapter II) which calculates the frequency of earthquakes as a function of their magnitude.

In chapter VII we will further describe the details of the probabilistic hazard calculation and apply CRISIS99 for the probabilistic seismic hazard analysis for Syria. CRISIS99 is a freeware computer program, operating under Windows, to compute seismic hazard in extended regions. It was developed at the Institute of Engineering, UNAM, Mexico. Basic input data are: geometry of the sources, seismicity of the sources, and attenuation relations. The steps in applying CRISIS99 for Syria are in the following:

Step 1, Defining source geometry: 1) area sources, using a polygon with at least three vertex; longitude, latitude and depth must be given for each vertex, so this type of source can be used to model, for instance, dipping plates or vertical strike-slip faults; 2) fault sources, using polylines; and 3) point sources are included essentially for academic purposes.

Step 2 Seismicity of the region: 1) Historical and instrumental catalogues; 3) Characteristic earthquakes; 3) Focal mechanism of the seismic sources.

Step 3, Modelling the seismicity of the sources:1) either as time-independent Poisson magnitude-frequency relations also smoothly truncated as Gutenberg-Richter curves, 2) for the characteristic earthquake processes, the program assumes Gaussian distribution of the magnitudes.

Step 4, Hazard computations: it can be performed, simultaneously, for several intensity measures, for instance, A_{max}, V_{max}, and several spectral ordinates. Required attenuation laws are given in the form of tables containing the median values of the intensity measures as a function of magnitude (the rows of the table) and focal distance (the columns of the table). Several attenuation models can be used in the same run, assigning one or several attenuation patterns to each source. Using a recursive triangularization algorithm, spatial integrations are performed to optimize the number of calculations. CRISIS99 will integrate more points for the nearest sources and less (or none) points for distant sources. Hazard estimations are made for points in a grid that is not necessarily rectangular.

Step 4, Visualization of hazard maps and diagrams: CRISIS99 includes a post-processing module that can be used to visualize the results, given in terms of maps of ground acceleration and intensity measures for arbitrary return periods for ground motion exceedance and rate curves for a selected site. Also, if several intensity measures are included in the computations, uniform-hazard spectra can be produced. The main results of a run are also written to ASCII files, so the user can use its own post-processing techniques.

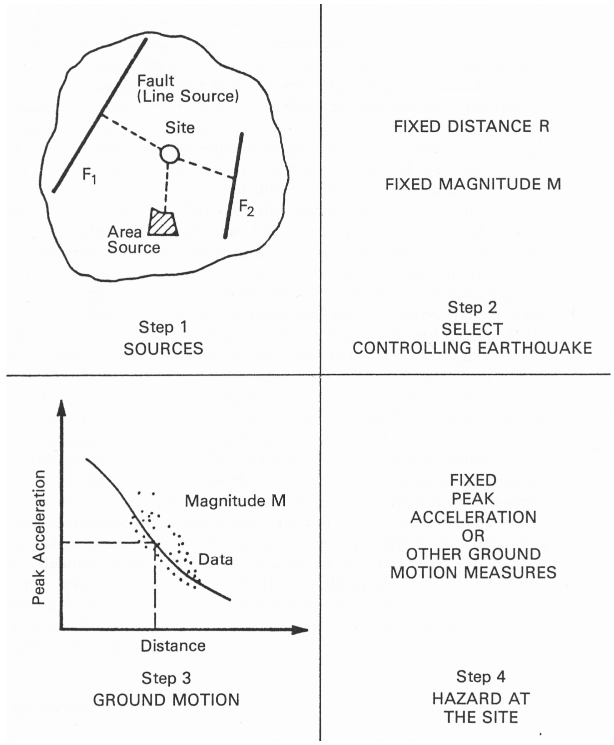

Figure 14: Basic steps of deterministic seismic hazard analysis (from Reiter, 1990)

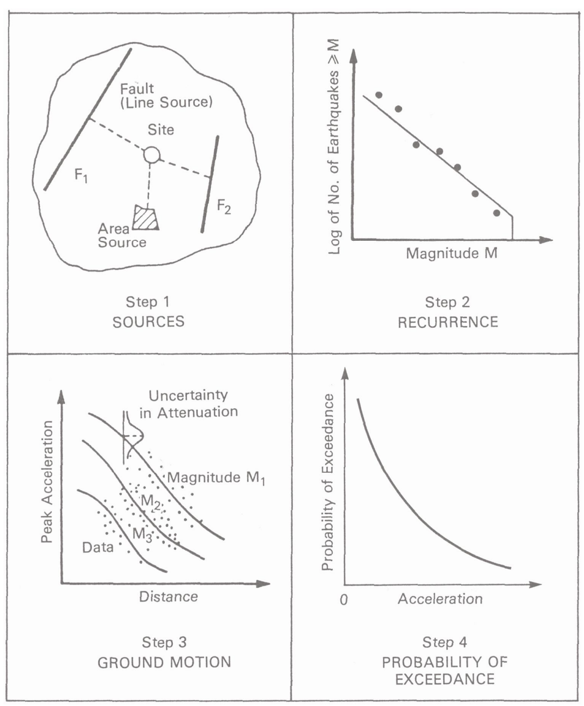

Figure 15: Basic steps of probabilistic seismic hazard analysis (from Reiter, 1990)

References

Allen, C. R. (1986). Seismological and paleoseismological techniques of research in active tectonics. In *Active Tectonics*: Studies in Geophysics (R. E. Wallace, chairman), pp. 148-154. Natl. Acad. Press, Washington, DC.

Akyuz H. S., E. Altunel, V. Karabacak, and C. C. Yalciner (2006). Historical earthquake Activity of the Northern Part of the Dead Sea Fault Zone, southern Turkey, Tectonophysics, 426, 281-293.

Anderson, E. M. (1942). The Dynamics of Faulting and Dyke Formation, with Applications in Britain. Edinburgh, Oliver and Boyd, p191.

Chinnery, M. A. (1969). Earthquake magnitude and source parameters, *Bull. Seism.Soc. Am.* 59, 1969-1982.

Cornell, C.A. (1968). Engineering seismic risk analysis. *Bulletin of the Seismological Society of America*, 58: 1583-1606.

Ellenblum R., S. Marco, A. Agnon, T. Rockwell, and A. Boas (1998). Crusader Castle Torn by Earthquake at down, 20 May 1202, Geology; April 1998, V. 26, No 4, p. 303-306, USA.

Grünthal, G. (Editor) (1993). European macroseismic scale 1992 (up-dated MSK-scale), Conseil de l'Europe, *Cen. Européen Géodyn. Seismol.,* 7, Luxembourg.

Kasahara K. (1985). Erthquake Mechnics, Cambredge University Press, USA.

Karcz I. and U. Kafri (1978). Evaluation of supposed Archaeoseismic Damage in Israel, Journal of Archaeological science, 5, 237-253.

McCalpin Jemes P., Alan R. Nelson (1996). The Scope of Paleoseismology, in Paleoseismology, James McCalpin (edit.), Acadimic Press, USA.

Marco H. E., A. Agnon, A. Ellenblum, R. Eidelman, A. Basson, and U. Boas (1997). 817 Year-old Walls offset Sinistrally 2.1 m by the Dead Sea Transform, Israel Journal of Geodynamics, v. 24, p. 11-20.

Meghraoui M., F. Gomez, R. Sbeinati, J. Van der Woerd, M. Mouty, A. N. Darkal, Y. Radwan, I. Layyous, H. Al-Najjar, R. Darawcheh, F. Hijazi, R. Al-Ghazzi, M. Barazangi (2003). Evidence for 830 years of seismic quiescence from Palaeoseismology, Archaeoseismology and Historical Seismicity along the Dead Sea Fault in Syria, Earth and Science Letters, 210, 35-52.

Reid, H.F. (1910). The Mechanics of the Earthquake, The California Earthquake of April 18, 1906, Report of the State Investigation Commission*,* Vol.2, Carnegie Institution of Washington, Washington, D.C.

Reiter, L. (1990). Earthquake hazard analysis – Issues and insight. Colombia University Press, New York, 254p.

Richter, C. F. (1958). Elementary Seismology. San Francisco: W. H. Freeman and Co.

Sbeinati M. R., R. Darawcheh, and M. Mouty (1994). Field archeological evidences of seismic effects in Syria, in *Materials of the CEC Project “Review of Historical Seismicity in Europe”* – vol. 2., Albini P. and A. (edit.), CNR – Consiglio Nazionale delle Ricerche, Milano, Italy.

Sbeinati, M. R. (1997). Catalogue of instrumentally recorded earthquakes in Syria and neighbouring regions, in the report presented to the International Atomic Energy Agency (IAEA) under the research project entitled *Seismic data fore sitting and site revalidation of nuclear facilities*, No. 6247/R3/RB), Atomic Energy Commission of Syria (AECS), Damascus, Syria.

Scholz Christopher H. (1990). The Mechanics of Earthquakes and Faulting, Cambridge University Press, USA.

Shebalin, N.V. (1970): Intensity: on the statistical definition of the term, in *Proc. X Ass. ESC*, Leningrad, 3-11 September 1968 (Acad. Sci. USSR, Soviet Geophysical Committee, Moscow).

Solonenko, V. P. (1973) in Paleoseismology, McCalpin (1996).

Stiros, S., R. E. Jones (Editors), (1996). Archaeoseismology, Institute of Geology & Mineralogy Exploration, Athens, Greece, and the British School at Athens, Athens, Greece.

Tocher, D. (1958). Earthquake energy and ground breakage, *Bull. Seis. Soc. Am.* 48, 147-153.

Yeats Robert S., Kerry Sieh and Clarence R. Allen (1997). The Geology of Earthquakes, Oxford University Press, NY, USA.

Wells, Donald L. and Kevin J. Coppersmith (1994). Bulletin of the Seismological Society of America, Vol. 84, No. 4, pp. 974-1002.

Wheeler, R. L. (1994). Persistent Segment boundaries on basin-range normal faults. In *fault segmentation and Controls of Rupture Initiation and Termination* (*D. P. Schwartz and R. H. Sibson, eds.*), *US Geol. Surv. Open File Rep.* 89-315, 432-444, (1994).

CHAPTER III

SEISMOTECTONIC SETTING OF WESTERN SYRIA

III Seismotectonic Setting of western Syria

III – 1. Tectonic Setting

Syria occupies the north-western corner of the Arabian Plate and the north-eastern section of the Sinai plate. In this situation, Syria seats on a plate boundary, i.e., the Dead Sea Fault that accommodates a remarkable portion of left-lateral strike slip movements (Figure 1). To the north, the continent/continent collision strikes in a roughly northwest direction at an estimated 18. ±2 mm/year between the Arabian and the Anatolian Plates (Reilinger et al., 2006). To the northwest of the Arabian Plate, the dextral North Anatolian Fault and the sinistral East Anatolian Fault accommodate tectonic movement of the Anatolian subplate that is escaping westward due to the Arabian-Eurasian convergence (McClusky et al., 2000). The Cenozoic Dead Sea fault forms the Arabian/African-Sinai plates boundary and it has a sinistral transform that runs between an extensional tectonic system to the south and a contractional plate boundary to the north. Indeed, the fault transforms southward the spreading oceanic lithosphere of the Red Sea into northward the contracting continental lithosphere at the junction with the East Anatolian Fault Zone and the Bitlis Suture Zone in Turkey. The active fault zone that accommodates the differential northward motion of the Arabian and African plates (Sinai subplates) includes the prominent Lebanese restraining bend (Figure 1) that extends further east as the Palmyrides contractional system. In fact, the NE trending Palmyrides fold-thrust belt starts from Damascus to the Euphrates River region and forms the main continental shortening in the northern part of the Arabian Plate (Chaimov, 1990).

The new tectonic map of Syria (Figure 2) and its description has been adopted from the comprehensive publication of the work of (Brew et al., 2001), with some modifications. The map shows the general tectonic structures and geological outcrop distribution on shaded relief imagery (srtm30). The faults and folds shown in black lines were mapped by (Dubertret, 1955 and 1966), (Ponikarov, 1966), (Searle, 1994), and from surface observations and limited remote-sensing imagery interpretation (Brew, 2001). The subsurface structure, in red, is modified from the top lower Cretaceous structure map. This level was chosen to represent the subsurface as most faulting cuts this horizon, yet it is still relatively close to the surface. The sense of motion on these faults may change according to the particular structural level that is considered. The authors have mapped many of the reverse faults that limit the Palmyrides anticlines as being reactivated (inverted) normal faults. The strike-slip activity is also difficult to map accurately in the subsurface and it is only noted where known with some certainty. Assuredly, many more faults have strike-slip components than are identified on this map. The map shows how most tectonic deformation in Syria is located within four major structural zones: the Palmyrides, the Abd el Aziz-Sinjar area (NE Syria), the Euphrates Fault System and the Dead Sea Fault System. These major structures have accommodated most of tectonic deformation in Syria throughout the Phanerozoic, whereas the intervening stable areas remained structurally high and relatively undeformed. The style of structural reactivation is dependent on the orientation of the tectonic zones to the prevailing stress pattern.

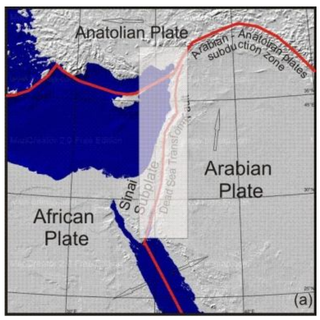

Figure 1: (a) The index map of regional plates with arrows showing the directions of the plate's movement and the tectonic map covering area. (b) General regional plate tectonic map of the Arabian and adjacent plates and the detailed segments of the Dead Sea Fault System. Focal mechanism are Harvard-CMTand GPS velocities are from Reilinger et al. (2006)

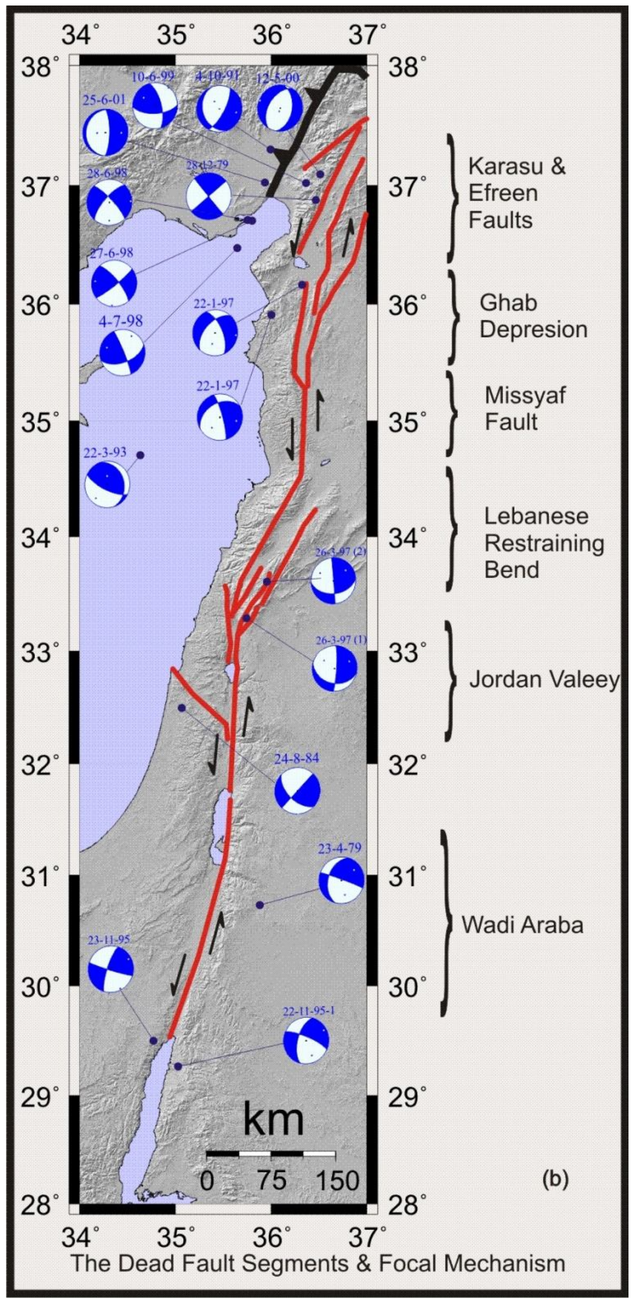

A brief description of the tectonic features shown in the map of Figure 2 is as following: The Lebanon and *Anti-Lebanon Mountains are* mainly uplifted as part of 'Syrian Arc' in the Paleogene. The *southwestern volcanic fields* consist on Neogene and Quaternary basalts erupted from prominent volcanic centers aligned in a NNW direction. The *Palmyrides* are late Cretaceous to present and with mainly Neogene SE-verging fault-propagation folding and very steep dipping southeastern forelimbs. The late Cretaceous *Baer-Bassit Ophiolite* that obducted from the north. The fault-bounded

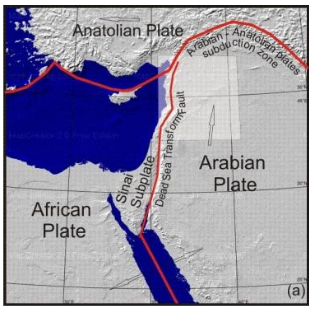

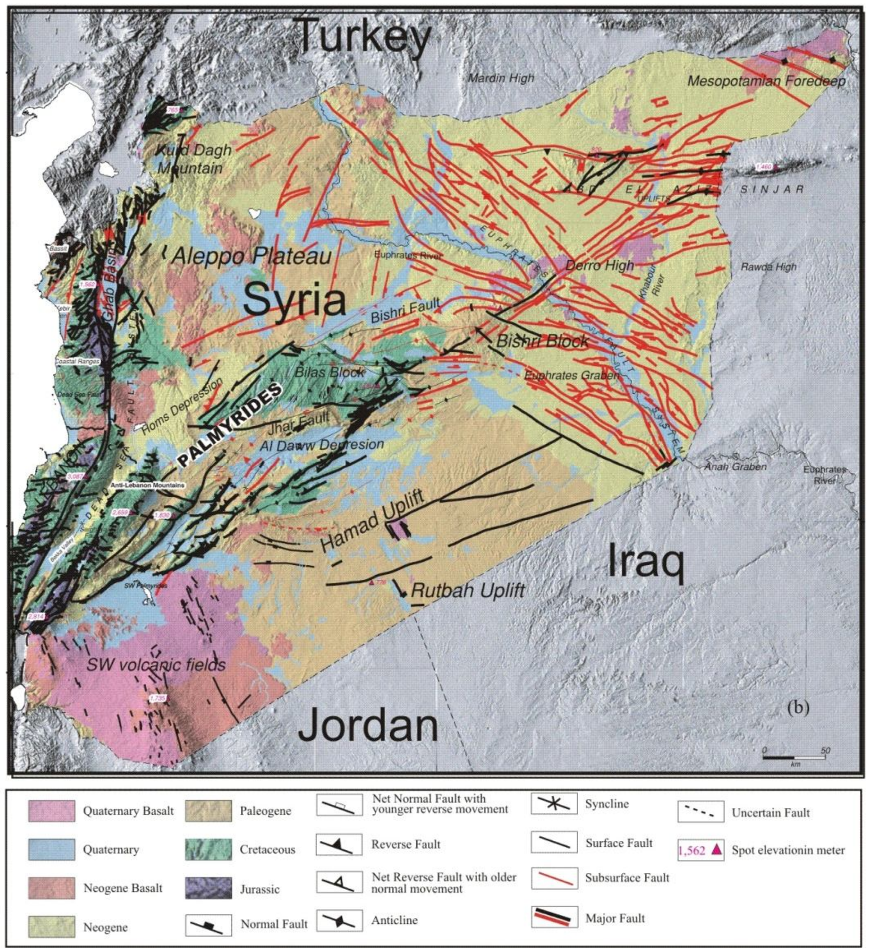

Figure 2: (a) The index map of regional plates with arrows showing the directions of the plate's movement and the tectonic map covering area. (b) The tectonic map of Syria showing the main tectonic features: main blocks, surface and subsurface faults, axes of folds and synclines, volcanic areas and geology (modified from Brew 2001).

Neogene depocenter *of Nahr Al-Kebir Depression* with up to 2-km-thick Neogene strata. The *northern Dead Sea Fault (in Lebanon and Syria)* formed since the late Miocene with <25 km of sinistral movement. The *Coastal Ranges* with ~2.5 km of post mid-Eocene uplift. *AL-Daww Depression*: Intermountain basin with ~2km of Cenozoic continental clastics. Furtehr east, The *Ghab Basin* shows up to 3.4 km of Pliocene/Quaternary alluvial deposits in a pull-apart basin along the Dead Sea Fault. The fault limits to the east the *Aleppo Plateau, a* structurally high topography and major crustal block in northern Syria, but with a crust thinner than in S. Syria. Other tectonic structures (such as the *Jhar Fault, Bishri Fault, Euphrates Graben, Derro High, Jebel Abd el-Aziz, Mesopotamian foredeep, Sinjar Uplift, Rawda High, Anah Graben, Rutbah Uplift, and Kurd Dagh mountains)* form mainly the tectonic framework of Syria not directly related to the Dead Sea fault system.

III – 2. The Dead Sea Fault System

The Dead Sea Fault System is a major left-lateral transform plate boundary separating Africa (Sinaï subplate) from Arabia and accommodates their differential movement. The total offset on the southern portion of the fault is well established to be around 105 km (Quennell, 1984). Some authors have suggested two episodes of strike-slip motion on the Dead Sea Fault System in agreement with a two phases Red Sea opening—Miocene slip of 60 to 65 km, and post-Miocene slip of 40 to 45 km (Freund et al., 1970; Quennell, 1984). Other authors (e.g., Steckler and ten Brink, 1986) have advocated a more constant Red Sea extension. Along the northern section of the fault (in Lebanon and Syria) the age and rates of faulting were not determined due to a lack of piercing points, although the total post-Miocene offset has been reported as less than 25 km (Trifonov et al., 1991). These observations added with the work in the Palmyride have been combined into a model in which the northern part of the Dead Sea Fault System has been active only during the second (post-Miocene) phase of faulting. In this model, 20 to 25 km of post-Miocene sinistral motion has been accommodated along the northern fault segment, and another 20 km in the shortening of the adjacent Palmyride fold and thrust belt (Chaimov et al., 1990), thus accommodating the full 40 to 45 km of post-Miocene slip. The northern segment of the Dead Sea Fault System strikes northward parallel to the coast through western Syria, and is clearly defined both topographically and structurally (Figure 2). Along the fault in western Syria is the deep Ghab Pliocene to Holocene pull-apart structure opened in response to a left-step, although sinistral motion fails to be fully transferred across the basin, resulting in the ‘horse-tailing’ of the fault system observed northward into Turkey. The Coastal Ranges have clearly been affected by the propagation of the Dead Sea Fault System and formation of the Ghab Basin, resulting in the steep eastern limb and the possible rotation of the block (Brew et al., 2001).

III – 3. Segmentation of northern DSF

The Dead Sea Fault can be roughly divided into two sections separated by the Lebanese restraining bend (Griffiths et al., 2000; Gomez et al., 2003). The southern section starts from the Golf of Aqaba in the south passing through Wadi Araba (Wadi Araba segment), forming the Dead Sea as a large pull-apart basin, continuing along the Jordan Valley and ends in the Hula Basin (Figure 1). Further north, the Lebanese restraining structure shows NNE trending fault branches, i.e., the Serghaya, Rashaya, Hasbaya, and Yammuneh Faults and NW trending Al-Roum Fault. The 200-km-long Yamouneh Fault forms the main continuation on the Dead Sea Fault to the North and ends at Al-Boukeyaa Basin where the N-S section starts in Syria. The northern section has three main segments from south to north: The Missyaf segment as single linear fault structure, and the Al-Ghab pull-apart region that separates into several fault branches with the main Jisser Al-Shoughur segment west of the basinand the Afamia and Ifreen Faults to the east of the basin. The northern DSFZ, in Syria and southern Turkey, is regarded as a series of transpressional stepovers, along which the left-lateral slip is apparently slower than the relative plate motion, because this slip is oblique to the relative plate motion (Gomez et al., 2007).

The late Quaternary tectonics and related slip rate along the Dead Sea Fault have been investigated by many authors applying geomorphological, paleoseismological, and geodetic (GPS) measurements methods. The main results summarized in Table 1 show that; 1) the slip rate estimation along the Dead Sea from the tectonic investigations is varying from 1.5-3.5 mm/yr to 9-15 mm/yr, while the GPS measurements give estimations of 4.5-4.8 mm/yr to 5.6-7.5 mm/yr. 2) The geological methods have higher level of slip rates than the GPS measurements. 3) There are some minor variations of slip rate between the northern and southern segments depending on each applied method of measurements and block models. Table 1 shows the different estimated slip rates along the Dead Sea Fault with the source and type of evidence.

III – 4. Historical Seismicity

The Earthquakes, as any natural catastrophic phenomena, have been described and recorded for more than 3000 years ago in the Middle-East region. Previous works have described the earthquake effects on nature and man-made structures, such as faulting rupture, coseismic deformation, landslide, springs appearing and disappearing, lives casualties, houses destruction, …etc. In our previous work, we have prepared the *historical earthquake catalogue of Syria and neighbouring regions (see Chapter IV)* which shows a parametric estimation of the textual descriptions of historical earthquake damage and effects (Sbeinati et al., 2005).

Fault segment	Evidence type	Amount of offset	Age of datum	locking depth km	Slip rate mm/y	Authors
DSF (general)	Geol.	65 km	~4Ma		~ 8.7	Westaway et al., 2001
			7–10 Ma		4–6	Freund et al., 1970
			3.1–3.7 Ma		9–15	Steinitz et al., 1978
			Pliocene-Pleistocene (4–5 Ma)		7–10	Garfunkel et al., 1981
			Last 1,000–1,500 yr		1.5–3.5	Garfunkel et al., 1981
	offset Miocene rocks	40–45 km	7–12 Ma		3.5–6	Freund et al., 1968
	GPS				4.5 – 4.8 ± 1	Reilinger et al., 2006
	GPS				5.6 – 7.5 ± 1	McClusky et al., 2003
Amik basin	Paleo	7.9 km	Pre-Quaternary		4.94±0.13	Karabacak 2009
	Paleo	42 m	6500 BC		?	Altunel et al., 2009
	Paleo	25 m	1500 BC		?	Altunel et al., 2009
Missyaf + Al-Ghab	Paleo.		Last 2000 years		6.9±0.1	Meghraoui et al, 2003
	GPS			5-16 km	1.8-3.3	Alchalbi et al, 2009
	GPS			15 km	4.2±0.3	Gomez et al, 2007
	GPS				4.8± 0.3	Reilinger et al, 2006
	GPS			13 km	4.7±0.4	Mahmoud et al., 2005
Yammuneh	Offset alluvial fans		25 ka		5.1 ± 1.3b	Daëron et al., 2004
	offset Homs basalts	8 km	Miocene- Pliocene		5–10	
	offset Litani river	5 km	1–2 Ma		5–10	Garfunkel et al., 1981
	GPS			15 km	3.9±0.3	Gomez et al, 2007
	GPS				3.5± 0.4	Reilinger et al, 2006
	GPS			13 km	3.4±0.4	Mahmoud et al., 2005
Roum	Paleo				0.86 – 1.05	Nemer et al., 2006
Serghaya	offset channels		10 ka		1.4±0.2	Gomez et al., 2003
	GPS				1.7-2.8	Wdowinski et al., 2004
South DSF	GPS				3.3 ± 0.4 - 3.7 ± 0.4	Wdowinski et al, 2004
Hula Basin	offset of walls	2.1 m	817 years		~ 2.5	Marco et al., 1997
	GPS			15 km	3.0±0.3	Gomez et al, 2007
Jordan Valley	Geol. offset gullies		the last 47.5 kyr		4.7 to 5.1	Ferry et al, 2007
	Paleo		Last 5 kyr		3 – 4	Marco et al., 2005
	offset channels	100–150 m	post-Lisan		10	Garfunkel et al., 1981
	Paleo		60,000 yr		0.5	Hamiel et al., 2009
	GPS			15 km	4.0±0.3	Gomez et al, 2007
	GPS				4.4 ± 0.3	Reilinger et al, 2006
	GPS			12 km	3.7±0.4	Wdowinski et al, 2004
	GPS			13 km	4.3±0.3	Mahmoud et al., 2005
Wadi Araba	offset gullies and fan surfaces on ributaries to Wadi Dahal	54 m 39 m 22.5 m	16–11 ka 9–6.5 ka 5.8 ka		3.4–4.9 4.3–6.0 3.9	Niemi et al., 2001
	offset of late pleisto. alluvial fan	500 m	77–140 ka		4	Klinger et al., 2000a
	Offsets in drainage basins and alluvial fans	15 km	Late Pliocene or early Pleistocene		3–7.5	Ginat et al., 1998
	slumps in Lisan deposits				6.4	El-Isa et al., 1986
	offset alluvial fans	3 km	0.3–0.6 Ma		5–10	Garfunkel et al., 1981
	offset alluvial fans	150 m	20–23 ka		7.5	Zak and Freund, 1966
	GPS			~12 km	4.9 ± 1.4	Le Beon et al, 2008
	GPS				4.5 ± 0.3	Reilinger et al, 2006
	GPS			13 km	4.4±0.3	Mahmoud et al., 2005

Table 1. Geologic and GPS estimate of lateral slip rates along the Dead Sea transform fault system.

The catalogue is presented as a list of earthquakes with its parameters ordered by date, time (whenever mentioned), epicentre, coordinates, estimated maximum intensity, calculated magnitude, intensity at affected localities, and the natural coseismic features.

The historical earthquake catalogue; extends the knowledge about the seismic activity for longer time span than the instrumental catalogue. In the Syrian case because of the rich civilization and historical heritage present in archaeology and literatures, the historical catalogue extended up to 1365 B.C. (Sbeinati, 2005), whereas the instrumental catalogue covers a more recent time beginning from 1900 A.D.. The completeness of the catalogue is for M = 6.5. In our case of long returning periods of destructive earthquakes in Syria, the historical catalogue (supplied with the archeoseismic and paleoseismic data) contains important information on the occurrence of large seismic events. Despite of the low level of instrumental seismicity and the absence of strong motion records, seismic parameters and fault activity along the active structures of the Dead Sea Fault associated with the historical earthquake data play a key role in estimating the seismic hazard for Syria.

The applied methodology in preparing the historical earthquake catalogue for Syria can be summarized in the following steps: (details are in the Chapter IV and the paper of Sbeinati et al., 2005), (see Figure II-12 in Chapter II): (1) Collecting all previous works about the historical seismicity of Syria and the neighbouring regions, such as seismological compilation, parametric catalogues, and individual events, (2) Systematic searching in all different types of historical sources, for collecting description on historical earthquakes, (3) Quality classification of the collected fragments of historical descriptions according to the restricted criteria: originality of the document or second-hand or translated, the author if contemporary or posterior, eye witness, transferred, position and socio-political conditions ,(4) Grouping the related description of each historical earthquake and ordering groups chronologically, (5) Quantifying the discretional texts of earthquake effects at each locality by means of applying the EMS-1992 intensity scale which is adopted from the MSK-64 intensity scale, (6) Drawing maps of intensities with localities and the isoseismal map for each earthquake, (7) Estimating the parameters of earthquake: date, epicentre coordinates, and magnitude (Shebalin, 1970), finally (8) producing the catalogue of the historical earthquakes, see Table 2: which shows the main destructive earthquakes with Ms > 5.9 along the Dead Sea Fault, these earthquakes have enough earthquake data to construct a parametric catalogue after (Sbeinati et al., 2005) and the map of earthquake epicentre distribution from 37 to 1900 A. D.)

No	Date (dd.mm.yyyy)	Lat. (°N)	Long. (°E)	Major affected localities	*I0* (EMS-92)	*H* (km)	*Ms*
01	37 A.D.	36.00	36.30	Antioch, Dafneh	VII-VIII	15	6.2
02	53	36.20	36.50	Antioch, Afamia, Manbej, Lattakia	VIII	30	6.6
03	303-304	33.80	34.30	Saida, Sur, Syria	VIII-IX	20	7.1
04	494	35.80	36.30	Antioch, Tripoli, Lattakia	VII-VIII	25	6.5
05	22.08.502	33.00	34.80	Akka, Sur, Saida, Beirut, Safad	VIII-IX	30	7.2
06	531-534	35.50	37.20	Area between Aleppo and Homs	VIII	15	6.5
07	09.07.551	34.00	35.50	Cities of Lebanese coast, Arwad	IX-X	28	7.2
08	565-571	36.00	36.20	Antioch, Seleucea, Kilikia, Anazrabo	VII-VIII	30	6.0
09	18.01.747	32.50	35.60	Mt. Tabor, Baalbak, Bosra, Nawa, Balqa, Al-Quds, Beit Qubayeh, Tabaryya, Damascus, Daraa	IX	25	7.2
10	24.11.847	34.40	36.30	In and around Damascus, Antioch, Al-Mosel	IX	35	7.5
11	30.12.859-29.01.860	35.70	36.40	Antioch, Lattakia, Jableh, Homs, Palmyra, Tarsus, Balis, Damascus, Adana, Ar-Raqqa	VIII-IX	33	7.4
12	05.04.991	33.70	36.40	Baalbak, Damascus	IX	22	7.1
13	30.07-27.08.1063	34.40	36.20	Tripoli, Lattakia, Akka, Sur	VIII	32	6.9
14	11.1114	37.30	38.50	Maskaneh, Maraash,	VIII-IX	40	7.4
15	11.1114	37.30	36.50	Samsat, Orfa, Harran	IX	40	7.7
16	27.09.1152	32.60	36.70	Bosra, Hauran, Syria	VIII	12	5.8
17	02-04.04.1157	35.50	36.50	Shaizar, Hama, Kafer Tab, Aleppo	VII	22	6.0
18	13.07.1157	35.20	36.60	Hama, Afamia, Kafer Tab, Homs, Tayma	VIII	25	6.6
19	12.08.1157	35.40	36.60	Shaizar, Kafar Tab, Afamia, Hama, Arqa, Aleppo, Homs, Lattakia, Tripoli, Antioch, Qalaat Al-Hosn, Maarret Annooman	IX-X	15	7.4
20	29.06.1170	34.80	36.40	Damascus, Homs, Hama, Lattakia, Baalbak, Shaizar, Barin, Aleppo	IX	35	7.7
21	20.05.1202	34.10	36.10	Mount Lebanon, Baalbak, Sur, Beit Jin, Banyas, Nablus, Al-Samyra, Damascus, Safita, Akka, Tripoli, Hauran, Beirut, Homs, Tartus	IX	30	7.6
22	02.01.1344	36.70	37.40	Al-Rawendan, Manbej, Aleppo	VIII	30	6.8
23	20.02.1404	35.70	36.20	Blatnes, Bkas, West of Aleppo, Qalaat Al-Marqeb, Tripoli, Lattakia, Jableh	VIII-IX	30	7.4
24	29.12.1408	35.80	36.10	Shugr, Bkas, Blatnes, Lattakia, Jableh, Antioch, Syrian coast	IX	25	7.4
25	10.10.1568	35.50	35.50	Lattakia, Famagusta	VIII	12	6.0
26	21.01.1626	36.50	37.10	Aleppo, Gaziantab, Hama	IX	20	7.3
27	22.09.1666	37.00	43.00	Al-Mousel, Sinjar, Sharqat	IX	35	6.9
28	24.11.1705	33.70	36.60	Yabroud, Al-Qastal, Damascus, Tripoli	VIII	35	6.9
29	15.04.1726	36.30	36.60	Jum, Aleppo	VIII	15	6.1
30	25.09.1738	36.70	36.50	Iskenderun, Bellen Bass, Antioch, Jabal Al-Amanus, Aleppo	VIII	10	6.2
31	30.10.1759	33.10	35.60	Al-Qunaytra, Safad, Akka,	VIII-IX	20	6.6
32	25.11.1759	33.70	35.90	Baalbak, Zabadani, Ras Baalbak, Al-Qunaytra, Damascus, Beirut, Saida, Safad, Sur, Tripoli, Homs, Hama, An-Nasra, Lattakia, Al-Quds, Gaza, Antioch	IX	30	7.4
33	26.04.1796	35.30	36.20	Qalaat Al-Marqeb, Al-Qadmous, Nahr Al-Kabir, Jableh, Bkas, Lattakia	VIII-IX	20	6.8
34	13.08.1822	36.10	36.75	Jisr Ash'Shoughour, Quseir, Aleppo, Darkoush, Antioch, Iskenderun, Idleb, Kelless, Armanaz, Sarmada, Lattakia, Homs, Hama, Maraash, Ram Hamadan, Bennesh, Maarret Missrin Safad	IX	18	7.0
35	01.01.1837	-	-		VIII		>7.0
36	03.04.1872	36.20	36.50	Harem, Armanaz, Lake of Al-Amq, Antioch, Aleppo, Suaidiya, Izaz, Idleb, Iskenderun	VIII-IX	10	7.2

Table 2; Main destructive earthquakes with Ms > 5.9 along the Dead Sea Fault, these earthquakes have enough data to construct a parametric catalogue.

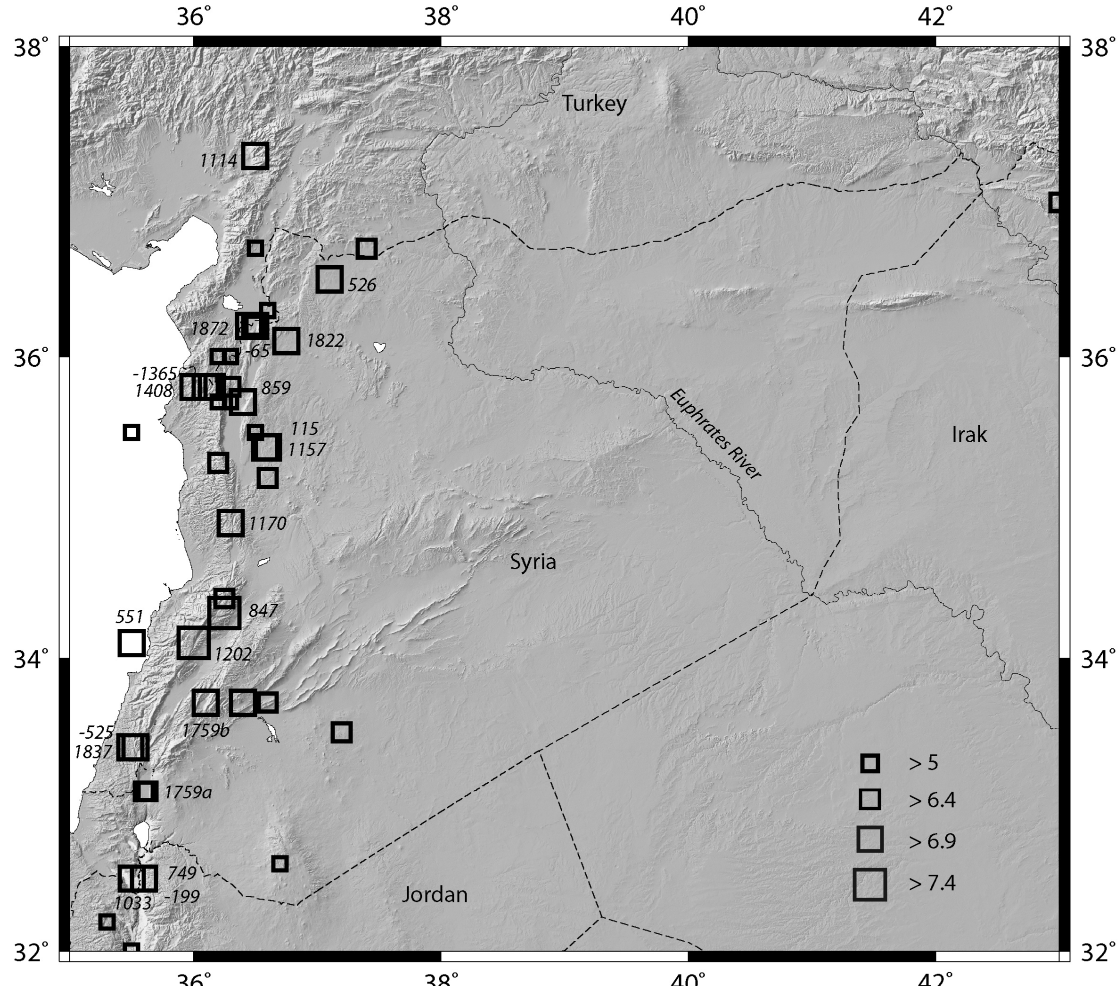

Figure 3: Map of historical seismicity from 37 A.D .to 1900 A.D.

III – 5. Instrumental Seismicity

The instrumental earthquake catalogue of Syria covers the period from 1900 to 2008 (Figure 4). The catalogue is a combination of two catalogues: the first one is the old version of catalogue (Sbeinati, 1997) covering the period 1900 – 1995 and the second covering the period from 1995 to 2008 (data from National Earthquake Centre of Syria, http://www.nec.gov.sy/).

The applied methodology in the first catalogue has been described in (Sbeinati, 1997), where the compiled of data were from different sources (mainly international data centres and seismic networks of the neighbouring countries). A special concern has been devoted to the fixed coordinates of epicentre location and unifying the magnitudes (the completeness of data includes M>2.5 depending on the time-window and the region. The second catalogue has been compiled after a download from the web page of the National Earthquake Centre (NEC-Syria) http://www.nec.gov.sy/, and from the International Seismological Centre (ISC) http://www.isc.ac.uk/, and the European-Mediterranean Seismological Centre (EMSC), http://www.emsc-csem.org/.

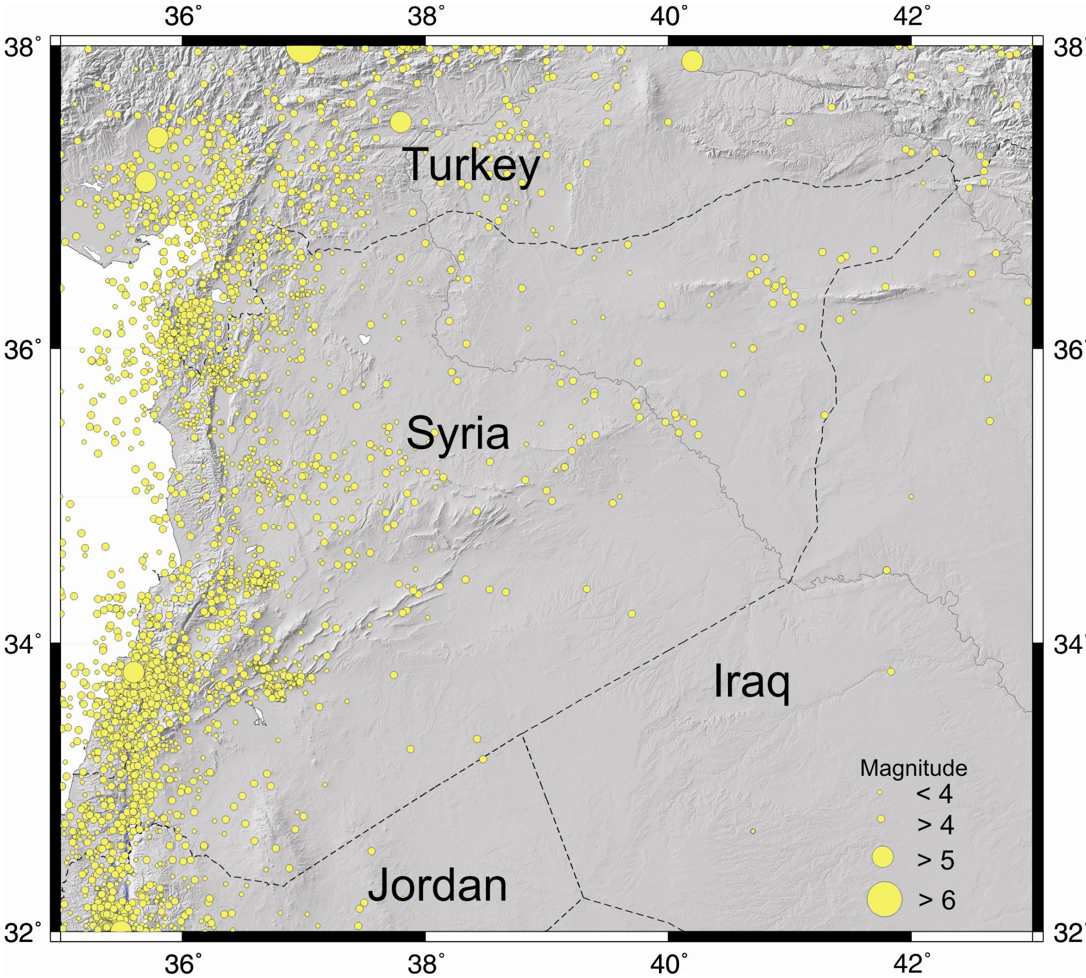

Fig. 4 Map of instrumental seismicity for 1900-2008

II - 6. Focal mechanism analysis

Analysis of focal mechanism solutions of the main recent events along the Dead Sea Fault, indicate a clear NNW-SSE trending of *P* axes with strike slip movements along faults such as the 22/11/95 event (M 7.3) in the golf of Aqaba, and the two events on the Serghaya Fault in 26/03/97 (M …, …) as seen in Figures 1 and 5 (Figure 1 is the Figure 1 in this chapter, Figure 5 is the map of focal mechanism and the GPS velocities). In Syria, the event mechanisms of 22/01/97 illustrate a transtension associated with the left-lateral pattern and show a component of normal faulting associated with the Ghab pull-apart basins. We present in Tables 4 and 5 all focal mechanisms calculated for Syria and neighboring regions (Reasenberg and Oppenheimer, 1985; Salamon, 2003; and Harvard-CMT solution). Earthquake mechanisms on the Dead Sea Fault Zone present a nearly N-S trending fault plane with left-lateral slip vector in accord with the P axe directions and inferred stress distribution. Unfortunately there is not enough recent large earthquakes (M>5) along the northern Dead Sea Fault that could document the stress distribution (Tables 4 and 5 represent the focal mechanism parameters according to Salmon, 2003 and Harvard-CMT solution).

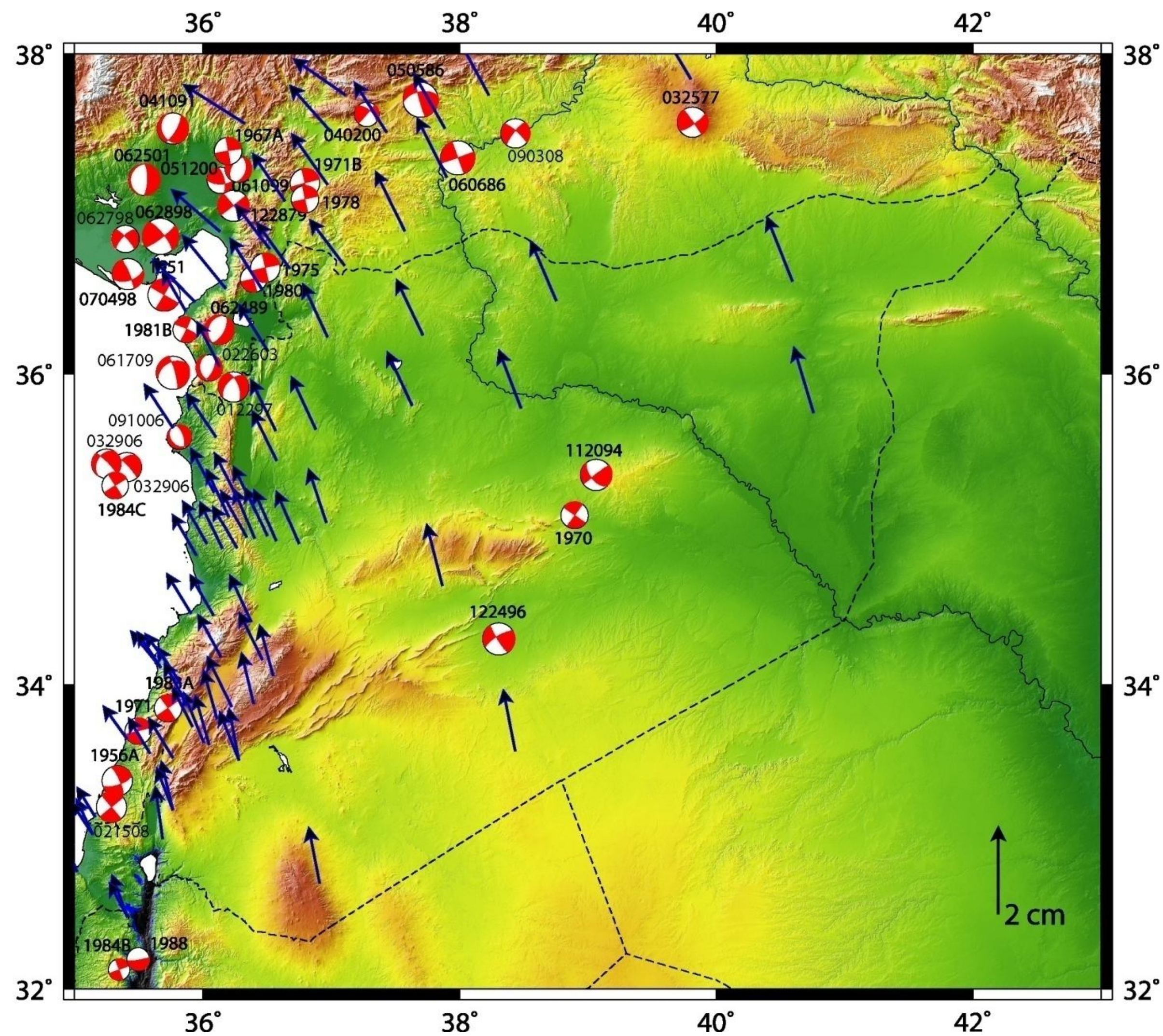

Figure 5: Map of focal mechanism (Harvard CMT, Reasenberg & Oppenheimer 1985 Salamon et al., 2003,and Pondrelli et al., 2002) and GPS velocities (Reilinger et al., 2006; Alchalbi et al., 2009).

Event										Parameters of fault plane solutions						
								P		T		First plane			Second plane		
No	Symbol	Origin time		*ML*	Lat.	Long.	Zone	φ	δ	φ	δ	φ	δ	*L*	φ	δ	*L*
1	4/51	1951	04082138	5.7	36.5	35.7	CA	66	41	17	263	30	105	−60	64	251	−106
2	3/56a	1956	03161932	5.2	33.3	35.3	DST	10	144	10	235	90	280	−15	75	10	−180
3	3/56b	1956	03161943	5.5	33.3	35.3	DST	18	155	34	51	50	288	12	80	190	140
4	3/68	1968	03261937	4.8	34.1	35.5	DST	27	251	0	341	70	120	−60	71	22	−21
5	10/70	1970	10051453	4.8	35.1	38.9	Plm	9	309	80	130	35	130	90	55	310	90
6	4/71	1971	04162127	4.6	33.7	35.5	DST	38	113	14	215	75	250	−40	51	352	−160
7	6/71	1971	06290908	5.0	37.1	36.8	NMTJ	11	312	62	65	40	160	130	60	292	61
8	7/71b	1971	07112012	5.1	37.2	36.8	NMTJ	30	134	60	314	75	135	90	15	315	90
9	8/71	1971	08170429	4.9	37.1	36.8	NMTJ	32	132	55	333	78	140	99	15	280	50
10	2/78	1978	02092110	4.5	37.07	36.84	NMTJ	17	11	66	233	30	170	60	64	23	106
11	1/80	1980	01021252	4.7	36.6	36.4	NMTJ	30	1	55	148	77	348	74	20	220	140
12	2/81	1981	02190241	4.7	36.35	36.42	DST	3	49	10	139	85	5	10	80	274	174
13	6/81	1981	06300759	4.7	36.18	35.89	DST	21	201	33	306	82	166	40	50	70	170
14	6/83a	1983	06030204	4.9	33.85	35.73	DST	65	77	5	179	55	200	−60	44	344	−125
15	11/83	1983	11240014	4.7	37.05	36.11	DST	21	184	6	91	70	316	−10	80	50	−160
16	12/84	1984	12181359	4.7	35.29	35.32	CA	1	337	51	69	58	305	42	55	190	140
17	6/87	1987	06160617	4.7	35.55	35.25	CA	55	53	30	266	77	253	−105	20	125	−40

Table 4: Parameters of the fault plane solutions of first P-wave arrivals, (Salamon et al., 2003). Abbreviations: Each event is noted by its symbol on the seismotectonic maps; origin time of year, month, day, hour and minute; local magnitude; and epicentral coordinates. Zones are: CA, Cypriot Arc; DST, Dead Sea Transform; NMTJ, Northeast Mediterranean Triple Junction; Plm, Palmyride fold belt; are given by the Plunge (φ) and the Trend (δ) of the Pressure (P) and Tension (T) axes; and Plunge (φ), Trend (δ) and Rake (L) of the two nodal planes.

No	**Origin time**		***mb***	**Long.**	**Lat.**	**Zone**	**Str1**	**Dip1**	**Slip1**	**Str2**	**Dip2**	**Slip2**	**Sm**
18	1979	12280309	5.1	35.85	37.52	NMTJ	141	90	180	231	90	0	1.47 e24
19	1989	06240309	4.9	35.93	36.72	NMTJ	203	28	−93	27	62	−88	5.04 e23
20	1991	04100108	5.2	36.14	37.31	NMTJ	160	27	−136	29	72	−70	12.91e23
21	1996	12242216	4.9	38.58	34.29	Plm	240	75	9	147	81	165	2.03 e24
22	1997	01221757	5.3	35.94	36.18	NMTJ	243	39	−15	345	81	−128	4.32 e24
23	1998	06271355	6.6	35.31	36.88	NMTJ	321	75	171	53	81	15	2.96 e25
24	1998	07040215	5.4	35.32	36.87	NMTJ	72	55	8	338	84	145	15.87 e23
25	2001	06251328	5.6	35.82	36.91	NMTJ	184	15	−88	2	75	−90	1.5 e24

Table 5: Parameters of CMT solutions done by Harvard, origin time, location and zones, are as in Table 2. Magnitude is mb according to NEIS. Mechanisms are given by Harvard conventions: strike, dip and slip of the two planes. Scalar moment (Sm) is given by abscissa and exponent.

Date	Lat.	Long.	Depth	*MW*	T-axes			N-axes			P-axes			Plane 1		
					σ	δ	ξ	σ	δ	ξ	σ	δ	ξ	σ	θ	λ
01/22/97	36.27	35.95	16.5	5.1	5.45	7	98	1.10	40	3	−6.55	49	196	224	52	−35
03/26/97	33.10	35.49	10.0	5.1	5.60	30	67	1.00	34	179	−6.59	42	306	104	35	−167
03/26/97	33.53	35.70	10.0	4.6	8.21	30	52	0.31	43	175	−8.52	32	301	87	43	−179
06/28/98	36.89	35.54	10.0	4.9	2.51	5	89	0.21	68	347	−2.72	22	181	223	71	−12
06/10/99	37.22	36.14	12.0	4.4	6.39	37	306	−1.02	53	133	−5.37	4	38	89	62	26
04/02/00	37.63	37.28	10.0	4.3	3.43	20	270	0.89	61	42	−4.31	19	172	311	61	179
05/12/00	37.29	36.28	16.9	4.7	1.20	1	292	0.11	11	22	−1.30	79	197	10	45	−106

Table 6: Focal mechanism parameters from Pondrelli et al. (2002)

We have 25 events from 1959 to 2001 with magnitude varying from 4.5 to 6.6; 12 events come from the Northeast Mediterranean Triple Junction among which 7 events correspond to the northern part of the Dead Sea Fault, 3 events are from the Cypriot Arc, and 2 from the Palmyride fold belt.

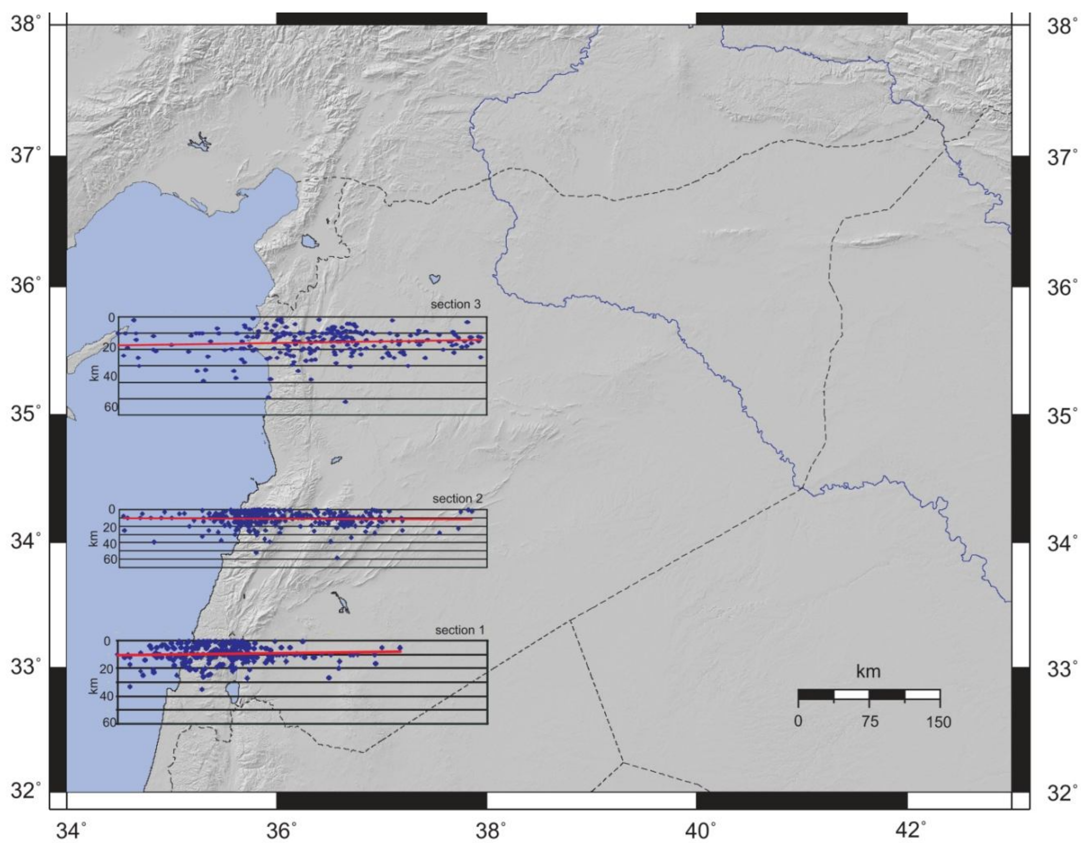

Figure 6: Sections of instrumental earthquakes from 1995 to 2008 (seismic data from ISC, NEC Damascus and Sbeinati, 1993).

III – 6. Crustal structures and active deformation

The Shebalin model of deriving historical earthquake parameters (Shebalin, 1974) shows that the estimated depth of large earthquakes varies from 10 – 35 km. The instrumental earthquake catalogue, (after assuming that all the epicenter analysis are well defined), gives a general trending of depth less than 20 km. Sections 1, 2, and 3 (Figure 6) show variations of seismicity depth and give an idea about the thickness variation of the crust across the northern Dead Sea Fault in Syria. The three different sections show that the seismogenic layer depth in southern part (section 1 & 2) ~ 10 km, is shallower than the northern part (section 3) of the fault estimated ~ 17 km. This observation shows a thinning of the seismogenic crust near the Lebanese Restraining Bend whereas the northern part shows a deeper seismogenic layer. On the other hand, the numerous seismic events in the western part of the fault and in the Lebanese Restraining Bend indicate a clear increase of activity. Although the depth determination is sometimes not very accurate (> 5 km), all three sections indicate that hypocenters do not exceed 40 km. However, one may observe that hypocenters in the Sinai-Africa plate have a higher depth (a large number between 20 and 40-km-depth) than seismic events in the Arabia plate. This implies that the Aleppo Plateau and Syria continental domain has a thin seismogenic layer .

References

Alchalbi, A., M. Daoud, F. Gomez, S. McClusky, R. Reilinger, M. Abu-Romeyeh, A. Alsouod, R. Yassminh, B. Ballani, R. Darawcheh, R. Sbeinati, Y. Radwan, R. Al Masri, M. Bayerly, R. Al Ghazzi, and M. Barazangi (2009). Crustal deformation in northwestern Arabia from GPS measurements in Syria: Slow slip rate along the northern Dead Sea Fault; *Geophys. J. Int*.

Erhan Altunel, E., M. Meghraoui, V. Karabacak, S. H. Aky¨uz, M. Ferry, C. Yalcıner1, and M. Munschy (2009). Archaeological sites (Tell and Road) offset by the Dead Sea Fault in the Amik Basin, Southern Turkey. *Geophys. J. Int.* (2009) doi: 10.1111/j.1365-246X.2009.04388.x

Brew, G., M. Barazangi, A. K. Al-Maleh, T. Sawaf (2001). Tectonic and Geologic Evolution of Syria. *GeoArabia*, Vol. 6, No. 4, p. 573-616. Gulf PetroLink, Bahrain.

Chaimov, T., M. Barazangi, D. Al-Saad, T. Sawaf and A. Gebran (1990). Crustal shortening in the Palmyride fold belt, Syria, and implications for movement along the Dead Sea fault system. Tectonics, v. 9, no. 6, p. 1369–1386.

Daeron, M., Benedetti, L., Tapponnier, P., Sursock, A., Finkel, R.C., 2004. Constraints on the post w25-ka slip rate of the Yammouneh fault (Lebanon) using in situ cosmogenic 36Cl dating of offset limestone-clast fans. Earth and Planetary Science Letters 227, 105e119.

Dubertret, L., 1955. Carte Géologique du Liban. Ministere des Travaux Publics, Beyrouth.

Dubertret, L., 1966. Liban, Syria et bordure des Pay Voisines: I, tableau stratigraphique et carte au millionieme. Extrait de Notes et Memoire Moyen-Orient VIII, Muséum National d'Histoire Naturelle, Paris.

El-Isa, Z.H. and Mustafa, H., 1986, Earthquake deformations in the Lisan deposits and seismotectonic implications, *Geophys. J. Royal Astron. Soc.* 86, 413–424.

European-Mediterranean Seismological Centre (EMSC), http://www.emsc-csem.org/

Ferry, M., Meghraoui, M., Karaki, N.A., Al-Taj, M., Amoush, H., Al-Dhaisat, S. & Barjous, M., 2007. A 48-kyr-long slip rate history for the Jordan Valley segment of the Dead Sea Fault, *Earth planet. Sci. Lett.,* 260, 394–406.

Freund, R., Zak, I. and Garfunkel, Z., 1968, Age and rate of the sinistral movement along the Dead Sea rift, *Nature* 220, 253–255.

Freund, R., Garfunkel, Z., Zak, I., Goldberg, M., Derin, B. and Weissbrod, T., 1970, The shear along the Dead Sea rift, *Philos. Trans. R. Soc. London*, Ser. A. 267, 107–130.

Garfunkel, Z., I. Zak and R. Freund (1981): Active faulting in the Dead Sea rift, *Tectonophysics,* 80, 1-26.

Ginat, H., Enzel, Y. and Avni, Y., 1998, Translocated Plio-Pleistocene drainage systems along the Arava fault of the Dead Sea transform, *Tectonophysics* 284, 151–160.

Gomez, F., G. Karam, M. Khawlie, S. McClusky, P. Vernant, R. Reilinger, R. Jaafar, C. Tabet, K. Khair, and M. Barazangi (2007). Global Positioning System measurements of strain accumulation and slip transfer through the restraining bend along the Dead Sea fault system in Lebanon, *Geophys. J. Int.*168, 1021–1028.

Gomez, F. *et al.,* 2003. Holocene faulting and earthquake recurrence along the Serghaya branch of the Dead Sea fault system in Syria and Lebanon, *Geophys. J. Int.,* 153, 658–674.

Griffiths, H.M., R.A. Clark, K.M. Thorp, and S. Spencer (2000). Strain accommodation at the lateral margin of an active transpressive zone: geological and seismological evidence from the Lebanese restraining bend. *Journal of the Geological Society, London,* 157: 289-302.

Grunthal, G. (Editor) (1993). European macroseismic scale 1992 (up-dated MSK-scale), Conseil de l'Europe, *Cen. Européen Géodyn. Seismol.,* 7, Luxembourg.

Hamiel, Y., R. Amit, Z. B. Begin, S. Marco, O. Katz, A. Salamon, E. Zilberman, and N. Porat (2009). The Seismicity along the Dead Sea Fault during the Last 60,000 Years. Bulletin of the Seismological Society of America, Vol. 99, No. 3, pp. 2020–2026, June 2009, doi: 10.1785/0120080218

Harvard-CMT solution, http://www.seismology.harvard.edu/projects/CMT/

International Seismological Centre (ISC) http://www.isc.ac.uk/,

Klinger, Y., J.P. Avouac, N. Abou Karaki, L. Dorbath, D. Bourles, J.L. Reyes (2000). Slip rate on the Dead Sea transform fault in the northern Araba Valley (Jordan),

Karabacak, V., E. Altunel, M. Meghraoui, and H.S. Akyüz (2010). Field evidences from northern Dead Sea Fault Zone (South Turkey): New findings for the initiation age and slip rate. Tectonophysics 480 (2010) 172–182.

Le Beon, M., Y. Klinger, A. Q. Amrat, A. Agnon, L. Dorbath, G. Baer, J.-C. Ruegg, O. Charade, and O. Mayyas (2008), Slip rate and locking depth from GPS profiles across the southern Dead Sea Transform, J. Geophys. Res., 113, B11403, doi:10.1029/2007JB005280.

Mahmoud, S., Reilinger, R., McClusky, S., Vernant, P. & Tealeb, A., 2005. GPS evidence for northward motion of the Sinai block: implications for E. Mediterranean tectonics, *Earth planet. Sci. Lett.,* 238, 217–227

Marco, S., Rockwell, T.K., Heimann, A., Frieslander, U., Agnon, A., 2005. Late Holocene slip of the Dead Sea Transform revealed in 3D palaeoseismic trenches on the Jordan Gorge segment. Earth and Planetary Science Letters 234, 189–205.

Marco, S., Agnon, A., Ellenblum, R., Eidelman, A., Basson, U. and Boas, A. (1997). 817-year-old walls offset sinistrally 2.1 m by the Dead Sea Transform, Israel, *J. Geodyn.* 24(1-4), 11–20.

McClusky, S., Reilinger, R., Mahmoud, S., Ben Sari, D., Tealeb, A., (2003). GPS constraints on Africa (Nubia) and Arabia plate motions. Geophysical Journal International 155, 126e138.

McClusky, S., et al. (2000), Global Positioning System constraints on plate kinematics and dynamics in the eastern Mediterranean and Caucasus, J. Geophys. Res., 105, 5695– 5719.

Meghraoui, M., F. Gomez, R. Sbeinati, J. Van der Woerd, M. Mouty, A. Darkal, Y. Radwan, I. Layyous, H. Al Najjar, R. Darawcheh, F. Hijazi, R. Al-Ghazzi, M. Barazangi (2003). Evidence for 830 years of seismic quiescence from palaeoseismology, archaeosesimology, and historical seismicity along the Dead Sea fault in Syria, *Earth planet. Sci. Lett.,* 210, 35–52.

National Earthquake Centre (NEC-Syria) http://www.nec.gov.sy/, and from

Nemer, T., and M. Meghraoui (2006). Evidence of coseismic ruptures along the Roum fault (Lebanon): a possible source for the AD 1837 earthquake. Journal of Structural Geology 28 (2006) 1483e1495

Niemi, T. M., H. Zhang, M. Atallah, and J. B. J. Harrison (2001). Late Pleistocene and Holocene slip rate of the Northern Wadi Araba fault, Dead Sea Transform, Jordan. *Journal of Seismology* 5: 449–474, 2001.

Pondrelli, S., A. Morelli, G. Ekström, S. Mazza, E. Boschi, and Dziewonski, A. M. 2002. European-Mediterranean regional centroid-moment tensors: 1997-2000. *Physics of the Earth and Planetary Interiors*, 130: 71-101.

Ponikarov, V.P. 1966. The geology of Syria. Explanatory Notes on the Geological Map of Syria, scale 1:200 000. Ministry of Industry, Syrian Arab Republic.

Quennell, A.M., 1984. The Western Arabia rift system, in *The Geological Evolution of the Eastern Mediterranean,* pp. 775–788, eds Dixon, J.E. & Robertson, A.H.F., Blackwell Scientific, Oxford.

Reasenberg, P. & Oppenheimer, D., 1985. *FPFIT, FPPLOT and FPPAGE:Fortran Computer Programs for Calculating and Displaying Earthquake Fault-plane Solutions,* USGS, Open-file report 85–739.

Reilinger, R. *et al*., 2006. GPS Constraints on Continental deformation in the Africa-Arabia-Eurasia continental collision zone and implications for the dynamics of plate interactions, *J. geophys. Res.,* 111, doi:10.1029/2005JB004051.

Salamon, A., Hofstetter, A., Garfunkel, Z. and Ron, H. 2003. Seismotectonics of the Sinai subplate - the eastern Mediterranean region. *Geophysical Journal International*, 155: 149-173.

Sbeinati, M. R. (1997). Catalogue of instrumentally recorded earthquakes in Syria and neighboring regions; Atomic Energy Commission of Syria, (A report presented to the International Atomic Energy Agency under the research project entitled Seismic data fore sitting and site revalidation of nuclear facilities, No. 6247/R3/RB).

Sbeinati, M.R., Darawcheh, R. & Mouty, M., 2005. Catalog of historical earthquakes in and around Syria, *Ann. Geofis.,* 48, 347–435.

Searle, M.P. 1994. Structure of the intraplate eastern Palmyride Fold Belt, Syria. Geological Society of America Bulletin, v. 106, no. 10, p. 1332–1350.

Shebalin, N.V. (1974): Principles and procedures of cataloguing, in *Catalogue of Earthquakes*, edited by N.V. Shebalin, V. Kanik and D. Hadzievski, *UNDP /UNESCOSurvey of Seismicity of the Balkan Region* (UNESCO, Skopje).

Shebalin, N.V. (1970): Intensity: on the statistical definition of the term, in *Proc. X Ass. ESC*, Leningrad, 3-11 September 1968 (Acad. Sci. USSR, Soviet Geophysical Committee, Moscow).

Steckler, M., and U. T. Brink (1986). Lithospheric strength variations as a control on new plate boundaries: examples from the northern Red Sea. Earth and Planetary Science Letters, v. 79, no. 1–2, p.120–132.

Steinitz, G., Bartov, Y. and Hunziker, J.C. (1978). K-Ar age determination of some Miocene-Pliocene basalts in Israel – their significance to the tectonics of the rift valley, *Geol. Mag.* 115(5), 329–340.

Trifonov, V.G., Tribukhin, V.M., Adzhamyan, Z., Dshallad, S., El-Khair, Y., Ayed, K. (1991). Levant fault zone in northwest Syria. Geotectonics 25, 145– 154.

Westaway, R., Arger, J. (2001). Kinematics of the Malatya–OvacVk fault zone. Geodin. Acta 14, 103– 131.

Wdowinski, S., Y. Bock, G. Baer, L. Prawirodirdjo, N. Bechor, S. Naaman, R. Knafo, Y. Forrai, and Y. Melzer (2004), GPS measurements of current crustal movements along the Dead Sea Fault, J. Geophys. Res., 109, B05403, doi:10.1029/2003JB002640.

Zak, I. and Freund, R. (1966). Recent strike-slip movements along the Dead Sea rift, *Isr. J. Earth Sci.* 15, 33–37.

Chapter IV

The historical earthquakes of Syria: an analysis of large and moderate earthquakes from 1365 B.C. to 1900 A.D.

MOHAMED REDA SBEINATI, RYAD DARAWCHEH and MIKHAIL MOUTY

ANNALS OF GEOPHYSICS

Vol. 48, N. 3, June 2005, pp. 347-435
ANNALS OF GEOPHYSICS, VOL. 48, N. 3, June 2005

The historical earthquakes of Syria: an analysis of large and moderate earthquakes from 1365 B.C. to 1900 A.D.

Mohamed Reda Sbeinati ([1]), **Ryad Darawcheh** ([1]) **and Mikhail Mouty** ([2])

([1]) *Department of Geology, Atomic Energy Commission of Syria, Damascus, Syria*

([2]) *Department of Geology, Faculty of Science, Damascus University, Damascus, Syria*

Abstract

The historical sources of large and moderate earthquakes, earthquake catalogues and monographs exist in many depositories in Syria and European centers. They have been studied, and the detailed review and analysis resulted in a catalogue with 181 historical earthquakes from 1365 B.C. to 1900 A.D. Numerous original documents in Arabic, Latin, Byzantine and Assyrian allowed us to identify seismic events not mentioned in previous works. In particular, detailed descriptions of damage in Arabic sources provided quantitative information necessary to re-evaluate past seismic events. These large earthquakes (I_0>VIII) caused considerable damage in cities, towns and villages located along the northern section of the Dead Sea fault system. Fewer large events also occurred along the Palmyra, Ar-Rassafeh and the Euphrates faults in Eastern Syria. Descriptions in original sources document foreshocks, aftershocks, fault ruptures, liquefaction, landslides, tsunamis, fires and other damages. We present here an updated historical catalogue of 181 historical earthquakes distributed in 4 categories regarding the originality and other considerations, we also present a table of the parametric catalogue of 36 historical earthquakes (table I) and a table of the complete list of all historical earthquakes (181 events) with the affected locality names and parameters of information quality and completeness (table II) using methods already applied in other regions (Italy, England, Iran, Russia) with a completeness test using EMS-92. This test suggests that the catalogue is relatively complete for magnitudes >6.5. This catalogue may contribute to a comprehensive and unified parametric earthquake catalogue and to a realistic assessment of seismic hazards in Syria and surrounding regions.

Key words *historical earthquakes – historical sources – seismic hazards – Dead Sea fault system – Eastern Mediterranean – Lebanon – Syria*

1. Introduction

The Middle East is one of the few regions worldwide where historical accounts of earthquakes can date back several hundred years B.C. When available, historical earthquake records are a critical database for characterizing earthquake sources and assessing seismic hazards. Previous compilations of historically documented earthquakes in Syria and adjacent regions indicate noteworthy seismic activity with large damage (*e.g.*, Sieberg, 1932; Ben-Menahem, 1979; Plassard and Kogoj, 1981; Guidoboni *et al.*, 1994; Ambraseys and Jackson, 1998). Despite these invaluable contributions to the understanding of seismicity in the Middle East, considerable information has remained unexploited in numerous original sources that provide important and quantitative input for developing a parametric catalogue.

Mailing address: Dr. Mohamed Reda Sbeinati, Department of Geology, Atomic Energy Commission of Syria, P.O. Box 6091, Damascus, Syria; e-mail: sbeinati@scs-net.org

Since 1990 and within the framework of the «Seismic Data for Siting and Site-Revalidation of Nuclear Facility» research project, under the patronage of the International Atomic Energy Agency (IAEA), the Seismology Section in the Department of Geology and Nuclear Ores at the Atomic Energy Commission of Syria (AECS) has investigated the historical seismicity of Syr-

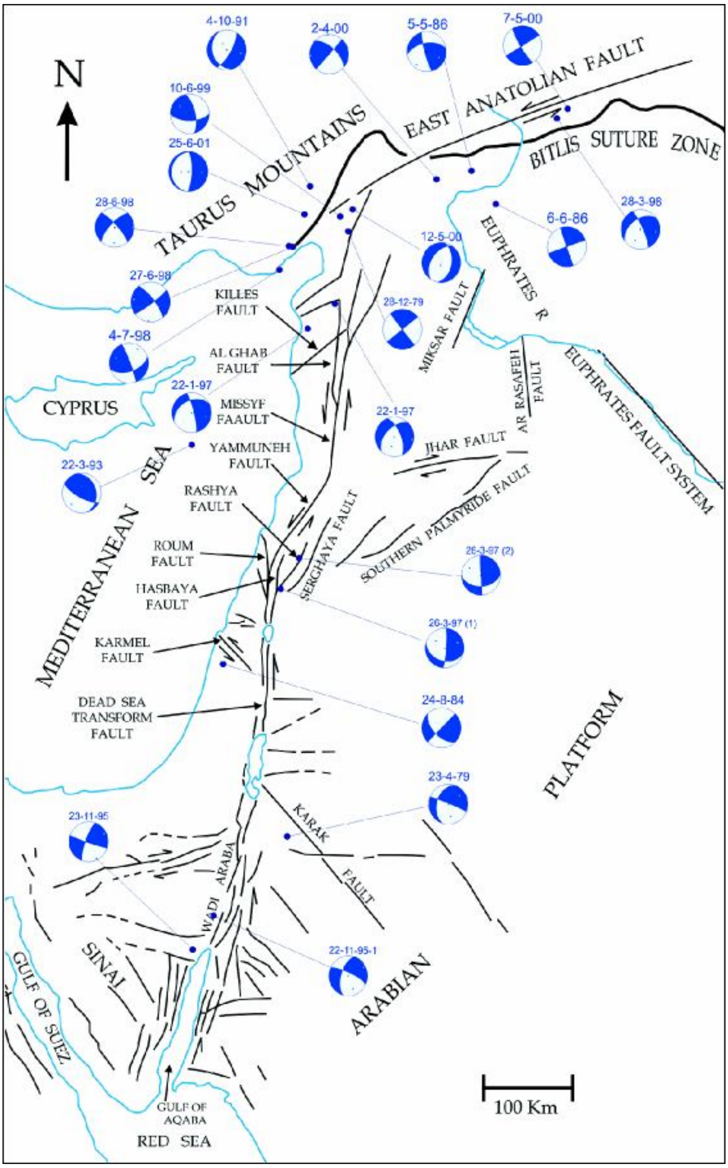

Fig. 1. Summary of major fault zones of the northern Arabian plate (redrawn from Garfunkel *et al.*, 1981; Barazangi *et al.*, 1993).

ia. Original sources were identified, located, and exploited to extract the necessary information for constructing a unified parametric catalogue. We studied 181 historical earthquakes, and estimated the related intensities for each locality with a standardized methodology. A final parametric catalogue for 36 major earthquakes reports the epicenter locations, maximum intensities and estimated magnitudes.

This paper documents historical earthquakes of Syria and addresses the following points: i) the study of new historical seismic events; ii) the re-appraisal of historical seismic events in the light of original and new sources; iii) re-evaluation of past events by means of a careful examination of all available references; iv) historical earthquakes in previous works, and finally a discussion on the distribution of large earthquakes along the main fault systems. In addition, all events are listed in table II which represents complete information about the historical earthquakes with estimated intensities at relevant localities and accompanying effects, with information completeness (A – complete; B – accepted; C – incomplete) and information quality factors (1 – good source quality; 2 – moderate source quality; 3 – poor source quality).

2. Seismotectonic setting

The study area is located in the northern part of the Arabian plate and encompasses Syria and Lebanon and adjacent areas of neighboring countries. It is bounded from the west, by the northern section of the Dead Sea Fault system (DSF), a plate boundary consisting of the northeast trending Al-Yammouneh Fault (YAF) and the north trending Al-Ghab Fault (GAF) (fig. 1). Northeast of Antioch, the DSF intersects the Eastern Anatolian Fault system (EAF) and the Bitlis Suture zone (BS), both of which comprise the northern border of the Arabian plate. Between Damascus and the Euphrates River, the northeast trending Palmyra fold-thrust belt is located within the northern Arabian plate (fig. 1). This belt consists of many asymmetrical elongated anticlines separated by narrow depressions.

The seismicity of Syria can be qualified as moderate during the last century (fig. 2). However, the historical seismicity indicates the occurrence of large earthquakes in the past. The main instrumental seismicity with many moderate earthquakes (5 < M_s < 6) is located along the East Anatolian Fault and the Dead Sea fault system (Sbeinati, 1993). An apparent lack of

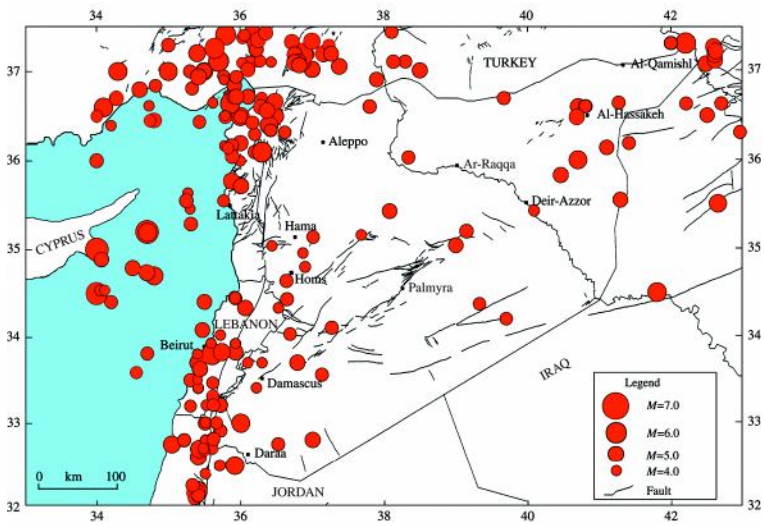

Fig. 2. Map of Syria showing the seismicity during 1900-1993 (Sbeinati, 1993).

seismicity can be observed along the Ghab fault zone and motivates a careful analysis of seismic documentation of the region.

Focal mechanisms of the main recent events indicate a NNW-SSE trending of *P* axes with strike slip movements along faults (see Harvard CMT Catalogue). These mechanisms illustrate the left-lateral pattern of active deformation with minor component of normal faulting associated with pull-apart basins along the Dead Sea Fault. The rate of active deformation and relative Arabia-Africa plate motion determined from GPS studies varies from 5.6 to 7.5 mm/yr from south to north, respectively (McCluskey *et al.*, 2003). Recent paleoseismic and archeoseismic investigations along the Missyaf segment south of the Ghab Basin show successive faulting with 13.6 m of left-lateral displacements during the last 2000 years yielding an average 6.9 mm/yr slip rate (Meghraoui *et al.*, 2003). In contrast, the intraplate area of Syria is generally aseismic, with infrequent earthquakes some of which can be of significant size (M_w 5.5) (fig. 2).

3. Previous works

Earthquake catalogues of the Middle-East are from Hoff (1840), Mallet (1853) and Perrey (1850) who compiled a list of earthquakes (see the parametric catalogues and seismological compilations in References Section). Tholozan (1879) mentioned information about earthquakes that hit the Middle-East between 7th and 17th centuries; Willis compiled in 1928 and 1933 (Willis, 1928, 1933a,b) an earthquake list for Palestine; catalogue of Sieberg (1932) is a global work with an incomplete description; Amiran prepared in 1950-1951 and 1952 a revised catalogue of Willis' work; Ergin *et al.* (1967) presented a parametric earthquake catalogue for Turkey and surrounding areas between 11 A.D. and 1964 A.D.; Al-Sinawi and Ghalib (1975) compiled a detailed and descriptive earthquake catalogue of Iraq and partly some adjacent countries using modern references; the parametric catalogue of Ben-Menahem (1979) is a real attempt at parameterization of the historical earthquakes specifically concerned with the Middle East; Taher (1979) presented a full corpus of texts from Arabic sources about the earthquakes that hit the Arab World; the work by Plassard and Kogoj (1981) is generally related to Lebanon and Syria; Russell (1985) used the available ancient textual and archaeological data in order to compile the seismic events of Palestine, Lebanon and Syria between the 2nd and the mid-8th century; Ambraseys *et al.* (1994) offered a seismic catalogue for Egypt, Arabia and the Red Sea; work of Guidoboni *et al.* (1994) represents a critical compilation and a historical review on the historical earthquakes that hit the Mediterranean area; Ambraseys and Finkel (1995) compiled a catalogue for Turkey and adjacent areas for the period 1500-1800; finally the compiled catalogue on Lebanon and parts of Syria presented by Abu Karaki (1992) is not based on primary sources.

On the other hand, there are two detailed papers dealing with the 1202 A.D. earthquake in the Eastern Mediterranean region (Ambraseys and Melville, 1988) and 1759 A.D. earthquake in Bekaa Valley (Ambraseys and Barazangi, 1989).

Although some of these catalogues consist of many usual and unusual problems, they are, to a large extent, valuable and helpful for preparing our catalogue.

4. Sources of the catalogue

Syria has been home to some of the world's earliest civilizations. It is located on the eastern shore of the Mediterranean Sea, at the crossroads of three continents (Asia, Europe and Africa).

The main sources for the pre-Islamic period are official letters, accounts of travelers who visited the affected regions shortly after the earthquakes, diaries, chronicles of historians written in Syriac and Greek. Most of these sources are not available in Syria. The rise of Islam in the early 7th century in Mecca, followed by many conquests for Syria and other regions represented the first step for real systematic documentation in the region. The Muslims paid considerable attention to the history of the Islamic World. Earthquakes are among natural phenomena that attract Muslim historians. Arabic chronicles are one of the main primary sources for the history of earthquakes for our region, from the 9th century till the 19th century. Between the 7th century and 1000 A.D., there were universal chronicles covering various events that happened in the Islamic Empire. Then and due to many known reasons, history was written to be more local. By the 17th century, the European sources started to mention events of our region in the form of travel literature and diplomatic correspondence reports. These latter were preserved in archives in Europe and Turkey.

An extensive bibliographical research has been performed as a base step and continued throughout the research period in order to dynamically improve the result (see References Section).

Scientific visits to the Turkish Atomic Energy Authority, Ankara, and ENEA, Rome, were made in 1994 and 1995, in an attempt to collect available sources and to better understand the methodology of studying historical earthquakes where many important historical sources on Byzantine and Ottoman eras were found.

Our investigations were achieved in the following libraries: Al-Assad National Library in Damascus, Syria (this cultural center represents one of the largest depositories in our Arabian region, containing a huge number of histories, mother books); the Institut Français de Damas in Damascus; Süleymaniye Library in Istanbul; the National Library in Ankara; the Vatican Library in Rome (by Dr. C. Margottini); Library of Pontificio Istituto Orientale in Rome (by Dr. C. Margottini).

There are numerous sources used for preparation this catalogue, these are original documents such as manuscripts, diaries, ambassador letters, existing catalogues and modern papers. To retrieve data already available in seismological literature, a supplement of research was devoted to a systematic reading of most sources.

Due to our belief that they are good interpretations, parameters of 1202 and 1759 events have been considered by this research as they are.

5. Methodology

For the study of historical earthquakes in and around Syria, all available relevant information concerning the history in the region was collected from libraries in Syria, Turkey, Lebanon and Italy. This information is translated, when needed, to the English language. Then, this information is assessed and evaluated. In addition, all other catalogues, monographs and books were also searched.

Both occidental and oriental sources containing useful data about earthquakes during the years under consideration have been identified, particularly Arabic, Greek, Syriac and to a lesser extent English, French and Ottoman.

Arabic chronicles are one of the main sources of information for the present catalogue, and they generally date earthquakes according to the Muslim calendar of 12 lunar months. The Muslim Era started in 622 A.D. (date of migration of the Prophet Muhammad from Mecca for Medina). Therefore, it is called the Hijiri (migration) calendar, which is indicated here by the suffix A.H. (*i.e.* After Hijira). In all cases, Gregorian calendar comes in the heading, while the Hijiri one is sometimes mentioned in the second part. On the other hand and for the sake of consistency, all needed conversions from Hijiri into their corresponding dates in the Christian calendar were made from the comparative tables in Wolseley Haig (1932) which takes 16 July 622 A.D. as the start of the Muslim Era. The Arabic documents are not without internal problems. As becomes clear below, the exact date of a earthquake is only rarely given in Arabic documents.

In principle, the applied methodology in this research is in accordance with the topology presented by the IAEA (1987) and by Stucchi (1994) as follows:

– Identifying the historical sources of information: historical sources (contemporary and near-contemporary), previous catalogues (parametric and compilations) and monographs have been investigated and collected from many libraries in Syria, Lebanon, Turkey and Italy.

– Grouping all available information relating to one historical earthquake and arranging it in chronicle order.

– Reading descriptions for each event in order to build up the earthquake flow and its date. Those descriptions which belong to the same event have been interpreted in terms of intensity for each affected locality using the European Macroseismic Scale 1992.

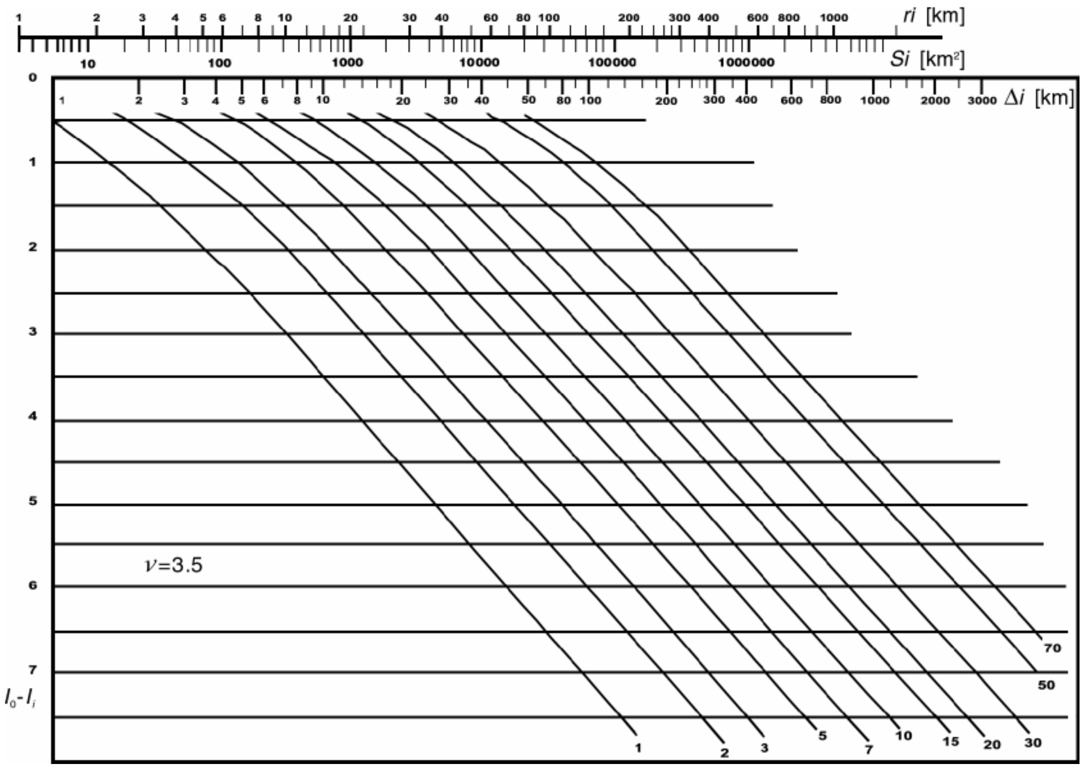

Fig. 3. Standard nomograph for determining local depht of shallow earthquakes from macroseismic data (area of isoseismal *Si*, their average radius *ri*, or distance to points of known intesity Δi), for attenuation coefficient ν=3.5 (Shebalin, 1970).

– Assessing parameters of each historical earthquake (date, epicentral location, epicentral intensity, locality intensity, depth and macroseismic magnitude), when the available descriptions are adequate to permit accurate assessment.

Date – Date of the earthquake is the first parameter that should be assessed. Date of the earthquake was assumed to be the most reliable one according to the nearest historical sources to the event in space and time.

Location – Latitude and longitude of the epicenter of the earthquake is the second parameter that should be also assessed. For the large earthquakes, this location was defined as a center of the isoseismal lines. However, all sources utilized in the catalogue give some idea of the location, with the indication of the area worst affected. In some cases, one locality was mentioned, so there is only a choice of locating the earthquake near this center. In other cases, two or more localities are reported, so there is a good chance for locating the epicenter in between.

Intensity – Effects of any earthquake on the environment should be evaluated using any descriptive scale. In our case, epicentral intensity (I_0) and intensities for each affected locality for the same earthquake have been assessed in accordance with the EMS Scale 1992. It is worth mentioning that the assessment of the intensity for each locality was defined on the basis of analyzing all sources taking into account their quality.

Depth – Depth of the earthquake foci can be evaluated when intensities of many localities are available. However, this assessment was performed according to the transparency of Shebalin (1970), with ν=3.5 where ν is coefficient

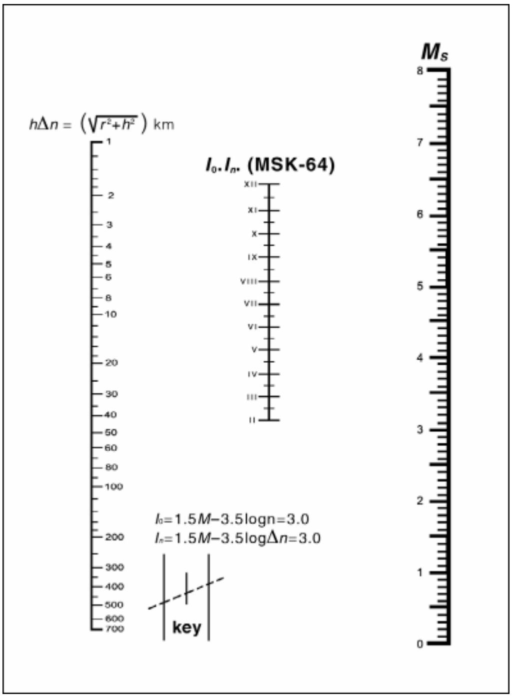

Fig. 4. Standard nomograph of M, h, Δ and I. It is averaged for shallow earthquakes (b = 1.5, ν= 3.5, c=3) (Shebalin, 1970).

of intensity attenuation (fig. 3). It is worth mentioning that the tectonic setting of western boundary of the Arabian plate (transform system) suggests that earthquakes originating in the study area are shallow events within the crust (44 km).

Magnitude – Size of the earthquake is the most important parameter that should be calculated. For large events in the catalogue, it is derived using the nomograph proposed by Shebalin (1970) (fig. 4).

6. Catalogue of historical earthquakes

This catalogue contains all historical earthquakes affecting Syria and neighboring regions, the 181 events distributed in four categories regarding the following parameters: 1) new sources for past unknown 14 events; 2) re-appraisal of 42 historical seismic events in the light of original and new sources; 3) re-evaluation of 116 seismic events; and 4) contains 9 historical seismic events without re-evaluation.

6.1. *New sources for past unknown events*

In this section, we present unknown historical earthquakes and their associated original sources which has never been referenced elsewhere. These references correspond to Arabic sources collected from different depositories.

(004) **331 B.C. Syria: VI.**
Sources
– Al-Boustani (1887): In the year of 331, there was a heavy earthquake causing many victims and destruction in Syria.

(069) **1046 July 8-1047 June 27 Diyar Bakr: ≥VII; Khlat: ≥VII.**
Sources
– Al-Suyuti: In the year 438 A.H. (1046 July 8-1047 June 27) many earthquakes occurred in Khlat and Dyar Bakr destroying the citadels and the fortresses, and killing people.

(073) **1094 April 20-May 18 Damascus: V-VI.**
Sources
– Ibn Al-Athir: In this month, 487 Rabi’ II A.H. (1094 April 20-May 18), there was a sequence of earthquakes in Bilad Al-Sham for a long time without a significant damage.
– Al-Dawadari: In this year there were 12 shocks for one day, causing destruction of the country and killing a great scientist [at Damascus].

(081) **1140 August 17-1141 August 6 Qalaat Sheizar: VI-VII.**
Sources
– Al-Dawadari: In this year [535 A.H.] [1140 August 17-1141 August 6] there was an earthquake in Sheizar, causing damaging its citadel.

(111) **1537 March 08 Damascus: IV.**
Sources
– Al-Ghazi: A slight shock was felt in Damascus on 27 Ramadan 943 A.H. (08 March 1537) (Badr Al-Ghazi).

(113) **1563 September 13 Damascus: VI.**
Sources
– Al-Ghazi: A strong shock hit (Damascus), accompanied by a sound from the earth, on Sunday early morning, 24 Muharram 971 A.H. (13 September 1563), causing a few houses to collapse and many fractures to appear on walls (Badr Al-Ghazi).

(117) **1604 March 13 Damascus: V; Bekaa: V.**
Sources
– Al-Nablsi: A strong shock was felt in Damascus and Bekaa on Friday night, 11 Shawwal 1012 A.H. (13 March 1604) (Al-Ghazi).

(118) **1606 October 19 Baalbak: IV.**
Sources
– Al-Nablsi: A shock was felt in Baalbak on Monday night, 17 Jamada II, 1015 A.H. (19 October 1606) (Al-Ghazi).

(121) **1618 July 8 Damascus: IV.**
Sources
– Al-Nablsi: A slight shock was felt [in Damascus] on Wednesday 15 Rajab 1027 A.H. (08 July 1618) at sunset time (Al-Ghazi).

(122) **1618 July 23-August 21 Damascus: IV.**
Sources
– Al-Nablsi: A slight shock was felt [in Damascus] in Sha'ban 1027 A.H. (23 July-August 21, 1618) (Al-Ghazi).

(123) **1619 December 8-1620 November 25 Darkoush. Landslide.**
Sources
– Al-Nablsi: A landslide, probably resulting from an earthquake, happened in Darkoush in the year of 1029 A.H. (1619 December 08-1620 November 25), destroying many houses and killing about 70 persons (Al-Ghazi).

(125) **1627 November 24. Damascus: V.**
Sources
– Al-Nablsi: A strong shock hit Damascus on Wednesday night, 15 Rabi'I 1037 A.H. (24 November 1627), but without any damage (Al-Ghazi).

(131) **1683 Safineh. Landslide.**
Sources
– Al-Nablsi: An earthquake occurred in a night of 1095 A.H. (1683), causing a village called Safineh in Al-Shouf region (Lebanon) to shift with its houses and trees from its location on the top of the mountain to the bottom of the valley, but without any damage.

(135) **1712 December 28 Damascus: IV.**
Sources
– Al-Nablsi: He reported that a shock was felt in Damascus on Wednesday night, 29 Zu-l-Qa' - da 1124 A.H. (28 December 1712).

6.2. *Re-appraisal of historical seismic events in the light of original and new sources*

The seismic events of this section have already been mentioned in previous works, but original documents and new sources of information (most of them from the Arabic and Byzantine period) provide new information on earthquake size and related damage distribution. Therefore, for some large events we provide a special section on «Sources» added to the «Parametric catalogues and previous studies» and «Seismological compilations».

(001) **~ 1365 B.C. Ugharit: VIII-IX. Tsunami, fire.**
Sources
– Schaeffer (1948): A violent earthquake hit Ugharit in the Recent Bronze Era between 1370 and 1360 B.C. (probably in 1365 B.C.). The layer of destruction that found in level I of Ugharit represents archaeological evidence for the catastrophe. Preliminary investigation in Ugharit permited that this layer caused by 1365 B .C. earthquake is corresponded with the text found in Tell Al-Amarneh in Syria, which was reported by Abimilki of Tyre to Amenophis IV as follows: «Ugharit, city of the king, was destroyed by the fire; half of the city burnt, other half was intact». Schaeffer estimated the intensity of this earthquake at Ugharit to be VIII after Mercalli scale or IX-X after the international scale. Detailed regional studies allow the establishment of the layers of destruction that found in Beit Mirsin, level CI, Recent Bronze II of Jerico and

probably those of Megiddo VIII, Bissan VII, Hésy V, Ascalan V ... were a result of the same earthquake of Ugharit. Farther away, the site of Troie in Asia Minor was subjected to serious damage due to an earthquake in the middle of XIV century (American excavations). In the center of Asia Minor, Boghazkeuy-Hattousas, the capital of Hittites was subjected to serious destruction during the time of 1365 B.C. earthquake.

– Saadeh (1982): A possible earthquake was in Ugharit. It was accompanied by a high sea-wave covered the region of Minet Al-Biada, and with a fire (indicated accidentally in a letter from the King of Tyre «Abimilki» to Pharoa of Egypt and archaeological excavation in Ugharit according to Schaeffer, 1954).

Parametric catalogues

– Plassard and Kogoj (1981): 1365 B.C., $I=$X, destruction in Ugharit and Byblus (*A letter from a King of Tyre to Akenton Pharoa*).

– Ben-Menahem (1979): In 1356 B.C., destruction of Ugarit, with tsunami at the Syrian coasts.

Other works

– Klengel (1985): Between 2100 and 1200 B.C., there was a catastrophe in Ras-Shamra (Ugharit) transferring the flourishing city into ruins and ash.

‹006› 148-130 B.C. February 21, afternoon Antioch: $\geq$VII.

Sources

– Al-Boustani (1887): 115 B.C., it was a heavy earthquake and many victims in Antioch.

Parametric catalogues

– Ben-Menahem (1979): 184, $M_L=$6.8, an earthquake was near Antioch (Willis).

Seismological compilations

– Sieberg (1932): 148 or 184, a destructive earthquake in Antioch.

– Guidoboni *et al.* (1994): Antioch IX $\leq I \leq$ XI, Antioch was suffered from the wrath of God. It could be dated at the year 130 B .C. (Malalas) regarding the confusion in Malalas dating or there were two separate earthquakes.

– Sieberg (1932): 140 B.C., a destructive sea wave was along the Syrian coast.

‹032› 502 August 22, Friday Akka: VIII; Tyre: VII-VIII; Sidon: VII-VIII; Beirut: VII; Palestine: VI; Safad: VI?; Reina: VI?

Sources

– Joshua the Stylite: 502 August 22, Friday: Ptolemais destroyed to the extent that nothing stayed standing. Half of Tyre and Sidon fell down. In Beirut, only the synagogue fell down.

Parametric catalogues

– Plassard and Kogoj (1981): 502 August 21-22, in Lebanon $I=$ IX, half of Tyre and Sidon were destroyed, at Beirut ($I=$ VII) some damage in houses, remarkably in the synagogue (Joshua the Stylite).

– Ben-Menahem (1979): 502 August 21 off coast Acre, $I_o=$ X, $M_l=$ 7.0, Acre destroyed. Destruction at Sur, Sidon, Beirut and Byblos. Latrun (Nicopolis) destroyed (Amiran; Plassard and Kogoj).

Seismological compilations

– Guidoboni *et al.* (1994): 502 August 22, Akka $I=$X, an earthquake happened between 501 and 502, where Akka was overturned and destroyed completely, half of Tyre and Sidon fell, the synagogue in Beirut fell down (Pseudo-Joshua's Chronicle). Palaces in Palestine were also affected (Russell).

– Russell (1985): 502 August 22, Akko was overturned by an earthquake at night and nothing left standing. Half of Tyre and Sidon fell. The synagogue at Beirut fell down (Chronicle of Joshua the Stylite). Safad and Reina in Galilee could be affected.

‹034› 526 May 20-29 Antioch: VIII; Dafneh: VII; Seluecea: VII. Aftershocks. Liquefaction at Antioch. Fire in Antioch.

Sources

– Malalas (1831): A large catastrophe occurred in Antioch. Citizens were buried under the debris. The houses, located only near the mountain, survived. The rest of the buildings were completely destroyed. Fire following the earthquake destroyed the Big Church (so was named the ancient church of Antioch) and the remaining houses. There were 250000 casualties because of holidays. Shocks lasted 18 months. Some buildings in Selucea and Dafneh fell down.

– John of Ephesus: In Antioch, the disaster was on the 7th hour, fire from the land and sky. City wall, houses and churches were destroyed. There was a fire following the earthquake. The Big Church was burned after 7 days and de-

stroyed completely. There were 255000 casualties ... as Malalas.
– Procopius of Caesarea: A severe earthquake occurred in Antioch where most of the buildings and the most beautiful ones fell down. There were 300000 casualties.
– Evagrius Scholasticus: An earthquake, followed by a fire, occurred in Antioch.
– Chronicon Edessenum (Urfa): A great earthquake ruined Antioch.
– Zachariah of Mitylene: A severe earthquake in Antioch. Houses fell down over their inhabitants.
– Giovanni Lido: The earthquake split Antioch and Selucea, no damage to the desert place between the mountain and the city where runs the river of Orontes.
– Marcellinus Comes: A severe earthquake destroyed Antioch. The fire, following the earthquake, increased by the wind.
– John of Nikiu: An earthquake and a fire were in Antioch. Houses were completely destroyed as well as a house located on the nearby hill. Many churches were destroyed or divided in two parts from the bottom to the top. The Big Church was destroyed. The casualties were 250000. Towns of Dafneh and Selucea at 20 miles from Antioch were destroyed.
– Theophanes: A large part of Antioch was destroyed by the earthquake. The survived citizens were killed by the fire.
– Chronicle of 819: A severe earthquake. Antioch was destroyed. The casualties were 255000.
– Georgius Monachus: An earthquake and a fire were in Antioch. There were many casualties.
– Leo Grammaticus: Most of Antioch was destroyed by the earthquake and fire.
– Georgius Cedrenus: There was an earthquake, followed by 6 days fire. There were many thousands of casualties.
– Michael Glykas: The earthquake produced a big opening. The fire killed the survivors.
– Chronicle of 1234: An earthquake and a fire occurred in Antioch, destroying all buildings and churches.
– Girgis Bar Hebraeus: An earthquake occurred in Antioch. The casualties were 255000. Shocks continued for one year and six months.

Parametric catalogue

– Plassard and Kogoj (1981): 526 May 29, in Lebanon I_0 V, Antioch was destroyed for the fifth time with a large number of victims (Michael the Syrian).
– Poirier and Taher (1980): 526 May mid-day 20-29, I_0 IX-X (MMS), very severe earthquake in Antioch.

Seismological compilations

– Guidoboni *et al.* (1994): 526 May mid-day 20-29, Antioch I_0 X, a disastrous earthquake was at Antioch, causing a great fire and thousands of deaths. There were fire and liquefaction resulted by the earthquake at Antioch, and everything had been destroyed, 250000 people perished (Malalas). Much of Antioch collapsed and vast numbers of people were killed (The Chronicle of Zacharia of Mitylene). Dafneh was struck by a violent earthquake which reduced the whole city to ruins and three hundred thousand Antioch perished (Procopius of Caesarea).
– Sieberg (1932): In 526, a strong earthquake, followed by a fire, destroyed Antioch with 250000 deaths (?). In Seleucea, there was damage.

(035) 528 November 29 Antioch: VII-VIII; Lattakia: VI-VII.

Sources

– Malalas (1831): in Antioch, duration one hour, terrible rumbling, all buildings which were rebuilt fell down, as well as the city wall and some churches. Damage to other cities near Antioch, with 5000 casualties. In the same year, Laodicia had the first earthquake, where its half was destroyed with 7500 casualties, the synagogue fell down but the church did not.
– John of Ephesus: A terrible earthquake with rumbling, ... as Malalas as well as the city gate fell down. The Big Church fell down and all the surviving houses and churches from the previous earthquake fell down except few numbers of buildings, villages in the vicinity 10 miles were destroyed. Seleucea and Dafneh did not affect. Surviving citizens of Antioch ran away to the open. In the 529 Laodicia was completely destroyed from the gate of Antioch to the Ghetto, but the left zone east of the church of S. Mother of God did not fall down, there were 7500 casualties without a fire.
– Evagrius Scholasticus: The earthquake split Antioch.
– Theophanes: A strong earthquake lasted for one

hour with terrible sound such as a bull's sound, all the constructions, the city wall and old constructions which survived from the previous earthquake fell down, there were 4870 casualties.
– Georgius Monachus: One hour duration, sound, the area 5 miles around Antioch fell down.
– Leo Grammaticus: An earthquake at Antioch.
– Georgius Cedrenus: A large earthquake lasted for one-hour duration, there was a terrible sound, all constructions were destroyed with 4870 buried casualties, emigration of survivors.
– Chronicle of 1234: There was a severe earthquake, followed by a sound from the sky like thunder and a sound from the earth like a bull's sound. City walls, churches and the surviving constructions from the previous earthquake were destroyed as well as the vicinity villages, there were 2740 casualties.
– Nicephorus Callistus: A severe earthquake at Antioch.
– Saadeh (1984): 529 January 2, a violent earthquake occurred in Lattakia, causing destruction of its large part and killing 7500 people.
Parametric catalogues
– Plassard and Kogoj (1981): 529 November 29, in Lebanon I=IV, Antioch was destroyed for the sixth time (Cedrenus; Michael the Syrian).
– Poirier and Taher (1980): 528 November 29, I_0=X-XI (MMS), Antioch, a mountain fell into the Euphrates at Quludhya, the Euphrates shifted its bed.
– Ben-Menahem (1979): 528 November 29, M_l=6.9, destruction of Antioch. Damage in Jerusalem and Damascus. Felt in Egypt, Turkey, Armenia and Mesopotamia (Ergin *et al.*; Plassard and Kogoj; Sieberg).
Seismological compilations
– Guidoboni *et al.* (1994): 528 November 28, Antioch and Lattakia I=IX, an earthquake struck Antioch destroying both the new buildings put up after the previous one (526), and those old buildings which had survived it, victims number was few thousands. Antioch suffered from an earthquake collapsing the new buildings, walls and some of churches, from one side and killing up to 5000 lives (Malalas). Laodicea suffered its first earthquake disaster by destroying its half and 7500 deaths (Malalas). Antioch was subjected to a violent earthquake causing all the buildings and walls to collapse (Theophanes).
– Sieberg (1932): In 528 November, a destructive earthquake was in Antioch, Dafneh and Betelma (?). There was damage in Seuleucea, Loadicea and Pompejopolis (?). In the latter, surface rupture appeared. There were 4870 victims.

(036) **531-534 Area between Aleppo and Homs: VI-VII; Antioch: VI; Mesopotamia: IV.**
Sources
– Malalas (1831): (earthquake between 531-534) After a short time, a terrible earthquake occurred at Antioch, but without damage.
Seismological compilations
– Sieberg (1932): 532, a destructive widespread earthquake in Syria. It destroyed the area from Aleppo to Homs. It was said that 130000 were killed. It was felt in Mesopotamia.
– Guidoboni *et al.* (1994): 532, An earthquake in Antioch without damage (Malalas). It dated back to between 531 and 534 (Downey, 1961).

(037) **551 July 9 Beirut: IX-X; Sur: IX-X; Tripoli: IX-X; Byblus: IX-X; Al-Batron: IX-X; Shaqa: IX-X; Sarfand: VII-VIII?; Sidon: VII-VIII; Arwad: III-IV. Tsunami along the Lebanese coast. Landslide near Al-Batron. Fire at Beirut** (fig. 5).
New original sources
The following publication summarizes the main information with new original sources on the earthquake of Beirut.
– Darawcheh *et al.* (2000): 551 July 9, 34.00N-35 .50E, M_s=7.2. This event destroyed several cities in Lebanon (Beirut, Tripoli, Saida, Djbil, Al-Batron, Tyre, Shakka and Sarfand) with great loss of lives. The shock was felt throughout the Eastern Mediterranean region. There were tsunami along the Lebenese coast, a local landslide near Al-B atron and a large fire in Beirut.
Among the main original references we mention:
– Theophanes: A large and terrible earthquake took place in the territories of Palestine, Arabia, Mesopotamia, Syria and Pheonicia. Tyre, Sidon, Beirut, Tripoli and Byblus suffered much damage and many thousands of people were killed. A part of the mountain named Lithoprosopus fell down forming a harbor in Botro, the sea went back for 1000 feet and many ships sunk.
– Georgius Monachus: A large and widespread

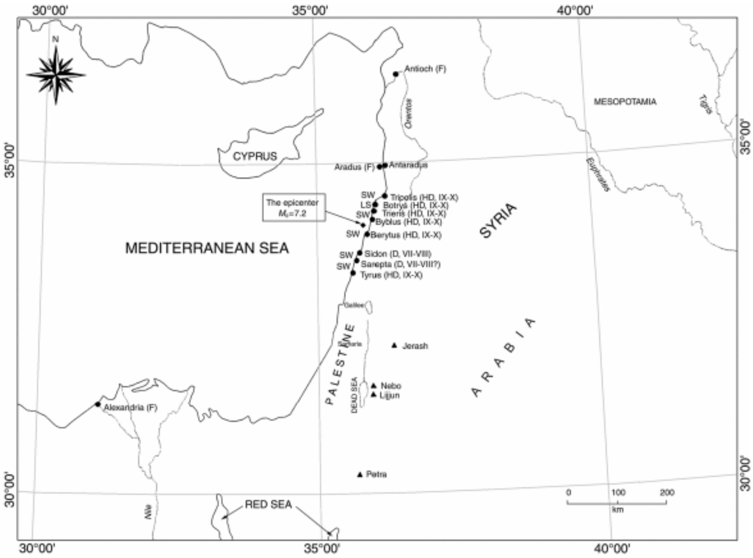

Fig. 5. Map of intensity distribution for July 9, 551 A.D. earthquake. F – felt; D – damage; LS – landslide, and SW – Sea-Wave. Triangles represent possible damaged archaeological sites (Darawcheh *et al.*, 2000).

earthquake. Most of the Earth shocked. The sea went back for two miles. This event caused destruction in Arabia, Palestine, Mesopotamia, Antioch and many others and near cities, killing large numbers of people.

– Georgius Cedrenus: A big earthquake destroyed houses, churches and the most part of the city wall near the Golden Gate. The sea went back for two miles. In Arabia, Palestine, Mesopotamia, and Antioch, many villages were destroyed. The earthquake destroyed most part of Nicomedia. Shocks continued for 40 days.

Parametric catalogues

– Plassard and Kogoj (1981): 551 July 6, in Lebanon $I_=$XI, an earthquake caused destruction of Beirut ($I_=$XI), Tripoli ($I_=$X), Sidon and Tyre ($I_=$VIII or IX) and 101 sites, a landslide occurred in the Lithoprosopon Mountain near Ras Chekka, Wujj Al-Hajar, creating a harbour near Al-Batron, there was a tsunami in Beirut and Tripoli in particular, where the sea retreated for two miles (Agathias; Fragment of Tusculum). – Ben-Menahem (1979): 551 July 09, off coast Beirut, $I_{0=}$XI-XII, $M_{L=}$7.8, destruction of Beirut, Sur, Sidon, Tripoli and Galilee. Felt in Egypt, Arabia and Mesopotamia. Tsunami. (Amiran; Al-Sinawi and Ghalib; Plassard and Kogoj; Sieberg; Willis).

Seismological compilations

– Guidoboni *et al.* (1994): 551 July 9, the earthquake affected the following localities: Byblus, Beirut and Tripoli $I_=$X, Sidon, Botrus (Al-Batron), Tyre, Arabia, Mesopotamia, Palestine and Syria, seismic sea wave and landslide, the principal damage was between Antioch and Tyre whereas there was apparently only minor damage further north and south. A disastrous earthquake along the Lebanese coast reducing many cities to ruins: Tripoli, Byblus, Beirut, Triaris, and killing thirty thousand known people in Beirut (Antoninus of Piacenza). A severe and tremendous earthquake occurred throughout the land of Palestine, in Arabia and in the land of Mesopotamia, Antioch, Phoenice Maritima and Phoenice Libanensis including Tyre, Sidon, Beirut, Tripoli, Byblus and parts of other cities, killing large numbers of people, cutting a large part of Lithoprosopon mountain at Botrus and accompanyied by a seismic sea wave (John of Ephesus; Malalas; Theophanes). Beirut was

completely ruined and many inhabitants were crushed to death under the weight wreckage (Agathias). It dated back to 557 (Michael the Syrian).
– Ambraseys *et al.* (1994): 551 July 9, 32.0N-36.0E, I_S VI, tsunami.
– Russell (1985): 551 July 9, a disastrous earthquake occurred throughout the regions of Palestine, Arabia, Mesopotamia, Syria and Phoenicia, to such an extent that Tyre, Sidon, Beirut, Tripoli and Byblus received great damage, and many thousands of people perished. In Botryos, a large part of the mountain called «Lithoprosopus» near the sea was separated and displaced into the sea. The water also withdrew for a mile out to a sea (Theophanes). Same description was mentioned by Cedrenus, but dated this event between August 550 through July 551. Agathius described the extensive damage to Beirut, without providing an exact date for this earthquake. He mentioned that this event was felt in Alexandria. Sites in the eastern delta may have been damaged, particularly Damieta.
– Sieberg (1932): 551 July 9, a vast earthquake occurred in Syria, Palestine, Egypt, Arabia and Mesopotamia. Beirut was completely destroyed with many deaths. It was said that 600 persons were buried under the debris. There was damage in the coastal cities between Tripoli and Tyre. Antioch, Apamea, Bosra and Alexandria were among the cities destroyed. The sea waves destroyed a large number of ships, especially in Botrys.

(040) 565-571 Antioch: VI-VII; Seleucea: VI-VII; Kiikia: VI; Anazrabo: VI; Orfa: IV.
Sources
– Procopius of Caesarea: Earthquakes destroyed Antioch and near Selucea.
– Theophanes: A severe event took place in Cilicia, Anazarbo, and Antioch.
– Georgius Cedrenus: A plague and earthquake occurred in Cilicia, Anazarbo and Antioch.
Parametric catalogues
– Ben-Menahem (1979): 565, M_l=6.7, strong in Baalbak and Damascus. It was felt in Palestine and Mesopotamia (Sieberg; Willis).
Seismological compilations
– Guidoboni *et al.* (1994): 570, a violent earthquake affected Antioch IX $\leq I \leq$ XI, Anazarbus, Edessa, Samosata, Seleucea Pieria, Cilicia and Syria. It is possible that there where two distinct earthquakes, but it is more likely that the date 570 is the result of confusion on the part of James of Edessa. A severe earthquake on 5 October with sound (Elias of Nisibis). The earth was shaking at Antioch, Seleucea and the two Cilicias collapsing them (Chronicle of 724). It was in 571 (Maronite Chronicle). It was in 560-561 at Cilicia, Anazarbus and Antioch (Theophanes). There were tremors at Edessa and Samosata (Micheal the Syrian). It was in 567 October (Chronicle of 1234).
– Seiberg (1932): 565, a destructive earthquake in Syria. Aleppo, Baalbak, Damascus, Apamea and Beirut were suffered. It was felt in Mesopotamia.
– Lemmens (1898): An earthquake was in Eastern Mediterranean.

(041) 580-581 Antioch: VI-VII; Dafneh: VI.
Sources
– Evagrius Scholasticus: 580-581, there was an earthquake in Antioch and Dafneh. In Antioch, public and private buildings were destroyed, some of these were completely. Dafneh was destroyed.
– Nicephorus Callistus: 580-581, as Evagrius Scholasticus.
– Agapius of Menbij: 580-581, a severe earthquake at Antioch, destroying two towers of the city wall.
Parametric catalogues
– Poirier and Taher (1980): 580-581, I_0=VIII-IX (MMS), Antioch, the suburb Dafneh was destroyed.
Seismological compilations
– Guidoboni *et al.* (1994): 580-581, Antioch-Dafneh I_∞ IX, a violent earthquake struck Theopolis (Antioch) and the suburb of Dafneh precisely at noon, causing total destruction of Dafneh and destroyed many public and private buildings in Antioch (Evagrius).
– Sieberg (1932): 579, Antioch and Dafneh were destroyed.

(042) 588 Antioch: VI-VII. Aftershocks.
Sources
– Evagrius Scholasticus [this author was an eyewitness because the earthquake took place during his marriage]: There was an earthquake with a big sound at Antioch. Many buildings

fell down. A part of the holy church fell down. The dome was inclined in north direction and fell down by the following shocks. Same happened for most of the district of Ostracina and Brisia. The buildings near the church of the Deipara Virgin fell down, except the Central Portico. The towers in the Kampos fell down while other buildings survived. A large number of persons were killed. No fire.
– John of Nikiu [no indication of the year can be found, except the name of the Emperor Maurice]: An earthquake destroyed Antioch. Many streets at the west and on the island were destroyed. Men were killed.
– Agapius of Menbij: An earthquake at Antioch. The big churches were destroyed as well as most of the city wall, trade square and houses.
– Nicephorus Callistus: Same as mentioned in Evagrius Scholasticus.
Parametric catalogues
– Plassard and Kogoj (1981): 589 October 21 or 31, $I =$ III, an earthquake caused destruction in Antioch with many victims (Perrey).
– Poirier and Taher (1980): 588 October 31, $I_0 =$ IX (MMS), Antioch destroyed with 60000 victims.
Seismological compilations
– Guidoboni *et al.* (1994): 587-588, Antioch VIII $\leq I \leq$ IX. In the year of 588 a disaster earthquake in Antioch causing thousands of deaths 60000), razing most buildings to the ground, accompanied by many aftershocks (Evagrius). Antioch suffered a great earthquake, many roads in the east were destroyed, as well as islands and countless victims (John of Nikiu). It was a violent earthquake in 587-588 destroying most of Antioch and killing the inhabitants (Ibn Batriq). It was in the winter of 587 (Michael the Syrian). It was in 588-589 (Chronicle of 1234; Barhebraeus). – Sieberg (1932): 587 September 30, a destructive earthquake in Antioch. It was said that it caused 60000 victims.

(043) 601-602 Kilikia; Syria. Surface faulting.
Sources
– Ibn Batriq: A severe earthquake in the Greek territory. In Syria, many cities were destroyed and many persons were killed.
– Michael the Syrian: Like Ibn Batriq but indicate only «Greek territory».
– Chronicle of 1234: A great earthquake took place in Syria and many cities were destroyed.
Seismological compilations
– Guidoboni *et al.* (1994): 601-602, Cilicia and Syria IX $\leq I \leq$ XI, with surface faulting. Towards the third hour of the day, there was a violent earthquake in the territory of Rum [Cillicia] destroying many cities in Syria and Cillicia, and killing a large number of people (Ibn Batriq). On 2 Nisan [April], in the year of 599, a destructive earthquake affected towns and villages burying their inhabitants, for the earth boiled and split open (Michael the Syrian). There was a great earthquake in Syria in 599, on Monday 19 Canun II [January], and many cities were laid waste (Chronicle of 1234).

(044) 634 Aleppo: VII-VIII; Palestine: IV-V. Aftershocks.
Parametric catalogues
– Poirier and Taher (1980): 634, $I_0 =$ VIII (MMS), Ramparts and fortress were destroyed in Aleppo.
Seismological compilations
– Guidoboni *et al.*(1994): 634, Aleppo VII $\leq I \leq$ VIII, an earthquake destroyed the fortress and walls of Aleppo (Ibn Shaddad).
– Ibn Shaddad: When Abu ‘Ubayda conquered the city of Aleppo in the year 15 of the Hegira, the walls and the citadel were restored, for an earthquake before the conquered had destroyed them.
– Theophanes: An earthquake in Palestine.
– Michael the Syrian: A severe earthquake. Churches of Resurrection and Golgotha and many places fell down.
– Agapius of Menbij: An earthquake in Palestine. – Erpenius: A large earthquake was in Palestine. Shocks lasted 30 days.

(046) 678 Batnan: VI-VII; Orfa: VI-VII; Mesopotamia: VI.
Sources
– Theophanes: A large earthquake took place in Mesopotamia. Church of Edessa was partly destroyed.
– Michael the Syrian: A violent earthquake. Batnan of Sarugi fell down, the church of Edessa was partly destroyed.
– Chronicle of 846: A violent earthquake destroyed Batnan of Sarugi and the ancient church of Edessa, a large number of people was killed.

– Chronicle of 819: A violent earthquake destroyed many places in Syria. Batnan of Sarugi was demolished, some destruction in the church of Edessa.
– Agapius of Menbij: An earthquake was at Beisan and Qatnan (unknown sites), city of Sarugi was struck, and the city wall and its houses fell down as Edessa and damage in many places.
– Chronicle of 1234: An earthquake destroyed Sarugi and partly the ancient church of Edessa.
– Chronicon Pseudo-Dionysus of Tell-Mahre: A big and violent shock. Batnan of Sarugi was destroyed and the ancient church of Edessa. There was a large number of casualties.
Seismological compilations
– Guidoboni *et al.* (1994): 679 April 3, an earthquake struck Batnan, the city of Edessa and Mesopotamia. A great earthquake struck Batnan of Sarug and the old church of Edessa collapsed and many people died (Chronicle of 846). There was a violent earthquake in 677-678, it struck Mesopotamia and the dome of the church of Edessa collapsed (Theophanes).
– Sieberg (1932): 678, a strong earthquake destroyed many cities in Syria. It was said that 170000 people were killed. Edessa and Batnae in West Mesopotamia were damaged.

⟨047⟩**713 February 28 Antioch: VI-VII; Aleppo: VI-VII; Kennesreen: VI-VII. Aftershocks.**
Sources
– Theophanes: A strong earthquake in Syria.
– Agapius of Menbij: A violent earthquake destroyed many buildings at Antioch.
– Chronicle of 819: A violent earthquake in all places of Syria, causing many casualties.
– Chronicle of 846: An earthquake destroyed in all Syria and many casualties.
– Chronicle of 1234: A violent earthquake, where many places were destroyed in the zone of Antioch, Aleppo and Qennesrin, all churches and temple fell down.
– Elias of Nisibis: Earthquakes lasted 40 days. Antioch fell down.
– Al-Isfahani: Earthquakes took place in some part of the world for 40 days. In Antioch, buildings and houses fell down.
– Notitia annorum 7 12-716 (information of the years 712-716): A shock and violent earthquake. Houses, villages, churches and many large cities fell down killing the inhabitants, some men were burned and other survivors in Antioch and district of Sidqa and Ksyut and coastal entire island, it was remaining until 1027.
– Ibn Al-Athir: In this year (713 A.D., 94 A.H.) there were earthquakes in Al-Sham which lasted for 40 days, causing destruction of the towns, particularly at Antioch.
– Al-Suyuti: In this year (713 A.D., 94 A.H.) March 20, earthquakes lasted for 40 days in the world, causing destruction of buildings (tall buildings). Most of Antioch fell down.
Parametric catalogues
– Plassard and Kogoj (1981): 713 February 28, in Lebanon $I_{=}$ IV, an earthquake caused destruction at Antioch, where there was a seismic crisis between December 712 and 715 (Berloty; Michael the Syrian; Perrey).
– Poirier and Taher (1980): 713 March 20, $I_{0=}$ IX (MMS), Antioch was completely destroyed.
– Ben-Menahem (1979): 713 February 28, $M_{l=}$ 7.0, destruction of Antioch. Felt in Egypt. (Ergin *et al.*; Plassard and Kogoj; Sieberg).
Seismological compilations
– Guidoboni *et al.* (1994): 713 February 28-March 10, Antioch, Aleppo and Qennesrin VI-II$_{\leq}I_{\leq}$X and other earthquake in 717 December, 24 in Mesopotamia and Syria. A violent earthquake struck Syria in 713, 28 February (Theophanes). On 28 February, 713 there was a tremor and severe earthquake causing many villages and towns to collapse on their inhabitants, some houses, villages and cities were swallowed up in the region of Antioch and district of Sidqa and Ksyut, and the whole coast and the islands, this earthquake or tremor lasted from 28 February to 715-716 (Notitia annorum 712 -716). During the year (7 October 712-25 September 713), earthquakes began in the world and lasted for 40 days, causing the collapse of high buildings and houses in Antioch (Al-Asfahani). There were earthquakes in Syria lasting for forty days, and the whole country collapsed, the strongest shocks took place at Antioch (Ibn Al-Athir). There was a tremor in every region of Syria, killing countless people (Syriac Chronicle of 846). Aleppo and Qennesrin were damaged by a violent earthquake on 28 February where many places collapsed in the region of Antioch, Aleppo and Qennesrin (Michael the Syrian).

– Sieberg (1932): 713 February 28, a strong earthquake occurred in Syria, destroying Antioch. The earthquake was felt in Egypt. Aftershocks continued for one month.

⟨048⟩**717 December24 Antioch: VI-VII; Batnan: VI-VII; Orfa: VI-VII. Aftershocks.**
Sources
– Theophanes: A violent earthquake in Syria.
– Agapius of Menbij: A violent earthquake took place, where many places were damaged.
– Chronicle of 846: A violent earthquake occurred and sound like a big torus.
– Michael the Syrian: A big earthquake.
– Georgius Cedrenus: An earthquake in Syria.
– Elias of Nisibis: An earthquake was in Mesopotamia, where many houses fell down. Shocks continued for 3 months.
– Chronicon Pseudo-Dionysus of Tell-Mahre: A big earthquake destroyed many places, temples, churches and the ancient church of Edessa and Batnan of Sarugi. Same happened for important tall constructions which fell down over the citizens [*note*: the author seems to be merging information from different dates or earthquakes 678].
Parametric catalogues
– Plassard and Kogoj (1981): 717, $I_=$III, an earthquake occurred at Antioch and Syria (Al-Suyuti; Anastase; Perrey).
Seismological compilations
– Guidoboni *et al.* (1994): In 717-718 a strong earthquake in Syria (Theophanes). A great earthquake on 24 December (Syriac Chronicle of 846). In 717-718 a severe and terrible earthquake destroyed many places, including temples, churches and great buildings, in particular Batan and the ancient church of Edessa were destroyed (Pseudo-Dionysius). In the year (14 August 7 17-2 August 718) an earthquake was in Mesopotamia, where many houses collapsed and the shocks lasted for six months (Elias of Nisibis).
– Sieberg (1932): 717 or 718, an earthquake in Syria.

⟨049⟩**749 January 18** (It seems to be that there are two earthquakes, the first is in Southern Syria while the second is in the northern part and Mesopotamia that Manbej could be affected). **Mount Tabor: VII-IX; Baalbak: VIII; Bosra: VII; Nawa: VIII; Balqa: VIII; Al-Quds: VII; Beit Qubayeh: VII-VIII; Tabaryya: VII; Al-Ghouta and Manbej: VII; Darayya: VI; Damascus and Daraa: V-VI; Ariha. Surface faulting and liquefaction in Mesopotamia. Landslide at Mount Tabor.**
Sources
– Al-Suyuti: In the year of 130 A.H. (started from 747 September 11) a shock occurred in Damascus causing panic and the Hens Souk fell down. In the year 131 A.H. (started from 748 August 31) a great shock occurred in Damascus, fracturing the roof of the Mosque.
– Al-Mansouri: In the year 132 A.H. (started from 749 August 20) there was an earthquake at Al-Sham.
– Theophanes: 749 January 18, a violent earthquake occurred in Palestine, Jordan and in all of Syria, many tens of thousands of casualties, churches and monasteries fell down especially near Jerusalem. Some cities were completely destroyed and some partly. In Mesopotamia, the land was opened for 2 miles where the eyewitness saw an ancient statue. Landslide for one city completely.
– Michael the Syrian: 749 January 18, an earthquake was in Damascus for some days; one fortress was completely destroyed and 800 casualties in the city. In Ghouta and Daraya, many casualties. Bosra, Nawa, Dar'a, Baalbak were completely swallowed up. In the region of Balqa (Mu'ab), a fortress was taken and thrown 3 miles away. City of Tiberias destroyed. Near the mount of Thabor, a village was moved for 4 miles without damage. A source of water near Ariha was moved 6 miles. In Maboug, the earthquake was during the prayer time.
– Chronicon Pseudo-Dionysus of Tell-Mahre: 749 January 18, in Manbej, and during the time of prayer, the church fell down.
– Chronicle of 1234: 749 January 18, there was an earthquake for some days in Damascus, a fortress at Beit Cubaya was destroyed, 800 casualties, the same in Ghuotah and Daraya, many casualties were heavily damaged, Bosra, Nawa and Baalbak fell down partially, a fortress in Mo'ab was thrown for 3 miles. The city of Tabaria was destroyed and a village near Thabor Mountain was shifted without damage. Mabboug was destroyed. – Elias of Nisibis: 749 January 18, many earth-

quakes occurred and many places fell down. A village near Tabor Mountain was shifted for 4 miles. The church of Mabboug fell down over the people.
– Agapius of Menbij: 749 January 18, a violent earthquake hit the coast of Palestine, many villages were hit and many casualties in Tiberias more than 100000 casualties
– Georgius Cedrenus: 749 January 18, a big earthquake took place in Palestine, Jordan and all of Syria. There were many thousands of casualties. Monasteries and temples fell down. – Nicephorus of Costantinopolis: 749 January 18, a violent earthquake hit Syria, the cities were swallowed up and some buildings were shifted for 7 miles. In Mesopotamia, a deep hollow was formed.
– Georgius Monachus: 749 January 18, a big earthquake destroyed the cities, some completely and other partially, the tall buildings fell down or shifted. In Mesopotamia, a deep hollow was formed for three miles.
– Al-Dhahabi: A strong earthquake in Syria. It was the strongest in Jerusalem, causing many casualties.
– Ibn Tagri Birdi: A violent earthquake in Syria destroyed Jerusalem.

Parametric catalogues
– Plassard and Kogoj (1981): They considered that there were two events, the first was on 746 January 18 (I=V) in Palestine with destruction (Anastase; Perrey; Sieberg) and the second was in 748 (I=VII) at Damascus with destruction (Al-Suyuti).
– Ben-Menahem (1979): 746, January 18, wednesday evening after 16 h, 32.0N, 35.5E, fault extended northwards over 120 km, I_0=XI, M_L=7 .3, felt in Egypt, Syria, Arabia and Mesopotamia. Great damage in Tiberias (30 synagogues destroyed), Jerusalem, led, Arad and to monasteries north of the Dead Sea. About 600 settlements in Judea, Samaria and Galilee were hit and many casualties reported. Destruction of Hisham palace near Jerico and the city of Gerasa. Tsunami in the Dead Sea and possible flooding of Dead Sea southern basin (Al-Sinawi and Ghalib; Amiran; Avi-Yonaha; Bahat *et al.*; Michel the Syrian; Neev and Emery; Plassard and Kogoj; Sieberg; Willis).

Seismological compilations
– Guidoboni *et al.* (1994): 749 January 18, Baalbak, Beit Qubayeh, Bosrah, Damascus, Daraa, Darayya, Al-Ghouta, Jerico, Jerusalem, Mabbug, Nawa, Tiberias, Mt. Tabor, Palestine, Mesopotamia and Syria (Jerusalem and Mabbug IX ≤ I ≤ X), in the mid 8th century, a powerful earthquake struck Palestine, inflicting serious damage at Jerusalem and Tiberias, and causing a landslide at a village near Mt. Tabor. There are two problems relating date of this event and either it was a single earthquake or a series of tremors, however it dated back to 18 January 749 (Tsafrir and Foerster, 1992). A powerful earthquake dated back to 18 January 747 occurred in Palestine, along the Jordan River and throughout Syria, killing thousands of people and collapsing churches and monasteries, especially in the desert near Jerusalem (Theophanes). There was a strong earthquake in Syria during the year (11 September 747-30 August 748), where the strongest shocks occurred in Jerusalem, causing the death of many conquering troops and others (Al-Dhahabi). There was a strong earthquake in Syria which destroyed Jerusalem, during the year (31 August 748-19 August 749) (Ibn Tagri Birdi). A severe and powerful earthquake in the West, the temple of Mambej collapsed totally in the year 747-748 (Pseudo-Dionysius). During the year (30 August 748-19 August 749) there were many earthquakes and many places were reduced to ruins, a village near Mt. Tabor moved four miles from its original position and in that year a church in Mambej collapsed (Elias of Nisibis). A tremor at Damascus lasted for days, a fortress in Beit Qubayeh collapsed and many people were killed, many myriads of people perished in Al-Ghouta and Dareya, while Bosra, Nawa, Dar'a and Baalbak were completely swallowed up, changing the color of water spring in the city, sea waves destroyed most of the cities and villages along the coast, the fortress of Balqa on the coast was uprooted, Tiberias collapsed, a village near Mt. Tabor was moved four miles with its houses and other buildings without any destruction, a water spring near Jerico changed its original place for six miles, destruction of churches and deaths in Mambej, most the buildings in Constantinople, Nicea and other cities collapsed (Michael the Syrian). Regarding (Tsafrir and Foerster, 1992) chronological analysis, they considered the Babylonian dating instead of the Antiochene sys-

tem, they dated this event back to 749 January, 18. An earthquake in Mesopotamia and Syria in the year of 749-750, causing various levels of destruction in many cities and large-scale surface faulting in Mesopotamia (Theophanes).

– Ambraseys *et al.* (1994): 747 January 18, morning, 31.8N-35.7E, $I_{\le}$VI. In 747 January 18, a large earthquake centering the Dead Sea region was felt in Egypt, some damage was caused in Damietta, in Fustat the shock was strongly felt and caused fear but no damage. There is a considerable confusion over the dating of this event, which the Arabic sources put in 130 A.H. began 11 September 747 (Al-Dhahabi; Al-'Ulami; Al-Suyuti; Caetani; Sibt Ibn Al-Jawzi; Taher), and January 748 has recently been proposed as the correct date (Ben-Menahem; Gil; Russell; Sieberg), the effects of the earthquake are frequently confused with those of another event that affected parts of Syria two years later (Al-Khwarazmi; Tsafrir and Foerster).

– Russell (1985): 748 January In January 18, 747, a great earthquake occurred in Palestine, around the Jordan, and in all of Syria, to such an extent that many innumerable and countless people perished in its power, and churches and monasteries collapsed (Theophanes). On 18th day of January at the 4th hour in the 6th year, there was a great earthquake in Palestine, and towards the Jordan, and throughout all of Syria. Many thousands of people perished, and churches and monasteries collapsed (Cedrenus). Russell evaluated the date to be from June 746 through May 747. That night there was a great earthquake in the land from the city of Gaza to the furthest extremity of Persia, many houses were ruined in all the cities, and none was saved from them. On the sea, many ships were sunk on that night. Six hundred cities and villages were wrecked with a vast destruction of men and beasts, but Egypt was uninjured, except Damietta. At Misr, there was only great fear without damage (Severus Ibn Al-Muqaff). There was an earthquake at Damascus which lasted for days, a fortress in Beit Qubayeh collapsed and many people were killed, many myriads of people perished in Al-Ghouta and Darayya, while Bosra, Nawa, Dar'a and Baalbak were completely swallowed up, sea waves destroyed most of the cities and villages along the coast, the fortress of Balqa on the coast was uprooted, Tiberias was destroyed except for a house, a village near Mt. Tabor was moved four miles with its houses and other buildings without any destruction, a water spring near Jericho changed its original place for six miles, destruction of churches and deaths in Mabbug (Michael the Syrian). Russell suggested a date between September 747 and August 748 for this event. There were many earthquakes where many regions gave way. A village near Mt. Tabor was displaced 4 miles along with houses and their possessions, but without damage. The church of the Jacobites in Mabbug collapsed on Sunday and many people perished in it (Elias of Nisibus). Russell also suggested that this event occurred between September 747 and August 748.

Monographs

– Tsafrir and Foerster (1992): A major earthquake occurred in 749 January 18 (according to Margaliot and archaeological evidences found in Bet Sheam), in Palestine and throughout Syria, destroying Jerusalem, Gerasa, Jericho, Pella, Capernaum, Sussita, Bet Sheam and many sites along the Jordan Valley, killing many tens of thousands of people (Cedrenus; Dionysus of Tellmahr; Ibn Tagri Birdi; Ibn Al-Muqaffa; Margaliot; Michael the Syrian; Sibt Ibn Al-Jawzi; Theophanes).

‹050› **757 March 9 Habura: VII; Mesopotamia; Syria; Palestine.**

Sources

– Theophanes: A strong earthquake in Syria and Palestine.

– Chronicon Pseudo-Dionysus of Tell-Mahre: A big and terrible shock in the region of Mesopotamia. Near Harbura, three villages fell down.

Seismological compilations

– Guidoboni *et al.* (1994): 757 March 9, Habura, Palestine, Syria and Mesopotamia $I_{=}$ IX. A powerful earthquake struck Syria and Palestine on 9 March 757 (Theophanes). In the year 756 on Tuesday 3 March, there was a great, violent and terrible earthquake in the land of Mesopotamia where three villages near Habura collapsed, many people there were crushed and perished (Pseudo-Dionysius).

– Russell (1985): An earthquake by no means mild, affected Palestine and Syria on 9 March 757 (Theophanes).

⟨054⟩835 January 5-December 25 Antioch: VI-VII. Aftershocks.

Sources

– Al-Suyuti: In the year 220 A.H. (started from 835 January 5) the earth shook for 40 days and Antioch destroyed.

Seismological compilations

– Guidoboni *et al.* (1994): 835 January 5-December 25, Antioch IX $\leq I \leq$ XI, the earth shook for forty days, and Antioch was destroyed (Al-Suyuti).

⟨055⟩ 846 August 28-847 August 16 Antioch: >VIII; Damascus: VII; Homs: VII; Antioch, Al-Jazira: VI; Al-Mousel: VI. Aftershocks.

Sources

– Al-Suyuti: During the year 232 A.H. (started from 846 August 28) many earthquakes occurred in the world in particular, in Morocco and Al-Sham. The walls of Damascus and Homs were collapsed. It was worst at Antioch. It caused destruction in Al-Jazira and Al-Mousel and lasted for many days.

Seismological compilations

– Sieberg (1932): 846, numerous places in Lebanon exposed to many sequences of shocks, to such an extent that landslides occurred.

⟨056⟩ 847 November 24 Damascus: VII-VIII; Al-Ghouta: VII-VIII; Al-Mazzeh: VII; Beit Lahya: VII; Darayya: VII; Antioch: VI; Al-Mousel: V.

Sources

– Al-Dhahabi: In 253 A.H. Rabi' II, it was a dreadful earthquake in Damascus which lasted for three hours, causing walls to fall down and people die under debris. It extended to Antioch killing 20000 as it was said, then to Al-Mousel where 50000 people were killed under debris as it was said.

– Al-Suyuti: In 253 A.H. 11 (847 A.D. November 25) there was a dreadful earthquake in Damascus where houses fell down and people died under debris. This earthquake extended to Antioch causing destruction, to Al-Jazira causing damage, and to Al-Mousel killing 50000 people as it was said. In his book *Al-Zalazel* (the earthquakes), Al-Hafez Ibn Asaker mentioned that there was an earthquake in Damascus on Thursday 11 Rab' 253, destroying a quarter of the Ommyad Mosque the great, the minaret fell down and bridges and houses collapsed, this earthquake reached Al-Ghouta where Darayya, Al-Mazzeh, Bait Lahya and others were destroyed.

New original sources

– Ibn Al-Imad: an earthquake caused heavy shaking in Damascus since morning for 3 h, destroying houses and displacing huge stones and breaking many windows of Souks and killing many people under debris. Many terraces of Ommyad Mosque the Great fell down, a quarter of its minaret fell down. A village in Al-Ghoutah was overturned on its inhabitants unless one person survived. It was strong at Antioch and Al-Mousel where more than 2000 houses collapsed over their residents and 20000 victims.

Parametric catalogues

– Plassard and Kogoj (1981) 847 November 24, $I =$ V in Lebanon, this earthquake caused destruction in Damascus and damage in Homs (Al-Suyuti).

– Ben-Menahem (1979): 847, $M_l =$ 6.2, destruction in Lebanon (Plassard and Kogoj; Sieberg; Willis).

Seismological compilations

– Guidoboni *et al.* (1994): 847 November 24, Antioch, Bayt Lahya, Damascus IX $\leq I \leq$ XI, Darayya, Al-Ghoutah, Al-Mousel and Al-Mazzah. A dreadful earthquake occurred at Damascus, causing the walls to collapse and people to die in the ruins, the earthquake reached Antioch and 20000 people died there and it reached Mawsel where 50000 people died in the ruins (Al-Dhahabi). The earthquake took place on 24 November 847, it was strong in Damascus, destroying a part of the Ommiad Great Mosque, the minaret fell down and bridges and houses collapsed, it reached Al-Ghouta, Darayya, Al-Mazzeh, Bayt Lahya and others were destroyed (Al-Suyuti).

⟨057⟩853 June 12-854 June 1 Tabariya: VIII-IX. Landslide.

Sources

– Ibn Al-Imad: The earth shook Tiberias at night, then a huge part (80 × 50 Zeraa) of its mountain split open, and many people were killed.

Parametric catalogues

– Plassard and Kogoj (1981): 853-854, *I*=III, a strong earthquake occurred in Tiberias (Al-Suyuti).

Seismological compilations

– Guidoboni *et al.* (1994): 853 June 12-854 June 1 ,Tiberias VIII≤*I*≤X, landslide, The earth shook at Tiberias, a huge part of the mountain split open, and so ... many people died (Ibn Al-Imad Al-Hanbali).

⟨058⟩ **859 December 30-860 January 29** (It could be two earthquakes, the first one is between Antioch and Lattakia while the second is on the Euphrates). **Antioch: VIII; Lattakia and Jableh: VIII; Homs: VII; Palmyra: VII; Tarsus: VI; Balis: VI; Damascus: VI; Adana: VI; Al-Quds: V-VI; Ar-Raqqa: V; Ras Al-Ein: V; Harran: V; Orfa: V; Egypt: IV** (fig. 6)**. Landslide.**

Sources

– Al-Mansouri: In the year 244 A.H. [858 April 19-859 April 7], a great earthquake occurred in Al-Sham, damaging Antioch, Homs and Palmyra.

– Al-Tabari: In Shawwal 245 A.H. (859 December 30-860 January 29), there was an earthquake at Antioch, collapsing 1500 houses, killing many people, half of the city wall and 90 towers fell down and people ran out to desert. A part of Jabal Al-Akraa was split and sank into the sea generating high waves, disappearing river there. It was said that inhabitants of Tnis (Egypt) heard a high noise which led to the killing of a large number of victims. In this year the earthquake shook Balis, Raqqa, Harran, Ras Al-Ain, Homs, Damascus, Al-Ruha, Tarsus, Adana and the Syrian coasts. In Lattakia the shock caused destruction of all houses and some survivals there escaped. Same happened to Jableh.

– Al-Suyuti: [...] The earthquake passed the Euphrates after destroying Balis and its around [...].

– Saadeh (1984): in the year 859-860, a violent earthquake occurred at Lattakia, causing destruction of most buildings with a large number of victims.

Fig. 6. Map of intensity distribution for the December 859-January 860 A.D. earthquake.

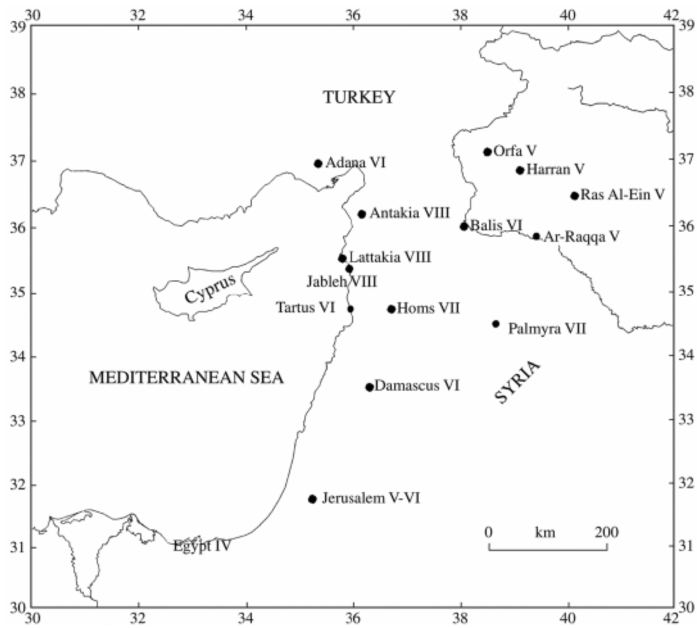

Parametric catalogues
– Plassard and Kogoj (1981): 859 April 18, in Lebanon I = VI, this earthquake caused destruction in Antioch and damage in Damascus and Homs (Al-Suyuti, Erpenius). Poirier and Taher (1980): 859 December, I_0 = X-XI (MMS), in Antioch 1500 houses were destroyed, 90 towers fell from the ramparts. Casios Montain (Jabal Al-Aqra'), 30 km SW of Antioch, fell into the sea. A river disappeared into the ground. Cities of Urfa, Adana, Tarsus, Misis, Homs and Damascus were destroyed.
– Ben-Menahem (1979): 859 April 8, 36.2N, 36.1E, I_0 = XII, M_L = 8.0, near Samandag, an inhabited mountain fell into the sea. Total destruction of Antioch. Felt in Mecca, Egypt, Turkey, Armenia, Mesopotamia. Damage in Jerusalem (Al-Sinawi and Ghalib; Amiran; Ergin *et al.*; Plassard and Kogoj; Sieberg).
Seismological compilations
– Guidoboni *et al.* (1994): [859 December 30-860 January 29] Adhana, Antioch, Balis, Damascus, Jableh, Harran, Homs, Laodicea IX ≤ I ≤ X, Al-Massisa, Edessa, Raqqa, Ra's al-'Ayn, Tarsus, Mt. Casius and Syria, landslide, in the year (30 December 859-29 January 860) there was an earthquake at Antioch, killing a large number of people and causing the collapse of 1500 houses and about 90 towers in the walls of the city, Mt. Casius (Jabal Al-Aqra'a) split open and rocks fell into the sea, which was stormy that day, people in Tinnis in Egypt were killed, there was another earthquake in the cities of Balis, Raqqa, Harran, Ra's Al-'Ayn, Hims, Damascus, Al-Ruha, Tarsus, Al-Massisa, Adhanah and along the Syrian coast, the earthquake reached Laodecea, where no home remained standing and only a small number of people escaped (Al-Tabari). Syria was struck by earthquakes which destroyed Laodicea and Jableh and many people were killed (Ya'qubi).
– Ambraseys *et al.* (1994): 860 January, 37.0N-38.0E, I ≤ VI. In one day of January 860, a large earthquake in Eastern Anatolia and North Syria, particularly destructive in Antioch, Jableh and Lattakia, was felt in Egypt (Al-Suyuti; Al-Tabari; Ibn Al-Athir; Taher). This earthquake could be dated in other catalogues on 859 and often under 8 April (Al-Sinawi and Ghaleb; Ben-Menahem; Kallner-Amiran; Poirier and Taher; Sieberg).
– Sieberg (1932): 859 April, a strong earthquake in Northern Syria. It was felt in Asia Minor, Armenia, Mesopotamia, Palestine and Egypt. It killed a large number of people. In Antioch, 1500 houses and 90 towers of the city rampart collapsed. Lattakia and Jableh lost most of their inhabitants. A part of Casius mountain fell into the sea. Damascus, Tarsus, Edessa, Baghdad, Homs, Balis, Adana Harran, Marsin and ...? affected. Minor damage in the mosque of Al-Aqsa in Al-Quds. Shocks lasted for 3 months.

(066) 1002 November 10-1003 October 29 Western Syria: ≥ VIII.
Sources
– Al-Suyuti: In the year 393 A.H. (1002 November 10-1003 October 29) an earthquake occurred in Al-Sham, cities and towns along the frontiers, causing citadels and fortresses to fall down, and people to die under the debris.
Parametric catalogues
– Poirier and Taher (1980): 1002, I_0 = VIII-IX (MMS), Syria, border zone much destruction.

(067) 1029 January 20- 1030 January 8 Damascus: VII.
Sources
– Al-Dawadari: in the year 420 A.H. (1029 January 20-1030 January 8) a heavy earthquake occurred in Damascus, collapsing its half and killing many people under the debris.
Parametric catalogues
– Plassard and Kogoj (1981): 1029 January 29, I = VII, this earthquake caused the destruction of half of Damascus (Perrey; Sieberg).
Seismological compilations
– Sieberg (1932): 1029 January 20, a strong earthquake in Syria destroying half of Damascus.

(068) 1042 August 21-1043 August 9 Palmyra: > VII; Baalbak: V; Tabriz: III; Egypt: III.
Sources
– Al-Suyuti: in the year 434 A.H. (1042 August 21-1043 August 8) an earthquake occurred in Palmyra and Baalbak. Most people in Palmyra were killed under the debris.
Parametric catalogues
– Ben-Menahem (1979): 1042 August 21, 35.1N, 38.9E, near Palmyra, M_L = 7.2, destruc-

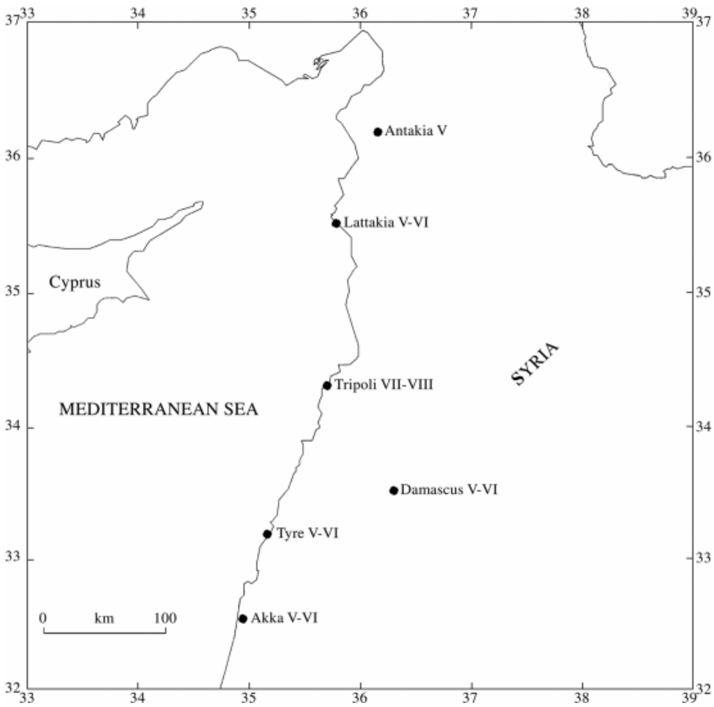

Fig. 7. Map of intensity distribution for July-August, 1063 earthquake.

tion of Palmyra. It was strong in Baalbak. It was felt in Tabriz and Egypt.

Seismological compilations

– Sieberg (1932): 1042 August 21, a strong widespread earthquake occurred to such an extent that it was felt in Tabriz and Egypt. The center of this earthquake seems to be at Palmyra, where it killed most of its inhabitants. It was felt strongly in Baalbak. Victims were evaluated to be 50000.

(070) **1063 July 30-August 27 Tripoli: VII-VIII; Lattakia: V-VI; Acre: V-VI; Sur: V-VI; Antioch: V** (fig. 7)**.**

Sources

– Al-Suyuti: In 455 A.H. Sha'ban (1063 July 30-August 27) there was a great earthquake at Waset, Antioch, Lattakia, Tyr, Akka, Al-Rum and Al-Sham, falling down a part of Tripoli wall.

– Abu Al-Fida: In this year (455 A.H.) (1063 January 4-1063 December 25), there was a great earthquake in Al-Sham, causing destruction of many cities. The wall of Tripoli collapsed.

– Ibn Kathir: In that year [455 A.H.] in Sha'ban [1063 July 30-August 27], there was a great earthquake in Al-Sham land, where it caused destruction of many towns. Wall of Tripoli was destroyed.

Parametric catalogues

– Plassard and Kogoj (1981): 1063 May, in Lebanon I= IX, this earthquake caused destruction in Tripoli and Akkar region (Al-Suyuti; Perrey).

– Poirier and Taher (1980): 1063 July, I_0=VIII (MMS), Antioch, Lattakia, Tripoli and Acre.

– Ben-Menahem (1979): 1063 August, M_L=7.1, damage in Antioch, Tripoli, Lattakia, Sur and Acre (Amiran; Ergin *et al.*; Willis).

Seismological compilations

– Sieberg (1932): 1063 or 1083, a strong earthquake occurred in the Syrian coast. Walls of

Tripoli collapsed. Antioch and Damascus suffered.

⟨072⟩ **1091 September 26 or October 6 Antioch: VI-VII.**
Parametric catalogues
– Plassard and Kogoj (1981): 1091, É=III (in Lebanon), an earthquake caused destruction at Antioch where 80 towers collapsed (Abu Al-Fida; Al-Suyuti; Berloty).
– Poirier and Taher (1980): 1091 September 17, I_0 = IX (MMS), in Antioch, 70 towers fell from the ramparts.
Seismological compilations
– Sieberg (1932): 1092, an earthquake was in Syria from Antioch to Damascus. Many buildings were destroyed.
– Ibn Al-Athir: In that year [484 A.H.] in Sha'ban 9 (1091 September 26) many earthquakes happened in Bilad Al-Sham and other countries, where people left their houses. In Antioch, it caused destruction of many houses with many victims under the debris, and 90 towers of its wall collapsed.
– Al-Dawadari: In 494 Sha'aban 19 (1091 October 6), an earthquake occurred in Antioch, causing the collapse of 70 towers of its wall.

⟨075⟩ **1114 November** (Two earthquakes could have happened; one at Maraash and other at Orfa). **Maskaneh: VIII; Maraash: VII-VIII; Samsat: VII-VIII; Orfa: VII-VIII; Harran: VII, Aleppo: V; Antioch: IV** (fig. 8)**. Landslide.**
Sources
– Ibn Al-Jawzi: In the year 508 A.H., the night of 18 Jamada II Sunday (1114 November 19), an

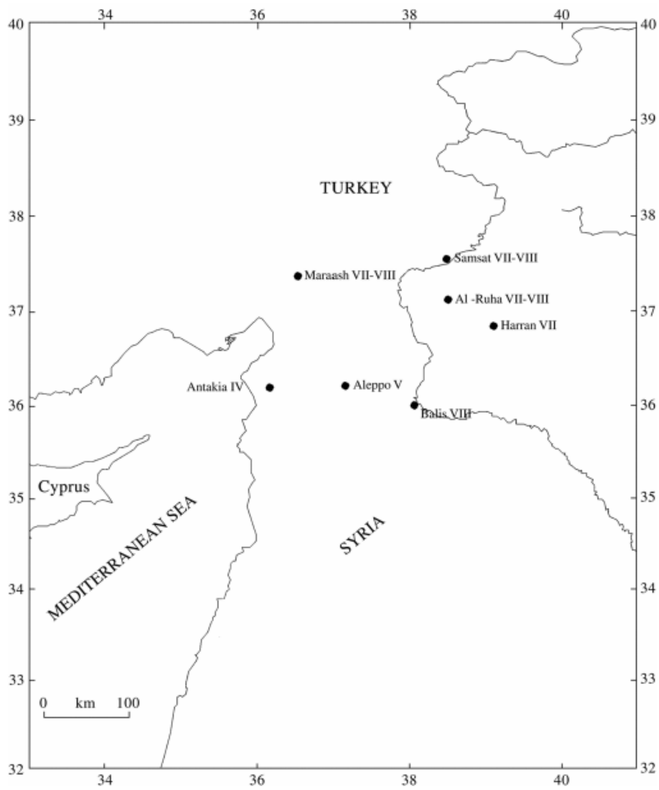

Fig. 8. Map of intensity distribution for November 1114 earthquake.

earthquake occurred, causing collapse of 13 towers of Al-Ruha Wall, a part of Harran Wall fell down and many houses collapsed on their inhabitants, Samasat was swallowed up, 100 houses and half of the citadel collapsed at Balis.
– Ibn Al-Athir: In this year (508 A.H.) in Jamada II (November 2-30), there was a strong earthquake in Al-Jazira area, Al-Sham and others, causing a wide destruction at Al-Ruha, Harran, Samsat, Balis and others, and many people killed under debris.
– Al-Dawadari: In this year (508 A.H.), there was an earthquake at Aleppo. Samsat and Marash were swallowed up and many people killed.
– Ibn Kathir: In this year (508 A.H.) (1114 January 7-1115 May 26), there was a great earthquake in Al-Jazira, causing destruction of 13 towers and many houses in Al-Ruha and some houses in Khurasan (?) and many houses in many countries where many of its inhabitants were killed about 100000 victims, and half of Harran castle was collapsed, Samsat was swallowed up and many people were killed under debris.
Parametric catalogues
– Plassard and Kogoj (1981): 1114 August 10 and November 13, in Lebanon $I=$II, there were two earthquakes, causing destruction in Cilicia with tsunami and damage in Antioch (Al-Suyuti; Sempad).
– Ben-Menahem (1979): 1114 August 10, 36.5N, 36.0E, $M_L=$7.0, destruction of Antioch. It was accompanied by a tsunami. It was strongly felt in Palestine. Jerusalem ($M_M=$ IV) (Amiran; Plassard and Kogoj; Sieberg).
– Ergin *et al.* (1967): Antioch was felt by the first event. The epicenter of the second one was between Urfa and Harran, the walls of Edessa city were ruined. Samsat, Marash, Antioch and Harran were felt.
– Ben-Menahem (1979): 1115 December 25, 37.0N, 38.9E, Urfa-Harran, Taurus mountains, $M_L=$7.5, Jerusalem ($M_M=$V). It was strong in Syria. Walls of Edessa destroyed (Amiran; Ergin *et al.*; Sieberg; Willis).
Seismological compilations
– Sieberg (1932): In 1114 August 10, a vast destructive earthquake started from southwest of Asia Minor through Cillicia and Cyprus to Egypt. There was large destruction in Antioch and minor damage in Aleppo. In 1114 November 13, repeating what happened in August in the same regions with the same damage.

(078) **1137 October 19-November 16 Syria: VII; Al-Jazira: VII; Al-Mousel: VII; Iraq: VII.**
Sources
– Ibn Al-Athir: In this year [532 A.H.] in Safar [1137 October 19-November 16], there was a great earthquake in Al-Sham, Al-Jazira, Diyar Bakr, Al-Mousel, Iraq and other countries, causing a lot of destruction in these regions and many people were killed under debris.
– Abu Al-Fida: In this year [532 A.H.] [1137 September 19-1138 September 08], there was a great earthquake in Al-Sham, Iraq and other countries, causing a lot of destruction and many people killed under debris.
Parametric catalogues
– Ben-Menahem (1979): 1137 September 13, NE Aleppo, $M_L=$ 7.2, felt in Mesopotamia and Egypt (Al-Sinawi and Ghaleb; Sieberg; Willis).
Seismological compilations
– Sieberg (1932): 1137 September 13, a destructive earthquake in Syria caused a large number of people to kill. It was felt in Mesopotamia and Aleppo. Aftershocks lasted for the next year.
– Ambraseys *et al.* (1994): 1138 October 15, afternoon, 36.5N-37 .0E, $I\leq$VI. Earthquake. Shocks were felt in Egypt, originating from the series of earthquakes that devastated Northern Syria.

(079) **1138 October 11-26 Al-Sham: VI-VII; Al-Jazira: VI-VII; Aleppo: VI-VII. Aftershocks.**
Sources
– Ibn Al-Athir: In this year [533 A.H.] in Safar [1138 October 11-26] there were many great earthquakes in Al-Sham, Al-Jazira and other countries, where the strongest were in Al-Sham lasting for many nights with many aftershocks, causing destruction of many towns such as Aleppo where people ran out leaving their houses to the desert. The earthquakes extended from Safar 4 to 19 in Al-Sham.
– Abu Al-Fida: Same description of Ibn Al-Athir.
Parametric catalogues
– Poirier and Taher (1980): 1139 November, $I_0=$X-XI (MMS), Aleppo was destroyed and the inhabitants evacuated.
Seismological compilations
– Plassard and Kogoj (1981): 1138 October, in

Lebanon $I=$ IV, there was an earthquake causing destruction in Aleppo (Al-Suyuti; Berloty; Ibn Al-Athir).
– Sieberg (1932): 1138 September 8, repeating of what happened in the same month of the last year, but it was stronger causing a large number of people to die in Aleppo and Ambar.

(082) **1152 September 27 Bosra: VII; Hauran: VII; Syria: VII.**
Sources
– Abu Shama: It was said that on 546 A.H. Jamada II 13 at night [1152 September 27], there was an earthquake, producing 3 shocks in Bosra and Horan regions, causing destruction of many house walls in Bosra and others. On Shawal 2 morning [1152 November 14] there was an earthquake, shaking the earth for 3 times and moving houses and walls.
Parametric catalogues
– Plassard and Kogoj (1981): 1152 March 22, $I=$ IV, it was an earthquake that caused a destruction in Afamea (Sieberg).
– Ben-Menahem (1979): 1151, 32.6N, 36.7E, Jabal Al-Arab (Hauran), $I_0=$ IX, $M_L=$ 6.2, destructive at Bousra and the Hauran. Felt in Palestine (Amiran; Plassard and Kogoj; Sieberg; Willis).
Seismological compilations
– Sieberg (1932): 1151, a destructive earthquake in the volcanic area in Al-Nuqra and Horan [Syria], where only Bosra was widely damaged. It was said that large areas of Syria were affected. In 1152 March 22, a destructive earthquake was in Syria, especially in Apamea and Qalaat Al-Madiq.

(083) **1156 September-1159 May Western Syria including Damascus. Foreshocks, aftershocks, surface faulting.**
New original sources
Depending on quality of the available historical sources, we consider that Ibn Al-Qalansi is the best eye-witness of this seismic crisis in the region during that period, and we summarize his text chronically with intensity evaluation of each described locality.
– Ibn Al-Qalansi: 1156 September 28 (551 Sha'aban 9), 3-4 strong shocks hit Damascus: III-IV. 1156 October 9 (551 Sha'aban 22), 6 shocks were felt in Damascus: II-III. 1156 October 12 (551 Sha'aban 25), 2 shocks hit Damascus: III-IV; Aleppo: V-VI; Hama: V-VI; Afamia: VI. 1156 October 17 (551 Sha'aban 29), 2 shocks was felt in Damascus: III. 1156 October 22 (551 Ramadan 5), there were 3 shocks in Damascus: IV. 1156 October 23 (551 Ramadan 6), 5 shocks were in Damascus: IV-V. 1156 October 31(551 Ramadan 15), 2 shocks in Damascus. 1156 November 1(551 Ramadan 16), 2 shocks in Damascus: III. 1156 November 4 (551 Ramadan 18), a strong shock was felt in Damascus: III-IV. 1156 November 8 (551 Ramadan 23), there was a strong shock in Damascus: III-IV. 1156 November 18 (551 Shawwal 2), there was a strong shock in Damascus: IV. 1156 November 22 (551 Shawwal 6), at noon, a shock was in Damascus: III. 1156 December 2 (551 Shawwal 16), there was a strong shock in Damascus: III. 1156 December 3 (551 Shawwal 17), 4 shocks in Damascus: IV. 1156 December 8 (551 Shawwal 23), many shocks in Damascus: IV-V. Aleppo: V-VI, Shaizar: VII-VIII; Kafar Tab: VI-VII; Hama: VI-VII. 1157 April 2 to 4 (552 Safar 19, 20 and 21), a shock was felt in Damascus: IV; Shaizar: VI; Hama: VI; Aleppo: V; Kafar Tab: VI. 1157 July 5(552 Jumada I 25), 4 strong shocks in Damascus: III-IV. 1157 July 13 (552 Jumada II 4), a great earthquake followed by anther one less stronger was in Damascus: IV-V. In Aleppo, it was a frighten earthquake: IV-V. In Homs, it was frighten earthquake with destruction: V-VI. In Hama and Kafar Tab, there was destruction: V-VII. Same was in Afamia: V-VII. In Tayma, there was damage: V. 1157 August 12(552 Rajab 4), a great earthquake was in Damascus, causing partial destruction: V-VI; Hama: VIII-IX; Shaizar: VIII-IX; Kafar Tab: VIII-IX.; Afamia: VIII-IX; Arqa: VIII-IX; Aleppo: VII-VIII; Homs: VII-VIII; Lattakia: VII-VIII; Tripoli: VII-VIII; Antioch: VII-VIII; Shmemis: VII-VIII; Qalaat Al-Hosn: VII-VIII; Maarret Annooman: VI-VII; Tel Harran:? (fig. 9). 1157 August 16, 17 and 18(552 Rajab 8, 552 Rajab 9, 552 Rajab 10), there were 4 main earthquakes and series of shocks in Damascus: III-IV. 1157 September 6 (552 Rajab 29), a frightening earthquake was in Damascus: IV-V. 1157 October 30 (552 Ramadan 24), many shocks were in Damascus: IV-V. In Aleppo, there was light damage to the houses: VI. In Hama, there were a destruction with sound: VII-VIII. 1157 November 14 (552 Shawwal 10), a strong

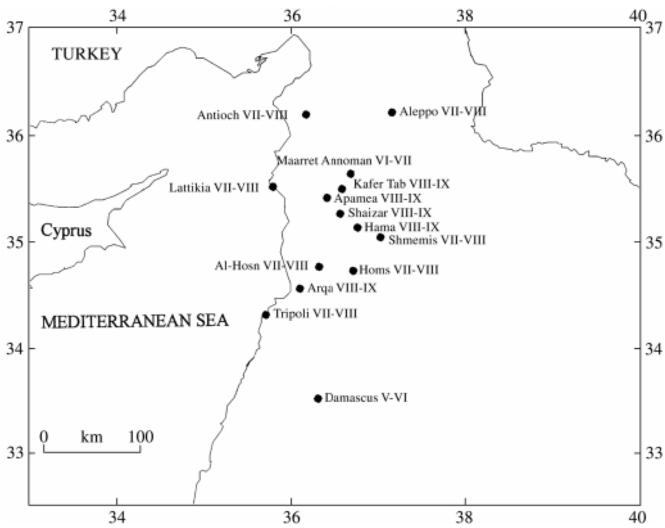

Fig. 9. Map of intensity distribution for August 12, 1157 earthquake.

earthquake caused a panic in Damascus: III-IV. 1157 December 13 and 14 (552 Dhul Qi'ada 10), there were 2 shocks in Damascus: III-IV. 1157 December 26 (552 Dhul Qi'ada 23), there was a shock in Damascus: IV. 1157 December 28 (552 Dhul Qi'ada 25), there were 6 shocks causing a panic in Damascus: IV-V. 1158 January 1 (552 Dhul Qi'ada 30), there were many shocks in Damascus: III-IV. 1158 April 16 (553 Rabi'a I 15), Aleppo was shaken: IV. 1158 April 25 (553 Rabi'a I 25), there was a shock in Damascus: III. 1158 August 20 (553 Rajab 23), there was a shock in Damascus: III. 1158 August 21 (553 Rajab 24), there was a shock in Damascus: III. 1159 January 23 (554 Muharram 1), there were 3 shocks in Damascus: III. 1159 April 12 (554 Rabi'a I 22), there was a shock in Damascus: IV-V. 1159 May 30 (554 Jumada I 10), there was a shock in Damascus: IV.

– Ibn Al-Athir: In this year [552 A.H.] in Rajab [1157 August 9-September 7], there were many strong earthquakes, causing destruction of many towns and killing a countless number of people. Hama, Shaizar, Kafar Tab, Maarret, Afamia, Homs, Crac Des Chevaliers, Arqa, Lattakia, Tripoli and Antioch were totally destroyed. The remaing towns in Bilad Al-Sham were partially destroyed. Ramparts of the towns and fortresses collapsed.

– Abu Al-Fida: In this year (552 A.H.), Rajab, there were strong earthquakes, causing destruction of Hama, Shaizar, Homs, Hosn Al-Akrad, Tripoli, Antioch and other places, to the extent that fortresses and walls fell down. Large number of people were killed under debris.

– Bar Hebraeus: And in this year, which is the year 552 of the Arabs (1157 A.D.), severe earthquakes took place in Syria destroying many towns. In Hamth [Hama], its fortress and all its large houses fell down. Old men, women, children, and tens of thousands of its inhabitants perished. The fortress of Shaizar fell down, every part of it, and only women and eunuch escaped. The people of Emessa went forth hastily and were delivered, but their monasteries and fortress perished. In the same manner, the people of Aleppo fled from the city, and stayed outside for a few days. Their houses in the city were thrown down with perishing of five hundred souls. Similar was in Kafar Tab and Afamia where no one escaped. Cities of Franks, Hosn Al-Akrad and Arqa fell completely. In Laodicea the great church only remained, and all those who were inside were delivered. The ground inside the church was rent

asunder, and a chasm which was full of clay appeared, and in the middle of the clay a molten image was standing upright. Similarly, most of Antioch and Tripoli were destroyed.
– Chronicle of 1234: And the year of 1462 arrived. In that year, there was a large earthquake and Sayzar [Shaizar] fell down. Forty thousand persons were killed. The governor and his children were among those who were killed. The citadel that was built on a mountain fell down. A great number of persons were killed in Hama, Salamiya and in many nearby villages.
– Michael the Syrian: And in this year, there were severe earthquakes in Syria and many places were destroyed. In Hamath, the fortress, the town and all large houses fell down upon the citizens. Old men, women, children and a myriad of persons were killed. The fortress of Saizar fell entirely, except a woman and a eunuch. And the people of Emessa were taken by the fear: they fled the town and were delivered. Their houses and the fortress were destroyed. And in same manner, the people in Aleppo fled from the city, and sat down outside it for a few days and were delivered, and their houses were thrown down, and only five hundred persons perished in it. Same was at Kaphar Tab, and Afamia, no one escaped, and many other places as far as Rahabot. Cities of the Franks, Hosn Al-Akrad and Arqa fell down completely. In Laodicea, the great church only remained, and all those who were in the church were delivered. In some cities, the earth was opened. In this city, the earth was opened and lying to watch a chasm full of mud, and in the center of the mud a statue, staying upright, was fusing. Similarly, the greater part of Antioch and Tripoli was destroyed.
– Saadeh (1984): In 1157, there was a very large earthquake in Northern Syria, causing heavy damages in Lattakia and other cities.
Parametric catalogues and previous studies
– Ambraseys and Barazangi (1989): 15 August 1157, 35.1N , 36.3E $M_s >$ 7.0 Hama.
– Ben-Menahem (1979): 1157, July 15, $M_l =$ 6.1, destruction of Baalbak (Amiran; Plassard and Kogoj; Sieberg).
– Plassard and Kogoj (1981): 1157 June 4, 14 and August 12, $I =$ VIII, there were earthquakes causing destruction in Tripoli, Krak, Homs, Hama and Sheizar. Hama and Sheizar citadel were the most affected sites. New earthquakes till 1158 (Al-Suyuti; Berloty; Ibn Al-Jawzi).

⟨084⟩ **1170 June 29 Damascus: VII-VIII; Homs: VII-VIII; Hama: VII-VIII; Al-Sham: VII-VIII; Lattakia: VII-VIII; Baalbak: VII-VIII; Shaizar: VII-VIII; Barin: VII; Aleppo: VII-VIII; Iraq: V; Al-Jazira: V; Al-Mousel: V** (fig. 10)**. Aftershocks, tsunami.**
Sources
– Abu Al-Fida: In this year [565 A.H.] [1169 September 25-1170 September 14], there was a great earthquake, destroying Al-Sham.

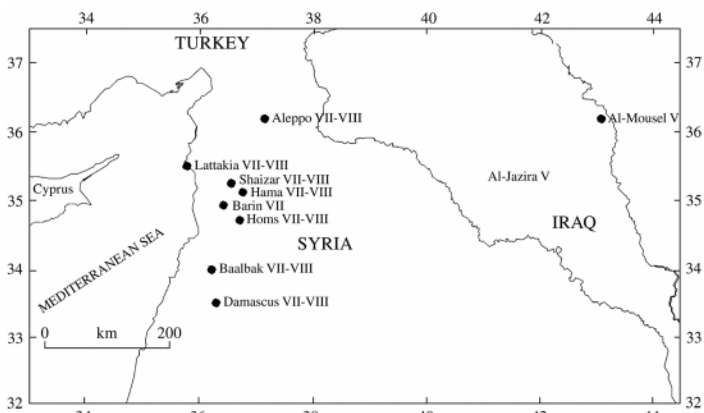

Fig. 10. Map of intensity distribution for June 29, 1170 earthquake.

– Ibn Al-Athir: Also in this year [565 A.H.] 12 Shawwal [1170 June 29], there were successive great terrible earthquakes which had never been seen before. Al-Sham, Al-Jazira, Al-Mousel, Iraq and other countries were affected. They were strongest in Al-Sham, where most of Damascus, Baalbak, Homs, Hama, Shaizar, Barin, Aleppo and others were destroyed, with their ramparts and fortresses, houses collapsed over their residents, killing countless numbers of people. Sultan Nur ed-Din visited these later towns and ordered to rebuild their ramparts and fortresses, while he found Aleppo had not been destroyed as these towns previously. Bilad Al-Firnj [in that time during the Crusader wars the Syrian coastal area was occupied by the Crusaders and called in Arabic Bilad Al-Firanj] was affected.
– Saadeh (1984) during the year of 1170, there was a very large earthquake that occurred in Northern Syria, causing heavy damage in Lattakia and other cities.
Parametric catalogues
– Ambraseys and Barazangi (1989): 1170 June 29, 35.9N-36.4E, $M_{S>}$7.0, tsunami.
– Plassard and Kogoj (1981): 1170 June 29, in Lebanon $I_=$ IX, there was an earthquake, causing destruction in Tripoli and Aleppo (Al-Suyuti; Berloty; Guillaume de Tyre; Perrey).
– Poirier and Taher (1980): 1170 June 30, $I_{0=}$ IX- X (MMS), Aleppo was totally destroyed with 80000 victims. Damage in Orontes Valley. In Antioch, St. Peters cathedral collapsed over the patriarch.
– Ben-Menahem (1979): 1170 June 29, 34.6N, 36.2E, $I_{0=}$XI-XII, $M_{L=}$7.9, damage and casualties in Palestine. It was felt throughout Mesopotamia, Cyprus and Upper Egypt. Tripoli ruined. Destruction at Damascus, Sur, Sidon and Baalbak (most columns fell down). Damage to the walls of Sur. Jerusalem ($M_{M=}$ V-VI). The obelisk at Caesaria may have been thrown down (Amiran; Humphrey; Plassard and Kogoj; Sieberg; Willis).
Seismological compilations
– Ambraseys *et al.* (1994): 1170 June 29, 35 .0N-36.5E, $I_\leq$ VI. A catastrophic earthquake in northwest Syria, felt in Egypt (Abu Shama; Ibn Al-Athir; Ibn Qadi Shuhba).
– Sieberg (1932): 1170 June 29, a destructive earthquake in Syria, killing 2000 persons. Lattakia and half of Hosn Al-Akrad were ruined. Antioch, Jableh, Tripoli and Jerusalem were also felt. Cyprus, Egypt and Mousel were also felt. Aftershocks lasted for three months.

‹095› **1287 March 22 Lattakia: VII-VIII; Palestine: IV; Armenia: IV.**
Sources
Saadeh (1984): In the year of 1287 March 22, a violent earthquake occurred in Lattakia, causing damage in some districts of Lattakia and its harbor, especially in the big tower.
Parametric catalogues
– Plassard and Kogoj (1981): 1287-1285, in Lebanon $I_=$ VI, it was an earthquake that caused destruction in Lattakia (Abu Al-Faraj; Al-Suyuti; Perrey).
– Ben-Menahem (1979): 1287, $M_{L=}$7.3, destructive in north Syria and Armenia. Lattakia ruined. It was felt in Palestine (Al-Sinawi and Ghaleb; Amiran; Plassard and Kogoj; Sieberg; Willis).
Seismological compilations
– Sieberg (1932): 1287, a strong earthquake in Northern Syria killed a large number of people. Lattakia was the most affected city to the extent that it was completely destroyed. It was felt in Palestine and Armenia.

‹098› **1322 January 20-February 19 Damascus: V.**
Sources
– Ibn Kathir: In this year (722 A.H.) of Muharram (1322 January 20-February 19), a great earthquake was felt at Damascus.
Parametric catalogues
– Plassard and Kogoj (1981): 1322 January-February, $I_=$IV, a strong earthquake occurred in Damascus (Al-Suyuti).

‹100› **1344 January 2 Al-Rawendan: VIII; Manbej: VII-VIII; Aleppo: VI-VII; Damascus: IV.**
Sources
– Abu Al-Fida: In this year [744 A.H.] of 15 Shaaban [1344 January 2], a great earthquake occurred, causing destruction of Aleppo and its vicinity. In Manbej, destruction was large and many people were killed under debris. Same was in Al-Rawendan castle.
– Ibn Kathir: In this year [744 A.H.] 15 Sha’ban, Saturday [1344 January 2], a slight shock was felt

by a few people in Damascus. News came from Aleppo mentioning that many houses were destroyed, a few towers of Aleppo citadel, mosques, monuments and walls fell down. Many citadels around Aleppo were destroyed. It was mentioned that most of Manbej had collapsed and most of its inhabitants were killed under the debris.
Parametric catalogues
– Plassard and Kogoj (1981): 1344, I = IV, there was a strong earthquake in Egypt and in Syria (Abu Al-Fida; Al-Suyuti; Perrey).

– Poirier and Taher (1980): 1343 January 1, I_0 = IX, Manbej was destroyed with 5700 victims. Aleppo fortress was destroyed.
Seismological compilations
– Ambraseys *et al.* (1994): 1344 January, a large earthquake in SE Anatolia was said to have been felt as far as Egypt (Al-'Aini; Anonymous; Ibn Al-Shihna; Ibn Habib; Poirier and Taher; Sibt Ibn Al-'Ajami; Taher). There is no effects in south of Damascus, where the shock was only slight (Ibn Kathir).
– Sieberg (1932): 1344, an earthquake was in Syria. It was felt in Egypt.

‹110› **1537 January 7 Antioch: VII; Damascus: IV; Dimyat: IV-V; Egypt: IV.**
New original sources
– Al-Ghazi: A slight shock was felt in Egypt and Damascus on 25 Rajab 943 A.H. (07 January 1537) (Badr Al-Ghazi).
Seismological compilations
– Ambraseys *et al.* (1994): 1537 January 8, Damietta was shaken by earthquakes that continued for four days, five times a day. These shocks may be associated with an earthquake reported to have shaken down many walls in Antioch the same year (Al-'Umari). Alternatively, there may be some connection with the shocks reported in Cairo and Damascus, noted above under 943-1537. Such associations imply a large earthquake in or offshore from Northern Syria, for which one would expect further details to be preserved, and it is more likely that the Antioch earthquake, at least, is a separate event.
– Al-Ghouneim (no date): In 944 A.H. (started from 1537 June 10), there was a great earthquake in Antioch where many walls fell down. Later on, Dimyat was shaken for 4 days, 5 times daily (Al-Jalabi).

‹114› **1565 July 26 Damascus: V.**
New original sources
– Al-Ghazi: A shock occurred on Wednesday early morning, 28 Zu-l-Hijja 972 A.H. (26 July 1565) in Damascus. It was accompanied by a sound from the earth (Badr Al-Ghazi).
Seismological compilations
– Sieberg (1932): 1566, a destructive earthquake was felt till Cyprus.

‹119› **1610 March 7 Aleppo: VI.**
New original sources
– Al-Nablsi: A great earthquake hit Aleppo at sunset time on 11 Zu-l-Hijja 1018 A.H. (07 March 1610) (Al-Ghazi).
Seismological compilations
– Ambraseys and Finkel (1995): A contemporary reports that Aleppo and its environs suffered a great earthquake on the evening of Sunday, 11 Zilhicce (Zulhijeh) 1018 A.H. (7 March 1610) (Al-Hafiz).

‹124› **1626 January 21 Aleppo: VIII-IX; Gaziantab: VIII-IX; Hama: VI-VII; Damascus: V** (fig. 11)**.**
Sources
– Al-Nablsi: A slight shock was felt in Damascus on Wednesday 22 Rabi' II 1035 A.H. (21 January 1626). In the meantime an earthquake hit Hama, causing the Souk Al-Dahsheh to collapse and killing many people under the debris (Al-Ghazi).
Seismological compilations
– Ambraseys and Finkel (1995): there was a great earthquake in the Middle East as result of which many places in the region of Aleppo and Gaziantep were ruined with great loss of life (LBS, BDP). This is most probably the earthquake of Wednesday, 22 Rebi-II 1035 A.H. (21 January 1626).

‹134› **1705 November 24 Yabroud: VIII; Al-Qastal VIII; Damascus: VII; Tripoli: VII. Aftershocks.**
Sources
– Al-Nablsi: He mentioned, as an eyewitness, that three main different sized shocks happened on Tuesday night, 7 Sha'ban 1117 A.H. (24 November 1705) in Damascus. The first one caused general panic while the second was the strong-

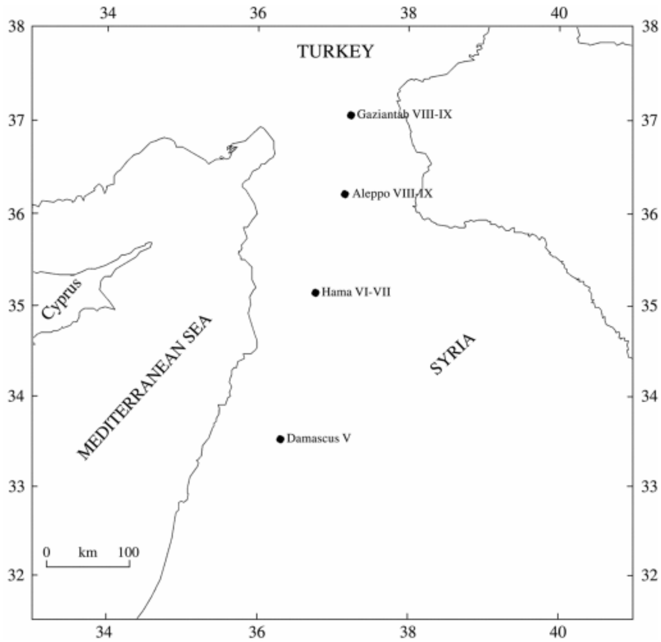

Fig. 11. Map of intensity distribution for January 21, 1626 earthquake.

est, causing houses to fall, walls to be destroyed in and around Damascus and top of the eastern minaret of the Umayyad Mosque to split, upper portion of the Murshidiyah minaret and Al-Afram minaret to fall, to the extent that large number of people in the villages were killed under the debris. In Al-Qastal village, its fortress collapsed as well as a monastery in Yabrud village. Light shocks continued to be felt till Ramadan [aftershocks were felt for one month].

Seismological compilations

– Ambraseys and Finkel (1993): A destructive earthquake occurred on Tuesday night, 7 Sha'ban 1117 A.H. (24 November 1705) in the northern part of the Bekaa Valley in Lebanon. It was preceded by a strong foreshock that caused panic in the area of Damascus. In Damascus, many strong aftershocks occurred, causing some houses to fall, walls to be destroyed, people to be killed in the debris, top of the eastern minaret of the Umayyad Mosque to split, upper portion of the Murshidiyah minaret and Al-Afram to fall. Fortress of Al-Qastal and its villages were destroyed. A monastery in Yabrud and many houses in the villages were also destroyed (Al-Nablsi). In Tripoli, roofs and walls of the city, some of the walls of the towers of the coastal fort and some of the quarters of the gar were destroyed.

(157) **1822 August 13, 09:50 p.m. (local time) Jisr Ash'Shoughour: IX; Quseir: IX; Aleppo: VIII-IX; Darkoush: VIII-IX; Antioch: VIII; Iskenderun: VIII; Idleb: VIII; Sarmeen: VIII; Kelless: VIII; Armanaz: VII-VIII; Sarmada: VII-VIII; Lattakia: VII; Homs: VII; Hama: VII; Maraash: VII; Ram Hamadan: VII; Bennesh: VII; Maarret Missrin: VII; Damascus: III; Gaza: III; Al-Quds: III; Black Sea: III; Cyprus: III** (figs. 12, 13 and 14)**. Faulting, tsunami.**

Parametric catalogues and previous studies

– Ambraseys (1989): 1822 August 13, 20:40 (LT), 36.7N-36.9E, M_s=7.4, I_0 (MSK) = X.

– Plassard and Kogoj (1981): 1822 August 13, in Lebanon I=V, an earthquake, causing destruction in Antioch, Aleppo and Lattakia with

tsunami. It was felt in Damascus and Cyprus (Blanckenhorn; Sieberg; Willis).
– Poirier and Taher (1980): 1822 August 13, I_0 = X-XI (MMS) , Aleppo destroyed at 60%, sea wave at Iskenderun.
– Ben-Menahem (1979): 1822 August 14, 36.4N-36.2E, I_0=X-XI, M_L=7.1, destruction of Antioch and Aleppo. Felt in Jerusalem and Cyprus. Tsunami at Beirut (Amiran; Kárník; Ergin *et al.*; Plassard and Kogoj; Sieberg).
– Ambraseys and Barazangi (1989): 36.7N-36.9E, M_S=7.4.
Seismological compilations
– Ambraseys (1989): 1822 August 13, this earthquake was the largest in the Border Zone in the last five centuries. It was felt from the coast of the Black Sea to Gaza, and it was followed by an aftershock sequence that lasted almost 2.5 years. The shock almost destroyed the region between Gaziantep and Antakia in Turkey and Aleppo and Khan Sheikhun in NW Syria, killing a very large number of people. Slight shocks began on August 5 and continued until August 12, reported from Aleppo and Antioch. At 8 h 10 min p.m. on August 13 a strong shock was felt in the region between Lattakia, Aleppo and Antioch, causing considerable concern. The main shock happened 30 min later. Gaziantep and its surrounding villages were almost completely destroyed with great loss of life. Damage was equally heavy in the districts of Shikaghi and particularly of Jum and in the settlements along the Aafrine River. The ground opened up for some distance. The Orontes River overflowed its

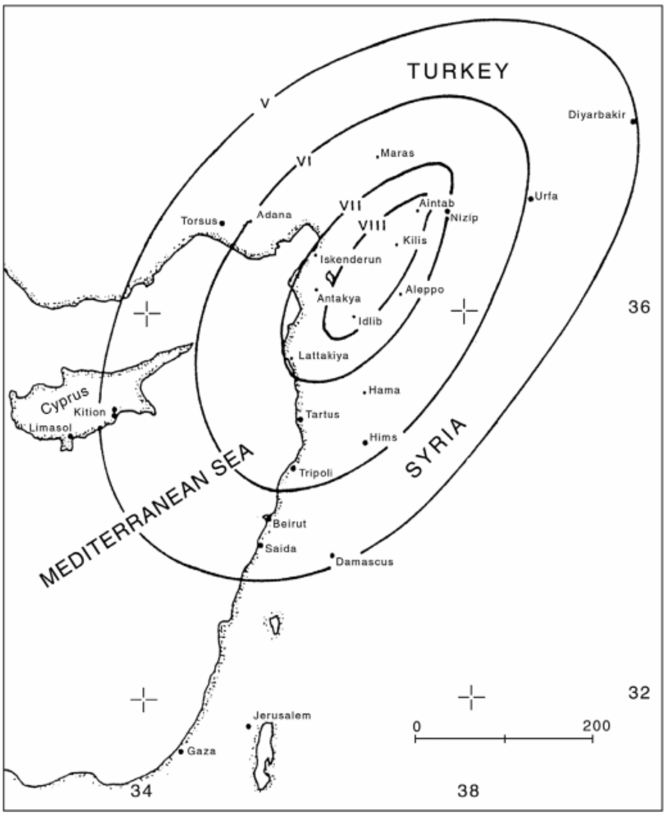

Fig. 12. Map of intensity distribution for August 13, 1822 earthquake (Ambraseys, 1989).

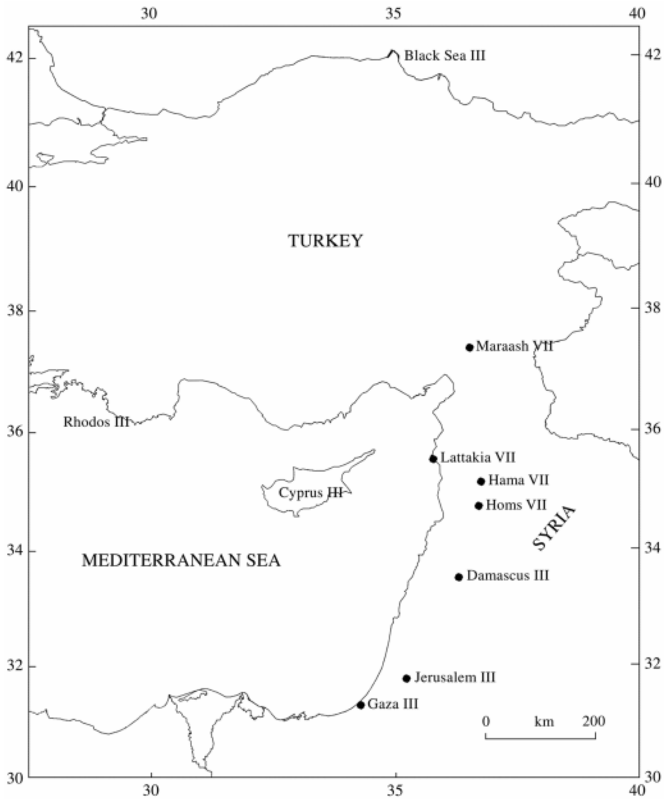

Fig. 13. Map of intensity distribution for August 13, 1822 earthquake.

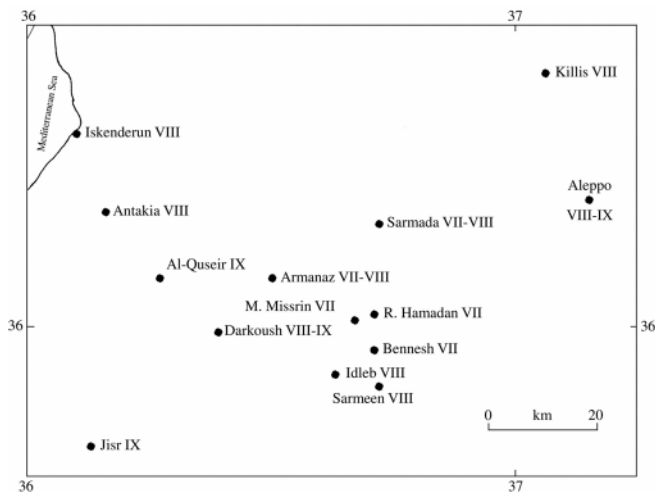

Fig. 14. Detailed map of intensity distribution for August 13, 1822 earthquake, between Antakia and Aleppo.

banks destroying bridges and embankments. Killis was destroyed with loss of life. Harem and Armanaz were totally destroyed. Darkush was ruined partly and a landslide blocked the Orontes River. Jisr As-Shugr was entirely destroyed with loss of life. Khan Sheikhun, Ariha, Idleb and particularly Maarat were almost completely ruined but the loss of life was not great. Houses collapsed in these places but large buildings, although shattered, were left standing, except in Maarat where they were brought down by aftershocks which also crevassed the banks of the Orontes. It is said that damage extended to Hama and that it suffered as much as Aleppo. Aleppo was ruined with 7000 deaths within the walls of the city. The walls of the citadel were ruined. Many houses, gates and *Souks* were ruined. It is said that before the earthquake the temperature of well water had increased. Antioch and its surrounding villages were ruined. Many small settlements in the upper and lower Quseir area were razed to the ground and there was a liquefaction of the ground near the town. Beilan was heavily damaged without casualties. In Iskenderun, number of houses were destroyed with liquefaction. At Payas, some houses sunk into the ground but without loss of life. One-third of Lattakia was destroyed and one-third damaged. In Marina, the fort, the mosque and the large khan collapsed, and houses and stores were considerably damaged. Jableh was more heavily damaged and people were killed. Damage was also reported from Markab and the castle of the Crusaders partly collapsed. Villages in the regions of Adana and Misis were ruined. Marash and Nizip also seem to have been affected. Tarsus was strongly affected by this event. At Homs it caused unspecified damage. At Tripoli and its dependencies, it was violent and caused damage. It was strongly felt at Beirut, Sidon, Jerusalem, Gaza, Trabzon, Tokat and Merzifon. It caused panic at Damascus. It was felt in Cyprus and Mesopotamia. It was felt at Urfa, Dyar Bakr and along the Euphrates and caused some damage. Destructive aftershocks occurred in 1822 August 15 and 23, September 5 and 29, October 18 and 1823 June 30, the sequence terminating in 1824 March. The total number of killed people varies between 30000 and 60000 (Consular Archives; Güzelbey and Yetkin; Press Reports).

– Sieberg (1932): 1822 August 13, a vast destructive earthquake in Northern Syria. It was said that 20000 people were killed. Antioch was a victim completely to that earthquake. In Aleppo, 2/3 of houses became not suitable for living and it was said that 1/3 inhabitants were killed. In Iskanderun and Lattakia, there was heavy damage to the houses. It was felt in Adana, Dayr Bakir, Damascus, Jerusalem and Cyprus. Aftershocks continued to the end of June 1823 in Aleppo and Lattakia.

– Al-Tabakh Al-Halabi (1925): Al-Sheikh Bakri Kateb [a religious leader in Aleppo] says that: «In August, many great earthquakes occurred causing the collapsing of the Jewish quarter, the *Souk* of Perfumery and Al-Aqaba [in Aleppo]. These earthquakes lasted 40 days for every day, collapsing schools and houses in the city [of Aleppo] to the extent people went out of the town. Minerat of the great Mosque was cracked». Jawdat Basha says that: «On the 3rd hour of the night of 6 Zu-L-Hijja 1237 A.H. [1822 August 23], a strong earthquake occurred in Aleppo, Kelless, Antioch and their vicinity, causing many buildings to collapse and large number of people to die under the debris». I [means Al-Tabakh Al-Halabi] catch a poem arranged by Mohammad Taqi ed-Din who lived in Aleppo during this year [1237 A.H.], describing these earthquakes and their effects in the localities. He says: «An awful earthquake occurred in Aleppo on the night of Wednesday [Tuesday], buildings fell, people were killed, khans collapsed, mosques ruined and the citadel of Aleppo collapsed with falling its stones in the surrounding trench. In Homs, Hama, Marash and Al-Maarat, people were killed. In Ariha and Salqein, the earth faulted. The earth in Gaziaintab and Atareb was shaking. Both Al-Quseir and Jisr Ash'Shougour cities were ruined and people were killed. Houses ruined and people killed in the villages of Aleppo. The ground in Al-Atareb and Ipin sunk. Ram Hamadan suffered. Idlib and Sarmeen became ruined completely. Bennesh and Maarret Missrin were ruined partially. In Darkoush, all houses fell, people were killed and sunk. In Armanaz, houses fell, some inhabitants ran away, others lost and others were injured. Kelless suffered as Aleppo. Sarmada and its vicinity collapsed and people ran away. In Antioch the tower, the city wall, khans and houses collapsed». Al-Sheikh Mohammad Al-Termanini from Aleppo (died in 1250 A.H.) says that: «On the 3rd hour of the night of 27 Zu-L-Qada 1237 A.H. [1822 August 14] there was an earthquake in and around Aleppo. While we were talking on the 3rd hour of that night, a terrible earthquake occurred causing great panic. At the beginning, we thought it was The Day of Judgment. This earthquake caused the collapse of houses, palaces, and the loss of about 10000 lives. We ran away to the desert. This earthquake caused also the collapse of houses, schools, mosques and soaks that were in front of the gate of the citadel [of Aleppo], starting from Khan Al-Farayin (in the west) to the Salt Square, Al-Mzaweq and Bab Al-Ahmar (in the east), and to the boundaries of Al-Qasileh and Al-Saphahiyya (in the north); only the school of Khessrow Basha, Mosque of Al-Atroush, the school of Al-Sultaniyya and the bath of Al-Nassiryya survived».

– ANF: A terrible earthquake occurred in 1822 August 13 at 09:50 p.m. (local time) lasted for one minute, causing great damage at Aleppo, destroying monuments, minarets, high buildings and walls of Aleppo, and killing many people. At Lattakia, half the city was destroyed and it was more terrible than the 1794 earthquake. Antioch was completely reduced to ruins and many open fractures appeared, producing smoke and lava (?). The Orontes River fled on the neighboring banks, destroying villages, bridges and dams. Iskenderun was destroyed. New springs appeared. The deeply affected area in north west Syria has a radius of 160 km. Villages of Aleppo district were demolished and others swallowed up. The seismic waves had vertical and horizontal components with East West direction. (In fact, this earthquake was followed by many big aftershocks from the date of the main shock up to writing this letter).

6.3. *Re-evaluated seismic events*

In this section we studied each historical earthquake by means of a careful examination of all available references. In addition we restimated all earthquake parameters (intensity, earthquake location, estimated magnitude; see table I) by a unified standard with the aim of providing a homogenous standard list of seismic events with the same characteristics.

‹002› **590 B.C. Tyre: VII? Tsunami at the Lebanese coast.**

Parametric catalogues

– Plassard and Kogoj (1981): 590 B.C., in Lebanon $I_=$IX, destruction in Tyre with tsunami.

– Ben-Menahem (1979): 590 B.C., $I_{0=}$IX-X, $M_{L=}$ 6.8, off Coast epicenter, flooding at Sur, tsunami at Lebanese coasts (Amos, Psal.).

Table I. Parametric catalogue of large historical earthquakes in Syria and its surroundings. The magnitude is calculated following Shebalin (1970), Ambraseys and Barazangi (1989) and Ambraseys (1997).

No.	Date (day.month.year)	Lat. (°N)	Long. (°E)	Major affected localities	I_0 (EMS-92)	H (km)	M_s
01	37 A.D.	36.00	36.30	Antioch, Dafneh	VII-VIII	15	6.2
02	53	36.20	36.50	Antioch, Afamia, Manbej, Lattakia	VIII	30	6.6
03	303-304	33.80	34.30	Saida, Sur, Syria	VIII-IX	20	7.1
04	494	35.80	36.30	Antioch, Tripoli, Lattakia	VII-VIII	25	6.5
05	22.08 .502	33.00	34.80	Akka, Sur, Saida, Beirut, Safad	VIII-IX	30	7.2
06	531-534	35.50	37.20	Area between Aleppo and Homs	VIII	15	6.5
07	09.07.551	34.00	35.50	Cities of Lebanese coast, Arwad	IX-X	28	7.2
08	565-571	36.00	36.20	Antioch, Seleucea, Kilikia, Anazrabo	VII-VIII	30	6.0

Table I (*continued*).

No.	Date (day.month.year)	Lat. (°N)	Long. (°E)	Major affected localities	I_0 (EMS-92)	H (km)	M_s
09	18.01.747	32.50	35.60	Mt. Tabor, Baalbak, Bosra, Nawa, Balqa, Al-Quds, Beit Qubayeh, Tabaryya, Damascus, Daraa	IX	25	7.2
10	24.11.847	34.40	36.30	In and around Damascus, Antioch, Al-Mosel	IX	35	7.5
11	30.12.859-29.01.860	35.70	36.40	Antioch, Lattakia, Jableh, Homs, Palmyra, Tarsus, Balis, Damascus, Adana, Ar-Raqqa	VIII-IX	33	7.4
12	05.04.991	33.70	36.40	Baalbak, Damascus	IX	22	7.1
13	30.07-27.08.1063	34.40	36.20	Tripoli, Lattakia, Akka, Sur	VIII	32	6.9
14	11.1114	37.30	38.50	Maskaneh, Maraash,	VIII-IX	40	7.4
15	11.1114	37.30	36.50	Samsat, Orfa, Harran	IX	40	7.7
16	27.09.1152	32.60	36.70	Bosra, Hauran, Syria	VIII	12	5.8
17	02-04.04.1157	35.50	36.50	Shaizar, Hama, Kafer Tab, Aleppo	VII	22	6.0
18	13.07.1157	35.20	36.60	Hama, Afamia, Kafer Tab, Homs, Tayma	VIII	25	6.6
19	12.08.1157	35.40	36.60	Shaizar, Kafar Tab, Afamia, Hama, Arqa, Aleppo, Homs, Lattakia, Tripoli, Antioch, Qalaat Al-Hosn, Maarret Annooman	IX-X	15	7.4
20	29.06.1 170	34.80	36.40	Damascus, Homs, Hama, Lattakia, Baalbak, Shaizar, Barin, Aleppo	IX	35	7.7
21	20.05.1202	34.10	36.10	Mount Lebanon, Baalbak, Sur, Beit Jin, Banyas, Nablus, Al-Samyra, Damascus, Safita, Akka, Tripoli, Hauran, Beirut, Homs, Tartus	IX	30	7.6
22	02.01.1344	36.70	37.40	Al-Rawendan, Manbej, Aleppo	VIII	30	6.8
23	20.02.1404	35.70	36.20	Blatnes, Bkas, West of Aleppo, Qalaat Al-Marqeb, Tripoli, Lattakia, Jableh	VIII-IX	30	7.4
24	29.12.1408	35.80	36.10	Shugr, Bkas, Blatnes, Lattakia, Jableh, Antioch, Syrian coast	IX	25	7.4
25	10.10.1568	35.50	35.50	Lattakia, Famagusta	VIII	12	6.0
26	21.01.1626	36.50	37.10	Aleppo, Gaziantab, Hama	IX	20	7.3
27	22.09.1666	37.00	43.00	Al-Mousel, Sinjar, Sharqat	IX	35	6.9
28	24.11.1705	33.70	36.60	Yabroud, Al-Qastal, Damascus, Tripoli	VIII	35	6.9
29	15.04.1726	36.30	36.60	Jum, Aleppo	VIII	15	6.1
30	25 .09.1738	36.70	36.50	Iskenderun, Bellen Bass, Antioch, Jabal Al-Amanus, Aleppo	VIII	10	6.2
31	30.10.1759	33.10	35.60	Al-Qunaytra, Safad, Akka, An-Nasra, Sidon, Saasaa	VIII-IX	20	6.6
32	25.11.1759	33.70	35.90	Baalbak, Zabadani, Ras Baalbak,	IX	30	7.4

Table I (*continued*).

No.	Date (day.month.year)	Lat. (°N)	Long. (°E)	Major affected localities	I_0 (EMS-92)	H (km)	M_s
				Al-Qunaytra, Damascus, Beirut, Saida, Safad, Sur, Tripoli, Homs, Hama, An-Nasra, Lattakia, Al-Quds, Gaza, Antioch			
33	26.04.1796	35.30	36.20	Qalaat Al-Marqeb, Al-Qadmous, Nahr Al-Kabir, Jableh, Bkas, Lattakia	VIII-IX	20	6.8
34	13.08.1822	36.10	36.75	Jisr Ash'Shoughour, Quseir, Aleppo, Darkoush, Antioch, Iskenderun, Idleb, Kelless, Armanaz, Sarmada, Lattakia, Homs, Hama, Maraash, Ram Hamadan, Bennesh, Maarret Missrin	IX	18	7.0
35	01.01.1837	-	-	Safad	VIII		>7.0
36	03.04.1872	36.20	36.50	Harem, Armanaz, Lake of Al-Amq, Antioch, Aleppo, Suaidiya, Izaz, Idleb, Iskenderun	VIII-IX	10	5.9

Seismological compilations
– Sieberg (1932): 590 B.C., a great shock occurred, causing a destructive sea wave in Tyre.

(003) **525 B.C. Tyre: VIII-IX; Sidon: VIII-IX; Kiklades island: III-IV; Eubea island: III-IV. Tsunami at the Lebanese coast.**
Parametric catalogues
– Plassard and Kogoj (1981): 525 B.C., in Lebanon I_0=X, destruction in Tyre and Sidon with tsunami, destruction in Bisri (Strabon).
– Ben-Menahem (1979): 525 B.C., off Coast Sur, I_0=XI, M_L=7.5, Sur destroyed. Sidon greatly damaged. Tsunami at Lebanese coast.
Seismological compilations
– Sieberg (1932): 525 B.C., Sure was completely destroyed. Two thirds of tall buildings in Sidon were ruined. Tsunami in the Lebanese coast. It was felt in Kiklades and Eubea Islands.

(005) **199-198 B.C. Sidon: VIII; Syria: ≤VII. Landslide at Sidon.**
Seismological compilations
– Guidoboni *et al.* (1994): 199-198, Sidon I_0=X, a series of shocks felt in Sidon and almost two thirds of it collapsed. A city above Sidon was swallowed up. It was less strongly in Syria with moderate intensity. There was a limited number of victims (Posidonois).

(007) **92 B.C. Syria: III-IV; Egypt: III-IV. Tsunami at the Syrian-Lebanese coasts.**
Parametric catalogues
– Plassard and Kogoj (1981): 92 B.C., I_0=VI, strong earthquake felt till Egypt.
– Ben-Menahem (1979): 92 B.C., February 28, SE Cyprus, M_L=7.1, big tsunami hit Levantine coastal cities. It was felt in Syria, Egypt and Palestine (NSH; Plassard and Kogoj; Talmud; Willis).
Seismological compilations:
– Sieberg (1932): 92 B.C., an earthquake occurred in Syria. It was felt in Egypt.

(008) **65 B.C. Syria: VII-VIII; Antioch: VII-VIII; Al-Quds: VI; Cyprus: III-IV; Salamis: III-IV; Famagusta: III-IV.**
Parametric catalogues
– Plassard and Kogoj (1981): 69 B.C., I_0=IV, destruction in Antioch.
– Ben-Menahem (1979): 64 B.C., M_L=7.7, 36.2N, 36.1E, destruction of Antioch. It was

felt in Cyprus. damage to the temple walls in Jerusalem (Amiran; Plassard and Kogoj; Sieberg; Willis; Yebamoth).

Seismological compilations

– Sieberg (1932): 69 B.C., a heavy earthquake destroyed many cities in Syria. Antioch was included in this destruction. It was said that 17 000 people were killed in Syria. Shocks reached Palestine and Cyprus (Salamis and Famagusta).

– Guidoboni *et al.* (1994): 65 B.C., Antioch, Syria I$_{\times\leq}I_{\leq\times}$I, a destructive earthquake hit Antioch causing one hundred and seventy thousands deaths and destroyed many cities (Pompeos Trogus and Malalas).

(009) **37 B.C. March 23, morning Dafneh: VI-VII; Antioch: V.**

Seismological compilations

– Guidoboni *et al.* (1994): 37 B.C. March 23, Antioch suffered and Dafneh was damaged (Malalas).

(010) **19 A.D. Sidon; Palestine; Syria; Asia Minor.**

Parametric catalogues

– Plassard and Kogoj (1981): 19 A.D., in Lebanon $I_{=}$ VI, a strong earthquake at Sidon (Sieberg).

– Ben-Menahem (1979): 19 A.D., off coast Sidon, $I_{0=}$IX-X, $M_{L=}$6.8, destruction at Sidon. It was felt in Palestine, Syria and Asia Minor (Amiran; Plassard and Kogoj; Willis).

Seismological compilations

– Sieberg (1932): 19 B.C., an earthquake was in Sidon.

(011) **37 A.D. Antioch: VII-VIII; Dafneh: VII; Al-Quds: IV.**

Parametric catalogues

– Plassard and Kogoj (1981): 37 A.D., $I_{=}$IV, a destructive earthquake at Antioch. It was felt at Jerusalem (Sieberg).

Seismological compilations

– Guidoboni *et al.* (1994): Antioch, Daphne VIII $_{\leq}I_{\leq x}$, Antioch suffered from an earthquake in the morning of 23 March 37. Dafneh area was also damaged (Malalas).

– Sieberg (1932): 37 B.C., a destructive earthquake in Antioch. It was felt in Jerusalem.

(012) **47 Antioch: VII.**

Seismological compilations

– Guidoboni *et al.* (1994): 47 A.D., Antioch VIII $_{\leq}I_{\leq x}$, a violent earthquake in Antioch (Philostratus). Antioch was shaken by an earthquake where the famous palaces collapsed and cracks appeared in many temples (Malalas).

(013) **53 Antioch: VII-VIII; Afamia: VI-VII; Manbej: VI-VII; Lattakia:VI-VII** (fig. 15)**.**

Parametric catalogues

– Plassard and Kogoj (1981): 53 A.D., $I_{=}$IV (in Lebanon), destructive earthquake at Antioch, Apamea and Lattakia (Sieberg).

– Poirier and Taher (1980): 52 A.D., $I_{0=}$VIII-IX (MMS), destruction in Antioch.

Seismological compilations

– Sieberg (1932): 53 A.D., there was an earthquake in Syria. In Antioch, temples of Diana and Hercules were destroyed. There was heavy damage in Menbej, Lattakia, Apamia.

(014) **82-94 Antioch: VI-VII, Syria. Aftershocks.**

Seismological compilations

– Sieberg (1932): between 82-94 A.D., a strong widespread earthquake struck Syria causing destruction of many houses at Antioch. Shocks lasted for 40 days.

(015) **115 December 13 Antioch: VII; Eleyah: VI-VII; Mirana: VI-VII; Rhodos: IV; Pitana. Tsunami at Caesaria, the Lebanese coast and Yavne.**

Parametric catalogues

– Plassard and Kogoj (1981): 115 December 3, $I_{=}$ VII (in Lebanon). It has an intensity VII at Beirut and all the Lebanese Coast. It was destructive at Antioch (Shalem).

– Poirier and Taher (1980): 115 A.D., $I_{0=}$X-XI (MMS), heavy destruction in Antioch.

– Ben-Menahem (1979): 115 December 13, at night, near Samandag, $M_{L=}$7.4, it was felt all over the near east and the Eastern Mediterranean up to Rhodos. Destruction of Antioch. Tsunami hit Yavne and Caesaria in Palestine (Ergin *et al.*; Plassard and Kogoj; Shebalin *et al.*; Sieberg; Willis).

*Seismological compilation*s

– Guidoboni *et al.* (1994): 115 December 13,

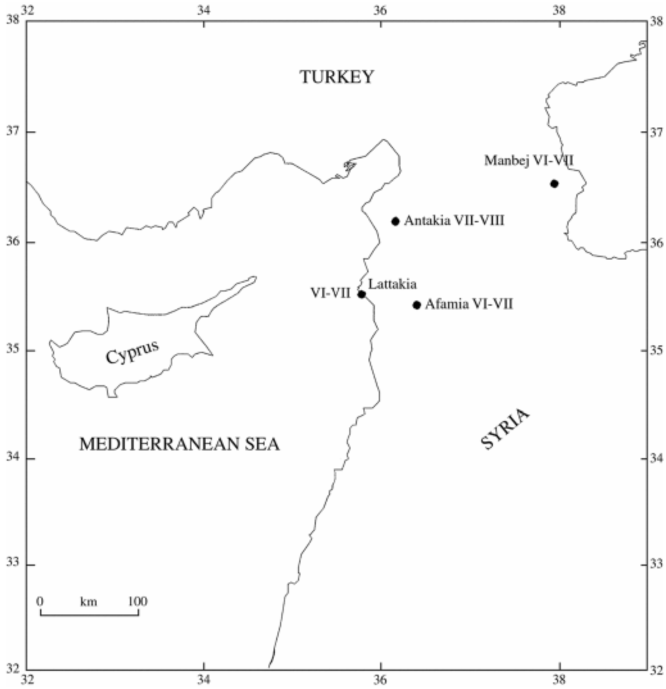

Fig. 15. Map of intensity distribution for the 53 A.D. earthquake.

Antioch Ix sIs xI, Antioch was struck by a violent earthquake, many cities were badly damaged, buildings were thrown into the air, large number of casualties and injured (Dio Cassius). Antioch, near Daphne, suffered from this earthquake (Malalas). An earthquake in Antioch (Incomplete Fragment XXXV in the Fasti Ostiensis).
—Sieberg (1932): 115 December 13, at night, an earthquake destroyed two thirds of Antioch. 1600 victims. Destruction of Eleyah, Mirina and Pitana (near Antioch). It was felt in Rhodos.

(016) **130 Damascus: V-VI; Baalbak: V; Eastern Mediterranean region. Aftershocks.**
Parametric catalogues
—Plassard and Kogoj (1981): in 130, there was an earthquake in Syria and Palestine. It was strongly felt in Baalbak.
—Ben-Menahem (1979): M_L 6.1, strong in Damascus (Plassard and Kogoj; Sieberg; Willis).
Seismological compilations
—Sieberg (1932): 130, a strong earthquake in Damascus and many aftershocks lasted for the next year.
—Lemmens (1898): in 131 A.D., there was an earthquake in the Eastern Mediterranean region and Syria.

(017) **160 October Dura Europos: VI.**
Seismological compilations
—Guidoboni *et al.* (1994): a morning in October 160, an earthquake struck Dura Europos (Baur and Rostovtzeff, 1931).

(018) **220 Antioch: VI. Aftershocks.**
Seismological compilations
— Sieberg (1932): 220 A.D., a destructive earthquake in Antioch. It was followed by a large number of shocks.

(019) **233 Damascus: VII.**
Parametric catalogues
— Ben-Menahem (1979): 233 A.D., M_L6.3, damage in Damascus.

Seismological compilations
- Sieberg (1932): 233 A.D., there was an earthquake in Syria causing destruction of many houses at Damascus.

(020) 242-245 Antioch: VI-VII; Syria: VI-VII; Egypt: III; Iran: III.
Parametric catalogues
- Ben-Menahem (1979): 245, M_L=7.5, near Antioch (Willis).

Seismological compilations
- Sieberg (1932): 242 or 245, a strong earthquake in Antioch and all over Syria. It was felt in Egypt and Iran.

(021) 272 Antioch: VI; Syria: VI.
Seismological compilations
- Sieberg (1932): 272 A.D., a strong earthquake in Antioch and all over Syria.

(022) 303-304 Sidon: VIII; Tyre: VIII; Syria: VII; Al-Quds: III-IV. Tsunami at Caesaria.
Parametric catalogues
- Plassard and Kogoj (1981): 306 A.D., in Lebanon I_0=IX, it was a destructive earthquake at Tyre and Sidon. There was a tsunami in Caesaria (Cesare) in Palestine (Eusèbe; Perrey).
- Ben-Menahem (1979): 306-308, off coast Sur, I_0=X, M_L=7.1, destruction at Sur and Sidon. Felt in Jerusalem. Tsunami at Caesaria (Amiran; Plassard and Kogoj; Sieberg; Willis).

Seismological compilations
- Guidoboni *et al.* (1994): 303-304, Sidon IX≤I≤XI, a terrible earthquake caused many buildings to collapse at Tyre and Sidon, and a large number of people were killed (Chronicon of Eusebius). An earthquake followed in Syria, as a result of which buildings collapsed everywhere, and thousands of people were crushed in Tyre and Sidon (Orosius). A date 303 for this event was mentioned by Hermann (1962).
- Russell (1985): 306, a terrible earthquake at Tyre and Sidon threw down many buildings, and in-numerable people were crushed (Chronicon of Eusebius). A date *ca.* 303 may be more nearly cor-rect (Ambraseys). Russell believes that sites in the Galilee would have been affected by this event.
- Sieberg (1932): 306, a strong earthquake in Syria. Tyre and Sidon were destroyed. The earthquake was felt in Jerusalem.

(023) 341 Antioch: VI-VII; Beirut: VII. Aftershocks.
Parametric catalogues
- Ben-Menahem (1979): 334, M_L=7.0, destruction of Antioch. Felt all over the near east (Ergin *et al.;* Sieberg; Willis).
- Plassard and Kogoj (1981): 344, destruction in Cyprus, in Lebanon I= IV (Theophanes; Perrey). - Poirier and Taher (1980): 340, I_0= IX (MMS), heavy destruction in Antioch.
- Ergin *et al.* (1967): an earthquake was in Antioch.

Seismological compilations
- Guidoboni *et al.* (1994): 341 A.D., a series of earthquakes occurred in the Eastern Mediterranean and in particular at Antioch for the whole year (Socrates). The church of Arian collapsed (Michael the Syrian). In the year 341, Antioch was shaken by a violent earthquake for three days (Theophanes). An earthquake at Antioch lasted for three days in the year 341-342 (Cedrenus). - Sieberg (1932): In 334, a strong earthquake in Syria and the near East. It was said there were 40000 victims. Antioch was destroyed. In 340, an earthquake destroyed Beirut, killing a large number of people. In 341, a destructive earthquake in Antioch, followed by many shocks.

(024) 348-349 Beirut: VII; Arwad: VI. Tsunami?
Parametric catalogues
- Plassard and Kogoj (1981): 349, I=X, a destructive earthquake at Beirut, I= X or IX, where most of the city was destroyed (Anstase). - Ben-Menahem (1979): 349-348, off coast Beirut, I_0=X, M_L=7.0, Syrian coast. Destruction at Beirut (Plassard and Kogoj; Sieberg; Willis).

Seismological compilations
- Guidoboni *et al.* (1994): 348-349, Beirut VIII ≤I≤ IX, a powerful earthquake destroyed most of Berytus (Theophanes; Cedrenus). Grumel in 1958 dates it to 348.
- Sieberg (1932): 348, a destructive earthquake in the Syrian coast, causing damage in Beirut and Arwad with tsunami.

⟨025⟩ **363 May 18-19, night This earthquake destroyed Palestine and parts of Jordan, Panyas: VII.**

Seismological compilations

– Guidoboni *et al.* (1994): 363 May 18-19 night, Jerusalem, Sebastia and Nicopolis I=X. A furious storm and earthquake occurred in Jerusalem, and the fire broke out in the temple and there was a light in the sky in the form of a cross (Gregory of Nazianzus). On the night, a mighty earthquake tore up the stones of the old foundations of the temple, and dispersed them all together with the adjacent edifices. Fire came down from heaven and consumed all the builders' tools (Socrates; Sozomen; Philostor-gius; Theodoret). The land shook considerably, and there were great tremors in the towns round about. Many Christians and the majority of the Jews perished in that scourge not only by the earthquake but also as a result of fire and in the heavy rain they had. More than half of Beit Gubrin, part of Baishan, Sebastia and its territory, Nicopolis and its territory, more than half of Lydda and its territory, about half of Ascalan, Antipatris and its territory, part of Caesarea, more than half of Samaria, a third of Paneas, half of Azotus, part of Gophna, more than half of Petra, more than half of Hada, a suburb of Jerusalem, more than half of Jerusalem. Fire came forth and consumed the teachers of the Jews. Part of Tiberias and its territory, more than half of Areopolis, Sepphoris and its territory, Aina d-gader, Haifa flowed with blood for 3 days, Japho perished. This event took place on Monday at the third hour, and partly at the ninth hour of the night. There was great loss of life here. It was on 19 Iyyar of the year 674 [May 363] of the kingdom of Alexander the Greek (Cyril of Jerusalem?). In 365 July 21, a great earthquake occurred in Areopolis, and the sea swept in over the shores of the whole wold, and the city walls collapsed that same night (Jerome in his Commentary on Isaiah). Many cities in Palestine were destroyed (Libanius). 21 cities were destroyed (Chronicle of 724; Chronicon Maroniticum). 22 cities were destroyed (Agapius of Menbij). It was a sudden fire rather than an earthquake (Ammianus; Ambrose; John Chrysostom). The Temple was destroyed (Coptic source). It was wrongly taken to be the 365 earthquake (Amiran).

– Russell (1985): 363 May 19, such as Cyril of Jerusalem' description as above.

– Sieberg (1932): 362, before June, a strong earthquake occurred at the eastern bank of the Dead Sea, causing a flood. Cities of Areopolis and Kerak were destroyed. At Jerusalem, the Temple suffered.

⟨026⟩ **394-396 Antioch: V-VI.**

Parametric catalogues

– Poirier and Taher (1980): 394 and 396, I_0=IX (MMS), heavy destruction in Antioch.

Seismological compilations

– Sieberg (1932): 396, a strong earthquake in Antioch.

⟨027⟩ **450-457 September Tripoli: VI-VII.**

Parametric catalogues

– Plassard and Kogoj (1981): 457, I=IV, a destructive earthquake at Antioch (Cedrenus; Perrey).

Seismological compilations

– Guidoboni *et al.* (1994): 450-457 September, Tripoli VIII≤I≤X, Tripoli in Syria suffered from the wrath of God, at night (Malalas).

– Sieberg (1932): In 445, a strong earthquake was in Tripoli.

⟨028⟩ **458 September Antioch: VII-IX.**

Parametric catalogues

– Poirier and Taher (1980): 458, I_0=IX (MMS), 80000 victims in Antioch.

Seismological compilations

– Guidoboni *et al.* (1994): 458 September 13-14, Antioch VIII≤I≤IX, a destructive earthquake struck Antioch with a large number of victims and homeless and habitant ran towards the mountain tops (Severus of Antioch). A dreadful trembling and shaking of the earth occurred in Antioch, destroying nearly all the buildings in the new city, towers and baths (John of Rhetorician). Antioch suffered its fourth calamity on Sunday 13th September (Malalas). Two parts of Antioch were destroyed and caused many deaths (Chronicle of 724). It was between 456 to 459 A.D. (Pseudo-Dionysius of Tellmahre). It was a terrible earthquake in 457-458 causing nearly all the city to reduce to ruins (Theophanes). It was in 457 (Cedrenus).

– Sieberg (1932): 457-458, a strong earthquake in Northern Syria destroyed a large part of Antioch.

⟨029⟩**475 September Jableh: VII-VIII.**
Seismological compilations
– Guidoboni *et al.* (1994): 475 September, Jableh VIII $\leq I \leq$ X, Jableh suffered (Malalas). It was dated on 478-479 (Pseudo-Dionysius of Tellmahre).
– Sieberg (1932): In 477, a strong earthquake in Jableh. In 479, a strong earthquake destroyed a large number of houses in Syria.

⟨030⟩**494 Antioch: VII; Tripoli: VI-VII; Lattakia: VI-VII; Beirut: V.**
Parametric catalogues
– Plassard and Kogoj (1981): 494 or 492 , $I =$ VIII, a destructive earthquake at Tripoli, causing panic at Beirut (Zacharie le Scolastique). *Seismological compilations*
– Sieberg (1932): 494 A.D., 90 villages and cities in Syria were destroyed. Laodicea and Tripoli were among these cities. The walls of Antioch fell down.

⟨031⟩**500 Antioch; Seleucea; Orfa; Safad.**
Parametric catalogues
– Ben-Menahem (1979): 500, 36.2N, 36.1E, $I_0 =$ XI, $M_L = 7.5$, destruction of Antioch. Damage to Safad. It was felt in Turkey and Greece (Amiran; Plassard and Kogoj; Sieberg; Willis).
– Ergin *et al.* (1967): an earthquake was in Samandag and Urfa.
Seismological compilations
– Sieberg (1932): 500, a heavy earthquake in Syria. It reached Palestine. Large destruction in Antioch and Seleucea. There was damage in Edessa and Safad.

⟨033⟩ **525 May Beirut: VII-VIII; Byblus: VII-VIII; Sidon: VI-VII; Antioch: VI-VII. Aftershocks.**
Parametric catalogues
– Ben-Menahem (1979): 525 May 29, off coast Sidon, I_0=IX-X, $M_L = 6.7$ (Ergin *et al.*; Plassard and Kogoj; Sieberg; Willis).
Seismological compilations
– Sieberg (1932): 525 May, a strong earthquake occurred in the coastal area of Syria with a large number of deaths. Berytos and Byblos were completely destroyed. In Sidon and Antioch, there was heavy damage to the buildings. Aftershocks continued till October.

⟨038⟩**553 Antioch: V.**
Seismological compilations
– Sieberg (1932): in 553, a strong earthquake was in Antioch.

⟨039⟩**557 Antioch: V.**
Seismological compilations
– Sieberg (1932): in 557, a strong earthquake was in Antioch.

⟨045⟩**639 Antioch: IV-V**
Seismological compilations
– Sieberg (1932): 639, a strong earthquake with a horrible noise occurred in Antioch.

⟨051⟩**775 Antioch: IV.**
Seismological compilations
– Sieberg (1932): 775, an earthquake was at Antioch.

⟨052⟩**791 Aleppo: V; Northern Syria; Palestine.**
Seismological compilations
– Sieberg (1932): 791, a strong earthquake in Aleppo and Northern Syria. It reached Palestine.

⟨053⟩**8th century Ar-Rassafeh: VII-VIII.**
Other works
– Klengel (1985): During the 8th century, Ar-Rassafeh hit by a strong earthquake, transferring its buildings into ruins.

⟨059⟩**881 May 16 Syria; Egypt; Mesopotamia; North Africa and Al-Andalus.**
Seismological compilations
– Guidoboni *et al.* (1994): In that year [267 A.H., 12 August 880-3 1 July 881], there was a strong earthquake in Syria, Egypt, some parts of Mesopotamia, North Africa and Andalusia (Ibn Al-Athir).

⟨060⟩**889 Aleppo: III-IV.**
Seismological compilations:
– Sieberg (1932): 889, several size-varied shocks (~ 6) occurred in Aleppo.

⟨061⟩ **894 Northern Syria.**
Seismological compilations
– Sieberg (1932): 894, an earthquake occurred in Northern Syria. It was felt in Armenia and Palestine.

⟨062⟩ **951 June 9-952 May 28 Aleppo: V-VI; Raaban?; Duluk ?; Tal Hamed ? Aftershocks.**
Parametric catalogues
– Poirier and Taher (1980): 951 September, I_0= VIII-IX, heavy destruction in Aleppo. Raaban and Duluk were destroyed.
Seismological compilations
– Guidoboni *et al.* (1994): 951 June 9-952 May 28, Aleppo VIII $\le I \le$ X, Duluk, Raaban, and Tall Hamid. In that year (9 June 951-28 May 952) there were many earthquakes in Aleppo and other cities, they lasted for 40 days, causing many victims and destroying the strongholds of Tall Hamid and those of the towns of Raaban and Duluk, three towers of the latter collapsed (Ibn Tagri Birdi).

⟨063⟩ **963 July Izaz: VII; Northern Syria: VI. Rock-falls.**
Seismological compilations
– Seiberg (1932): 963 July, Izaz was destroyed by an earthquake. Many other places in Northern Syria were damaged. It was accompanied by rock-falls.

⟨064⟩ **972 Antioch: VI-VII; Damascus: V.**
Parametric catalogues
– Plassard and Kogoj (1981): 972-3, I= III, a strong earthquake occurred in Al-Sham (= Southern Syria) (Al-Suyuti).
– Poirier and Taher (1980): 972, I_0= IX (MMS), Antioch, Emperor Johannes Shamshik sent 12000 workers to rebuild the city.
Seismological compilations
– Guidoboni *et al.* (1994): 972, Antioch VII $\le I \le$ VIII and Damascus. There was an earthquake in Antioch, and a large part of its walls collapsed (Al-Antaki). An earthquake affected Damascus and surrounding area, many towers in Antioch collapsed (Al-Maqrizi).

⟨065⟩ **991 April 5, night Baalbak: VIII-IX; Damascus: VII-VIII; Egypt: III-IV. Landslide, tsunami, aftershocks.**
Parametric catalogues
– Plassard and Kogoj (1981): 991 April 5, I= VII, this earthquake caused destruction of 1000 houses at Damascus and a village near Baalbak (Erpenius).
Seismological compilations
– Guidoboni *et al.* (1994): Baalbak and Damascus I= IX. On the night of 5 April 991, there was an earthquake at Damascus collapsing more than 1000 houses and a large number of people died, a village near Baalbak was swallowed up by the earth, other tremors occurred in Damascus and the surrounding area of Baalbak (Al-Antaki).
– Seiberg (1932): 991 April 5, an earthquake occurred in Syria. It was accompanied by a tsunami. In Damascus, more than 1000 houses collapsed with many victims. A village near Baalbak vanished. Aftershocks lasted for six weeks. The earthquake was felt in Egypt.
– Ben-Menahem (1979): 991 April 5, I_0= IX-X, M_L= 6.5, great destruction and many casualties in Damascus and Baalbak. Felt as far as Egypt (Plassard and Kogoj; Seiberg; Willis).

⟨071⟩ **1089 Palmyra: ≥ VIII.**
Seismological compilations
– Sieberg (1932): 1089, a strong earthquake was in Syria. It ruined Palmyra.

⟨074⟩ **1098 January Antioch: III; Aleppo: III.**
Seismological compilations
– Sieberg (1932): 1098 January, a slight earthquake was in Antioch, Aleppo and other places in Northern Syria.

⟨076⟩ **1128 Tyre. Surface faulting?**
Seismological compilations
– Sieberg (1932): 1128, a destructive earthquake killed a large number of people in Sure. Cracks appeared in the ground.

⟨077⟩ **1135 Syria.**
Seismological compilations
– Sieberg (1932): 1135, an earthquake was in Syria.

⟨080⟩ **1139 Aleppo.**
Seismological compilations
– Sieberg (1932): 1139, many strong shocks occurred in Aleppo for two weeks.

(085) **1182 Bosra: VII; Judea: VI; Nablus: VI.**
Parametric catalogues
– Ben-Menahem (1979): 1182, 32.6N, 36.7E, Jabal Al-Arab, I_0= IX-X, M_L= 6.7, destructive at Bosra and Southern Syria. Destructive in Judea and Nablus (Amiran; Plassard and Kogoj; Seiberg; Willis).
Seismological compilations
– Sieberg (1932): 1182, a destructive earthquake hit Southern Syria. It was felt in Judea.

(086) **1202 May 20, early morning Mount Lebanon: IX; Baalbak: IX; Tyre: IX; Nablus: VIII; Beit Jin: IX; Banyas: VIII+; Al-Samyra: VIII+; Damascus: VIII; Safita: VII; Akka: VII; Hauran:VIII; Hama: VIII; Tripoli: VIII; Safad: VII; Al-Quds: VI; Bosra: VII-VIII; Al-Batron: VII; Jbeil: VII; Beirut: VII; Marqab and Hosn Al-Akrad: VII; Barin: VII; Homs: VII; Tartus: VI; Aleppo: V; Antioch: V; Al-Mousel: IV-V; Mesopotamia: IV; Cairo: IV; Alexandria: IV; Dimyat: IV; Qus: IV; Iraq: IV; Cyprus: VII?; Lesser Armenia: IV; Sicily: IV; Khlat: IV; Ceuta: III?; Constantinople: IV** (fig. 16)**. Tsunami, landslide, aftershocks.**
Parametric catalogues
– Plassard and Kogoj (1981): 1201 June and July, I=X, there was an earthquake that caused a destruction in Tyr, Beirut, Damascus, Baalbak, Palestine (Nablus, Acre and Safad), and Homs in Syria, with tsunami in Cyprus (Al-Suyuti; Ernoul; Perrey).
– Ben-Menahem (1979): 1201 July-August, 34.5N, 36.8E, I_0= XI, M_L=7.3, felt in Mesopotamia, Anatolia, Upper Egypt, Cyprus. Destructive in Tripoli, Sur, Acre, Nablus. Many monuments and temples at Baalbak collapse. Many victims (Al-Sinawi *et al.*; Amiran; Ergin *et al.*; Plassard and Kogoj; Seiberg; Willis).
– Ben-Menahem (1979): 1202, May 20, at down, 32.5N, 35.5E, near Bissan, I_0=X-XI, M_L= 6.8, destruction in Central Palestine. Nablus destroyed. Safad, Bissan and Banyas experienced M_M=IX. It was felt in Syria, Cyprus, Egypt and Mesopotamia. Jerusalem M_M= V. Acre M_M= VIII. Tiberias M_M= IX, damage to the city walls (Al-Sinawi and Ghalib; Amiran; Plassard and Kogoj; Sieberg).
Seismological compilations
– Ambraseys *et al.* (1994): 1202 May 20,

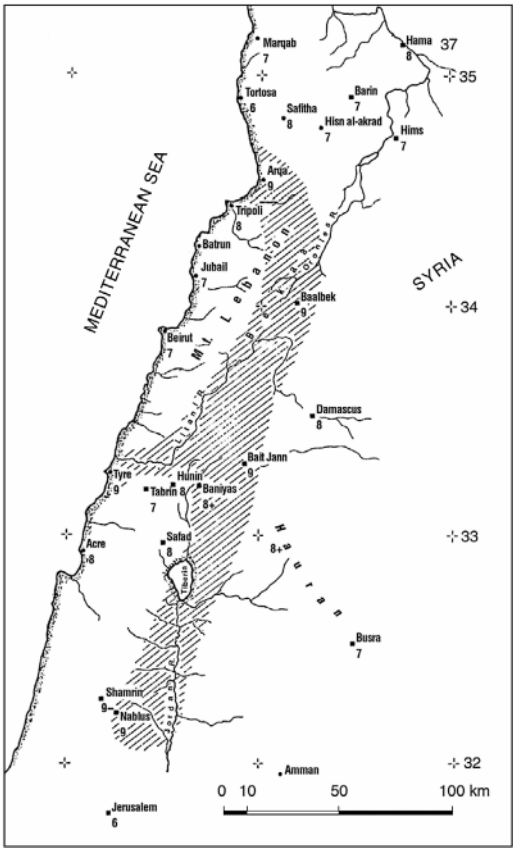

Fig. 16. Map of intensity distribution for May 20, 1202 earthquake (Ambraseys and Melville, 1985). Shaded zone is the most affected region.

33.5N-36.0E, VI≤I≤VII, tsunami and faulting. A major earthquake in the upper Jordan and Litani Valleys was responsible for tens of thousands of casualties in the Eastern Mediterranean region, it was felt throughout Egypt, causing great concern but little damage (Abd Al-Latif). The main shock was felt from Sicily to Azarbaijan in NW Iran, and from Constantinople to Aswan (Ambraseys and Melville).
– Sieberg (1932): 1202 May 20, a strong earthquake at Samaria and Galilia, causing a large number of victims and destroying Nablus. Akka and Safad were suffered. There was a large sea wave along the Syrian coast destroying

many ships and settlements. In 1202, a destructive earthquake destroyed Baalbak. There was destruction in Homs and Crac des Chevaliers. It was felt in Mesopotamia and Cyprus.

Monographs

– Ambraseys and Melville (1988): A shallow, large magnitude multiple earthquake was widely felt in the Middle East around daybreak on the morning of 20 May 1202. The main shock was felt from Lesser Armenia, parts of Anatolia and northwest Iran to Qus in upper Egypt, and from Sicily in the west to Iraq and Mesopotamia in the east (radius of 1200 km). It was associated with tsunamis. This event caused serious damage in Syria and to a lesser extent in Cyprus, with great loss of life. The epicenter was evaluated to be 34.1N and 36.1E, with estimated magnitude $M_{s=}7.5$. Both Acre and Tyre were severely damaged with heavy loss of life. Contemporary letters (Mayer, 1972) speak of damage to walls and towers in both cities, including the palace at Acre. The house of the Temperas in Acre was spared. All but 3 towers and some outlying fortifications were destroyed in Tyre, along with churches and many houses. Intensities in Tyre may be assessed higher than those in Acre, respectively around IX and VIII. In Shamrin (Samaria) and Houran, damage was equally severe (VIII). Safad was partially destroyed, with the loss of all (VIII). At Bait Jann, not even the foundations of walls remained standing, everything having been swallowed up (IX). In Nablus, there was total destruction (IX). In Houran province, most of the towns were so badly damage (Abd Al-Latif; Sibt Al-Jwazi). One of the villages around Busra is said to have been completely destroyed, perhaps by landslides (Ibn Al-Athir). Jerusalem suffered relatively lightly (Abd Al-Latif) at intensities not exceeding VI. Damascus was strongly shaken (VIII): a large number of houses collapsed, major buildings near the citadel were damaged, the Umayyad mosque lost its eastern minaret and 16 ornamental battlements along its north wall, one man was killed in the collapse of the Jirun gate of the mosque, the lead dome of the mosque was split in two and one other minaret fissured (Le Strange), the Kallasa mosque was ruined, killing a North African and a Mamluk slave (Abu Shama). The shock in Damascus was of long duration. Another slight shock was felt early on the following morning (Abu Shama), and aftershocks continued for at least four days (‘Abd Al-Latif). In Jubail, houses are said to have collapsed (VII). The walls of Beirut are said to have been repaired around this time following earthquake damage (VII). Rockfalls in Mount Lebanon overwhelmed about 200 people from Baalbak. Baalbak itself was destroyed (‘Abd Al-Latif) (IX). In Tripoli, there was heavy loss of life (Mayer) and heavy damage (Ibn Al-Athir) (VIII). Tartus and the Templar citadel seem largely to have been spared (Berchem and Fatio; Enlart) (VI). The strongholds at Marqab and Krak (Hosn Al-Akrad) were badly damaged (Geoffrey of Donjon; Sibt Al-Jawzi) (VII). Castle of Barin was also damaged (Abd Al-Latif) (VII). In Homs, the shock was experienced at similar intensities (VII), where a watchtower of the castle was thrown down (Sibt Ibn Al-Jwazi). The earthquake in Hama was experienced as two shocks, destroying its castle, along with many houses (Ibn Al-Athir) (VIII). In and around Aleppo, the earthquake is said to have been felt (Sibt Ibn Al-Jawzi) (V), and also in Antioch (V). This event was reported also in Al-Mousel (IV-V) and throughout the districts of Mesopotamia (IV), as far as Iraq, though without destruction of houses. Azarbaijan, Armenia, parts of Anatolia are said to have experienced the earthquake (Ibn Al-Athir; Sibt Ibn Al-Jawzi). The shock was felt throughout Egypt from Qus to Alexandria: in Cairo, the shock caused arousing sleepers who jumped from their beds in fear (V). Three violent shocks were reported, shaking buildings, doors and roofs (Abd Al-Latif). In Cyprus, the earthquake damaged churches and other buildings and was strongly felt (Abd Al-Latif; Annales 5689; Ibn Al-Athir) (VII?). The sea between Cyprus and the coast parted and mountainous waves were piled up, throwing ships up onto the land (Arabic authors). Eastern parts of the island were flooded and numbers of fish were left stranded (Abd Al-Latif; Ibn Mankali in Taher). The earthquake is said to have been felt as far as Sicily (Ibn Al-Athir) (IV) and Ceuta (Ibn Wasil) (III?). It is very likely that the shaking reported on or after 1 March 1202 felt in and around Constantinople was from the earthquake of 20 May (Nicetas) (IV). The loss of life caused by this earthquake and its aftershocks is high. A figure frequently quoted in Arab sources is 1100000 dead (Al-Dhahabi; Al-Suyuti) for the year 597-598 A.H. (1201-1202). This includes those dying of famine and the epidemic consequent on the failure of the Nile floods, graphically described by Abd Al-Latif, who noted 111000 deaths in Cairo along between 596 and 598 A.H. Aftershocks were reported from Hama, Damascus and Cairo, for at least four days (Abd Al-Latif).

(087) **1212 Antioch.**
Seismological compilations
– Sieberg (1932): 1212, an earthquake in Antioch.

(088) **1222 Kelless.**
Seismological compilations
– Sieberg (1932): 1222, there was a lava in Killis.

(089) **1236 Northern Syria: VI-VII.**
Seismological compilations
– Sieberg (1932): 1236, an earthquake in Northern Syria, causing minor damage.

(090) **1242 Syria.**
Seismological compilations
– Sieberg (1932): 1242, an earthquake was in Syria.

(091) **1254 Northern Syria.**
Seismological compilations
– Sieberg (1932): 1254, an earthquake caused minor damage in Northern Syria.

(093) **1274 Syria.**
Seismological compilations
– Sieberg (1932): 1274, an earthquake was in Syria.

(094) **1281 Syria.**
Seismological compilations
– Sieberg (1932): 1281, a slight earthquake hit Syria, but without damage.

(096) **1290 Syria.**
Seismological compilations
– Sieberg (1932): 1290, an earthquake was in Syria.

(097) **1303 August 8** (It seems to be two different events). **Cairo: VII; Alexandria: VII; Damanhur: VII; Safad: VII; Damascus: VI; Hama: VI; Antioch: IV; Tunis: IV; Barqa: IV; Morocco: IV; Cyprus: IV; Istanbul: IV; Sicily: IV. Tsunami, flood.**
Parametric catalogues
– Plassard and Kogoj (1981): In 1303 August 8, I_0 V, there was an earthquake causing destruction in Alexandaria with tsunami and Cairo. It was felt in Damascus (Abu Al-Fida; Al-Suyuti; Perrey).
Seismological compilations
– Al-Ghouneim (no date): In [702 A.H.] Zu-l-Hijja 23 Thursday (1303 August 9) early morning, it was mentioned that a strong earthquake was in many towns and cities in Egypt. Many places in Cairo, Eskandariyeh, Damenhur were destroyed or fell down. It was felt in Barqa, Tunis, Sicily and Morocco. Cyprus was destroyed to the ground. It was felt in Antioch, Constantinople the great (Al-Dawadari). In this year [702 A.H.] of Zu-l-Hijja 23, a great earthquake in Egypt. In Cairo, many mosques, minarets and schools were destroyed. There was flooding of the Nile River with great sound. There was a sea wave in Eskandariyeh. A part of Safad citadel was collapsed and the sea in Akka was retread. Cracks appeared in the walls of Omyyad mosque at Damascus (Al-Maqrizi).
– Sieberg (1932): 1303, an earthquake in Syria. Part of walls of Hama was collapsed.

(099) **1339 January 13-February 11 Tripoli: VII; Palestine: IV.**
Parametric catalogues
– Plassard and Kogoj (1981): 1339 January-February, I_0 IX, an earthquake occurred causing destruction in Tripoli (Al-Suyuti).
Seismological compilations
– Al-Ghouneim (no date): In 739 A.H. Rajab (1339 January 13), an earthquake occurred at Tripoli, killing 60 persons.
– Sieberg (1932): 1338 July 20, an earthquake was in Syria. It was strong in Tripoli. It was felt in Palestine.

(102) **1399 September 20 Damascus: III-IV.**
Seismological compilations
– Al-Ghouneim (no date): In 802 A.H. Muhar-

ram 17 (1399 September 20), a shock was felt at Damascus (Al-Asqalani).

(103) **1403 December 18 Aleppo: IV-V.**
Seismological compilations
– Ambraseys and Melville (1995): 1403 December 18 Tuesday, 806 A.H. Jamada II 3 Friday, a shock was felt in Aleppo and its dependencies, but without damage (Atsiz; Ibn Hajar).

(104) **1404 February 20 Qalaat Blatnes: VII-II; Bkas: VIII; West of Aleppo: VII-VIII; Qalaat Al-Marqeb: VII-VIII; Tripoli district: VII; Lattakia: VII; Jableh: VII. Tsunami, landslide.**
Parametric catalogues
– Ambraseys and Barazangi (1989): 1404 February 22, 35.9N-36.3E, large.
– Plassard and Kogoj (1981): 1403-1404 December-January, in Lebanon I=V, there was an earthquake which caused destruction in Aleppo with tsunami in the Syrian coast (Al-Suyuti; Perrey).
– Poirier and Taher, 1980: 1404 February 11, I_0=IX (MMS), heavy destruction in Aleppo, while Lattakia fortress was destroyed.
Seismological compilations
– Ambraseys and Melville (1995): 1404 February 20, 806 Sha'ban 8, a damaging earthquake took place affecting the region west of Aleppo, where many places were destroyed. There was a long sequence of aftershocks which caused considerable concern, particularly to the west of Aleppo (Ibn Hajar; Ibn Al-Shihna). Other accounts mentioned that the most effects were experienced in the district of Tripoli, where many buildings were destroyed (Al-Jauhari). Either as a result of this shock, or of further strong aftershocks, part of the castle of Marqab collapsed at the beginning of Ramadan (mid March), together with other structures elsewhere (Al-Jauhari; Al-Maqrizi).
– Al-Ghouneim (no date): In 806 A.H. Sha'ban (from 1404 February 13), news received that a great earthquake was at Tripoli region, destroying many buildings including a part of Qalaat Al-Marqab, Lattakia, Jableh, Blatnes citadel, Bkas and other towns in the mountain and the coastal areas, killing many people under the debris (Al-Maqrzi). In this year [806 A.H.] Shaaban 8, a strong earthquake was in and around Aleppo, destroying many places. It was shacked on mid-day of Friday 3rd Jamada II. Many shocks were felt during this year (Al-Asqalani). In the latest third of Sha'ban, news brought from Tripoli region, that there was a great earthquake destroying many buildings and most parts of Qalaat Al-Marqab fell down (Al-Sayrafi).
– Sieberg (1932): 1402, an earthquake was in Syria, causing landslides with damage in a few cities. There were sea waves in the coastal area.

(105) **1404 November 5-December 4 Aleppo: V.**
Parametric catalogues
– Poirier and Taher (1980): 807 A.H. Jamada I (1404 December 5), I_0=VII (MMS), there were three shocks in Aleppo.
Seismological compilations
– Ambraseys and Melville (1995): 1404 November 7, 807 A.H. Jamada I 3 at midday, The shock was of long duration and was widely felt in other towns of the region. It caused great alarm, and was followed by a few aftershocks, but no damage was reported (Al-Suyuti; Ibn Hajar).
– Al-Ghouneim (no date): 807 A.H. Jamada I (from 5 November 1404), a great earthquake in Aleppo, causing a large panic without damage (Al-Asqalani).
– Sieberg (1932): 1404, an earthquake in Syria.

(106) **1407 April 9-May 8 Antioch: VII; Cyprus: V. Surface faulting.**
Parametric catalogues
– Plassard and Kogoj (1981): 1407 April-May, I=IV, there was an earthquake that caused destruction in Antoich (Al-Suyuti).
– Ambraseys and Barazangi (1989): 1407 April 29, 35.7N-36.3E, M_S=7.0, faulting.
Seismological compilations
– Ambraseys and Melville (1995): 1407 April, 809 A.H. Zu-L-Qa'da, a shock was in Antioch, killing 100 people or more (Al-Suyuti; Ibn Hajar). An earthquake felt strongly throughout Cyprus on 29 April 1407 may be the same event.
– Al-Ghouneim (no date): In 809 A.H. Zu-l-Qa'-da (from 1407 April 09), a great earthquake was at Antioch, killing a large number of people, 100 or more, under the debris (Al-Asqalani).

(107) **1408 December 29 Shugr: VIII-IX; Bkas: VIII-IX; Blatnes: VIII; Lattakia: VII;**

Jableh: VII; Antioch: VII; Syrian coast: VI (fig. 17)**. Faulting between Sfuhen and Al-Quseir. Landslide in Sfuhen. Tsunami in Lattakia.**

Parametric catalogues

– Plassard and Kogoj (1981): 1408-1409 December-January, in Lebanon I_0 IX. They are earthquakes which caused destruction in Tripoli and Aleppo (Al-Suyuti).

– Poirier and Taher (1980): 1408 December 30, I_0 X-XI (MMS), heavy destruction was in Antioch and Aleppo, the ice fell off the top of Jabal Al-Akraa. Between Al-Qucir and Saltuhum, a fissure 1 mile long appeared. A sea wave in Lattakia.

Seismological compilations

– Ambraseys and Melville (1995): 1408 December 29, 811 A.H. Sha'ban 10, there was a great earthquake in Shugr and Antioch, where Shugr and its region were destroyed (Atsiz). A great earthquake affected the districts belonging to Aleppo and Tripoli, and destroyed a number of places in Lattakia, Jableh and Balatunus. The castle of Balatunus collapsed and 15 people were killed. 15 people were killed in Jableh. Shugr Bakas was totally destroyed with its castle, and all but 50 of its inhabitants were killed. The ground fissured and was thrown down over the distance of a stage, from the town of Qusair to Salt(f)uham (?) – a town on the top of a mountain – about a mile of which moved during the night, carrying with it trees, buildings and their inhabitants, who were unaware of what was happening. The shock also affected Cyprus, where many

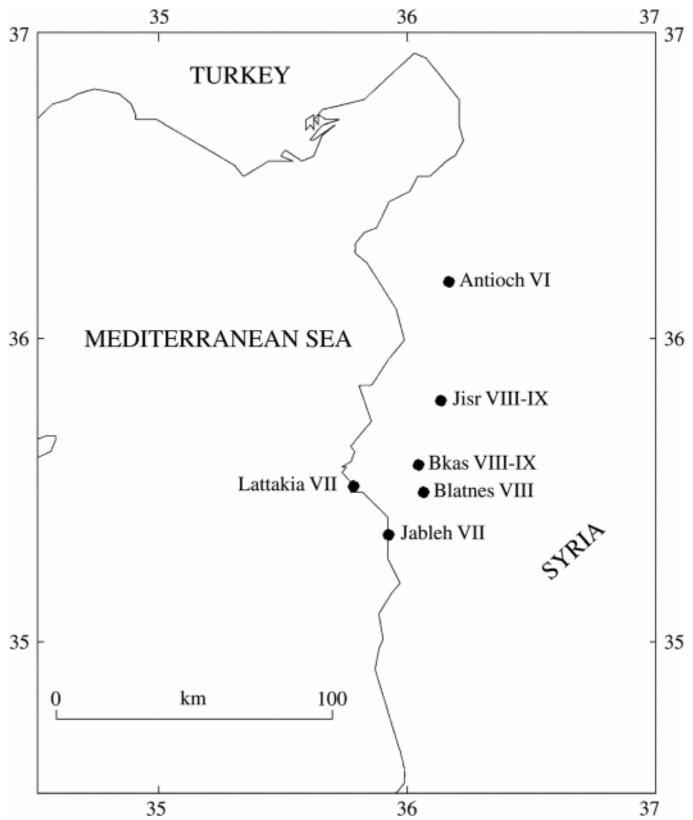

Fig. 17. Map of intensity distribution for December 29, 1408 earthquake.

places were destroyed in the mountains and the plains. Snow was seen on the top of Jabal Al-Akraa, and the sea receded for 10 farsakhs (*ca.* 60 km) and then returned. Ships at sea touched the bottom before the water returned to normal, without hurting anyone (Ibn Hajar). According to Ambraesys' point of view, the available evidence suggests that surface faulting extended for a distance of at least 20 km from Qusair, either southwest in the direction of the coast, or south along one or more strands of the Dead Sea Fault. – Al-Ghouneim (no date): In 811 A.H. Sha'ban 10 (1408 December 30), a great earthquake in Aleppo, Tripoli and their vicinity. Many places in Lattakia, Jableh and Blatnes were destroyed. Fortress of Platnes fell down, killing 15 persons under the debris. In Jableh, 15 persons were killed. Both citadels of Bkas totally collapsed and all their residents were killed and only 50 persons survived. The earth was opened between Salfouhum and Al-Qusair. Salfouhum moved from the top of the hill down along one mile with its inhabitants, trees, springs and animals, but without damage. In Cyprus, many places were destroyed. It was felt in the coastal area of Syria. The ice masses on the Jabal Al-Aqra were seen moving down. In the sea, sailors mentioned that the sea retreated then returned back without any damage (Al-Maqrizi).

(108) **1484 March 29-April 27 Aleppo: V-VI.**
Seismological compilations
– Al-Ghouneim (no date): In 889 A.H. Rabi I (started from 1484 29 March), Aleppo was shaken by 6 strong shocks (Al-Suyuti).

(109) **1491 April 24 Nicosia: VII; Limassol: VII; Famagusta: VII; Paphos: VII; Damascus: IV; Cairo: IV; Crete: IV.**
Seismological compilations
– Ambraseys *et al.* (1994): 1491 April 24, two slight shocks a week apart were reported from Damascus, Cairo and Crete, both earthquakes caused heavy damage in Cyprus, where the forts at Limassol, Paphos and Famagusta and buildings in Nicosia were destroyed (Anonymous Pilgrim; Archivo Ducale Sforzesco-Milan; Ben-Menahem; Darrouzes; Dietrich von Schachtem). In Damascus, the first shock, which was not widely felt, occurred after the sunset prayers on 16 Jumada II-evening of 25 April; the second was before sunrise on 22 Jumada II-1 May (Ibn Tulun). In Egypt, the earthquake was alarming, shaking buildings and lasting a *daraja* or more ('Abd Al-Basit; Al-Sakhawi). The second shock was slight (Al-Suyuti; Ibn Iyas).

(112) **1546 September 29 Nablus: VI-VII; Damascus: V; Al-Quds: VI; Yafa: VI; Tripoli: VI; Famagusta: V. Tsunami at Cyprus.**
Parametric catalogues
– Plassard and Kogoj (1981): 1546 September 29, I_0 VI, there was an earthquake which caused destruction in Nablus, it was strong in Damascus and Famagusta in Cyprus (Perrey; Sieberg). There was a tsunami in Cyprus (Shalem Nathan).
Seismological compilations
– Sieberg (1932): 1546 September 29, a strong earthquake was in Samaria, causing heavy damages in Nablus. Damages were recorded in Jerusalem, Yafa, Tripoli, Damascus and Famagusta. It was accompanied with a sea wave.

(115) **1568 October 10 Lattakia: VII; Famagusta: V; Limassol: IV; Nicosia: IV.**
Seismological compilation
– Ambraseys and Finkel (1995): An order from the Kadi of Lazkiya (Lattakia), dated 18 Rebi-II A.H. (10 October 1568), says that 'The great earthquake ruined the walls and roofs of many mescids (mosques), mihrabs and imarats in the town and villages; in particular, some walls of the great old mosque built by Sultan Alaeddin are demolished and some walls are cracked (BBA). Limassol and Nicosia were affected by some shocks of varying intensity, Famagusta was also shaken for eight days and many people moved out and camped in the countryside (Lusignano). This earthquake seems probable in Lattakia associated with the fore- and aftershock activity of the same event, a possible location of which would be between the Syrian coast and Cyprus.

(116) **1577 Northern Syria: VI-VII; Palestine: IV; Cyprus: IV; Armenia: IV. Aftershocks.**
Parametric catalogues
– Plassard and Kogoj (1981): 1577, I_0 IV, there was an earthquake that caused a destruction in Northern Syria and Cyprus. It was felt in Palestine (Perrey; Sieberg).

Seismological compilations
– Sieberg (1932): 1577, a destructive earthquake was in Northern Syria. It was felt in Palestine and Armenia. Aftershocks lasted four months.

(120) **1616 July 22 Aleppo: VI.**
Seismological compilations
– Ambraseys and Finkel (1995): 1616 July 22, a strong earthquake was experienced on the feast of S. Maria della Neve by Pietro della Valle while he was in Aleppo. The shock did not last long and caused no damage in the town (Valle).
– Sieberg (1932): 1616 August 27, a destructive earthquake in Aleppo collapsed its walls.

(126) **1640 Damascus: VI; Syria; Tabriz.**
Parametric catalogues
– Plassard and Kogoj (1981): 1640, I= VI, it was an earthquake that caused destruction in Damascus (Perrey ?).
Seismological compilations
– Sieberg (1932): 1640, an earthquake was in Syria. Some buildings in Damascus fell down. It was felt in Tabriz.

(127) **1656 February Tripoli: VII; Palestine: IV.**
Parametric catalogues
– Plassard and Kogoj (1981): 1656 February, in Lebanon I= VII, an earthquake occurred in Tripoli, causing some damages (Perrey; Willis).
– Ben-Menahem (1979): 1656 February, 34.9N, 36.2E, I_0=X, M_L=7.0, destruction of Tripoli. It was felt in Palestine (Al-Sinawi and Ghaleb; Amiran; Plassard and Kogoj; Sieberg; Willis).
Seismological compilations
– Sieberg (1932): 1656 February, an earthquake in Syria ruined half of Tripoli. It was felt in Palestine. Shocks repeated in November.

(128) **1657 Aleppo: IV.**
Seismological compilations
– Ambraseys and Finkel (1995): 1657, during this year four earthquakes were felt in Aleppo within a period of two months (Besson).

(129) **1666 September 22 Al-Mousel: VII-VIII; Sinjar: VI-VII; Sharqat: VI-VII; Aleppo: V; Tabriz: V; Van: V. Landslides, aftershocks.**
Parametric catalogues
– Ambraseys (1989): 1666 September 22, 37.0 N-43.0 E, M_S=6.6, I_{max} (MSK) = IX.
Seismological compilations
– Ambraseys (1989): 1666 September 22, news of the disaster was reported from Aleppo where the shock was apparently felt. In Al-Mousel and its surroundings the shock was particularly strong. Many houses were destroyed in Al-Mousel and also the cathedral that housed the tomb of Nebi Yunus. Monasteries to the north of the town were ruined. In addition, 5 towns and 45 villages were totally destroyed, and damages extended to Sinjar and Sharqat. It is said that as a result of the earthquake «four great mountains were raised up from the ground and thrust against each other reducing themselves into dust», an allusion, perhaps, to landslides. Destructive shocks continued for several days. It appears that the earthquake was felt strongly in Van and Tabriz (Fiey; Hammer; Theatrum Europeum).
– Sieberg (1932): 1666, Aleppo and 44 places affected deeply by an earthquake.

(130) **1680 March 22-23 Aleppo: IV.**
Seismological compilations
– Ambraseys and Finkel (1995): Slight shocks on 22 and 23 March 1680 were felt by a European traveler in Aleppo (d'Arvieux).

(132) **1693-94 Northwestern Iraq. Landslides.**
Seismological compilations
– Ambraseys and Finkel (1995): In 1105 A.H. (2 September 1693-21 August 1694) in the region of Jabal Sinjar in NW Iraq, there was a mighty noise which heard and an area 50 cubits long by 30 wide sank down beneath the mountain (Al-'Umari). It is note necessary to be assumed that an earthquake was responsible for triggering what appears to be landslide or rock-fall.

(133) **1701 Aleppo: IV.**
Seismological compilations
– Ambraseys and Finkel (1995): 1701, it seems that an earthquake was felt in Aleppo during this year (Panzac).

(136) **1719 March Aleppo: VII.**
Parametric catalogues
– Plassard and Kogoj (1981): 1719 March, I=IV, it was an earthquake that caused destruc-

tion in Aleppo, 200 houses of Aleppo affected (Sieberg).
Seismological compilations
– Ambraseys and Finkel (1995): An earthquake shook Aleppo during this month, damaging three mosques and ruining more than 200 houses (Berryat).
– Sieberg (1932): 1719 March, a destructive earthquake in Syria caused destruction of three mosques and 200 houses in Aleppo.

⟨137⟩ **1722-1723 Aleppo: VII.**
Seismological compilations
– Ambraseys and Finkel (1995): A near-contemporary source says that: in 1135 A.H. (1722-1723) Aleppo was afflicted by a terrible earthquake, which destroyed most of its houses and killed many people (Al-Ghazi). Modern author (Panzac) repeated this information.

⟨138⟩ **1726 April 15 Jum: >VII; Aleppo: VII; Iskenderun: IV; Famagusta: III.**
Seismological compilations
– Ambraseys and Finkel (1995): 1726 April 15, this earthquake occurred at quarter past noon and caused considerable damage in the region of Jum, particularly at Harim, but details are lacking (ANF; Panzac). It was violent in Aleppo, where some walls were thrown down, and caused panic in Iskenderun (PMdF). It was perceptible in Famagusta at the same hour, but there is no evidence in French consular correspondence that it was felt in Antioch (ANF).
– Sieberg (1932): 1726 April 15, three shocks caused collapsing the old walls of Aleppo. News brought that an earthquake occurred in Iskandaroun.

⟨139⟩ **1738 September 25 Iskenderun: VIII; Bellen Bass: VII-VIII; Antioch: VII; Jabal Al-Amanus: VII; Aleppo: V-VI; Kelless: V; Bereket: V.**
Seismological compilations
– Ambraseys and Finkel (1995): 1738 September 25, this earthquake caused considerable damage in the region of Amanus, ruining a number of villages on the east side of the Belen Bass (Riggs). Part of Antioch's walls and some houses collapsed according to European traveler (Pococke). A part of castle between Bayas and Iskenderun has been demolished (BBA). Probably, it was demolished by this earthquake. The shock, according to an eyewitness, was strongly felt in Aleppo without damage (Kort). This is certainly the same event that was also felt in Kilis (Kilisli Kadri) and in other parts of the region of Bereket (Riggs). – Sieberg (1932): 1737, a destructive earthquake in Antioch destroyed completely many old ruins.

⟨140⟩ **1752 July 21 Lattakia: VII; Tripoli: V. Tsunami at the Syrian coast.**
Parametric catalogues
– Plassard and Kogoj (1981): 1752 July 21, in Lebanon $I_=$ VII, a strong earthquake occurred in Tripoli, Lattakia and along the entire Syrian coast, generating a tsunami (Sieberg; Willis).
– Ben-Menahem (1979): 1752 July 21, off coast Lattakia, $I_{0=}$ X, $M_{l=}$ 7.0, destruction at Tripoli and Lattakia. Tsunami at Syrian coasts (Amiran; Plassard and Kogoj; Sieberg; Willis).
Seismological compilations
– Sieberg (1932): 1752 July 21, an earthquake occurred in the Syrian coast, generating a destructive sea wave. Great damage was in Lattakia. It was felt in Tripoli. It was said that there were 20000 deaths.

⟨141⟩ **1759 February 17 Aleppo: V.**
Seismological compilations
– Sieberg (1932): 1759 February 17, a strong earthquake occurred in Aleppo.

⟨142⟩ **1759 June 10 Aleppo: IV.**
Seismological compilations
– Ambraseys and Finkel (1995): 1759 June 10, an eyewitness reports that a slight earthquake was felt in and around Aleppo in the morning (Russell).
– Sieberg (1932): 1759 June 10, a weak shock was felt in Aleppo.

⟨143⟩ **1759 October 30, 03:45 (local time) Al-Qunaytra: VIII; Safad: VII; Acre: VI; An-Nasra: VI; Sidon: VI; Saasaa: VI; Damascus: V; Aleppo: IV; Al-Quds: IV; Beirut: IV; Antioch: IV; Gaza: IV; Cyprus: IV. Landslides at the west of Damascus and Tabariya. Tsunami at Acre and Tripoli. Aftershocks.**
Parametric catalogues
– Plassard and Kogoj (1981): 1759 October 30,

I_o VIII (in Lebanon), it was an earthquake that caused destruction in Safad and large damage in Al-Chouf (Jalfaq).
– Ben-Menahem (1979): 1759, October 30, 02 h, 33.0N, 35.5E, I_0 IX, M_L 6.5, heavy destruction and many casualties in Safad. Tiberias city wall overthrown. Area of damage extend to Damascus. Tsunami in the sea of Galilee. Damage in Sidon MM=VII (Amiran; Barslawy; Plassard and Kogoj; Sieberg; Willis).
Seismological compilations
– Sieberg (1932): 1759 October, a set of shocks started for three months in ... and Bekaa Valley. It was said that 30000 persons were killed due to these events, from which 20000 deaths in Bekaa.
Monographs
– Ambraseys and Barazangi (1989): 1759 October 30, 33.1N-35.6E, M_s 6.6. This earthquake is considered as a foreshock of the main event of November 25. It was affected the region of Safad and a mountain area to the NE where many villages were destroyed with the loss of about 2000 lives. Safad and Qunaitra were almost totally ruined, and many of the inhabitants were killed. In Sidon, Saasaa, Nazareth and Acre, few houses collapsed without casualties. In and around Damascus, this earthquake caused considerable concern and widespread minor damage, one or two houses collapsed, a few were damaged, many were cracked, many public buildings such as minarets and tall buildings were damaged, the water supply of Damascus was affected by rock falls. In Tiberias, a landslide took place but without loss of life. Antioch, Aleppo, Jerusalem and Gaza were felt, and it was reported by sailing boats between Cyprus and Beirut. In Acre and Tripoli, there was a seismic sea wave that flooded them without damage. This earthquake was followed by a series of strong aftershocks, some of which were felt as far as Aleppo, that added to the damage (Al-Budayri; ANF; Archives British Legations; Archives Historiques Ch. Comm. Marseille; Ben Zvi; Dahman; Findikli; Vitaliano; Yaari).

(145) 1760 January Qadicha: V; Aleppo: VI. Earthquake.
Parametric catalogues
– Plassard and Kogoj (1981): 1760 January, I_o VII (in Lebanon), a strong earthquake occurred in Qadicha (Deir-Marjerjius and Qanobin), it was stronger in Aleppo (Perrey; Sieberg).
Seismological compilations
– Sieberg (1932): 1760 January, aftershocks continued to occur, destroying Deir-Marjerjius. It was felt in the mountain of Lebanon.

(146) 1765 Tripoli: V; Aleppo: IV.
Parametric catalogues
– Plassard and Kogoj (1932): 1764 February 14, 19 h, I_o VI (in Lebanon), a strong earthquake hit Tripoli. It lasted 6 seconds (Perrey).
Seismological compilations
– Ambraseys and Finkel (1995): 1765, during the year there were earthquakes in the region between Aleppo and Tripoli (Lemmens).
– Sieberg (1932): 1764 January/February, a shock was in Aleppo. In 1764 February 14, a strong shock was in Syria. It was felt in Tripoli.

(147) 1778 May 5 Aleppo: IV.
Seismological compilations
– Ambraseys and Finkel (1995): 1778 May, at 5 h 10 min there was an earthquake in Aleppo without damage (PGF).
– Sieberg (1932): 1778 May 5, a shock was felt in Aleppo.

(148) 1779 June 8 Aleppo: V-VI.
Seismological compilations
– Ambraseys and Finkel (1995): 1779 June 8, preceded by an earthquake at the beginning of the month, a strong earthquake occurred in Aleppo on June, causing considerable concern (BRG). Another eyewitness reports the same event on Tuesday, 10 June, between 23 h and midnight, stating that it caused no damage save the collapse of inhabited houses (Evens). 8 June fell on Tuesday.

(149) 1783 December 14 Aleppo: VI; Tripoli: IV.
Parametric catalogues
– Plassard and Kogoj (1981): 1783 July 20, I_o IV (in Lebanon), an earthquake felt in Tripoli and Aleppo (Sieberg).
Seismological compilations
– Ambraseys and Finkel (1995): 1783 December 14, a strong shock was felt in Aleppo (BV; Guys; Volney).

– Sieberg (1932): 1783 July 20, an earthquake occurred in Northern Syria. In Aleppo, there was minor damage. It was felt in Tripoli and the whole of Lebanon.

⟨150⟩**1783 December 4 Aleppo: IV**.
Seismological compilations
– Sieberg (1932): 1783 December 4, a slight shock occurred in Aleppo.

⟨151⟩**1795 January Aleppo: VI.**
Seismological compilations
– Ambraseys and Finkel (1995): 1783 December, at 14 h 10 min, two shocks in Aleppo, the second being strong enough to damage many houses (Olivier).
– Sieberg (1932): 1795 January, two shocks caused some damages in houses at Aleppo.

⟨152⟩**1796 April 26 Qalaat Al-Marqeb: VI-II; Al-Qadmous: VIII; villages along Nahr Al-Kabir: VII-VIII; Jableh: VII-VIII; Bkas area: VII-VIII; Lattakia: VII; Saida: V; Aleppo: IV; Tripoli: V. Landslides, liquefaction.**
Parametric catalogues
– Plassard and Kogoj (1981): 1796 May 5, $I=$ V (in Lebanon), an earthquake caused destruction in Lattakia, where one-third of the city houses were destroyed (Blanckenhorn; Sieberg; Willis).
– Ambraseys and Barazangi (1989): 1796 April 26, 35.7N-36.0E, $M_S=6.6$.
– Ambraseys (1989): 1796 April 26, 09:05 (LT), 35.5N-36.0E, $M_S=6.6$, I_{max} (MSK) = VIII.
Seismological compilations
– Ambraseys and Finkel (1995): 1796 April 26, this was a destructive shock in the Sahel region of Lattakia on the Syrian littoral (Ambraseys, 1989). The earthquake occurred on 18 Shawal 1210 A.H. (Nuri). At about 9 h (Olivier) without foreshocks and lasted with intermissions for about one minute. In Lattakia so violent that almost everything collapsed with the first shock. The traveler Olivier, who had been there 22 months earlier, found the town barely recognizable. In the port area the old fort at the entrance of the harbor (Morana) and the tobacco stores of the customs-house and the han (BBA), solidly-built structures, collapsed instantly killing the *Aga,* his officers, 400 people and many animals (AMAE CADN). Out of a population of about 5000, 1500 (Olivier)-2000 (Guys) people were killed and many injured. One-third of the houses was destroyed and the remainder more or less ruined. Damages were equally heavy in Jableh where most of the houses were destroyed and the minaret of the mosque of Ibrahim fell: farmers lost their lives in surrounding villages; the castles of Markab and Qadmus were completely ruined (Nuri). There was also loss of life in the Bucak area north of Lattakia and settlements along the Nahr Al-Kebir River suffered in particular (ANF). The shock was felt between Aleppo and Tripoli and in Saida (Sidon) (Browne). It is said that as a result of the earthquake the surface of the ground around Lattakia rose (Olivier) but this may be an exaggeration.
– Ambraseys (1989): 1796 April 26 morning, a destructive earthquake occurred in the Sahel district of Lattakia. It lasted for about 1 min, almost totally ruining the coastal plain between Jableh and Bucak. Most of the houses collapsed in Jableh, and water wells caved in and became dry. Most of the miri villages in the Nahr Al-Kebir plain were ruined. In Lattakia, 1500 out of a population of 5000 were killed. One-third of Lattakia collapsed and the remainder was damaged. The old castle, minarets, watchtowers and large buildings fell down. In the port area, the tobacco customs-house fell in and killed 400 people. It is said that the shock raised the surface of the ground several toises. It was strongly felt at Saida. Aftershocks continued to be felt for two months (Consular Archives; Cevdet; Olivier, 1807).
– Sieberg (1932): 1796 April 26 or May 5, a destructive earthquake was in Northern Syria. 1/3 of the houses in Lattakia was destroyed and there were 1500 victims. In 1796 June, many weak shocks were felt in Lattakia.

⟨153⟩**1802 Baalbak: VI; Palestine: III.**
Parametric catalogues
– Ben-Menahem (1979): 1802, 34.0N, 36.2E, $I_0=$ VIII-IX, $M_l=6.2$, great damage at Baalbak. It was felt in Palestine (Amiran; Karnik; Plassard and Kogoj; Seiberg).
Seismological compilations
– Sieberg (1932): 1802, a vast earthquake occurred in Central Syria. Minor damage occurred in Al-Bekaa and Baalbak. It was felt in Palestine.

(155) **1814 Al-Laja: VI-VII. Rock-falls.**
Seismological compilations
– Sieberg (1932): 1814, there was a strong earthquake at the edge of the volcanic area in Al-Laja. It was accompanied by large rock-falls.

(156) **1819 February Syria: IV-V.**
Seismological compilations
– Sieberg (1932): 1819 end of February, a strong shock was felt in Syria.

(158) **1822 September 5 Aleppo: VII.**
Parametric catalogues
– Poirier and Taher (1980): 1822 September 5, destruction of what remained in Aleppo, with 20000 victims.

(159) **1830 Aleppo: III.**
Seismological compilations
– Sieberg (1932): 1830, a shock was felt in Aleppo.

(160) **1831 February 22 Aleppo: V.**
Seismological compilations
– Sieberg (1932): 1831 February 22, a very strong shock was felt in Aleppo.

(162) **1844 September 19 and 30 Aleppo: V.**
Seismological compilations
– Sieberg (1932): 1844 September 19 and 30, strong shocks were felt in Aleppo.

(164) **1846 December 3 Aleppo: V.**
Seismological compilations
– Sieberg (1932): 1846 December 3, there was a strong shock in Aleppo.

(165) **1850 February 12 Beirut: III; Ain Hamadeh: III.**
Parametric catalogues
– Plassard and Kogoj (1981): 1850 February 12, I_0 III (in Lebanon), an earthquake was felt in Beirut and Ain Hamadeh (Sieberg).
Seismological compilations
– Sieberg (1932): 1850 February 12, a slight shock was in Beirut. It was felt in Ain Hamadeh.

(166) **1854 Antioch: III; Suaidiya: III; Beirut: III; Aleppo: III; Yafa: III.**
Parametric catalogues
– Plassard and Kogoj (1981): 1854, I_0 III (in Lebanon), an earthquake was felt in Beirut, Aleppo and Yafa (Blackenhorn; Willis).
Seismological compilations
– Sieberg (1932): 1854, an earthquake was felt in Syria. It was felt in Swedieh, Antioch, Aleppo, Beirut and Yafa.

(167) **1859 January 24 Tripoli: III; Beirut: III; Damascus: III; Aleppo: III.**
Parametric catalogues
– Plassard and Kogoj (1981): 1859 January 24, I_0 IV, an earthquake was felt in Tripoli, Beirut, Damascus and Aleppo (Blachenhorn; Sieberg; Willis).
Seismological compilations
– Sieberg (1932): 1859 January 24, three shocks were felt in Damascus and Tripoli.

(168) **1864 August 15 Aleppo: IV.**
Seismological compilations
– Sieberg (1932): 1864 August 15, a strong shock was felt in Aleppo.

(169) **1868 April 16 Aleppo: III.**
Seismological compilations
– Sieberg (1932): 1868 April 16, a shock was felt in Aleppo.

(170) **1870 January 2 Aleppo: III.**
Seismological compilations
– Sieberg (1932): 1870 January 2, a shock was felt in Aleppo.

(171) **1872 April 3 Harem: VIII; Armanaz: VIII; Buhyret Al-Amq: VII-VIII; Antioch: VII-VIII; Aleppo: VII; Suaidiya: VII; Izaz: VI-VII; Idleb: VI-VII; Iskenderun: VI-VII; Hama: IV; Homs: IV; Tripoli: IV; Damascus: III; Beirut: III; Sidon: III; Diyar Bakr: III; Egypt: III; Rhodos: III** (figs. 18 and 19)**. Faulting at Baghras. Liquefaction, tsunami, aftershocks.**
Parametric catalogues
– Ambraseys (1989): 1872 April3, 07:40 (LT), 36.4N-36.5E, M_s=7.2, I_0 (MSK) =X.
– Ambraseys and Barazangi (1989): 1872 April 3, 36.4N, 36.5E, M_s=7.2.
– Plassard and Kogoj (1981): In Lebanon I_0 IV,

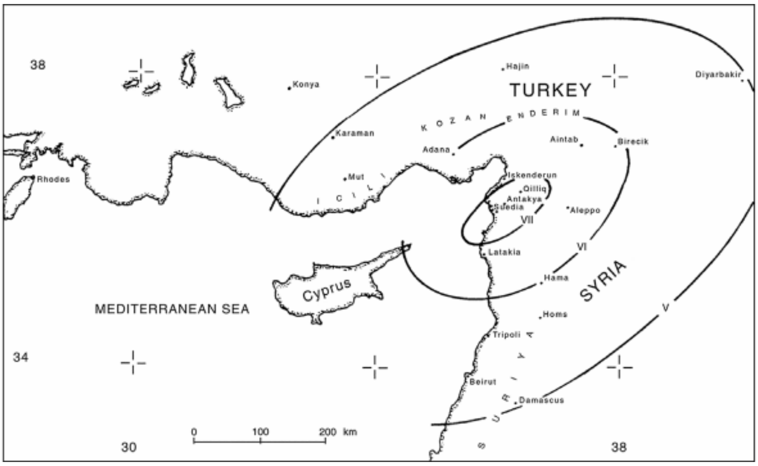

Fig. 18. Map of intensity distribution for April 3, 1872 earthquake (Ambraseys, 1989).

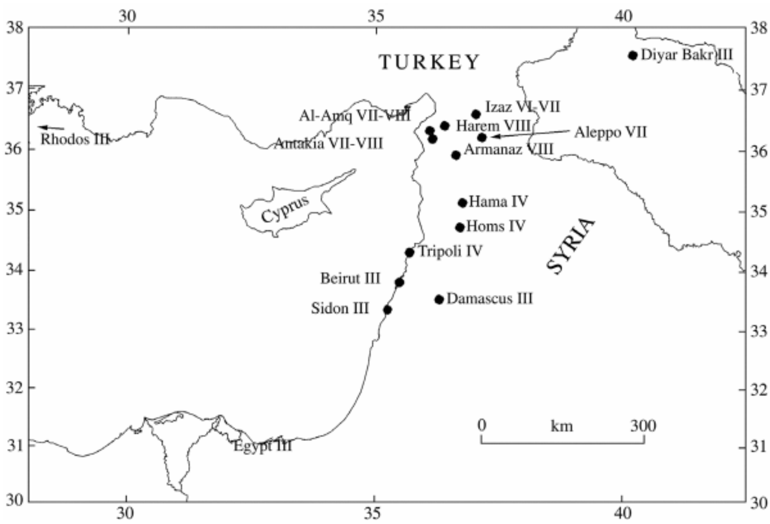

Fig. 19. Map of intensity distribution for April 3, 1872 earthquake.

at 07 h 50 min an earthquake caused destruction in Antioch and Swedieh, it was felt in Beirut and Tripoli (Fuchs, 1886). In April 28, an earthquake was felt in Sidon, Beirut and Antioch (Diaire des Pères Jésuites de Saida; Journaux Contemporains des Événments).

– Poirier and Taher (1980): 1872 April 2, Antioch was destroyed at 30%, 500-1800 victims.

– Ben-Menahem (1979): 1872 April 2, 07 h 45 min, 36.2N, 36.2E, near Samandag, I_0=X-XI, M_L=7.3, destruction of Antioch. Felt in Palestine and Egypt. Strong aftershocks on April 10 and May 15 (Amiran; Ergin *et al.*; Karnik; Plassard and Kogoj; Sieberg).

Seismological compilations

– Ambraseys (1989): 1872 April 3, a large earthquake occurred at 7:40 a.m., affecting the reaches of the Orontes where the river empties into the Mediterranean. The shock almost totally destroyed Antioch as well as its seaport of Suaidiya. At Antioch, the shock lasted 40 s, killing 500 people and injuring an equal number. 1960 houses of 3003 were totally destroyed and 894 so damaged. There were a further 1331 other buildings, *i.e.* shops, mosques, churches, etc., of which there remained 349 shops, one mosque and one soap factory; thus, of the 4334 buildings of all kinds, only 500 were left standing. The Greek cathedral, completed before the earthquake, and the American Protestant church and premised collapsed, killing four members of the community. The East and North gates (of Bab Bulus) were thrown down and part of the citadel walls collapsed. The old Roman bridge of four arches was breached in several places and all manor houses, including that of the Scotsman Yate, were destroyed. By contrast with the lower part of the town, the upper part suffered less severely. Thirty-eight villages between Suaidiya and Beilan were totally destroyed. 2150 houses were destroyed in Suaidya, and more than 300 people killed or seriously injured. The nearby villages of Kabusi, Jedida and Laushiya were razed to the ground with loss of life. The sea rose after the earthquake, allegedly to a great height, flooding the coast. Qaramut and its district were completely destroyed. In the town itself there were 170 dead and 187 wounded; in addition to shops and public buildings, 3552 houses were razed to the ground. Heavy damage extended to east of Amik Glü. Qilliq was totally ruined with the loss of 300 lives, and neighboring villages suffered similarly. Here, it is said, the earthquake split the ground in places and yellow sand filled the area, a description suggesting widespread liquefaction. Also, between Batrakan and Quaralu, the valley to the east of hills is said to have dropped as a result of the earthquake and the ground was 'rent' all the way to Baghras, an allusion to faulting. Damage was very heavy and there was great loss of life to the north and south of Qilliq, particularly in the region of Harim and Armanaz, but details are lacking. In Aleppo, the shock lasted 72 s and caused great panic. About 100 houses were badly damaged or collapsed, killing 7 and injuring 3 people. Part of the citadel fell down. Damage extended to Izaz, Basut, Zirbeh and Idleb as well as to settlements along the Mediterranean coast such as Arsuz and Iskenderun. Damage to the south of Afsiyeh became known many months after the earthquake, as did damage to bridges and hans. The Orontes bridge at Jisr Al-Hadid was damaged and its defense towers were thrown down. The shock was very strongly felt at Adana, Aintab, Birecik, Hama, Homs and Tripoli. It was reported from Rhodes, Konya, Diyar Bakr, Beirut and Damascus. The earthquake was not felt in Egypt as alleged by modern writers. Aftershocks continued to be felt with decreasing severity throughout April and May, but did not cease altogether until 1873 February (Consular Archives; Press Reports).

– Sieberg (1932): 1872, a destructive earthquake in Northern Syria, killing 1800 persons. 2/3 of Antioch and Swedieh were ruined and rebuilt again using stones of the ramparts of the city. Iskandarun and Aleppo felt by this event, but without damage. It was felt in Urfa, Diyar Bakir, many places in Mesopotamia, Damascus, Yafa, Egypt, Tripoli (of Libya), Rhodos and Smyrna. Aftershocks lasted till August, that were felt in Antioch, Aleppo and Smyrna.

‹172› **1873 February 9 Aleppo: III.**

Seismological compilations

– Sieberg (1932): 1873 February 9, a shock was felt in Aleppo.

‹173› **1873 February 14 Tyr: V; Beirut: III; Al-Quds: III; Akka: III.**

Parametric catalogues

– Plassard and Kogoj (1981): 1873 February 14, in Lebanon $I_=$V, an earthquake felt in Tyr, Beirut and Palestine (Fuchs; Sieberg).

– Ben-Menahem (1979): 1873 February 14, off coast Sur, $M_{L=}$6.2, strong at Sur. Felt in Jerusalem and Cairo (Amiran; Plassard and Kogoj; Sieberg).

Seismological compilations

– Sieberg (1932): 1873 February 14, a strong shock was reported in Tyre. It was felt in Beirut, Akka and Jerusalem.

‹177› **1884 June 6 Aleppo: V.**
Seismological compilations
– Sieberg (1932): 1884 June 6, a strong shock was felt in Aleppo.

‹178› **1896 February 20 Damascus: V.**
Parametric catalogues
– Plassard and Kogoj (1981): 1896 February 20, I_0 III? (in Lebanon), an earthquake caused damage in Damascus (Sieberg).
Seismological compilations
– Sieberg (1932): 1896 February 20, a slight earthquake occurred in Damascus. It was followed by a shock at night.

‹179› **1896 May 12 Baalbak: V.**
Parametric catalogues
– Plassard and Kogoj (1981): 1896 May 12, I_0 VI, two shocks were felt at Baalbek (Sieberg).
Seismological compilations
– Sieberg (1932): 1896 May 12, two strong shocks were felt in Baalbak. The second was stronger.

‹180› **1896 May 14 Antioch: V; JisrAsh'Shoughur: III; Lattakia: III; Aleppo: III; Kelless: III.**
Seismological compilations
– Sieberg (1932): 1894 May 14, an earthquake occurred in Northern Syria. It was strong in Antioch. It was weak in Jisr Ash'Shoughur, Lattakia, Aleppo and Kelless.

‹181› **1896 June 29 Syria: IV; Bisri: IV; Shouf: IV; Palestine: IV; Cairo: IV.**
Parametric catalogues
– Plassard and Kogoj (1981): 1896 Jun. 29, I_0 VI, an earthquake was felt at Bisri, Chouf in Lebanon, Syria, Palestine and Cairo (Blanckenhorn, 1905; Willis, 1928, 1933a,b; Sieberg, 1932).
Seismological compilations
– Sieberg (1932): 1896 June 29, an earthquake caused heavy destruction at Lymasol.

6.4. *Historical seismic events without re-evaluation*

‹092› **1268 Kiikia.**
Parametric catalogues
– Plassard and Kogoj (1932): 1268, I_0 III, an earthquake caused destruction in Cilicia (Abu Al-Faraj; Al-Suyuti).

‹101› **1355 Syria; Armenia; Palestine.**
Seismological compilations
– Sieberg (1932): 1355, an earthquake in Syria caused minor damage. It was felt in Armenia and Palestine.

‹144› **1759 November 25, 19:23 (local time) Baalbak: >VIII; Serghaya: >VIII; Zabadani: >VIII; Ras Baalbak: VIII; Al-Qunaytra: VIII; Damascus: VII-VIII; Beirut: VII-VIII; Sidon: VII-VIII; Safad: VII-VIII; Sur: VII-VIII; Tripoli: VII; Acre: VII; Homs: VI-VII; Hama: VI-VII; An-Nasra: VI-VII; Hosn Al-Akrad: VI-VII; Lattakia: V-VI; Al-Quds: V-VI; Gaza: V-VI; Antioch: V-VI; Aleppo: V; Tarba: V; Anatolia: IV; Egypt: IV** (fig. 20)**. Faulting along the Bekaa valley. Landslides near Mukhtara and Deir Marjrjos. Tsunami at Acre. Aftershocks.**
Parametric catalogues
– Plassard and Kogoj (1981): 1759 November 25, I_0 X, it was an earthquake that caused destruction in Shouf and 100 persons were killed, it also caused destruction in Baalbak, Ras Baalbak, Hasbaya, Beit Jin and Northern Syria (Jalfaq; Perrey; Sieberg).
– Ben-Menahem (1979): 1759 November 25, 33.8N, 36.2 E, I_0 X-XI, M_L 6.8, great destruction at Baalbak. A part of Damascus destroyed. Damaged area extends to Antioch and Yafa. Safad M_M VIII. Many thousands of persons were reported to have perished in the Bekaa (Amiran; Plassard and Kogoj; Seiberg).
Seismological compilations
– Sieberg (1932): 1759 November 25, a destructive earthquake destroyed 1/3 of Damascus. Many places in Lebanon were strongly damaged. In Baalbak, there was heavy damage, 12 huge columns of the Temple fell down. It was felt in Antioch and Yafa. Aftershocks continued to the end of the month, causing a few houses to fell.
Monographs
– Ambraseys and Barazangi (1989): 1759 November 25, 33.7N-35.9E, M_S 7.4, tsunami and faulting. It is the main shock of the 1759 earthquakes, lasted about 50 s. It destroyed totally all villages in a narrow zone extending to the NE

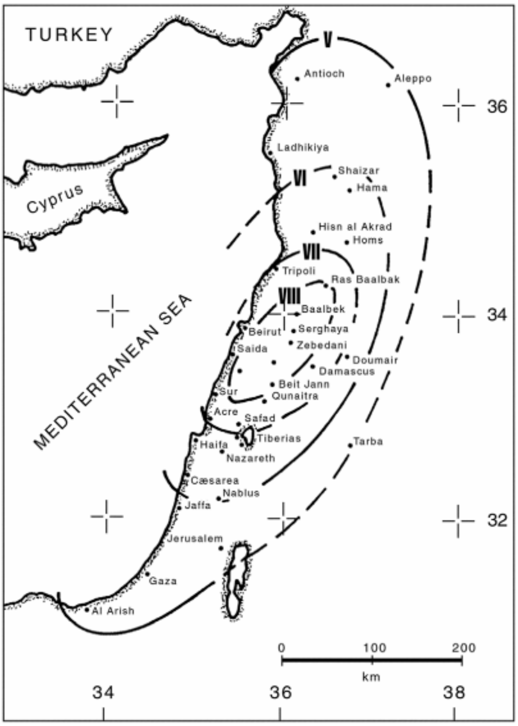

Fig. 20. Map of intensity distribution for November 25, 1759 earthquake (Ambraseys and Barazangi, 1989).

for about 120 km along the Litani and the Bekaa Valleys into the upper reaches of the Orontes River in NW Syria. Safad was almost totally destroyed with loss of life. The Metwali settlements, Bshara and in the Shouf region, were razed to the ground. Near Mukhtara and Mar Djerjos, rock falls and landslides took place and added to the damage. In Serghaya and Hasbaya, there was heavy destruction. Baalbak was totally destroyed with great loss of life, a landslide was dammed the supplied water up. Heavy damage extended to Ras Baalbak. The available evidence suggests that within this area of maximum damage the earthquake was associated with extensive faulting for at least 100 km. In Damascus district, many villages in the Ghutah and Marj suffered mainly from foundation failures. The shock caused great panic in Damascus with several casualties and damage, of the 15000 mainly adobe houses, very few collapsed completely but many were badly cracked, the Umayyad mosque, other mosques, medreses, gates, baths and walls suffered different degrees of damage, a few minarets were thrown down causing additional damage to adjacent houses, part of the Damascus Citadel crumbled into the Banas canal damming its flow, in Salihiyeh (north part of Damascus), damage was more serious, European consuls estimated loss of life at a few handred lives as compared to 6000-20 000 given by local sources in Damascus. It was strongly felt in Antioch and Lattakia, causing some panic and collapse of a number of old houses. In Aleppo, it lasted two minutes and a few walls were fissured. It was also felt in Tarba, Gaza and Al-Arish and a few old Khans were damaged. The shock was felt throughout Anatolia as far as Nakhichevan and in Egypt. A seismic sea wave associated with this earthquake was noted as far south as the Nile Delta without any damage. In Acre, ships were thrown onto the shore with some casualties. The total estimated killed number by various temporary writrers vary between 10000-40000. Aftershocks continued to be felt till August 1760 (Al-Budayri; Archives British Legations; Archives Historiques Ch. Comm. Marseille; ANF; Ben Zvi; Dahman; Findikli; Vitaliano; Yaari).

(154) **1810 Baalbak: VI; Tripoli: VI; Syria: III; Palestine: III.**

Parametric catalogues

– Plassard and Kogoj (1981): 1810, I_0 VII, an earthquake caused light damage near Baalbak and in Lebanon, a house in Tripoli was destroyed, it was felt in Syria and Palestine (Diaire des Pères Lazaristes de Tripoli; Willis).

(161) **1837 January 1, 04:00 p.m. (local time) Safad: VII-VIII; Nablus: VII-VIII; Beit Lahm: VII-VIII; Al-Khalil: VII-VIII; Tabariya: VII; Beirut: VI-VII; Damascus: VI. Tsunami at the lake of Tabariya. Aftershocks.**

Parametric catalogues

– Ben-Menahem (1979): 1837, January 1, 14h 34m, 33.0N, 35.5 E, near Safad, I_0 IX, M_L 6.4, destructive in Safad and Tiberias. 5000 victims. Damage at Sur, Sidon, Damascus and Beirut. Tsunami in the lake of Galilee (Amiran;

Braslawy; Karnik; Plassard and Kogoj; Sieberg; Vered and Striem; Willis).
– Plassard and Kogoj (1981): 1837 January 1, I_0 IX, an earthquake caused destruction in Shouf, Palestine, Safad (5000 persons killed?) and Tiberias (700 persons killed and there was agitation of the lake water and elevation of temperature of the thermal sources), in Beirut there was large damage and panic, there was damage in Damascus (Shalem; Sieberg).
Seismological compilations
– Sieberg (1932): 1837 January 1, a destructive earthquake in the Galilea killed a large number of people. It was felt in Cyprus. Safad was near completely destroyed and it was said that 1000-5000 were killed. In Tabrias, most of the houses and a large part of its wall fell down, with a loss of 700 lives. Temperature of the springs increased. There was a tsunami in the lake of Al-Huleh. Zone of destruction extended from Jesreel niderung till Beirut. Another zone of destruction extended from Nablus through Beit Lahm till Al-Khalil. Aftershocks continued till end of January in the Galilea region, especially in Safad. On 24 January many houses at Sur were destroyed.
Monographs
– Ambraseys (1997): 1837 January 1 at about four in the afternoon, its epicentral area extended from beyond Safad into Lebanon, M_s 7.0, there is no conclusive field evidence that this event was associated with surface faulting. There was a destructive earthquake lasting about 20 s which caused heavy damage in Southern Lebanon and Northern Palestine. Destruction was done along the relatively narrow zone which extended from the coastal area of Saida through the inland ikilmi of Al-Touffa, Marjuyum, Bshara to lake Taberias. In Beirut, the earthquake caused panic and about eight houses collapsed killing two people. Saida was almost totally ruined with the loss of 7 lives. Much of Banyas was ruined. Sur suffered considerable damage where 40 houses collapsed killing 16 and injuring 36 people. Bint Jubayl was ruined with the loss of 8 lives. In Safad, the largest of places affected with 2158 deaths. At Acre, about houses fell, 4 people were killed and several injured. Also in the district of Acre, 141 people were killed. In Tiberias, about two thirds of the houses collapsed killing 822 people and injuring 65. In Nazareth, only one house collapsed and one quarter of the dwellings suffered killing 7 people. In Nablus, one quarter of the houses and a number of shops were ruined causing the loss of 48 lives. In Damascus, about 2000 houses were slightly damaged, 4 minarets and several houses were destroyed and about 10 people were killed or injured. Bazaars were damaged and parts of the city gates as well as several. At the port of Jaffa the shock threw merchandise from stacks while it was slow in Ramala. In Jerusalem, the earthquake was not very strong. The shock was felt all along the coast such as in Tripoli, Lattakia, Antioch as well as in Aleppo and at Kilis. Also it was felt in the Nile Delta, at Damietta and Cairo. The earthquake was also felt in Famagusta and Larnaca. Aftershocks continued to be felt for almost 4 months *e.g.*, 16, 22, 25 January and 20 May were the most important. The loss of life due to this earthquake and its aftershocks was larger than 6000-7000 deaths (AMAE CADN; Archives Dép. des Bouches du Rhône; Archives Société de Géographie; Archives: Abdin Palace, Athene, Correspondenzblatt, L'Echo du Monde Savante, Journal de Smyrne, Das Morgenland, Natur und Heilkunde; FO).

(163) 1845 February 21 Antioch: V; Cyprus: III.
Parametric catalogues
– Plassard and Kogoj (1981): 1845 February 21, I_0 III, a strong earthquake occurred in Antioch. It was felt in Cyprus (Ambraseys, 1961, 1963).

(174) 1873 November 4 Sidon: III.
Parametric catalogues
– Plassard and Kogoj (1981): 1873 November 4, I_0 III (in Lebanon), an earthquake was felt at Sidon (Diaire des Pères Jésuites de Saida; Journaux Contemporains des Événments).

(175) 1877 February 26 Sidon: III.
Parametric catalogues
– Plassard and Kogoj, 1981: 1877 February 26, I_0 III, an earthquake was felt at Sidon (Diaire des Pères Jésuites de Saida; Journaux Contemporains des Événments).

(176) 1881 January 23, 17:45 (local time) Sidon: III.
Parametric catalogues

– Plassard and Kogoj (1981): 1881 January 23, I_0 III (in Lebanon), an earthquake was felt at Sidon (Diaire des Pères Jésuites de Saida; Journaux Contemporains des Événments; Sieberg).

7. Discussion and conclusions

This catalogue represents a comprehensive databank on the historical earthquakes for Syria and the surroundings covering 35 centuries, and will serve in studying the seismic hazards of the region. It is a unified seismological compilation and parametric catalogue. While it is certain that many small earthquakes must be missing due to many reasons, we can say that the total number of the historical earthquakes in and around Syria for the period between the 14th century B.C. and the 19th century A.D. amounts to 181 events. The 1365 B.C. earthquake in Ugharit was the first documented one to be mentioned in the catalogue. The most extensive and disastrous appear to have been those of 53 A.D., 494, 502, 551, 747, 849, 859-860, 1114, 1157, 1170, 1202, 1404, 1408, 1705, 1759, 1796, 1822, 1837 and 1872. They caused considerable damage and killed a large number of people in Syria and Lebanon. Most these events were preceded and followed by some damaging shocks, some of them causing significant destruction and large loss of life. On the other hand, they were associated with earthquake hazards such as faulting raptures, liquefaction, landslides, tsunamis and fires.

Parameters of 36 historical events are included in table I. Also, fig. 21 is a distribution of these events. These destructive earthquakes and others

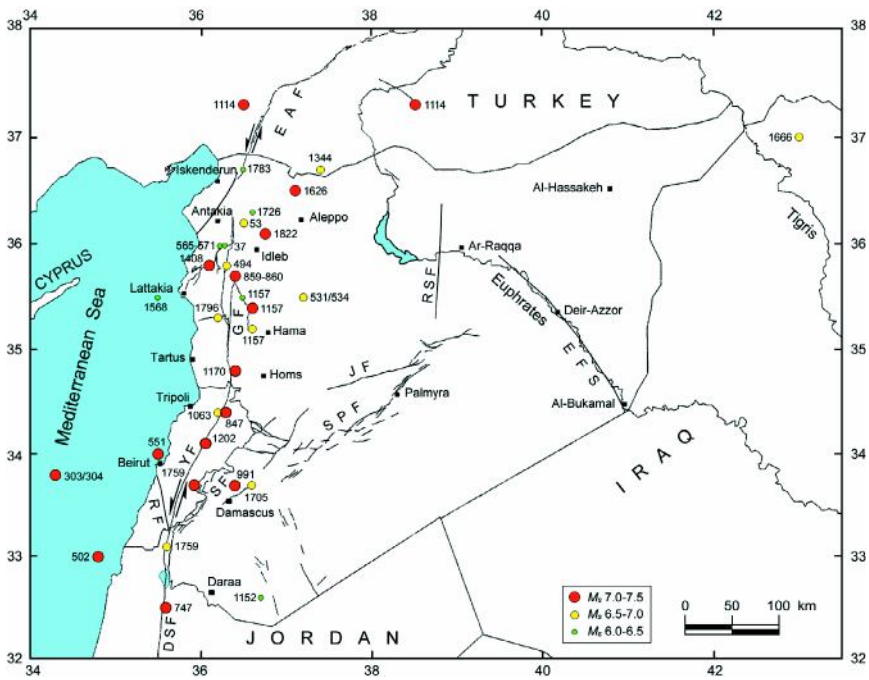

Fig. 21. Map of Syria and the surroundings showing the distribution of historical earthquakes epicenters (circles). Dates of earthquakes are listed in table I. DSF – Dead Sea Fault system; EAF – Eastern Anatolian Fault system; EFS – Euphrates Fault System; GF – Al-Ghab Fault; RSF – Ar-Rassafeh Fault; RF – Roum Fault; SF – Serghaya Fault; SPF – Southern Palmyride Fault; YF – Al-Yammouneh Fault (faults are compiled from McBride *et al.*, 1990; Barazangi *et al.*, 1993; Gomez *et al.*, 2001).

presented in the catalogue occurred primarily as a result of movement of the northern segment of the Dead Sea fault system (Al-Yammouneh in Lebanon and Al-Ghab in Syria) and of the Eastern Anatolian fault system. While few large earthquakes occurred along the Palmyra, Ar-Rassafeh and the Euphrates faults. Table II is a complete list of historical earthquakes with estimated intensities at relevant localities and accompanying effects, with information completeness (A– complete; B – accepted; C – uncomplete) and information quality factors (1 – good source quality; 2 – moderate source quality; 3 – poor source quality).

The general conclusion of this paper is that the historical seismicity of Syria is relatively-well documented now, and that Western Syria and Lebanon are the most seismic regions, while the Palmyra, Ar-Rassafeh, the Euphrates and the Jabal Al-Arab regions have less seismic activity. Consequently, the earthquake hazards may be genuine in the Western Syria and Lebanon, the region that is the most densely populated where both regions include the larger cities such as Damascus, Beirut, Aleppo, Homs, Hama, Tripoli, Idleb, Lattakia, Tartus, Daraa, Akka, Saida, Zahleh, Baalbak Al-Qunaytra and Antakia.

Comparing both instrumentally recorded (figs. 2 and 22) and historical earthquakes (figs. 21 to 23) for the northern extension of the DSF in Syria and Lebanon, one can easily see that there is a clear difference between these two periods. In fact, the instrumental seismicity represents an apparent quiescence that does not reflect the potential hazard. It is, therefore, recommended that consideration of historical period is essential when assessing seismic hazard in this region.

Table II. A complete table of historical earthquakes with estimated intensities at relevant localities and accompanying effects, with information completeness (A – complete; B – accepted; C – incomplete) and information quality factors (1 – good source quality; 2 – moderate source quality; 3 – poor source quality)

No.	Date	Intensity distribution	Surface effects	Completeness	Quality
001	~ 1365 B.C.	Ugharit: VIII-IX.	Tsunami, fire.	C	2
002	590 B.C.	Tyre: VII?	Tsunami at the Lebanese coast.	C	3
003	525 B.C.	Tyre: VIII-IX; Sidon: VIII-IX; Kiklades island: III-IV; Eubea island: III-IV.	Tsunami at the Lebanese coast.	B	3
004	331 B.C.	Syria: VI.		C	3
005	199-198 B.C.	Sidon: VIII; Syria: ≤VII.	Landslide at Sidon.	C	3
006	148-130 B.C. February 21, afternoon	Antioch: ≥ VII.		C	3
007	92 B.C.	Syria: III-IV; Egypt: III-IV.	Tsunami at the Syrian-Lebanese coasts.	C	3
008	65 B.C.	Syria: VII-VIII; Antioch: VII-VIII; Al-Quds: VI; Cyprus: III-IV; Salamis: III-IV; Famagusta: III-IV.		B	3
009	37 B.C. March 23, morning	Dafneh: VI-VII; Antioch: V.		C	3
10	19 A.D.	Sidon; Palestine; Syria; Asia Minor.		C	3
011	37 A.D.	Antioch: VII-VIII; Dafneh: VII; Al-Quds: IV.		C	3

Table II (*continued*).

No.	Date	Intensity distribution	Surface effects	Completeness	Quality
012	47	Antioch: VII.		C	3
013	53	Antioch: VII-VIII; Afamia: VI-VII; Manbej: VI-VII; Lattakia:VI-VII (fig. 15).		B	3
014	82-94	Antioch: VI-VII; Syria.	Aftershocks.	C	3
015	115 December 13	Antioch: VII; Eleyah: VI -VII; Mirana: VI-VII; Rhodos: IV; Pitana.	Tsunami at Caesaria, the Lebanese coast and Yavne.	B	2
016	130	Damascus: V-VI; Baalbak: V; Eastern Mediterranean region.	Aftershocks.	C	3
017	160 October	Dura Europos: ≥ VI.		C	3
018	220	Antioch: VI.	Aftershocks.	C	3
019	233	Damascus: VII.		C	3
020	242-245	Antioch: VI-VII; Syria: VI- -VII; Egypt: III; Iran: III.		B	3
021	272	Antioch: VI; Syria: VI.		C	3
022	303-304	Sidon: VIII; Tyre: VIII; Syria: VII; Al-Quds: III-IV.	Tsunami at Caesaria.	B	2
023	341	Antioch: VI-VII; Beirut: VII.	Aftershocks.	C	2
024	348-349	Beirut: VII; Arwad: VI.	Tsunami?	C	3
025	363 May 18-19, night	This earthquake destroyed Palestine and parts of Jordan, Panyas: VII.		C	2
026	394-396	Antioch: V-VI.		C	3
027	450-457 September	Tripoli: VI-VII.		C	3
028	458 September	Antioch: VII-IX.		C	2
029	475 September	Jableh: VII-VIII.		C	3
030	494	Antioch: VII, Tripoli: VI-VII; Lattakia: VI-VII; Beirut: V.		B	3
031	500	Antioch; Seleucea; Orfa; Safad.		C	3
032	502 August 22, Friday	Akka: VIII; Tyre: VII-VIII; Sidon: VII-VIII; Beirut: VII; Palestine: VI; Safad: VI?; Reina: VI?		A	2
033	525 May	Beirut: VII-VIII; Byblus: VII-VIII; Sidon: VI-VII; Antioch: VI-VII.	Aftershocks.	A	3
034	526 May 20-29	Antioch: VIII; Dafneh: VII; Seluecea: VII.	Aftershocks. Liquefaction at Antioch. Fire in Antioch.	B	1
035	528 November 29	Antioch: VII-VIII; Lattakia: VI-VII.		C	1
036	531-534	Area between Aleppo and Homs: VI-VII; Antioch:		C	2

Table II (*continued*).

No.	Date	Intensity distribution	Surface effects	Completeness	Quality
		VI; Mesopotamia: IV.			
037	551 July 9	Beirut: IX-X; Sur: IX-X; Tripoli: IX-X; Byblus: IX-X; Al-Batron: IX-X; Shaqa: IX-X; Sarfand: VII-VIII?; Sidon: VII-VIII; Arwad: III-IV.	Tsunami along the Lebanese coast. Landslide near Al-Batron. Fire at Beirut (fig. 5).	A	1
038	553	Antioch: V.		C	3
039	557	Antioch: V.		C	3
040	565-57 1	Antioch: VI-VII; Seleucea: VI-VII; Kilikia: VI; Anazrabo: VI; Orfa: IV.		B	1
041	580-58 1	Antioch: VI-VII; Dafneh: VI.		C	1
042	588	Antioch: VI-VII.	Aftershocks.	C	1
043	601-602	Kilikia; Syria.	Surface faulting.	C	1
044	634	Aleppo: VII-VIII; Palestine: IV-V.	Aftershocks.	C	1
045	639	Antioch: IV-V.		C	3
046	678	Batnan: VI-VII; Orfa: VI-VII; Mesopotamia: VI.		C	1
047	713 February 28	Antioch: VI-VII; Aleppo: VI-VII; Kennesreen: VI-VII.	Aftershocks.	C	1
048	717 December 24	Antioch: VI-VII; Batnan: VI-VII; Orfa: VI-VII.	Aftershocks.	C	1
049	747 January 18 (It seems to be that there are two earthquakes, the first is in the Southern Syria while the second is in the northern one and Mesopotamia that Manbej could be affected.)	Mt. Tabor: VII-IX; Baalbak: VIII; Bosra: VII; Nawa: VIII; Balqa: VIII; Al-Quds: VII; Beit Qubayeh: VII-VIII; Tabaryya: VII; Al-Ghouta and Manbej: VII; Darayya: VI; Damascus and Daraa: V-VI; Ariha.	Surface faulting and liquefaction in Mesopotamia. Landslide at Mt.Tabor.	A	1
050	757 March 9	Habura: VII; Mesopotamia; Syria; Palestine.		C	1
051	775	Antioch: IV.		C	3
052	791	Aleppo: V; Northern Syria; Palestine.		C	3
053	8th century	Ar-Rassafeh: VII-VIII.		C	3
054	835 January 5--December 25	Antioch: VI-VII.	Aftershocks.	C	3
055	846 August 28--847 August 16	Antioch: > VIII; Damascus: VII; Homs: VII; Antioch; Al-Jazira: VI; Al-Mousel: VI.	Aftershocks.	A	3

Table II (*continued*).

No.	Date	Intensity distribution	Surface effects	Completeness	Quality
056	847 November 24	Damascus: VII-VIII; Al-Ghouta: VII-VIII; Al-Mazzeh: VII; Beit Lahya: VII; Darayya: VII; Antioch: VI; Al-Mousel: V.		A	1
057	853 June 12- -854 June 1	Tabariya: VIII-IX.	Landslide.	C	3
058	859 December 30- -860 January 29 (It could be two earthquakes, the first one is between Antioch and Lattakia while the second is on the Euphrates.)	Antioch: VIII; Lattakia and Jableh: VIII; Homs: VII; Palmyra: VII; Tarsus: VI; Balis: VI; Damascus: VI; Adana: VI; Al-Quds: V-VI; Ar-Raqqa: V; Ras Al-Ein: V; Harran: V; Orfa: V; Egypt: IV (fig. 6).	Landslide.	A	1
059	881 May 16	Syria; Egypt; Mesopotamia; North Africa and Al-Andalus.		C	3
060	889	Aleppo: III-IV.		C	3
061	894	Northern Syria.		C	3
062	951 June 9- -952 May 28	Aleppo: V-VI; Raaban?; Duluk ?; Tal Hamed ?	Aftershocks.	C	3
063	963 July	Izaz: VII; Northern Syria: VI.	Rock-falls.	C	3
064	972	Antioch: VI-VII, Damascus: V.		C	2
065	991 April 5, night	Baalbak: VIII-IX; Damascus: VII-VIII; Egypt: III-IV.	Landslide, tsunami, aftershocks.	C	3
066	1002 November 10- -1003 October 29	Western Syria: ≥ VIII.		C	3
067	1029 January 20- -1030 January 8	Damascus: VII.		C	3
068	1042 August 21- -1043 August 9	Palmyra: > VII; Baalbak: V; Tabriz: III; Egypt: III.		B	3
069	1046 July 8- 1047 June 27	Diyar Bakr: ≥ VII; Khlat: ≥ VII.		C	3
070	1063 July 30- -August 27	Tripoli: VII-VIII; Lattakia: V-VI; Acre: V-VI; Sur: V-VI; Antioch: V (fig. 7).		B	1
071	1089	Palmyra: ≥ VIII.		C	3
072	1091 September 26 or October 6	Antioch: VI-VII.		C	1
073	1094 April 20- -May 18	Damascus: V-VI.		C	1

Table II (*continued*).

No.	Date	Intensity distribution	Surface effects	Completeness	Quality
074	1098 January	Antioch: III; Aleppo: III.		C	3
075	1114 November (Two earthquakes could be happened; one at Maraash and other at Orfa.)	Maskaneh: VIII; Maraash: VII-VIII; Samsat: VII-VIII; Orfa: VII-VIII; Harran: VII; Aleppo: V; Antioch: IV (fig. 8).	Landslide.	A	1
076	1128	Tyre.	Surface faulting?	C	3
077	1135	Syria.		C	3
078	1137 October 19 -November 16	Syria: VII; Al-Jazira: VII; Al-Mousel: VII; Iraq: VII.		B	1
079	1138 October 11-26	Al-Sham: VI-VII; Al-Jazira: VI-VII; Aleppo: VI-VII.	Aftershocks.	C	1
080	1139	Aleppo.		C	3
081	1140 August 17 -1141 August 6	Qalaat Sheizar: VI-VII.		C	2
082	1152 September 27	Bosra: VII; Hauran: VII; Syria: VII.		C	2
083	1156 September -1159 May	Western Syria including Damascus.	Foreshocks, aftershocks, surface faulting.	C	1
084	1170 June 29	Damascus: VII-VIII; Homs: VII-VIII; Hama: VII-VIII; Al-Sham: VII-VIII; Lattakia: VII-VIII; Baalbak: VII-VIII; Shaizar: VII-VIII; Barin: VII; Aleppo: VII-VIII; Iraq: V; Al-Jazira: V; Al-Mousel: V (fig. 10).	Aftershocks, tsunami.	A	1
085	1182	Bosra: VII; Judea: VI; Nablus: VI.		C	3
086	1202 May 20, early morning	Mount Lebanon: IX; Baalbak: IX; Tyre: IX; Nablus: VIII; Beit Jin: IX; Banyas: VIII+; Al-Samyra: VIII+; Damascus: VIII; Safita: VII; Akka: VII; Hauran: VIII; Hama: VIII; Tripoli: VIII; Safad: VII; Al-Quds: VI; Bosra: VII-VIII; Al-Batron: VII; Jbeil: VII; Beirut: VII; Marqab and Hosn Al-Akrad: VII; Barin: VII; Homs: VII; Tartus: VI; Aleppo: V; Antioch: V; Al-Mousel: IV-V; Mesopotamia: IV; Cairo: IV; Alexandria: IV; Dimyat: IV; Qus: IV; Iraq: IV; Cyprus: VII?; Lesser Armenia: IV; Sicily: IV; Khlat: IV; Ceuta: III?; Constantinople: IV (fig. 16).	Tsunami, landslide, aftershocks.	A	1
087	1212	Antioch.		C	3
088	1222	Kelless.		C	3

Table II (*continued*).

No.	Date	Intensity distribution	Surface effects	Completeness	Quality
089	1236	Northern Syria: VI-VII.		C	3
090	1242	Syria.		C	3
091	1254	Northern Syria.		C	3
092	1268	Kilikia.		C	3
093	1274	Syria.		C	3
094	1281	Syria.		C	3
095	1287 March 22	Lattakia: VII-VIII; Palestine: IV; Armenia: IV.		C	3
096	1290	Syria.		C	3
097	1303 August 8 (It seems to be two different events.)	Cairo: VII; Alexandria: VII; Damanhur: VII, Safad: VII; Damascus: VI; Hama: VI; Antioch: IV; Tunis: IV; Barqa: IV; Morocco: IV; Cyprus: IV; Istanbul: IV; Sicily: IV.	Tsunami, flood.	A	2
098	1322 January 20- -February 19	Damascus: V.		C	2
099	1339 January 13 -February 11	Tripoli: VII, Palestine: IV.		C	3
100	1344 January 2	Al-Rawendan: VIII; Manbej: VII-VIII; Aleppo: VI-VII; Damascus: IV.		B	1
101	1355	Syria; Armenia; Palestine.		C	3
102	1399 September 20	Damascus: III-IV.		C	3
103	1403 December 18	Aleppo: IV-V.		C	3
104	1404 February 20	Qalaat Blatnes: VIII; Bkas: VIII; West of Aleppo: VII-VIII; Qalaat Al-Marqeb: VII-VIII; Tripoli district: VII, Lattakia: VII; Jableh: VII.	Tsunami, landslide.	A	2
105	1404 November 5- -December 4	Aleppo: V.		C	3
106	1407 April 9- -May 8	Antioch: VII; Cyprus: V.	Surface faulting.	C	3
107	1408 December 29	Shugr: VIII-IX; Bkas: VIII- -IX; Blatnes: VIII; Lattakia: VII; Jableh: VII; Antioch: VII; Syrian coast: VI (fig. 17).	Faulting between Sfuhen and Al-Quseir. Landslide in Sfuhen. Tsunami in Lattakia.	A	2
108	1484 March 29- -April 27	Aleppo: V-VI.		C	3
109	1491 April 24	Nicosia: VII; Limassol: VII; Famagusta: VII; Paphos: VII; Damascus: IV; Cairo: IV; Crete: IV.		A	2
110	1537 January 7	Antioch: VII; Damascus: IV; Dimyat: IV-V; Egypt: IV.		B	1

Table II (*continued*).

No.	Date	Intensity distribution	Surface effects	Completeness	Quality
111	1537 March 08	Damascus: IV.		C	2
112	1546 September 29	Nablus: VI-VII; Damascus: V; Al-Quds: VI; Yafa: VI; Tripoli: VI; Famagusta: V.	Tsunami at Cyprus.	A	3
113	1563 September 13	Damascus: VI.		C	2
114	1565 July 26	Damascus: V.		C	2
115	1568 October 10	Lattakia: VII; Famagusta: V; Limassol: IV; Nicosia: IV.		B	3
116	1577	Northern Syria: VI-VII; Palestine: IV; Cyprus: IV; Armenia: IV.	Aftershocks.	B	3
117	1604 March 13	Damascus: V, Bekaa: V.		C	2
118	1606 October 19	Baalbak: IV.		C	2
119	1610 March 7	Aleppo: VI.		C	2
120	1616 July 22	Aleppo: VI.		C	3
121	1618 July 8	Damascus: IV.		C	2
122	1618 July 23-- -August 21	Damascus: IV.		C	2
123	1619 December 8- -1620 November 25	Darkoush.	Landslide.	C	2
124	1626 January 21	Aleppo: VIII-IX; Gaziantab: VIII-IX; Hama: VI-VII; Damascus: V (fig. 11).		B	2
125	1627 November 24	Damascus: V.		C	2
126	1640	Damascus: VI; Syria; Tabriz.		C	3
127	1656 February	Tripoli: VII, Palestine: IV.		C	3
128	1657	Aleppo: IV.		C	3
129	1666 September 22	Al-Mousel: VII-VIII; Sinjar: VI-VII; Sharqat: VI-VII; Aleppo: V; Tabriz: V; Van: V.	Landslides, aftershocks.	A	2
130	1680 March 22-23	Aleppo: IV.		C	3
131	1683	Safineh.	Landslides.	C	3
132	1693-1694	Northwestern Iraq.	Landslides.	C	3
133	1701	Aleppo: IV.		C	3
134	1705 November 24	Yabroud: VIII; Al-Qastal: VIII; Damascus: VII; Tripoli: VII.	Aftershocks.	B	2
135	1712 December 28	Damascus: IV.		C	2
136	1719 March	Aleppo: VII.		C	3
137	1722-1723	Aleppo: VII.		C	3
138	1726 April 15	Jum: > VII; Aleppo: VII; Iskenderun: IV; Famagusta: III.		B	2

Table II (*continued*).

No.	Date	Intensity distribution	Surface effects	Completeness	Quality
139	1738 September 25	Iskenderun: VIII; Bellen Bass: VII-VIII,; Antioch: VII; Jabal Al-Amanus: VII; Aleppo: V-VI; Kelless: V; Bereket: V.		A	2
140	1752 July 21	Lattakia: VII; Tripoli: V.	Tsunami at the Syrian coast.	C	3
141	1759 February 17	Aleppo: V.		C	3
142	1759 June 10	Aleppo: IV.		C	3
143	1759 October 30, 03:45 (local time)	Al-Qunaytra: VIII; Safad: VII; Acre: VI; An-Nasra: VI; Sidon: VI; Saasaa: VI; Damascus: V; Aleppo: IV; Al-Quds: IV; Beirut: IV; Antioch: IV; Gaza: IV; Cyprus: IV.	Landslides at the west of Damascus and Tabariya. Tsunami at Acre and Tripoli. Aftershocks.	A	1
144	1759 November 25, 19:23 (local time)	Baalbak: > VIII; Serghaya: > VIII; Zabadani: > VIII; Ras-Baalbak: VIII; Al-Qunaytra: VIII; Damascus: VII-VIII; Beirut: VII-VIII; Sidon: VII-VIII ; Safad: VII-VIII; Sur: VII-VIII; Tripoli: VII; Acre: VII; Homs: VI-VII; Hama: VI-VII; An-Nasra: VI-VII; Hosn Al-Akrad: VI-VII; Lattakia: V-VI; Al-Quds: V-VI; Gaza: V-VI; Antioch: V-VI; Aleppo: V; Tarba: V; Anatolia: IV; Egypt: IV (fig. 20).	Faulting along the Bekaa valley. Land-slides near Mukhtara and Deir Marjrjos. Tsunami at Acre. Aftershocks.	A	1
145	1760 January	Qadicha: V; Aleppo: VI.		C	3
146	1765	Tripoli: V; Aleppo: IV.		C	3
147	1778 May 5	Aleppo: IV.		C	3
148	1779 June 8	Aleppo: V-VI.		C	3
149	1783 December 4	Aleppo: IV.		C	3
150	1783 December 14	Aleppo: VI; Tripoli: IV.		C	2
151	1795 January	Aleppo: VI.		C	3
152	1796 April 26	Qalaat Al-Marqeb: VIII; Al-Qadmous: VIII; villages along Nahr Al-Kabir: VII-VIII; Jableh: VII-VIII; Bkas area: VII-VIII; Lattakia: VII; Saida: V; Aleppo: IV; Tripoli: V.	Landslides, liquefaction.	A	2
153	1802	Baalbak: VI; Palestine: III.		C	3
154	1810	Baalbak: VI; Tripoli: VI; Syria: III; Palestine: III.		B	3
155	1814	Al-Laja: VI-VII.	Rock-falls.	C	3
156	1819 February	Syria: IV-V.		C	3
157	1822 August 13, 09:50 p.m.	Jisr Ash'Shoughour: IX; Quseir: IX; Aleppo: VIII-IX;	Faulting, tsunami.	A	1

Table II (*continued*).

No.	Date	Intensity distribution	Surface effects	Completeness	Quality
	(local time)	Darkoush: VIII-IX; Antioch: VIII; Iskenderun: VIII; Idleb: VIII; Sarmeen: VIII; Kelless: VIII; Armanaz: VII-VIII; Sarmada: VII-VIII; Lattakia: VII; Homs: VII; Hama: VII; Maraash: VII; Ram Hamadan: VII; Bennesh: VII; Maarret Missrin: VII; Damascus: III; Gaza: III; Al-Quds: III; Black Sea: III; Cyprus: III (figs. 12, 13 and 14).			
158	1822 September 5	Aleppo: VII.		C	3
159	1830	Aleppo: III.		C	3
160	1831 February 22	Aleppo: V.		C	3
161	1837 January 1, 04:00 p.m. (local time)	Safad: VII-VIII; Nablus: VII-VIII; Beit Lahm: VII-VIII; Al-Khalil: VII-VIII; Tabariya: VII; Beirut: VI-VII; Damascus: VI.	Tsunami at the lake of Tabariya. Aftershocks.	A	3
162	1844 September 19 and 30	Aleppo: V.		C	3
163	1845 February 21	Antioch: V; Cyprus: III.		C	3
164	1846 December 3	Aleppo: V.		C	3
165	1850 February 12	Beirut: III; Ain Hamadeh: III.		C	3
166	1854	Antioch: III; Suaidiya: III; Beirut: III; Aleppo: III; Yafa: III.		B	3
167	1859 January 24	Tripoli: III; Beirut: III; Damascus: III; Aleppo: III.		B	3
168	1864 August 15	Aleppo: IV.		C	3
169	1868 April 16	Aleppo: III.		C	3
170	1870 January 2	Aleppo: III.		C	3
171	1872 April 3	Harem: VIII; Armanaz: VIII; Buhyret Al-Amq: VII-VIII; Antioch: VII-VIII; Aleppo: VII; Suaidiya: VII; Izaz: VI-VII; Idleb: VI-VII; Iskenderun: VI-VII; Hama: IV; Homs: IV; Tripoli: IV; Damascus: III; Beirut: III; Sidon: III; Diyar Bakr: III; Egypt: III; Rhodos: III (figs. 18 and 19).	Faulting at Baghras. Liquefaction, tsunami, aftershocks.	A	1
172	1873 February 9	Aleppo: III.		C	3
173	1873 February 14	Tyr: V; Beirut: III; Al-Quds: III; Akka: III.		B	3
174	1873 November 4	Sidon: III.		C	3
175	1877 February 26	Sidon: III.		C	3
176	1881 January 23, 17:45 (local time)	Sidon: III.		C	3

Table II (*continued*).

No.	Date	Intensity distribution	Surface effects	Completeness	Quality
177	1884 June 6	Aleppo: V.		C	3
178	1896 February 20	Damascus: V		C	3
179	1896 May 12	Baalbak: V.		C	3
180	1896 May 14	Antioch: V; Jisr Ash'Shoughur: III; Lattakia: III; Aleppo: III; Kelless: III.		B	3
181	1896 June 29	Syria: IV; Bisri: IV; Shouf: IV; Palestine: IV; Cairo: IV.		B	3

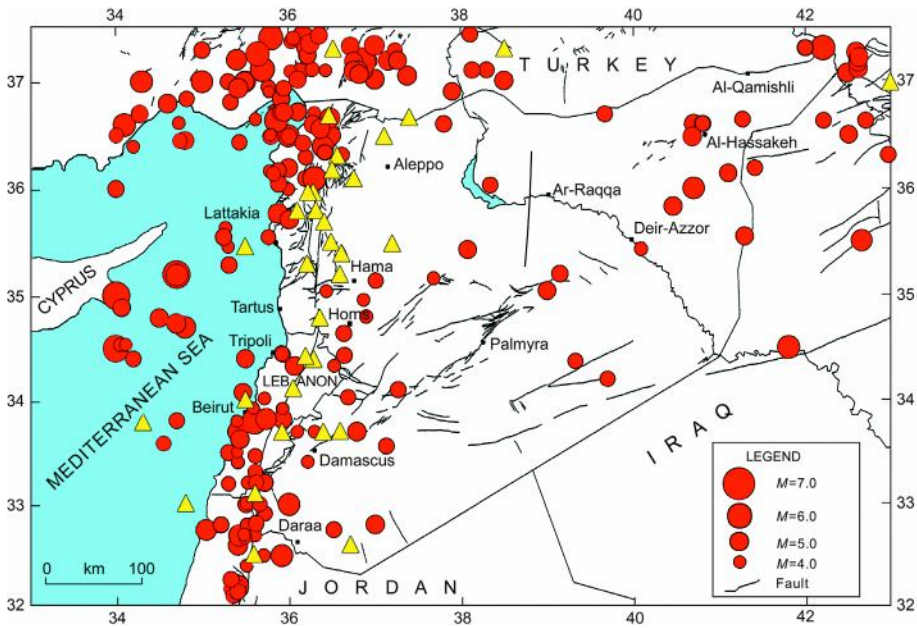

Fig. 22. Map of instrumental (red circles) and historical (yellow triangles) seismicity of Syria and surrounding region.

From the statistical point of view, a completeness test is applied to the parametric catalogue. It is found that its completeness was estimated to be at magnitude *M*6.5. The reason that this magnitude-threshold is very high, can be explained through two factors: i) the parametric assessing of some historical earthquakes is only performed for the earthquakes that have complete descriptions and in the meantime affected many localities; and ii) there is some inhomogeneity with respect to the density of the description flow of the historical earthquakes along the whole time-window of the catalogue. Figure 24 shows the completeness plot of the parametric catalogue.

We believe that the coverage, to some extent, in this catalogue is still not uniform in space or

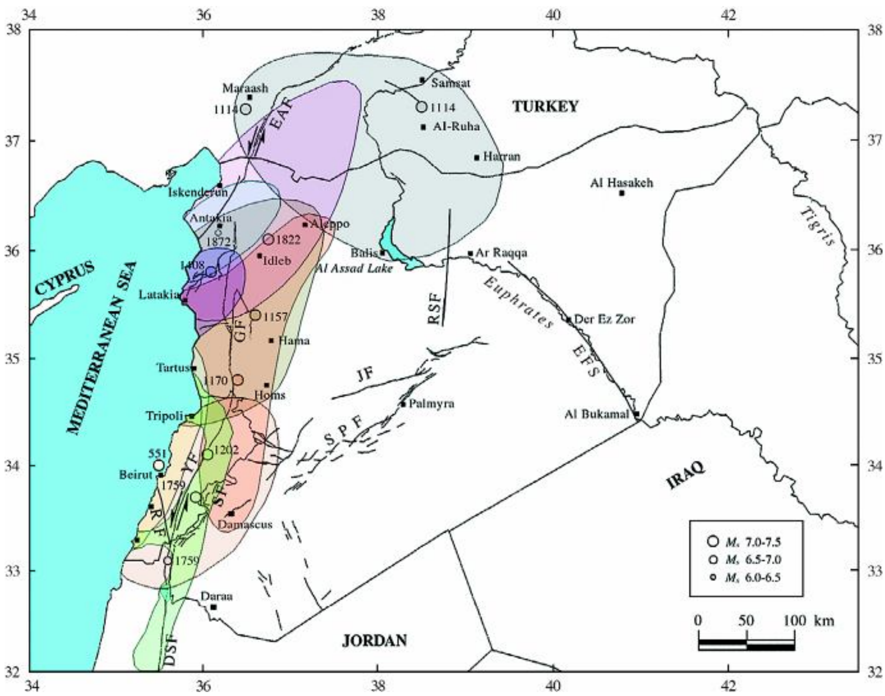

Fig. 23. Map of cumulative main historical earthquake damage distribution in Syria and surrounding region.

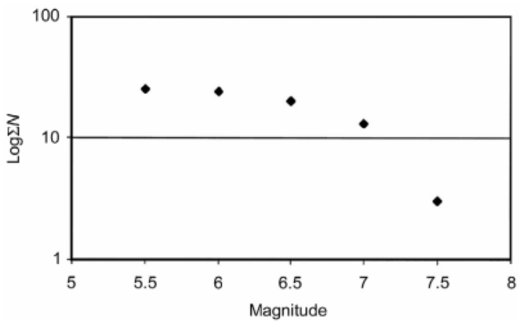

Fig. 24. The completeness plot of the parametric catalogue (N: number of earthquakes).

time. This requires further archival searches to discover unknown earthquakes and improve the data, and studies of earthquake and faulting behavior through palaeoseismic analyses should be done to identify seismotectonic behaviors of these active faults.

It is hoped that this catalogue represents a comprehensive databank on the historical seismicity covering 35 centuries, and will serve in studying the seismic hazards of the country.

Acknowledgements

We wish to thank Prof. Ibrahim Othman, Director General of the AECS.

We would also like to thank Profs. Abdul Karim Rafek, Nazem Kallas, Mohamed Muhafel and Souhail Zakkar from Damascus University, Faculty of Literatures, Department of History; Dr. Muammer Ülker, Head of the Süleymaniye Library in Istanbul and Dr. Salvatore Paolini from ENEA in Rome, for providing some historical sources. Dr. Claudio Margottini contributed in providing and analyzing some historical sources.

We thank Profs. Nicholas A. Ambraseys (Imperial College of London) and Massimiliano Stucchi (INGV-Milan) for their review of manuscript and their comments. We are deeply indebted to Prof. Muawia Barazangi (Cornell University), Dr. Mustapha Meghraoui (IPG Strasbourg) and Dr. Francisco Gomez (Missouri University) who made thorough reading in early and recent versions of the manuscript. We are grateful to Mme. Micheline Berthélemy (Damascus) for her re-writing of the manuscript of 1822 earthquake. Many thanks to Mr. Tony Nimr (IPG Strasbourg) for his help in preparing the fig. 1. Special thanks to our colleagues from AECS-Department of geology Mr. Ihssan layyous, Mme. Rahil Saadeh and Mr. Adnan Hasan for their helping drawing some figures, and also to Mr. Youssef Radwan for reading in the manuscript.

More information on the historical seismicity database is in <http://apamea.u-strasbg.fr>.

The preparation of the catalogue and related specific studies and investigations on individual earthquakes were funded by the International Atomic Energy Agency (contract No. 6247/R3/RB) and partially by the APAME EC project (contract No. ICA-CT-2002-10024) General Directorate of Antiquities and museums (Ministry of Cultural).

Appendix I. Information about authors or texts cited in the catalogue.

Abû Al-Fidâ, E. (672-732 A.H., 1273-1331 A.D.): He was born in Damascus and lived partially in Cairo. He was a prince of Hama, the scientist and the historian. His book *Al-Mukhtasar fi Akhbar Al-Bashar* (A Summary of Human Beings News) was known and appreciated in Europe during the 17th century. It represents his most famous work, in which many earthquakes were described.

Abu Shama, Shihab Ed-Din Abdl Rahman Al-Maqdisi (559-665 A.H., 1203-1268 A.D.): He was born in Damascus. After studying, he traveled to Mecca and Al-Quds. In the year 628 A.Hi1231 A.D., he was named a teacher at *Rukniya* and in the 662-1264 he was named teacher of the most important school of law called *Al-Asrafiya*. His book *Al-Roudhtein fi Akhbar Al-Dawlatein* (The Two Gardens in Both Countries) is the history of both sultans *Nur Ed-Din* and *Salah Ed-Din*. In his work, he copied from some sources adding personal events or his father's events.

Agathius Scholasticus (*ca.* 536-582): A Byzantine poet, historian and lawyer from Myrina, who lived in Constantinople. His history of his own times begins where that of his model, Procopius of Caesarea, ends. His historical account of the reign of emperor Justinian covers events from 552 to 558, but the work was unfinished, and was continued by Menander Protector.

Al-Antaki, Abu'l-Faraj Yahya Ibn Sa'id (980?- 1066 A.D.): An Arab historian and physician, well known for his continuation of the *Chronicle* of Eutychius of Alexandria. He was a Melchite Christian, and lived in Egypt for the first forty years of his life. From 1014 onwards, he lived in Antioch under Byzantine rule. His sources are Islamic, Greek and Antiochene Christian.

Al-Boustani, Botrus (1234-1300 A.H., 1819-1883 A.D.): An Arab knowledgeable scientist who was born in *Al-Dbiyya* (Lebanon). His work, *Dairet Al-Maaref* (Cycle of the knowledge), is an encyclopedia that contains a section of *Zlzala* (earthquake).

Al-Budayri Al-Halak, Ahmad (18th century A.D.): He was a barber who was born at Damascus. His career assisted him to write a valuable historical book entitled *Hawadith Dimashq Al-Yawmiyya bayn 1741 wa 1762* (Damascus daily events between 1741-1762 A.D.) which represents an eyewitness account of the 1759 A.D. earthquake.

Al-Dhahabi, Shams Ed-Din Muhammad Ibn Abdallah (1274-1348 A.D.): An Arab historian and theologian who was born in Damascus or Mayyafariqin (east of Diyar Bakr, Southern Turkey) and educated in Cairo. His major work is a Chronicle dealing with the history of Islam from its origin to the 14th century.

Al-Ghazi, Kamal Ed-Din (586-660 A.H., 1191-1262 A.D.): He was born in Aleppo. He studied the law and was a historian and traveler. His most important work is *Tarikh Halab (*History of Aleppo). He took some information from ancient sources and personal, or parents', memories.

Al-Ghazi, Mohamad Al-Najm (?-1061 A.H., ?-1651 A.D.): A historian and writer of literature who compiled many texts. He died in Damascus.

Al-Hamoui, Yakut (547-626 A.H., 1178-1229 A.D.): He is a geographic chronicler. His origin was Byzantine, captured when he was a boy and sold as a slave in Baghdad, he was released by a merchant who educated him. His surname was probably derived from his Master *Askar Al-Hamoui*. In his work *Moujam Al-Bouldan* (Dictionary of Towns), he described places, cities, towns and villages he visited.

Al-Maqrizi, Taqi Ed-Din Abul Abbas Ahmad (766-845 A.H.,1346-1442 A.D.): An Arab historian who was born in Cairo. Most of his life was in *Misr* (Egypt) except sometimes in Damascus. He worked in government, but then left public administration to follow his vocation as a historian. His work *Al-Suluk li Maarefet Dual Al-Muluk* describes the events that occurred between 568 and 845 A.H.

Al-Nablsi, Abd Al-Ghani (?-1143 A.H., ?-1731 A.D.): A Damascene historian, poet and literature who compiled many texts of earthquakes. He died in Damascus.

Al-Suyuti, Jalal Ed-Din (849-911 A.H., 1445-1505 A.D.): An Arab polygrapher and historian, who was born in Cairo. His well work *Kashf Al-Salsala an Wasf Al-Zalzala* (... Description of the Earthquake) represents the first compilation for about 108 earthquakes that occurred in the Arab World before and during Islam till 905 A.H.

Al-Tabakh, Mohammad Ragheb (1293-1370 A.H., 1877-195 1 A.D.): An Arab historian, who was born and died at Aleppo. In his work *Aalam Al-noubala 'a bi Tarikh Halab Al-Shahba 'a* (The Famous Noblemen in the History of Aleppo), the 1237 A.H. earthquake (1822 A.D.) was mentioned in detail according to four eyewitnesses from Aleppo namely Bakri Kateb, Jawdat Basha, Mohammad Al-Termanini and Mohammad Taqi Ed-Din.

Al-Tabari, Muhammad Ibn Jarir (224-3 10 A.H., 839-923 A.D.): The most famous Arab historian. He was born at Amil (Tarbastan), and lived and died in Baghdad. After studying in Baghdad and then in Basra and Kufeh, he returned to Baghdad, where he spent the rest of his life as a teacher. His work *Tarikh Al-Russol wa Al-Mouluk* (History of Prophets and Kings), covers the period from the beginning of the Islam and the year 302 A.H., and containing ten earthquakes.

Antonini Placentini Itinerarium (6th century A.D.): This is one of the itineraries written for the use of pilgrims visiting the Holy lands in Palestine. It dates to 6th century.

Badr Al-Ghazi, Mohamad (?-984 A.H.,?-1576 A.D.): A theology teacher and writer who lived in Damascus. He is a father of *Mohamad Al-Najm Al-Ghazi*.

Chronicle of Edessa (540 A.D.): A Syriac source written by an unknown author around 540. It mentions the 528 earthquake.

Chronicle of 724 (8th century A.D.): It was a Syriac chronicle by an unknown author covering the period from Adam to 724. It was probably written at the time of the Caliph Hisham.

Chronicle of 1234 (13th century A.D.): An anonymous Syriac chronicle written about half a century after the chronicle of Michael the Syrian. It is divided into two parts, of which one is devoted to secular history (to 1234) and the other to ecclesiastical history (to 1207).

Dio Cassius Cocceianus (2nd-3rd century A.D.): A senator during the reign of the Roman emperor Commodus (180-192 A.D.), who subsequently held other important positions. He wrote in Greek a history of Rome from its origin to 299 A.D., of which the books covering the years 68-10 B .C. have survived in their entirety. The period 9 B .C.-46 A.D. survives in abbreviated form, and the other parts are to be found in the epitomes of Xiphilinus (11th century) and Zonaras (12th century). Dio Cassius' work is based on late republican histories, the tradition imperial annals and, for contemporary events, his own experience.

Elias of Nisibis (975-1049 A.D.): He was born at *Nisibis* in Northern Syria, and became metropolitan of the city in 1008. He wrote a *Chronography* in Syriac and Arabic, the first part of which is historiographical work coming down to 1018 and modeled on the *Chronicon* of Eusebius. He mentions various earthquakes in his work, but some of his dating have to be corrected in the light of other Byzantine sources.

Evagrius Scholasticus (*ca.* 536-600): He was born at Epiphania in Syria, and worked as a lawyer, probably at Antioch, where he wrote his *Historia Ecclesiastica* in 6 books. It narrates events from 431 to 594 and treats both ecclesiastical and secular history. He used sources which are now partly lost.

Fragmenta Tusculana (6th century A.D.): These fragments were discovered in the Abbey of Santa Maria at Grottaferrata (Rome). They are probably dated to the 6th century A.D.

Georgius Cedrenus (late 11th-early 12th century A.D.): A Byzantine chronicler who compiled a chronicle of the world history from the creation to the reign of the emperor Isaac I Comnenus (1057). His material comes from earlier chroniclers such as Joannes Scitre and Joannes Scylitzes.

Georgius Monachus (9th century A.D.): He is a Byzantine historian. Between 842 and 867, he wrote a chronicle covering the period from the creation to the year 842. He brought together material from many ancient sources as well as from some nearer to his own day. It is very difficult to identify his ancient sources, but those for the Byzantine period are the works of Theophanes, Malalas and Nicephorus.

Ibn Al-Athir, Ezz Ad-Din (555-630 A.H., 1160-1232 A.D.): An Arab historian who was born, lived and died in Al-Mousel. He traveled often to many cities such as Baghdad, Aleppo, Damascus and Al-Quds. His book *Al-Kamil fi Al-Tarikh* (The Complete in History), which covers the period from the creation up to the end of 1230 A.D. and contains 56 earthquakes, represents the most famous one. He took some information from Ibn Al-Qalansi.

Ibn Al-Dawadari, Abu Bakr Ibn Abdallah (14th century A.D.): An Arab historian who was born in Egypt and lived between Egypt and Syria. His *Chronicle* is an important source for the history of the *Fatimites, Ayyoubites* and *Mamluks* periods.

Ibn Al-Jawzi, Abdul Rahman (510?-597 A.H., 1113?-1200 A.D.): An Arab historian who was born, lived and died in Baghdad. His work *Al-Mountazam fi Tarikh Al-Mouluk wa Al-Oumam* (The Regular in the History of Kings and Nations) is a general history, including earthquakes, from the creation up to 1185 A.D.

Ibn Al-Qalanisi, Hamzeh Ibn Assad (465-555 A.H., 1073-1160 A.D.): He was born and lived in Damascus. Following his studies in Letters, Law and Theology, he began an administrative career. He was *ra'is* (president) of Damascus twice. His *Chronicle* is the best source relating the first and second Crusader stages and the first years of Nur Ed-Din. His work *Tarikh Dimashq* (history of Damascus) was used by Ibn Al-Athir.

Ibn Al-Wardi, Omar (691-749 A.H., 1292-1348 A.D.): An Arab grammarian and historian, who was born at Maarret Annooman and died at Aleppo. In his work *Tarikh Ibn Al-Wardi* (History of Ibn Al-Wardi), numerous earthquakes occurring in Arabia before and during his life have been mentioned.

Ibn Batriq (877-940 A.D.): An Arab historian, who was Melchite Patriarch of Alexandria from 933, and opposed the Coptic Jacobites. He wrote a number of works in Arabic, notably a Chronicle, which was continued by his nephew Al-Antaki. It includes several theological discussions.

Ibn Kathir Al-Dimashqi, Ismail Abu Al-Fida Al-Hafez (710-774 A.H., 1310-1372 A.D.): An Arab chronicler who was born in the village of Bosra and lived most of his life in Damascus. His work *Al-Bidaya wa Al-Nihaya* (The Beginning and the Finale) covers the period from the creation to the year 767 A.H., and includes 46 earthquakes that occurred in and around Syria.

Ibn Tagri Birdi, Abu'l-Mahasin Jamal Ed-Din yusuf (1410?-1470 A.D.): An Arab historian who was born and died in Cairo. He was a military official during the Egyptian *Mamluk* dynasty. He covered many important positions. He wrote a *Chronicle* of this dynasty, which is a primary source for the study of post-*Fatimite* Egypt.

John of Ephesus (507-586 A.D.): A Bishop of Ephesus and a monophysite. He wrote an ecclesiastical history in Syriac before the year 581 A.D.

Klengel, Horst: He was a director of the Berlin's museum in the 1950s.

Lammense, Henri (1278-1356 A.H., 1862-1937 A.D.): An orientalist who was born in Belgium. He studied theology in England then lived in Beirut. He was a compiler of many books on the Arabs and Islam. He died at Beirut.

Malalas, John (*ca.* 491-578): He was a chronicler. His name Malalas is a Greek adaptation of the Syriac word *melel*, meaning «lawyer» or «rhetorician». His *Chronographia*, in 18 books, provides a confused and sometimes ill-ordered narrative of world history since the creation. It makes use of an extraordinary variety of sources, often misunderstanding dates and confusing events. When he comes to the 5th and 6th centuries A.D., however, he is closest to his own day, and provides interesting information, intermingled with accounts of wonders and prodigies. The fact that he shows a great deal of interest in Antioch, suggests that the work was written there.

Maronite Chronicle (2nd half of the 7th century A.D.): An anonymous Syriac chronicle, covering the period from the reign of Alexander the Great (336-323 B.C.) to the mid 660s, but there is a great lacuna from 361 to 658. It must have been composed shortly after the latest events it covers.

Michael the Syrian (1126-1199 A.D.): A Syrian historian who was born at Melitene (Malatya). He was named patriarch of the Jacobites from 1166 onwards, and wrote a universal history from Adam to 1195 in 21 books. It has come down to us in a number of manuscripts, but all of them have eliminated certain parts. It was also translated into Arabic and Armenian. The Armenian translation, which is of only slightly later date, contains certain details which add to the surviving Syriac texts. The original work was arranged in three parallel columns, which dealt respectively with Church history, secular history and reports of prodigious events such as eclipses, earthquakes, famine etc.

Pompeus Trogus (29 B.C.-14 A.D.): A Latin historian who was born in Gallia and lived in Augustan times. He wrote *De animallibus* and *Historiae Philippicae*, the latter surviving only in an abbreviated version by Justin.

Posidonius (135-51/50 B.C.): A stoic philosopher who was born at Apamea (Turkey) and lived in Athens, Rome and Rhodes. His work embraced all areas of philosophy and natural science, but only fragments have survived. His theory of earthquakes was elaborated by his disciple Asclepiodotus and has come down to us through Seneca.

Procopius of Caesarea (end of the 5th century-after 565 A.D.): A Byzantine historian who was born at Caesarea in Palestine. All his writings are of a historical nature, except for *Aedificia* , which he wrote between 553 and 555 to describe and praise Justinian's building work throughout the Empire. He also wrote a *Historia Arcana*. The gothic War is his most important work.

Pseudo-Dionysius of Tellmahre (8th century A.D.): It is a chronicle written by a Christian author of about the 8th century, because it was formerly attributed to the 9th century Syrian patriarch Dionysius of Tellmahre, whose *Chronicle* in 16 books (of which only a few echoes re-main) covered events from 582 to 843. A more correct name for our work is *Chronicle of Zuquin*, and it is divided into two parts, the first consisting of freely adapted *excerpta* from the historical works of Eusebius (the *Chronicon* and the *Ecclesiastical History*).

Pseudo-Joshua the Stylite (5th-6th century A.D.): Attributed to this Syrian writer is a chronicle of Edessa for the years around 497-505/507, which was subsequently reworked by the Jacobite patriarch Pseudo-Dionysius of Tellmahre.

Saadeh, Gabreal (1922-1997 A.D.): A Syrian historian about Lattakia and Ugharit who was born and died recently in Lattakia. He had the degree of law from Beirut in 1944, then had many positions in Lattakia. His work *Al-Mukhtasar fi Tarikh Al-Lathiqyeh* (A Summary in the History of Lattakia) consists of 7 historical earthquakes that hit Lattakia (529, 859/860, 1157, 1170, 1287, 1796 and 1822).

Severus of Antioch (465-538 A.D.): Born at Sozopolis in Pisidia (Turkey), he was monophysitic patriarch of Antioch from 512 to 518. As a result of presecution by the Chalcedonians, he was forced to flee to Alexandria in Egypt, where he spent many years. He wrote in Greek, but scarcely any of his works have survived in that language, being preserved instead in Syriac translation.

Socrates Scholasticus (380-439/450 A.D.): He is a Byzantine writer. His *Historia Ecclesiastica* continues the work of Eusebius from 305 A.D. up to 439. He is primarily interested in the history of the Church.

Strabo (64 B .C.-23? A.D.): A Greek geographic historian who was born at Amasea in Pontus. His historical writings were lost, but the 17th books of his *Geographia* have survived. Books 3-11 are about Europe; books 11-16 are about Asia and book 17 is about Africa.

Theophanes (*ca.* 760-818): A Byzantine chronicler who wrote a history of events from 284 to 813 A.D. for the western and eastern empires. His sources are ecclesiastical histories and chronicles, as well as historians such as Procopius and Agathias. He is the principle source for the dating of a number of earthquakes.

Zonaras, John (12th century A.D.): A Byzantine historian and writer on ecclesiastical subjects, who held an official position at the court of Constantinople. He became a monk around 1118 and retired to the Monastery of Mt. Athos. In addition to an epitome of world history from the creation to the year 1118, he wrote various commentaries on canon law and some hymns. His sources include such important historians as Herodotus, Xenophon, Plutarch and Dio Cassius.

Appendix II. Different historical names of localities cited in the catalogue.

[Format: **Current locality name(s) in Arabic and English (description):** *Ancient name*(*s*), location.]
Aafrine: see Ifreen.
Acre: see Akka.
Adana (town): Southern Turkey.
Afamia (archaeological site): *Apamea*, north-west of Hama.
Afsiyeh: see Aq-Saya.
Aina d-Gader (village?): near Salt, North-western Jordan.
Ain Hamadeh: near Beirut.
Akka, Acre (city): *Ptolemais, Akkô*, southern Lebanese littoral.
Akkar (town): east of Tripoli, Northern Lebanon.
Akkô: see Akka.
Al-Andalus: see Espania.
Al-Assi, Orontes (river): *Orontes*, Western Syria.
Al-Batra, Patra, Petra (archaeological site): Southern Jordan.
Al-Batron (town): *Botrys, Botro*, south of Tripoli.
Al-Dbiyya (village): in Lebanon.
Aleppo: see Halab.
Al-Eskandariyeh, Alexandria (city): Northern Egypt.
Alexandria: see Al-Eskandariyeh.

Al-Fustat: see Al-Qahira.
Al-Ghouta (plain): it surrounds Damascus from south and east.
Al-Harbyeh: see Dafneh.
Al-Hejaz, Hejaz (region): in Saudi Arabia.
Al-Jalil, Galilee (region): Northern Palestine.
Al-Jazira, Mesopotamia (region): NE of Syria and N of Iraq.
Al-Karak, Kerak (city): Central Jordan. **Al-Khalil, Hebron (city):** *Hebron,* Central Palestine.
Al-Laja (hill): south of Damascus. **Al-Lathiqiyeh, Latakia (city):** *Rameta, Mazbada, Laodicea*, Syrian coast.
Al-Led, Lod, Lydda (town): *Diospolis*, northwest of Al-Quds, Central Palestine. **Al-Mazzeh:** a Damascene suburb.
Al-Mazzeh: a Damascene suburb.
Al-Mousel, Mosul (city): *Mousel*, Northern Iraq.
Al-Qadmous (town): northeast of Tartus.
Al-Qahira, Cairo (city): *Al-Fustat,* Northern Egypt.
Al-Qastal (village): northeast of Damascus.
Al-Quds, the Holy City, Jerusalem (city): *Al-Quds*, Central Palestine.
Al-Qunaytra (city): southeast of Damascus, Southern Syria.
Al-Rafiqa: see Ar-Raqqa.
Al-Ruha: see Orfa.
Al-Salameyeh, Salamiya (town): *Salamias,* southeast of Hama.
Amid: see Diyar Bakr.
Amil: in Tarbastan.
Amik Glü: see Buhyret Al-Amq.
Andalusia: see Espania.
An-Nasra, Nazareth (town): Northern Palestine.
Antakia, Antakya, Antioch (city): *Theopolis, Antioch*, Northwestern Syria.
Antakya: see Antakia.
Antaradus: see Tartus.
Antharidus: see Arwad.
Antioch: see Antakia.
Apamia: see Afamia.
Aq-Saya, Afsiyeh (village): east of Antioch, NW of Syria.
Aradus: see Arwad.
Areopolis: see Moab.
Ariha, Riha (town): 13 km south of Idleb, Western Syria.
Ariha, Jericho (city): *Jericho,* Central Palestine.
Armanaz (town): west of Aleppo.
Arra: see Maarret Annooman.
Ar-Raqqa (city): *Ar-Raqqa*, *Al-Rafiqa*, NE Syria.
Ar-Rassafah (archaeological site): *Rasaba*, *Sergiopolis*, southwest of Ar-Raqqa.
Arwad (island): *Aradus, Antharidus*, Syrian coast, southwest of Tartus.
Ascalan (town): *Ascalon,* Southern Palestinian Littoral.
Ascalon: see Ascalan.
Ash-Sham: see Dimashq.
Ash-Sham, Bilad as-Sham (region): Syria, Lebanon, Palestine and Jordan.
As-Salihiyeh (archaeological site): *Dura Europos*, southeast of Deir Ez-Zor, Eastern Syria.
As-Samyra, Samaria, Shamrin (archaeological site): *Sebastia*, northwest of Nablus.
As-Suweida (city): *Soada*, Southern Syria.
Atareb (town): southwest of Aleppo.
Azotus (archaeological site): south of Jaffa, southern Palestinian littoral.
Baalbak (town): *Heliopolis*, Eastern Lebanon.
Baghdad: in Iraq.
Baghras (village): in Antioch district.
Baishan: see Bissan.
Bakas: see Bkas.
Balis: see Maskaneh.
Bambyce: see Manbej.
Banyas (village): *Banyas*, southwest of Damascus.
Banyas Al-Sahel, Banyas (town): Syrian Littoral.
Barin (village): Western Syria.
Bar Lyas (village): south of Zahleh, Lebanon.
Barqa (city): in Libya.
Basut: see Basuta.
Basuta, Basut (village): NW of Aleppo.
Batnan (town): Southern Turkey.
Batrakan (village): in Antioch district.
Beilan (town): south of Iskenderun.
Beirut (city): *Bêrytus*, Lebanese coast.
Beit Jin (village): southwest of Damascus.
Beit Jubrin (village): southwest of Al-Quds.
Beit Lahm, Bethlehem (town): south of Al-Quds, Central Palestine.
Beit Lahya (ruins of a village): few kilometers northeast of Damascus.

Beit Qubayeh (village): around Damascus.
Beit Saho (village): east of Damascus.
Benghazi, Benighazi (city): in Libya.
Benighazi: see Bebghazi.
Bennesh (village): 7 km northeast of Idleb.
Beroea: see Halab.
Bêrytus: see Beirut.
Bethlehem: see Beit Lahm.
Bilad Al-Andalus: see Espania.
Bissan, Baishan (town): Northern Palestine.
Bkas, Bakas (archaeological site): near Jisr Ash'Shoughour.
Bosra: see Bosra Al-Sham.
Bosra Al-Sham, Bosra (town): *Bostra*, Southern Syria.
Bostra: see Bosra Al-Sham.
Botro: see Al-B atron.
Botrys: see Al-Batron.
Bucak (?): Western Syria.
Buhyret Al-Amq, Amik Glü (lake): north Antioch.
Byblus: see Jbeil.
Caesarea (town): Northern Palestinian coast.
Cairo: see Al-Qahira
Casius Mount: see Jabal Al-Aqraa.
Ceasar: see Qalaat Sheizar.
Chalcis: see Kennesreen.
Cilicia: see Kilikia.
Constantinople: see Istanbul.
Crac des Chevaliers: see Qalaat Al-Hosn.
Cyprus: see Qubrus.
Dafneh, Al-Harbyeh (town): 9 km southwest of Antioch.
Damanhur (city): Northern Egypt.
Damascus: see Dimashq.
Dameska: see Dimashq.
Dameski: see Dimashq.
Damietta: see Dimyat.
Daraa (city): *Daraat*, Southern Syria.
Daraat: see Daraa.
Darayya (village): 3 km south of Damascus.
Darkoush, Darkush (village): NWW of Idleb.
Darkush: see Darkoush.
Deir Marjrjos (village and archaeological site): west of Homs.
Dimashq, Ash-Sham, Damascus (city): *Dameski, Dameska*, *Ash-Sham*, Southern Syria.
Dimyat, Damietta (city): NW Egypt.
Diospolis: see Al-Led.
Diyar Bakr (town): *Amid,* Northern Syria.
Douma (town): 7 km northeast of Damascus.
Duluk (village and fortress): near Gaziantab, Southern Turkey.
Dura Europos: see As-Salihiyeh.
Edessa: see Orfa.
Edlib: see Idleb.
Eleutherus: see Nahr Al-Kabir.
Emessa: see Hims.
Epiphania: see Hama.
Espania, Spain (country): Al-Andalus, Bilad Al-Andalus, Andalusia.
Euphrates: see Nahr Al-Furat.
Famagusta (city): western coast of Cyprus.
Galilee: see Al-Jalil.
Gaza (town): southern Palestinian coast.
Gaziantab, Iantab (town): Southern Turkey.
Gerasa: see Jarash.
Germanicia: see Marash.
Gophna: see Jifna.
Habur, Habura (village): east southeast of Mardin, Southern Turkey.
Habura: see Habur.
Halab, Aleppo (city): *Harabu, Beroea, Halab*, Northern Syria.
Hama (city): *Epiphania*, *Hamat, Hamath,* Central Syria.
Hamat: see Hama.
Hamath: see Hama.
Harabu: see Halab.
Harem, Harim (town): west of Aleppo.
Harim: see Harem.
Harran (town): southeast of Sanliurfa, Southern Turkey.
Hauran (region): *Hauran*, region of Daraa, Southern Syria.
Hazart: see Izaz.
Hebron: see Al-Khalil.
Hejaz: see Al-Hejaz.
Heliopolis: see Baalbak.
Herapolis: see Manbej.
Hims, Homs (city): *Emessa*, *Homs*, Central Syria.
Homs: see Hims.
Hosn Al-Akrad: see Qalaat Al-Hosn.
Iantab: see Gaziantab.
Ibin (village): north of Idleb.
Idleb, Idlib (city): Northwestern Syria.
Ifreen, Aafrine (town): northwest of Aleppo.
Iskenderun (city): *Miryandrous* , Northwestern Syria.

Istanbul (city): *Constantinople*, Western Turkey.
Izaz (town): *Hazart,* north of Aleppo.
Izmir (city): *Smyrna*, Western Turkey.
Jabal Al-Akraa (mountain): *Casius Mount*, Northwestern Syria.
Jabal Al-Amanus (mountain): *Jabal Al-Lkam,* Northwestern Syria.
Jabal Al-Lkam: see Jabal Al-Amanus.
Jabala: see Jableh.
Jableh (town): *Jabala*, Syrian coast, south of Latakia.
Jaffa: see Yafa.
Japho: see Yafa.
Jarash, Jerash (town): *Gerasa*, Northern Jordan.
Jbeil (town): *Byblus*, Lebanese coast, north of Beirut.
Jedida (village): in Antioch district, NW of Syria.
Jerash: see Jarash.
Jericho: see Ariha.
Jerusalem: see Al-Quds.
Jifna, Gophna (?): in Jordan.
Jisr Ash'Shoughour (town): southwest of Idleb.
Judea (region): Central Palestine.
Jum (village): NW of Aleppo.
Kabusi (village): in Antioch district, NW of Syria.
Kafer Tab (village): north of Hama.
Kelless, Killes, Killis (town): north of Aleppo.
Kennesreen (archaeological site): *Chalcis, Qenneshrin*, 20 km south of Aleppo.
Kerak: see Al-Karak.
Khan Sheikhoun, khan Sheikhun (town): 30 km north of Hama.
Khan Sheikhun: see Khan Sheikhoun.
Khlat: northeast of Diyar Bakr, Southern Turkey.
Kilikia, Cilicia (region): Southern Turkey.
Killes: see Kelless.
Killis: see Kelless.
Konya (town): Turkey.
Kufeh: in Iraq.
Labruda: see Yabroud.
Laodicea: see Al-Lathiqiyeh.
Laryssa: see Qalaat Sheizar.
Latakia: see Al-Lathiqiyeh.
Laushiya (village): in Antioch district.
Lefkosia (city): Central Cyprus.
Lejjun (citadel): Western Jordan.
Limassol (city): southern littoral of Cyprus.
Lod: see Al-led.
Lydda: see Al-Led.
Maarat: see Maarret Annooman.
Maarret Annooman, Maarat (town): *Arra,* south of Idleb.
Maarret Missrin (village): 12 km north of Idleb.
Mabbog: see Manbej.
Mabbug: see Manbej.
Makkeh, Mecca (city): in Western Saudi Arabia.
Malatya, Melitene (city): in Turkey.
Manbej (town): *Bambyce, Hierapolis*, *Mabbug, Mabbog*, northeast of Aleppo.
Maras: see Marash.
Marash, Maras (town): *Germanicia,* Southern Turkey.
Marsin (town): in Kilikia, Southern Turkey.
Masada (village): Central Palestine.
Maskaneh (town): *Balis*, southeast of Aleppo.
Mazbada: see Al-Lathiqiyeh.
Mecca: see Makkeh.
Melitene: see Malatya.
Mesopotamia: see Al-Jazira.
Miryandrous: see Iskenderun.
Misis (town): *Moposueste*, Southern Turkey.
Moab (town and archaeological site): *Areopolis*, east of Dead Sea, in Jordan.
Moposueste: see Misis.
Mosul: see Al-Mousel.
Naba (mountain and archaeological site): *Nebo*, northwest of the Dead Sea, Western Jordan.
Nablus (city): Northern Palestine.
Nahr Al-Kabir, Nahr Al-Kebir (river): *Eleutherus,* Northwestern Syria.
Nahr Al-Furat, Euphrates (river): in Northern and Eastern Syria.
Nahr Al-Kebir: see Nahr Al-Kabir.
Nawa (village): *Neve,* north of Daraa, Southern Syria.
Nazareth: see An-Nasra.
Nebo: see Naba.
Neve: see Nawa.
Nusaybin, Nisibis (town): Northern Syria.
Nisibis: see Nusaybin.
Orfa, Urfa, Sanliurfa, Al-Ruha (town): *Edessa*, Southern Turkey.
Orontes: see Al-Assi.
Palmyra: see Tadmor.
Patra: see Al-Batra.

Payas (village): Northwestern Syria.
Petra: see Al-Batra.
Phoenician coast: coasts of Syria, Lebanon and Palestine.
Ptolemais: see Akka.
Qalaat Balatunus: see Qalaat Blatnes.
Qalaat Blatnes, Qalaat Al-Mahalbeh, Qalaat Balatunus (citadel): east of Latakia.
Qalaat Al-Hosn, Hosn Al-Akrad, Crac des Chevaliers (citadel): west of Homs.
Qalaat Al-Mahalbeh: see Qalaat Blatnes.
Qalaat Al-Marqeb (citadel): North Tartus, Syrian coast.
Qalaat Sheizar (citadel): *Laryssa, Ceasar*, northwest of Hama.
Qaramut (village): south of Iskenderun.
Qatana (town): 17 km southwest of Damascus.
Qenneshrin: see Kennesreen.
Qilliq (village): in Antioch district.
Quaralu (village): in Antioch district.
Qubrus, Cyprus (island and country): Eastern Mediterranean region.
Quseir (mountain): it includes Dafneh and three villages, Northwestern Syria.
Rameta: see Al-Lathiqiyeh.
Ram Hamadan (village): 10 km northeast of Idleb.
Rasaba: see Ar-Rassafah.
Ras Al-Ein (town): Northeastern Syria.
Ras Baalbak (village): Northern Lebanon.
Ras Shamra, Ugharit (archaeological site): *Ugharit*, 10 km north of Latakia.
Riha: see Ariha of Syria.
Saasaa (village): northeast of Al-Qunaytra.
Safad (town): *Zefat*, Northern Palestine.
Safita (town): southeast of Tartus.
Saida, Sidon (city): *Sidon*, Southern Lebanese littoral.
Salamias: see Al-Salameyeh.
Salamis (town): Western Cyprus.
Salamiya: see Al-Salameyeh.
Salfouhum: see Sfuhen.
Salqein (town): northwest of Idleb.
Samandag, Samandag˘i (town): southwest of Antioch.
Samandag˘i: see Samandag.
Samaria: see As-Samyra.
Samosta: see Samsat.
Samsat (?): *Samosata*, Turkey.
Sanliurfa: see Orfa.

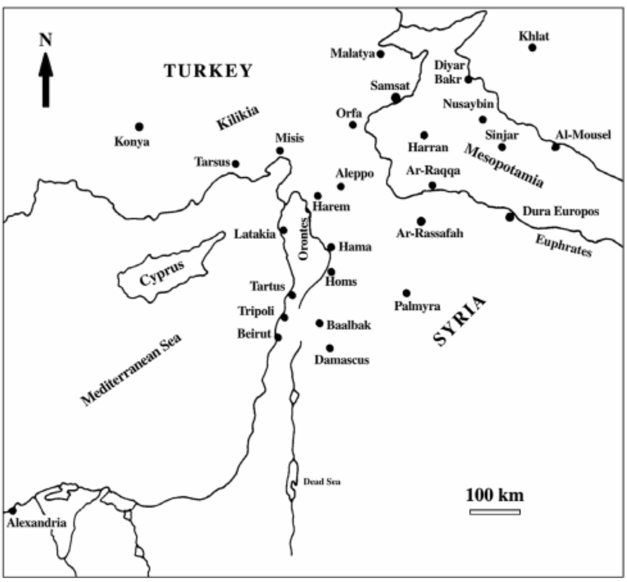

Fig. A.1. Major cities affected by the historical earthquakes in Syria and the surroundings.

Sarakeb (town): southeast of Idleb.
Sarepta: see Sarfand.
Sarfand (village and archaeological site): *Sarepta*, Lebanese littoral.
Sarghaya (town): northwest of Damascus.
Sarmada (village): north of Idleb, Northwestern Syria.
Sarmeen (village): 8 km southeast of Idleb.
Sarugi (?): see Suruc.
Sebastia: see As-Samyra.
Seleucea: see Suaidiya.
Sepphoris (?): Palestine.
Sergiopolis: see Ar-Rassafah.
Sfuhen (village and archaeological site): *Salfouhum*?, west of Maarret Annooman.
Shamrin: see As-Samyra.
Shaqa (village): *Triaris*, Lebanese coast.
Sharqat (?): in Iraq.
Sicily: see Siqilliya.
Sidon: see Saida.
Sinjar (mountain): Northern Iraq.
Siqilliya, Sicily (island): Southern Italy.
Sis (town): in Kilikia, Southern Turkey.
Smyrna: see Izmir.
Soada: see As-Suweida.
Sur, Tyre (city): *Tyre*, southern Lebanese littoral.
Suruc (?): *Sarugi*, between Harran and Orfa, Southern Turkey.
Suaidiya, Sweidiyeh (town): *Seleucea,* near Antioch.

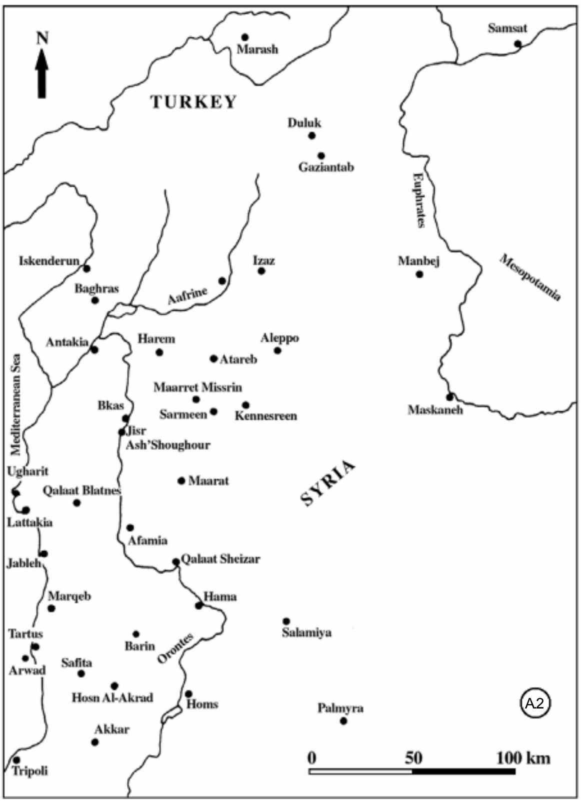

Fig. A.2. Localities affected by the historical earthquakes in Western and Northern Syria.

Fig. A.3. Localities affected by the historical earthquakes in and around Palestine.

Sweidiyeh: see Suaidiya.
Tabariya, Tiberias (town): Northern Palestine.
Tadmor, Palmyra (town and archaeological site): *Tadmor*, Central Syria.
Taftanaz (village): 15 km northeast of Idleb.
Tarablus Ash-Sham, Tripoli (city): northern Lebanese littoral.
Tartus (city): *Antaradus, Tortosa*, Syrian littoral.
Tarsus (town): Southern Turkey.
Tel Aviv: see Yafa.
Theopolis: see Antakia
Tiberias: see Tabariya.
Tinnis (village): NE Egypt.
Tortosa: see Tartus.
Triaris: see Shaqa.
Tripoli: see Tarablus Ash-Sham.
Tyre: see Sur.
Ugharit: see Ras Shamra.
Urfa: see Orfa.
Yabroud (town): *Labruda,* northeast of Damascus.
Yafa, Jaffa, Tel Aviv (city): *Japho*, Palestinian littoral.
Zabadani (town): northwest of Damascus.
Zahleh (city): Eastern Lebanon.
Zefat: see Safad.
Zerba, Zirbeh (village): SW of Aleppo, NW of Syria.
Zirbeh: see Zerba.
(For location of the most of these localities, see figs. A.1., A.2. and A.3.).

REFERENCES

Bibliographical list of all types of historical and modern references.

Abbreviations

AE = Archives Etrangères (in AN).
AN = Archives Nationales, Paris.
BBA = Basbakanlik Arsivi, Istanbul.
BL = British Library, London.
Bodleian = Bodleian Library, Oxford.
CFHB = Corpus fontium historiae Byzantinae.
CSCO Arab. = Corpus Scriptorum Christianorum Orientalium, Scriptores Arabici.
CSCO Syr. = Corpus Scriptorum Christianorum Orientalium, Scriptores Syri.
CSHB = Corpus Scriptorum Historiae Byzantinae.
FO = Foreign Office archives, Public Record Office, London.
Leiden = Bibliotheek der Rijksuniversiteit te Leiden.
MD = Mühimme Defteri (in BBA).
MMD = Maliyeden Müdevver Defterler (in BBA).
MGH, AA = Monumenta Germaniae Historica, Auctores Antiquissimi.
PG = Patrologiae cursus completus, series Graeca.
SP = State Papers (in FO).

Sources

‘ABD AL-BASIT, *Nail Al-amal fi Dhail Al-Duwal*, Bodleian Ms. Huntington 610.
‘ABD AL-LATIF, *Kitab Al-Ifada*, facsimile edited and translated by K.H. ZAND, J.A. VIDEAN and I.E. VIDEAN, The Eastern Key, London 1965; also translated by SILVESTRE DE SACY, Relation de l’Egypte, Paris 1810.
ABU’L-FADA’IL, *Tarikh Mansuri*, facsimile edited by P.A. GRYAZEVITCH, Moscow 1960.
ABU’L-FADA’IL, *Al-Tarikh Al-Mansuri*, facsimile edited by ABU AL-EID DOUDOU, Damascus 1982.
ABU AL-FIDA, E., *Al-Mukhtasar fi Akhbar Al-Bashar*, vols. 2-4, Dar Al-kitab Al-Lubnani, Beirut 1970.
ABU AL-FARAJ (Bar Hebraeus), *Chronography*, translated by E.A.W. BUDGE, London 1932.
ABU SHAMA, *Al-Raudhtein fi Akhbar Al-Dawlatein*, edited by MUHAMMAD HILMI MUHAMMAD AHMAD, 2 vols., Cairo 1956-1962.
ABU SHAMA, *Dhail ‘ala Al-Raudatain*, edited by M. ZAHID AL-KAUTHARI, Cairo 1947.
AGAPIUS OF MENBIJ, *Kitab Al-Un wan*, edited by A. VASILIEV, Patrologia Orientalis, VIII, Fasc. 3, Paris 1921.
AGATHIAS, in Patrologie Grecque (PG), edited by J.P. MIGNE, 88, col. 1359, 1360.
AGATHIAS, *Historiae*, edited by R. KEYDELL, CFHB 2, Berlin 1967; translated by J.D. FRENDO, The Histories, Berlin and New-York 1975.
AL-’AINI, *Iqd Al-Juman fi Tarikh ahl Al-Zaman*, Paris Ms. Arabe 1543 (621-79 H) and 1544 (799-832 H).
AL-ASQALANI, Ibn Hajar, *Anbaa’Al-Ghamer bi A’nbaa’Al-Oumer*, edited by HASAN HABASHI, Cairo 1969-1972.
AL-ASSADI, KH. (1984): *Ahiyaa Halab wa Asswaqouha*, Ministry of Education (Pub.), Damascus.
ALBERT MILIOLI, *Cronica Imperatorum*, Mon. German Hist. Ss. vol. 31.
AL-BOUSTANI, B., *Dairet Al-Maaref* (Arab Encyclopedia), vol. 9, Beirut 1887, 239-242.
AL-BUDAYRI AL-HALAK, A, *Hawadith Dimashq Al-Yawmiyya bayn 1741 wa 1762*, edited by A.I. KARIM, Cairo 1959.
AL-DA’UDI, continuator of Al-Suyuti, in *Kashf Al-Salsala*, 62-64; also edited by AL-HAFIZ, 1982.
AL-DAWADARI, Abu Bakr Ibn Aybak, *Kanz Al-Durar wa Jamea Al-Ghurar*, Cairo 1972.
AL-DHAHABI, *Tarikh Al-Islam wa-Tabaqat Mashahir Al-Islam,* edited by H.D. AL-QADSI, V, Cairo no date (?1369/1950).
AL-DHAHABI, *Kitab Al-’ibar fi Khabar Man Ghabar*, edited by S. MUNAJJID, 5 vols., Kuwait 1960-1966. AL-DWYHY, Astafanos, Tarikh Al-Azmineh, *Al-Mashreq Journal*, vol. 44, Beirut 1951.
AL-GHAZI, K.A. (N.D): The seismicity in Damascus region, *Al-Mashreq Journal*, vol. 6.
AL-GHAZZI, Kamil, *Nahr Al-thahab fi Tarikh Halap*, 3 vols., Maronian Publisher, Aleppo 1926.
AL-HAMAWI, Yaqut, see YAQUT AL-HAMAWI.
AL-HAMAWI, Muhammad Ibn Ali (1963): *Al-Tarikh Al-*

Mansouri, Moscow.
AL-HAMAWI, Muhammad Ibn Ali, *Mukhtasar Siyar Al-Awail wa Al-Muluk wa Wasilat Al-Abd Al-Mamluk*, Bibliotheque Nationale, Ms. Ar. 1507, 177a.
AL-ISFAHANI, *Kitab Ta'rikh Sani Muluk Al-Ard wa'l-Anbiya*, edited by GOTTWALD, Leipzig 1848.
AL-ISFAHANI, Hamza, *Tarikh Sini Muluk Al-Ard wa Al-Anbiya*, Berlin 1921.
AL-JALABI, D., *Ikhtiar Zoubdet Al-Athar Al-Jaliya fil 'L-Hawadith Al-A rdiya*, Al-Najaf 1974.
AL-MAQRIZI, *Itti'az Al-Hunafa fi Akhbar Al-A'imma Al-Fatimiyyin Al-Khulafa*, edited by J. SHAYYAL, 3 vols., Cairo 1967-1973.
AL-MAQRIZI (1970-1973): *Al-Suluk Li-maarifat Dual Al-Muluk*, edited by MOUHAMMED MUSTAFA ZIYADAH, voll. 1-2, Cairo 1939-1958; edited by SA'ID ABD AL-FATTAH ASHOUR, voll. 3-4, Cairo.
Al-Mashreq Journal, Damascus.
AL-NABLSI, Abd Al-Ghani, Manuscript (see AL-HAFIZ).
AL-SAKHAWI, *Al-Dau Al-lami' Li-ahl Al-qarn Al-tasi'*, 12 vols., Cairo 1934-1936.
AL-SAYRAFI, Ali Ibn Dawood, *Nuzhet Al-nufus wa Al-Abdan fi Tawarikh Al-Zaman*, edited by HASAN HABASHI, Cairo 1973.
AL-SHIHABY, A., *Al-Ghouras Al-Hissan fi Twarikh Hawadeth Al-Azman*, Egypt 1900.
AL-SUYUTI, Jalal Ed-Din, *Kashf Al-Salsala an Wasf Al-Zalzala*, edited by A. SAADANI, Fez 1971; French translation by S. AL-NAJJAR, Cahiers du Centre Universitaire de la Recherche Scientifique, Rabat 1974.
AL-SUYUTI, Jalal Ed-Din, *Kashf Al-Salsala an Wasf Al-Zalzala* (Al-Dar Library), edited by A.A. AL-FRYOUAI, AL-MADINEH AL-MOUNAWRA 1984.
AL-TABAKH AL-HALABI, Ragheb, *Mouthakarat Tarikhieh Lemadinet Halap*, 3 vols., Aleppo 1925.
AL-TABAKH AL-HALABI, Ragheb, *Aalam Al-Noubala'a bi Tarikh Halab Al-Shahba'a*, Aleppo.
AL-TABBAKH, Muhammad (1923): *Ilam Al-Nubala*, I, Aleppo, 205.
AL-TABARI, M. Ibn Jarir, *Tarikh Al-Russol wa Al-Muluk*, edited J.M. DE GOERJE, 3 vols. in 15, Leiden 1879-1901.
AL-TABARI, M. Ibn Jarir, *Tarikh Al-Oumam wa Al-Mouluk*, vol. 8, Cairo 1939.
AL-TABARI, M. Ibn Jarir, *Tarikh Al-Russol wa Al-Muluk*, edited by MOUHAMMED ABUL-FADHEL IBRAHIM, voll. 1-10, Cairo 1960-1969.
AL-'ULAMI, *Al-Uns Al-Jalil Bi-tarikh Al-Quds wa 'l-Khalil*, Cairo 1283/1866; abr. translated by J. SAUVAIRE, Histoir de Jerusalem et d'Hebron, Paris 1876; also 2 vols., Najaf 1388/1968.
AL-'UMARI, Y. Al-Khatib, *Ghayat Al-Masary fi Tarikh Al-Mahasen*, Bagdad 1917.
AL-'UMARI, Y. Al-Khatib, *Ghraeb Al-Athar fi Hawadith Rouba Al-Karn Al-Thaleth Ashar*, Mosel 1940.
AL-'UMARI, Y. Al-Khatib, *Mouniet Al-Oudabaa fi Tarikh Al-Mosel Al-Hadbaa*, Mosel 1955.
AL-'UMARI, Y. Al-Khatib, *Al-Athar Al-Jaliya fi'l-hawadith Al-A rdhiya*, Ms. Iraqi Academy, Baghdad, also BL Or. 6300.
AL-YA'QUBI, *Tarikh*, edited by T. HOUSTSMA, 2 vols., Leiden 1883.
AL-YA'QUBI, *Tarikh Al-Ya'qubi*, voll. 1-2, Beirut 1960.
ANASTASE LE BIBLIOTHÉCAIRE, *Histoire Ecclésiastique* (Byzantin IX).
Annales 5689, Annales Terrae Sanctae, Bibliotèque Nationale de France, Paris, Fond Latin, no. 5689, Extr. Archives de l'Orient Latin, vol. 2.
Annales de Terre Sainte, edited by G. RAYNAUD and R. ROHRICHT, Archives de l'Orient Latin, vol. 2b, 1884.
ANONYMOUS, *Manah Al-Rabaniyya*, Paris Ms. Arab. 1536.
ANONYMOUS, *Chronicum*, CSCO 56, 254-255.
ANONYMOUS PILGRIM, in Queen's College Oxford, Ms. 357, fol. 33ro.; also BL Ms. Haerleian 2333, fol. 30ro.
ARCHIVES HISTORIQUES CH. COMM. MARSEILLE, AA/340/1759-60.
ARCHIVES NATIONALES (ANF), Affaires Etrangères (AE). (Bi/978 'Acre'), (Bi/973 'Aleppo'), (Cor. Pol., Turquie voll. 193, 194), (Libraries & Archives), Paris.
ARCHIVES NATIONALES (ANF), Affaires Etrangères (AE), vol. 26, 177-181, (Libraries & Archives), Paris.
ATSIZ, C.N. (1961): *Osmanli Tarihine ait Takvimler*, Istanbul.
BAETHGEN, F., *Fragmente Syrischer und Arabischer Historiker*. Abbandlungen f. die Kunde des Morgenlandes, VIII/3, Leipzig 1884.
BAR HEBRAEUS, Girgis Abu Al-Faraj, *Chronography*, edited by P. BEDJAN, Gregorii Bahebraei Chronicon Syriacum, Paris 1890; translated by E.A.W. BUDGE, The chronography of Gregory Abul-Faraj, London 1932.
Barletta Ms. in KOHLER (1900-1901).
BAŞBAKANLIK OSMANLI ARŞIVI (BBA), Mühimme Defteri (MD), (7.797), (Libraries & Archives), Istanbul.
BAŞBAKANLIK OSMANLI ARŞIVI (BBA), Cevdet-Maliye (CM), (27741), (Libraries & Archives), Istanbul.
BAŞBAKANLIK OSMANLI ARŞIVI (BBA), Maliyeden Müdevver Defterler (MMD), (3609.570), (Libraries & Archives), Istanbul.
BEN ZVI (Editor), *Edut Bi-Jhossef*, Daron 40, Jerusalem 1933.
BIBLIOTHEEK RIJKSUNIVERSITEIT (BRG), (Ms., no. 997, 90-91), (Libraries & Archives), Gnt.
BIBLIOTHEK VADIANA (BV), (Ms., no. S. 66d, p. 40), (Libraries & Archives), St. Gall.
BROUGHTON, TH.R.SH. (1935): Some non-colonial coloni of Augustus, *Trans. Proc. Am. Philol. Assoc.*, **66**, 18-24.
BROUGHTON, TH.R.SH. (1938): *An Economic Survey of Ancient Roma* (The Johns Hopkins Press, Baltimore), vol. IV.
BÜCHELER, F. (1882): *Coniectanea*, Kleine Schriften, II, Leipzig-Berlin 1927, 444-463.
CAETANI, L. (1913-1923): *Chronographia Islamica ossia Riassunto Chronologico della Storia di Tutti i Popoli Musulmani*, 5 vols., Paris.
CAMERON AVERIL (1970): *Agathias*, Oxford.
CEDRENUS, Georgios, *Histoir* (XI Byzantin) in PG, edited by J.P. MIGNE, col. 569, 719.
CEDRENUS, Georgius, *Synopsis Historiarum*, edited by I. BEKKER, Bonn 1838-1839.
CHANDLER, Tertius (1964): Date of the earthquake at Ugharit, *J. Syria*, XLI, 8 1-182.
CEVDET, 1309/1893, *Cevdet tarhi*, Istanbul.
Chronicle of 724 = Chronicon Miscellaneum ad A.D. 724 Pertinens, edited by E.W.BROOKS, in Chronica minora, II, CSCO 3 Syr. 3, Louvain 1960 (repr.), 77-155; Latin translation by J.B. CHABOT, CSCO 4 Syr. 4, Louvain 1960 (repr.), 61-119.
Chronicle of 819 = Chronicon Anonymum ad A.D. 819 Pertinens, edited by A. BARSAUM, CSCO 81 Syr. 36, Lou-

vain, 1953 (repr.), 3-22; Latin translation by J.-B. CHABOT, CSCO 109 Syr. 56, Louvain 1937, 1-16.

Chronicle of 846 = Chronicon A.D .846 pertinens, edited by E.W. BROOKS, in *Chronica minora*, II, CSCO 3 Syr. 3, Louvain 1960 (repr.), 157-238; Latin translation by J.B. CHABOT.

Chronicle of 1234 = Chronicon ad Annum Christi 1234 Pertinens, edited by J.B. CHABOT, 2 vols., CSCO 8 1-82 Syr. 36-37, Louvain 1953 (repr.); Latin translation of Part I by J.B. CHABOT, CSCO 109 Syr. 56, Louvain 1937; French translation of part II by A. ABOUNA, CSCO 354 Syr. 154, Louvain, 1974.

Chronicon Edessenum, edited by I. GUIDI, in *Chronica minora*, I, CSCO 1 Syr. 1, Louvain 1960 (repr.), 1-13; Latin translation by I. GUIDI, CSCO 2 Syr. 2, Louvain 1955 (repr.), 1-11.

Chronicon Maroniticum, edited by E.W. BROOKS, in Chronica minora II, CSCO 3 Syr. 3, Louvain 1960 (repr.), 43-74; Latin translation by J.-B. Chabot, CSCO 4 Syr. 4, Louvain 1960 (repr.), 37-57.

Chronicon Pseudo-Dionysus of Tell-Mahre, *Incerti Auctoris Chronicon Pseudo-Dionysianum Vulgo Dictum*, edited by J.B. CHABOT, CSCO, vol. 121, *Scripores Syri*, no. 66, Louvain 1949.

Chronique de Terre Sainte, 1131-1224, in Gestes des Chiprois, edited by G. RAYNAUD, Publ. Soc. de l'Orient Lat., vol. 5, Paris 1887 (repr. Osnabruck 1968).

Chronography, edited by BAR HEBRAEUS, II, 144.

CLEMENTONI, G. (1989): *Tiberio e il Problema della Protezione Civile*, in SORDI (1989a), 167-183.

CONSULAR ARCHIVES: Foreign Office. London (FO 195/ 39.1796. Aleppo. Istanbul. Alexandria: FO, 78/110-112.1822-3 Aleppo. Istanbul also FO 195/1 12: also for other years under Levant); India Office Records. London (IO SP 105/140.1822-4. Aleppo. Antioch. Suedia; also for other years); Archives Nationales, Paris (AN B1/1042/169-204,1822 Aleppo, Saida, Levant; also for other years).

DAHMAN, M.A. (Editor) (1948): Zalzal sanat 1173, *Al-Mashriq*, **42**, 333-337.

DAHMAN, M.A. (1982): *Fi Rihab Dimashq* (published by Dar Al-Fikr, Damascus), 194-216.

DARGON, G. (1974): *Naissance d'une Capitale*, Paris.

DARROUZÉS, J. (1954, 1957, 1958): Notes pour servir à l'histoire de Chypre, *Kypriakai Spoudai*, vol. 17, 83-102; vol. 20, 33-63; vol. 22, 224-250, Nicosia.

D'ARVIEUX, L., *Mémoires du Chevalier d'Arvieux etc.*, 6 vols., Paris 1735.

DEUTSCHE PRESSEFORSCHUNG (BDP), Universitatsbibliothek, (Libraries & Archives), Bremen-Zeitung, (Z. 20, no. 18, 1626.4.18).

DE VAUX, Vincent O.P., *L'Archéologie et les Manuscrits de Mer Morte*, British Academy, Oxford 1962.

Diaire des Pères Lazaristes de Tripoli (XIX), 1834.

Diaire des Pères Jésuites de Saida (XIX).

DIETRICH VON SCHACHTEM, in *Deutshe Pilgerreisen nach dem Heiligen Lande*, edited by R. RÖHRICHT and K. MEISNER, Berlin 1880 (new edition, Innsbruck 1900).

DIO CASSIUS COCCEIANUS, *Historia Romana, Xiphilini Epitome*, edited by U.P. BOISSEVAIN, Berlin 1895-1931; *Dio's Roman History*, edited by E. CARY, London-Cambridge (Mass.) 1914-27; *The Roman History: the Region of Augustus*, translated by I. SCOTT-KILVERT, Harmondsworth 1987.

DOWNEY, G. (1938a): Seleucid chronology in Malalas, *Am. J. Archaeol.*, **42**, 106-20.

DOWNEY, G. (1951): *Nizam Al-Miyah fi Antakia fi Al-Ussor Al-Kadimah*, translated by G. HADDAD, *Journal of Al-Hawlyat Al-Atharia As-Souria* I, Part II, Damascus, 28 1-283.

DOWNEY, G. (1961): *A History of Antioch in Syria*, Princeton.

ELIAS OF NISIBIS, *Opus Chronologicum*, I, edited by E.W. BROOKS, CSCO 62 Syr. 21; Latin translation by E.W. BROOKS, CSCO 63 Syr. 23, Paris 1910.

ERNOUL, *Chronique d'Ernoul et de Bernard le Trésorier*, edited by MAS LATRIE, Paris 1871.

ERPENIUS, *Historia Sarracernorum*, translated by GIRGIS IBN AL-MANSUR, Leyde 1625.

EUSÈBE, *Histoir de Ecclésiastique* (Byzantin V, dans Patrologie Grecque).

EUSÈBE, *Les Martyrs de Palestine*.

EUSEBIUS, *Chronicon*, edited by R. HELM, GSC 47, Berlin 1956.

EUSEBIUS, *I Martiri della Palestina*, edited by G. DEL TON, Scrinium Patristicum Lateranense, Roma 1964.

EUSEBIUS, *Praeparatio Evangelica*, edited by G. DINDORF, Leipzig 1867.

EUTYCHIUS, see IBN BATRIQ.

EVAGRIUS SCHOLASTICUS, *Historia Ecclesiastica*, edited by J. BIDEZ and L. PARMENTIER, London 1898 (repr. Amsterdam 1964).

EVENS, S. (1784): *Journal Kept on a Journey from Bassora to Otranto*, Hrsham.

FIEY, J.M., *Assyrie Chretienne*, vol. 2, Impremerie Catholique, Beyrouth 1965.

FINDIKLI, *Mür'it-tavanli*, Bayzit Library Ms. F. 429, Istanbul.

FOSTER, R. (1902): *De Libanio, Pausania, Templo Apollinis Delphico*, Album gratultorium in honorem H. van Herwerden, Utrecht, 45-54.

Fragmenta Historica Tusculana, edited by A. MAI, 1808-1826.

FRANCESCO AMADI, *Chroniques d'Amadi et de Strambaldi*, Chronique d'Amadi, edited by MAS LATRIE, Coll. de doc. inedit. sur l'Hist. de France, vol. 1, Paris.

GAZETT DE FRANCE (PGF), (1778.8.10, 9.11), (Press), Paris.

GENNADIUS, *De Viribus Illustribus*, edited by W. HERDING, Leipzig 1879 (repr. 1924).

GEOFFREY OF DONJON, *Letter* in MAYER (1972).

GEORGE THE MONK, *Chronicle*, edited by C. DE BOOR, BT, 2 vols., Leipzig 1904.

GEORGIUS CEDRENUS, see CEDRENUS.

GEORGIUS MONACHUS, see GEORGE THE MONK.

GEORGIUS SYNCELLUS, see SYNCELLUS.

GIL, M. (1992): *A History of Palestine*, Cambridge, 634-1099.

GIOVANNI LIDO, *De Magistratibus Romanis*, CSHB, 246-247, Bonnae 1837.

GROSDIDIER DE MATONS, J., *Romanos le Mélode*, Hymnes V, Paris 1981.

GRUMEL, V. (1958): *Traité d'Études Byzantines: la Chronologie*, Paris.

GLYKAS, Michael, see MICHAEL GLYKAS.

GUILLAUME DE TYRE (XII), *Histoire*, livre 20, chap. 18 (ouvrage écrit en latin, traduit et continué après lui sous les titres de Chroniques d'Eracles et d'Ernoul).

GÜZELBEY, C. and H.YEKTIN (1970): *Gaziantep Ş̦er'i Mahkeme Sicillerinden Örnekler*, vol. 140, Gaziantep, 57-58.

HADDAD, G. (1951) *Anaser Al-Sukkan fi Antakia fi Al-Asr*

Al-Helnesti (The journal of Al-Hawlyat Al-Atharia As-Souria), 1, Part I, Damascus, p. 126.
HAKIM MEMET, *Vakayi Name* (I), Ms. Bagdad Kosku 231, Topkapi Sarrayi Library, Istanbul.
HAMMER, J. von, *Geschichte des Osmanischen Reiches*, 10 vols., Pest.
HETHUM OF GOR'IGOS, *Table Chronologique*, Rec. Hist. Croisades. Arm., vol. 1.
HETHUM PATMIC, *Chronicle*, in HAKOBYAN (1956, p. 61).
HONIGMANN, E. (1952): *Á propos de Pompéïopolis de «Mysie»*, Byzantion 22, 301-304.
HROZNY, B. (1932): *Les ionien à Ras Shamra*, Arch. Or., IV, 169-178.
IBN AL-ATHIR, Ezz Ad-Din, *Al-Kamil fi Al-Tarikh* (Dar Sader), voll. 8, 9, 10, 11, 12, Beirut 1982.
IBN AL-ATHIR, Ezz Ad-Din, *Al-Kamil fi Al-Tarikh*, edited by C.J. TORNBERG, Leiden 1851-1876.
IBN AL-FURAT, *Tarikh Al-Duwal wa 'l-Muluk*, edited by HASSAN AL-SHAMMA, vol. IV/I-V/I, Basra 1969.
IBN AL-IMAD, Al-Hanbali, *Shatharat az-Zahab fi Akhbar men Zahab*, Beirut.
IBN AL-JAWZI, *Ajaib*, Arabes 1567, 26a.
IBN AL-QALANISI, Hamzah Ibn Assad, *Tarikh Dimashq*, edited by S. ZAKKAR, Damascus 1983.
IBN AL-SHIHNA, *Raudat Al-Munazir fi Akhbar Al-Awa'il wa'l-Awakhir*, British Library Ms., Or., Add. 23,336.
IBN AL-SHIHNA, *Raudat Al-Munazir*, on the margins of Ibn Al-Athir, edited by BULAQ, vols. VII-IX, Cairo 1874.
IBN AL-WARDI, Omar, *Tarikh Ibn Al-Wardi*, voll. 1-2, Cairo 1879.
IBN BATRIQ, *Al-Ta'rikh Al-Majmu' ala Al-Tahqiq wa'l-Tasdiq* (Eutychii Patriachae Alexandrini Annales-Pars Prior), edited by L. CHEIKHO, CSCO Arab., Series tertia, vol. 6, Beyrout-Paris 1906.
IBN HABIB, *Tadhkirat Al-Nabih*, edited by M.M. AMIN, 3 vols., Cairo 1976-1986.
IBN HAJAR, see Al-Asqalani.
IBN IYAS, Mohammad Ibn Ahmad, *Bada'i' Al-Zuhur fi waqa'i' Al-Duhur*, edited by P. KAHLE and M. MOSTAFA, 5 vols., Cairo and Wiesbaden 1960-1975. Partly translated by G. WIET, Histoire des Mamlouks Circassiens, II, Cairo 1945; and G. Wiet, Journal d'un Bourgeois du Caire, 2 vols., Paris 1955, 1960.
IBN JARIR AL-TABARI, M., see AL-TABARI.
IBN JUBAIR, *The Travels of Ibn Jubayr*, edited by W. WRIGHT; 2nd edition by J.M. DE GOEJE, Gibb Memorial Series, vol. 5, London 1907.
IBN KATHIR, *Al-Bidaya wa Al-Nihaya fi 'l-Tarikh*, 13 vols., Cairo 1351-1358/1932-1939.
IBN KATHIR AL-DIMASHQI, *Al-Bidaya wa Al-Nihaya*, voll. 11, 12, 13, Beirut 1988.
IBN MANKALI, *Al-Ahkam Al-Mulukiyya*, vol. 37, quoted in TAHER(1979, p. 125).
IBN QADI SHUHBA, *Al-Kawakib Al-Duriyya fi 'l-Sirat Al-Nuriyya*, edited by M. ZAYIDH, Beirut 1971.
IBN SHADDAD, *Al-A'laq Al-Khatira fi Dhikr Umara' Ash-Sham wa'l-Jazira*, edited by D. SOURDEL, Damascus 1953.
IBN SHAKIR AL-KUTUBI, *Uyun Al-Tawarikh*, Bibliotheque Nationale Ms. Arab. 1588, 88a.
IBN TAGRI BIRDI, *Al-Nujum Al-Zahira fi Muluk Misr wa'l-Qahira*, Cairo 1932.
IBN TULUN, *Mufakaat Al-Khillan fi Hawadith Al-Zaman*, edited by M. MOSTAFA, 2 vols., Cairo 1962,1964.
IBN WASIL, *Mufarrij Al-Kurub fi Akhbar Bani Ayyub*, edited by M. SHAYYAL, vol. III, Cairo 1962.
IOHANNES MALALAS, see MALALAS.
IOHANNES ZONARAS, see ZONARAS.
JACOB OF EDESSA, *Chronicle*, edited by E.W. BROOKS, in Chronica minora III, CSCO 5 Syr. 5, Louvain 1961 (repr.), 261-330; Latin translation by E.W. BROOKS, III, CSCO 6 Syr. 6, Louvain 1960 (repr.), 197-258; English translation by E.W. BROOKS, The Chronological Canon of James of Edessa, *Zeitschrift der deutschen morgenlandischen Gesellschaft*, **53** (1899), 261-327, 550; **54** (1900), 100-102.
JALFAQ, B., Évêque de Saida-Lettres publiées dans les Nouvelles (Riçalat) de l'Abbaye de Mar Mukhallès près Saida.
JEFFREYS, E., M. JEFFREYSand R. SCOTT(Translators) (1986): *The Chronicle of John Malalas*, Sydney, N.S.W.
JOSHUA THE STYLITE, *The Chronique of Joshua the Stylite composed in Syriac, A.D. 507*, translated by DE WRIGHT, Cambridge 1882.
JOHN OF EPHESUS, *Ecclesiastical History*, Fragments of Part II, edited by J.P.N. LAND, Anecdota Syriaca, 2, Leiden 1868, 289-329; Latin translation by W.J. VAN DOUWEN and J.P.N. LAND, Ioannis Ephesini episcopi Commentarii de beatis orientalibus et Historiae ecclesiasticae fragmenta (Verhandelingen van de Kkoninklijke Akademie van Wetenschappen. Afdeeling Letterkunde, 18), Amsterdam 1889, 216-243; Part III, edited by E.W. BROOKS, CSCO 105 Syr. 54, Louvain 1935; Latin translation by E.W. BROOKS, CSCO 106 Syr. 55, Louvain 1936.
JOHN OF NIKIU, *The Chronicle of John Bishop of Nikiu*, translated to English by R.H. CHARLES, 135-137, London 1916.
Journaux Contemporains des Événements.
KILISLI, Kadri (1932): *Kilis Tarihi*, Istanbul.
KORTE, J. (1741): *Jonas Kortens Reise nach Egypten dem Berg Libanon etc.,* Altona.
LANDESBIBLIOTHEK (LBS), (Libraries & Archives), Stuttgart-Zeitung (Allgem. G., qt. 407, 1626.5.1).
LEO GRAMMATICUS, *Chronographia*, edited by I. BEKKER, CSHB, Bonn 1842.
Les Gestes des Chyprois, Rec. Hist. Croisades. Arm., vol. 2.
L'Estoire d'Eracle, Rec. Hist. Croisades. Occ., vol. 2.
LIEBESCHUETZ, J.H.W.G. (1972): *Antioch: City and Imperial Administration in the Later Roman Empire*, Oxford.
LIGORIO PIRRO (1574-1577): *Libro o Trattato di diversi terremoti, raccolti da diversi Autori per Pyrro Ligorio cittadino romano, mentre la città di Ferrara è stata percossa et ha tremato per un simile accidente del moto della terra*, Archivio di Stato di Torino, Antichità romane, cod. 28.
LUSIGNANO, S. (1950): *Descripion de Toute l'Isle de Chypre etc.*, translated by G. CHAUDIÈRE, Paris.
MALALAS, IOHANNES (1831): *Chronographia*, edited by L. DINDORF, CSHB, Bonn 1831; translated by E. JEFFREYS, M. JEFFREYS and R. SCOTT, The Chronicle, Sydney, N.S.W. 1986.
MARCELLINUS COMES (1894): *Chronicon*, edited by TH. MOMMSEN, MGH, AA 11, Chronica minora, vol. 2, Berlin, 37-104.
MARINO SANUTO, THE ELDER, *Liber secretorum* (Secrets for the Crusaders) *or Gesta Dei per Francos*, book III/XI, ch. 1, Hannover 1611.

McGING, B.C. (1986): *The Foreign Policy of Mithridates VI Eupator King of Pontus*, Leiden.
MERCUREDE FRANCE (PMdF), (1726.10, p. 2349), (Press), Paris.
MICHAEL GLYKAS, *Annales*, edited by J.P. MIGNE, PG 158, Paris 1866.
MICHAEL THE SYRIAN, *Chronicle*, translated by J.-B. Chabot, 4 vols., Paris 1899.
MINISTÈREDES AFFAIRES ETRANGÈRES, Centre des Archives Diplomatiques de Nantes (AMAE CADN), (CCC, Turquie vol. 14, Lattaquie, entry dated 1822.8.28), Nantes.
MUHAMMED AL-TABAKH, see AL-TABAKH.
MUKHTARBASHA, Muhamed, *Al-Tawfiqat Al-Ilhamyeh*, Boulaq 1893.
MÜNZER, TH. (1930): s.v. Marcius 92, RE 14.2, cols. 1584-1585.
NASIR-I-KHUSRAU, *Sefer Nameh*, Relation du Voyage de Nassiri Khusrau en Syria, en Palestine, et Egypte, en Arabe ..., Charles Schefer, Paris 1881, 17-18.
NICEPHORUS CALLISTUS, *Historia Ayntomo*, edited by C. DE BOR, BT, Leipzig 1880.
NICEPHORUS PATRIARCHA, *Short History*, edited by C. MANGO, Washigton D.C. 1990.
NICETAS CHONIATES ACOMINATOS, *Historia Chronicon*, edited by I. BEKKER, Corp. Script. Hist. Byz., Bonn 1835.
OBERHUMMER, E., *Die Insel Cypern. Eine Landeskunde auf historischer Grundlage*, edited by TH. ACKERMAN, München 1903, 139-146.
OBERMEYER, J., *Die Landschaft Babilonien im Zeitalter des Talmuds und des Gaonats*, Frankfort a.M 1929.
OLIVIER, G.A. (1807): *Voyage dans l'Empire Othoman, L'Egypte et la Perse,* 3 vols., Paris.
OPPENHEIMER, A. (1983): *Babylonia Judaica in the Talmudic Period*, Wiesbaden.
Oracula Sibyllina, edited by A. KURFESS, München 1951; edited and translated by H.N. BATE, Sibylline oracles (books III-V), London 1918.
OROSIUS PAULUS, *Historiarum Adversus Paganos Libri VII*, edited by A. LIPPOLD, Milano 1976.
PANZAC, D. (1985): *La Peste dans l'Empire Ottoman*, 1700-1850, Louvain.
PAYNE SMITH, R. (Editor) (1879): *Thesaurus Syriacus*, Oxford.
PHILIP OF PLESSIS (1972): *Letter* in MAYER.
PHILOSTRATUS THE ATHENIAN, *Vita Apolloni*, edited by C.L. KAYSER, I, Leipzig 1870; translated by F.C. CONYBEARE, *The Life of Apollonius of Tyana*, London 1912; translated by J.S. PHILLIMORE, *Philostratus in Hinour of Apollonius of Tyana*, Oxford 1912; translated by C.P. Eells, *Life and times of Apollonius of Tyana*, Stanford 1923.
Press Reports: Varius: most important. Istanbul (Levant Herald, Stanboul, Neologos, Ikdam, Sabah). Izmir (Amaltheia, Courier de Symrne). Paris (Moniteur, Journal des Debats, Nouvelles Missions du Levant).
POCOCKE, R.A. (1743-1745): *A Description of the East etc.*, 2 vols., Bowyer, London.
PROCOPIUS OF CAESAREA, *Anecdota*, in Opera omnia, edited by J. HAURY and G. WIRTH, III, Liepzig 1953; translated by G.A. WILLIAMSON, Secret history, London, 1990.
PROCOPIUS OF CAESAREA, *Bella*, in Opera omnia, edited by J. HAURY and G. WIRTH, I-II, Liepzig 1952-1953.
PROCOPIUS OF CAESAREA, *De Aedificiis*, in Opera omnia, edited by J. HAURY and G. WIRTH, IV, Liepzig 1954.
RAFEQ, A.K. (no date): The provance of Damascus.
RALPH OF COGGESHALL, *Chronicon Anglicanum*, edited by J. STEVENSON, Rolls Ser., vol. 66.
Res gestae Divi Augusti, edited by P.A. BRUNT and J.M. MOORE, Oxford 1967.
RIZZO, F.P. (1963): *Le Fonti per la Storia della Conquista Pompeiana della Siria*, Palermo.
ROBERT, L. (1962): *Villes d'Asie Mineure* (2nd edition), Paris.
ROBERT OF AUXERRE, *Chronicon*, Mon. German. Hist. Ss. vol. 26; also edited by BOUQUET, Rec. Hist. Gaule et de la France, vol. 18.
RUNCIMAN, S. SIR (1971): *A History of the Crusades* ,Harmondsworth, 3 vols..
SAADEH, G. (1984): *Al-Moukhtasar fi Tarikh Al-Lathiqieh* (A Summary in the History of Lattakia), Lattakia.
SAADEH, S. (1982): *Ugharit, Mu'assaset Al-Fikr lil'abhath we Al-Nasher* (1st edition), Beirut.
SALIMBENE DE ADAM, *Cronica*, Mon. German. Hist. Ss., vol. 32.
SCHAEFFER, C.F.A. (1948): *Stratigraphie Comparée et Chronologie de l'Asie Occidentale (IIIe et IIe millénaires),* (Oxford University Press, London).
SCHENK VON STAUFFENBERG, A. (1931): *Die romische Kaisergeschichte bei Malalas*, Stuttgart.
SEMPAD LE CONNÉTABLE, *Chronique du Royaume de Petite Arménie*, Cf KSA 6, p. 29 (Reports of Ksara Observatory).
SEVERUS OF ANTIOCH, *Homily 31*, edited with French translation by M. BRIÈRE and F. GRAFFIN, Les Homiliae cathedrales de Sévère d'Antioche. Traduction syriaque de Jaques d'Edesse. Homélies XXVI à XXXI, PO 36/4= =170, Turnhout 1974, 106-31.
SIBT IBN AL-'AJAMI, *Kunuz Al-Dhahab fi Tarikh Halab*, translated by J. SAUVAGET, Matériaux pour servir à l'histoire de la ville d'Alep, Beirut 1950.
SIBT IBN AL-JAUZI, *Mir'at Al-Zamn*, vol. VIII, Hyderabad 1951.
SIBT IBN AL-JAWZI, A., *Al-Mountazam fi Tarikh Al-Mouluk wa Al-Oumam*, vols. 7, 8, 9, 10, Haydarabad 1938.
SIBT IBN AL-JAWZI, A., *Al-Mountazam fi Tarikh Al-Mouluk wa Al-Oumam*, British Library Ms. Or. 3004, 19b.
SOCRATES, *Historia Ecclesiastica*, edited by J.P. MIGNE, PG 67, Paris 1864.
STEIN, E., *Histoire du Bas-Empire II*, edited by J.-R. PALANQUE, Bruges 1949.
STRABO, *Geographica*, edited by A. MEINEKE, Leipzig 1877; edited by G. AUJAC and F. LASSERE, Paris 1966-89; edited by H.L. JOHNES, *The Geography of Strabo*, London-Cambridge (Mass.)1917-1928.
STRABON, *Géographe Grec (a vécu de 58 à 21-25)*, *Auteur de «Geographica»*.
SUETONIUS, C. Tranquillus, *De Vita Caesarum*, edited by H. AILLOUD, Paris 1961-1964; translated by R. GRAVES, *The twelve caesars*, Harmondsworth 1989.
SYNCELLUS, Georgius, *Chronographia*, edited by G.B. NIEBUHR, CSHB, Bonn 1829; edited by A.A. MOSSHAMMER, Leipzig 1984.
TACITUS, Publius Cornelius, *Annales ab Excessu Divi Augusti*, edited by E. KOESTERMANN, Leipzig 1971; translated by M. GRANT, The annals of imperial Rome, Harmondsworth 1989.
The Book of the Wanderings of Felix Fabri (1480-83), vol. 9, London 1893 (repr. AMS, New York 1971).
THE GREAT CHRONOGRAPHER, in *Beitrage zur antiochenis-*

chen und zur kostantinopolitanischen Stadtchronik, edited by A. FREUND, Jena 1882, 38-53.
Theatrum Europeum, edited by J.P. ABELIN, 21 vols., Frankfurt 1617-1712.
THEOPHANES, *Theophanis Chronographia*, CSHB , vol. 26/i, Bonn 1839.
THEOPHANES, *Chronographi*, edited by C. DE BOOR, Leipzig 1883-85 (repr. Hildesheim 1963).
THEOPHANES CONTINUATUS, edited by I. BEKKER, CSHB, Bonn 1838.
TSUGITAKA, S. (1988): The Syrian coastal town of Jabala: Its history and present situation, *Studia Culturae Islamicae,* **35** (Institute for the Study of Languages and Cultures of Asia and Africa, Tokyo).
Tusculum (Fragments of Tusculum), D'avant l'an 565, découvert par Angelo May, Fragment IV, in PG, edited by J.P. MIGNE, 85, coll. 1821-1824.
VALLE, Pietro della (1662-63): *Viaggi di Pietro della Valle il Pellegrino etc.*, 4 vols., Roma.
Vita Symeonis Iunioris, edited by P. VAN DEN VEN, Brussels 1962-1970.
VITALIANO DONATI, *Giornal del Viaggio*, Bibl. Reale Ms. 291, Torino.
VOLNEY, C.F. (1787): *Travels through Syria and Egypt in the Years 1783, 1784 and 1785*, 2 vols., London.
WHITBY, M. and M. (Translators) (1989): *Chronicon Paschale 284 -628 A.D.*, Liverpool.
WILBRANDUS OF OLDENBORG, *Travels*, edited by J.C.M. LAURENT, Peregrinatores medii aevi quatuor (2nd edition), Leipzig 1873, 161-191.
WILLIAM OF NANGIS, *Chronicon*, Rec. Gaule et de la France, vol. 20.
WINNETT, F.V. and W.L. REED (1970): *Ancient Records from North Arabia*, Toronto.
YAARI, A. (1951): *Sinai*: *28.349*, Jerusalem.
YAHYA IBN SAID, *Histoire*, edited and translated into French by I. KRATCHKOVSKY and A. VASILIEV, Pat Orientalis, XVIII, Fasc. 5, Paris 1957.
YAHYA IBN SAID AL-ANTAKI, *Dhayl ta'rikh Ibn Batriq*, edited by L. CHEIKHO *et al.*, CSCO Arab., Series tertia, vol. 7, Beirut-Paris.
YAQUT AL-HAMAWI, *Mu'jam Al-Buldan*, edited by WUSTENFELD, 4 vols., Leipzig 1866-1873.
Yebamoth (from The Bobylonian Talmud), edited by I.W. SLOTKI, London 1936.
ZACHARIAH OF MITYLENE, *The Syriac Chronicle*, translated by F.J. HAMILTON and E.W. BROOKS, London 1899.
ZACHARIE LE SCOLASTIQÛE, *Vie de Sévère d'Antioche*, Patrologie Orientale (2nd edition), Graffin-Nau.
ZAKARAYA, W. (1984) *Jawla Athariya fi Baedh Al-Bilad Al-Shamiya*, Dar Al-Fikr (Pub.), Damascus.
ZONARAS, Iohannes, *Epitome Historiarum Libri I-XII*, edited by B.G. NIEBUHR, CSHB, Bonn, 1844; *Epitome Historiarum Libri XIII-XVIII*, edited by Th. BÜTTNER-WOBST, CSHB, Bonn 1897.

Parametric catalogues

ABOU KARAKI, N. (1987): Synthèse et carte sismotectonique des pays de la bordure orientale de la Méditerranée : sismicité du systéme de failles du Jordain-Mer Morte, *Thèse de Doctorat* (Université Louis Pasteur, Strasbourg).
AL-HAKEEM, K. (1988): Studying of historical earthquakes activity in Syria, in *Proceedings of the Workshop on Historical Seismicity of Central-Eastern Mediterranean Region*, edited by C. Margottini and L. Serva, 27-29 Ottobre 1987, ENEA CRE Casaccia, Roma, 19-32.
AL-SINAWI, S.A. and H.A.A. GHALIB (1975): Historical seismicity of Iraq, *Bull. Seismol. Soc. Am.,* **65** (5), 541-547.
AMBRASEYS, N.N. (1961): On the seismicity of South-West Asia: data from a XVth century Arabic manuscript, *Rev. Etud. Calamités,* **37**, 18-30.
AMBRASEYS, N.N. (1962): A note on the chronology of Willis's list of earthquakes in Palestine and Syria, *Bull. Seismol. Soc. Am.*, **52**, 77-80.
AMBRASEYS, N.N. (1963): The seismicity of Cyprus, *Publications of Imperial College*, London.
AMBRASEYS, N.N. (1965): The seismic history of Cyprus, *Rev. Union Int. Secours,* **3**, 25-48.
AMBRASEYS, N.N. (1975): Studies in historical seismicity and tectonics, in *Geodynamics Today* (Royal Society, London), 7-16.
AMBRASEYS, N.N. (1978): Middle East: a reappraisal of the seismicity, *Q. J. Eng. Geol.,* **11**, 19-32.
AMIRAN, D.H.K. (1950-1951, 1952): Arevised earthquake-catalogue of Palestine, *Isr. Explor. J.,* **1**, 223-246; **2**, 48-62.
ANDREASYAN, H. (1970): Ermeni Kaynaklarindan Derlenmis Deprem Listesi, *Yayinlanmamis*, Prof. Dr. H. Soysal Arsivi, Istanbul.
BÅTH, M. (1979): *Introduction to Seismology* (2nd edition), Basel, Boston, Stuttgart, p. 139.
BEN-MENAHEM, A. (1979): Earthquake catalogue for the Middle East (92 B .C. to 1980 A.D.), *Boll. Geofis. Teor. Appl.,* **21**, 245-313.
BERLOTY, B. (1931) : Tremblements de terre et séismologie, *Almanach de l'Imprime Catholique*, 24-38.
CALVI, V.S. (1941): Erdbebenkatalog der Turkei und Einiger Benaehbarter Gebiete, *Yayinlanmamis*, Rep. No. 276, MTA Enstitüsü, Ankara.
ERGIN, K., U. GÜÇLÜ and Z. UZ (1967): *A Catalogue of Earthquakes for Turkey and Surrounding Area (11 A.D. to 1964 A.D.)*, Technical University of Istanbul, Istanbul.
GALANOPOULOS, A.G. and N.D. DELIBASIS (1965): The seismic activity of the Cyprus Area (26 B.C.-1963 A.D.), in *Proc. Athens Academy*, 387-405.
GANSE, R.A. and J.B. NELSON (1981): Catalogue of significant earthquakes (2000 B.C.-1979 A.D.), *Rep. SE-27*, *World Data Center Afor Solid Earth Geophysics*, pp. 154.
ISMAIL, A. (1960): Near and local earthquakes of Helwan (1903-1950), *Helwan Obs.,* **49**, pp. 32.
KÁRNÍK, V. (1971): *Seismicity of the European Area* (D. Reidel Publishing Company, Dordrecht, Holland), 2.
LERSCH, *Erdbeben-Chronik für die Zeit von 2362 v. Chr. bis 1897*, Ms., Archives of the Zentralinstitut für Physik der Erd, Jena.
LOMNITZ, C. (1974): Global tectonics and earthquake risk, *Dev. Geotect.*, **5**, *Elsevier Sc. Publ. Com.*, p. 320.
LYONS, H.G. (1907): Earthquakes in Egypt, *Survey Notes*, Cairo, I (10), 277-86.
MAAMOUN, M. and A. ALLAM (1981): Neotectonics of Eastern Arabian region – Regional studies, *Bull. Helwan Inst. Astron. Geophys.*, I, Ser. B, 173-235.
MEYERS, H.M. and C.A. VON HAKE (1976): Earthquake data file summary, *National Geophysical and Solar Terrestrial Data Center*, Boulder, CO.

MILNE, J. (1911): Catalogue of destructive earthquakes A.D. 7 to A.D. 1899, *Report of the 81st Meeting of the British Association for the Advancement of Science*, London, 694-740.

MORELLI, C. (1942): Carta sismica dell'Albania, *Reale Academia d'Italia, Commissione Italiana di Studio per i Problemi del Soccorso alle Popolazioni*, 10, Firenze, p. 121.

MOUTY, M. and M.R. SBEINATI (1988): Historical earthquake catalogue for Syria and adjacent areas, *Atomic Energy Commission of Syria*, *Internal Rep.*, Damascus.

ÖCAL, N. (1961): Kurze Liste der Erdbeben in der Türkei bis 1800 (*I*≥IX), Ms., 2.

ÖCAL, N. (1968): Türkiyenin sismisitesi ve zelzele cografyasi, 1850-1960 Yiliari Için Zelzele Katalogu, *Kandilli Rasathanesi Yayinlari No. 8*, Istanbul.

PINAR, N. and E. LAHN (1952): Türkiye depremleri izahli katalogu, *Bayindirlik Bakanligi, Yapi ve Imar Isleri Reisligi Yayinlarindan*, Ser. 6, Sayi 36, Ankara, p. 153.

PLASSARD, J. and B. KOGOJ (1981): Seismicité du Liban: catalogue des séismes ressentis (3rd edition), *Collection des Annales-Mémoires de l'Observatoire de Ksara*, IV, Beirut.

POIRIER, J. and M. TAHER (1980): Historical seismicity in the Near and Middle East, North Africa, and Spain from Arabic documents (VIIth-XVIIIth century), *Bull. Seismol. Soc. Am.*, **70**, 2185-220 1.

RIGGS, H.H. (1905-1909): *Monthly Earthquake Reports*, Euphrates College Seism. Station, Harpoot.

RUSSELL, P. (1760): An account of the late earthquake in Syria, *Philos. Trans.*, **51**, London, 529-534.

SCHMIDT, J.F. (1879): *Studien üeber Erdbeben*, Leipzig.

SCHMIDT, J.F. (1881): *Studien über Vulkanen und Erdbeben* (2nd edition), Leipzig.

SHALEM, N. (1952): La seismicité au Levant, *Bull. Res Counc. Isr.*, **2**(1), 1-16.

SHALEM, N. (1954): The Red Sea and the Erythrean disturbances, in *Congrès Géologique International, C., R., de la 19e session*, Alger, 222-231.

SHALEM, N. (1956) Seismicity and Erythrean disturbances in the Levant, *Publ. BCIS*, S.A., Tr. Sc. F. 19, 267-275.

SHALEM, N. (1960): Seismicity in Palestine and neighboring areas (macroseismical investigation), *Ms.*, 79.

SHEBALIN, N.V., V. KÁRNÍK and D. HADZIEVSKI (1974): *Catalogue of earthquakes, Part I: 1901 -1970; Part II: prior to 1901*, UNESCO, Skopie.

SOYSAL, H., S. SIPAHIäLU, D. KOLÇAK and Y. ALTINOK (1981): *Türkiye ve çevresinin tarihsel deprem katalogu (M.Ö. 2100-M.S. 1900)*, Tubitak, Matematik - Fiziki Ve Biyolojik Bilimler Arastirma Grubu, *Project. No. TBAG 341*, Istanbul.

THOLOZAN, J.D. (1879): Sur les tremblements de terre qui ont eu lieu en Orient du VII au XVII siecle, *Compte Rendus de l'Académie des Sciences de Frances,* **88**, 1063- 1066.

TÜRKELLI, N., A. NECIOäLU and A. AL-AMRI (1990): Seismicity of the Eastern Mediterranean, in *Proceedings of the Workshop on Historical Seismicity and Seismotectonics of the Mediterranean Region* (Bektur, ed.), Istanbul, 37-129.

US CONGRESS (1888): *Great Earthquakes* (Washington D.C.), 1.

WILLIS, B. (1928): Earthquakes in the Holy Land, *Bull. Seismol. Soc. Am.,* **18**, California, 73-103.

WILLIS, B. (1933a): Earthquakes in the Holy Land: a correction, *Bull. Seismol. Soc. Am.,* **23**, 88-89.

WILLIS, B. (1933b): Earthquakes in the Holy Land: a correction, *Science,* **77**, p. 351.

World Map of Natural Hazards (1978), Münchener Rückversicherungs-Gesellschaft, Munich, Federal Republic of Germany.

Seismological compilations

AL-GHOUNEIM, A.Y. (no date): *Asbab Al-Zlazel wa Houdutheha fi Al-Tourath Al-Arabi* (Causes of Earthquakes and their Events in the Arabic Literature).

AL-HAFEZ, M.M. (1982): Nusus ghair manshura an al-zalazil men 914-1124 A.H./1508-1712 A.D., *Bull. Etud. Orientales,* 32-33, Damascus, 256-264.

ALONSO-NÚÙEZ, J.-M. (1992): *La Historia Universal de Pompeyo Trogo*, Madrid.

AL-SANAWI, S. and H.A. GHALIB (1975): Historical seismicity of Iraq, *Bull. Seismol. Soc. Am.*, **65**, 541-547.

AMBRASEYS, N.N. (1961): On the seismicity of South-West Asia: data from a XV century Arabic manuscript, *Rev. Etud. Calamités*, **37**, 18-37.

AMBRASEYS, N.N. (1962): Data for the investigation of the seismic sea-waves in the Eastern Mediterranean, *Bull. Seismol. Soc. Am.*, **52**, 895-913.

AMBRASEYS, N.N. (1988) Engineering seismology, *J. Earthquake Eng. Struct. Dyn.*, **17**, 1-105.

AMBRASEYS, N.N. (1989): Temporary seismic quiescence: SE Turkey, *Geophys. J.*, **96**, 311-331.

AMBRASEYS, N.N. and C.F. FINKEL (1993): Material for the investigation of the seismicity of the Eastern Mediterranean region during the period 1690-1710, in *Materials of the CEC Project* '*Review of Historical Seismicity in Europe'*, edited by M. STUCCHI, CNR Milano, 1, 173-194.

AMBRASEYS, N.N. and C. FINKEL (1995): The seismicity of Turkey and adjacent areas: a historical review (1500-1800), *Muhittin Salih EREN Publ.*, Istanbul.

AMBRASEYS, N.N. and J.A. JAKSON (1998): Faulting associated with historical and recent earthquakes in Eastern Mediterranean region, *Geophys. J. Int.*, **133**, 390-406.

AMBRASEYS, N.N. and C.P. MELVILLE (1995): Historical evidence of faulting in Eastern Anatolia and Northern Syria, *Ann. Geofis*., **XXXVIII** (3/4), 337-343.

AMBRASEYS, N.N. and D. WHITE (1997): The seismicity of the Eastern Mediterranean region 550-501 B.C.: a reappraisal, *J. Earthquake Eng.*, **1** (4), 603-632.

AMBRASEYS, N.N., C.P. MELVILLE and R.D. ADAMS (1994): *The Seismicity of Egypt, Arabia and the Red Sea: a Historical Review* (Cambridge University Press).

ANDREASYAN, H. (1973): XIV ve XV. Yuzyil Turk Tarihine Ait Ufak Kronolojiler, Kolafanlar, Ist. Uni. Ede. Fak. Tarih Ens. Dergisi, Sayi 3, Istanbul.

ARINCI, R. (1945): Arzda ve Yerdumuzda Zelzele Bolgeleleri, Corumlu Mcmuasi, Corum Halkevi Yayini, Yil 4, Sayi 29, Corum.

BARBIERI, G. (1970): Pompeo Macrino, Asinio Marcello, Bebio Macro e i Fasti Ostiensi del 115, *Mélanges d'Archéologie et d'Histoire de l'Ècole Française de Rome,* **82** (1), 263-78.

BAUR, P.V.C. and M.I. ROSTOVTZEFF (1931): *The Excavations at Dura-Europos*, II, New Haven.

BERRYAT, J. (1761): Liste chronologique des éruptions de Volcans, des Tremblements de Terre etc., *Collect. Académique*, **6**, Paris, 488-676.

BESSON, J. (1660): *La Syrie Sainte* ... Henault, Paris.

BLANCKENHORN, Max (1905): Die Erdbeben in Palästina und die erforschung künftiger, *Zeitschrift des deutschen Palätinavereins*, 28, part 1, 216-218.

BONITO, M. (1691): *Terra tremante, o vero continuatione de' terremoti dalla Creatione del Mondo sino al tempo presente* ..., Napoli 1691 (reprint, Sala Bolognese 1980).

BURNARND, Y. (1984): Terrae Motus, La documentation épigraphique sur les tremblements de terre dans l'Occident romain, in *Tremblements de terr* , 173-82.

CAPELLE, W. (1924): s.v. Erdbebenforschung, RE, Suppl. IV, coll. 344-374.

Catalogo epigrafi (1989) = Catalogo delle epigrafi latine riguardanti terremoti, in GUIDOBONI (1989), 135-68.

CAVASINO, A. (1931a): Note sur catalogo dei terremoti distruttivi dal 1501 al 1929 nel bacino del Mediterraneo, 29-36, *R. Acad. Nat. Lincei, Publ. della Com. It. per lo Studio delle Grandi Calamita,* vol. II, Mem. Sci. Technol., Roma.

CAVASINO, A. (1931b): Catalogo dei terremoti avertiti nel bacino del Mediterraneo del 1501 al 1929, 37-60, *R. Acad. Nat. Lincei, Publ. della Com. It. per lo Studio delle Grandi Calamita*, vol. II, Mem. Sci. Technol., Roma.

COLLECTION ACADÉMIQUE, Tome VI de la Partie Etranger et Premier, Tome de la Physique Experimentale Séparée.

FRANCIS, I. (1947): *Bizanz Kaynaklarina*, Gore Orta Sark'ta Vukubulan Zelzeleler, 1st. Uni. Ed. Fak. Cog. Bl. Doktora tezi, Ist. Uni. Kitapligi No. 1420.

FUCHS, C.W.C. (1886): Statistik der Erdbeben von 1865-1885, *Sitzungsberichte d.M. Mathem.-Naturw. Ges.*, Bd. XCII, Heft. 3, 215-625, Vienna.

GATIER, P.L. (1984): Tremblements du sol et frissions des hommes, Trois séismes en Orient sous Anastase, in *Tremblements de terre* , 87-94.

GHAWANMEH, Y. (1989): Earthquakes effects on Belad Al-Sham settlements, *Paper presented at IVe Congrés sur l'Histoire et L'Archéologie de Jordanie*, 30 May-4 June, Lyon.

GUIDOBONI, E. (Editor) (1989): *I Terremoti Prima del Mille in Italia e nell'Area Mediterranea, Storia Archeologia Sismologia* (ING, Roma-SGA, Bologna), pp. 768.

GUIDOBONI, E., A. COMASTRI and G. TRAINA (1994): *Catalogue of Ancient Earthquakes in the Mediterranean Area up to the 10th Century* (ING, Roma-SGA, Bologna), pp. 504.

HENRY, M. (1985): Le témoignage de Libanius et les phénomènes séismiques du IVe siècle de notre ère, *Essai d'Interprétation*, Phoenix, 39, 36-61.

HERMANN, A. (1962): s.v. Erdbeben, Reallexikon für Antike und christentum 5, cols. 1070-10113, (Contributions to the geology and palaeobiology of the Caribean and adjacent areas), Verhandlungen der Naturforschenden Gesellschaft in Basel 84, 101-52.

HOFF, K.E.A. von (1840): Chronik der Erdbeben und Vulkan-Ausbrüche etc., *Gesch. Überlief. Nachgew. Natürl. Veräender. Erdoberfläche*, IV, Gotha.

KALLNER-AMIRAN, D. (1951): A revised earthquake catalogue of Palestine, *Is. Explor. J.*, vol. I, 223-46; vol. II, (1952), 48-65.

LEMMENS, H.J. (1898): *Al-zalazil fi Suriah*, *Al-Mashreq*, 1, 303-304 and 337-342, Beirut.

MALLET, R. (1853): Third report on the facts of earthquakes phenomena, *Report of the 22nd Meeting of the British Association for the Advancement of Science*, 1-176.

MALLET, R. and J.W. MALLET (1858): The earthquake catalogue of the British Association, *Trans. Br. Ass. Adv. Sci.*, 1852 to 1858, London.

MANETTI, Giannozzo (1457): *De Terraemoto Libri Tres*, Biblioteca Apostolica Vaticana, cod. Urbinate Lat. 5; cod. Palatino Lat. 1076, 1077 and 1604.

MONTANDON, F. (1953): *Les Tremblements de Terre Destructeurs en Europe* (Union Internationale de Secours, Genève), p. 160 séisme de 334.

PERREY, A. (1850): Mémoire sur les tremblements de terre ressentis dans la Péninsule Turco-Hellénique et en Syrie, *Mém. Acad. R. Belg.,* **23**, Bruxelles.

POIRIER, J.P., B.A. ROMANOWICZ and M.A. TAHER (1980): Large historical earthquakes and seismic risk in Northwest Syria, *Nature,* **285**, 2 17-20.

ROBERT, L. (1978): Documents d'Asie Mineure V. Stèle funéraire de Nicomédie et séismes dans les inscriptions, *Bull. Corresp. Hellèniqque*, **102**, 395-408.

RUSSELL, K.W. (1985): The earthquake chronology of Palestine and Northwest Arabia from the 2nd through the Mid-8th century A.D., *Bull. Am. Sch. Oriental Res.,* **260**, 37-59.

SIEBERG, A. (1932): Untersuchungen übar erdbeben und bruchscholenbau im Östlichen mittelmeergebiet, *Denkschrifften der Medizinsch-Naturwissenschaft Gesellschaft zu Jena*, **18**, 161-273.

SWISS REINSURANCE COMPANY (1978): *Atlas on Seismicity and Volcanism* (October 1977, Switzerland).

TAHER, M.A. (1979): Corpus des textes arabes relatifs aux tremblements de terre et autres catastrophes naturelles de la conquête arabe au XII H/XVIII JC, *Thesis de Doctorat d'Etat* (Univ. Paris 1, Sorbonne), 2 vols.

TUCKER, W. (no date): *The Effects of Earthquakes in the Medieval Islamic World* (Dept. of History, Univ. of Arkansas, Fayeteville).

WORLDDATA CENTER FOR SOLID EARTH GEOPHYSICS, *Catalogue of Significant Earthquakes (2000 B.C.-1979 A.D.).*

Monographs

AL-HAKEEM, K. (1986): Analysis of the 1759 A.D. earthquake, *Atomic Energy Commission of Syria, Internal Rep.*, Damascus.

AMBRASEYS, N.N. (1997): The earthquake of 1 January 1837 in Southern Lebanon and Northern Israel, *Ann. Geofis.*, **XL** (4), 923-935.

AMBRASEYS, N.N. and M. BARAZANGI (1989): The 1759 earthquake in the Bekaa Valley: implications for earthquake hazard assessment in the Eastern Mediterranean region, *J. Geophys. Res.*, **94**, 4007-4013.

AMBRASEYS, N.N. and C.P. MELVILLE (1988): An analysis of the Eastern Mediterranean earthquake of 20 May 1202, in *History of Seismography and Earthquakes of the World*, edited by W.H. LEE (Academic, San Diego, CA), 181-200.

DARAWCHEH, R., M.R. SBEINATI, C. MARGOTTINI and S. PAOLINI (2000): The 9 July 551 A.D. Beirut earthquake, Eastern Mediterranean region, *J. Earthquake Eng.*, **4**, 403-414.

GUYS, C.E. (1822): Le tremblement de terre qui a bouleversé la Haute-Syrie en Août 1822, *Bull. Soc. Géogr.,* Paris, 1, 301-305.

MARGALIOT, M. (1960): The date of an earthquake at Taberias, *Tarbiz,* **29**, 339-44.

TRAINA, G. (1994): From Crimea to Syria. Re-defining the alleged historical earthquake of 63 B.C., *Ann. Geofis.*, **XXXVIII** (5/6), 479-489.

TSAFRIR, Y. and G. FOERSTER (1992): The dating of the 'Earthquake of the Sabbatical year' of 749 C.E. in Palestine, *Bull. Sch. Oriental African Stud.*, 55/ii, London, 23 1-235.

VERED, M. and H. STRIEM (1976): The Safad earthquake of 1.1.1837 and its implications on risk evaluation in Israel, *Isr. A.E.C.*, No. IA-LD-1-105.

Other works

BARAZANGI, M. (1983): A summary of the seismotectonics of the Arabia region, in *Assessment and Mitigation of Earthquake Risk in the Arab Region*, edited by K. CIDINSKY and B. ROUHBAN, *Ass. Mit. Earthq. Ris. Arab Reg.*, UNESCO, 43-58.

BARAZANGI, M., D. SEBER, T. CHAIMOV, J. BEST and R. LITAK (1993): *Tectonic Evolution of the Northern Arabian Plate in Western Syria* (Kluwer Academic Publishers), 117-140.

BEST, J., M. BARAZANGI, D. AL-SAAD, T. SAWAF and A. GEBRAN (1990): Bouguer gravity trends and crustal structure of thePalmyride mountain belt and surrounding northern Arabian platform, *Geology,* **18**, 1235-1239.

BREW, G., M. BARAZANGI, A.K. AL-MALEH and T. SAWAF (2001): Tectonic and geological evolution of Syria, *GeoArabia,* **6**, 537-616.

GARFUNKEL, Z., I. ZAK and R. FREUND (1981): Active faulting in the Dead Sea rift, *Tectonophysics,* **80**, 1-26.

GOMEZ, F., M. MEGHRAOUI, A.N. DARKAL, R. SBEINATI, R. DARAWCHEH, C. TABET, M. KHAWLIE, M. CHARABE, K. KHAIR and M. BARAZANGI (2001): Coseismic displacements along the Serghaya fault: an active branch of the Dead Sea fault system in Syria and Lebanon, *J. Geol. Soc.*, **158**, 405-408.

GRÜNTHAL, G. (Editor) (1993): European macroseismic scale 1992 (up-dated MSK-scale), Conseil de l'Europe, *Cen. Européen Géodyn. Seismol.,* 7, Luxembourg.

IAEA (INTERNATIONAL ATOMIC ENERGY AGENCY) (1979): Earthquakes and its associated topics in relation to nuclear power plant siting, *IAEA Safety Series 50-SG-S1*, Vienna.

IAEA (INTERNATIONAL ATOMIC ENERGY AGENCY) (1987): Methodology and procedures for compilation of historical earthquakes data, *IAEA-TECDOC-434*, Vienna.

KLENGEL, H. (1985): *Syria Antiquity*, translated by KASSEM TWER, Ministry of Culture, Damascus, 47-48 and 127.

MCBRIDE, J., M. BARAZANGI, J. BEST, D. AL-SAAD, T. SAWAF, M. AL-OTRI, and A. GEBRAN (1990): Seismic reflection structures of intracratonic Palmyride fold-thrust belt and surrounding Arabian platform, Syria, *Am. Assoc. Pet. Geol. Bull.,* **74**, 238-259.

MCCLUSKY, S., R. REILINGER, S. MAHMOUD, D. BEN SARIand A. TEALEB(2003): GPS constraints on Africa (Nubia) and Arabia plate motions, *Geophys. J. Int.*, **155**, 126-138.

MEGHRAOUI, M., F. GOMEZ, R. SBEINATI, J. VAN DER WOERD, M. MOUTY, A.N. DARKAL, Y. RADWAN, I. LAYYOUS, H. AL-NAJJAR, R. DARAWCHEH, F. HIJAZI, R. AL-GHAZZI and M. BARAZANGI (2003): Evidence for 830 years of seismic quiescence from palaeoseismology, archaeoseismology and historical seismicity along the Dead Sea fault in Syria, *Earth Planet. Sci. Lett.*, **210**, 35-52.

PONIKAROV, V.P (Editor) (1964): *Tectonic Map of Syria, Scale 1:1000000* (Ministry of Industry, Damascus, Syria).

SBEINATI, M.R. (1993): Instrumental catalogue of earthquakes in Syria and adjacent areas from 1900 to 1993, *ICTP Res. Rep.*, Trieste (unpublished).

SHEBALIN, N.V. (1970): Intensity: on the statistical definition of the term, in *Proc. X Ass. ESC*, Leningrad, 3-11 September 1968 (Acad. Sci. USSR, Soviet Geophysical Committee, Moscow).

SHEBALIN, N.V. (1974): Principles and procedures of cataloguing, in *Catalogue of Earthquakes*, edited by N.V. SHEBALIN, V. KÁRNÍK and D. HADZIEVSKI, *UNDP/UNESCO Survey of Seismicity of the Balkan Region* (UNESCO, Skopje).

STUCCHI, M. (1994): Recommendations for the compilation of a European parametric earthquake catalogue, with special reference to historical records, in *Materials of the CEC Project* '*Review of Historical Seismicity in Europe'*, edited by P. ALBINIand A. MORONI, CNR Milano, 2, 181-190.

WOLSELEY HAIG, LT.-COLONEL SIR (1932): *Comparative Tables of Muhammadan and Christian Dates* (Luzac and Co., London).

(received December 19, 2003;
accepted November 12, 2004

CHAPTER V

ARCHEOSEISMOLOGY AND PALEOSEISMOLOGY IN SYRIA

V. Archeoseismology and Paleoseismology in Syria

V – 1. Framework of field investigations in Syria

Archeoseismology can be introduced as the Earthquake Archeology. This identification can be understood as the study of the impact of pre-historical and historical earthquakes on ancient sites. The time coverage may extend as a function of the richness of the cultural heritage of a region and the preservation of the archeological and historical sites. The importance of archeoseismology can be measured in the ability to play a key role in presenting field evidence of coseismic destruction and faulting, landslide and liquefaction of the ancient earthquakes. The advantage of archeological evidence in the study of past earthquakes is the potential for establishing precise dates of unrecorded past seismic events using associated cultural materials, and for guiding a better estimate of earthquake parameters. Finally, the misinterpretation of archeological data can be avoided by means of a confrontation and comparison between field evidences and historical documents.

The Eastern Mediterranean Region is one of the historically and culturally richest regions worldwide. Indeed, Syria hosted the early human being and rising up of the 1 million years old Homo-erectus at Palmyra and Neher Al-Kabir Al-Shemali sites, till the early kingdoms in 5000 B.C. close to Damascus and at Tell Sabi Abiedh in Al-Raqqa NE Syria. A striking cultural event is the first creation of the alphabet about 2000 B.C. in Ugarit (NE Syria, immediately north of Lattakia), followed by the Hellenistic, Roman, Byzantine eras, and the different Islamic periods: Umayyad, Abbasid, Fatimi, Mamluki, Seljuk, and finally the Ottoman period. All the past civilizations left many traces in Syria and this richness in heritage allows more than 100 foreign and local archeological missions to conduct field investigations and discover sometimes evidence of past earthquakes.

The proximity of a plate boundary (see also chapter III) represented by the Dead Sea Fault and related destructive earthquakes obviously left many traces preserved in the archeological layers. These traces of the coseismic impacts can be discriminated from other types of damage such as wars, floods, erosion, and other human and natural causes.

According to Stiros (1996) in its identification of earthquakes from archaeological data "*The principal effects of seismic waves on a construction manifest themselves in two forces: one horizontal force exerted at the top of the construction, and a vertical force exerted at its foundations. These forces are alternating in direction. The response of a construction to an earthquake depends on the parameters of the earthquake, such as its magnitude, structural characteristics, the characteristic frequency of the building and the dominant frequency of the seismic waves, building orientation relative to the direction of the seismic wave's propagation*".

Based on what ismentioned above, such as ancient brittle masonry structures in Roman temples and Byzantine churches can accommodate the effect of seismic waves through different behaviour: i - from a small horizontal displacements of the stones structure, ii - or an opening arch as seen in Figure 22 or a fracture (Figure 25) as in Krak des Chevaliers, to tracing the surface waves on the tall walls in Deir Dahess (Figure 41), and finally ii – as a total destruction of a building as in Apamea (Figure 30).

The main types of earthquake damages fall into five categories according to the recognized earthquake-deduced typology, as seen in the work of Sbeinati (1994), Stiros and Jones (1996) and Marco (2008). In many archeological sites in Syria (Figure 1) and along the Dead Sea Fault these categories of earthquake damage can be classified as:

- Ancient building structures may have been cracked, ruptured and/or displaced and separated due to surface faulting as seen for the Al-Harif Roman aqueduct site along the Missyaf Fault (Meghraoui, 2003).
- The waving walls and opening arches as the effect of surface wave propagation observed in the Samaan citadel (Saint Simon) citadel that can be interpreted as a result from high signal amplitude with low frequency.
- A unidirectional orientation of fallen building structure elements dominated in a site (columns, towers, long walls) as seen in the famous ancient city of Apamea (Figure 30) probably resulting from the effect of high horizontal ground acceleration.

- The opening of the structure pieces as battles of flower and spread out of destruction such as in Kherbet Maez site that may be resulted from site effect and the structure resonance phenomena.
- The X shape cracks in walls and windows resulting from the shaking of building structures as seen in modern structure.

Other coseismic features such as landslides and liquefaction effects can be easily recognised and dated as observed and documented in the Agora site of Apamea city and Hussen Suleiman (Zeus temple).

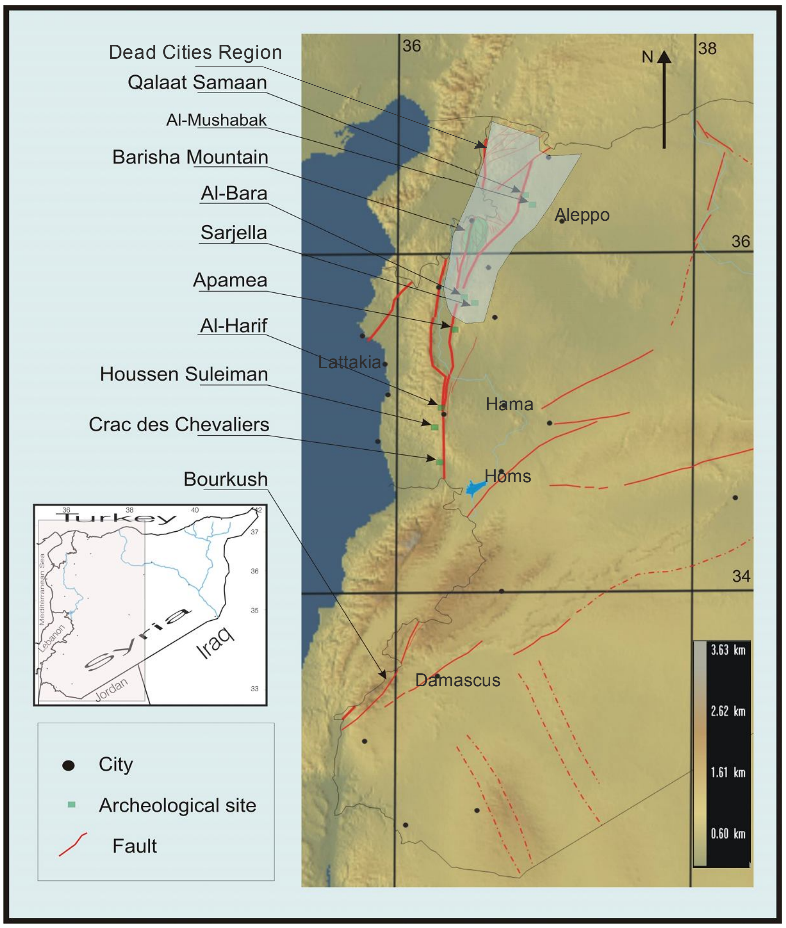

Figure 1: Map of Syria showing the studied Archeological sites and the major faults.

Our archeoseismological investigations have been achieved in two stages: 1) The reconnaissance stage as seen in the reports and publication of the AECS report for the IAEA Project (Sbeinati, 1994; Sbeinati et al., 1994; Sbeinati et al., 1997; see also appendixes 2 and 3). 2) The detailed investigations, as seen in the AECS-DGAM annual and final reports prepared for the 3-year EC funded APAME Project (Sbeinati et al., 2006), (Meghraoui, 2003) and in the following paragraphs.

The work in the first stage concentrated in exploring and describing all archeological sites in Syria which have clear indications of earthquake damage. Twenty sites were considered to have fairly reliable evidences of ancient earthquake scars in Syria and are hereafter mentioned; The Dead Cities: Babisqa, Darqita, Kouknaya, Kerbet Maez, Samaan Citadel (Saint Simon), Al-Mshabek Palace (Church), Sarfud Palace (Al-Breij), and Deir Dahess are along the Afrin Fault. The Qalaat Salah-Addin (Fortress of Sahyoun) on the costal mountain chain and Ugharit site on the coastline. The Al-Bara, Sergella, and Apamea cities are along the Ghap depression, while the Al Harif Aqueduct, Hussen Suleiman and Crac des Chevaliers fortresses are along the Missyaf fault. The Kharaeb As-Sukari and Palmyra cities are on the Palmyride fold zone and Ar-Rassafah site on the Rassafeh fault. Finally, the Halabeh and Zalabieh villages on the Euphrates fault. Each site is classified following the gathered data with regard to: different names, geographical and geological environment, historical information and dates of historical earthquakes, building materials, present-day conditions, types of earthquake damage, and grade of damage according to EMS-98 scale (Grünthal, 1998).

The work in the second stage consists in more detailed investigations in the archeological sites along the Dead Sea Fault in Syria. The AECS reports for the APAME project (Appendix 1) contains summarized descriptions of earthquake damage in Kerbet Maez, Samaan Citadel (Saint Simon), Al-Mshabek Palace (Church), Sarfud Palace, Deir Dahess, Al-Bara, Sergella, Apamea, Al-Harif, Hussen Suleiman, Crac des Chevaliers are and Bourkush (Figure 1).

The APAME project allowed us to perform detailed investigations at four sites: Al-Harif Roman aqueduct, Krak des Chevaliers, Apamea, and Deir Dahess. The main objectives were to move up from descriptive or analytical methods to quantitative analysis. Our objective was to provide precise dating of past seismic events and related faulting parameters, and analyse the type of destruction at each site using geomorphology and paleoseismology, archaeology and architecture, aided with techniques of sounding, trenching and isotopic (mostly C^{14}) dating.

I present the detail study of the four sites in the following sections.

Timing of earthquake ruptures at the Al Harif Roman Aqueduct (Dead Sea fault, Syria) from archeoseismology and paleoseismology

Sbeinati Mohamed Reda [1 & 2], Meghraoui Mustapha [2 *], Suleyman Ghada [3], Francisco Gomez[4], Grootes Pieter [5], Nadeau Marie-Josée [5], Haithem Al Najjar [1], & Riad Al-Ghazzi [6]

1) *Dept. of Geology, Atomic Energy Commission, Damascus, Syria*
2) *Laboratory of Active Tectonics, Institut de Physique du Globe, UMR 7516, Strasbourg, France*
3) *Directorate General of Antiquities and Museums, Damascus, Syria*
4) *Dept. of Geological Sciences, Missouri University, USA*
5) *Leibniz-Labor für Altersbestimmung und Isotopenforschung, Kiel University Germany*
6) *Higher Institute for Applied Sciences and Technology, Damascus, Syria (now at the virtual University, Damascus)*

* Corresponding author

Submitted to the Geological Society of America Bulletin
Special Volume on "Ancient Earthquakes"
Accepted April 2010

Abstract.

We study the faulted Al Harif Roman aqueduct located on the north-south trending and ~ 90-km-long Missyaf segment of the Dead Sea Fault (DSF) using 4 archeological excavations, 3 paleoseismic trenches and the analysis of 6 tufa cores. Damage to the aqueduct wall exhibits successive left-lateral fault offsets that amount 13.6 ± 0.2 m since the aqueduct construction younger than BC 65. Radiocarbons dating of sedimentary units in trenches, building cement of the aqueduct wall and tufa cores constrain the late Holocene aqueduct history. The building stone types, related cement dating and tufa deposits of the aqueduct indicate 2 reconstruction-repair episodes in AD 340 ±20 and AD 720 ±20. The combined analysis of trench results, successive building and repair of aqueduct wall, and tufa onsets, growths and interruptions suggests the occurrence of 4 faulting events in the last ~ 3500 years with a cluster of 3 events in AD 160 - 510, AD 625 - 690 and AD 1010 - 1210, the latter being correlated with the 29 June 1170 large earthquake. Our study provides the timing of late Holocene earthquakes and infers a lower and uppr bound 4.9 – 6.3 mm/yr slip rate along the Missyaf segment of the Dead Sea Fault in Syria. The inferred successive faulting events, fault segment length and related amount of coseismic slip yield M_w = 7.3 - 7.5 for individual earthquakes. The identification of the temporal cluster of large seismic events suggests periods of seismic quiescence reaching 1700 years along the Missyaf fault segment.

1- INTRODUCTION

Large strike slip faults are continental tectonic structures and sources of seismic strain release during recurrent large earthquakes. The ~ 850-km-long Dead Sea Fault (DSF) constitutes a north-south trending plate boundary that accommodates most of the left-lateral active deformation between the Africa (Sinai sub-plate) and Arabia plates (Garfunkel et al., 1981; Barazangi et al., 1993; Figures 1 a and b). The total left-lateral offset along the fault reaches 105 km among which ~ 45 km are post-Miocene slip as a result of the sea-floor spreading in the Red Sea (Quennel, 1984). However, the northern DSF shows less than 25 km left-lateral post-Miocene offset (Trifonov et al., 1991), the ~20 km missing slip being possibly absorbed by the shortening along the Palmyrides fold belt (Chaimov et al.; 1990). Kinematic models of the northern DSF imply a transpressional fault system that suggest an oblique relative plate motion and relative rotation at about 31.1°N 26.7°E at 0.40 ±0.028 Ma^{-1}.(Westaway, 2004; Gomez et al., 2006). The northern section of the DSF (i.e., in Lebanon and Syria) can be considered among the main seismogenic zones in the region since it has a long (since 1365 BC), rich and well-documented history of large destructive earthquakes that severely damaged many ancient cities (Figure 1 a; Ambraseys and Melville, 1988a; Guidoboni, 1994; Sbeinati et al., 2005). In contrast, the instrumental seismicity during the last century along the plate boundary is of low level and does not reflect the hazardous nature of the fault (Salamon et al., 2003). The long term faulting behavior needs to be investigated and a better constrain on the rate of active faulting is required for the seismic hazard assessment.

The DSF has been the source of numerous large earthquakes with surface faulting in the historical time (Ambraseys and Jackson, 1998). Although no recent surface ruptures have been observed in recent times, the combined analyses in historical seismology, paleoseismology and archeoseismology contributed in a better understanding of the relationship between large historical earthquakes (Mw > 7) and fault segments. The most recent large earthquake reached Mw 7.2 and took place in 22 November 1995 offshore in the Gulf of Aquaba at the southern end of the DSF. Historical earthquake-faulting related studies included from north to south (Figure 1 a), the 1408 earthquake and Jisr-Al-Shuggur Fault (Ambraseys and Melville, 1988a), the 1157 and 1170 earthquakes and Apame and Missyaf Fault segments, respectively (Meghraoui et al., 2003; Sbeinati et al, 2005), the 1202 earthquake and the Yammouneh fault (Ambraseys and Melville, 1988b; Ellenblum et al., 1998; Daeron et al., 2005, 2007), the 1759 earthquake sequence and the Serghaya-Rachaya Fault branches (Gomez et al., 2003, Nemer et al., 2008), the 1837 earthquake and the Roum Fault branch of the Lebanese restraining band (Nemer and Meghraoui, 2006), the AD 749 earthquake and the Jordan Valley Fault (Marco et al., 2003; Ferry et al., 2007), and the 1068 earthquake and south Araba Valley Fault (Amit et al., 2006).

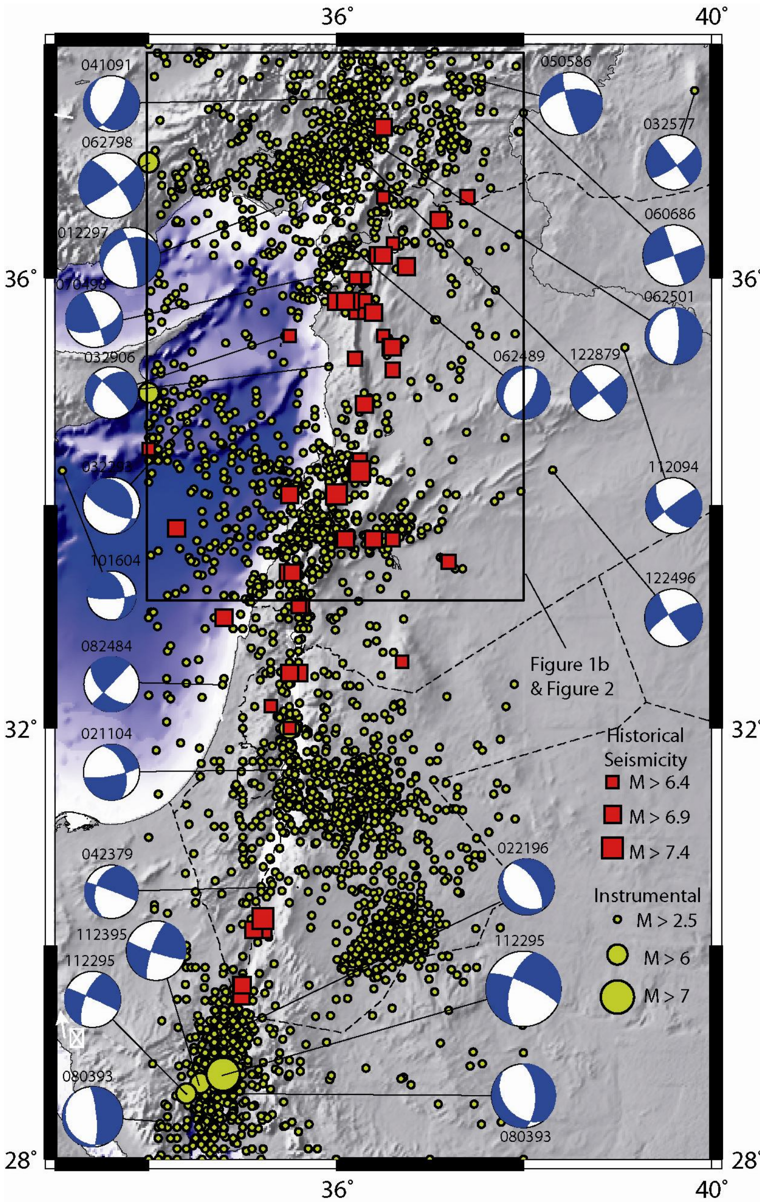

Figure 1 a) Seismicity (historical before 1900 and instrumental till 2004) along the Dead Sea fault (data from merged ISC, EMSC and the APAME Project catalogue). Focal mechanism solutions are from Harvard CMT. The black frame indicates the Missyaf fault segment (see also Figure 3).

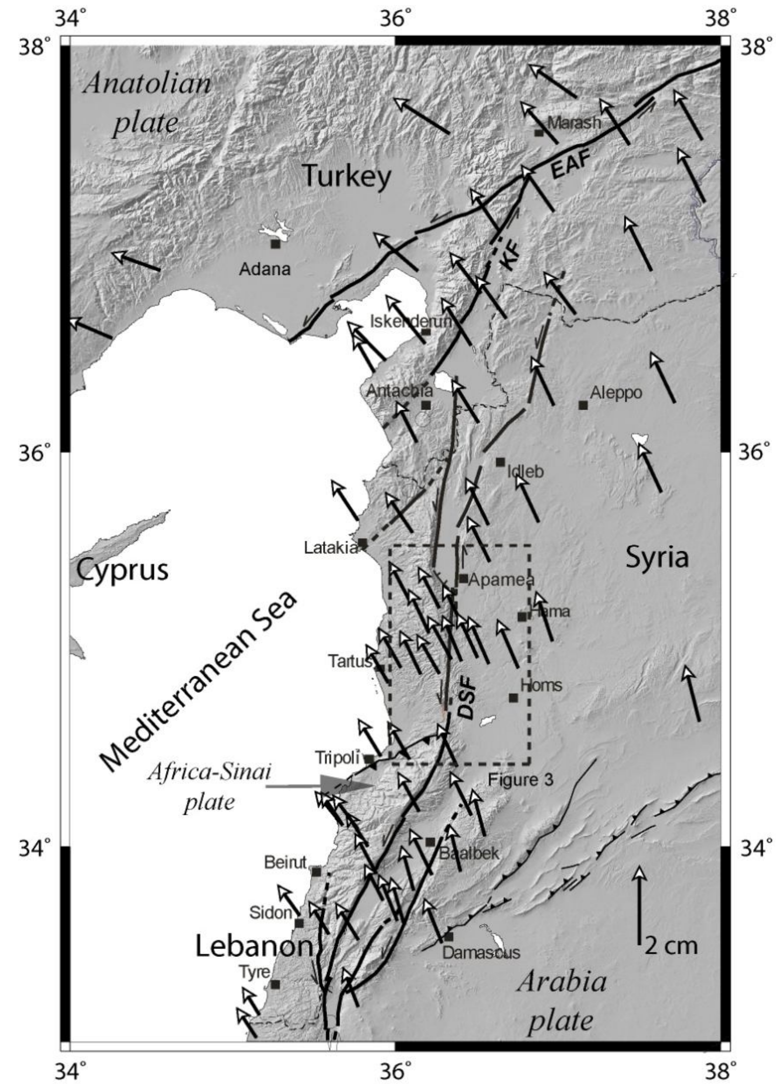

Figure 1 b) Fault zone (black line; Meghraoui et al., 2003; Gomez et al., 2003; Elias, 2006; Nemer et al., 2008) and GPS velocities (red arrows with Eurasia fixed; Reilinger et al., 2006; Gomez et al., 2007; Le Beon et al., 2008; Alchalbi et al., 2009) emphasizing the left-lateral movements between the Sinai Block and Arabia plate. Thick line is strike slip fault; thin line is thrust fault.

The study of historical seismic events of the DSF and related area of maximum damage was associated to investigations on the possible extent of surface ruptures and related major geometrical barriers. Earthquake parameters that include individual or cumulative left-lateral offsets and rate of slip can be obtained from paleo-earthquake studies along the DSF. Numerous fault slip rates have been inferred from offset geological units and geomorphologic features along the DSF and the more recent investigations including stream offsets and paleoseismic studies yield 4 to 7 mm/yr measured at time scales ~ 10 to 100 Ka (Garfunkel et al., 1981; Ginat et al., 1998; Klinger et al., 2000; Niemi et al., 2001; Daeron et al., 2004; Gomez et al., 2007; Ferry et al., 2007; Karabacak et al., 2010) and younger than 10 Ka (Marco et al., 2003; Meghraoui et al., 2003; Gomez et al., 2003; Akyuz et al., 2006). Although an accurate measurement of the present-day active deformation across the DSF requires a dense geodetic network combined with consistent block models, the 3 to 6 mm/yr GPS velocities appear to be comparable to the geologic rate of slip (McClusky et al., 2003; Wdowinsky et al., 2004; Reilinger et al., 2006; Gomez et al., 2007; Le Beon et al., 2008; Alchalbi et al., 2009).

The DSF crosses regions with abundant archeological sites that evidence records of direct (fault offsets) or indirect (damage to building) coseismic features. Previous studies of archeological sites from field investigations or textual documents revealed the occurrence of "earthquake storms" probably associated to the DSF (Nur and Cline, 2000). Indirect earthquake features are, however, very often problematic and unless dedicated to the specific study of known historical earthquake damage (Stiros and Jones, 1996; Marco, 2008), most of archeological reports can hardly provide usable earthquake parameters (Ambraseys, 2006). Recent studies that combine archeoseismic excavations and paleoseismic trenching provide some constraints of the left-lateral strike-slip movements and related past earthquake events. The Jordan Fault segment and related past earthquake ruptures offset the Vadum Jacob Crusader Castle and Holocene deposits visible in trenches at Beyt Zayda near the Sea of Galilee yielding 3 to 4 mm/yr. slip rate (Ellenblum et al., 1998; Marco et al., 2005). North of our study area, archeological sites are largely spread in the Amik Basin where the fault crosses the ~5000 BC Tell Sicantarla and reveals 42.4 ±1.5 m cumulative left-lateral movement thus yielding 6.0 ±0.2 mm/yr slip rate (Altunel et al., 2009).

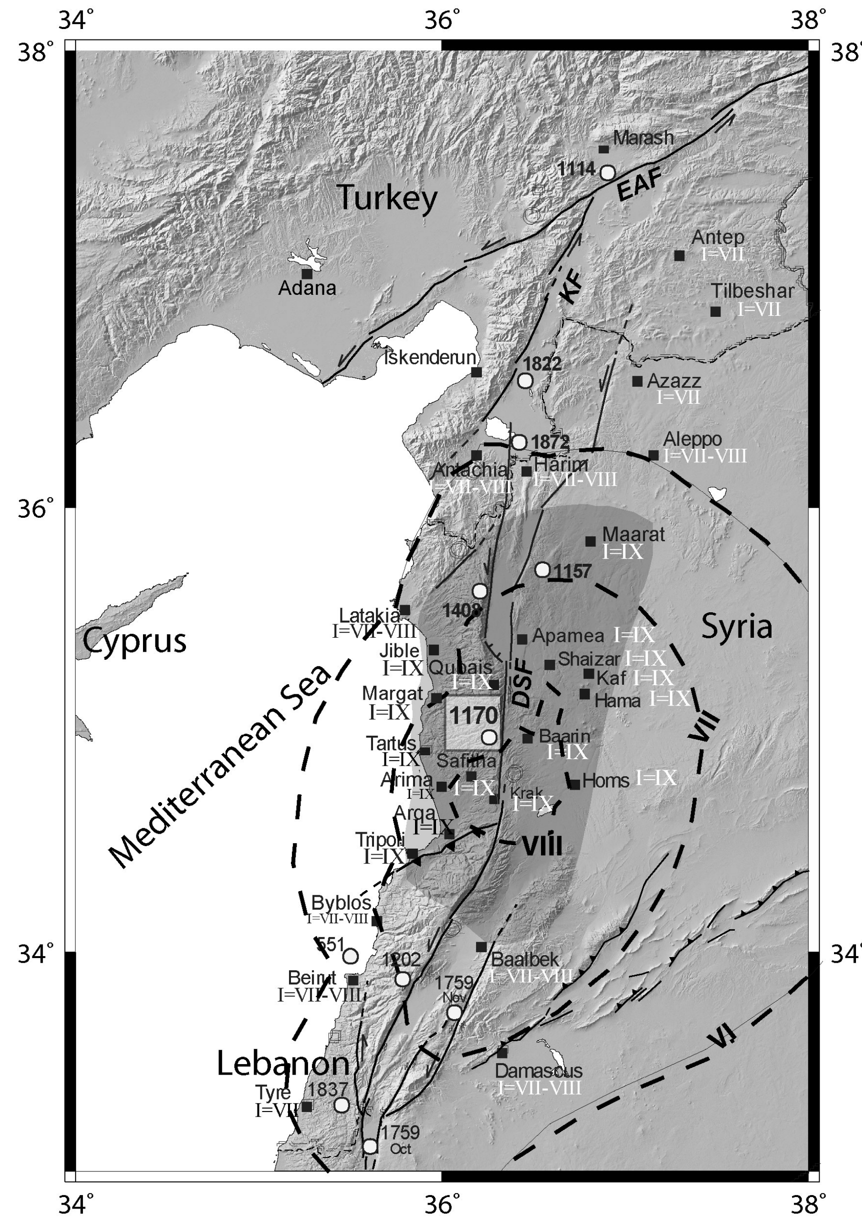

Figure 2: Major historical earthquakes (white dots) and areas of maximum damage (shaded) for the 29 June 1170 earthquake (Io=IX using EMS98 intensity definition of Grunthal, 1998) as recorded along the northern Dead Sea Fault (local intensities are from Guidoboni, 2004 and Sbeinati et al., 2005). The shaded area of maximum damage (Io = IX) for the AD 1170 large earthquake is along the Missyaf fault segment and Ghab Basin (see also Figures 1b and 3 for legend) and overlaps with the maximum intensity VIII (MSK, black dashed line) as drawn by Ambraseys (2009).

Previous archeo-paleoseismic work on the faulted Al Harif Roman aqueduct revealed 13.6 m left-lateral offset and 6.9 ±0.1 mm/yr slip rate that result from at least 3 earthquakes (Meghraoui et al., 2003). The early aqueduct study and trench A shed light on the relationships between the Roman building and repeated faulting events but left open questions on: 1) The earthquake events scenarios and related rebuild and repair of the aqueduct after each coseismic slip; 2) the estimated long term averaged slip-rate versus a temporal cluster of seismic events over the last 2000 years and its comparison to the present-day geodetic rate; 3) the constraint of the ~ 800-years-long temporal and spatial seismic gap on the Missyaf segment and the recurrence interval of large earthquakes along the northern DSF. In addition of the paleoseismic trenching and archeoseismic excavations, the tufa accumulation since the aqueduct building may constitute a real archive of the aqueduct history that records the successive earthquake damages. Our study infers that the aqueduct remains, the related tufa deposits and faulted Holocene sedimentary units contain comparable records of the most recent surface rupturing events along the Missyaf fault segment.

In this paper, we present the study of the faulted Al Harif Aqueduct site using archeological excavations, paleoseismic trenching across the fault zone coupled with total station surveys and the coring of tufa accumulation on the aqueduct walls. We first describe the geomorphologic features and clear late Quaternary active tectonics of the fault zone that belongs to the Missyaf segment of the DSF. Archeological excavations of the aqueduct walls and bridge combined with 3 trenches dug across the nearby fault zone and related radiocarbon dating illustrate the timing of successive faulting episodes. The dated onset, major discontinuities and interruptions of tufa cores are correlated to the faulting events. The analysis and interpretations of earthquake damage with probable rebuilding phase of aqueduct wall and coseismic ruptures constrain the timing of successive faulting events. The Holocene faulting activity and related seismic cycle of the Missyaf Fault segment reveal the long term seismic strain release and hence determine the potential for a future large earthquake along the DSF.

2- ACTIVE FAULTING AND SEISMOTECTONIC SETTING OF THE MISSYAF SEGMENT

The Missyaf fault segment (MFS) is a section of the northern DSF located in the western coastal part of Syria (Figures 1 b, 2 and 3). The ~200-km-long northern DSF is made of: 1) a 90 ±10 km-long linear fault zone, i.e., the Missyaf segment limited by the Al Boqueaa and the Lebanese restraining bend to the south and the Ghab pull-apart basin to the north, and 2) the ~ 10-km-wide Ghab pull-apart basin and related fault accompanied in its northern termination by a complex system of fault branches when reaching the Amik Basin and Karasu Valley in Turkey (Figures 2 and 3).

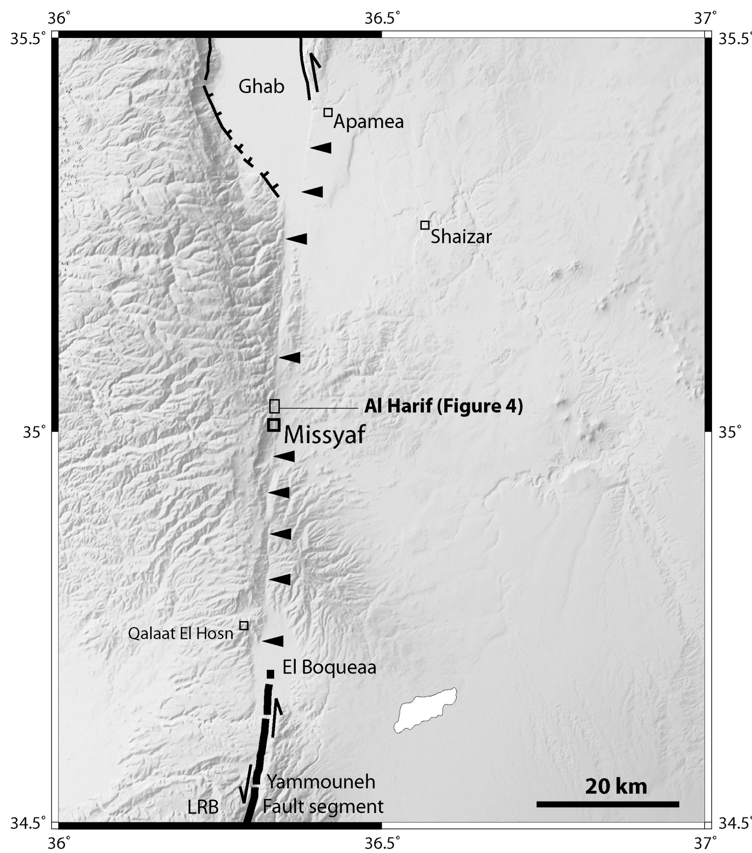

Figure 3: The 80-km-long Missyaf fault segment and the Al Harif Roman Aqueduct site. The background topography (SRTM 30 arc-sec posting digital elevation model; Farr and Kobrick, 2000) clearly delineates the fault segment (arrowheads) in between the Ghab and Al Boqueaa pull-apart basins. The Roman aqueduct at Al Harif (see also Figure 4)

was designed to bring fresh water from western ranges to Apamea and Shaizar. LRB is for Lebanese Restraining Bend.

The MFS has a nearly north-south linear trend that limits the coastal ranges to the west from the Mesozoïc-Cenozoïc plateau to the east (Figure 3). Near Al Boqueaa Basin, the fault affects the Neogene basaltic formation of the Sheen Mountains. Further north, the fault crosses the Neogene volcanic and sedimentary formations and shows ~ 10 to 50-m-wide gouge zone, breccias and rupture planes that affect the Mesozoic limestone of the coastal ranges. From Missyaf city to the Ghab Basin area, the fault limits the Mesozoic limestone mountain range to the west from the Quaternary basins and Mesozoic-Cenozoic Aleppo plateau to the east (Dubertret, 1955).

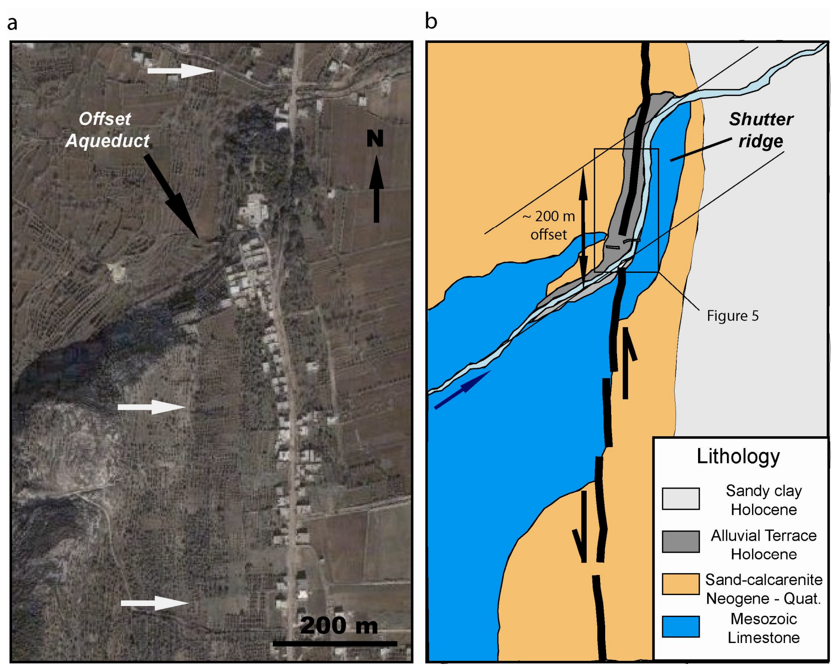

Figure 4: a) Satellite view from Google Earth showing offset Al Harif Aqueduct (black arrow) along the DSF (white arrows); b) local geomorphologic framework of the aqueduct site as interpreted from Figure 4a indicating a shutter ridge (Mesozoic limestone east of the fault) and ~ 200 m of left-lateral offset. Blue arrow is for stream flow. See Figure 5 for the detailed aqueduct map and location of excavations and trenches.

The left-lateral fault exhibits a clear geomorphologic expression along strike with neotectonic features consistent with the structural characteristics of the Al Bouqueaa and Ghab pull-apart basins (Figure 3). The left-lateral movements are indicated by the en-echelon right stepping fault strand, faulted alluvial fans, deflected large and small streams that flow from the western mountain range and shutter ridges made of either volcanic or limestone units (Figures 3 and 4). The left-lateral slip is also expressed in outcrops where fault breccias in limestones also display en-echelon structures. Estimated from main channel deflections, observed in aerial photographs or satellite images or measured using total station, systematic left-lateral offsets visible at different scales range from as low as 9 ± 1 m along strike to a few hundred meters (Figures 3 and 4).

The instrumental seismicity along the MFS is scarce in comparison with that of the Lebanese restraining bend to the south or the Karasu Valley and junction with the East Anatolian fault to the north (Figures 1 a and b). Although the fault zone corresponds to the Africa-Arabia plate boundary, the instrumental seismicity is low-level and magnitudes (M_l) are less than 4.5. Focal mechanisms (CMT Harvard) of the few events with Mw > 4.5 in the northern DSF show strike slip faulting with predominant north-south trending left-lateral fault plane mixed with normal faulting solutions near the pull-apart basins.

The historical seismicity along the northern DSF reports the occurrence of large and destructive earthquakes in BC 1365, AD 115, 526, 859, 1063, 1139, 1156, 1170 and 1408 (Ambraseys and Melville, 1988a; Guidoboni et al., 2004 a and b; Sbeinati et al., 2005). Only a few historical contemporaneous manuscripts, however, account for accurate damage distribution and sometimes for coseismic surface breaks with enough details that allow the correlation with fault segments (Ambraseys and Melville, 1988b). Most contemporaneous manuscripts and inscriptions from Byzantine, Crusader and Arabic sources provide accurate damage descriptions of castles, churches and mosques, villages and cities often accompanied with an estimate of casualties. Based on our work on the catalogue of historical earthquakes of Syria and paleo-archeoseismic investigations (Mouty and Sbeinati, 1988; Meghraoui et al., 2003; Sbeinati et al., 2005) we have shown that the damage distribution associated with the 29 June 1170 earthquake suggests a correlation with the MFS. Using numerous historical documents that report the 1170 earthquake damage, Guidoboni et al. (2004 b) provide a comparable damage distribution and suggest an epicentral location on the Missyaf fault. However, overestimated damages at Aleppo (from misinterpretations of the Arabic chronicler Ibn Al Athir [1160-1233]) and poorly constrained seismotectonics inferences brought the authors to the erroneous conclusion that the 90 ±10 km-long MFS alone could not generate the Mw 1170 seismic event (Guidoboni et al., 2004b). Zones of maximum damage should be identified primarily from contemporary eyewitness accounts in manuscripts, corroborated by present-day field investigations on the active fault and damage of ancient buildings. Furthermore, the geometrical structures (i.e., the Al Boqueaa pull apart and Lebanese restraining bend to the south and the Ghab pull apart to the north) that limit the fault segment are major obstacles to a coseismic rupture propagation and hence, constrain the earthquake fault dimension.

3- ARCHEOSEISMOLOGY AND PALEOSEISMOLOGY

3. 1. Site description

The Al-Harif Aqueduct is located ~ 4 km north of the city of Missyaf, immediately west of a limestone shutter ridge and related ~200 m left-lateral stream deflection (Figures 3 and 4). According to the remaining aqueduct walls and related mills in the region, the aqueduct was built during the Roman time (younger than BC 65 in the Middle East) to drain fresh water collected from springs of the western mountain range to the eastern semi-arid plains. The remaining ruins of the aqueduct suggest a ~ 40-km-long building that may have included several bridges over streams and landscape gorges.

The aqueduct building description and related age has not been reported so far in any archive, manuscript or in the literature. It has, however, an interesting anecdotal story from the local tradition that it has been built by a local prince to supply potable water to Apamea and/or Sheizar cities located northeast of the aqueduct (Figure 3). Apamea during that time was the most famous and strategic city during the Hellenistic & Roman period, whereas Sheizar is known as an important political and military fortress during the Middle age (Ibn Al Athir, 1982).

In their description of the DSF in Syria, Trifonov et al. (1991) mentioned the existence of a faulted aqueduct near the city of Missyaf but neither the precise location nor the accurate amount of offset walls were given. However, this early tectonic observation was helpful and allowed us to discover the site and consider a detailed study (Meghraoui et al., 2003) which is extended here using combined methods in archeoseismology, paleoseismology and tufa investigations. In addition, a microtopographic survey of measurements accompanied all field studies (Figure 5).

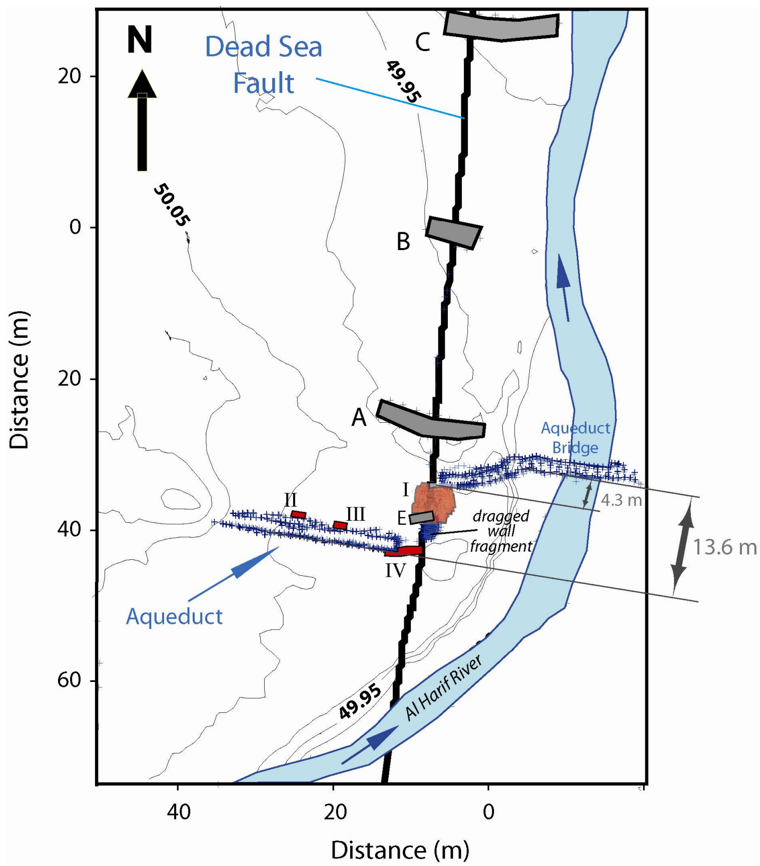

Figure 5: Microtopographic survey (0.05 m contour lines) of the Al-Harif Aqueduct and related flat alluvial terrace. The aqueduct (thin blue crosses) shows a total 13.6 ±0.20 m of left-lateral slip along the fault zone (Meghraoui et al., 2003). Roman numbers indicate archeseismic excavations (in reddish and orange labeled I to IV) and letters indicate paleoseismic trenches (in grey and black labeled A, B, C and E). The dragged wall fragment is located between excavation IV and trench E and is marked by a dense cluster of survey points.

Previous investigations on the aqueduct (Meghraoui et al., 2003) established: 1) an evaluation of its age based on an account of the large size blocks, the dating of sedimentary units below the aqueduct wall foundation and dating of early tufa deposits on the aqueduct wall, and 2) the identification of the seismic faulting origin of damage in nearby trench A. The building style with typical bridge arch and large stone size disposition (*Opus caementum*) suggested a Roman age which was confirmed by the radiocarbon dating of sedimentary layers below the walls and the early tufa deposits on the walls. The faulted aqueduct revealed 13.6 ±0.20 m of total left-lateral offset and called for detailed investigations on the characteristics and history of the successive fault movements.

The aqueduct design with an open canal on top of the 4-m-high wall allowed fresh and carbonate saturated water to overflow and induce an important tufa accumulation from 0.30 m to 0.83 m in section (Figures 6 a and b, Figure 7). The carbonate-rich and cool water collected from the nearby western range is associated to a semi-arid and karstic area of the Mesozoic limestone (Figure 4) that favors fast carbonate precipitation and tufa accumulation. The Tufa deposits show successive growths of lamination carbonate with high porosity, banded texture and rich organic encrustations (Ford and Pedley, 1996). Field observations show that tufa accumulation developed on both eastern and western sections (from the fault line) but only on the north facing wall likely due to a slight tilt of the damaged aqueduct wall probably after the two first earthquakes (Figure 7).

The following paragraphs present the field investigations that consisted in: 1) four archeoseismic excavations near the aqueduct walls and remains, 2) four paleoseismic trenches across the fault zone and the alluvial sediments, and 3) four cores of tufa deposits collected from different sections of the aqueduct. More than 200 samples of organic matter, charcoal fragments and tufa core pieces were taken for radiocarbon analysis in order to characterize the timing of successive faulting and related damage of the aqueduct building. All radiocarbon dating are calibrated (2σ range, 95.4% probability density) using Oxcal v4.0 (Bronk Ramsey, 2001) and INTCAL04 calibration curve of Reimer et al. (2004).

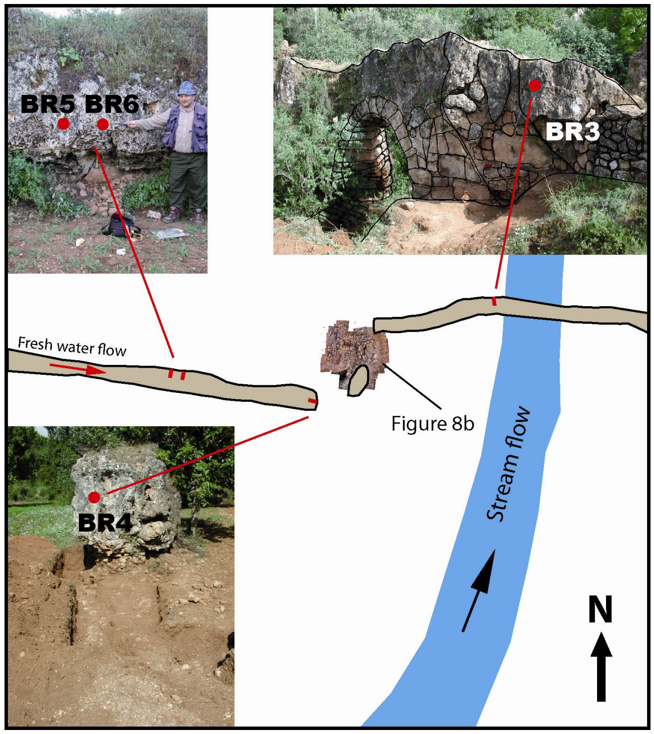

Figure 6 a) Schematic sketch of the aqueduct and locations of the selected cores BR3, 5 and 6; BR4 core sample consists in tufa accumulation at the location of the missing (broken) piece of the aqueduct wall near the fault. Mosaic of the archeological excavation I is detailed in Figure 8 b (see also location in Figure 5).

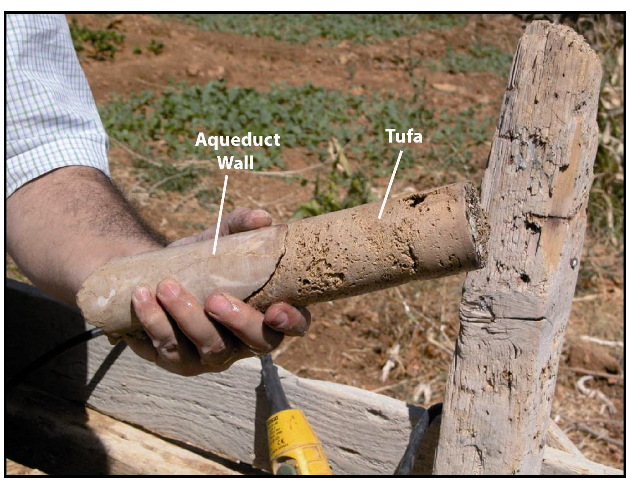

Figure 6 b) Core section BR4 showing the limit between the wall stone and tufa deposits.

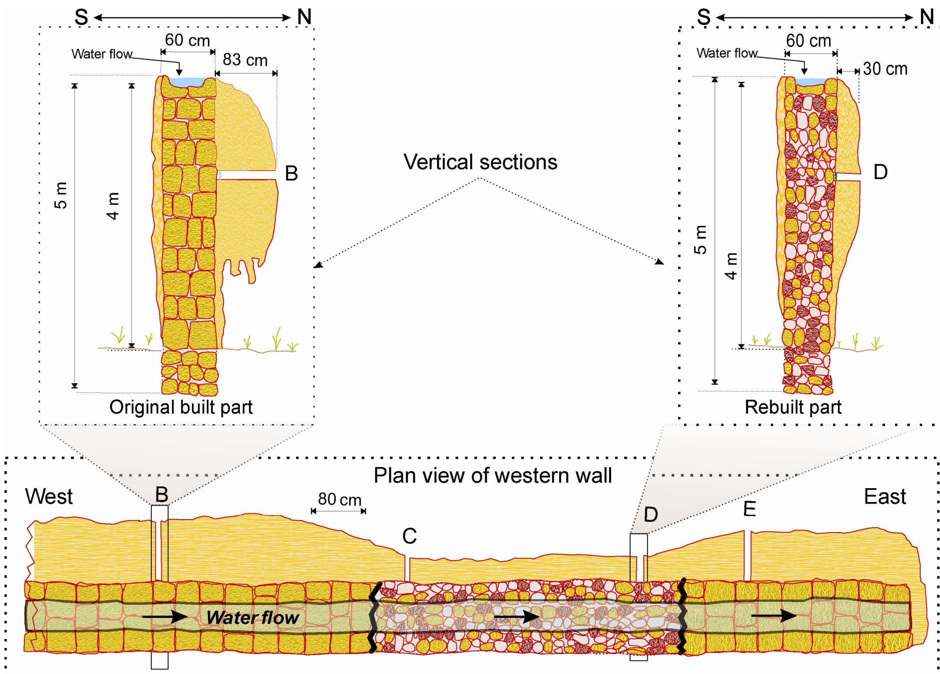

Figure 7: Schematic sections of the aqueduct western wall and related tufa deposits (B, C, D and E indicate earlier core sections of tufa deposits (Meghraoui et al., 2003). Tufa samples AQ-Tr B13 and AQ-Tr D5 (Table 1) are from cores B and D, respectively. The right and left vertical sections show the relative tufa thickness of the original built part (with Opus caementum and quadratum stones) and the rebuilt part, respectively. The plan view indicates the variation of tufa deposition and shows the cores distribution and related depths along the western wall of the aqueduct.

3. 2. Archeoseismic excavations

The remaining aqueduct building forms a ~ 50-m-long, ~ 5-m-high and 0.60-m-thick wall that includes a ~ 15-m-high arch bridge in its eastern section (Figures 5 and Figure 6 a). The outer part is coated by a thick layer of tufa deposits probably due to a long time standing fresh water flow. The construction material that may vary with the successive building and repair ages is made of: 1) large size limestone blocks (*Opus quadratum*, 1.0 m x 0.5 m x 0..5 m; see also http://www.romanaqueducst.info/aquasite/) similar to the typical Roman archeological constructions and visible at the lower bridge (pier section) and wall sections, 2) medium size limestone blocks (*Opus incertum*; 0.50 m x 0.30 m x 0.30 m) that form the foundation or the upper half wall section and show visible small portions of cement, and 3) small size of mixed stones of irregular shape with significant portions of mortar (cement) mostly visible in the apparently rebuilt part of the wall. Figures 5 and 6 a also show a detached small piece of the aqueduct wall made of small size stones and related cement at about 3.5 m away from the eastern wall. Therefore, four areas (noted I to IV in Figure 5) were excavated near the aqueduct using proper archeological methods.

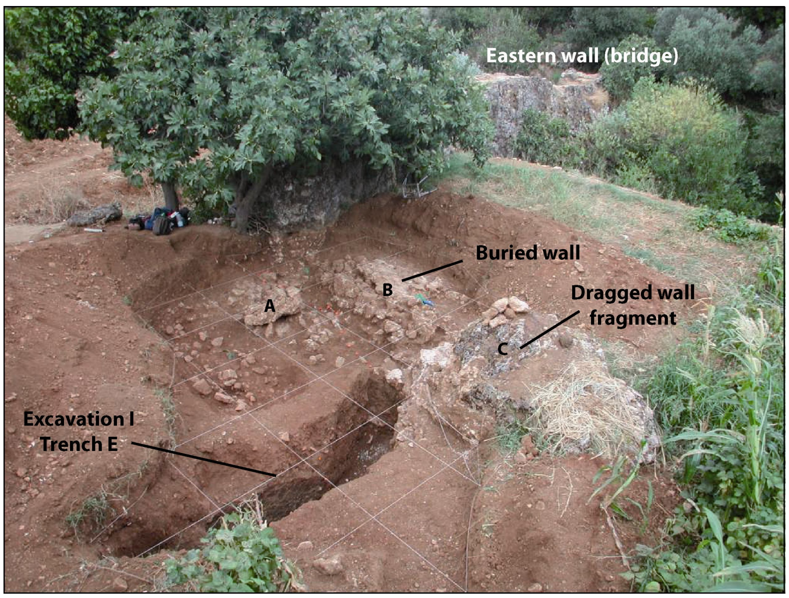

Figure 8 a) view of the fault zone from the western aqueduct wall, the dragged wall piece and eastern wall (string grid is 1 m x 1 m). Log of trench-excavation E is in Figure 7c (facing NE ditrection).

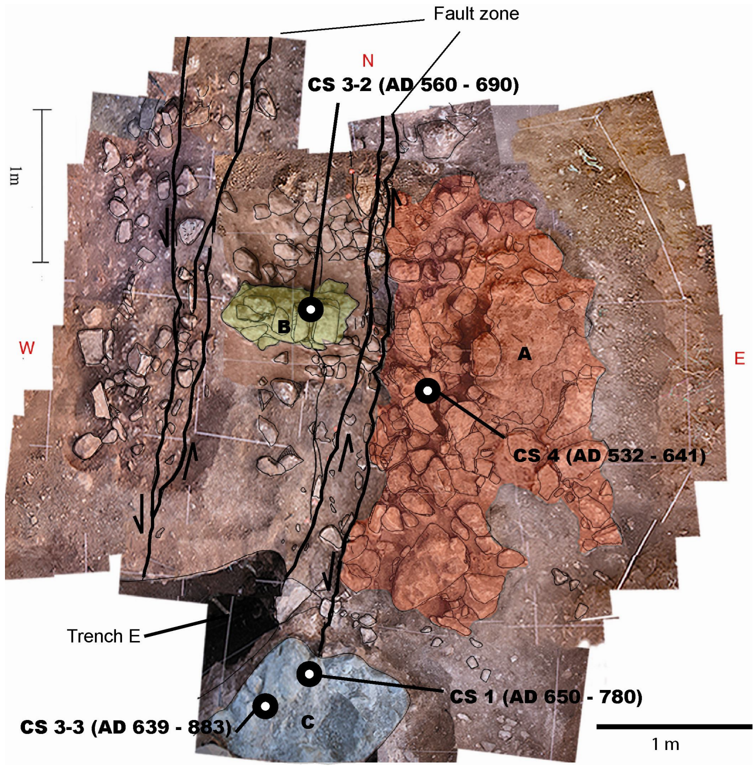

Figure 8 b) Oblique photo of mosaic of excavation I exhibits the main fallen wall (A and B) and dragged wall piece (C), scattered wall pieces and the fault zone; note also location of cement sample CS 1 to 4 (see text for explanation);

The large excavation I was dug on the fault zone near the dragged wall fragment, in the area between the eastern and western aqueduct walls (Figures 5 and 8 a and b). The purpose of excavation is here to study the relationships between the fault zone and aqueduct. The excavation that has ~ 4.5 x 4.5 m surface and ~ 0.6 m depth exposed missed parts of the aqueduct. A buried and fallen wall piece rotated and dragged parallel to the fault and a remaining wall piece in an oblique position between two shear zones were discovered. The buried wall fragments are not comparable to the *Opus caementum* (*quadratum*) of the original construction and suggest a rebuilding phase. The excavation floor displays oriented gravels and pebbles that mark the shear zones and related fault branches also visible in the inner trench section E (Figures 8 b and c).

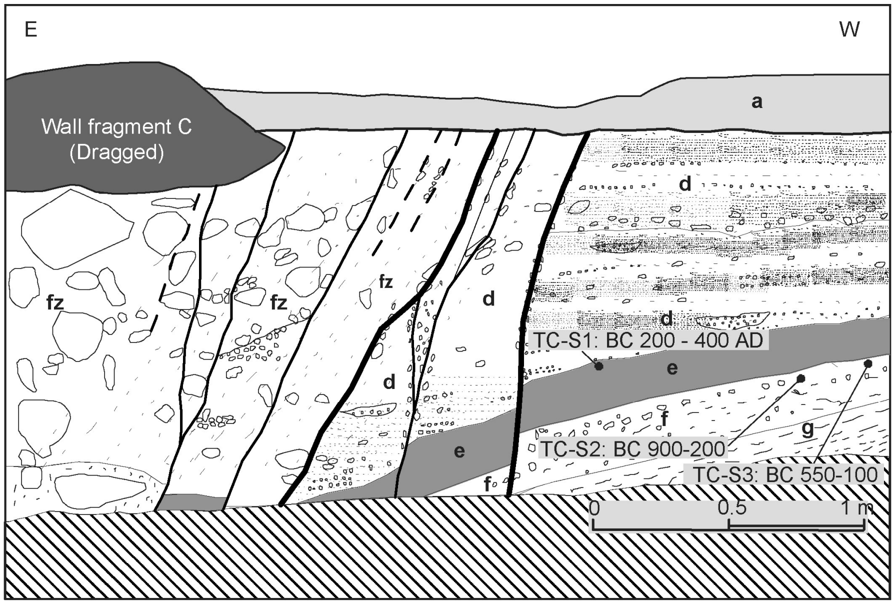

Figure 8 c) Trench E (excavation I, south wall) exposes faulted sedimentary units below the archeological remains and wall fragment C visible in bottom of Figure 7 b; fz is for fault zone, sedimentary units are similar to those of trenches A, B and C (see also Figure 9) and dating characteristics are in Table 1.

We collected four samples in the fallen wall sections labeled A, B and C of excavation I (Figure 8 b): Two cement samples (AQ – CS-1 and AQ-CS-4) found in between building stones are made of typical medieval rubble mortars (mainly mud, gypsum and lime); the two other samples (AQ-CS-2 and AQ-CS-3) are tufa deposits preserved on building stones. All four samples contain enough organic matter that allowed radiocarbon dating (Table 1). Two dating of cement yield AD 532 – 641 (section A, AQ - CS4) for the large fallen wall in excavation I and AD 650 - 780 (section C, AQ - CS-1) for the wall fragment piece in between the walls (Figure 8 b). In addition, two tufa deposits on wall stones provide consistent ages AD 560 – 690 (section B, AQ - CS3-2) and AD 639 – 883 (section C, AQ - CS3-3) with cement ages. The two different cement dating of the fallen wall and dragged wall fragment can be correlated to the new tufa deposits that testify for two rebuilding phases. The dated buried fallen wall in section B (CS3-2) obtained from a thin (~ 5 cm) tufa accumulation correlates with the similarly fallen wall in section A and related cement date of CS-4 (Figure 8 b and Table 1). In section C, the tufa deposits and related dated sample CS3-3 correlate with cement age of CS-1. The type and size of stones (opus incertum) and thin tufa accumulation in sections A and B suggest an early rebuilding phase postdating the 1st damaging event that may have occurred between the 1st and 6th century AD. The different building layout of section C made of small size of mixed stones of irregular shape, and dating of cement sample CS-1 (AD 650 – 780) and tufa accumulation CS3-3 (AD 639 – 883) indicate a repairing and rebuilding period postdating a 2nd damaging event at the end of the Byzantine time and beginning of the Islamic period (7th to 8th century AD). The damaged and dragged most recent wall section C along the fault indicates the occurrence of a 3rd event after which the aqueduct was definitely abandoned.

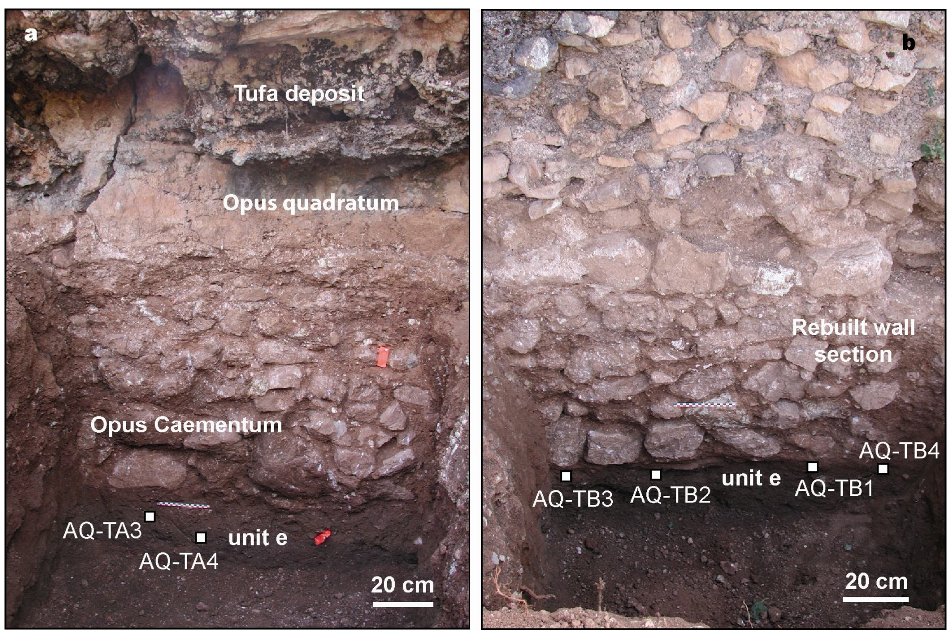

Figure 9: Excavations II (a) and III (b) that expose the aqueduct wall foundation (see also Figure 5) and related sedimentary units e underneath. The difference in the size of stones (e.g., Opus quadratum and caementum) between excavation II (a) and excavation III (b) implies a rebuilding phase of the latter wall (facing S direction).

Three small excavations II, III and IV (1.5 m to 3.0-m-long, 1.0-m-wide and 1.50-m-deep) were dug in the base layer of the western aqueduct wall in order to expose its foundation and related underneath sedimentary units that predate the early building phase

(Figures 5 and 9). Excavations II and III were dug under the wall section with maximum (> 0.80 m) and minimum (~ 0.30 m) thickness of tufa deposition, respectively (Figures 9 a and b). Excavation IV already described in Meghraoui et al. (2003) exposed the faulted foundation of the missing section of western wall edge. The wall foundation reaches 1 m depth and shows regular patterns of medium size cut limestone blocks (0.50 m x 0.30 m x 0.30 m) built over a dark brown clayey layer (unit e).

Charcoal samples collected in excavations I (trench E) II and III from unit e yield C^{14} dating with an age spanning ~ 3 centuries BC to 3 centuries AD (see samples AQ-TA, TB and TC in Table 1, and Figure 8 c and Figures 9 a and b). Although in these excavations the age range of unit e seems quite large (probably due to charcoal mixing), the younger age that is here 350 BC to 130 AD (sample AQ-TA-4) is consistent with other radiocarbon ages of unit e and related stratigraphic succession in trenches (see section 3.3 herein). In excavation II, the large stone shape (*Opus quadratum*) with small amount of cementing material and pottery fragments found on the same level near the building base can be correlated with the early Roman era (Figure 9 a). Large stones and tufa thickness led us to consider this section of the aqueduct wall in original condition i.e., probably undamaged by large earthquakes.

Excavation III (1.65-m-long, 1.0-m-wide and 1.2- m-deep; Figure 9 b) is similar to excavations II and IV but the 1-m-deep wall foundation and upper section show irregular shapes of mixed medium and small size cut limestone blocks (0.10 x 0.20 x 0.15). Excavation III was realized at the location of the thinnest tufa deposits (< 0.30 m). The size of stones, cement texture and irregular shape of building wall suggest that this building section was rebuilt (Figure 9 b). C^{14} dating of unit e below the wall yield comparable age range obtained in excavations II (see AQ-TA, TB and TC in Table 1).

Sample ID	Sample Name	Fraction	Trench- Excav. Unit & Core level	Analysed carbon (mg)	Carbon content %)	^{14}C Date (years BP)	^{14}C Age Calibrated BC/AD (95.4 %)
Al Harif - Trenches							
KIA 14261	BAL TA N23	Charcoal, Alkali Residue	b & c (A)	5.87	71.9%	1015 ± 35	AD 960 – 1060
KIA 14263	BAL TA N27	Charcoal, Alkali Residue	f (A)	4.09	67.4%	2335 ± 30	BC 520 - 350
KIA 14262	BAL TA N25	Charcoal, Alkali Residue	e (A)	0.42	24.9%	2090 ± 50	BC 350 – 30 AD
AA 43995	EH I – S7	Charcoal, Alkali Residue	e (A)	-	-	2195 ± 40	BC 390 - 160
AA 43993	EH I - TA S33	Charcoal, Alkali Residue	d (A)	4.33	-	1287 ± 36	AD 650 - 810
KIA 14264	BAL TA N31	Charcoal, Alkali Residue	a (A)	1.95	63.3%	875 ± 35	AD 1030 - 1250
KIA 14268	BAL TN 61	Charcoal, Alkali Residue	a (A)	1.02	1.0%	4555 ± 40	BC 3490 - 3090
KIA 14265	BAL TA N47	Charcoal, Alkali Residue	g (A)	1.71	3.6%	7410 ± 45	BC 6400 - 6100
KIA 23856	AQ TA 3	Charcoal, Alkali Residue	e (II)	1.83	22.6%	2295 ± 30	BC 410 -210
KIA 23855	AQ TA 4	Charcoal, Alkali Residue	e (II)	0.24	4.7%	2050 ± 70	BC 350 – 130 AD
KIA 23861	AQ TB1	Charcoal, Alkali Residue	e (III)	1.77	22.4%	2250 ± 30	BC 400 - 200
KIA 23862	AQ TB2	Charcoal, Alkali Residue	e (III)	1.64	25.9%	2200 ± 40	BC 390 - 160
KIA 23863	AQ TB3	Charcoal, Alkali Residue	e (III)	4.23	49.8%	2235 ± 30	BC 390 - 200
KIA 23857	AQ TB4	Charcoal, Alkali Residue	e (III)	0.38	4.0%	2460 ± 60	BC 770 - 400
KIA 23858	AQ TC S1	Charcoal, Alkali Residue	e (I - E)	0.17	2.1%	1930 ± 110	BC 200 – 400 AD
KIA 23859	AQ TC S2	Charcoal, Alkali Residue	f (I - E)	0.13	1.6%	2450 ± 140	BC 900 - 200
KIA 23860	AQ TC S3	Charcoal, Alkali Residue	f (I - E)	0.28	9.5%	2280 ± 70	BC 550 - 100
KIA 23903	EH II 7S	Charcoal, Acid Residue	a (C)	0.49	128.9%	290 ± 40	AD 1480 - 1800
KIA 23880	EH II 2 N	Charcoal, Alkali Residue	a (C)	4.16	50.7%	280 ± 25	AD 1510 - 1670
KIA 23917	EH II 16 S	Charcoal, Alkali Residue	b1 (C)	5.62	69.0%	1465 ± 30	AD 540 - 650
KIA 23911	EH II 11 S	Charcoal, Acid Residue	f (C)	2.11	51.7%	2135 ± 30	BC 360 - 50
KIA 23915	EH II 10 S	Charcoal, Alkali Residue	f (C)	1.54	57.5%	2150 ± 30	BC 360 - 60
KIA 23910	EH II 12 S	Charcoal, Alkali Residue	f (C)	4.66	62.3%	2160 ± 30	BC 360 - 90
KIA 23920	EH II 18 S	Charcoal, Acid Residue	f (C)	0.97	9.3%	2525 ± 40	BC 800 - 510
KIA 23909	EH II 5 S	Seed, Alkali Residue	f (C)	0.03	4.5%	3420 ±570	BC 3400 - 300
KIA 23895	EH III 8 S	Charcoal, Acid Residue	e (B)	2.40	38.4%	2110 ± 35	BC 350 - 40
KIA 23896	EH III 7 S	Charcoal, Acid Residue	e (B)	1.19	45.2%	2215 ± 35	BC 410 - 90
KIA 23897	EH III 6 S	Charcoal, Acid Residue	Fault zone (B)	0.24	6.3%	2390 ± 80	BC 800 - 200
KIA 23900	EH III 3 S	Charcoal, Acid Residue	Fault zone (B)	1.05	64.0%	4375 ± 40	BC 3100 - 2980
KIA 23893	EH III 10 S	Charcoal, Alkali Residue	d? (B)	0.12	5.5%	2680 ± 170	BC 1300 - 350

Sample ID	Sample Name	Fraction	Trench- Excav. Unit & Core level	Analysed carbon (mg)	Carbon content %)	^{14}C Date (years BP)	^{14}C Age Calibrated BC/AD (95.4 %)
Al Harif – Cores & cement							
KIA 16627	AQ - Tr D5	Tufa, Acid Residue	D, 0 – 5 cm	1.13	80.1%	1863 ± 29	AD 80 - 240
KIA 16628	AQ - Tr B13	Tufa, Acid Residue	B, 0 – 5 cm	2.39	2.7%	2030 ± 25	BC 110 – 60 AD
KIA 16628	AQ - Tr B13	Tufa, Humic Acids	B, 0 – 5 cm	3.72	41.3%	1880 ± 25	AD 70 - 230
KIA 22189	AQ - CS 1	Cement, Alkali Residue	I - Wall piece	0.50	0.4%	1314 ± 37	AD 650 - 780
KIA 22191	AQ - CS 3-2	Tufa, Alkali Residue	I – Fallen wall	0.99	2.9%	1400 ± 35	AD 560 - 690
KIA 22191	AQ - CS 3-3	Tufa, Alkali Residue	I – Fallen wall	0.57	1.9%	1283 ± 44	AD 639 - 883
KIA 22192	AQ - CS 4	Cement, Alkali Residue	I - Fallen wall	5.33	0.3%	1497 ± 24	AD 532 - 641
KIA 26056	BR-3-1/SYR Al Harif	Tufa, Alkali Residue	3-1, 0-0.5 cm	0.53	17.3%	1570 ± 35	AD 410 - 600
KIA 26056	BR-3-4/SYR Al Harif	Tufa, Alkali Residue	3-4, 32.5-33 cm	2.28	2.3%	1180 ± 20	AD 770 - 940
KIA 26057	BR-4-1/SYR Al Harif	Tufa, Alkali Residue	4-1, 10.5-11 cm	0.71	6.7%	1465 ± 35	AD 530 - 660
KIA 26057	BR-4-3/SYR Al Harif	Tufa, Alkali Residue	4-3, 23.5-24.5 cm	0.14	22.6%	1310 ± 110	AD 540 - 980
KIA 26058	BR-5-2/SYR Al Harif	Tufa, Alkali Residue	5-2, 4.5 - 5.0 cm	0.51	1.7%	1995 ± 45	BC 110 – 130 AD
KIA 26058	BR-5-7/SYR Al Harif	Tufa, Humic Acids	5-7, 32 - 33.5 cm	3.44	40.5%	1090 ± 25	AD 890 - 1020
KIA 26059	BR-6-1/SYR Al Harif	Tufa, Alkali Residue	6-1, 0 - 0.5 cm	0.15	1.1%	2020 ± 110	BC 400 – 250 AD
KIA 26059	BR-6-8/SYR Al Harif	Tufa, Alkali Residue	6-8, 38 - 39 cm	0.58	1.2%	1020 ± 35	AD 900 – 1160

Table 1: Sample list and radiocarbon dating (AMS) at the Al Harif aqueduct site. All samples have been calibrated using the Oxcal program v3.5 (Bronk-Ramsey, 2001) and calibration curve INTCAL04 (Reimer et al., 2004) and adopted age ranges are equivalent to calibrated 2σ ranges (94.5%), in AD and BC. Trench and excavation units are marked in parenthesis from trenches A, B and C and excavations I, I-E, II and III. Location of cores B and D is in Figure 7.

Trench section E (4.30-m-long, 0.70-m-wide and 1.30-m-deep, Figures 5 and 8 a, b and c) was dug within excavation I in order to see in section the fault zone that affects the archeological floor units. The trench wall exposes similar sedimentary units visible in excavations II, III and IV, and affected by two main fault branches of the shear zone visible in the floor layer of excavation I. C^{14} dating of samples AQ-TC-S1, S2 and S3 of units f and e indicate 900 BC - 400 AD maximum and minimum age range, respectively, (Figure 8 c and Table 1) comparable to the age range obtained in excavations II and III for unit e (Figures 9 a and b, Table 1). However, as here again the large age range can be due to charcoal mixing, the dating of unit e is obtained by comparison to the dated stratigraphic succession of units in trenches (see section 3.3).

3. 3. Paleoseismic trenches

Two trenches B, and C (Figure 5 and Figures 10, trenches B and C) were dug across the DSF north of the aqueduct in addition of the previously studied trench A (Figure 10 A; Meghraoui et al., 2003). The two trenches exposed a ~ 1.5-m-wide fault zone that affects a succession of 2 to 3-m-thick fine and coarse alluvial sedimentary layers similar to the alluvial deposits of trench A. Alluvial units visible in all trenches exhibit here similar textures, structures and colour, and correspond to the same layers that belong to the same alluvial terrace. Although the three trenches A, B and C may not expose a completed stratigraphic section, the comparison between sedimentary units, faulting events, archeoseismic observations and tufa accumulation limits the possibility of a missing earthquake event that affected the aqueduct.

In trench B (south wall), the fault zone shows three main fault branches (labelled I to IV in trenches of Figure 10) that affect sedimentary units g to d and form a negative flower structure. The central and western main branches III and IV are truncated by unit a that forms stratified 0.3 – 0.4-m-thick deposit of coarse gravels in a sandy matrix. The eastern fault branch II is buried below unit d made of well-sorted reddish fine gravels. Unit e, a 0.2 – 0.5-m-thick dark-brown silt-clay thickens towards east. Units f and g are made of scattered clasts in a massive clay matrix of dark brown and light brown color, respectively. Although intense warping and faulting is marked by contrasting color and texture of unit e, faulted sedimentary layers of this trench do not allow the identification of all faulting events. However, buried fault branch II and IV indicate a faulting event postdated by unit d (event X) while the other fault branches I and III show at least another faulting event (event Z) overlain by unit a. While clearly visible in other trench walls, event Y is here likely concealed by the complex fault branches truncated by unit a.

Trench C (Figure 10 C) exposes a stratigraphic succession affected by at least five main fault branches (labeled I to V in Figure 10 C). From trench bottom, fault branch I that affects unit g is overlain by unit f. A similar observation can be made for fault branch II that also affects all units below unit d. Furthermore, the trench-wall exposes a ~0.60-m-thick well-stratified, coarse and fine gravels above unit e and across the fault zone. Unit d thins significantly west of fault branch III and is overlapped by relatively thick coarse gravel units which display a mixed fine and coarse gravels between fault branches III and IV, and show a succession of well stratified alluvial units west of fault branch IV (Figure 10 C). Taking into account its alluvial origin made of well stratified fine and coarse gravels, and west of fault branch IV unit d is sub-divided into d1, d2, d3 and d4. Faulting movements at this site allows truncation of unit d1 (equivalent to d east of fault branch III) and sedimentation of units d2 to d4 (in a likely small pull-apart basin). Unit d3 consists in ~0.20-m-thick dark brown silt-sand overlain by unit d4 made of light-brown fine silt-sand. Below the plough zone a2, the well stratified unit a1 showing flat laying pebbles and gravels and intercalated fine gravels cover previous units and the fault zone.

Fault branches I to V in trench C indicate a negative flower structure that intersects a sedimentary sequence and reveal at least 4 faulting events (Figure 10 C): 1) Event W identified on fault branch I is older than BC 800-510 (EH II-18 S) of lowermost layers of unit f and younger than unit g dated with sample EH-II-5 S (BC 3400 – 300). 2) Next to fault branch II buried below unit d, the vertical offsets between unit e and units d and d1 across fault branch III, and the absence of unit e between fault branches III and IV, determines the faulting event X between unit e and unit d. Since unit d overlain an erosional surface of unit e, faulting event X may have formed a depression (i.e., a small pull-apart basin) that allowed the deposition of d1 to d4 next to a thick unit d east of fault branch III. The faulting event X is here predated by BC 360-90 (EH II-12S), BC 360-50 (EH II-11 S) and BC 360-60 (EH II-10 S) of uppermost layers of unit f (event X is postdated by sample EH I-TA-S33 of Trench A). 3) Faulting event Y can be identified at the westernmost fault branch V between unit d2 and unit d3. The dating of sample EH II – 16S in d3 postdate event X younger than AD 540 – 650 which we consider as a reliable age taking into account its high carbon content (event Y is predated by sample EH I-TA-S33 of Trench A). 4) Faulting event Z corresponds to the main fault branches III and IV overlain by the stratified unit a2 below the plough zone. Fault rupture IV affects unit d4 and indicates that the faulting event Z is older than radiocarbon age AD 1480-1800 (EH II-7S) and AD 1510-1670 (EH II-2N) of unit a2 and younger than unit d4.

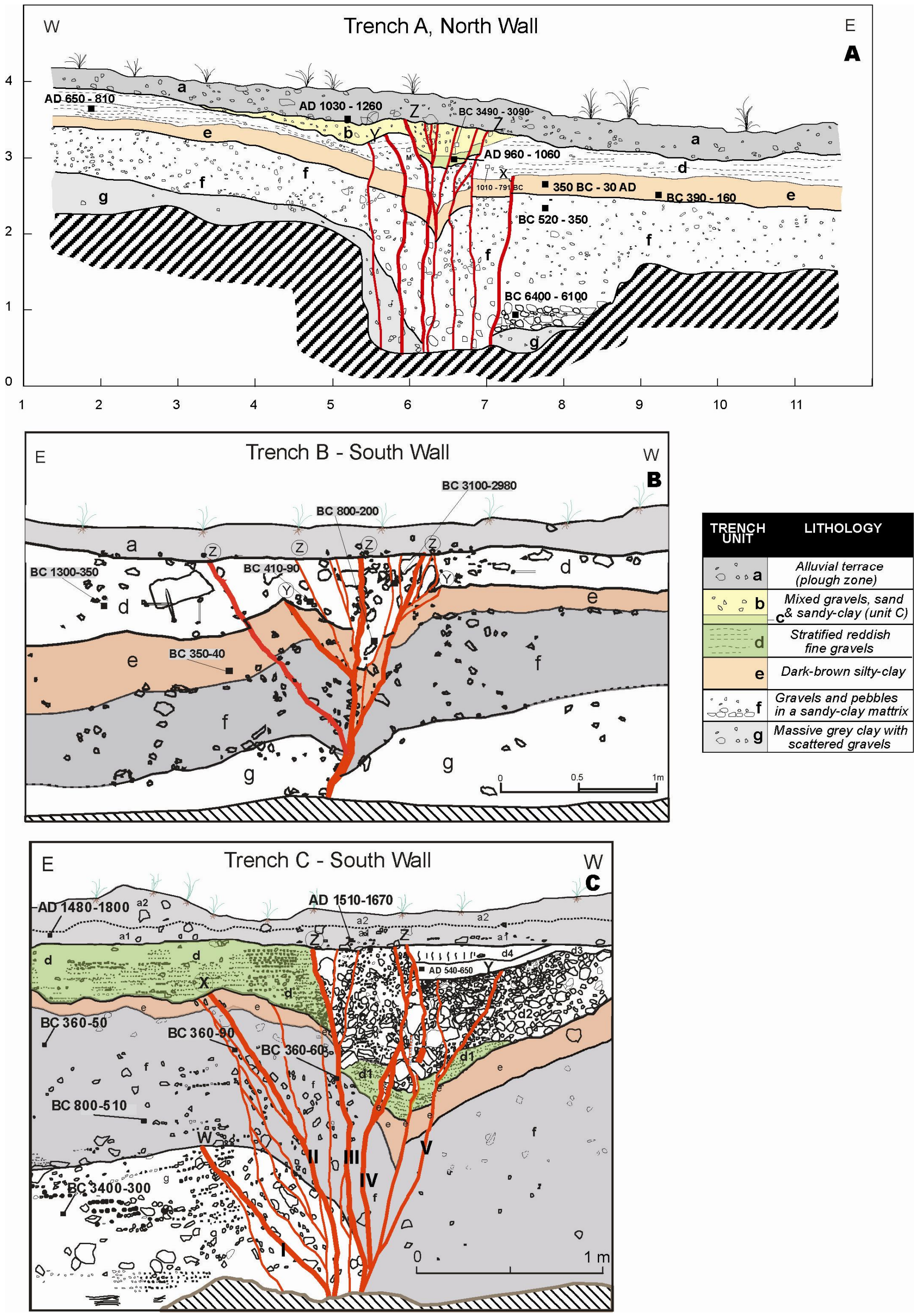

Figure 10: Trench logs A, B and C north of the aqueduct site (see location in Figure 5). All trenches display the Dead Sea fault zone as a negative flower structure affecting all alluvial units below unit a. Calibrated C^{14} dating are in Table 1. Fault branches in trench C are labeled I to V (see text for explanation). The sedimentary units are very comparable and show 3 to 4 faulting events denoted W to Z (see text for explanation).

3. 4. Summary of faulting events from archeoseismology and paleoseismology

The analysis of faulting events from the aqueduct (damage and rebuild) and from trenches A, B and C can be presented as following:

- Event W is older than unit f (i.e., BC 800 - 510) and younger than unit g (i.e., BC 3400 – 300) of trench C. The bracket of event W is here difficult to assess since the detrital charcoal sample in unit f was not taken from the base of unit f. According to C^{14} dates the faulting event can be estimated as younger than BC 3400 and older than BC 510. However, taking into account the rate of sedimentation in unit f, we may estimate a minimum BC 962 age for W.
- Event X, the first faulting event that affects the aqueduct is bracketed between the 1st and 6th century AD. In trenches, a large bracket of this event is between BC 350 – 30 AD and AD 650-810 (as obtained from dated units of trench A).
- Event Y characterized from paleoseismology appears to be older than AD 650-810 (unit d, Trench A) and younger than AD 540-650 (unit d3 in Trench C). The results of archeoseismic investigations indicate that dating CS-1 (AD 650 – 780) and tufa accumulation CS3-3 (AD 639 – 883) postdate event Y.
- Event Z is the last faulting event that affects the aqueduct after which it was definitely abandoned. In trenches A and C, event Z is younger than AD 1480-1800, AD 1510-1670 and AD 1030-1260 and older than AD 960-1060 .

4- TUFA OF THE AL-HARIF AQUEDUCT

The tufa thickness accumulated on the northern face of aqueduct wall suggests a continuous water flow during a relatively long period of time and may include the record of large earthquakes that affected the aqueduct. Hence, the relationships between tufa accumulation and earthquake events are established through the simultaneous major tufa interruptions and restarts observed in different cores. Except during major changes in the water flow conditions, the permanent water flow coming from the nearby spring was responsible of the tufa accumulation that, in principle, did not interrupt on the western wall section (with regards to the fault). On the eastern wall section (and bridge) and broken pieces of western wall, however, the tufa accumulation was likely episodic due to the earthquake damage and related faulting events; new tufa accumulation appears in subsequent building-repair. Previous radiocarbon dating of early tufa deposits (AD 70 – 230 and AD 80 – 240, Table 1) post-dated the initial construction of the aqueduct and revealed a Roman age consistent with the dates obtained from the archeological and paleoseismic investigations (Meghraoui et al., 2003).

Six tufa cores (named Tr B13, Tr D5 and BR 3, BR 4, BR 5 and BR 6) reaching the stone construction were collected from the aqueduct wall in order to date major catastrophic events and infer the relationship with large earthquakes (Figure 11). Tr B13 and Tr D5 were previously collected and analysed mainly to date the early tufa deposits which provide the maximum age of the aqueduct construction (Meghraoui et al., 2003). A subsequent selection of core location on both eastern and western sections of the aqueduct wall was performed to study the completed tufa accumulation and successive growth. Figure 6 shows the drilled wall location with the early cores Tr B13 and Tr D5 and 3 cores (BR 4, BR5 and BR 6) on the western wall and 1 core (BR 3) on the eastern wall next to the bridge. Cores BR 5 and BR 6 correspond to the thickest tufa section. BR 4 is on the eastern edge of the west aqueduct wall, a section probably exposed after an earthquake damage that induced the collapse of a 2.5 m-long wall-section next to the fault zone.

Each core is described to illustrate fabric (structure, texture and color), lamination changes, which provide evidence of tufa precipitation and successive growths (Figure 11). Although marked by a high porosity, the cores were carefully drilled in order to preserve their structure and length continuity. An analysis in progress of cores using computer tomography (CT) and climatic-stratigraphy correlation details the physico-chemical and biochemical processes of tufa growth (Grootes at al., 2006). The cores show a variety of porous, dense and biogenic tufa with growth laminae and stromatolitic markers of different colors. The location of end of tufa growth (i.e., very porous tufa in Figure 11) and onset of biogenic tufa (indicating only a seasonal growth) can be interpreted as episodes of decrease in accumulation, or a significant decrease in the chemical precipitation due a major change in the environmental conditions (Figure 11).

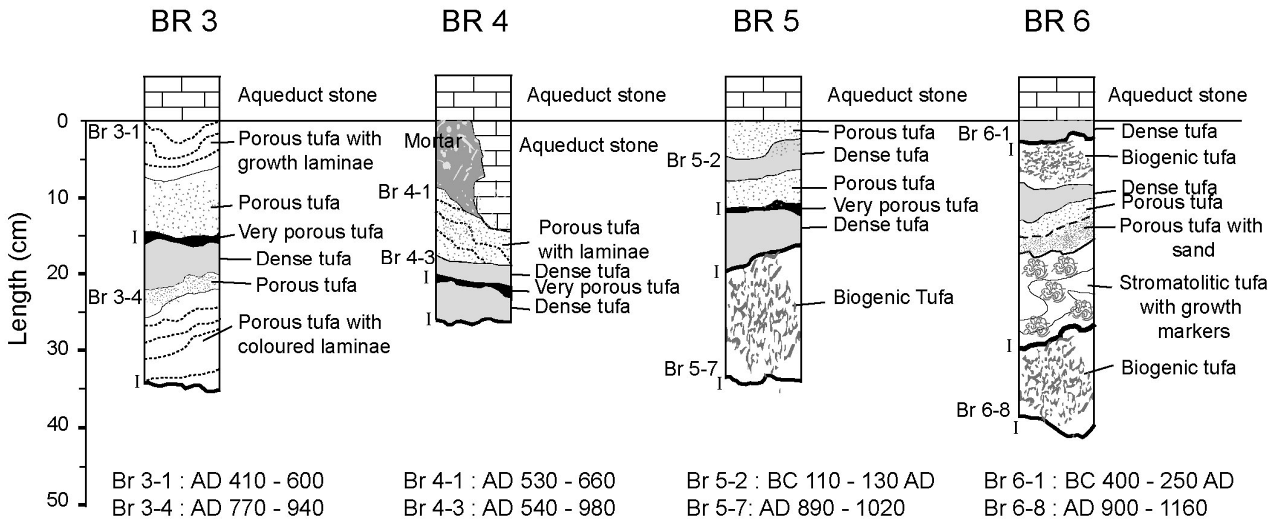

Figure 11: *Synthetic description of cores with lithologic content and sample number for radiocarbon dating (see Table 1 and Figure 6 for core locations); I stands for major interruption. The very porous tufa indicates major interruptions in tufa growth (e.g., a major interruption of core growth in BR3 is visible at about 22 cm (Br 3-4 sample; see text for explanation). The correlation between major interruptions of tufa growth and faulting events in trenches and archeoseismic building constrains the timing of repeated earthquakes along the Missyaf segment of the Dead Sea Fault.*

Discontinuities of tufa deposits marked by the interruption of core growths and initiation of biogenic tufa are interpreted as major changes in environment with a possible correlation with large earthquakes. The early tufa deposits (core B of Figure 11) on the aqueduct wall provide AD 70 – 230 and AD 80 - 240 (samples Tr B13 and Tr D5 in Table 1) which postdate the aqueduct building and early function (Meghraoui et al., 2003). The tufa accumulation in BR 3 (core in eastern wall near the bridge, Figure 6) started sometimes before AD 410 - 600 (sample Br 3-1, Table 1) and may result from a repair of the aqueduct with water overflowing the eastern wall (and bridge) after a major damaging event. Similarly, the location of a growth interruption (very porous tufa, Figure 11) in BR 5 at about 6 cm after Br 5-2 (BC 110-130 AD) and onset of biogenic tufa in

BR 6 after Br 6-1 (BC 400 – 250 AD) coincide with the occurrence of the first damaging event X. In parallel, the beginning of BR 4 with tufa accumulation at the damaged eastern edge of the western wall, (Figure 6) and sample Br 4-1 dated AD 530-660 (Figure 11 and Table 1) postdates the occurrence of a major damaging event. Both Br 3-1 and Br 4-1 postdate here the record of a major damaging event that affected the aqueduct. However, while BR 4 can accumulate only after a major damage, BR 3 deposits can accumulate only after the repair of aqueduct. It implies that the first major damaging event on the aqueduct took place between AD 70 – 230 and AD 410 – 600.

The interruption of tufa growth in BR 3 a few cm before sample Br 3-4 dated AD 770-940 results probably from a second damaging event. This observation coincides with the restart of BR 4 after a major interruption 3 to 4 cm after Br 4-3 dated and AD 540-980 (Figure 11 and Table 1). Furthermore, the sharp change (second interruption) from dense tufa to biogenic tufa in BR 5 and BR 6 may also be contemporaneous of the damaging event. The age of this second damaging event can be bracketed between Br 4-3 (AD 540-980) and Br 3-4 (AD 770-940). Unless simply broken, the definite interruption of BR 3 (about 10 cm after sample Br 3-4) marks the end of water overflow on the eastern aqueduct wall (and bridge)after the second damaging event.

The growth of dense tufa in BR 4 and biogenic tufa in BR 5 and BR 6 in final sections of cores indicate a continuous water flow on the western aqueduct wall after the second damaging event. The almost simultaneous arrest of tufa growth ~ 2 cm after Br 5-7 (AD 890-1020), ~ 1 cm after Br 6-8 (AD 900-1160) and ~ 7 cm after Br 4-3 (AD 540-980) suggest the occurrence of a major damaging event. Indeed, the arrest of tufa accumulation (in core samples Br 3-4, Br 5-7 and Br 6-8) occurred probably after A.D. 900 - 1160 years (Br 6-8, Table 1) and indicate the final stop of water flow over the aqueduct.

5- TIMING OF EARTHQUAKE FAULTING AND CORRELATION BETWEEN ARCHEOSEISMIC EXCAVATIONS, PALEOSEISMIC TRENCHES AND CORES

The analysis of field data in archeoseismology, paleoseismology and tufa coring provide some constraints on the successive past earthquakes along the DSF at the Al Harif Roman aqueduct site (Figures 12 and 13). The damage and repair of the aqueduct are here related to the total 13.6 m of left-lateral fault offset since the aqueduct building (Figure 5). In addition, the tufa successive growth and interruptions visible in cores provide a direct relation between the water flow and the aqueduct function east and west to the fault zone. The correlation and timing coincidence between the faulting events visible in trenches, aqueduct building damage and repair (see also section 3.4), combined with tufa growth and interruptions provide a better constraint on the timing of the successive large earthquakes:

- Event W observed in trench C occurred before BC 800-510 (unit f) and after BC 3400 – 300 (unit g). This faulting event can be determined only in trench C and hence cannot be correlated with damaging events in the aqueduct archeoseismic excavations and tufa cores. However, we suggest two possible ages for this event: i - according to the textual inscriptions found in different archeological sites in Syria, a damaging earthquake sequence around BC 1365 affected Ugharit near Latakia in Syria, and Tyre further south in Lebanon and east of the DSF (Sbeinati et al., 2005) may be correlated to event W; ii – the rate of sedimentation in unit f of trench C imply a minimum BC 962 for event W.
- Event X identified in trenches A and C between BC 350 – 30 AD and AD 532 – 641 postdates the aqueduct building (younger than 65 BC i.e., the onset of Roman time in the Middle East and older than AD 70 – 230 of early tufa deposits). Event X also predates the onset of BR 3 tufa growth (see Br 3-1 dated AD 410-600). Similarly, the tufa growth interruption in BR 5 (after Br 5-2 dated BC 110-130 AD) and onset of tufa in BR 6 (after Br 6-1 dated BC 400 – 250 AD) coincide with the occurrence of the first damaging event

X. The first earthquake faulting that damaged the aqueduct took place between AD 70 – 230 and AD 410 – 600.

- Event Y is younger than AD 650-810 (unit d in trench A) and older than AD 540-650 (unit d3 in trench C). This event postdates the first rebuilding phase of the aqueduct recognized from the fallen wall in excavation I and related cement sample AQ - CS4 (AD 532 – 641) and tufa sample AQ - CS3-2 (AD 560 – 690). Event Y predates the dragged wall fragment and related cement sample AQ-CS1 (AD 650 – 780) and tufa sample AQ - CS3-3 (AD 639 – 883, Table 1). Core samples of tufa deposits provide a bracket of the second damaging earthquake faulting between Br 4-3 (AD 540-980) and Br 3-4 (AD 770-940). The second interruption in both BR 5 and BR 6 may also be contemporaneous of the damaging event. Taking into account only the archeoseismic results, we can conclude that Event Y likely occurred between AD 560 – 690 and AD 650 – 780; however, the consistency between all dates of paleoseismic, archeoseismic and tufa analysis suggest an earthquake event close to AD 650. Cement samples CS-1 and tufa sample CS3-3 also indicate a rebuilding period after event Y, at the end of the Byzantine time and beginning of the Islamic period (5^{th} to 6^{th} century AD).
- Event Z observed in trenches A, B and C is identified as younger than AD 960-1060, and older than AD 1030-1260. The definite interruption of tufa growth in all cores and mainly BR 5 and BR 6 indicates the final stop of water flow over the bridge section. The interruption postdates sample Br 6-8 (A.D. 900 – 1160) and can be correlated with the 29 June1170 large earthquake that affected the Missyaf region (Mouty and Sbeinati, 1988; Sbeinati et al., 2005).

Figure 12: a) Calibrated dating of samples (with calibration curve INTCAL04 from Reimer et al. (2004) with 2σ age range and 94.5% probability) and sequential distribution from Oxcal program (see also Table 1; Bronk Ramsey C., 2001). The Bayesian distribution computes the time range of large earthquakes (events W, X, Y and Z) at the Al Harif Aqueduct according to faulting events, building and repair of walls, starts and interruptions of the tufa deposits (see text for explanation).

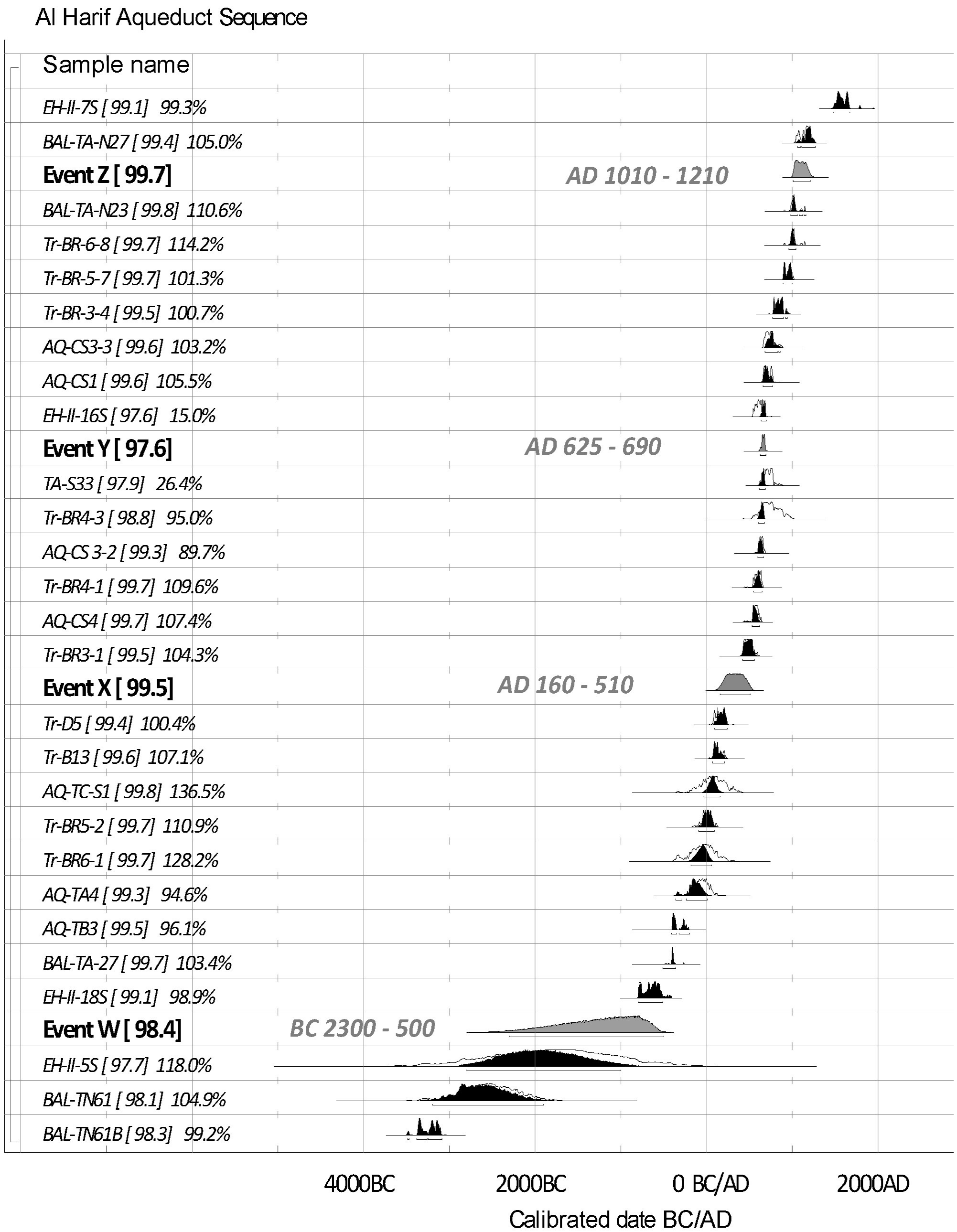

Figure 12: a) Calibrated dating of samples (with calibration curve INTCAL04 from Reimer et al. (2004) with 2σ age range and 94.5% probability) and sequential distribution from Oxcal program (see also Table 1; Bronk Ramsey C., 2001). The Bayesian distribution computes the time range of large earthquakes (events W, X, Y and Z) at the Al Harif Aqueduct according to faulting events, building and repair of walls, starts and interruptions of the tufa deposits (see text for explanation).

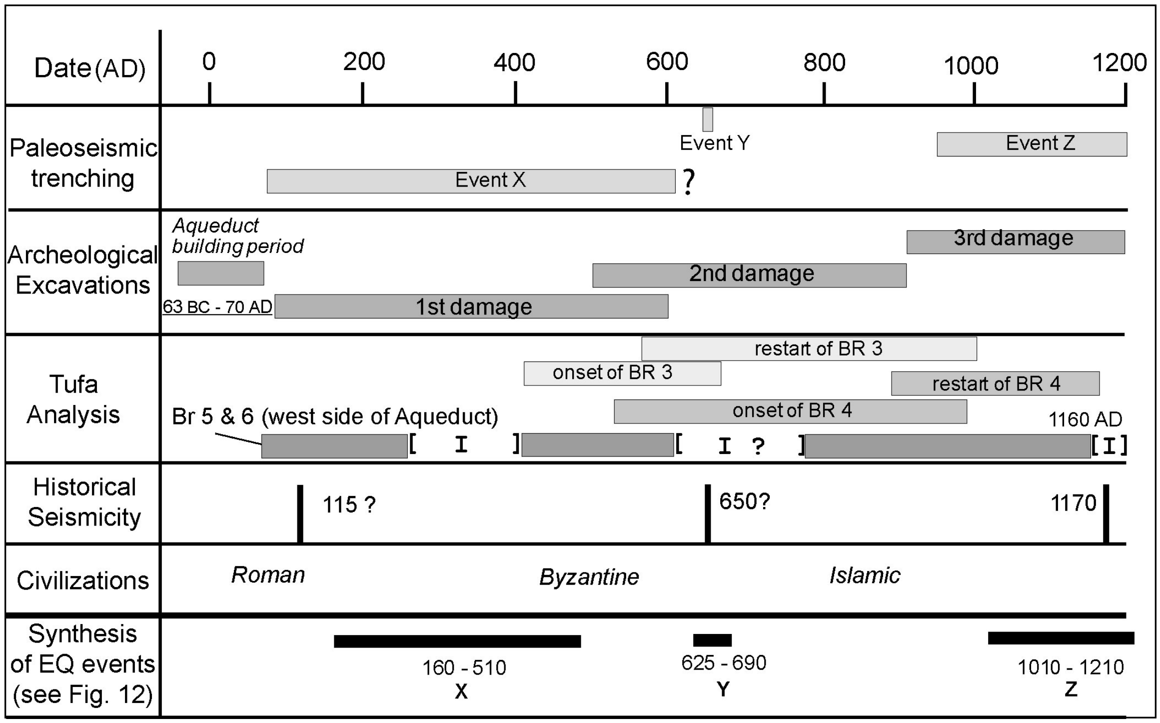

Figure 13) Correlation of results between paleoseismic trenching, archeoseismic excavations and tufa analysis. In paleoseismic trenching, the youngest age for event X is not constrained but it is, however, limited by event Y. In archeoseismic excavations, the period of first damage overlaps with that of the second damage due to poor age control. In tufa analysis, the onset and restart of Br3 and Br4 mark the damage episodes to the aqueduct; The growth of Br5 and Br6 shows interruptions [I] indicating the occurrence of major events. Except for the 29 June 1170, previous events have been unknown in the historical seismicity catalogue. The synthesis of large earthquake events results from the timing correlation between the faulting events, building repair and tufa interruptions (also summarized in Figure 12 and text). Although visible in trenches (faulting event X), archeoseismic excavations (first damage) and first interruption of tufa growth (in Br5 and Br6 cores), the AD 160 - 510 AD age of event X has a large bracket. In contrast, event Y is relatively well bracketed between AD 625 - 690 with the overlapped dating from trench results, the second damage of the aqueduct and the interruption and restart of Br3 and onset of Br4. The occurrence of the 1170 earthquake correlates well with event Z of trenches, the age of 3rd damage to the aqueduct, and the age of interruption of Br4, Br5 and Br6.

The Missyaf segment of the Dead Sea Fault experienced four large earthquakes with event W in BC 3400 – 510, event X in AD 70 - 600, event Y in AD 560 – 780 (probably close to AD 650) and event Z in AD 960 – 1260 (probably in AD 1170). Using the Oxcal program (Bronk Ramsey, 2001) an attempt of sequential ordering of dates and events presented in Figure 12 provides a time probability density function for W (BC 2300 – 500), X (AD 160 – 510), Y (AD 625 – 690) and Z (AD 1010 – 1210). The timing of events obtained from the correlation and sequential distribution clearly indicate a temporal clustering of 3 large seismic events X, Y and Z (Figure 12) after event W that may indicate a relatively long period of quiescence. Although our data and observations cannot precisely constrain event W, it may be correlated with the BC 1365 large earthquake that affected several sites between Lattakia and Tyre as reported in the historical seismicity catalogue of Syria (Sbeinati et al., 2005). The Missyaf fault behavior is comparable to the temporal cluster of large seismic events that occurred on other comparable major strike-slip faults (e.g., San Andreas Fault; Weldon et al., 2004; Jordan Valley Fault segment of the DSF, Ferry et al., 2007).

6- DISCUSSION AND CONCLUSION

We conducted 4 archeoseismic excavations, 3 paleoseismic trenches and obtained the radiocarbon dating of 6 cores at the Al Harif Aqueduct site along the Missyaf segment of the DSF. The combined study allows us to obtain a better constrain on the timing of past earthquakes with 4 large seismic events during the last ~ 3400 years. The occurrence of 3 seismic events X, Y and Z (AD 70 - 600, ~ AD 650 and AD 1170, respectively) since the aqueduct building is attested by faulting events in trenches, the damage and repair of the aqueduct wall and the tufa growth and interruptions since the Roman time (Figure 13). These results point out a temporal clustering of 3 large earthquakes between AD 70 and AD 1170 along the Missyaf Fault segment (Figure 14).

The 90 ±10-km-long and linear Missyaf segment experienced the AD 1170 earthquake recorded in trenches, aqueduct building and tufa deposits. In this tectonic framework, the large (10-km-wide) Ghab pull-apart basin to the north and the Al Bouqueaa pull-apart and onset of the restraining bend to the south (Figure 3) may constitute endpoints for earthquake rupture propagation as observed for other large continental strike-slip faults (Klinger et al., 2005; Wesnousky, 2006). The size of the Ghab Basin and the sharp bend of the Lebanese fault system may act as structural control of the fault-rupture initiation and propagation. Furthermore, the damage distribution of the AD 1170 earthquake well located on the Missyaf segment is limited to the north by the AD 1156 large earthquake and to the south by the AD 1063 and AD 1202 earthquakes (Figure 2, Sbeinati et al., 2005). The 20-km-thick seismogenic layer (Brew et al., 2001) correlates with the ~ 90 km fault length estimated from field mapping (Figure 3). Fault dimensions are consistent with the ~ 4.3 m maximum characteristic slip inferred from the warping of the aqueduct wall east of the fault (and west of the bridge). Here, we assume that successive faulting episodes maintain the early ~ 4.3 m warping of an already ruptured strong building. Taking an average 2.0 m coseismic slip along the fault, the obtained seismic moment is $Mo=1.05\ 10^{20}$ N.m (Mw 7.3, Wells and Coppersmith, 1994) which is comparable for instance to the seismic moment of the 1999 Izmit large earthquake (Mw 7.4) of the North Anatolian Fault.

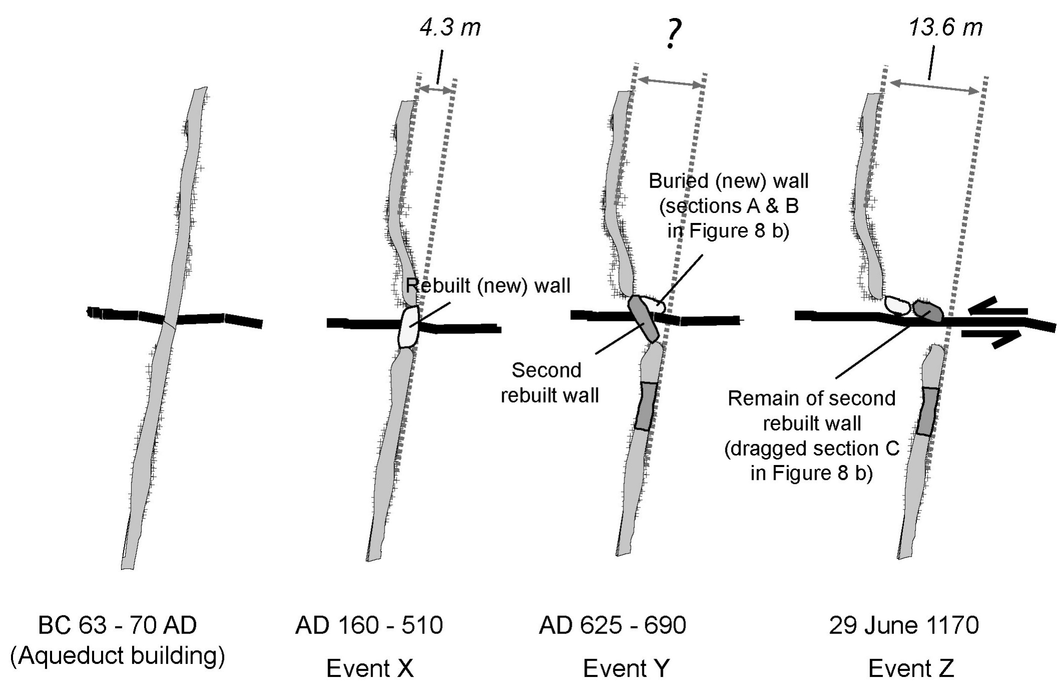

Figure 14: Schematic reconstruction (with final stage from Figure 5) of the AD 160 - 510, AD 625 - 690 and AD 1170 large earthquakes and related faulting of the Al Harif

Aqueduct. Except for the AD 1170 earthquake (see historical catalogue of Sbeinati et al., 2005), the dating of earthquake events are from Figure 12. The white small section is the rebuilt wall after event X (see buried wall A and B in Figure 8 b); the subsequent grey piece corresponds to the rebuilt wall after event Y (see wall section C in Figure 8 b) which was damaged and dragged after event Z. The earlier aqueduct deformation (warping of the eastern wall near the fault rupture) may have recorded ~ 4.3 m of coseismic left-lateral slip well preserved during the subsequent fault movements.

6. 1. The faulted aqueduct : Earthquake damage and successive offsets

The consistency between the timing of faulted sedimentary units in trenches, the age of building and repair of the aqueduct wall and the dating of tufa interruptions and restart determines the completeness of a sequence of earthquake events. The dating of 3 episodes of fault slip X, Y and Z are consistent with the 2 phases of aqueduct wall repair, and the two interruptions of the longest tufa deposits BR5 and BR6, and interruptions and restart in BR3 and BR4. Our observations indicate that the aqueduct was repaired after the large seismic events X and Y but abandoned after the most recent faulting event Z. The building repair after a damaging earthquake is very often necessary because it is a vital remedial measure of water supply in order to avoid a decline of the local economy (Ambraseys, 2005). The repair has the benefit to leave critical indicators of previous damage and in some cases on the fault slip characteristics. For instance, the eastern wall of the Al Harif aqueduct shows a clear warping that confirms the left-lateral movement near the fault zone. As observed for coseismic surface ruptures crossing buildings, fences and walls during the large strike-slip earthquakes (Yeats et al., 1997), warped walls that may record a coseismic slip are often observed along strike slip faulting. The warping that amount 4.3 m can be interpreted as the individual coseismic slip during event X. The warping can be due to the opposite lateral movements across the fault constrained by the bridge cohesion to the east and wall solidity to the west. While the western aqueduct wall section is built straight on the flat alluvial terrace and ends abruptly against the fault, only the section between the bridge and the fault zone (which is partly built on loose sediments and bridge ballast) presents some warping and dragging (possibly separated from the alluvial substratum; Figure 14). The warped section near the bridge displays one generation of cracks filled with tufa that attests for the early bridge damage and possible correlation with event X (Meghraoui et al., 2003). Similar warped walls and fences were observed after the 17 August 1999 earthquake and along the North Anatolia fault in Turkey (Barka et al., 2002). Subsequent faulting movements Y and Z would affect an already broken aqueduct wall (even if rebuilt) with less strength at the fault zone than for the initial building conditions (Figure 14). Furthermore, the 4.3 m can be considered as a characteristic slip at the aqueduct site; such characteristic behavior with repeated same amount of coseismic slip has already been observed and inferred from paleoseismic trenches along major strike slip faults (Klinger et al., 2005; Rockwell et al., 2009). If the warped aqueduct wall is random and not representative of a coseismic slip, the alternative solution is quite similar if we consider a 4.5 m average individual slip from the cumulative 13.6 m left-lateral offset and the X, Y and Z large seismic events at the aqueduct site.

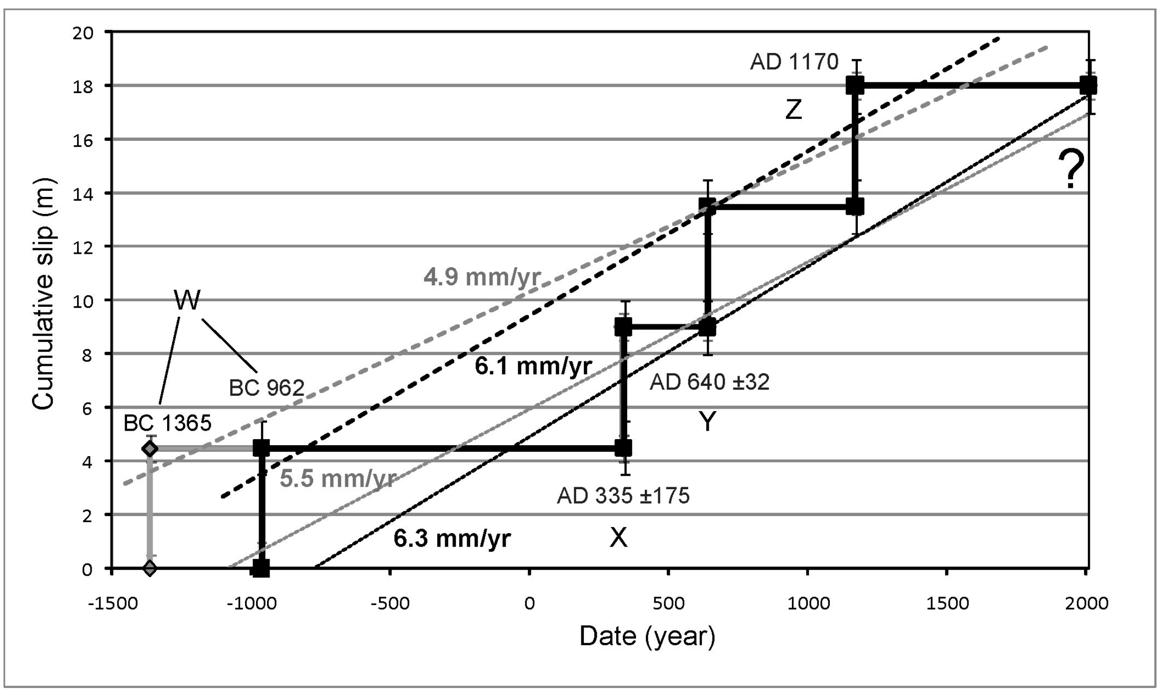

Figure 15: Estimated fault-slip behavior and related slip rates (obtained from regression lines) from two scenarios of possible earthquake occurrence taking into account timing for paleo-earthquakes as in Figure 12 (with average X (AD 160 - 510) 375 ±175, average

Y (AD 625-690) 640 ±32, Z (AD 1170) and two different timeframes for W (historical event of 1365 BC and . In both cases, the two regression lines indicate a minimum a maximum slip rate estimate. In parallel, we assume an average 4.3 m characteristic individual slip consistent with the cumulative 13.6 m measured on the aqueduct (Figure 5). a). If we assume a minimum age AD 962 for W (according to the dating in unit f, related rate of sedimentation and the interface between unit f and unit g in trench C) the slip rate ranges between 6.1 mm/yr and 6.3 mm/yr (dark regression line with 80% correlation coefficient) implying that a large seismic event is overdue. If we consider the historical catalogue and the BC 1365 earthquake sequence along the DSF for W (grey regression line with 78% correlation coefficient), the slip rate reduces to 4.9 – 5.5 mm/yr. The question mark indicates that for both scenarios a large earthquake is overdue along the Missyaf fault segment (according to the seismic gap and the 4.0 slip deficit). The temporal cluster of 3 large earthquakes in less than 1000 years suggests a Wallace model of fault behavior with periods of seismic quiescence reaching ~ 1700 years.

6. 2. Earthquake records in cores

Another key issue is the relationships between the aqueduct damage, the start and interruption of tufa with past earthquakes (Figures 11 and 13). Indeed, the water flow may be interrupted anytime due to, for instance, the actions of man (warfare) or the onset of a drought period and climatic fluctuations that may influence the water flow. These possibilities seem here unlikely because the only two interruptions in cores BR5 and BR6 coincide with earthquake events X and Y and no other additional interruptions were here recorded. This is also attested by the two interruptions in cores BR3 and BR4 that correlate with earthquake events X and Y. The difference between the tufa accumulation in BR4, BR5 and BR6 located on the wall section west of the fault, and BR3 located on the wall section next to the bridge, east of the fault provides a consistent aqueduct damage history (Figure 13). The onset of BR3 after event X is the sign of an extensive damage that tilted the bridge and allowed overflow with tufa accumulation on the aqueduct northern side. The subsequent interruption (repair) and restart of BR3 that coincides with event Y illustrate the successive aquaduct damage. Located on the broken western wall section (Figure 6), the onset of BR4 after event X and restart after event Y is consistent with BR3 tufa growth and accumulation. As illustrated in Figure 13, the coincidence between faulting events X, Y and Z from paleoseismic trenches, the three building damage and repair from archeoseismic investigations, with tufa growth and interruption constrains the earthquake-induced damage and faulting episodes across the aqueduct.

6. 3. The Missyaf segment seismic gap and fault-rupture behavior

The Al Harif aqueduct located at the mid-distance of the Missyaf fault segment documents the size and rate of fault slip associated with large earthquakes. The numerous stream deflections observed along the fault segment imply cumulative left-lateral coseismic offsets consistent with the total aqueduct wall displacement. Stream deflections and wall offset result from the succession of large earthquakes and illustrate the long term and short term fault behavior, respectively. The previous 6.9 mm/yr slip rate obtained from the temporal cluster of large earthquakes X, Y and Z (Meghraoui et al., 2003) clearly overestimates the long term fault behavior because limited to the last 2000 years time-window. The occurrence of earthquake events W, X, Y and Z in the last 3500 years or so and related inferred 4.3 m characteristic left-lateral fault slip lead to 4.9 to 6.3 mm/yr slip rate (Figure 15). Although the inferred age of event W from trench C is not well constrained, the correlation with the BC 1365 seismic sequence and related extension of damage from Latakia (in Syria) to Tyre (in Lebanon) reported in the historical catalogue (Sbeinati et al., 2005) suggest a 1700 to 1300 years of seismic quiescence in the sequence. The fault activity is here comparable to the Wallace-type behavior that describes the succession of temporal clusters of large earthquakes separated by periods of seismic quiescence (Shimazaki and Nakata, 1980). The mean recurrence time of large seismic events on the Missyaf fault segment can be estimated between 550 and 850 years during the temporal cluster. This recurrence time increases to ~ 1077 if we take into account the maximum estimated age of event W obtained from the whole earthquake sequence of Figure 12. A comparable ~ 1100 year mean return period is obtained from a ~ 6000 year paleo-earthquake record on the juxtaposed southern Yammouneh fault segment (Daeron et al., 2007). With a limited number of radiocarbon ages and a possible overlap of the 1408 and 1872 earthquake ruptures, Akyuz et al.

(2006) suggest a minimum 464 to 549 year recurrence interval of surface faulting in the last 1000 years on the northern end of the DSF. However, the inferred large estimate of 500 to 1100 year recurrence interval of earthquake faulting confirms the variability of earthquake occurrence and slip rates determined by the relatively long periods of quiescence along the DSF (Ferry et al., 2007).

The instrumental seismicity in Figure 1 a shows a seismic gap in Syria that also corresponds to more than 800 years quiescence since the AD 1170 earthquake along the Missyaf segment. The seismic strain distribution is time predictable if we assume a constant characteristic slip at the aqueduct location. Taking into account a minimum BC 962 age of event W (Figure 15), the 6.1 - 6.3 mm/yr slip rate along the fault is comparable to other slip rates along the northern DSF obtained from geology or GPS (McClusky et al., 2003; Altunel et al., 2009; Karabacak et al., 2010; Figure 15). If the BC 1365 large earthquake involved the Missyaf fault segment, it implies a 4.9 – 5.5 mm/yr slip rate in agreement with other long term slip rates of the southern DSF (Klinger et al., 2000; Niemi et al., 2001; Daeron et al., 2004; Marco et al., 2005; Reilinger et al., 2006; Ferry et al., 2007; Gomez et al., 2007; Le Beon et al., 2008). The estimated 5.5 mm/yr slip rate and seismic quiescence since AD 1170 advocate ~ 4.0 m slip deficit and indicate that more seismic stress accumulation (which may correspond to 1 to 2 centuries to reach a 4.3 m characteristic slip) is needed for a rupture initiation. Our study shows that the integration of results from archeoseismology, paleoseismology, tufa deposits and historical seismicity is helpful to constrain the timing and characteristics of past earthquakes. However, the Dead Sea fault and related Wallace type behavior requires further paleoearthquake investigations that span several temporal clusters of seismic events.

Acknowledgments: This research was funded by the EC funded APAME Project (Contract ICA3-CT-2002-10024) and by the UMR 7516 of CNRS in Strasbourg. This research benefited with field support from the Syrian Atomic Energy Commission (SAEC), the Directorate General of Antiquities and Museums (DGAM) and the Higher Institute of Applied Sciences and Technology (HIAST) in Damascus. We are grateful to Ibrahim Osman (director general of the Atomic Energy Commission of Syria), Muawia

Barazangi (Cornell University), Abdal Razzaq Moaz and Tammam Fakoush (DGAM) and Mikhail Mouty and Khaled Al-Maleh (Damascus University) for their constant support during the 5-year study of the Al Harif archeo-paleoseismology site. We are indebted to Tony Nemer, Ihsan Layous, Ryad Darawcheh, Youssef Radwan and Abdul Nasser Darkal for field assistance and to Matthieu Ferry and Ersen Aksoy for critically reading an earlier version of this manuscript. We thank the two anonymous reviewers who significantly helped to improve our manuscript. Some figures were prepared using the public domain GMT software [Wessel and Smith, 1998].

References

Akyuz S., Altunel, E., Karabacak, V., Yalciner, C., 2006, Historical earthquake activity of the northern part of the Dead Sea Fault Zone, southern Turkey, Tectonophysics, v. 426, 281–293.

Alchalbi et al., and 15 authors, 2009, Crustal deformation in northwestern Arabia from GPS measurements in Syria: Slow slip rate along the northern Dead Sea Fault, Geophys. J. Int., doi: 10.1111/j.1365-246X.2009.04431.x

Altunel,E., Meghraoui, M., Karabacak. V., Akyüz, S. H., Ferry, M., Yalçıner, C. and Munschy, M., 2009, Archeological sites (Tell and Road) offset by the Dead Sea Fault in the Amik Basin, southern Turkey", Geophys. J. Int., v. 179, 1313–1329.

Ambraseys, N & Melville, C. P., 1988 a, Historical evidence of faulting in Eastern Anatolia and northern Syria, Annali di Geofisica, v. 28, 337 – 343

Ambraseys, N & Melville, C. P., 1988 b, An analysis of the eastern Mediterranean earthquake of 20 May 1202, in Historical Seismograms and Earthquakes of the World, Academic Press, San Diego, p. 181-200.

Ambraseys, N.N., & Jackson, J. A., 1998, Faulting associated with historical and recent earthquakes in the Eastern Mediterranean region, Geophys. J. Int., v. 133, 390-406.

Ambraseys, N. N., 2006, Earthquakes and Archeology, J. Archaeo. Sci., v. 33, 1008-1016.

Ambraseys, N. N., 2009, Earthquakes in the Mediterranean and Middle East, A multidisciplinary study of seismicity up to 1900, Cambridge University Press (UK), 947 p.

Barazangi, M., Seber, D., Chaimov, T., Best, J., Litak, R., Al-Saad, D., and Sawaf, T., 1993, Tectonic evolution of the northern Arabian plate in western Syria, Boschi, E., et al., (Eds.), Recent Evolution and Seismicity of the Mediterranean Region, pp. 117– 140.

Barka, A., and 21 authors, 2002, The surface rupture and slip distribution of the 17 August 1999 Izmit earthquake (M 7.4), North Anatolian fault, Bull. Seism. Soc. Am. v. 92, 43–60.

Brew, G., Lupa, J., Barazangi, M., Sawaf, T., Al-Imam, A., and Zaza, T., 2001, Structure and tectonic development of the Ghab basin and the Dead Sea fault system, Syria, J. Geol. Soc. London, v. 158, 665-674.

Bronk Ramsey C., 2001, Development of the Radiocarbon Program OxCal, Radiocarbon, v. 43, 355-363.

Chaimov, T.A., Barazangi, M., Al-Saad, D., Sawaf, T., and Gebran, A., 1990. Crustal shortening in the Palmyride fold belt, Syria, and implications for movement along the Dead Sea fault system, Tectonics, V. 9, 1369–1386.

Daeron, M., Benedetti, L., Tapponnier, P., Sursock, A. and Finkel, R., 2004, Constraints on the post _25-Ka slip rate of the Yammouneh fault (Lebanon) using in situ cosmogenic 36Cl dating of offset limestone-clast fans. Earth and Planet. Sci. Letters, v. 227, 105–119.

Daeron, M., Klinger, Y., Tapponnier, P., Elias, A., Jacques, E. and Sursock, A., 2005, Sources of the large A.D. 1202 and 1759 Near East earthquakes. Geology, v. 33, 529–532.

Daeron, M., Klinger, Y., Tapponnier, P., Elias, A., Jacques, E. and Sursock, A., 2007, 12,000-year long Record of 10 to 13 Paleo-Earthquakes on the Yammouneh Fault (Levant Fault System, Lebanon), Bull. seism. Soc. Am., v. 97, 749–771.

Dubertret, L., 1955, Carte géologique de Syrie avec notice explicative. République Syrienne, Ministère des travaux publics (1:200,000).

Elias, A., 2006, Le chevauchement de Tripoli-Saıuml;da: Croissance du Mont Liban et risque sismique (Ph.D. thesis): Institut de Physique du Globe de Paris, 230 p.

Ellenblum, R., Marco, S., Agnon, A., Rockwell, T., and Boas, A., 1998, Crusader castle torn apart by earthquake at dawn, 20 May 1202: Geology, v. 26, p. 303-306.

Farr, T., and Kobrick, M., 2000, Shuttle radar topography mission produces a wealth of data, EOS Trans. AGU, v. 81, 583–585.

Ferry, M., M. Meghraoui, N. Abou Karaki, M. Al-Taj, H. Amoush, S. Al-Dhaisat, and M. Barjous, 2007, A 48-kyr-long slip rate history for the Jordan Valley segment of the Dead Sea Fault, Earth Planet. Sci. Lett., v. 260, 394-406,

Ford, T. D., and Pedley, H. M., 1996, A review of tufa and travertine deposits of the world, Earth Science Reviews, v. 41, 117-175.

Ginat, H., Enzel, Y. and Avni Y., 1998, Translocated Plio-Pleistocene drainage systems along the Arava Fault of the Dead Sea Transform, Tectonophysics, v. 284, 151-160,

Garfunkel, Z., Zak, I., and Freund, R., 1981, Active faulting in the Dead Sea rift, Tectonophysics, v. 80, 1-26.

Gomez, F., Meghraoui, M., Darkal, A., Hijazi, F., Mouty, M., Sulaiman, Y., Sbeinati, R., Darawcheh, R., Al-Ghazzi, R. and Barazangi, M., 2003, Holocene faulting and earthquake recurrence along the Serghaya branch of the Dead Sea fault system in Syria and Lebanon. Geophys. J. Int., v. 153, 658–674.

Gomez, F., Khawlie, M., Tabet, C., Darkal, A.N., Khair, K. and Barazangi, M., 2006. Late Cenozoic uplift along the northern Dead Sea transform in Lebanon and Syria, Earth Planet. Sci. Lett., v. 241, 913–931.

Gomez, F., et al., 2007, Global positioning system measurements of strain accumulation and slip transfer through the restraining bend along the Dead Sea Fault system in Lebanon, Geophys. J. Int., v. 168, 1021-1028.

Gomez, F., T. Nemer, C. Tabet, M. Khawlie, M. Meghraoui and M. Barazangi, 2007, Strain partitioning of active transpression within the Lebanese restraining bend of the Dead Sea Fault (Lebanon and SW Syria), Geological Society, London, Special Publications, v. 290, p. 285-303 doi:10.1144/290.10.

Grootes, P.M., Nadeau, M. J., and Rieck, A., 2004, ^{14}C-AMS at the Leibniz-Labor:

Radiometric dating and isotope research. Nucl. Inst. Meth, B223-224, 55-61.

Grootes, P.M., Nadeau, M. J., Roth, S., Andersen, N., Huels, M., Meghraoui, M., and Sbeinati, R., 2006, 1000 years of usage: The life story of a Roman Aqueduct provides tectonic information, American Geophysical Union, Fall meeting 2006, abstract T13B-0500.

Grünthal, G., 1998, European Macroseismic Scale, 1998.,Cahiers du Centre Européen de Géodynamique et de Seismologie. Conseil de l'Europe. 230 p.

Guidoboni, E., A. Comastri, and G. Traina, 1994, Catalogue of ancient earthquakes in the Mediterranean area up to the 10th century, ING-SGA, Bologna, 504 p.

Guidoboni, E., F., Bernardini and A. Comastri, 2004 a, The 1138-1139 and 1156-1159 destructive seismic crisis in Syria, south-eastern Turkey and northern Lebanon, *J. Seismology* 8, 105-127.

Guidoboni, E., F. Bernardini, A. Comastri, and E. Boschi, 2004 b, The large earthquake on 29 June 1170 (Syria, Lebanon, and central southern Turkey), J. Geophys. Res., v. 109, B07304, doi:10.1029/2003JB002523.

Ibn Al-Athir, Ezz Ad-Din (AH 491-541, AD 1097-1146), 1982, Al-Kamil fi Al-Tarikh (The complete in history), v. 8, 9, 10, 11, 12, Dar Sader, Beirut.

Karabacak, V., Altunel, E., Meghraoui, and M., Akyüz, S., 2010, Field evidences from northern Dead Sea Fault Zone (South Turkey): New findings for the initiation age and slip rate, Tectonophysics, v. 480, 172–182.

Klinger Y., Avouac, J. P., Abou Karaki, N., Dorbath, L., Bourles, D. and Reyss, J. L., 2000, Slip rate on the Dead Sea transform in northern Araba Valley (Jordan), Geophys. J. Int., v. 142, 755-768.

Klinger, Y., Sieh, K., Altunel, E., Akoglu, A., Barka, A., Dawson, T., Gonzalez, T., Meltzner, A., and Rockwell, T., 2005, Paleoseismic Evidence of Characteristic Slip on theWestern Segment of the North Anatolian Fault, Turkey, Bull. Seismol. Soc. Am., v. 93, 2317–2332, doi:10.1785/ 0120010270.

Le Beon, M. et al., 2008. Slip rate and locking depth from GPS profiles across the southern Dead Sea Transform, J. geophys. Res., v. 113, B11403, doi:11410.11029/12007JB005280.

Marco, S., Rockwell, T.K., Heimann, A., Frieslander, U., and Agnon, A., 2005, Late Holocene activity of the Dead Sea Transform revealed in 3D paleoseismic trenches on the Jordan Gorge segment. Earth Planet. Sci. Lett., v. 234, 189–205.

Marco, S., 2008, Recognition of earthquake-related damage in archaeological sites—3 Examples from the Dead Sea fault zone, Tectonophysics, v. 453, 148–156.

McClusky, S., Reilinger, R., Mahmoud, S., Ben, D., and Tealeb, A., 2003, GPS constraints on Africa (Nubia) and Arabia plate motions, Geophys. J. Int., v. 155, 126-138,

Meghraoui, M., Gomez, F., Sbeinati, R., Van der Woerd, J., Mouty, M., Darkal, A., Radwan, Y., Layyous, I., Najjar, H, Darawcheh, R., Hijazi, F., Al-Ghazzi, R., and M. Barazangi, 2003, Evidence for 830 years of seismic quiescence from paleoseismology, archeoseismology and historical seismicity along the Dead Sea fault in Syria, Earth Planet. Sci. Lett., v. 210, 35-52.

Mouty, M. and Sbeinati, R., 1988, Historical earthquake catalogue for Syria and adjacent areas, Atomic Energy Commission of Syria, Internal Report, Damascus, 70 p.

Nemer, T. and Meghraoui, M., 2006, Evidence of coseismic ruptures along the Roum fault (Lebanon): a possible source for the AD 1837 earthquake, J. Struct. Geol., v. 28, 1483–1495.

Nemer, T., Meghraoui, M. and Khair, K., 2008, The Rachaya-Serghaya fault system (Lebanon): Evidence of coseismic ruptures, and the AD 1759 earthquake sequence, J. Geophys. Res., v. 113, B05312, doi:10.1029/2007JB005090.

Niemi, T., Zhang, H., Atallah, M., and Harrison J. B. J., 2001, Late Pleistocene and Holocene slip rate of the Northern Wadi Araba fault, Dead Sea Transform, Jordan, J. Seismol., v. 5, 449-474,

Nur, A., and Cline, E. H., 2000, Poseidon's Horses: Plate tectonics and earthquake storms in the late Bronze age Aegean and Eastern Mediterranean, J. Archaeo. Sci., v. 27, 43-63.

Quennell, A.M., 1984, The western Arabia rift system. In: Dixon, J.E., Robertson, A.H.F., The Geological Evolution of the eastern Mediterranean, Geol. Soc. Sp. Pub., v. 17, 775–788.

Reilinger, R., McClusky, S. et al., 2006, GPS constraints on continental deformation in the Africa–Arabia–Eurasia continental collision zone and implications for dynamics of plate interactions. J. Geophys. Res., v. 111, doi:10.1029/2005JB004051.

Reimer, P. J., and 28 authors, 2004, IntCal04 Terrestrial radiocarbon age calibration, 26 - 0 ka BP. Radiocarbon, v. 46, 1029-1058.

Rockwell, T., and 12 authors, 2009, Paleoseismology of the North Anatolia fault near the Marmara Sea: Implications for fault segmentation and seismic hazard, Geol. Soc. London Special Publications, v. 316, 31-54. DOI: 10.1144/SP316.3.

Salamon, A., Hofstetter, A., Garfunkel, Z. and Ron, H., 2003, Seismotectonics of the Sinai subplate–the eastern Mediterranean region, Geophys. J. Int., v. 155, 149–173.

Sbeinati, M. R., Darawcheh R., and Mouty, M., 2005, The historical earthquakes of Syria: an analysis of large and moderate earthquakes from 1365 B.C. to 1900 A.D, Ann. Geophys., v. 48, 347-435.

Shimazaki, K. and Nakata, T., 1980, Time-predictable recurrence model for large earthquakes, Geophys. Res. Letters, v. 7, 279-282.

Stiros, S. and Jones, R. E., 1996, Archeoseismology, Fitch Laboratory occasional paper 7, British School of Athens, Greece, 268 p.

Trifonov, V. G., et al., 1991, Levant Fault zone in northwest Syria, Geotectonics, v. 25, 145-154.

Wdowinski, S., Bock, Y., Baer, G., Prawirodirdjo, L., Bechor, N., Naaman, S., Knafo, R., Forrai, Y., and Melzer, Y., 2004, GPS measurements of current crustal movements along the Dead Sea fault, J. Geophys. Res., v. 109, B05403,

Weldon, R., Scharer, K., Fumal, T., and Biasi, G., 2004, Wrightwood and the earthquake cycle: What a long recurrence record tells us about how faults work, GSA Today 14, 4-10.

Wells, D. L., and Coppersmith, K. J., 1994, New empirical relationships among magnitude, rupture length, rupture width, rupture area, and surface displacement, Bull. Seism. Soc. Am., v. 84, 974–1002.

Westaway, R., 2004, Kinematic consistency between the Dead Sea Fault Zone and the Neogene and Quaternary left-lateral faulting in SE Turkey, Tectonophysics, v. 391, 203–237.

Wesnousky, S. G., 2006, Predicting the endpoints of earthquake ruptures, Nature, v. 444, 358-360.

Wessel, P., and Smith, H. F., 1998, New, improved version of the Generic Mapping Tools Released, EOS Trans. AGU, v. 79, 579.

Yeats, R., Sieh, K., and Allen, C., 1997, The geology of earthquakes, Oxford University Press, 568 p.

Zilberman, E., Amit, R., Porat, N., Enzel, Y., and Avner, U., 2005, Surface ruptures induced by the devastating 1068 AD earthquake in the southern Arava valley, Dead Sea Rift, Israel, Tectonophysics, v. 408, 79 – 99.

V – 3. Ruptures in Krak des Chevaliers

This castle is one of the most famous fortresses in the world, and the one of the biggest construction with well developed defence system and decoration (Karak means fortress in Syriaque). It is located on the top of basaltic hill (750 m ASL, and 300 m above Al-Boukeaa basin) at about 60 Km west of Homs and 35 Km the Mediterranean Sea (see Figures 17, 18 and 19). Many names were given to this castle such as: Castle of Slope *'Houssen Al-Safeh'*, Castle of Kurdish *'Houssen Al-Akrad'*, Castle of Knights *'Krak des Chevaliers'*, castle of fortress *'Kalaat Al-Houssen'*, where Al-Houssen in Arabic means fortress in English (sea Figure 4).

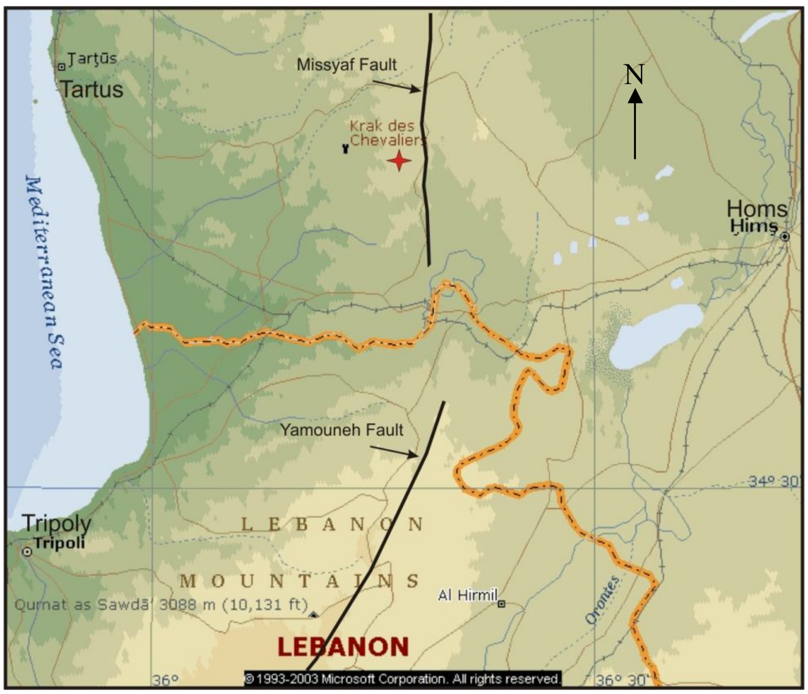

Figure 17: location map of Krak des Chevaliers.

3 – 1. History of the fortress:

The castle was first a small fortress built by a group of Kurdish in 1031 during the Fatimid reign (969 - 1171 AD). The castle faced a lot of attacks by the Byzantine then by the Crusaders and it fallen in 1142 when the Kurdish sold the castle to the Hospitallers troops after a long time of struggling. In 7 April 1271, the castle was liberated by the king Al-Zaher Bibars and later the castle became part of Tripoli district governed for a long time under the control of many important families, the latter one being the Al-Dandisheh family until ~1800 AD. Lately and finally, the castle was registered in the UNESCO patrimony since 2006.

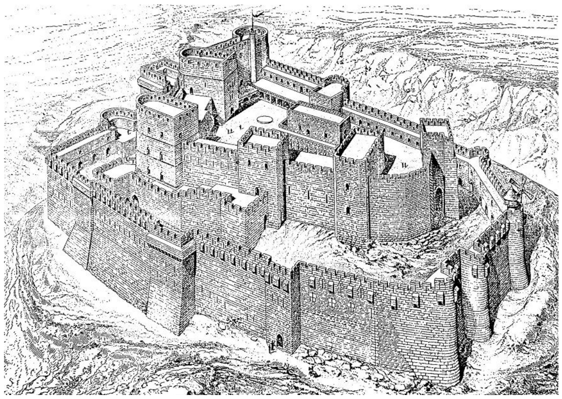

Figure 18: Draw by Baron Ray 1859. Facing SW direction (from Tlass, 1990).

Figure 19: General view of the castle (facing NE direction).

3 – 2. The Construction:

The castle lay on the top of consolidated massif basalt; it was first assessed by a Kurdish group then some parts were added by the Crusaders and finally took its final shape during the Mamluk reign (1250 - 1517). The castle consists of a main central building composed by many big halls, this central part surrounded by two fences separated by a deep trench (inner and outer) were the outer fence has many towers. The general shape of the castle is like a semi-diagonal where the base is the southern wall (see Figures 20 and 21).

3 – 3. Historical Earthquakes:

The castle endured several times wars because of its strategic location. However, it was also affected by many destructive historical earthquakes because of its proximity to the Dead Sea Fault (the Missyaf fault segment, Figure 17). The earthquake damage and destructions were recovered immediately after the historical events because of its military importance, either by the Crusaders or by the Muslims, even though, the scars of earthquakes can be noticed in the citadel. The description of historical buildings, wars and date of past damaging earthquakes are listed in the following (Tlas et al., 1990 and Sbeinati et al., 2005):

- 20 Jan. 1029: the castle was projected by the order of Shibl Al-Dawleh Al-Merdasi and built in 1031.
- May 1063: A large to moderate earthquake is recorded (no damage)
- 13 Nov.1114: A large earthquake is felt.

- 27 Sep. 1156 to mid of 1158 a group of destructive earthquakes hit the central of the western region in Syria.
- 29 June 1170 the most destructive earthquake destroyed many important parts of the castle.
- 1201, 1202 and 1203 earthquakes destroyed many parts of the castle.

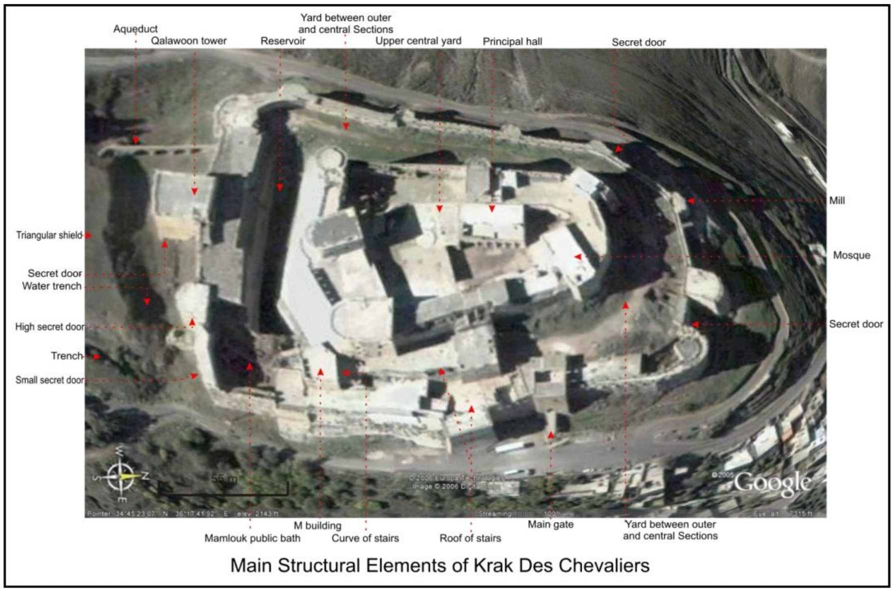

Figure 20: Space photo of Krak des Chevaliers showing its main structural elements, and the excavation site (oblique projection).

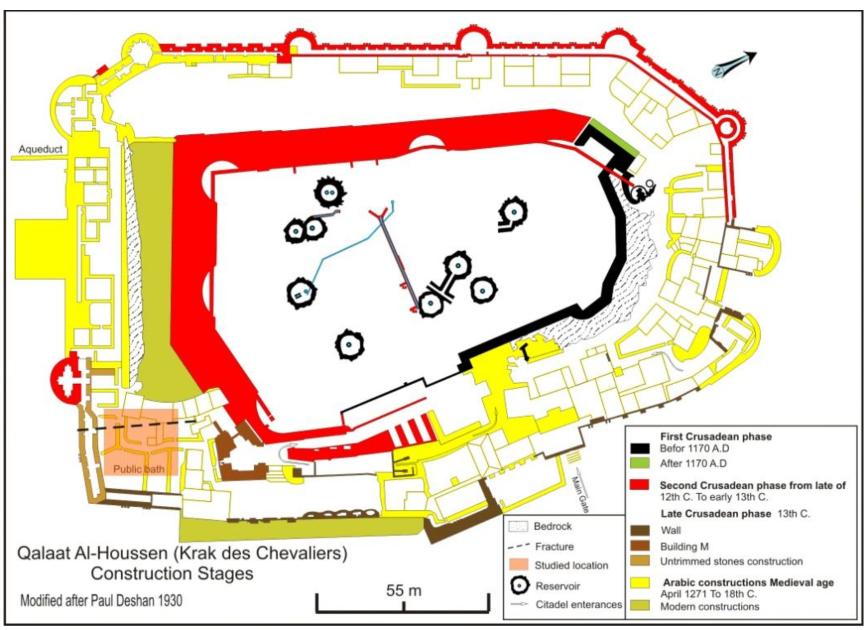

Figure 21: the construction stages of the Castle, the Mamluk bath and the fracture extension (oblique projection).

3 – 4. Field Investigations:

A group of Syrian seismologists and archaeologist conducted field investigations in Krak des Chevaliers during the third field work season of the APAME Project. The work was conducted by M. Reda Sbeinati in collaboration with Ghada Suleiman, Haytham Al-Najjar and Evelyn Samaan. We performed a detailed study of fractures along the southern outer wall and inside the castle in the Mamlouk Hammam (Bath) with the southern backyard in between. We also explored the surrounding geological outcrops outside north and south of the citadel, and observed that the fracture continues in the bedrock in a north-south direction (Figure 21), and are clearly visible vertically on the outer wall (Figures 22 and 23).

This several meter long crack is interpreted as an evidence of coseismic rupture of a historical earthquake affecting both the construction and the bedrock. From this observation, our objective was to: 1) Differentiate the building stages in the southern part of the outer wall-fence; 2) Identify this fracture from other features, such as the interval of limestone building rocks along the outer wall also built of massif untrimmed basaltic rocks. Another striking observation is a deflection in the wall-fence direction of about 10 degrees and its relationship with the cracks (Figures 22, 23, and 24); and 3) Date the crack rupture. We have followed the crack extension and have made an excavation to unearth the basalt bedrock of the wall-fence beneath the fracture in the Mamluk bath, see (Figures 21, 22, and 24). Fifteen samples were taken from different levels of the excavation for AMS C^{14} analysis.

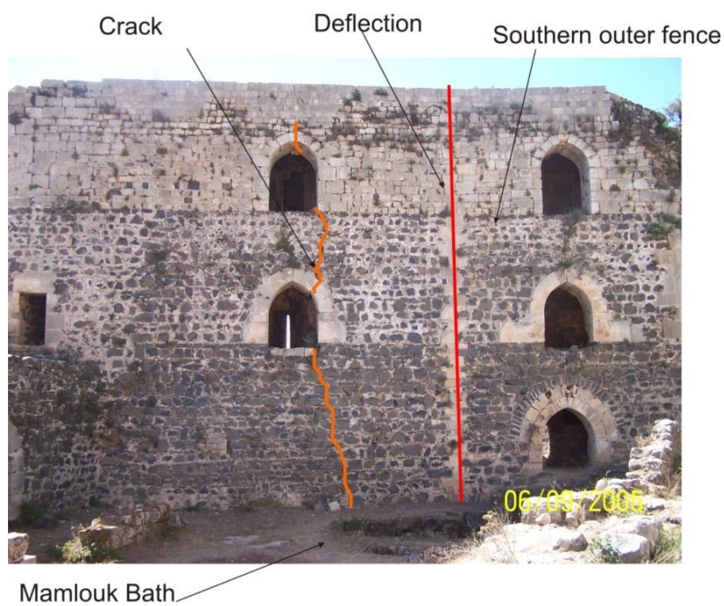

Figure 22: The inner part of the southern outer fence, showing the deflection in the basaltic wall (red line) and the crack (orange line), the Mamlouk Bath (facing S direction).

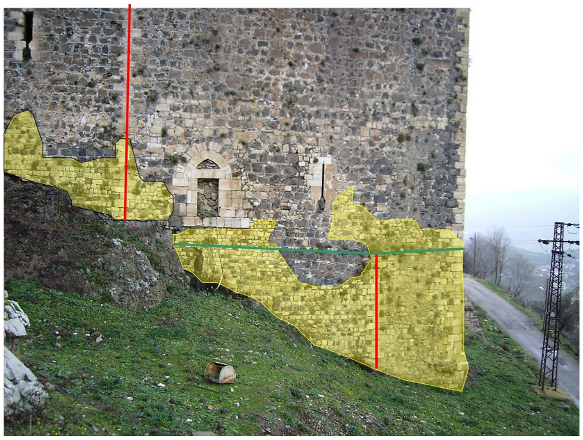

Figure 23: The outer part of the southern outer wall-fence, showing the deflection in the basaltic wall as a constructing system (red lines) in the upper and lower levels; the yellow stone represents the rebuilding stage during the French excavation 1936(facing N direction).

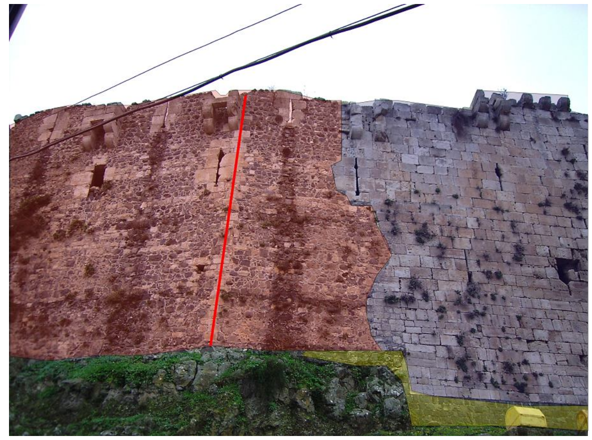

Figure 24: The north-eastern part of the outer wall-fence, showing different stages of building and the red line marking the deflection in the wall as a construction system to strengthen the basaltic wall (facing W direction).

Figure 25: Upper photo facing south direction, lower photo vertical shows the horizontal projection, it showing the trench in the basement of the southern outer wall-fence; orange line: crack; brown: building stones (limestone); red: bedrock (basaltic rocks); dark brown: soil; blue: disposal water of the bath; bright brown: building stones of the channel of disposal water.

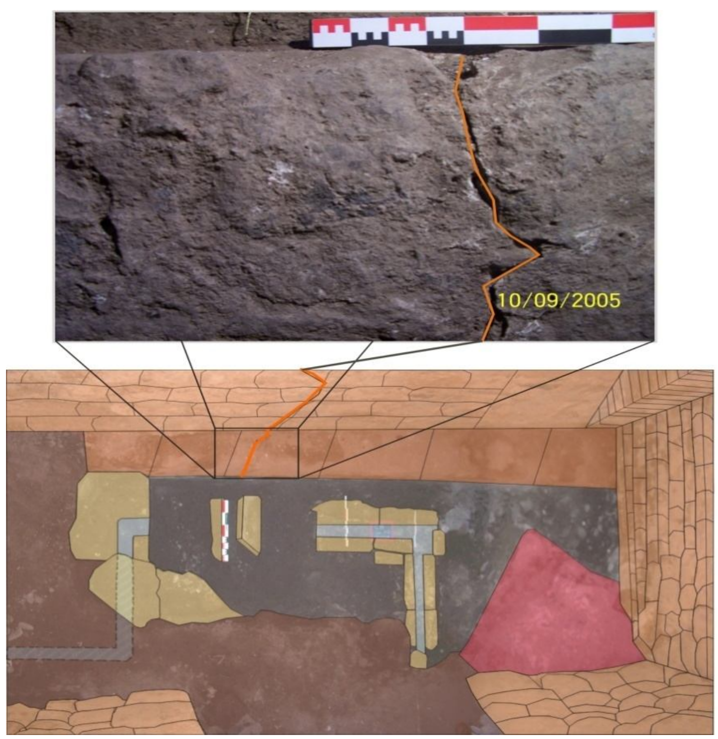

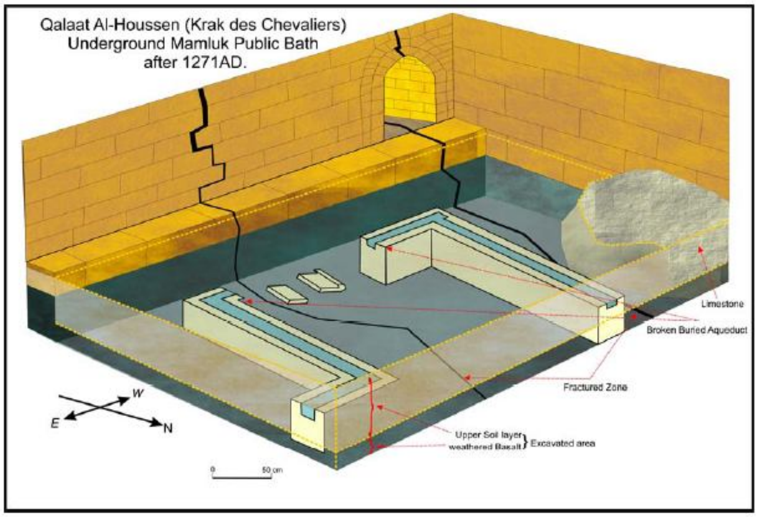

Fig. 26: 3 Dimension of the underground public bath at the southern wall of the Krak des Chevaliers Castle and related earthquake rupture affecting a buried canal.

Sample ID	Sample Name	Fraction	Current (% of normal)	Amount of carbon analysed (mg)	Fraction carbon content (%)	14C Age (years BP)	Calib. age (95.4% AD-BC)
28943	CH-2/SYR	Charcoal, Alkali Residue	100	5.48	69.4%	715 ± 25	1250-1380
28944	CH-3/SYR	Slag, Alkali Residue	88	0.87	0.1%	770 ± 30	1215-1285
28945	CH-4/SYR	Charcoal, Alkali Residue	99	1.82	69.2%	570 ± 25	1300-1420
28945	CH-4/SYR	Charcoal, Humic Acids	69	5.23	61.5%	640 ± 25	1280-1400
28946	CH-5/SYR	Charcoal, Alkali Residue	101	5.85	73.7%	915 ± 20	1030-1170
28947	CH-6/SYR	Charcoal, Humic Acids	100	5.17	51.5%	945 ± 25	1020-1160
28947	CH-6/SYR	Charcoal, Alkali Residue	47	0.30	14.9%	1080 ± 70	770-1160
28948	CH-7/SYR	Charcoal, Alkali Residue	99	3.53	65.9%	645 ± 20	1280-1400
28949	CH-8/SYR	Charcoal, Alkali Residue	94	5.82	71.4%	535 ± 20	1320-1440
28954	CH-13/SYR	Charcoal, Alkali Residue	112	5.47	71.4%	645 ± 20	1280-1400
28950	CH-9/SYR	Charcoal, Alkali Residue	101	5.68	72.4%	870 ± 25	1040-1230
28950	CH-9/SYR	Charcoal, Humic Acids	87	3.62	66.3%	740 ± 25	1225-1290
28951	CH-10/SYR	Charcoal, Alkali Residue	102	5.36	70.4%	545 ± 20	1320-1430
28952	CH-11/SYR	Charcoal, Alkali Residue	102	5.50	70.5%	480 ± 20	1415-1450
28953	CH-12/SYR	Charcoal, Alkali Residue	103	6.30	63.7%	550 ± 20	1310-1430

Table 2: Detailed measurements presented here give proper insights regarding the quality (amount of carbon should be larger than 1 mg) of collected samples; the possibility of sample fraction (alkali residue, humic acids) enhances the dating accuracy. The 2σ-calibrations were performed using the OxCal 3.5 software (Bronk Ramsey, 2001) and the atmospheric data (INTCAL04) are from PJ Reimer et al. (2004). Level 1, Level 2, Level 3, Level 4.

Level 1: First level West the trench, beside the outcrop in the corner of the basement.

Level 2: Second level North the trench, directly above the channel cover, close to the door.

Level 3: Third level West the trench, same as the level of the channel cover.

Level 4: Forth level Centre the trench, beneath the broken part of the channel & along the crack.

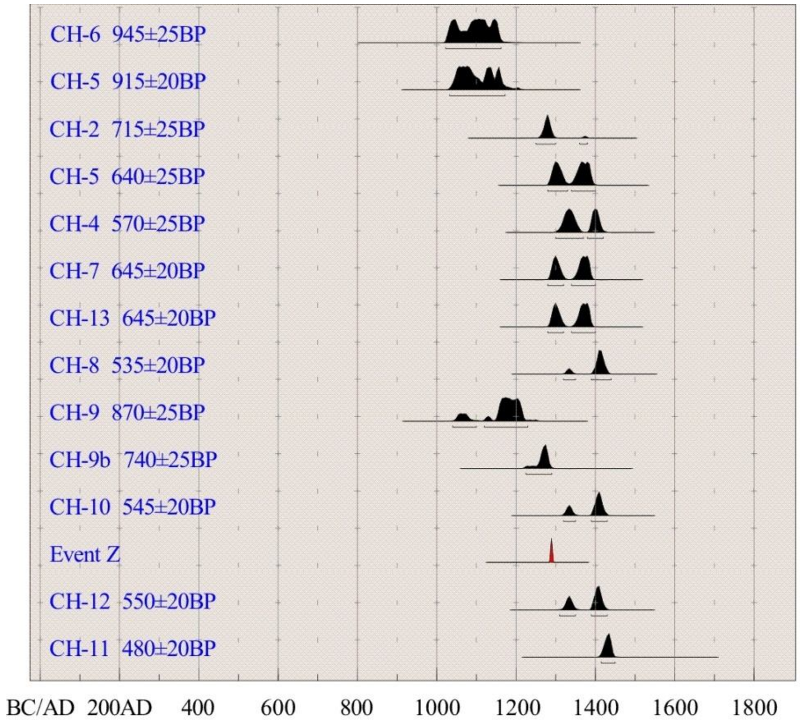

Figure 27: Probability distribution of C^{14} ages (Table 2) obtained from sequential radiocarbon dates and the Event Z age (1275-1295 AD) using the OxCal 3.5 software (Bronk Ramsey, 2001) and the atmospheric data (INTCAL04) are from PJ Reimer et al. (2004). The age range of the seismic event (red) is determined using the Bayesian analysis probability distribution in Oxcal.

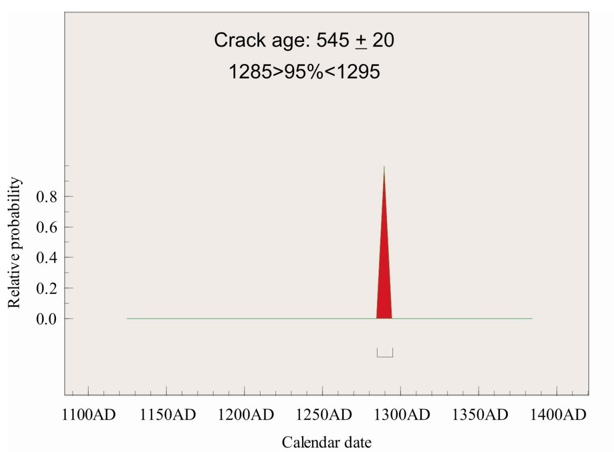

*Figure 28: Probability distribution of the Event Z age (1285-1295 A**D)** obtained using the OxCal 3.5 software (Bronk Ramsey, 2001) and the atmospheric data (INTCAL04) are from PJ Reimer et al. (2004).*

3 – 5. The analysis of damaged parts and the radiocarbon dating results:

According to the excavation in the Mamluk bath and radiocarbon dating results accompanied by the fortress exploration and surrounding area, and from the history (Tlas, 1990), , we may conclude to the following conclusions:

- The southern part of the outer wall-fence was rebuilt rapidly after the 29 June 1170 earthquake by the Hospitallers and in 1217 by the king Andrew II of Hungary. They strengthened the outer walls and financed the guarding troop, untrimmed new basaltic rocks (to replace previous limestone rock pieces of wall) as seen in bright brown colour in Figure 21 and in red in Figure 24. Some restoration works has been done by the French archeological mission during 1936; the used stones are small cut limestone blocks as seen in yellow in Figure 23.
- The 10° sharp deflections in the basaltic walls are clear in the southern part and in the northern eastern one of the outer wall-fence. It corresponds to a construction design system to strengthen the long standing walls presented in strait red lines (Figures 22, 23, and 24). This deflection that is of the same age of the outer wall-fence rebuilding has actually no relation with the studied fracture and it has no continuation in the bedrock.
- The crack in the southern outer fence extends in the Mamlouk bath and the basaltic bedrock in N-S direction in parallel to the Missyaf fault (Figures 17, 22, and 25).
- The trench dug in the Mamlouk bath discovers a channel of water disposal affected by the crack (Figures 25 and 26).
- The crack caused the rotation of the building stones of the discovered channel which are on the same trend of the crack; this was quiet surprising and gave the possibility to be dated. Since there is no indication of landslide, or deferential load of the structure, the crack can be interpreted as a coseismic feature.

The fifteen charcoal samples were taken from different levels in the trench, (i.e. beneath the channel of disposal water, from the level of the channel, from the level of disturbed part by the crack of the channel, from the level cupping the channel, and from the surface soil), in order to determine the ages of the crack and channel. As seen in (Table 2), the obtained results of C^{14} analysis and the probability density function of the event Z, which postdates the channel construction and predates the age overlain soil, provides the date bracket between 1275 AD and 1295 AD (Figure 27). Although with a seismic intensity VII – VIII (EMS 98) in Lattakia This event can be correlated to the earthquake of 22 March 1287). However, , the dated crack in the Mamluk bath may also shed light on the possibility of an unknown local and moderate earthquake in the region.

V – 4. Collapsed columns in the Agora of Apamea

4 – 1. The Apamea ancient city site

Apamea is an antique city of Syria situated on the right bank of the Orontes river overlooking the Al-Ghab plain and at about 55 km northwest of the city of Hama (Figure 1). Since Apamea is one of the most famous archeological sites in the Middle-East because of its richness, coloured culture for long time, and strategic location important for trading, military, religious and architectural levels. Apamea is also one of the archeological sites sitting very close to the Dead Sea fault. Hence, Apamea can be considered as an archeological archive of seismic events that recorded the most destructive earthquakes along the Dead Sea fault. The archeological site preserved the earthquake-induced destruction and damage of the old buildings and columns (all the historical and archeological information were taken from Balty, 1999; and Zakariyya, 1984).

4 – 2. History

Apamea was erected in 300 BC by Saluqas Nikator (a lieutenant of Alexander the Great), the first king of the Seleucides in Syria. He named the city it after his Persian wife Afamia. The city flourished to an extent that its population numbered half a million in the early days of Christianity. Most ruins of Apamea dated back to the Roman and Byzantine eras. It is distinguished for its long walls, its colonnaded street (2 km X 87m) (Figure 26) and its theatre; the main parts of the Apamea city and the locations of the excavation sites are shown in (Figure 28).

During its life-time, Apamea was destroyed by the destructive earthquakes of: 53, 115, 525, 526, 1157 and 1170 and by the wars of 583, 992 AD. and 1110 AD. and by a fire in 997 AD.

4 – 3. The buildings of Apamea city

The focal point of the ruins of Apamea is its central main street. The buildings include a number of Christian churches and Basilicas. There are also many features dating to the city's heyday. The building materials used are of different size blocks of massive limestone and granite, brick, and cements. We present in the following a brief description of the main remarkable features and among them the Agora because it was selected as our field of excavation:

- The Colonnaded Street. This is a 2-km-long Apamea's main street that is longer than the main thorough fare of Palmyra city. The street terminates in the Antioch Gate to the north and the Homs Gate to the south. It was constructed in the second century AD, re-erected in the 1930s, and took its name from the continuous colonnaded porticos that line its pavements on both sides of the road. Many of the 10 metre high 1200 columns have a unique twisted pattern not seen in any other Greek or Roman cities. The capitals are sculpted with vegetative patterns with the faces of city leaders and emperors.

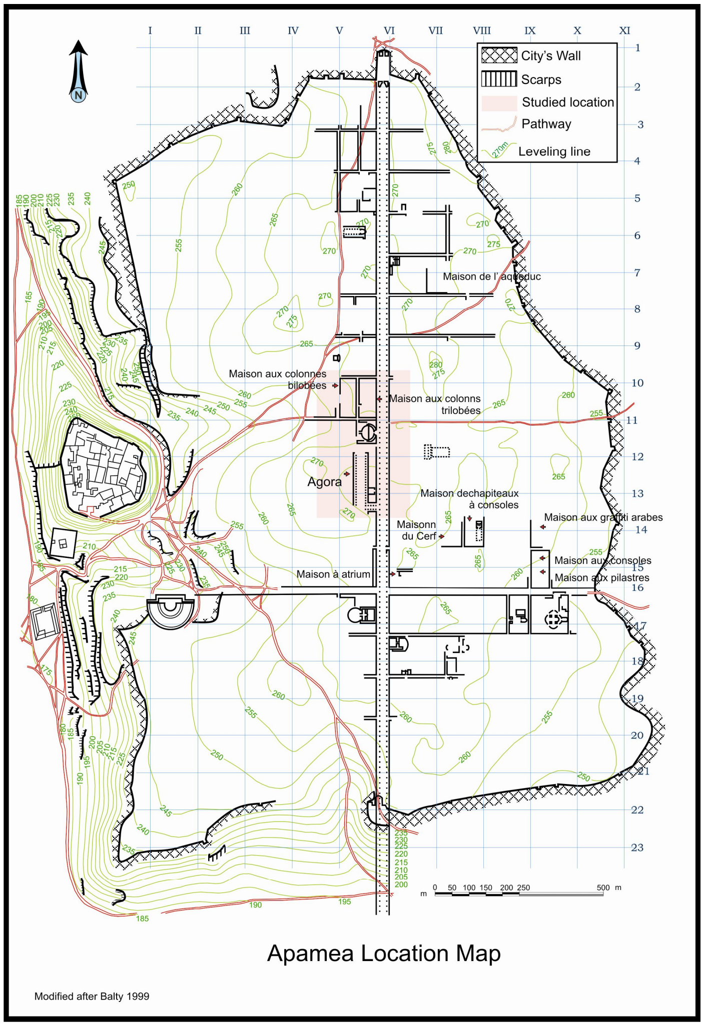

Figure 29: Location map of Apamea; the pink shaded rectangle is the excavation site (map modified from Balty, 1999).

- The Agora or forum is located to the east of the colonnaded street and corresponds to a rectangular space of 150m long and 25m wide. The Agora was connected to the colonnaded street by a small road and a monumental entrance way which included a colonnaded portico topped with a triangular pediment. The toppled columns indicated that this entrance was destroyed in the most recent earthquake that devastated the city. It was reassembled when reconstruction of the city commenced in ….

4 – 4. Types of earthquake damage

Among the main impressive feature of earthquake damage in Apamea is the unified ESE-WNW direction of collapse of a large number of columns, and the liquefaction effect observed especially in the Agora site (Figures 30). A horizontal displacements were noticed in the base of the some structure elements, as seen in Figure 30. To the north of the Agora (~ 30 m), a previous archeological excavations of archeological mission from Belgium in the "*maison aux colonnes bilobées*", it can be noticed in the excavated sections, the patterns of successive layers having the signs of different destruction building and rebuilding stages. The Apamea city is almost totally in a ruinous state and mostly covered by a thick layer of debris, except the area of the works of reinstallation in the colonnaded street and the excavation parts of the archeological mission from Belgium.

4 – 5. The excavation pit in the Agora:

The city of Apamea has a wide spreading area as seen in (Figure 29), and because of the restriction of the permission for archeological excavation in Apamea, and limitation in time, we choose the Agora as one of representative examples for Apamea city destruction. According to the field investigation; the fallen columns of the Agora have been untouched since its fallen date, and the liquefaction effect is well exposed on the rocky plates of the its floor. In this regards; A pit was digged beside the base of the first column in the Agora, this column is the only one remaining standing up among all the rest of columns in the Agora (it may be refer to the thickness of covering debris above it), but it was broken from the middle, (Figure 30) shows the place of the pit, and (Figure 31-b) showing the covering debris thickness above the column, the pit has with 2.5 X 1 m length and width, and ~ 2.5 m depth. The pit location determined on the bases of exploring the thickest accumulation of debris in the Agora site, in the base of the pit; we have reached the oldest level of the Agora at depth of 1.9 m where the base of the column.

The section of the accumulated debris is composed of two main portions: the down one is about (~ 1.5 m) of dark grey fine soil filled by a dense accumulation of sharp angular gravels of broken stone, alternated by lenses of ash (in the top this level we reach the upper most base stone of the column), above we have (~ 30 cm) a big size building stone cupping the down portion of the debris (it seams to be imposed to protect the Agora from debris and uplifting the Agora base floor), the upper portion, above the big building stone, is composed of a light grey fine soft accumulation of soil alternated by scattered angular gravels (see Figure 31-b). In the base of the pit we found a complete jaw of animal beneath the fallen building stone, the age of the jaw may indicates to date of the debris accumulation, as seen (Figure 34), a) showing the total section of the debris from the base of the column, b) showing the animal jaw at the base of the pit.

4 – 6. The analysis of the "maison aux colonnes bilobées" section:

From previous excavations of archeological mission from Belgium in the "*maison aux colonnes bilobées*" (to the north of the Agora ~ 30 m), we can notice patterns of successive layers having the signs of different destruction building and rebuilding phases. They consists of, from down to top, a ~ 70 cm-thick layer of dark grey clay with high percentage of charcoals, ~ 10 cm of blanc-sale chalky layer as remains of the oldest floor layer (lens) of the house, ~ 25 cm mixture of yellow wish soil with fine remains of bricks and scattered pieces of roof bricks, ~ 10 cm of white chalky fine layer with mosaics represents the second floor, ~35 cm of mixture of debris with medium size broken pieces of bricks, ~ 20 cm of dense and thick broken roof tiles, ~ 25 cm of dark grey ashy layer with high percentage of charcoal pieces, ~ 15 cm thin layer of whit choky which represent the third floor of the house, and in the top a cupping layer of ~ 3m of soil and debris, (Figures 32 a and c) show the section of different layers of debris; and (Figure 33) shows the excavation and the three different floors and the thickness of the final debris layer, (Figure 32 C) were the contact is clear between the old wall of the house and the sequence of the debris, and the second old mosaic floor level covered by a thin white sandy layer for protection, in (Figure 32 b) we can see the western entrance of the house how it was originally, wide (> 2 m) with two big cylindrical columns on the both sides, and its original base level at the same with columns and the old base layer of mosaic in the second floor, which covered by white sand, and latter; how it was modified to a width to became (~ 1 m) and uplifting its base to be higher on the same level of the newer floor level (third floor); by altering additional big size building stones, this giving indication of the same architectural system of the original construction and the destruction was recovered fast.

Regarding to the above description of the analysis of the exposed sections of the debris in the "*maison aux colonnes bilobées*", the dating the dating of the cement of the wall from lower level in contact with the debris, will indicates to the date of the first construction, dating the debris sequence will indicate to the functioning periods of the house and its death.

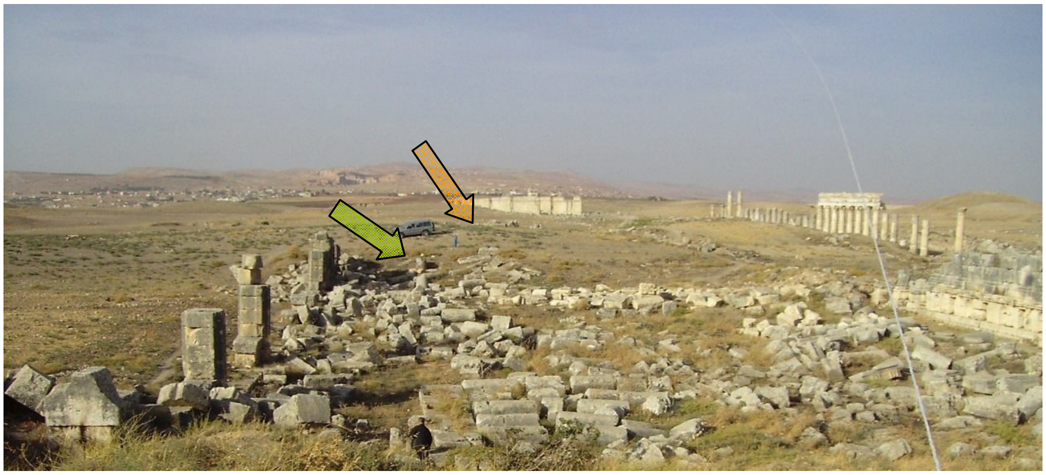

Figure 30: General view of the Agora location, showing the direction of the fallen columns. The photo is facing north direction, the green and orange arrows indicate to the excavation in the Agora and the house ”maison aux colonnes trilobées”, respectively (facing N direction).

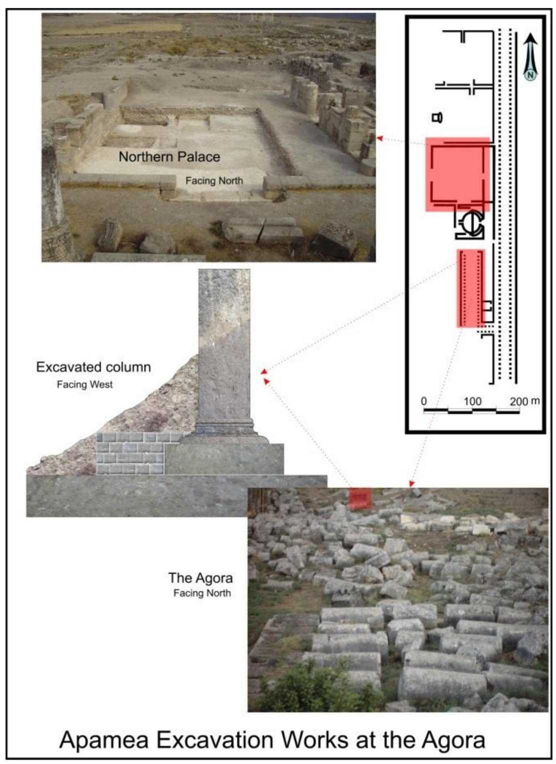

Figure 31: The excavation locations, upper photo is the northern palace ‘maison aux colonnes bilobees’, photo in middle shows the section in base of the excavated column in the Agora

(the debris thickness above the base of the base of the column), and the photo down showing the location of the excavated column.

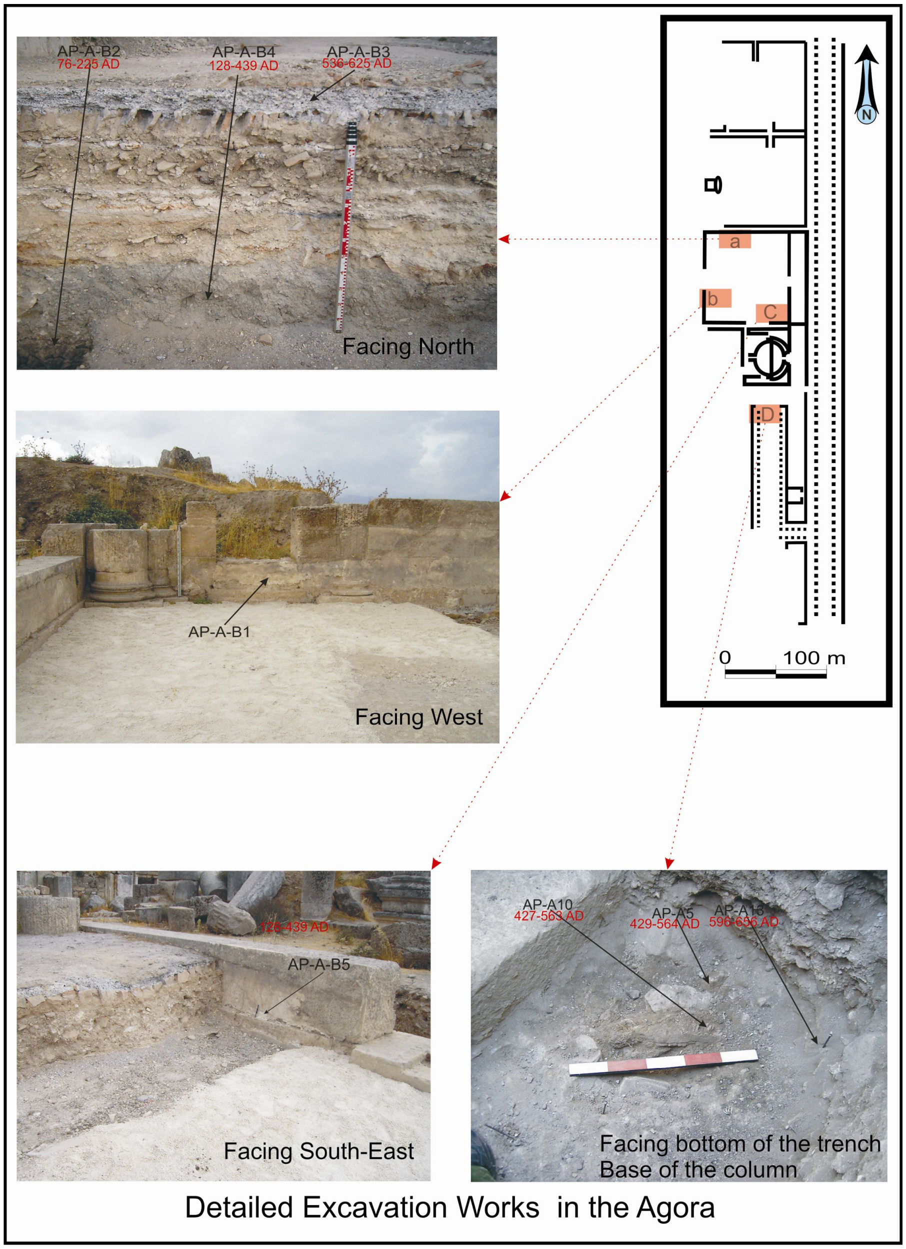

Figure 32: showing the sample locations for radiocarbon dating and related results; photos a, b and c, are sampling in the 'maison aux colonnes trilobees' to the north of the Agora, photo d shows the base of the pit and sample distribution.

Figure 33: Showing the excavation and the three different floors and the thickness of the final debris layer (facing north).

Figure 34: the pit in the Agora, a) Showing the north wall's section of debris in the pit beside the base of the column, b) Showing the jaw of animal in the base level of the column.

4 – 7. The AMS C^{14} dating analysis

Four samples were take from the base of the column in the Agora (collection APA-A), which possibly prost-date the first earthquake. Five samples were taken from the described section of the debris in the '*maison aux colonnes trilobées'* (collection APA-B); in order to know the dates of destruction stages, and from the cement of the base of wall building, which should indicate the first building stage. (Table 3: Showing the samples with radiocarbon dating) and Figures 33 and 34: the probability distribution of C^{14} ages and probability distribution of event Z age (420 – 570 AD) respectively.

Sample ID	Sample Name	Fraction	Current (% of normal)	Amount of carbon analysed (mg)	Fraction carbon content (%)	14C Age (years BP)	Calib. age (AD/BC)
26040	AP-A-0/SYR Apamea	Cement, Alkali Residue	104	4.20	1.7%	1375 ± 25	615-680
26041	AP-A-5/SYR Apamea	Charcoal, Alkali Residue	109	6.44	78.1%	1550 ± 25	420-570
26042	AP-A-10/SYR Apamea	Bone, Collagen	96	3.38	41.7%	1555 ± 25	420-570
26043	AP-A-13/SYR Apamea	Charcoal, Alkali Residue	102	5.64	70.8%	1445 ± 25	570-650
26044	AP-A-B-1/SYR Apamea	Cement, Alkali Residue	97	1.26	8.5%	104.3 ± 0.4 pMC (> AD 1954)	
26044	AP-A-B-1/SYR Apamea	Cement, Humic Acids	102	3.72	49.7%	230 ± 25	
26045	AP-A-B-2/SYR Apamea	Charcoal, Alkali Residue	98	9.06	103.0%	1875 ± 25	70-220
26046	AP-A-B-3/SYR Apamea	Charcoal, Alkali Residue	104	3.86	72.4%	1495 ± 25	530-640
26047	AP-A-B-4/SYR Apamea	Gery dust, Alkali Residue	63	0.25	0.5%	1730 ± 70	120-530
26048	AP-A-B-5/SYR Apamea	Cement, Alkali Residue	25	0.11	0.9%	1670 ± 150	50-500
26049	AP-A-B-6/SYR Apamea	Charcoal, Alkali Residue	104	6.04	73.3%	1275 ± 25	

Table 3: Detailed measurements presented here give proper insights regarding the quality (amount of carbon should be larger than 1 mg) of collected samples, the possibility of sample fraction (alkali residue, humic acids) enhances the dating accuracy. The 2σ-calibrations were performed using the OxCal 3.5 software (Bronk Ramsey, 2001) and the atmospheric data (INTCAL04) are from PJ Reimer et al. (2004).

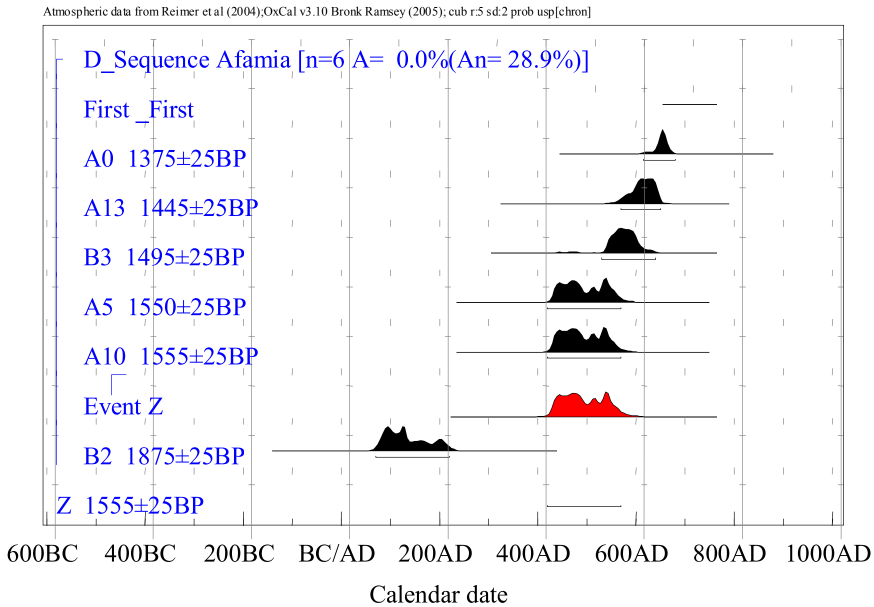

Figure 35: Probability distribution of C^{14} ages (Table 3) after ignoring the unqualified samples obtained from sequential radiocarbon dates using the OxCal 3.5 software (Bronk Ramsey, 2001); the atmospheric data (INTCAL04) are from PJ Reimer et al. (2004). The calibrated dates (black) are presented with 2σ age range (95.4 % density). The age range of the seismic event (red) is determined using Bayesian analysis probability distribution.

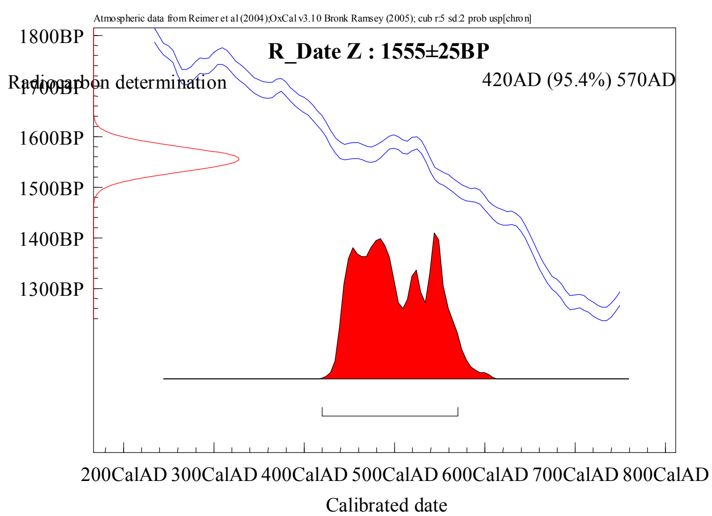

Figure 36: Probability distribution of the Event Z age (420 – 570 AD), presented with 2σ age range (95.4 % density). and obtained using the OxCal 3.5 software (Bronk Ramsey, 2001) and the atmospheric data (INTCAL04) from PJ Reimer et al. (2004).

4 - 8. **The results:**

From the pit of the Agora, the analysis of the debris section in the '*maison aux colonnes trilobées*', and the radiocarbon dating of the collected samples, we have obtained the following results:

- The radiocarbon dating provide the dating of an earthquake in the VI Century, with the calibrated date bracket 420 – 570 AD. In comparison with the historical earthquake catalogue (Sbeinati et al., 2005) this event can be well corelated with the destructive earthquake of May 526 AD, this earthquake had a wide spread destructive effect in the western part of Syria and southern Turkey.
- The Agora shows a partial destruction, as we can noticed from the excavated base of the column, where no horizontal shifting, but only buried fallen stones. We couldn't date the earthquake which destroyed the Agora, and the liquefaction effect.
- The '*maison aux colonnes btrilobees*', shows a total destruction by the VI Century earthquake, and many stages of building, destruction and rebuilding are clear in the section of the debris in the house.
- The estimated intensity in the site can be (VII – VIII) according to EMS-98 scale (Grünthal, 1998).
- The most recent destruction and the liquefaction effect in the Agora appear to be the effect of either the 1157 AD large earthquake or 1170 AD large earthquake (Sbeinati et al., 2005), and the estimated intensity in the site can be (VIII – IX) according to EMS-98 scale (Grünthal, 1998).

V – 5. Collapse the monastery of Deir Dahess

5 – 1. Deir Dahes Site and history

The Deir Dahess (Dahess Monastery complex) is a part of the ancient village Dahess, on the road between Harem and Aleppo city, and it is one of hundreds archeological sites in NW Syria called the Dead Cities as seen in the (Figure 1) in mountain of Barisha and the surrounding region. These sites flourished during the Byzantine time in the 5th and 6th centuries as mentioned by Yakut Al-Hamoui (1178-1229 AD.; see also Al-Hamwi, 1906), a geographer and historian, who visited the region at that time. They are remarkable for their splendid stone building and beautiful design. Castles, villas, monasteries, and temples are scattered over the mountain of Barisha.

The first well documented description of the Dead Cities comes from the tremendous work of Tchalenko in 1953 (Tchalenko, 1953). Deir Dahess represents a typical classical history era with its impressive structures; it consists of church, tower, courtyard, oil press, and domestic rooms, isolated from the Dahess village by a few hundreds of meters. The building material is medium to large size blocks of limestone as seen in the photo of the tower (Figure 43). In the present day condition, one can notice that these monasteries are in ruinous state with remains of some free-standing individual walls and arches. The dates of historical earthquakes that affected the village is difficult to assess due to its location at the junction of the Dead Sea Fault (Ghab segment) and the East Anatolian Fault. Deir Dahess was probably affected by most historical earthquakes that hit northwestern Syria see also chapter III and Figures 35 and 36. The types of destructions related to earthquakes appear as clear fractures, horizontal shifting rocking and waving at the tower, waving walls of the monastery and annex with enlarging, tilting and twisting of buildings. (Figure 43 shows the main parts of the site and Figure 38 indicates the destruction of the tower).

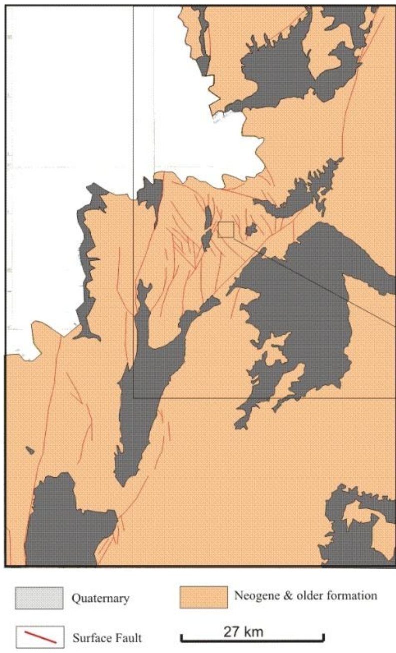

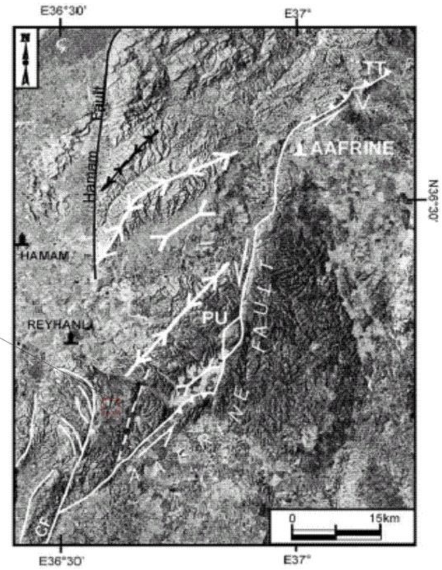

Figure 37: Simplified geological map of Dahess region (modified from Ponikarov, 1963),.

Figure 38: Space photo of Dahess region.

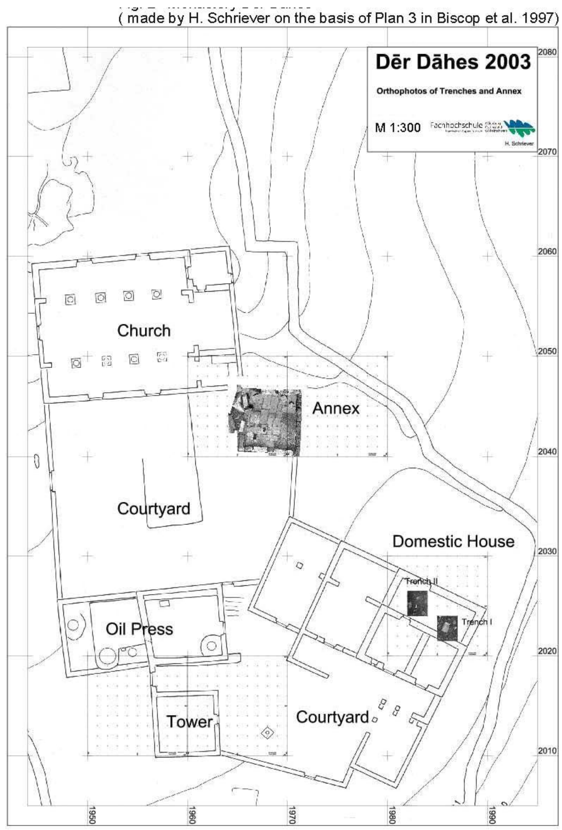

Figure 39: The main parts of Deir Dahess and location of excavation works, redrawn from Biscop (1997) modified by Finkbeiner (2005)

5 – 2. Deir Dahess excavations

We have conducted this field work at Deir Dahess site in the frame of a close collaboration between the German archeological group from Tubingen University, and seismologists from the Syrian Atomic Energy Commission. The preliminary field investigations and previous studies (Sbeinati et al., 1994) show traces of past earthquake destruction such as: waves shape of the fence wall, opened arches in the church, loosing and separation of the stone building and bending wall with destruction to the tower, unified direction of destruction, and finally collapse of somr rooms. The work as we will see in the following paragraphs was concentrated on the annex, the dwelling-house ("Bâtiment d'habitation"), the tower and the Church, in order to discover the buried parts of the complex monastery, dating the destruction and documenting the type of destruction of the tower.

The annex (Figure 39)

This annex is a room at the southeast corner of the church (Biscop et al. 1997, Figure 39); the function of the room at the time of the earthquake is difficult to be determined (Attora, 2005). The building material is made of large size of limestone blocks (200 cm X 60 cm X 60 cm). The room was totally destroyed, except two walls that remained standing; the northern one is still well preserved because of the floor level of the room is ~ 2 m beneath the floor level of the contacting church. Therefore, the opposed side of the wall is in contact with the bedrocksand gives additional strength to the northern wall. In the eastern part of the room, the second wall is partly destroyed and the stone building appears unstable; the remaining amount of the stone building were thrown down to the west direction and the floor was paved by the same type and size of the wall stones. This type of destruction and damage may be attributed to a destructive earthquake and the dating of a trapped thin layer of debris (~ 20 cm) between the fallen wall stones and the floor stones led us to determine the age of destruction; many samples were collected from this trapped debris for radiocarbon dating proposes (Table 4).

The dwelling-house, "Bâtiment d'habitation" (Figure 39)

Since the function of the house host the daily activity, the target of investigating this house is to explore the sequence of destruction which is not removed and kept onsite. This sequence allows us to date the structure composition (remains of the roof pillars) and the rest of the room contents; this features allow us to date the construction and the destruction dates. According to the report of Finkbeiner et al. (2005) "*Studying the documentation it became clear that in the northwest corner of test-trench I, there exists a continuous partition wall, so that in the plan of Biscop et al. (1997, 32, Pl. 2, 3 and 11), the long room of the* *northern enlargement was divided into two rooms. This wall was probably added later, as it does not connect to the two vertical walls. Therefore, the two test-trenches were opened in two different rooms of the later enlargement in the north, and not in one and the same room, as seemed to be the case in the publication of Biscop et al. (1997)*".

A detailed description of test-trench I and test-trench II exists in Finkbeiner et al., 2005 (see also Figures 40, 41 and 42.

Figure 40: A vertical section in the northern wall of the trench I, facing North, it shows the debris of the stone building and the roof tiles.

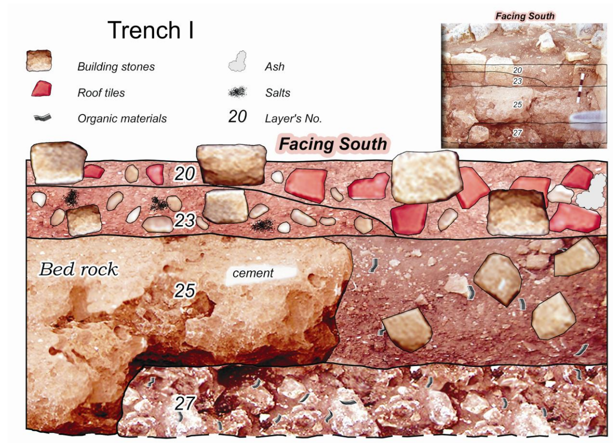

Figure 41: A vertical section in the southern wall; of the trench I, facing South direction, it shows the debris of the stone building and the roof tiles, and the charcoal peaces in dark grey which may the remains of the roof pillars.

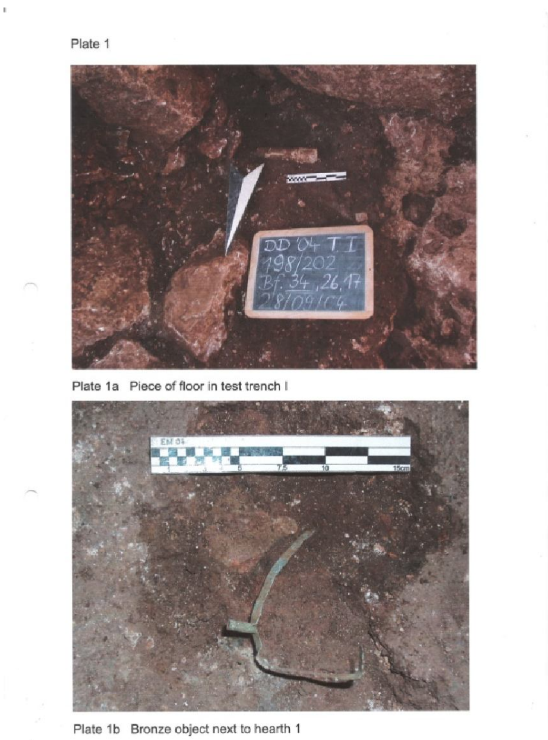

Figure 42: A horizontal section of the base of the trench II, it shows the remains of ashes and animal bones and ash.

The Church

In the church we collected three samples taken from the two layers of the floor and one taken from the cement of the wall, in order to date the age of building and rebuilding stages see (Figure 43).

The Tower

In the tower; a small pit has been done in order to take samples from beneath the fallen stones of the tower. Three samples of charcoal were taken and a coin beneath the corner of the entrance in order to determine the date of its destruction, (Figure 45).

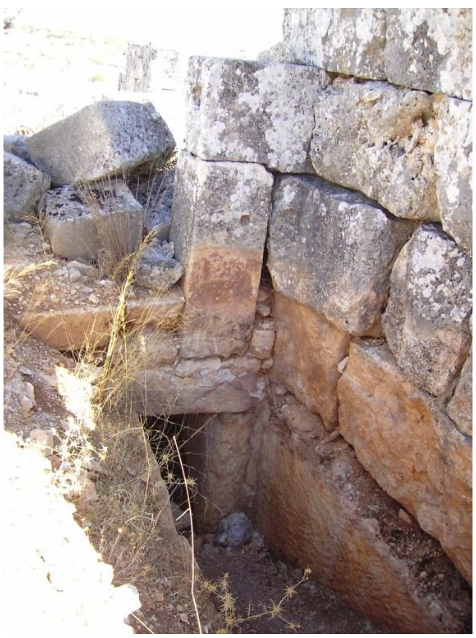

Figure 43: The entrance to a tomb beneath the church showing the location of the taken samples from the cement of the wall and the two floor layers (facing east).

Figure 44: The remaining northern façade wall of the tower showing the bending and the reckoning of the building stones and the destruction (facing SE direction).

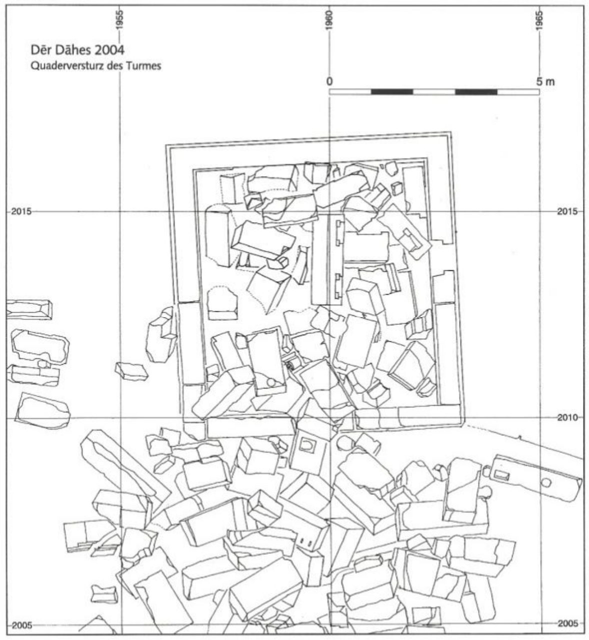

Figure 45: The draw of distribution of the fallen building stones of the tower, and the location of the small pit the coin location by eng. Ellen Schneiders (Finkbeiner, 2005).

Coins and dating results

Two coins were founds in the site: the first one was in the debris in the base layer of the trench I, and the second from the tower (Figure 45). The first one was not so clear and needs farther treatment, the one corresponds to the early VI Century according to the determination of Mr. Kiwan from the Museum of Damascus (personal communication, see also Figure 46 that shows the photo of the coin from the tower).

*Figure 46: Coin from the early Byzantine period; it was also used until the early Islamic period (*Mr. Kiwan personal communication*)*

5 – 3. The results of C14 dating analysis

In order to date the historical , various samples were taken from layers in the annex and from both test-trenches I and II, in the dwelling-house, from the base of the tower, and from the floor and the wall cement of the church. Samples from the annex: Most of them stem from different stratigraphic units of test-trench II. In detail, the samples come from the fallen layer of roof-tiles above *floor 1*, from *floor1*, from the fill between the two floors (*floors 1* and *2)* and from *floor 2*. Samples of ashes were taken from the hearths (*hearths 1, 2* and *3*). Other samples come from test-trench I and from the tower and the church. The results of analysis of the total number of samples for the two campaigns are shown in Table 4 and from Figure 47.

The two events age took place in the following brackets:
Event Z: the wider range from 430 to 940 AD, the narrow range from 650 to 940 AD.
The Event Y: the wider range from 1270 to 1960 AD, the narrow range from 1390 to 1660 AD.

Sample Name	Fraction	Current (% of normal)	Amount of carbon analysed (mg)	Fraction carbon content (%)	14C age (years BP)	Calib. age (BC/AD)
T-4/SYR Deir Dahess	Charcoal, Alkali Residue	102	5.88	74.1%	1100 ± 20	890-990
T-5/SYR Deir Dahess	Charcoal, Alkali Residue	95	5.93	74.2%	960 ± 25	1020-1160
C-10/SYR Deir Dahess	Cement, Alkali Residue	100	1.59	0.3%	1190 ± 20	
C-10/SYR Deir Dahess	Cement, Humic Acids	103	3.62	40.0%	1175 ± 20	770-940
T-1/SYR Deir Dahess	Charcoal, Alkali Residue	102	6.22	77.0%	166 ± 20	1660-1960
F-2/SYR Deir Dahess	Cement, Alkali Residue	99	2.14	0.2%	675 ± 25	1270-1390
A-50/SYR Deir Dahess	Charcoal, Alkali Residue	10	0.05	2.3%	1870 +340/ -320	
A-50/SYR Deir Dahess	Charcoal, Humic Acids	89	0.59	10.7%	1490 ± 40	430-650
A-56/SYR Deir Dahess	Cement, Alkali Residue	100	1.24	0.6%	1500 ± 25	460-640
A-52/SYR Deir Dahess	Charcoal, Humic Acids	92	0.62	7.9%	1955 ± 40	40BC-130AD
F-1/SYR Deir Dahess	Cement, Alkali Residue	101	1.42	0.2%	2110 ± 25	BC 250-50

Table 4: Detailed measurements presented here give proper insights regarding the quality (amount of carbon should be larger than 1 mg) of collected samples, the possibility of sample fraction (alkali residue, humic acids) enhances the dating accuracy. The 2σ-calibrations were performed using the OxCal 3.5 software (Bronk Ramsey, 2001) and the atmospheric data (INTCAL04) are from PJ Reimer et al. (2004); Samples with low carbon content (< 1 mg)do not provide reliable age and are are not considered in the analysis..

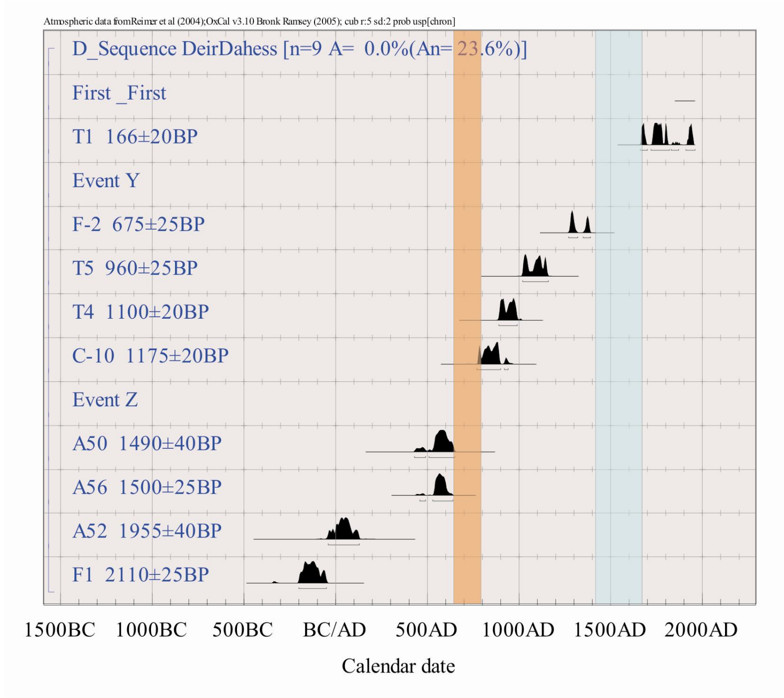

Figure 47: Probability distribution of C^{14} ages (Table 15) after ignoring the unqualified samples obtained from sequential radiocarbon dates using OxCal 3.10 (Bronk Ramsey, 1998). The calibrated dates (black) are presented with 2σ age range (95.4 % density). The age range of the first seismic Event Z is the first earthquake (orange rectangle), the Event Y is the second earthquake (light blue rectangle), is determined using Bayesian analysis probability distribution.

The collected samples of the first year, have been analysed separately as two series: Series A were taken from the annex gives the date of destruction in the annexed room within the range 1426 to 1486 AD which may be correlated to the earthquake of 1408 AD. Series B were taken from the dwelling-house between 500 and 600, with the curve of distribution the data suggesting a date of 530 A.D. This date may be correlated with the large earthquake of 526 A.D. that took place in the region of Aleppo and Antioch (Figures 48, 49, and 50).

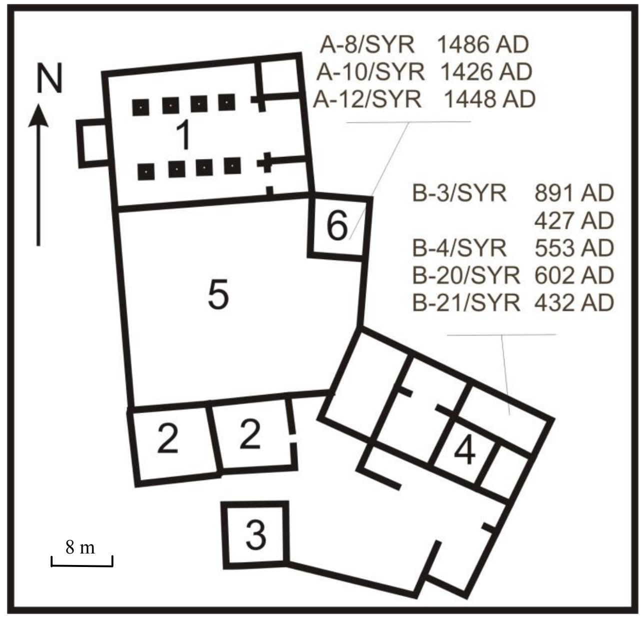

Figure 48: Simplified location map of Deir Dahess and the dating results of samples taken from no. 4 and no. 6 sites,1) Church, 2) Olive oil press, 3) Tower, 4) Domestic rooms, 5) Back yard, 6) Annexed room.

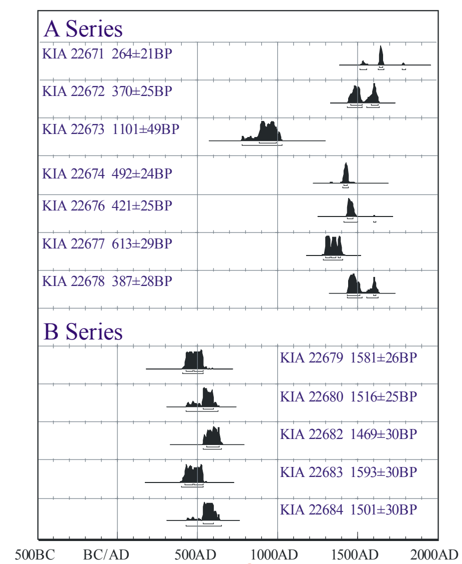

Figure 49: Probability distribution vs calendar age for the main fractions of all sample. The 2σ-calibrations were performed using the OxCal 3.5 software (Bronk Ramsey, 2001) and the atmospheric data (INTCAL04) are from PJ Reimer et al. (2004).

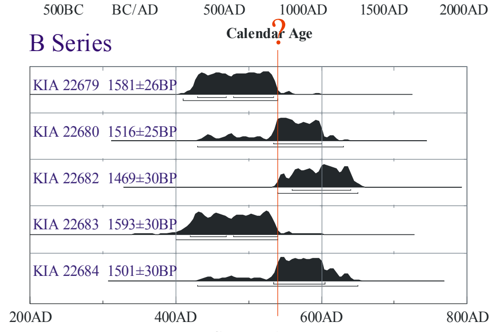

Figure 50: Probability distribution vs calendar age for the main fractions of the samples from Series B. The 2σ-calibrations were performed using the OxCal 3.5 software (Bronk Ramsey, 2001) and the atmospheric data (INTCAL04) are from PJ Reimer et al. (2004).

5 - 4. The results:

The monastery complex of the Deir Dahess had been affected deeply by two destructive earthquakes:

- The first earthquake: took place between the dates of construction of: 1) the church (age of wall cement and the first layer of the floor), 2) the two excavated rooms (the age of the wood remains of the roof pillars in the roof tiles level and the base of the trenches I and II), and the destruction dates of: 1) the second floor age of the church, 2) the two excavated rooms (the debris level directly beneath the roof tiles). This earthquake is represented as event Z in the results of radiocarbon dating analysis within the age of wider range from 430 to 940 AD, and narrow range from 650 to 940 AD. In comparison with the historical earthquake catalogue (Sbeinati et al., 2005) showing a close coloration with the earthquake of 526 AD. The estimated seismic intensity in the site is I > VIII on EMS-98 scale (Grünthal, 1998).

- The second earthquake took place after the age of the coin taken from the tower and the age of the trapped debris under the fallen building stones in the annex. This earthquake is represented as Event Y in the results of the radiocarbon dating analysis within the age of wider range from 1270 to 1960 AD, the narrow range from 1390 to 1660 AD. In comparison with the historical earthquake catalogue (Sbeinati et al., 2005) showing a close coloration with the earthquake of 1408 AD. The estimated seismic intensity in the site is I > VIII, on EMS-98 scale (Grünthal, 1998).

V – 6. Conclusion

From the obtained results of the detailed paleoseismological and archeoseismological investigations, the analysis of destruction types, radiocarbon dating analysis and the comparison with the historical earthquake catalogue for the four archeological sites of Al-Harif, Krak des Chevaliers, Apamea, and Deir Dahes, we can conclude to following points:

6 – 1. Al-Harif:

The analysis of field data in archeoseismology, paleoseismology and tufa coring provide some constraints on the successive past earthquakes along the DSF at the Al Harif Roman aqueduct site (Figures 12 and 13). The damage and repair of the aqueduct are here related to the total 13.6 m of left-lateral fault offset since the aqueduct building (Figure 5). In addition, the tufa successive growth and interruptions visible in cores provide a direct relation between the water flow and the aqueduct function east and west to the fault zone. The correlation and timing coincidence between the faulting events visible in trenches, aqueduct building damage and repair (see also section 3.4), combined with tufa growth and interruptions provide a better constraint on the timing of the successive large earthquakes:

- Event W observed in trench C occurred before BC 800-510 (unit f) and after BC 3400 – 300 (unit g). This faulting event is visible only in trenches and hence cannot be correlated with damaging events of archeoseismic and tufa cores. However, according to the textual inscriptions found in different archeological sites in Syria, a damaging earthquake sequence around BC 1360-1370 affected Ugharit near Latakia in Syria, and Tyre further south in Lebanon and east of the DSF (Sbeinati et al., 2005) may be correlated to event W.

- Event X identified in trenches A and C between BC 350 – 30 AD and AD 532 – 641 postdates the aqueduct building (younger than 65 BC i.e., the onset of Roman time in the Middle East and older than AD 70 – 230 of early tufa deposits). Event X also predates the onset of BR 3 tufa growth (see Br 3-1 dated AD 410-600). Similarly, the tufa growth interruption in BR 5 (after Br 5-2 dated BC 110-130 AD) and onset of tufa in BR 6 (after Br 6-1 dated BC 400 – 250 AD) coincide with the occurrence of the first damaging event X. The first earthquake faulting that damaged the aqueduct took place between AD 70 – 230 and AD 410 – 600.

- Event Y is younger than AD 650-810 (unit d in trench A) and older than AD 540-650 (unit d3 in trench C). This event postdates the first rebuilding phase of the aqueduct recognized from the fallen wall in excavation I and related cement sample AQ - CS4 (AD 532 – 641) and tufa sample

AQ - CS3-2 (AD 560 – 690). Event Y predates the dragged wall fragment and related cement sample AQ-CS1 (AD 650 – 780) and tufa sample AQ - CS3-3 (AD 639 – 883, Table 1). Core samples of tufa deposits provide a bracket of the second damaging earthquake faulting between Br 4-3 (AD 540-980) and Br 3-4 (AD 770-940). The second interruption in both BR 5 and BR 6 may also be contemporaneous of the damaging event. Taking into account only the archeoseismic results, we can conclude that Event Y likely occurred between AD 560 – 690 and AD 650 – 780; however, the consistency between all dates of paleoseismic, archeoseismic and tufa analysis suggest an earthquake event close to AD 650. Cement samples CS-1 and tufa sample CS3-3 also indicate a rebuilding period after event Y, at the end of the Byzantine time and beginning of the Islamic period (5^{th} to 6^{th} century AD).

- Event Z observed in trenches A, B and C is identified as younger than AD 960-1060, and older than AD 1030-1260. The definite interruption of tufa growth in all cores and mainly BR 5 and BR 6 indicates the final stop of water flow over the bridge section. The interruption postdates sample Br 6-8 (A.D. 900 – 1160) and can be correlated with the 29 June1170 large earthquake that affected the Missyaf region (Mouty and Sbeinati, 1988; Sbeinati et al., 2005).

The Missyaf segment of the Dead Sea Fault experienced four large earthquakes with event W in BC 3400 – 510, event X in AD 70 - 600, event Y in AD 560 – 780 (probably close to AD 650) and event Z in AD 960 – 1260 (probably in AD 1170). Using the Oxcal program (Bronk Ramsey, 2001) an attempt of sequential ordering of dates and events presented in Figure 12 provides a time density function for W (BC 2300 – 500), X (AD 160 – 510), Y (AD 625 – 690) and Z (AD 1010 – 1210). The timing of events obtained from the correlation and sequential distribution clearly indicate a temporal clustering of 3 large seismic events X, Y and Z (Figure 12) after event W that may indicate a relatively long period of quiescence and event W. Although our data and observations cannot precisely constrain event W, it may be correlated with the BC 1365 large earthquake that affected several sites near the Missyaf fault segment as reported in the historical seismicity catalogue of Syria (Sbeinati et al., 2005). The Missyaf fault behavior is comparable to the temporal cluster of large seismic events that occurred on other comparable major strike-slip faults (e.g., San Andreas Fault; Weldon et al., 2004; Jordan Valley Fault segment of the DSF, Ferry et al., 2007).

6 – 2. Krak des Chevaliers:

- The fortress has the scars of different stages building and rebuilding stages, and evidences of earthquake destructions.

- the investigation of the rupture of the Mamluk bath indicates the existence of minor effects induced by the earthquake after 1271 AD the starting date of the Mamluk domination the citadel (the building age of the bath)and lays in the range between 1275 AD and 1295 AD (according the results of the radiocarbon dating). This event is not clearly identified in the historical earthquake catalogue, but the only one that could be correlated is that of 22 March1287 with a seismic intensity VII – VIII in Lattakia. This studied crack of the Mamluk bath refers to a possible unknown moderate earthquake if local (or a large distant one in the region), and with a seismic intensity of about VI – VII on the EMS-98 scale (Grünthal, 1998).

- The southern part of the outer wall-fence was rebuilt rapidly after the 29 June 1170 earthquake by the Hospitallers and in 1217 by the king Andrew II of Hungary. They strengthened the outer walls and financed the guarding troop, untrimmed new basaltic rocks (to replace previous limestone rock pieces of wall) as seen in bright brown colour in Figure 21 and in red in (Figure 24). Some restoration works has been done by the French archeological mission during 1936; the used stones are small cut limestone blocks as seen in yellow in (Figure 23).

- The 10° sharp deflections in the basaltic walls are clear in the southern part and in the northern eastern one of the outer wall-fence. It corresponds to a construction design system to strengthen the long standing walls presented in strait red lines (Figures 22, 23, and 24). This deflection that is of the same age of the outer wall-fence rebuilding has actually no relation with the studied fracture and it has no continuation in the bedrock.

- The crack in the southern outer fence extends in the Mamlouk bath and the basaltic bedrock in N-S direction in parallel to the Missyaf fault (Figures 17, 22, and 25).

- The trench dug in the Mamlouk bath discovers a channel of water disposal affected by the crack (Figures 25 and 26).

6 – 3. Apamea:

The obtained results from the pit of the Agora, the analysis of the debris section in the 'maison aux colonnes bilobées', and the radiocarbon dating of the collected samples yield:

- The radiocarbon dating results sign to an earthquake in the VI Century, having the calibrated date (420 – 570 AD) with (95.4 % density). In comparison with historical earthquake catalogue (Sbeinati et al., 2005) this event is very convenient with the destructive earthquake of May 525 AD, this earthquake had a wide spread destructive effect on the western part of Syria and Lebanon.

- The Agora shows a partial destruction, as we can noticed from the excavated base of the column, where no horizontal shifting, but only buried fallen stones. We couldn't date the last earthquake which destroyed the Agora totally, and the well presented liquefaction effect, it is more probable to be the effect of earthquake 1170 AD according to the comparison with the historical earthquake catalogue (Sbeinati et al., 2005), and the estimated intensity in the site can be (VIII – IX) according to EMS-98 scale (Grünthal, 1998).

- The 'maison aux colonnes bilobees', had been totally destroyed during the VI Century earthquake, and many stages of building, destruction and rebuilding are clear in the section of the debris in the house.

- The estimated intensity in the site can be (VII – VIII) according to EMS-98 scale (Grünthal, 1998).

6 – 4. Deir Dahess:

The monastery complex of the Deir Dahess was severely affected by two destructive earthquakes:

- The first earthquake: took place between the dates of construction of: 1) the church (age of wall cement and the first layer of the floor), 2) the two excavated rooms (the age of the wood remains from the roof pillars in the roof tiles level and the base of the trenches I and II), and the destruction dates of: 1) the second floor age of the church, 2) the two excavated rooms (the debris level directly beneath the roof tiles). This earthquake is represented as event Z ranging from a wide period between 430 and 940 AD obtained from the radiocarbon dating analysis , and a narrow range from 650 to 940 AD. The comparison with the historical earthquake catalogue (Sbeinati et al., 2005) indicates a close correlation with the earthquake of 526 AD. The estimated seismic intensity in the site is I > VIII on the EMS-98 scale (Grünthal, 1998).

- The second earthquake took place after the age of the coin taken from the tower and the age of the trapped debris under the fallen building stones in the annex. This earthquake is represented as Event Y in the probability analysis of the radiocarbon dating and corresponds to wider age range from 1270 to 1960 AD; the narrow range is from 1390 to 1660 AD. The comparison with the historical earthquake catalogue (Sbeinati et al., 2005) allows a correlation with the earthquake of 1408 AD. The estimated seismic intensity in the site is I > VIII, on EMS-98 scale (Grünthal, 1998).

References

Al-Hamoui, Y., (1906) *Moujam al-bouldan* (Dictionary of twons and cities), Eds ? Cairo, pp ?

Altunel et al., (2009). Archeological sites (Tell and Road) offset by the Dead Sea Fault in the Amik Basin, southern Turkey", *Geophys. J. Int.* (in press).

Ambraseys, N & Melville, C. P., (1988 a). Historical evidence of faulting in Eastern Anatolia and northern Syria, *Annali di Geofisica* 28, 337 – 343

Ambraseys, N & Melville, C. P., (1988 b). *An analysis of the eastern Mediterranean earthquake of 20 May 1202,* in *Historical Seismograms and Earthquakes of the World,* pp. 181-200, ed Lee, W., Academic Press, San Diego.

Ambraseys, N.N., & Jackson, J. A. (1998). Faulting associated with historical and recent earthquakes in the Eastern Mediterranean region, *Geophys. J. Int.* **133**, 390-406.

Ambraseys, N. N. (2006), Earthquakes and Archeology, *J. Archaeo. Sci.*, *33*, 1008-1016,

Attoura, H. (2005). Bericht über die archäoseismologischen Untersuchungen in Dēr Dahess (Syrien) 2003; in Baghdader Mitteilungen 35.

Balty, J. et J.-C. (1999). *Apamée : site et musée*, Damas, (Ministry of Culture of the Syrian Arab republic).

Biscop, J.-L. (avec la collaboration de D. Orssaud et M. Mundell Mango) (1997). 'Dair Déhès, monastère d'Antiochène; Étude Architecturale', *Bibliothèque Archéologique et Historique - T. CXLVIII* (Beyrouth).

Brew, G., Lupa, J., Barazangi, M., Sawaf, T., Al-Imam, A., Zaza, T., (2001). Structure and tectonic development of the Ghab basin and the Dead Sea fault system, Syria, *J. Geol. Soc. London* 158, 665-674.

Bronk Ramsey C., (2001). Development of the Radiocarbon Program OxCal, Radiocarbon, 43 (2A) 355-363.

Daeron, M., Benedetti, L., Tapponnier, P., Sursock, A. & Finkel, R. (2004). Constraints on the post _25-Ka slip rate of the Yammouneh fault (Lebanon) using in situ cosmogenic 36Cl dating of offset limestone-clast fans. *Earth and Planet. Sci. Letters* 227, 105–119.

Daeron, M., Klinger, Y., Tapponnier, P., Elias, A., Jacques, E. & Sursock, A. (2005). Sources of the large A.D. 1202 and 1759 Near East earthquakes. *Geology*, 33, 529–532.

Dubertret, L., 1955. Carte géologique de Syrie avec notice explicative. République Syrienne, Ministère des travaux publics (1:200,000).

Ellenblum, R., Marco, S., Agnon, A., Rockwell, T., and Boas, A., (1998). Crusader castle torn apart by earthquake at dawn, 20 May 1202: *Geology*, v. 26, p. 303-306.

Farr, T., and M. Kobrick (2000). Shuttle radar topography mission produces a wealth of data, *EOS Trans. AGU* **81,** 583–585.

Ferry, M., M. Meghraoui, N. Abou Karaki, M. Al-Taj, H. Amoush, S. Al-Dhaisat, and M. Barjous (2007). A 48-kyr-long slip rate history for the Jordan Valley segment of the Dead Sea Fault, *Earth Planet. Sci. Lett.*, *260*, 394-406,

Finkbeiner, U. et al., (2005). Report for the year 2004/2005 from Tübingen University to APAME Project (ICA3 – 2002 – 10060 INCO – MED).

Ford, T. D., and H. M. Pedley, (1996) A review of tufa and travertine deposits of the world, Earth Science Reviews 41, 117-175.

Galli, P. (1999). Active tectonics along the Wadi Araba-Jordan Valley transform fault, *J. Geophys. Res.* 104, 2777-2796,

Ginat, H., Y. Enzel, and Y. Avni (1998). Translocated Plio-Pleistocene drainage systems along the Arava Fault of the Dead Sea Transform, *Tectonophysics*, *284*, 151-160,

Garfunkel, Z., Zak, I., & Freund, R. (1981). Active faulting in the Dead Sea rift, *Tectonophysics* **80**, 1-26.

Gomez, F., Meghraoui, M. et al.. (2003). Holocene faulting and earthquake recurrence along the Serghaya branch of the Dead Sea fault system in Syria and Lebanon. *Geophys. J. Int.*, 153, 658–674.

Gomez, F., et al., (2007). Global positioning system measurements of strain accumulation and slip transfer through the restraining bend along the Dead Sea Fault system in Lebanon, *Geophys. J. Int.* 168, 1021-1028.

Gomez, F., T. Nemer, C. Tabet, M. Khawlie, M. Meghraoui and M. Barazangi, (2007). Strain partitioning of active transpression within the Lebanese restraining bend of the Dead Sea Fault (Lebanon and SW Syria), *Geological Society, London, Special Publications* 2007; v. 290; p. 285-303 doi:10.1144/290.10.

Grootes, P.M., Nadeau, M. J., and Rieck, A. (2004). ^{14}*C-AMS at the Leibniz-Labor: Radiometric dating and isotope research.* Nucl. Inst. Meth. *B223-224*, 55-61.

Grootes, P.M., Nadeau, M. J., Roth, S., Andersen, N., Huels, M., Meghraoui, M., and Sbeinati, R. (2006). 1000 years of usage: The life story of a Roman Aqueduct provides tectonic information, *American Geophysical Union, Fall meeting* 2006, *abstract* T13B-0500.

Grünthal, G. (1998) European Macroseismic Scale 1998. Cahiers du Centre Européen de Géodynamique et de Seismologie. Conseil de l’Europe.

Guidoboni, E., A. Comastri, and G. Traina (1994). *Catalogue of ancient earthquakes in the Mediterranean area up to the 10th century*, 504 pp., ING-SGA, Bologna.

Guidoboni, E., F., Bernardini and A. Comastri, (2004). The 1138-1139 and 1156-1159 destructive seismic crisis in Syria, south-eastern Turkey and northern Lebanon, J. Seismology 8, 105-127.

Ibn Al-Athir, Ezz Ad-Din *(AH 491-541, AD 1097-1146)*, *Al-Kamil fi Al-Tarikh (The complete in history),* vol. 8, 9, 10, 11, 12, Ed. Dar Sader, Beirut 1982.

Issar, A.S. (2003). *Climate changes during the Holocene and their impact on hydrological systems*. International Hydrology Series. Cambridge University Press, Cambridge, 127 pp.

Klinger Y., J. P. Avouac, N. Abou Karaki, L. Dorbath, D. Bourles, J.L. Reyss, (2000). Slip rate on the Dead Sea transform in northern Araba Valley (Jordan), *Geophys. J. Int.* 142755-768.

Marco, S., M. Hartal, N. Hazan, L. Lev, and M. Stein (2003). Archaeology, history, and geology of the A.D. 749 earthquake, Dead Sea Transform, *Geology (Boulder)*, *31*, 665-668.

Marco, S., Rockwell, T.K., Heimann, A., Frieslander, U., Agnon, A., (2005). Late Holocene activity of the Dead Sea Transform revealed in 3D paleoseismic trenches on the Jordan Gorge segment. Earth Planet. Sci. Lett. 234, 189–205.

Marco, S., (2008). Recognition of earthquake-related damage in archaeological sites—3 Examples from the Dead Sea fault zone, *Tectonophysics* 453, 148–156.

McClusky, S., R. Reilinger, S. Mahmoud, S. D. Ben, and A. Tealeb (2003). GPS constraints on Africa (Nubia) and Arabia plate motions, *Geophys. J. Int.*, *155*, 126-138,

Meghraoui, M., F. Gomez, R. Sbeinati, J. Van der Woerd, M. Mouty, A. Darkal, Y. Radwan, I. Layyous, H. M. Najjar, R. Darawcheh, F. Hijazi, R. Al-Ghazzi, and M. Barazangi (2003). Evidence for 830 years of seismic quiescence from paleoseismology, archeoseismology and historical seismicity along the Dead Sea fault in Syria, *Earth Planet. Sci. Lett.*, *210*, 35-52,

Nemer, T. and M. Meghraoui, (2006). Evidence of coseismic ruptures along the Roum fault (Lebanon): a possible source for the AD 1837 earthquake, *J. of Struct. Geol.* 28, 1483–1495.

Nemer, T., Meghraoui, M. and Khair, K., (2008). The Rachaya-Serghaya fault system (Lebanon): Evidence of coseismic ruptures, and the AD 1759 earthquake sequence, *J. Geophys. Res.*, 113, B05312, doi:10.1029/2007JB005090.

Niemi, T. M., H. Zhang, M. Atallah, and J. B. J. Harrison (2001). Late Pleistocene and Holocene slip rate of the Northern Wadi Araba fault, Dead Sea Transform, Jordan, *J. Seismol. 5*, 449-474, Nur, A., and Cline, E. H., (2000). Poseidon's Horses: Plate tectonics and earthquake storms in the late Bronze age Aegean and Eastern Mediterranean, *J. Archaeo. Sci.* 27, 43-63.

Ponikarov, V.P. 1963. The geological map of Syria, scale 1:200 000. Ministry of Industry, Syrian Arab Republic.

Reilinger, R., McClusky, S. et al. (2006). GPS constraints on continental deformation in the Africa–Arabia–Eurasia continental collision zone and implications for dynamics of plate interactions. *J. Geophys. Res.* 111, doi:10.1029/ 2005JB004051.

Reimer, P. J., and 28 authors, 2004, IntCal04 Terrestrial radiocarbon age calibration, 26 - 0 ka BP. *Radiocarbon* 46:1029-1058.

Sbeinati et al., (2010), Timing of Earthquake Ruptures at the Al Harif Roman Aqueduct (Dead Sea fault, Syria) from Archeoseismology, Paleoseismology and Tufa Cores, submitted to Geological Society of America Bulletin, Special Issue on "Ancient Earthquake".

Sbeinati, M. R.(2006). First Annual Report by DGAM and AECS for the EC Project APAME entitled: 'The Impact of Large Earthquakes on the Archeological sites and Cultural Heritage in the Middle East'. Sbeinati, M. R., R. Darawcheh and M. Mouty (2005). The historical earthquakes of Syria: an analysis of large and moderate earthquakes from 1365 B.C. to 1900 A.D, *Ann. Geophys.*, *48*, 347-435.

Sbeinati, M. R., R. Darawcheh (1997). Archaeological evidences of earthquake damage in Syria**",** Atomic Energy Commission of Syria, (A report presented to the International Atomic Energy Agency under the research project entitled Seismic data fore sitting and site revalidation of nuclear facilities, No. 6247/R3/RB), 1997.

Sbeinati M. R., R. Darawcheh, and M. Mouty (1994). Field archeological evidences of seismic effects in Syria, in *Materials of the CEC Project "Review of Historical Seismicity in Europe"* – vol. 2., Albini P. and A. (edit.), CNR – Consiglio Nazionale delle Ricerche, Milano, Italy.

Sbeinati, M. R. (1994). "Evidences of seismic effects on selected archaeological sites in Syria", internal report on scientific field study, AECS-G/RSS 78, Atomic Energy Commission of Syria, Damascus.

Shimazaki, K. and T. Nakata, (1980). Time-predictable recurrence model for large earthquakes, *Geophys. Res. Letters* 7, 279-282.

Stiros, S. C. and Jones, R. E., (1996). *Archeoseismology*, Fitch Laboratory occasional paper 7, British School of Athens, Greece, 268 pp.

Stiros, S. C. (1996). Identification of earthquakes from archaeological data: methodology, criteria and limitations, in Archeoseismology, edited by (Stiros, S. C. and Jones, R. E.), Fitch Laboratory occasional paper 7, British School of Athens, Greece, 268 pp. 129-152.

Stuiver, M., P. J. Reimer, E. Bard, J. W. Beck, G. S. Burr, K. A. Hughen, B. Kromer, G. McCormac, J. van der Plicht, and M. Spurk (1998). INTCAL98 Radiocarbon Age Calibration, 24000-0 cal BP, *Radiocarbon*, *40*, 1041-1083,

Tchalenko, G. (1953). Villages antiques de la Syrie Nord, le massif du belus à l'époque Romaine, I – IV, *Institut Franccais d'archeologie de Beyrouth, Bibliotheque archeologique et historic, Tome L*.

Tlas, M., and M. W. Al-Jallad (1990). Kalaat Al-Houssen (Huussen Al-Akrad), by *Dar Tlas Publisher,* ***city, number of pages*** .

Trifonov, V. G., et al. (1991). Levant Fault zone in northwest Syria, *Geotectonics* 25, 145-154.

Wdowinski, S., Y. Bock, G. Baer, L. Prawirodirdjo, N. Bechor, S. Naaman, R. Knafo, Y. Forrai, and Y. Melzer (2004). GPS measurements of current crustal movements along the Dead Sea fault, *J. Geophys. Res.*, *109*, B05403,

Weldon, R., K. Scharer, T. Fumal, G. Biasi, (2004). Wrightwood and the earthquake cycle: What a long recurrence record tells us about how faults work, *GSA Today* 14, 4-10.

Wells, D. L., and K. J. Coppersmith (1994). New empirical relationships among magnitude, rupture length, rupture width, rupture area, and surface displacement, *Bull. Seism. Soc. Am.* 84**,** 974–1002.

Wesnousky, S. G., (2006). Predicting the endpoints of earthquake ruptures, *Nature* 444, 358-360.

Wessel, P., and H. F. Smith (1998), New, improved version of the Generic Mapping Tools Released, *EOS Trans. AGU*, *79*, 579.

Zakariyya, W. (1984) *Jawla athariyya fi baed al-bilad al-Chamiyya* (An archaeological tour at some Syrian towns), Dar al-Fikr, Damascus.

Zilberman, E., R. Amit, N. Porat, Y. Enzel, and U. Avner, (2005). Surface ruptures induced by the devastating 1068 AD earthquake in the southern Arava valley, Dead Sea Rift, Israel, *Tectonophysics* 408, 79 – 99.

CHAPTER VI

SEISMIC HAZARDS OF SYRIA

VI. SEISMIC HAZARDS OF SYRIA

VI – 1. Introduction

This chapter presents the main results of our analysis of the earthquake databank of Syria and neighbouring regions as integrated into the seismic hazard evaluation. As described in previous chapters, the catalogue of seismic events that includes the instrumental and historical seismicity, archeoseismicity and paleoseismicity constitutes our databank. Seismic sources are mapped fault segments fault branches of the northern Dead Sea Fault accompanied by their parameters (fault dimensions, average slip and slip rate, focal mechanism, and the attributed maximum magnitude). Previous seismic hazard assessments of the Dead Sea Fault regions covered the whole Middle East and were mainly based on compiled seismicity catalogues that span ~ 4000 years (Ben Menahem, 1979; Plassard and Kogoj, 1981; Amiran, 1990; Guidoboni, 1994; Ambraseys, 2001; Al Tarazi et al., 2007). The used fault mapping were very often approximative and their parameters roughly determined or inexact. The seismic hazard assessment of the northern Dead Sea Fault in Syria needed further investigations on fault segments using multidisciplinary approach in order to better understand the seismic cycle and earthquake generation.

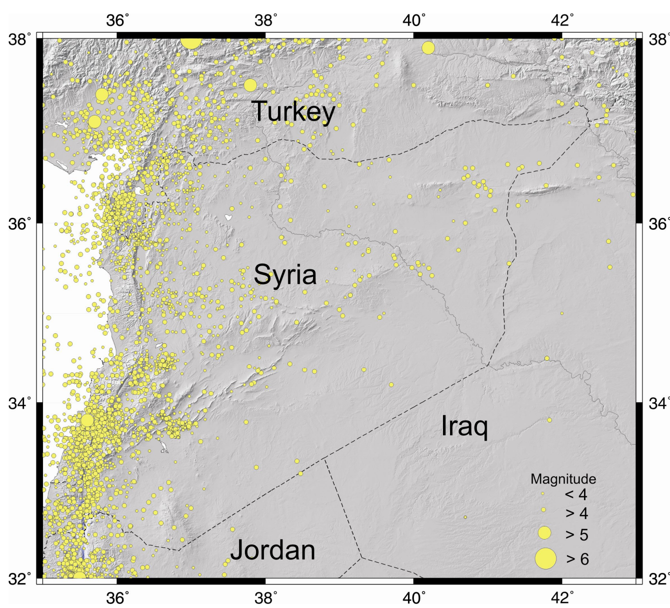

Fig. 1 Map of instrumental seismicity for 1900-2008

The previous databank of instrumental seismicity very often depended on the ISC (International Seismological Centre) and the record of local recent earthquakes (more recent than

1980). The used historical seismicity also depended mainly on previous published catalogues without any further analysis of new documents that may justifies the seismicity parameters.

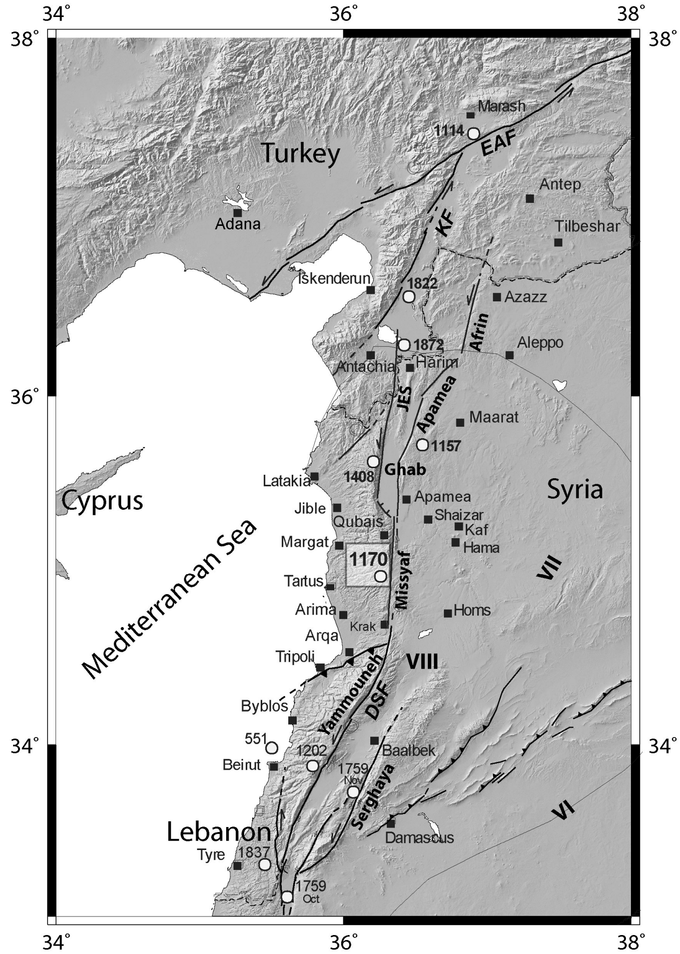

Figure 2: Major historical earthquakes (yellow dots) and areas of maximum damage for the 29 June 1170 earthquake (in yellow, with white Roman number for EMS98 intensity; Grunthal, 1998) as recorded along the northern Dead Sea Fault (Guidoboni, 2004; Sbeinati et al., 2005). The area of maximum damage (Io = IX) for the AD 1170 large earthquake is along the Missyaf fault segment and Ghab (see GF and Figure 3) and overlaps with the maximum intensity VIII (MSK, black dashed line) as drawn by Ambraseys (2009).

The long term seismicity of Syria of the last 4000 years indicates the occurrence of large earthquakes that are replaced by a period of quiescence in the last ~ 200 years (Figures 1 and 2). The combination between the instrumental seismicity and historical seismicity shows the existence of a seismic gap along the Missyaf segment of the Dead Sea Fault (Figure 1). Large earthquakes reaching a magnitude as high as Mw 7.6 (along the Yammouneh fault segment in Lebanon) are homogeneously distributed along the Dead Sea Fault (Figure 2; Ambraseys and Jackson, 1998). The recorded low-level seismicity with M < 5 during the last century roughly delimits the Dead Sea

Fault and does not represent the fault capability and related hazard level. Previous seismic hazard evaluation from deterministic models in Damascus region indicate values of acceleration ranging between 0.3 and 0.6 g (Nemer, 2005), whereas probabilistic models show 0.17 g although with a return period of 2500 years (Elnashai and El-Khoury, 2004). This large difference between estimated accelerations reflects the effect of the multidisciplinary approach (seismicity catalogue, fault characteristics and parmeters and paleoseismic results used by Nemer (2005) in the databank construction and indicates the level of uncertainties when using only a compiled seismicity catalogue.

Our objective in this work is to construct a realistic seismic hazard assessment and map based on: i – The seismicity catalogue of Syria covering the last century and based on 2 main sources, i.e., the local and neighbouring seismic networks (Syria, Turkey, Lebanon, Jordan and Israel) and the ISC, added with the focal mechanism solutions (from Harvard CMT and recent studies; see chapter III); ii – the recently developed parametric and unified historical seismicity catalogue (see Chapter IV); iii – The detailed mapping of active fault zones in Syria, Lebanon, Turkey and Jordan (Figure 2), and the study of their parameters, including results of slip rate determination; and iv – the archeoseismic and paleoseismic results obtained from our field investigations.

VI – 2. Applied methodology

Several approaches were developed recently for the seismic hazard assessment in seismically active regions (Reiter, 1991). Most of recent works use 1) the deterministic hazard assessment that defines the seismic source area which may generate an earthquake of specified size (Magnitude), and a peak ground acceleration calculated at the specific distance to the site (Costa et al., 1993); or 2) the probabilistic seismic hazard analysis based on the Gutenberg-Richter law (see also chapter II) and the statistical analysis of the earthquake activity (Cornell, 1968). The probabilistic approach has the advantage of statistical analysis of input data that corresponds to time-independant (Poisson) analysis or time-dependant (conditional probability) calculations.

I applied in this work the probabilistic approach using the earthquake databank and its analysis that include the characteristic earthquake determination as untruncated value of magnitudes. This approach takes into account the uncertainty of the magnitude determination as calculated from the modified Gutenberg-Richter relation (b-value). The fault parameters support the size of characteristic earthquakes and associated long term rate of active deformation (seismic moment rate) as obtained from empirical relations (Wells and Coppersmith, 1994).

In order to generate maps of probabilistic seismic hazards PSHA for the Syrian territory, I applied the CRISIS 2007 software developed by M. Ordaz, A. Aguilar and J. Arboleda at the

Instituto de Ingeniería, UNAM, Mexico. CRISIS computes seismic hazard using a probabilistic model that considers the rates of occurrence, attenuation characteristics and geographical distribution of earthquakes. As input data, I prepared a dataset of seismicity using the parametric catalogue and statistical analysis in order to test the thresholds of data completeness through a de-aggregation analysis, and obtain the modified Gutenberg-Richter relation. The main steps adopted for the seismic hazards calculation consist in the preparation of grid of sites, source geometry, source seismicity and attenuation data. For this latter parameter we use SEA99 model (Spudich et al., 1999; Spudich and Boore, 2005) because it has a wider spectrum of ground shaking frequency calculated for rock and soil characteristics. Since there are no significant strong motion records of a regional or local large events (Mw>5.5), it is difficult to calculate an attenuation law in Syria; therefore, I have chosen to use an already build-in table that can be applied to our rock and soil conditions. In our case, we chose rock conditions in the processing. In addition, I consider the type of distance as the closest distance from the site to the rupture area. Finally, using different seismic sources, the results can be presented as a collection of seismic hazard maps taking into account different return periods (500 years and 1000 years), and two spectral ordinate frequencies (0.5 Hz and 1Hz).

VI – 3. Data analysis and input parameters

The developed seismicity catalogue that includes instrumental, historical, archeoseismic and paleoseismic events was prepared as a unified parametric list of earthquakes with their main characteristics. In order to derive the optimum *b* value for the Dead Sea fault, we have to apply the degraded Gutenberg-Richter relation relationship by illustrating the annual rate of exceedence versus the corresponding magnitude range (0.5 magnitude step) applying the following steps:

- Dividing the list of earthquake magnitudes into groups of events that have the same range of magnitude by 0.5 steps, such as: 3.6-4.0, 4.1-4.5…..7.1-7.5.
- For each magnitude group, I draw the line of cumulative number of earthquakes starting from the recent time to the starting date of the earthquake list.
- By repeating the above step on all groups of magnitudes, I get all lines of cumulative number of earthquakes (as seen in Figures 4 &5).
- In order to derive the annual rate of exceedence, I define the period of years corresponds each group of magnitudes. It is defined by the point of changing inclination of the line of cumulative number of earthquakes (as seen in Figures 4 &5).
- Then I select the number of earthquakes from each magnitude group during the defined period of years and I divided by the corresponding number of years and the result is the annual rate of exceedence. For example, in Figure 3 the M 3.5 – 4.0 appears to be complete for the period corresponding to the most recent 25 years. Furthermore, I calculate the rate of exceedance by dividing the number of events by the related complete period and obtain the mean exceedance rate.
- I plot the values of annual rate of exceedence versus the groups of magnitudes, I and by applying the least-square method I derive the Gutenberg-Richter relationship and the optimised *b* value. I calculate the *a* and *b* values in the modified Gutenberg-Richter relation by plotting the mean rate of annual exceedance versus magnitude (Figure 5). The analysis of all events made through a least-square method yields $a = 3.42$ and $b = 0.774$ and the latter value shows a moderate slope (< 1) which indicate the value of input data from studied historical earthquakes and archeo-paleoseismic results (Figure 5). In fact, the diagram of Figure 5 shows that the catalogue covers the whole spectrum of magnitude including magnitudes > 6.5 and reaching a maximum M 7.3.

However, a gap of magnitudes between 5 and 5.5 can be observed and may represent a lack of data due to an incomplete coverage of magnitudes by the instrumental seismicity, and lower than the threshold of completeness of the historical catalogue.

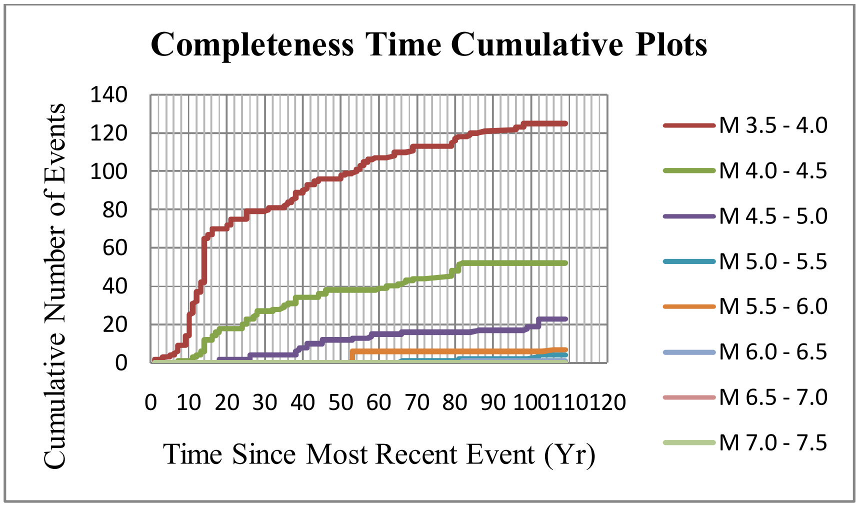

Figure 3: De-aggregated completeness time of seismicity (AD 0 – 2008) for the whole spectrum of magnitudes; magnitudes higher than 5.5 do not appear in this diagram because of their low frequency.

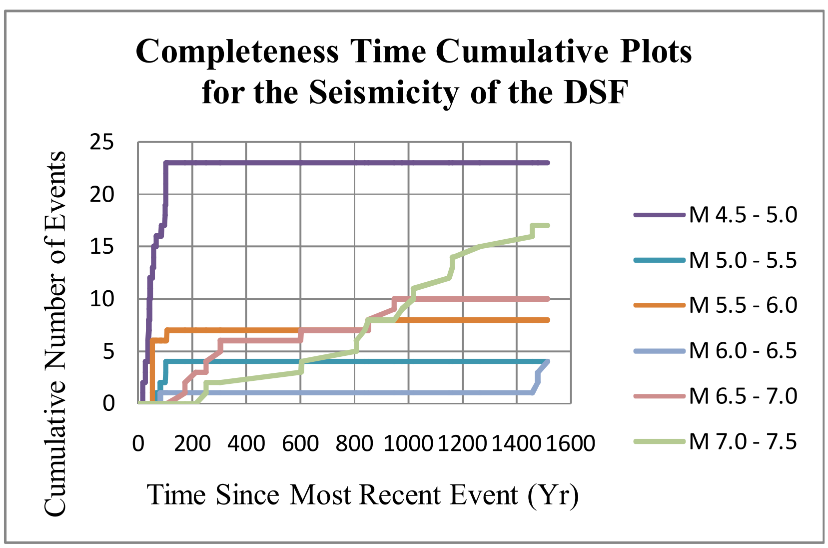

Figure 4: De-aggregated completeness time of seismicity (AD 0 – 2008) for magnitudes higher than 4.5 to 7.5.

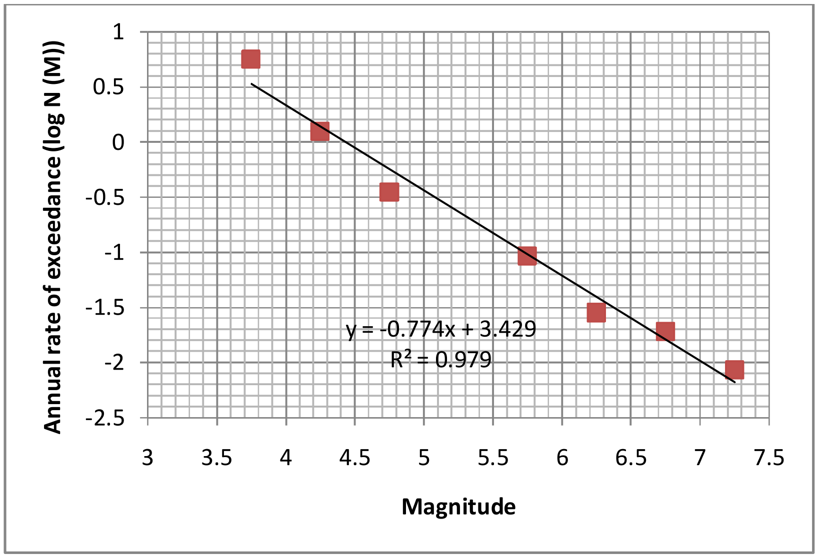

Figure 5: Annual rate of exceedance versus magnitude that corresponds to the modified Gutenberg-Richter relation. The b-value (0.774) and the input data for large magnitudes (M>6.5) illustrate the completeness of the catalogue. R^2=97% corresponds to the correlation coefficient.

– The source geometry is taken from both field investigations along the Dead Sea Fault (in Lebanon and Syria) and the related seismicity (Figure 2). The active tectonics and seismic parameters allow me to identify six main sources named Yammuneh, Serghaya, Missyaf, Apamea, Jissr el-Shoughur (JES), and Afrin, I consider the type of sources as line sources. Tables 1 and 2 prepared for the Poissonian model, they present for each segment the characteristic earthquake, the input parameters obtained from the multidisciplinary approach adopted in my work.

Source	Thresh. Mag.	Return period	b value	R^2	Exp. Mag.	Er. Mag.	Min. Mag.	Max. Mag.
Yammuneh	4.5	1.1324	0.774	0.02	7.5	0.3	7.2	7.6
Serghaya	4.5	1.1324	0.774	0.02	7.3	0.3	6.8	7.5
Missyaf	4.5	1.1324	0.774	0.02	7.4	0.3	7.0	7.5
Apamea	4.5	1.1324	0.774	0.02	7.3	0.3	7.0	7.5
JES	4.5	1.1324	0.774	0.02	7.4	0.3	7.0	7.5
Afrin	4.5	1.1324	0.774	0.02	6.8	0.3	6.2	6.8

Table 1 : Main input parameters of active faults for Poissonian Model. Fault zones are shown in Figure 2.

Source	Return period of Char. Eq.	R^2 of Char. Eq.	Min. Char. Eq.	Max. Char. Eq.	Elapsed time of Char. Eq.	Expected Char. Eq.
Yammuneh	1000	0.3	7.2	7.6	810	7.6
Serghaya	1500	0.3	6.8	7.4	250	7.2
Missyaf	1000	0.3	7.0	7.4	840	7.2
Apamea	1000	0.3	7.0	7.3	853	7.15
JES	1000	0.3	7.0	7.4	602	7.2
Afrin	1500	0.3	6.2	6.8	1484	6.5

Table 2 : Main input parameters of active faults for Characteristic Model. Fault zones are shown in Figure 2.

VI – 4. Results of data treatment and seismic hazard maps

In this processing, I chose to produce seismic hazard maps for the whole active region of western Syria and Lebanon that includes all seismic sources along the Dead Sea Fault (see also Tables 1 and 2). The analysis of seismic sources and related parameters are tested for 500 years and 1000 years return period, with the attenuation law obtained from SEA99 (Spudich et al., 1999), and the frequency ordinate of 0.5 Hz and 1 Hz.

From the resulted seismic hazards maps we can conclude the following results:

- The active seismic sources have a high probability to produce high accelerations with maximum exceeding 0.6g for the 1 Hz and return periods 500 and 1000 years, and exceeding 0.8 and 0.9g for the 0.5 Hz and return periods 500 and 1000 years as seen in the Figures 6 a and b and Figures 7 a and b, respectively.
- The comparison between the acceleration contours in Figures 6a and 6b and Figures 7 a and 7b shows that the acceleration can be correlated with higher frequency.
- All major cities (Damascus, Beyrut, Aleppo, Lattakia, Homs and Antioch) in the studied region are exposed to accelerations higher than 0.4 even for 500 return period, regardless of site effects.
- A more sophisticated analysis requires field data for building a regional attenuation law and developing a databank of rock and soil frequencies for the study of site effects and microzonation.

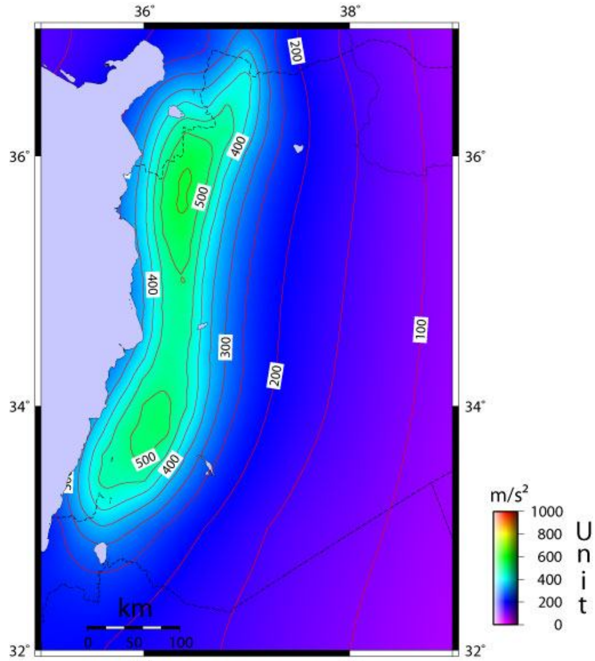

Figure 6a: Seismic hazard map obtained from the input data of Tables 1 and 2 for a Poissonian model and for a 1Hz frequency and 500 years of return period. Values correspond to acceleration in cm/s². The maximum acceleration reaching 0.6g is concentrated along the Yammouneh fault and JES and Apamea faults (see Figure 2 for fault segment names).

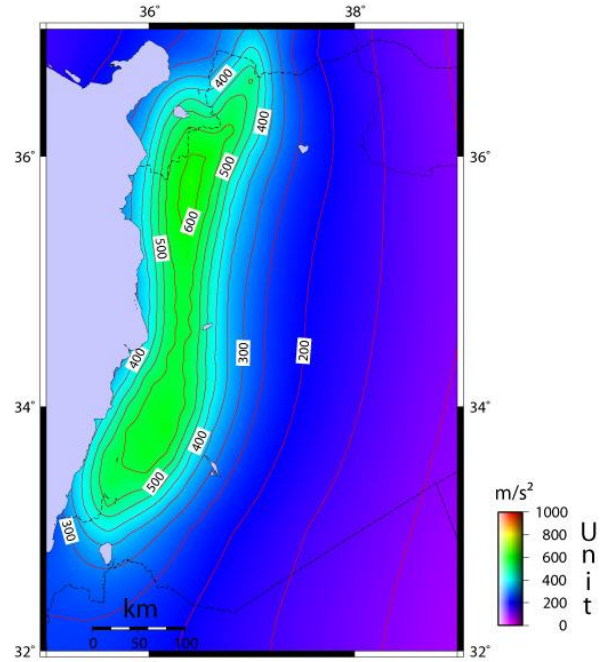

Figure 6b: Seismic hazard map obtained from the input data of Tables 1 and 2 for a Poissonian model and for a 1Hz frequency and 1000 years of return period. Values correspond to acceleration in cm/s². The maximum acceleration exceeds 0.6g situated along the Yammouneh, Serghaya, Missyaf, JES and Apamea faults with a minor increase of acceleration for the Afrin fault.

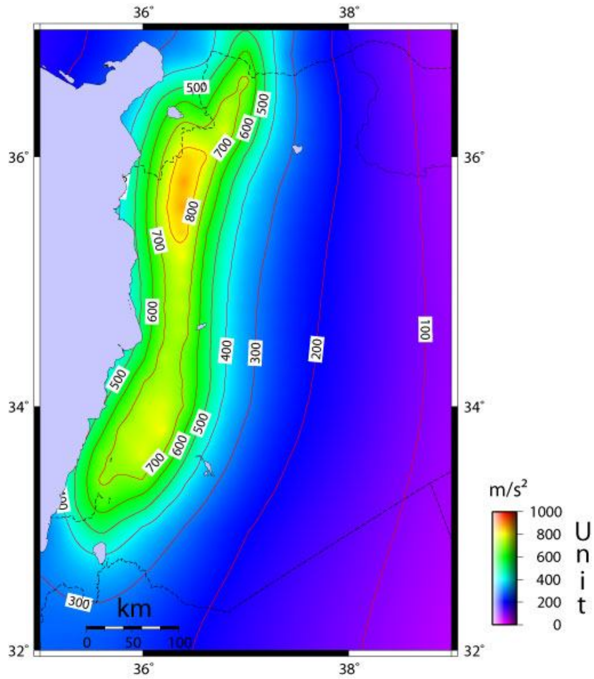

Figure 7a: *Seismic hazard map obtained from the input data of Tables 1 and 2 for a Poissonian model and for a 0.5Hz frequency and 500 years of return period. Values correspond to acceleration in cm/s^2. The maximum acceleration exceeding 0.8g is concentrated in the Ghab area. Other high acceleration is along the Yammouneh, Serghaya, Missyaf and Afrin faults (see Figure 2 for fault segment names).*

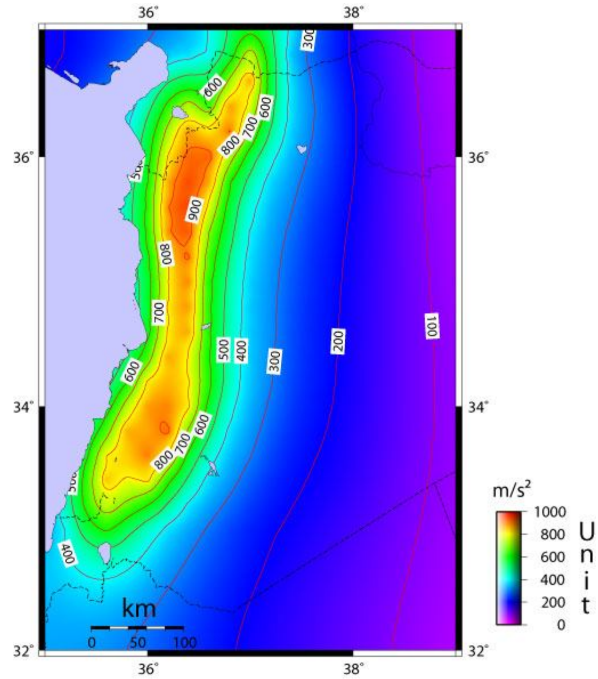

Figure 7b: *Seismic hazard map obtained from the input data of Tables 1 and 2 for a Poissonian model and for a 0.5 Hz frequency and 1000 years of return period. Values correspond to acceleration in cm/s^2. The maximum acceleration exceeding 0.9g is concentrated along the JES, Apamea, Serghaya, Missyaf and Yammouneh fauls.*

References

Al Tarazi, E., and Sandvol, E., 2007, Alternative models of seismic hazard evaluation along the Jordan-Dead Sea Transform, Earthquake Spectra, vol. 23, 1-19.

Ambraseys, N.N., & Jackson, J. A. (1998). Faulting associated with historical and recent earthquakes in the Eastern Mediterranean region, *Geophys. J. Int.* **133**, 390-406.

AMBRASEYS, N. (2001): Far-field effects of Eastern Mediterranean earthquakes in Lower Egypt, *J. Seismol.,*5, 263-2001.

Amiran, D.H.K., E. Arieh, T. Turcotte (1990). Earthquakes in Israel and adjacent areas : macroseismic observations since 100 B.C.E.

Ben-Menahem, A. (1979): Earthquake catalogue for the Middle East (92 B.C.-1980 A.D.), *Boll. Geof. Teor. Appl.*, 21 (84), 245-310.

Guidoboni, E., A. Comastri, and G. Traina (1994). *Catalogue of ancient earthquakes in the Mediterranean area up to the 10th century*, 504 pp., ING-SGA, Bologna.

Cornell, C.A. (1968). Engineering seismic risk analysis. *Bulletin of the Seismological Society of America*, 58: 1583-1606.

Costa, G., G. F. Panza, P. Suhadolc and F. Vaccari (1993). Zoning of the Italian territoryin terms of expected peak ground acceleration derived from complete synthetic seismograms. Journal of Applied Geophysics, 30: 149-160.

Elnashai A. S. And R. El-Khoury (2004). Earthquake hazard in Lebanon. Imperial College Press. P. 171.

Nemer, T. (2005). Seismotectonique et comportement sismique du relais tranpressif de la faille du Levant: role et effets branches de failles sur l'alea sismique au Liban. Thesis, University of Luis Pasteur Strasbourg.

Plassard and Kogoj, 1981;

Reiter, L. (1990). Earthquake hazard analysis – Issues and insight. Colombia University Press, New York, 254p.

Spudich, P., W. B. Joyner, A. G. Lindh, D. M. Boore, B. M. Margaris, and J. B. Fletcher (1999). SEA99: A Revised Ground Motion Prediction Relation for Use in Extensional Tectonic Regimes, Bull. Seism. Soc. Amer. 89, 5, pp. 1156-1170.

Spudich, P., and D.M. Boore (2005). ERRATUM to SEA99: A Revised Ground Motion Prediction Relation for Use in Extensional Tectonic Regimes, Bull. Seism. Soc. Amer., 95, 3, p. 1209.

Wells, D. L., and K. J. Coppersmith (1994). New empirical relationships among magnitude, rupture length, rupture width, rupture area, and surface displacement, *Bull. Seism. Soc. Am.* 84**,** 974–1002.

CHAPTER VII

CONCLUSIONS

VII - CONCLUSIONS

In the thesis, my attempt is to show the benefits of applying the multidisciplinary approach of applying active tectonics, paleoseismology, archeoseismology, historical and instrumental seismicity studies as an integrated work conducted along the northern Dead Sea Fault (NDSF). This approach allows to reach a better understanding of the long term behavior of the northern Dead Sea Fault throughout: **i** - the analysis of past earthquakes through their seismic intensity at the investigated sites (e.g., Al-Harif, Krak des Chevaliers, Apamea and Deir Dahess); **ii** – the estimation of the paleo-earthquake distribution, seismic cycle and related slip-rate of the Missyaf segment; **iii** – the discrimination between the different destruction types of earthquake-induced damages and those of non seismic origin; **iv** - the introduction of a new generation of seismic hazard maps complying with the new results and parameters obtained from the integrated methodologies of investigations.

The field investigations in active tectonics and the previous works in the frame of the APAME project allows me to use the new field mapping and conduct archeoseismic and paleoseismic studies of the NDSF segments (Yammouneh, Serghaya, Missyaf, Apamea, Jisr Al-Shoughor and Afrin faults). Other dataset are selected from focal mechanism solutions and slip rates, and the estimated seismic parameters for each segment as presented in Table 1 of Chapter III. The plotting of hypocenters of the last Century seismic events on three different sections crossing the NDSF shows that hypocenter depths and therefore the seismogenic layer do not exceed 40 km. The hypocenter distribution in the Sinai-Africa plate and western block along the NDSF has higher depth values (20 – 40 km) than in the Arabian plate (10 – 20 km east of the NDSF). The estimated depth of large earthquakes varies from 10 – 35 km, according to the macro-earthquake distribution presented in Chapter IV.

The results of the thorough investigation of the historical earthquake documents show the occurrence of 181 historical earthquakes (Table 2, Chapter IV) that hit the studied region most of them were generated by the NDSF and EAF. The analysis of each historical event yielded the determination of the complete parameters of 36 events among the 181 ones (see Table 1 of Chapter IV) containing magnitudes of M $\geq$ 7.0 and completeness threshold for M = 6.5.The historical seismicity of the NDSF spanning more than 3500 years (Chapter IV) and the comprehensive investigations of paleo-archeoseismological studies at some significant (with earthquake faulting and damage) sites located along the NDSF (Krak des Chevaliers, Al-Harif, Apamea, Deir Dahess, see Chapter V) present strong evidences that the DSF generates destructive earthquakes with magnitudes M 6.0 to 7.5. The earthquake activity was of high level during the Middle Age centuries and using the arche-paleoseismic record, the fault behavior shows long return periods (ranging 250 – 1000 years). I also observe that the return period of the characteristic earthquakes for each fault segment varies from1000 to 1500 years as presented in Table 1 of Chapter VI.

The comparison between the distribution of epicenters obtained from the historical and instrumental seismicity along the NDSF shows a concentration earthquake activity along the southern part of the NDSF (Yammouneh, Rashaya, Serghaya faults) and the northern part of the NDSF at the junction zone with the East Anatolian fault EAF. One may, however, observe a significant lack of seismicity in the central part (Missyaf, Apamea and southern part of the Jisr Al-Shoughor faults), which is the site of a long elapsed time since the last characteristic earthquakes (since 1170 Missyaf and 1157 Apamealarge earthquakes).

The detailed paleo-archeoseismological investigations at Al-Harif Roman aqueduct site, through the integrated interpretation of the results obtained from the three paleoseismic trenches, the four archeological excavations and the six tufa cores gives a clear field evidence of a temporal clusters of three large earthquakes among for three characteristic earthquakes along the Missyaf segment named W, X, Y and Z, (Figure 13, Chapter V) during the past 3400 years with 13.6 m. of left-lateral coseismic offset identified on the Roman aqueduct for the last 3 events, and 4.3 m for the characteristic slip. Event W observed in trench C probably occurred before BC 510 (unit f) and after BC 3400; however, it minimum age can be estimated as BC 962 according to the calculation of the rate of sedimentation in unit f. Event W may also be correlated with the historical event of BC. 1365 that affected Ugarit near Lattakia. The occurrence of the three seismic events X, Y and Z is dated AD 70 - 600, ~ AD 650 and AD 1170, respectively. The estimated slip-rate of Missyaf segment is ~5.5 mm/year, and the seismic quiescence since AD 1170 advocate ~ 4.0 m slip deficit and indicate that more seismic stress accumulation (which may correspond to less than 1 to 2 centuries) to reach a 4.3 m characteristic slip is needed for a seismic rupture initiation. The Missyaf fault segment likely corresponds to an earthquake-prone area and must be taken in a high consideration for the seismic hazard preparedness procedures in Syria and Lebanon.

The interpretation of the archeoseismological excavations in the Mamlouk Bath (1271 AD.) and the analysis of the different building stages of the Krak de Chevaliers lead us to the following:

i - The southern fence wall shows a coseismic crack with a date ranging between 1275 AD and 1295 AD. The observed damage and estimated seismic intensity of VI – VII at this site, the historical earthquake can be correlated to the 22 March 1287 seismic event that generated a seismic intensity level of VII – VIII in Lattakia (western Syria).

ii - The damage related to the 29 June 1170 earthquake, has been recovered soon after the event by rebuilding the southern and north-eastern fence walls by untrimmed new basaltic rocks taken from the nearby quarries (as seen from the bedrocks outcrops). Initially, the extensive length of long standing walls of the southern and the north-eastern parts of the outer fence apparently obliged the engineers to strengthen them by an a 10^{o} artificial bending; After the earthquake damage to the walls, the gaps in the basaltic building stones were filled by well cut limestone blocks.

The earthquake damage interpretations of the Apamea city in the two explored sites (the Agora and the "*maison aux colonnes bilobees*") expose the earthquake effects of the of the VI Century earthquake (AD 526) with seismic intensity (VII – VIII) and either or both earthquakes 1157 and 1170 with cumulative seismic intensity (VIII – IX).

At Deir Dahess monastery; the detailed archeological sounding in the two dwelling rooms, the dating of the trapped soils and remains under the big size collapsed wall stones of the annex, the dates of building and reconstruction of the church, and the small sounding in the tower as well as the dating of a coin, lead us to conclude that the site was exposed to two destructive earthquakes. The first one was during the VI Century with seismic intensity I ≥ VIII, and the second one lays in the AD 1390 to 1660 range of date which may correspond to the AD 1408 earthquake.

The new obtained results obtained mainly from field investigations are constructed to compose the input parameters for the seismic hazard model covering the northern part of the Dead Sea Fault and western part of Syria, mid-southern Turkey (Antioch area) and Lebanon regions. Using the CRISIS2007 software and applying the probabilistic model, the analysis of input data leaded to a collection of seismic hazard maps for 1 and 0.5 Second structure frequencies, for 500 and 1000 years of return periods.

The presented maps in Chapter VI lead to the following results:

- The active seismic sources are analysed with a high probability to produce high accelerations exceeding 0.6 g for the 1 Hz shaking frequency (on rocks) and 500 to 1000 years return periods, and exceeding 0.8 and 0.9g for the 0.5 Hz and 500 to 1000 years return periods (see Figures 6 a and b and Figures 7 a and b, respectively, in Chapter VI).
- The comparison between the acceleration contours for different frequencies (1 and 0.5 Sec.) shows that the acceleration increases with higher frequency.
- All major cities (Damascus, Beyrut, Aleppo, Lattakia, Homs and Antioch) in the studied region are exposed to accelerations higher than 0.4 g even for a 500 return period, regardless of the site effects.

The main implications inferred from the evaluation of fault behaviour and seismic cycle, and seismic intensities of past earthquakes at archeological sites reside in a realistic seismic hazard assessment. The results contained in this thesis may contribute effectively in the processing of different earthquake hazard scenarios and calculation of the seismic loads for the urban planning and seismic design of industrial construction projects.

Finally and since I have a strong believe about the necessity of improving our knowledge about the seismic behavior of active faults in Syria, I may suggest the following perspectives for the development of future research topics:

- Applying the dynamic analysis models, for some representative archeological structures: Al-Harif, Saint Simon, Deir Dahess and Apamea.
- Conducting more detailed paleoseismic trenching on other sites along the Missyaf segment (further north and south from the Roman Aqueduct site)
- Further archeoseismological investigations with integration of shallow geophysical methods such as GPR or magnetic in the main archeological sites of western and north-western Syria (i.e., Apamea, Kherbet Maez, Saint Simon, and Bourkush).
- Conducting further paleoseismological investigations along the other active segments of the NDSF (Jisr Al-Shoughor, Apamea and Afrin faults).
- A more sophisticated analysis of the regional seismic hazard and risk assessments that require field measurements (and a dense seismic and strong motion network) for building a regional attenuation law and developing a databank of rock and soil frequencies for the study of the site effects and microzonation.

Appendix

List of Appendix

Sbeinati M. R., R. Darawcheh, and M. Mouty (1994). Field archeological evidences of seismic effects in Syria, in Materials of the CEC Project "*Review of Historical Seismicity in Europe*" – vol. 2., Albini P. and A. (edit.), CNR – Consiglio Nazionale delle Ricerche, Milano, Italy.

Darawcheh, R., Sbeinati, M.R., Margottini, C., and Paolini, S., (2000), The 9 July 551 A.D. Beirut earthquake, eastern Mediterranean region: *Journal of Earthquake Engineering*, v. 4, p. 403–414, doi: 10.1142/S1363246900000229.

Gomez, F., Meghraoui, M., Darkal, A., Sbeinati, R., Darawcheh, R., Tabet, C., Khawlie, M., Charabe, M., Khair, K., and Barazangi, M., (2001), Coseismic displacements along the Serghaya Fault: an active branch of the Dead Sea Fault System in Syria and Lebanon, *J. Geol. Soc. London* 158, 405 – 408.

Meghraoui, M., Gomez, F., Sbeinati, R., Van der Woerd, J., Mouty, M., Darkal, A., Radwan, Y., Layyous, I., Najjar, H., M., Darawcheh, R., Hijazi, F., Al-Ghazzi, R., & Barazangi, M., (2003), Evidence for 830 years of seismic quiescence from paleoseismology, archeoseismology and historical seismicity along the Dead Sea fault in Syria, *Earth. Planet. Sci. Letters* 210, 35-52.

Alchalbi et al., and 15 authors (2009), Crustal deformation in northwestern Arabia from GPS measurements in Syria: Slow slip rate along the northern Dead Sea Fault, *Geophys. J. Int.* (2009), doi: 10.1111/j.1365-246X.2009.04431.x

Historical Investigation of European Earthquakes

2

Materials of the CEC project
Review of Historical Seismicity in Europe

Paola Albini and Andrea Moroni
editors

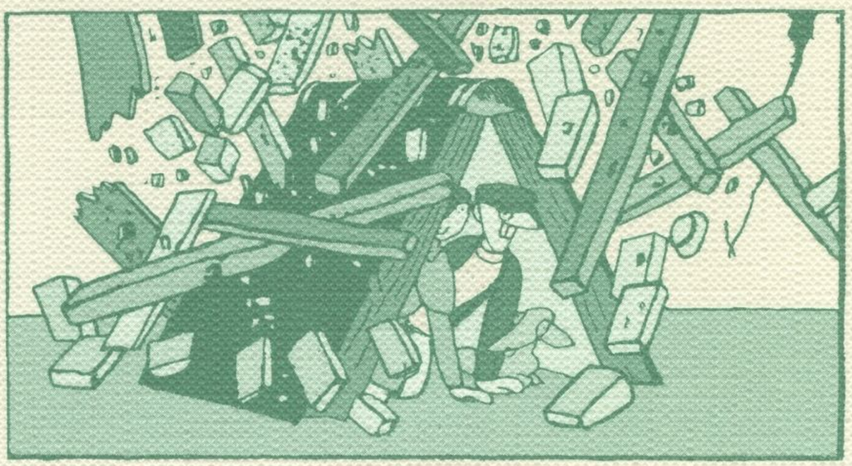

CNR - Istituto di Ricerca sul Rischio Sismico

Mohamed Reda Sbeinati *, Ryad Darawcheh *
and Mikhail Mouty *

Field archaeological evidences of seismic effects in Syria

Introduction

It is of fundamental importance to collect all available information to reconstruct the maximum ground motion which occurred at archaeological sites in the proximity of which critical facilities are planned to be erected (Gürpinar and Margottini, 1994).

As Syria is rich in archaeological sites, field research was carried out to define the historical earthquake effects at archaeological sites located in north-western Syria along the northernmost part of the Syrian Lebanese Fault (SLF). This fault, which represents the northern extension of the Dead Sea transform fault system in Syria, is one of the most seismogenic fault zones in the region.

This study deals with five examples of archaeological sites. Fig. 1 shows location map of these monuments. This study involves:

- desk work oriented to define the archaeological sites damaged by earthquakes, their names during their life-times, time of their foundation and date of latest reconstruction;
- field investigation to define the type of earthquake damage and to distinguish seismic effects from non-seismic ones.

History

The history of archaeological sites investigated is briefly reviewed as follows:

- Qalaat Samaan (citadel of St. Simeon): situated on a limestone hill, it has splendid Byzantine monuments of the 5th century AD.
  The cathedral surrounding the pillar, on top of which St. Simeon lived, is considered among the largest churches in the ancient world. The church was converted into a stronghold citadel during Sayf Ad Dawla Al-Hamadani's rule. There are ruins of a city on the slope of the hill (Zakariyya, 1984; Sha'ath, 1983).

---

* *Department of Geology and Nuclear Ores, Atomic Energy Commission of Syria, P.O. Box 6091, Damascus, Syria.*

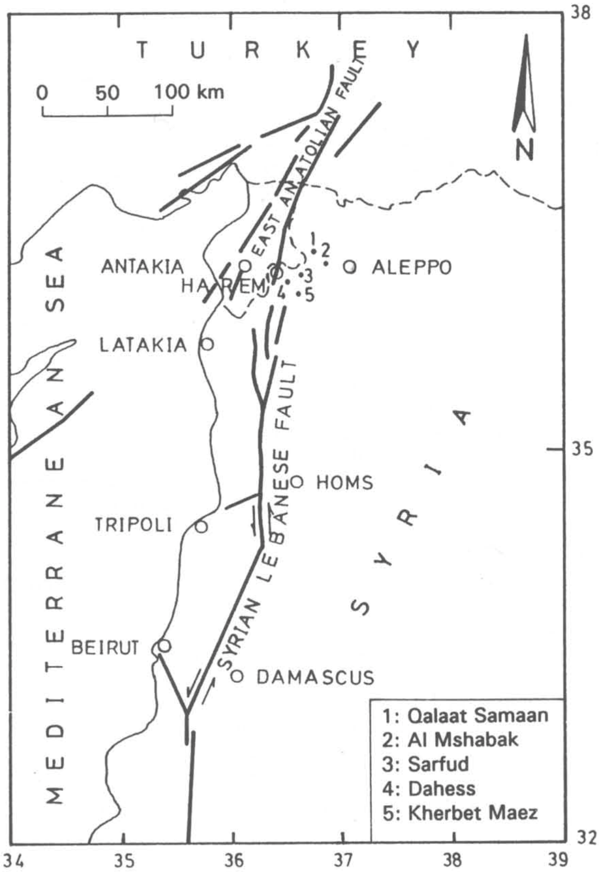

Fig. 1 - Location of the investigated archaeological sites.

- Qasr Al-Mshabak: located between Aleppo and Qalaat Samaan (3 Km. far from Daret Ezzeh), it has the shape of a rectangular church and probably it dates back to the Byzantine era. Unfortunately, historical information on this site is lacking.
- The archaeological sites in Barisha mountain (3 sites): located north-west of Idlib near the Turkish-Syrian border, they contain more than 200 of the so called "Dead Towns". These sites flourished during the Byzantine time and,

N	Archaeological site (Monument)	Time of construction	Building material	Dates of damaging earthquakes (Ambraseys and Barazangi, 1989)	Present condition	Type of evidence	Fig.	Grade of Damage according to MSK-64
1	Qalaat Samaan (Citadel) = St. Simeon	Byzantine	Large size blocks of limestones	526, 1137, 1170, 1719, 1822	Cathedral partially restored. Ruins of a city on the slope of the hill	- Fractures - Horizontal shifting - Twisting - Waving	2 2 - 3	4-5
2	Qasr Al-Mshabak (Palace)	n.d. (Byzantine?)	Medium size blocks of limestones		Church ceiling completely destroyed	- Horizontal shifting - Waved walls - Extension	- 4 5	2
3	Dahess (Ruins)	n.d.	Large size blocks of limestones	Most of earthquakes which hit Antioch	In ruinous state with remaining individual wall	- Rocking - Horizontal shifting - Waving	6 7 7	4-5
4	Sarfud = Al-Braeje (Convent)	Byzantine	Large size blocks of limestones	Most of earthquakes which hit Antioch	Partly destroyed	- Fractures - Horizontal shifting - Tilting	8 9 -	3-4
5	Kherbet Maez (Ruins)	Byzantine	Large size blocks of limestones	Most of earthquakes which hit Antioch	Ruined considerably	- Deformation - Horizontal shifting - Waving	10 - -	4-5

Tab. 1 - Main characteristics of the investigated monuments.

for instance, they were described by Yakut al-Hamoui (1906), a geographer and historian who lived between 1178 and 1229, and occasionally visited them (Zakariyya, 1984). Among them, Sarfud, Kherbet Maez and Dahess are to be mentioned. The several churches, monasteries and temples in Barisha reflect the prosperous life enjoyed by the population. There are only few references available on these sites, poor in details (Tchalenko, 1953; Al-Satea, 1975).

Tab. 1 summarises the main characteristics of the five sites.

Seismological and seismotectonic setting

The area where Samaan and Barisha mountains are located is very close to the Syrian Lebanese fault, and also close to another very active seismic zone, the Eastern Anatolian fault (EAF), outcropped to the north of the area (Fig. 1). The SLF, northern part of Dead Sea fault (DSF) is a N-S trending interplate transform fault between the Arabian plate (east) and the Sinai plate (west). It displays a left lateral displacement with minor components of extension and compression. Morphological and geological evidences for neotectonics along the SLF were evaluated by Radwan and Al-Najjar (1991). Moderate to large earthquakes occurred along the entire extension of this fault (Ministry of Electricity, 1988; Ambraseys and Barazangi, 1989; Sbeinati, 1994).

The area of Samaan and Barisha, like other areas along the DSF, seems to be stricken by large earthquakes ($M \geq 6.5$) with long return period (200-350 years) (Ambraseys and Barazangi, 1989).

Evidences of possible seismic damage

Very frequent fracturing in the walls of these monuments can be observed. The origin of this fracturing is uncertain, i.e. they can be interpreted as effects of earthquake(s) or of deterioration of their structure (Fig. 2 and 9). The extension observed in Fig. 5 can be considered as a characteristic feature of the effects of seismic ground motion. An interesting example is displayed in Fig. 7, where the rocking of the western wall (Dahess) can be considered as a clear effect of seismic ground motion. Other evidence is shown in Figs. 3, 4, 6, 8 and 10. In Tab. 1, column 7 "Type of evidence", many types of possible seismic damage, observed at the investigated monuments, are listed.

Concluding remarks

The examples shown suggest that the study of archaeological sites can be a useful tool in understanding seismic history.

Archaeological evidence can be used to establish, in a very preliminary way, an upper limit of the seismic effects recorded at the site, if one assumes that:

- today evidence corresponds to the original earthquake record;
- the earthquake struck the site when it stood in good conditions and its

vulnerability was the lowest possible.

If these two circumstances are not met, the archaeological evidence should be assumed as the result of lower shakings.

Following this point, Tab. 1 presents a very preliminary determination of the maximum macroseismic intensity which in principle might be correlated with the evidence rise.

In short, investigation on archaeological sites may give preliminary information on seismic effects, though they bear great uncertainties which necessitate concerted efforts to improve the reliability of the results.

Acknowledgements

This study is part of a research project entitled "Seismic Data for the Siting and Site Re-Validation of Nuclear Facilities" (No. 6247/RB), funded by International Atomic Energy Agency at Vienna. The authors express their sincere gratitude to the Director General of Syrian Atomic Energy Commission for his constant encouragement and support. We would also like to thank M. Stucchi and P. Albini for their valuable suggestions and remarks.

References

Al-Hamoui,Y., 1906. Moujam al-bouldan. Cairo [n. pub.].

Al-Satea, A. and Al-Satea, F., 1975. Al-Dalil al-Akhdar lil siyyaha wa al-athar. Dar al-Fukr, Damascus.

Ambraseys, N. and Barazangi, M., 1989. The 1759 earthquake in the Bekaa Valley: Implications for earthquake hazard assessment in the Mediterranean region. Journal of Geophysical Research, 94, B4: 4007-4013.

Gürpinar, A. and Margottini, C., 1994. Possible evidences of past seismic ground motion(s) in the historical town of Hatra (Central Mesopotamia). Proc. of the Regional Workshop on Archaeoseismicity in the Mediterranean region, Damascus (in press).

Ministry of Electricity, 1988. Report of macroseismic research in areas of NPP sites location (in English), Aleppo.

Radwan, Y., Al-Najjar, H. and Darawcheh, R., 1991. Investigations of active tectonics along the major faults in Syria using geomorphic techniques. In: S. Riad, A. Morelli and M. Miele (Editors), Proc. of the First Regional Seminar on Earthquake Research Activity and Risk Assessment in the Mediterranean region, Cairo.

Sbeinati, M. R., 1994. Evidences of seismic effects on selected archaeological sites in Syria. Report on scientific field study, Atomic Energy Commission of Syria, Damascus, pp. 4-28 [not public].

Sha'ath, Sh., 1983. Qalaat Samaan. The Directorate General of Antiquities and Museums, Damascus.

Tchalenko, G., 1953. Villages antiques de la Syrie du Nord. Librairie Orientaliste, Paris.

Zakariyya, W., 1984. Jawala athariyya fi baed al-bilad al-chamiyya. Dar al-Fukr, Damascus.

Fig. 2 - Fracturing and horizontal shifting in the western wall of a building at Samaan city.

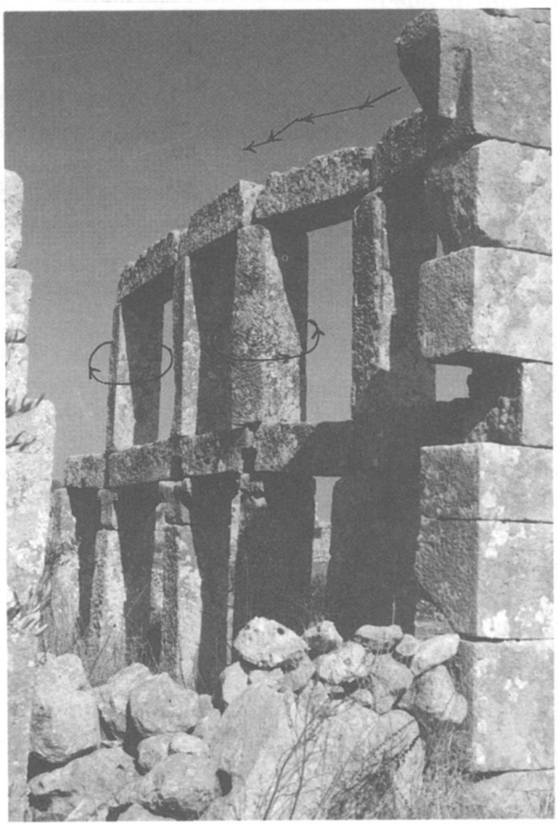

Fig. 3 - Rotated pillars and waved wall at Samaan city.

Fig. 4 - Characteristic deformation of major earthquake at Al-Mshabak site.

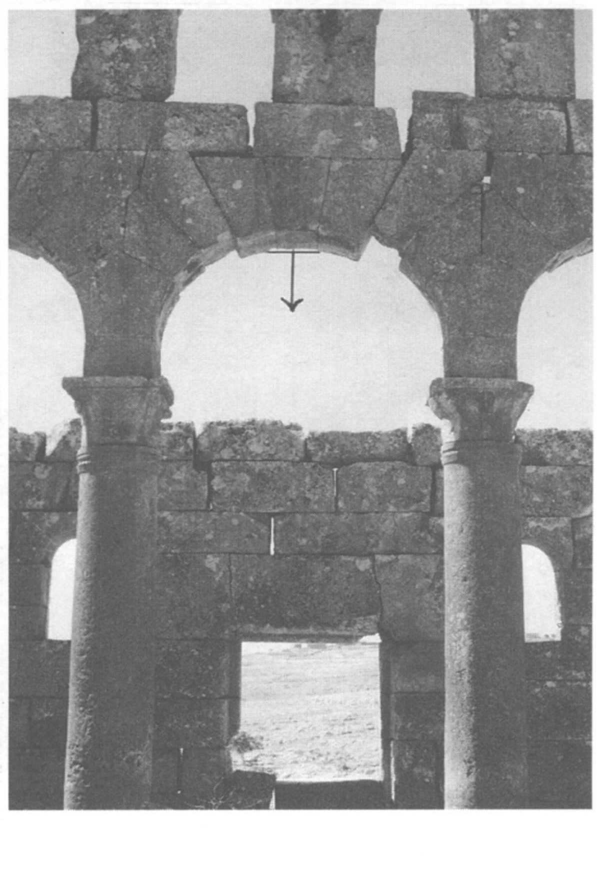

Fig. 5 - Lateral extension and down sliding of the central key stones of one internal arches: a characteristic feature of earthquake effects at Al-Mshabak site.

Fig. 6 - Rocking of the western wall at Dahess site.

Fig. 7 - Horizontal shifting and waving in the southern wall at Dahess site.

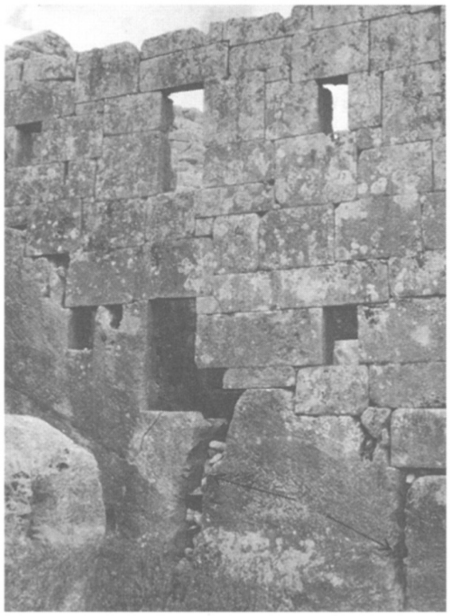

Fig. 8 - Cracks in the bedrock (basement of the building), Sarfud (Al-Breige) site.

Fig. 9 - Breakage and tilting of the pillar that supports a water reservoir, Sarfud (Al-Breige) site.

Fig. 10 - Flower-petals-like splitting of the western church at Kherbet Maez: stones rotation and fall are usually resulted by long seismic duration effect.

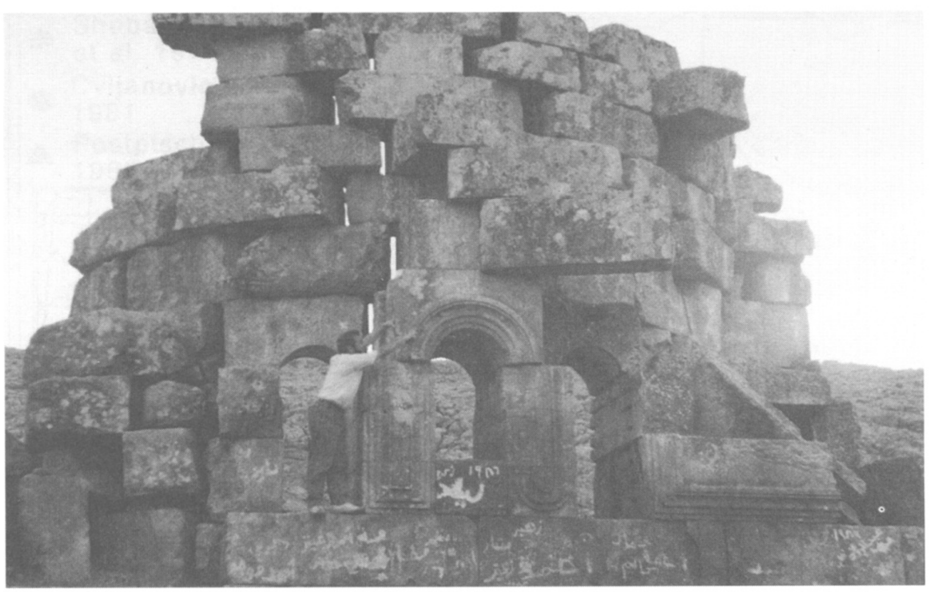

Journal of Earthquake Engineering, Vol. 4, No. 4 (2000) 403–414

THE 9 JULY 551 AD BEIRUT EARTHQUAKE, EASTERN MEDITERRANEAN REGION

RYAD DARAWCHEH and MOHAMED REDA SBEINATI

Atomic Energy Commission of Syria,
P.O. Box 6091, Damascus, Syria

CLAUDIO MARGOTTINI

Italian Agency for New Technology, Energy and Environment,
S.P. 67 – Via Anguillarese,
301 – 00060 S. Maria di Galeria, Rome, Italy

SALVATORE PAOLINI

Italian Agency for New Technology, Energy and Environment,
P.O. Box 65 – 00044 Frascati, Rome, Italy

Received 18 August 1998
Revised 16 December 1998
Accepted 15 May 2000

Analysis of the Byzantine primary and secondary sources for identifying the historical earthquakes in Syria and Lebanon reveals that a large earthquake ($Ms = 7.2$) occurred in July 9, 551 AD along the Lebanese littoral and was felt over a very large area in the eastern Mediterranean region. It was a shallow-focus earthquake, associated with a regional tsunami along the Lebanese coast, a local landslide near Al-Batron town, and a large fire in Beirut. It caused heavy destruction with great loss of lives to several Lebanese cities, mainly Beirut, with a maximum intensity between IX–X (EMS-92). The proposed epicentre of the event is offshore of Beirut at about 34.00°N, 35.50°E, indicating that the earthquake appears to be the result of movement along the strike-slip left-lateral Roum fault in southern Lebanon.

Keywords: Seismology, historical earthquakes, historical primary sources, Lebanon.

1. Introduction

Studying a moderate to large historical earthquake in any region, when historical sources are available, should lead to the assessment of the parameters of that earthquake (i.e. date, coordinates, intensity and magnitude) and consequently the definition of a possible causative fault. This assessment together with others for many historical earthquakes in the region, then, will be used in the earthquake hazard assessment for particular sites, on both local and regional scales.

This paper deals with the 551 AD earthquake, the event that is described as probably the highest magnitude event in the Eastern Mediterranean Region [USGS-UNESCO, 1993].

Several pre-1900 AD catalogues mentioned this earthquake such as those of Bonito [1691] and Perrey [1850]. Also it is listed in the 20th century catalogues: Sieberg [1932] presented the first scientific study on this event when he described its effects in eastern Mediterranean region. Amiran [1952], using a noncontemporary source, had considered the event to be of grade ≥ 9 (MCS). Ben-Menahem [1979] used earthquake catalogues to place the earthquake's epicentre off coast of Beirut. While Plassard and Kogoj [1981] reviewed four historical sources to describe, especially, this event of Beirut. Abou Karaki [1987] had considered this event as a duplicated one and the real date, according to him, was in 1156 AD resulted from dating error between Hejira and Gregorian calendars, without presenting any evidence. Russell [1985] defined the path of destruction from Palestine through northwest Arabia by providing two noncontemporary sources and discussing another contemporary one. In addition, he noted that the destruction at Jerash, Nebo, Petra and Lijjun (today in western Jordan) caused by the 551 AD earthquake, that were proposed by Crowfoot [1938]; Saller and Bagatti [1949]; Hammond [1981] and Parker [1982; 1983] may be an interpretive error. Recently, Ambraseys *et al.* [1994] cited that this earthquake was in Palestine and felt across a large area. Also they suggested that the earthquake's epicentre is in the Jordan Rift Valley. Meanwhile, Guidoboni [1989] and Guidoboni *et al.* [1994] presented three historical original texts of the earthquake, showing the affected area along the Lebanese coast and indicating, in the same time, that the epicenter is located offshore of Beirut. Table 1 shows the available parameters of the earthquake as assessed by some of aforesaid authors. Although most of these series of the related works are valuable, we believe that the earthquake should be re-appraised for two reasons. Firstly, when reviewing the results of Guidoboni *et al.* [1994] and those of Ambraseys *et al.* [1994], we see that there is a clear discrepancy between them, with regard to the location of the epicenter. Secondly, no author has assessed the complete parameters of this earthquake.

Hence, the purpose of this paper is (1) to assess the complete parameters of the earthquake by analyzsing the macroseismic data based on original sources and applying modern methods of intensity and magnitude determinations, (2) to demon-

Table 1. Parameters of the 9 July 551 earthquake from the previous literature.

Author(s)	Date	Epicenter °N-°E	Intensity (I)	Magnitude (M)
Sieberg [1932]	551, July 9	/	/	/
Ben Menahem [1979]	551, July 9	/	I0=XI–XII (MM)	$M_L = 7.8$
Plassard & Kogoj [1981]	551, July 6	/	I=XII (Lebanese scale)	/
Russell [1985]	551, July 9	/	/	/
Ambraseys *et al.* [1994]	551, July 9	32.0–36.0	I Ω VI (MSK)	/
Guidoboni *et al.* [1994]	551, July 9	/	I=X (EMS)	/

strate the expected causative fault of the event and (3) to present an account of this event at the cities of the Lebanese coast in general and in Beirut in particular, in a region that has shown relative seismic quiescence during the 20th century.

2. Seismotectonic Setting

The area where the 551 AD earthquake occurred is located in the northern flank of the Arabian plate. This platform is bounded by the left-lateral strike-slip, north–south oriented Levant fault system (LEF) from the west, and by the Bitlis Suture system and the left-lateral strike-slip East Anatolian fault system from the north [Best *et al.*, 1990]. The relative left-lateral movement along the LEF is estimated at around 4–6 mm/year [Barazangi, 1983]. This movement causes collision of Arabian plate with the Eurasian plate. The LEF extends for about 1000 km from the Gulf of Aqaba to the border between Syria and Turkey near Antakya. Its extension in Lebanon consists of two main strike-slip left-lateral faults namely the Yammouneh fault (YAF) of N30°E, which runs through the western Bekaa Valley, and the Roum fault (ROF) that strikes N07°W in southern Lebanon. The ROF extends for more than 50 km from the Hula depression to the city of Beirut. The northernmost part of the YAF in Syria trends again N–S defining the significant strike-slip left lateral Al-Ghab fault (GHF) and intersects the East Anatolian fault system just north of Antakya [Ambraseys and Barazangi, 1989]. Figure 1 shows the main faults of the LEF zone in Lebanon and Syria.

The seismic instrumental monitoring during the 20th century reveals that there is a moderate earthquake activity in Lebanon and western Syria [Sbeinati, 1994]. This activity is concentrated along the main segments of the LEF in Lebanon and western Syria. Two recent moderate earthquake activities occurred due to the ROF and felt widely in southern Lebanon and western Damascus. The first one represents by the double shocks of March 26, 1997 (at 04:22 and 13:20 GMT) of duration magnitude 4.9 and 4.5, respectively [Darawcheh and Sbeinati, 1998], whereas the second event is the shock of June 20, 1999 (at 10:44 GMT) of duration magnitude 3.4 [Sbeinati and Darawcheh, 1999]. Clearly this shows that the ROF is capable and active. Historically, the northern extension of LEF is the site of numerous large earthquakes ($Ms \geq 6.5$) [Ambraseys and Barazangi, 1989; Mouty *et al.*, 1998] with return period of 200–350 years [Ambraseys and Barazangi, 1989].

The importance of the 551 earthquake lies in the fact that Lebanon and western Syria have generally shown relatively seismic tranquillity in the 20th century and most important cities and economical pools are located in the vicinity of the YAF, GHF and ROF.

3. Methodology and Sources of Information

The methodology of study of the historical earthquakes is now available in the literature (e.g. IAEA [1987]; Ambraseys *et al.* [1983, 1997]; Vogt [1993]; Stucchi [1994]).

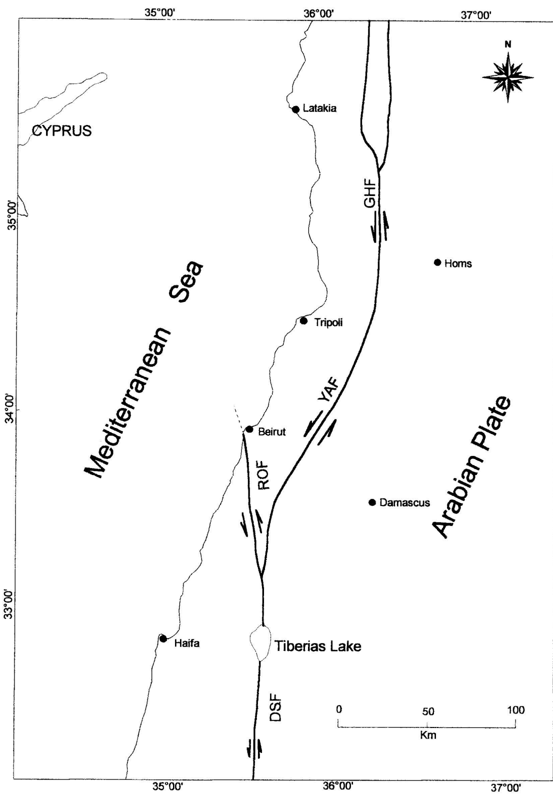

Fig. 1. The main faults of the Levant fault zone in Lebanon and Syria. Note that YAF: Yammouneh Fault; ROF: Roum Fault; GHF: Al-Ghab Fault; DSF: Dead Sea Fault.

In short, we have retrieved the relevant macroseismic data from the available historical sources from two depositories, the Vatican and Pontificio Istituto Orientale, then we reviewed and studied these macroseismic data; in order to reassess the parameters of the earthquake (i.e. date of the earthquake, epicentral location, epicentral intensity and locality intensity, focal depth and macroseismic magnitude) using some relevant rules.

The sources of information for our earthquake are well-known chroniclers who lived in the time of the event. They are Malalas (Mal.) (ca. 491–578 AD), Agathias (Agath.) (ca. 532–580 AD) and John of Ephesus (John Eph.) (ca. 507–586 AD). In addition, there is an itinerary dated to ca. 560–570 written by a traveller named Antoninus Placentinus (Anton.) who visited a part of the affected region shortly after the earthquake. Also, we used an account named De Fragmentis Historicis Tuscolanis (Frag. Hist. Tusc.) dated back to 6th/7th century written by anonymous chronicler. Normally these sources exist only in quotation by later writers (see historical sources of the references). With the exception of the last source, these sources are documented in Guidoboni *et al.* [1994]. Also we used the late 9th century AD source Chronicon pseudo-Dionisyaum (Chron. pse. Dionis.) despite it is the late one, as it mentioned localities that not reported by the above-mentioned sources.

Although there are problems in some of these sources, they contain good descriptions of the 551 AD earthquake with its physical effects.

We avoided using noncontemporary, but Byzantine sources that are attributed to Theophanes (ca. 758–818), Georgius Monachus (9th century AD), Georgius Cedrenus (ca. 1081–1118) and Michael the Syrian (1126–1199 AD), since they derived their materials from original ones and consequently add no further information.

However, we believe that the historical information available about the earthquake is barely sufficient to allow us to construct the earthquake including its parameters.

4. The Earthquake: Analyses of Data

The exact date of this event is doubtful, and still not very clear. The date reported in the *Chronographia* of Theophanes seems to be the most reliable, being probably extracted from one of the earlier versions of Malalas. Nevertheless, the same Malalas chronicle was largely used from the posterior authors, but with errors and misinterpretations, such as John of Ephesus (year 558/559), or the anonymous authors of the Chronicon pseudo-Dionisyanum (552/3 and 558/9).

Other authors, in example Agathias Scholasticus, are too vague.

In the year 551 AD, July 9, there was a destructive earthquake occurred during the reign of the Byzantine Emperor Justinian (ca. 527–565) along the entire Lebanese littoral. The earthquake destroyed several cities in Maritima (modern Lebanese coast). The affected cities were Berytus [John Malalas, John of Ephesus, Agathias Scholasticus, Antoninus Placentinus, De Fragmentis Historicis Tuscolanis, Chronicon pseudo-Dionisyanum] which is modern Beirut, Tripolis [John Malalas, Antoninus Placentinus, De Fragmentis Historicis Tuscolanis, Chronicon pseudo-Dionisyanum] which is modern Tripoli, Sidon [John Malalas, De Fragmentis Historicis Tuscolanis, Chronicon pseudo-Dionisyanum] which is modern Saida, Byblus [John Malalas, Antoninus Placentinus, De Fragmentis Historicis Tuscolanis, Chronicon pseudo-Dionisyanum] which is modern Djbil, Botrys [John Malalas, De Fragmentis Historicis Tuscolanis] which is modern Al-Batron, and Tyrus [John Malalas, De Fragmentis Historicis Tuscolanis, Chronicon pseudo-Dionisyanum] which is modern Tyre or Sur, to an extent that they received financial assistance from the Emperor for reconstruction [John Malalas]. Moreover, there is a 6th/7th century AD source (De Fragmentis Historicis Tuscolanis) added that 101 towns, not named in the source but located in the vicinity of these cities, fell down, and a great myriad of men and animals were killed in them. With the exception of Beirut, detailed description is lacking for other affected Lebanese cities and regions. In Berytus, most of the buildings including the famous structures fell down with the loss of a great number of people under the debris [Agathias Scholasticus]. The Bishop of Beirut (an eyewitness of the earthquake) said that there were 30,000 deaths due to the earthquake, except the foreign residences [Antoninus Placentinus]. This figure is probably reasonable for a city that was flourishing to the extent it was called pearl of the Phoenician coast at that time. Nevertheless, John of Ephesus reported that the survivors were exhausted by the thirst due to the destruction of the city aqueduct. He added that there was a large fire, continuing for almost two months. The School of Law, one of the outstanding features in Berytus and one of the important centers for legal studies in the Byzantine Empire during that time was destroyed to the extent it was temporary transferred to Sidon [Agathias Scholasticus]. On the other hand, it was mentioned that at the time of the earthquake the sea retired for a mile then returned drowning many ships [John Malalas]. More details about this phenomenon in Beirut are supplied by John of Ephesus. He says: "before the earthquake happened, the sea retired roughly two miles, then the people were rushed in the seabed to find wealth at the sunken ships, then an immense wave returned, flooding the shore and drowning ships as well as the people who were in the seabed and along the coast". Although this last detailed description is somewhat strange and it is difficult to verify its reality, obviously the earthquake was associated with a tsunami. The horrible news of Beirut have reverberated across the entire Empire to an extent that the 6th century Hellenistic poet from Spain John Barbacallus wrote a verse elegizing Beirut [cited in Hitti, 1972]. Based on Beirut's available data, the intensity can be assessed as IX–X (EMS-92). Historical sources, from the other side, have mentioned that Beirut was in chaos and easily conquered by the Persians, Byzantines and Arabs in the year 600 AD [Collinet, 1925].

The city of Sidon suffered with a large number of deaths [John Malalas]. The process of transferring School of Law from Beirut to Saida [Agathias Scholasticus] gives an impression that the degree of damage in Saida was less than that in Beirut. Therefore, a seismic intensity range VII–VIII in Saida may be assigned. In the town of Botrys, a part of Mount Lithoprosopos broke off and fell into the sea forming a harbour [John Malalas]. This description indicates that there was a local landslide. The cities of Byblus, Tyrus and Tripolis were also destroyed with their inhabitants [John Malalas, Antoninus Placentinus, De Fragmentis Historicis Tuscolanis, Chronicon pseudo-Dionisyanum]. Tyre was also destroyed with its inhabitants [John Malalas, De Fragmentis Historicis Tuscolanis, Chronicon pseudo-Dionisyanum]. A similar fate befell the town of Trieris [Antoninus Placentinus], modern Shikka. Although the description is very short, intensity range of IX–X has been allocated to these former towns for geographical considerations. When Antoninus arrived at the island of Antharidus near Syria during his way to the Holy Land, which is probably the sole island of Aradus (modern Arwad) belonging to Syria and not Antaradus (modern coastal city of Tartus), he was silent about the earthquake's effects at the island. Taking into consideration that the earthquake was felt farther north at Antioch (as it will be shown later on) and that this island is very small that did not allow him to observe any effect, it is believed that Aradus should has only felt this earthquake. The end 8th century chronicle [Chronicon pseudo-Dionisyanum] mentioned that Sarepta (modern Sarfand) was also destroyed with its people. Despite this source is a very late one and so should be treated with caution, this earthquake probably damaged or destroyed Sarepta as it lies between Sidon and Tyre. If this is so, this indicates an intensity range VII–VIII?

On the mainland, the earthquake was severe and tremendous in Palestine [John Malalas, De Fragmentis Historicis Tuscolanis], to such an extent that many cities and villages, not named, in both regions of Galilee (modern Aj-Jalil) and Samaria (modern As-Samyra) were destroyed [John of Ephesus, Chronicon pseudo-Dionisyanum]. To the east, similarly happened to the province of Arabia, which is western Jordan today, [John Malalas, John of Ephesus, De Fragmentis Historicis Tuscolanis, Chronicon pseudo-Dionisyanum]. In this regard, archaeological evidences suggest that the 551 AD earthquake is responsible for destruction or damage of a number of historical sites in Arabia (Jerash, Nebo, Lijjun and Petra) [Crowfoot, 1938; Saller and Bagatti, 1949; Hammond, 1981; Parker,1982, 1983]. However, due to the missing of objective evidence we cannot verify any severe damage to these sites.

This event was strongly felt in Syria including regions of Antioch (modern Antakya) and Mesopotamia [John Malalas, De Fragmentis Historicis Tuscolanis]. In the time of this earthquake, Agathias Scholasticus mentioned that Alexandria was felt by an earthquake causing concern and no one remained in his house. We think that it may be the same event.

The total number of deaths is rather difficult to evaluate. However, as a result of the earthquake side-effects (tsunami and fires) we believe that a myriad of people were killed along the Lebanese coast, particularly in Beirut.

The available macroseismic data makes impossible to construct the isoseismal curves for the 551 AD earthquake, from which the earthquake's epicenter can be assessed. Alternatively, we proposed distribution of the damage severity and earthquake intensity (according to EMS-92 [Grünthal, 1993]) for the affected Lebanese cities as shown in Fig. 2. However, we believe that the most probable position of the earthquake's epicentre seems to be a near-field location of Beirut, the locality that has the highest intensity due to this earthquake from one hand, and alternatively, offshore of Beirut on the other hand. The evidences for the latter is as follows: firstly, the earthquake was preceded by a retreating of the sea for a period of time that allowed people to rush downward the exposed bottom of the sea to search for treasures before they felt the land shaking. Secondly, there is the large extent and the severity of the tsunami along the whole Lebanese coast. Considering that there is no evidence that the earthquake affected or even was felt in Cyprus [Pantazis, 1996], we estimate the earthquake's epicentre at 34.00°N and 35.50°E. These coordinate fit with the conclusions of Guidoboni *et al.* [1994].

Locating the earthquake's epicentre near the sole strike-slip Roum fault suggests that the earthquake is the result of its movement. This northwest fault that extends

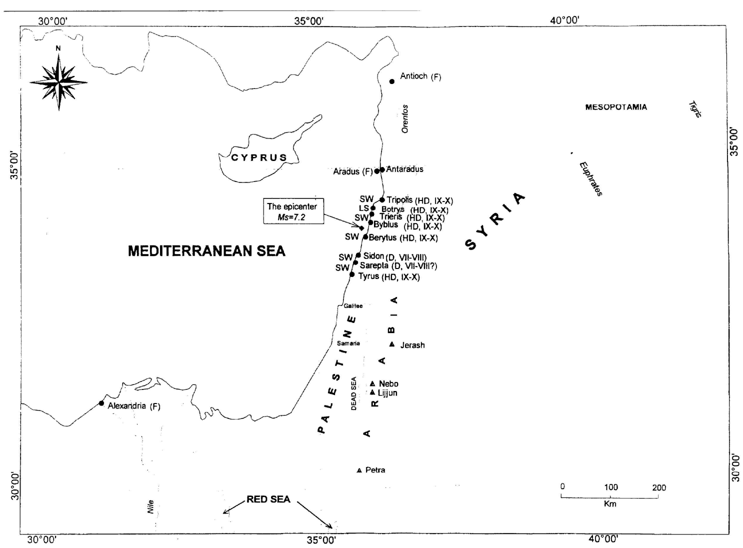

Fig. 2. Distribution of the damage severity and the intensity (EMS-92) for the 9 July, 551 AD earthquake, and its proposed epicentre. Note that F: Felt; D: Damage; HD: Heavy Damage; LS: Landslide and SW: Sea-Wave. Triangles represent possible damaged archaeological sites from the previous literature.

from north of Tiberias Lake to city of Beirut is a branch of a major fault system that forms the western boundary of the Arabian platform of the transform nature. This fact, together with the results of the seismic monitoring in the region during the 20th century suggests that the focal depth is shallow.

Taking into consideration the above-mentioned effects of the event in the area, we believe that the earthquake is of large size. To assess surface wave magnitude Ms of the earthquake, three methods were used:

1 — Using the Shebalin's nomograph [1974], $Ms = 7.3$ is calculated.

2 — Applying Ambraseys' equation [1988] that correlates between observed length of strike-slip surface fault L (in km) and Ms for the Middle East:

$$Ms = 4.63 + 1.43 \log(L) \tag{1}$$

and assuming that this event may be attributed to the 50-km-long, strike-slip Roum fault, we obtain $Ms = 7.1$.

3 — Adopting the empirical formula of Bonilla *et al.*, 1984 that correlates also between Ms and L for numerous strike-slip faults:

$$Ms = (6.10 \pm 0.25) + (0.70 \pm 0.13) \log L \tag{2}$$

by taking into account the five possible cases (4 with errors and one without errors), Ms has been calculated to be 7.3. The results obtained by the above reported formulae are scattered between the values $Ms = 7.1$–7.3 which can be assumed as final magnitude.

Moreover these values seems to be reasonable as compared with the historical descriptions of the effects produced by this earthquake.

Although historical sources did not mention occurrence of aftershocks, it is more likely that this large earthquake should be followed by at least one less-magnitude (felt) aftershock. Sometimes this is encountered, as the historical sources report only the larger events.

5. Discussion and Conclusions

The re-appraisal of the 9 July 551 AD earthquake has led to the following conclusions:

1 — Location of three new affected sites: these are the island of Aradus (modern Arwad), the towns of Trieris (modern Shikka) and Sarepta (modern Sarfand).
2 — Estimating the seismic intensities for the previous localities, as well as the towns of Tyrus, Sidon and Botrys.
3 — Assessment of the average surface-wave magnitude of the earthquake (Ms), to be of the order of 7.1–7.3.
4 — Suggesting that the strike-slip left-lateral Roum fault is a possible causative fault of the earthquake.
5 — Locating the earthquake's epicentre at 34.00°N and 35.50°E.

In general, this paper shows that the 9 July 551 AD earthquake represents one of the largest seismic events in and around Lebanon during the Byzantine period. It destroyed several Lebanese coastal cities and chiefly the city of Beirut. The earthquake was associated with a tsunami along the Lebanese coast, with a local landslide near Al-Batron and with an eruption of a large fire in Beirut, continuing for almost two months.

The general conclusions are shown in Fig. 2.

Returning to Fig. 1, the Roum fault (ROF), which seems to be responsible of this earthquake, represents a branch of the major fault system criss-cross Lebanon and western Syria. This major fault system consists of two main faults namely the Yammouneh fault (YAF) and the Al-Ghab fault (GHF), which are both responsible for generating many destructive historical earthquakes in Syria and Lebanon. In this regard, the YAF has generated earthquakes in 1202 ($Ms = 7.5$), 1705 ($Ms = 6.9$) and 1759 ($Ms = 6.6$ and 7.4) [Ambraseys and Melville, 1988; Ambraseys and Barazangi, 1989; Ambraseys and Finkel, 1993; Mouty *et al.*, 1998]. While the Al-Ghab fault has generated destructive historical earthquakes in western and northwestern Syria, such as earthquakes of 1157 ($Ms > 7.0$), 1170 ($Ms > 7.0$), 1404 ($Ms = 7.4$), 1407 ($Ms \sim 7.0$), 1796 ($Ms = 6.6$), 1822 ($Ms = 7.4$), 1872 ($Ms = 7.2$) [Ambraseys and Barazangi, 1989; Mouty *et al.*, 1998]. Taking into consideration that the return period between these large historical earthquakes that occurred in Lebanon and western Syria is 200–350 years [Ambraseys and Barazangi, 1989] from one hand, and that the region with its urban and economic density, on the other hand, has shown relatively seismic quiescence during the 20th century, we believe that the earthquake hazards of these may be genuine in many cities in the area in the near future. In other words, there may be a probable rupture of one of the aforesaid faults, in the form of a large earthquake ($M \geq 6.5$). This implies that results of these historical earthquake studies must be used in seismic hazard assessment for particular sites and on both local and regional scales for Lebanon and Syria, and that huge efforts of multidisciplinary approaches should be done by architects and engineers by designing structures within acceptable safety margins and strengthening existing structures. And this, in turn, will help in mitigating the seismic risk in our region.

Acknowledgements

We would like to thank Dr. A. Gürpinar from IAEA for his valuable support and for the fruitful coordinating of our activities in the frame of IAEA-AECS project entitled "Seismic Data for the Siting and Site Revalidation of Nuclear Facilities". We express our gratitude also to Prof. I. Othman, Director General of the Atomic Energy Commission of Syria for his encouragement. We are also grateful to Prof. M. Mouty, the main investigator of IAEA project in Syria for his reviewing of this paper. Many thanks are due to Profs. N. N. Ambraseys and M. Barazangi for their critical reviewing, comments and effective guidance. For their useful suggestions, comments and constructive criticism of the manuscript, thanks are due to both anonymous reviewers. Authors would like to thank Geol. B. Kattaa for digitising the maps. This paper has been written within the framework of IAEA-AECS research project, and in collaboration with the Italian Agency for New Technology, Energy and Environment.

References

Historical primary and secondary sources

Agathias Scholasticus (Agath.), *Historiarum libri quinque*, ed. J. P. Migne, PG, 88, Paris, 1864.

Antoninus Placentinus (Anton.), *Itinera Hierosolymitana saec, IV–VIII*, ed. P. Geyer, CSEL 39, Praha-Wien-Leipzig, 1898.

Chronicon pseudo-Dionisyanum (Chron. pse. Dionis.), tr. Hespel, Corpus Scriptorum Christianorum Orientalium, Script. Syri, t. 213, Louvain, 1989.

De Fragmentis Historicis Tuscolanis (Frag. Hist. Tusc.), ed. J. P. Migne, PG, 85, Paris, 1864.

Georgius Cedrenus, *Compendium Historiarum*, ed. J. P. Migne, PG, 121, Paris, 1894.

Georgius Monachus, *Chronicon*, ed. J. P. Migne, PG, 110, Paris, 1863.

John of Ephesus (John Eph.), *Joannis Ephesini episcopi Commentarii de beatis orientalibus et Historiae ecclesiaticae fragmenta*, tran. W. J. Van Douwen and J. P. N. Land, Amsterdam, 1889.

John Malalas (Mal.), *The Chronicle*, tr. E. Jeffrey, M. Jeffrey, R. Scott, Melbourne, 1986.
Michael the Syrian, *Chronicle*, ed. and French tr. J.-B. Chabot, *Chronique de Michel le Syrien*, Paris, 1899–1910.
Theophanes, *Chronographia*, ed. C. De Boor, 1, Leipzig, 1883.

Catalogues and literature

Abou Karaki, N. [1987] "Synthèse et carte sismotectonique des pays de la bordure orientale de la Méditerranée: sismicité du systéme de failles du Jordan-Mer Morte," Thèse de Doctorat, Université Louis Pasteur, Strasbourg.
Ambraseys, N., Banda, E. *et al.* [1983] "Note on historical seismicity," BSSA 73, 1917–1920.
Ambraseys, N. [1988] "Magnitude-fault length relationships for earthquakes in the Middle East," ed. Lee, W. H. *History of Seismography and Earthquakes of the World*, Academic, San Diego, Calif., 309–310.
Ambraseys, N. and Melville, C. [1988] "An analysis of the eastern Mediterranean earthquake of 20 May 1202," ed. Lee, W. H. *History of Seismography and Earthquakes of the World*, Academic, San Diego, Calif., 181–200.
Ambraseys, N. and Barazangi, M. [1989] The 1759 earthquake in the Bekaa valley: Implications for earthquake hazard assessment in the eastern Mediterranean region, *J. Geophys. Res.* **94**, 4007–4013.
Ambraseys, N. and Finkel, C. [1993] "Material for the investigation of the seismicity of the eastern Mediterranean region during the period 1690–1710," ed. Stucchi, M. *Hist. Invest. European Earthq.* **1**, 173–194.
Ambraseys, N., Melville, C. and Adams, R. [1994] *The Seismicity of Egypt, Arabia and the Red Sea: A Historical Review* (Cambridge University Press).
Ambraseys, N. and White, D. [1997] "The seismicity of the Eastern Mediterranean region 550–501 BC: A re-appraisal," *J. Earthq. Engrg.* **1**(4), 603–632.
Amiran, D. K. [1952] "A revised earthquake catalogue of Palestine," *Isr. Explor. J.* **1**, 223–246.
Barazangi, M. [1983] "A summary of the seismotectonics of the Arab region," eds. Cidinsky and Rouhban *Ass. Mit. Earthq. Ris. Arab Reg.*, UNESCO, 43–58.
Ben-Menahem, A. [1979] "Earthquake catalogue for the Middle East," *Boll. Geofis. Teor. Appl.* **21**, 245–313.
Best, J. A., Barazangi, M., Al-Saad, D., Sawaf, T. and Gebran, A. [1990] "Bouguer gravity trends and crustal structure of the Palmyride Mountain belt and surrounding northern Arabian platform," *Geology* **18**, 1235–1239.
Bonilla, Mark and Lienkaemper [1984], In: Bullen, K. E. and Bolt, B. A. *An Introduction to the Theory of Seismology* (1993), 4th ed., Cambridge.
Bonito, M. [1691] "Terra tremante, o vero continuatione de' terremoti dalla Creatione del Mondo fino al tempo presente," Napoli 1691 (reprint, Sala Bolognese, 1981).
Collinet, P. [1925] "Histoire de l'Ecole de droit de Beyrouth," Paris.
Crowfoot, J. W. [1938] "The Christian churches in Gerasa: city of the Decapolis," ed. C. H. Kraeling, New Haven, *Amer. Sch. Orient. Res.*, 171–262.
Darawcheh, R. and Sbeinati, M. R. [1998] "Earthquakes in and around Syria during 1997: Bulletin No. 7," (in Arabic), unpublished *AECS*-G\RSS 233, Damascus.
Grünthal, G., ed. [1993] "European macroseismic scale 1992 (up-dated MSK-scale)," Conseil de l'Europe, *Cen. Européen Géody. Séis.* 7, Luxembourg.
Guidoboni, E., ed. [1989] "I terremoti prima del Mille in Italia e nell'area mediterranea," Bologna.

Guidoboni, E., Comastri, A. and Traina, G. [1994] "Catalogue of ancient earthquakes in the Mediterranean area up to the 10th century," *Publ. Ist. Nazion di Geofisica*, Rome, 332–336.

Hammond, P. C. [1981] "Cult and cupboard at Nabatean Petra," *Archaeology.*

Hitti, Ph. [1972] "Tarikh Lobnan: History of Lebanon," (in Arabic), *Publ. Dar Ath-Thaqafah*, tr. by Anis Freha, Beirut.

International Atomic Energy Agency [1987] "Methodology and procedures for compilation of historical earthquake data," IAEA-TECDOC-434, Vienna.

Mouty, M., Sbeinati, M. R. and Darawcheh, R. [1998] "Seismic Data for Siting and Site-Revalidation of Nuclear Facilities — Part I: Catalogue of historical earthquakes in and around Syria," Unpublished *AECS* Research Report No. G\FRSR 176, Damascus.

Pantazis, Th. [1996] "Archaeseismicity of Cyprus," *Proc. Reg. Workshop Archaeoseis. Med. Region*, AECS, Damascus, 81–89.

Parker, S. T. [1982] "Preliminary Report on the 1980 Season of the Central Limes Arabicus Project," *Bull. Am. Sch. Orie Res.* **247**.

Parker, S. T. [1983] "The Central Limes Arabicus Project: The 1982 Campaign," *Annual of the Department of Antiquities of Jordan 27.*

Perrey, A. [1850] "Mémoire sur les tremblements de terre ressentis dans la péninsule turco-hellénique et en Syrie," *Mém. Cour. Mém. Sav. Etr. Acad. R.* Belgique 23, Bruxelles.

Plassard, J. and Kogoj, B. [1981] "Sismicité du Liban: Catalogue des séismes ressentis," *Annals-Mem. Obs.* de Ksara IV, Beirut.

Russell, K. W. [1985] "The earthquake chronology of Palestine and Northwest Arabia from the 2nd through the Mid-8th century AD," *Bull. Am. Sch. Ori. Res.* **260**, 37–59.

Saller, S. J. and Bagatti, B. [1949] "The Town of Nebo (Khirbet El-Mekhayyat) with a Brief Survey of Other Ancient Christian Monuments in Transjordan," *Publication of the Studium Biblicum Franciscanum* **7**.

Sbeinati, M. R. [1994] "Instrumental catalogue of earthquakes in Syria and adjacent areas from 1900 to 1993," Unpublished *ICTP* Research Report, Trieste.

Sbeinati, M. R. and Darawcheh, R. [1999] "A preliminary report on the June 20, 1999 earthquake," (in Arabic), unpublished *AECS* report, Damascus.

Shebalin, N. V. [1974] "Principles and procedures of cataloguing. In Catalogue of Earthquakes," eds. Shebalin, Kárník and Hadžievski, UNDP/UNESCO survey of seismicity of the Balkan region (Skopje: UNESCO).

Sieberg, A. [1932] "Untersuchungen über Erdbeben und Bruchscholenbau im Östlichen Mittelmeergiet," *Denkschriffen der Medizinsch-Naturwissenschaft Gesellschaft zu Jena* **18**, 161–273.

Stucchi, M. [1994] "Recommendations for the compilation of a European parametric earthquake catalogue, with special reference to historical records," eds. Albini, P. and Moroni, A., *Hist. Invest. European Earthq.* **2**, 181–190.

USGS-UNESCO [1993] "Cooperative program for reducing earthquake losses in the EMR," Cairo, Oct. 16–21, p. 21.

Vogt, J. [1993] "Historical seismology: Some notes on the sources for seismologists," ed. Stucchi, M., *Hist. Invest. European Earthq.* **1**, 15–24.

Geophys. J. Int. (2003) 153, 658–674

Holocene faulting and earthquake recurrence along the Serghaya branch of the Dead Sea fault system in Syria and Lebanon

Francisco Gomez,[1] Mustapha Meghraoui,[2] Abdul Nasser Darkal,[3] Fouad Hijazi,[4] Michel Mouty,[4] Youssef Suleiman,[4] Reda Sbeinati,[5] Ryad Darawcheh,[5] Riad Al-Ghazzi[4] and Muawia Barazangi[1]

[1] *Institute for the Study of the Continents, Snee Hall, Cornell University, Ithaca,* NY 14853, *USA. E-mail: fgomez@geology.cornell.edu*
[2] *EOST, Institut de Physique du Globe,* UMR 7516, *Strasbourg, France*
[3] *Department of Geology, Damascus University, Damascus, Syria*
[4] *Higher Institute of Applied Sciences and Technology, Damascus, Syria*
[5] *Department of Geology, Syrian Atomic Energy Commission, Damascus, Syria*

Accepted 2003 January 4. Received 2002 November 25; in original form 2002 July 24

SUMMARY

The Serghaya fault, located approximately along the Syrian–Lebanese border, is a prominent structure within the 200 km restraining bend in the left-lateral Dead Sea fault system. This study documents palaeoseismic and geomorphic expressions of Holocene movements on the Serghaya fault based on trench excavations and radiocarbon dates. Trenches were excavated across and parallel to a 4.5 m fault scarp where Late Pleistocene sediments are faulted against Holocene alluvium and colluvium. Locally oblique slip on the Serghaya fault has produced a sequence of fault-derived colluvial wedges that distinguishes individual palaeoseismic events. In addition, the trench excavations also depict a sequence of buried and displaced channels. Our palaeoseismic study reveals evidence for five surface-rupturing events within the past ~6500 yr. The last event involved 2–2.5 m of primarily left-lateral displacement and may correspond to one of two historically documented earthquakes during the 18th century (in 1705 and 1759). The displaced channels provide an estimated slip rate of approximately 1.4 ± 0.2 mm yr^{-1} during the Holocene. The chronological relationships between the colluvial wedges and faulted channels demonstrate an average left-lateral displacement of about 2 m per event, suggesting that such events correspond to earthquakes of $M \gtrsim 7$ with a mean return time of about 1300 yr. These results demonstrate that the Serghaya fault may present a previously overlooked earthquake hazard for populations in the vicinity of the AntiLebanon Mountains, including the cities of Damascus and Beirut. In a regional context, the inferred slip rate along the Serghaya fault accounts for about 25 per cent of the total expected motion of Arabia relative to Africa along the Dead Sea fault system. The fact that the Serghaya fault accounts for only a fraction of the expected plate motion implies that the remaining strike-slip and shortening must be accommodated by other active fault branches within the large restraining bend of the Dead Sea fault system. These results contradict suggestions that the northern Dead Sea fault system in Lebanon and Syria is presently inactive as a result of an evolving regional stress field in the eastern Mediterranean region.

Key words: Dead Sea fault, earthquakes, Lebanon, slip rate, Syria.

1 INTRODUCTION

Spanning nearly 1000 km from the Gulf of Aqaba in the south to the Taurus Mountains in southern Turkey, the Dead Sea fault system (DSFS) ranks among the largest strike-slip fault systems in the world and represents a key element of the eastern Mediterranean tectonic framework. The DSFS is the left-lateral transform boundary between the Arabian and African plates and accommodates their differential convergence relative to Eurasia (e.g. Freund *et al.* 1970; Ben Menahem *et al.* 1976). However, recent debates concerning the slip rate and kinematics of the DSFS, especially the activity of the northern ~500 km of the DSFS in Lebanon and Syria (e.g. Girdler 1990; Butler *et al.* 1997), attest to the limited understanding of the DSFS as an active and seismogenic system.

The general structure of the left-lateral DSFS consists of two relatively simple northern and southern sections, joined by a ~200 km

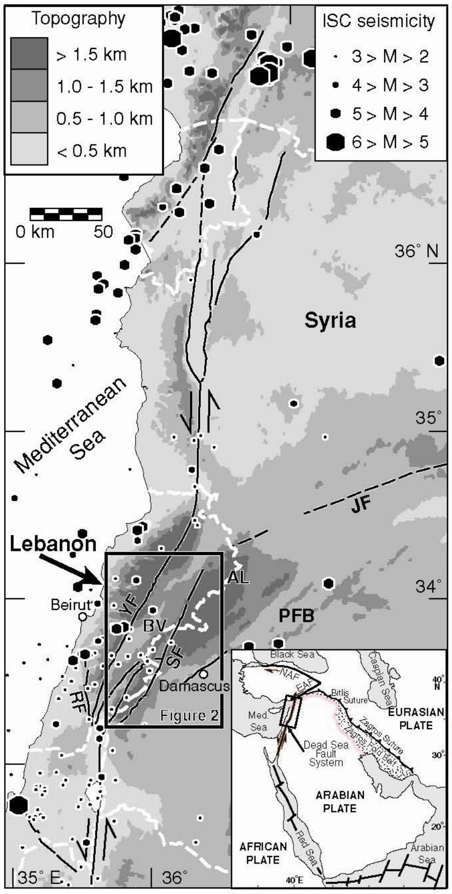

Figure 1. Simplified topography and tectonic map of the northern Dead Sea fault system. Tectonic and physiographic features: SF = Serghaya fault, YF = Yammouneh fault, RF = Roum fault, JF = Jhar fault, AL = AntiLebanon Mountains, PFB = Palmyride fold belt, BV = Bekaa Valley. The inset depicts the plate tectonic context of the Dead Sea fault system. Faults are simplified from Dubertret (1962).

long restraining bend located mostly in Lebanon (see Fig. 1; Garfunkel *et al.* 1981; Quennell 1984; Beydoun 1999). Within this restraining bend, the fault system comprises several distinct fault branches (e.g. Walley 1988). An understanding of which structures are active, along with their kinematics, is essential to unravelling the nature and tectonic evolution of this part of the plate boundary and how it links the structurally simpler sections of the DSFS to the north and south.

Another motivation for studying active tectonics of the DSFS is a better understanding of the regional earthquake hazard in the eastern Mediterranean. The DSFS, in particular, presents a special opportunity to integrate several millennia of historical records of large earthquakes with palaeoseismic methods in order to understand the processes of earthquake recurrence in the plate boundary deformation. Historical accounts testify to large and devastating earthquakes along the DSFS over the past several millennia (e.g. Poirier & Taher 1980; Ambraseys & Barazangi 1989; Ambraseys *et al.* 1994; Amiran *et al.* 1994; Darawcheh *et al.* 2000; Sbeinati *et al.* 2002).

For the central and northern DSFS, these historical records contrast with instrumental records of seismicity during the past century depicting little earthquake activity (e.g. Ambraseys & Jackson 1998). This apparent behaviour of seismic quiescence punctuated by large earthquakes underscores the need for geological studies of past earthquakes (i.e. palaeoseismology and tectonic geomorphology) to understand the patterns of large earthquake recurrence along this plate boundary. During the past decade, palaeoseismic investigations along the southern DSFS have proven successful in identifying surface ruptures associated with historical earthquakes (e.g. Ellenblum *et al.* 1998; Ken-Tor *et al.* 2001), as well as documenting evidence for long-term earthquake behaviour such as temporal clustering (e.g. El-Isa & Mustafa 1986; Marco *et al.* 1996; Zilberman *et al.* 2000). Aside from one recent study at the site of a faulted Hellenistic or Roman aqueduct in Syria (Meghraoui *et al.* 2003), similar studies are, in general, lacking for the central and northern DSFS in Lebanon and Syria (i.e. from the restraining bend northward). In addition to earthquake recurrence histories, fundamental kinematic parameters such as rates of fault slip are not well documented. Hence, the DSFS presents a poorly understood earthquake hazard for the surrounding populations, particularly in the central and northern sections. In the case of the restraining bend, the relative activity of different active branches will have implications for earthquake hazard assessment, particularly if concepts such as stress triggering and fault interactions are considered (e.g. Stein *et al.* 1997; Mohamad *et al.* 2000).

This study examines the Serghaya fault, a branch of the DSFS within the restraining bend that, until recently, has been generally regarded as inactive since the Pliocene (e.g. Walley 1988; Girdler 1990; Butler *et al.* 1997). This study presents detailed observations and analyses that build upon our previously reported reconnaissance work in the region (Gomez *et al.* 2001). These new results demonstrate that the Serghaya fault has important implications in terms of regional tectonics and earthquake hazard. Palaeoseismic and geomorphic evidence demonstrates a record of Holocene earthquakes and provides a Holocene slip rate for this fault branch. After discussing the implications for the regional earthquake hazard, these results are placed within the context of present-day regional tectonics of the DSFS.

1.1 Regional tectonic and seismotectonic setting

The present-day relative motion between Arabia and Africa is estimated to be 4–8 mm yr^{-1}, based on plate tectonic models (e.g. Joffe & Garfunkel 1987; Jestin *et al.* 1994) and recent GPS observations (e.g. McClusky *et al.* 2000, 2003). This is consistent with geological estimates of Quaternary slip rates for the southern DSFS (e.g. Garfunkel *et al.* 1981; Klinger *et al.* 2000a), as well as an estimated slip rate, averaged over ~2000 yr, from the aforementioned faulted aqueduct in Syria (Meghraoui *et al.* 2003). Interestingly, almost all models of instantaneous (i.e. present-day) plate motions predict a general northward increase in the rates of slip along the DSFS, as well as increasing the component of relative convergence between the Arabian and African plates across the DSFS. This assumes that all of the relative plate motion is accommodated by the DSFS. The present episode of tectonic activity of the DSFS is believed to have initiated during the end of the Miocene or early Pliocene (e.g. Hempton 1987).

Available seismotectonic observations, although limited, are consistent with the general model of a continental transform system. The kinematics of the large Gulf of Aqaba earthquake in 1995 ($M \sim 7.3$) demonstrated predominantly left-lateral motion along the southern DSFS (Pinar & Turkelli 1997; Klinger *et al.* 1999). The paucity of large, instrumentally recorded earthquakes has precluded accurate assessment of seismic moment release along the plate boundary (e.g. Jackson & McKenzie 1988). However, some have suggested 6–10 mm yr^{-1} of slip by inferring seismic moment and other parameters of large, historically documented earthquakes (e.g. Westaway 1994). The morphological expression of the DSFS from remotely sensed imagery also shows a general spatial correspondence with seismicity patterns (e.g. Al Ghazzi 1992).

The 200 km long northeast–southwest striking restraining bend encompasses the Mt Lebanon and AntiLebanon ranges. At the southern end of this restraining bend, the relatively simple trace of the southern DSFS branches into several distinct fault splays, including the Yammouneh, Serghaya, Rachaya, Hasbaya and Roum faults (Fig. 1) (e.g. Walley 1988; Heimann & Ron 1993). Of all of these fault branches, the Yammouneh fault is the only throughgoing structure that connects the northern and southern sections of the DSFS.

Adjacent to the restraining bend, the Palmyride fold belt is another regionally prominent tectonic element (Fig. 1). This Cenozoic fold belt corresponds to a Late Palaeozoic–Early Mesozoic (Neo-Tethyan) rift basin that was tectonically inverted during the Cenozoic (e.g. Chaimov *et al.* 1990). Scattered seismicity suggests that the Palmyride region is still tectonically active (e.g. Chaimov *et al.* 1990; Brew *et al.* 2001). Hence, the Palmyrides represent some internal deformation of the Arabian plate that might have some kinematic relationship with the plate boundary deformation of the DSFS.

1.2 Serghaya fault and Zebadani valley

Branching from the southern DSFS in the Golan Heights, the Serghaya fault can be traced approximately 125 km through the AntiLebanon Mountains to the eastern edge of the Bekaa Valley (Fig. 2). A detailed map of the Serghaya fault zone (Fig. 2) has resulted from the analysis of remote sensing imagery (satellite imagery and aerial photos), a high-resolution (20 m pixel) digital elevation model (DEM), information from published geological maps (e.g. Dubertret 1955), and ground-truth from field investigations. Fig. 2 also depicts the morphology of the region using the DEM to generate a shaded relief image. The gross geomorphic expressions of the Serghaya fault include the alignment of linear valleys and large stream valley deflections. Almost all valleys show clear leftward deflections implying long-term, tectonic control of the landscape. Furthermore, left steps in the fault zone correspond to the elongate basins, suggesting these are pull-apart basins.

Along the southern half of the Serghaya fault, the uplift of the Mt Hermon block in the AntiLebanon Mountains forms within an apparent strike-slip duplex comprising the Serghaya and Rachaya faults (Fig. 2). This interpretation of a crustal sliver trapped between two strike-slip faults is consistent with reported vertical-axis rotations of the Mt Hermon region observed with palaeomagnetic data (e.g. Ron 1987; Heimann & Ron 1993). Field evidence for Quaternary strike-slip faulting along the Serghaya fault is observed as far north as the village of Aarsal, near the edge of the Bekaa Valley (Fig. 2). North of this point, the trace of the Serghaya fault is obscure. Existing geological maps and overhead imagery depict neither geomorphic nor structural indications to suggest that the northern Serghaya fault reconnects with the transform boundary (Fig. 2). Such a linkage would be expected to involve local extension and subsidence (a leftward step in a left-lateral fault system), and these phenomena are not apparent.

Although the Serghaya fault primarily traces through the Mesozoic carbonate bedrock of the AntiLebanon Mountains, the fault occasionally passes through Quaternary basins, providing an opportunity to observe the expressions of recent fault movements. In the Zebadani Valley of Syria (Fig. 2), the focus of this study, the Serghaya fault bounds the eastern side of the valley. The stereonet in Fig. 3 depicts the fault planes and associated striations measured in faulted Late Pleistocene lake sediments in the southern Zebadani Valley. Shear indicators (e.g. slickenside striations and tool marks) demonstrate predominantly left-lateral slip. Rakes of 10°–20° are observed on subvertical fault planes, implying a ratio of strike-slip to dip-slip between 4:1 and 5:1. A 4.0–4.5 m fault scarp results from the oblique fault slip along this portion of the Serghaya fault. Locally, the fault scarp preserves a free face, attesting to recent fault movement. The free face heights suggest approximately 0.5 m of dip slip for the last episodic movement (Gomez *et al.* 2001).

Small hillslope drainage deflections also coincide with the fault scarp (Fig. 4). Many of these deflections have been measured and interpreted as true fault displacements (Gomez *et al.* 2001). All of these small drainages depict minimum deflections of 1.9–2.5 m, as well as larger, composite stream deflections (Fig. 3). The proportion of strike-slip to dip-slip suggested by the stream deflections and scarp free faces, respectively, is consistent with the fault kinematic indicators (stereonet in Fig. 3). Hence, these recent movements are most likely to be contemporaneous.

One colluvial wedge corresponds to the remnant of the free face, suggesting that the free face represents only one palaeoseismic event (e.g. McCalpin 1996). Radiocarbon dating has constrained this paleoseismic indicator within the past 300 yr (Gomez *et al.* 2001). Hence, the free faces and minimum drainage displacements are probably the expressions of the last surface rupturing earthquake, and this event may correspond to one of two well-documented earthquakes that strongly affected the AntiLebanon Mountains and surrounding regions in the early and mid 18th century (i.e. in 1705 and 1759; see Table 1). The recent timing of this event is also supported by the preservation of a fault scarp free face in Late Pleistocene lake sediments.

2 PALAEOSEISMIC STUDY: METHODS AND RESULTS

The presence of an active fault with an apparent coseismic displacement during recent history motivated our effort to extend the record of past earthquakes and their associated displacements back through the Holocene. The evidence of a prominent, young fault scarp and consistent left-lateral stream offsets, along with lacustrine and alluvial deposits, suggested that the southern Zebadani valley might be a promising site for palaeoseismic investigation. Our study focused on a site near the village of Tekieh (see Figs 3, 5 and 6) where the fault juxtaposes recent alluvium against Late Pleistocene lacustrine sediments. Microtopographic mapping and analysis was combined with a trench excavation in order to document the earthquake history of the Serghaya fault.

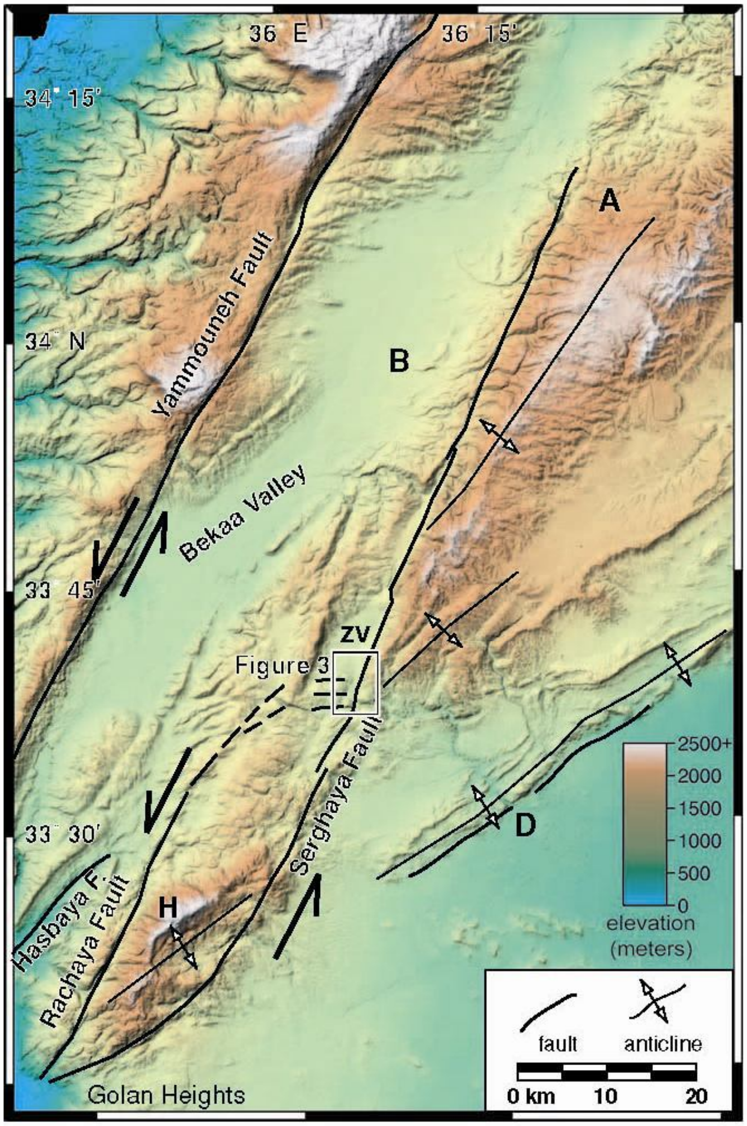

Figure 2. Shaded relief image depicting the gross morphology of the Serghaya fault. Faults and the main anticlinal hinges are shown. Geographic features: ZV = Zebadani Valley, H = Mt Hermon, D = Damascus, B = Baalbek, A = Aarsal. See Fig. 1 for location.

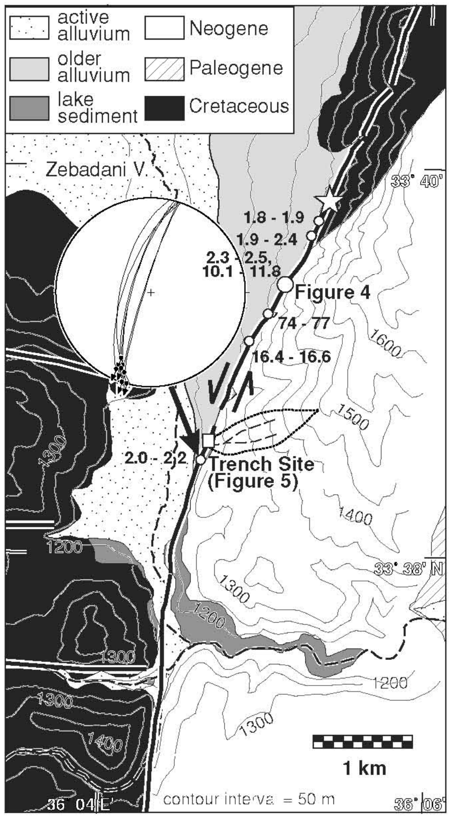

Figure 3. Geology of the southern Zebadani Valley (Syria). See Fig. 2 for location. Stereonet depicts fault planes and associated striations from faulted Late Pleistocene lake sediments. The dotted line depicts the catchment for the hillslope drainage at the trench site (white square). The white star denotes the excavation of the upper colluvial wedge described in Gomez *et al.* (2001). White discs denote small drainage deflections (values in metres), including the example shown in Fig. 4. Topographic contour interval = 50 m.

2.1 Local morphology

The Serghaya fault is represented by a composite fault scarp ~4.0–4.5 m high and comprising the boundary between the mountain front and the Late Quaternary alluvial apron (Fig. 6). As shown in the topographic profile (Fig. 5b), the lower alluvial surface appears to correspond to the bevelled bedrock in the upper surface. About 150 m to the south can be found some of the free faces reported by Gomez *et al.* (2001).

The up-thrown eastern block of the fault comprises Late Quaternary lacustrine sediments (calcareous silt and gravel) and Pliocene–Quaternary conglomerates (Fig. 5). Radiocarbon dating of a charcoal fragment from a roadcut exposure of the lacustrine sediments about 0.5 km to the south yielded a radiocarbon age of 44.6 kyr BP (sample LS-1 in Table 2).

At the trench site, a hillslope drainage with a small catchment area of approximately 0.25 km^2 exits the mountain front (Fig. 3). This ephemeral stream feeds a young alluvial fan that attains up to about 1 m of relief above the surface of the older alluvial apron (Fig. 5). Although today partially truncated on the north side by an orchard, the northern limit of the younger fan was mapped from aerial photos dating to 1983.

Emerging from the mouth of the drainage at the fault scarp, the active, ephemeral streambed deflects southward (i.e. left-lateral) approximately 2 m (Fig. 5). This deflection is consistent with the minimum deflections observed in other small drainages in the southern Zebadani Valley (Fig. 3; Gomez *et al.* 2001). Hence, we interpret this deflection as a displacement corresponding to the last surface-rupturing earthquake in the early or mid 18th century.

2.2 Palaeoseismic trenching

The system of three trenches shown in Figs 5 and 6 was designed to take advantage of both the vertical and lateral components of the locally oblique fault slip. The trenches were excavated using a backhoe, and the walls were subsequently cleaned by hand. A 1 m grid facilitated the careful logging of all six trench walls (three trenches with two walls each) at a scale of 1:20. Within the study site, we mapped the precise positions of the trenches with respect to the present-day stream channel and fault scarp using a total station.

Trench 1 spanned approximately 8 m across the fault zone and exposed the Late Pleistocene lacustrine deposits and the alluvial sediments. This trench was excavated to depths from 2.5 to 4 m and provided a view of the relationships between faulting and different colluvial/alluvial deposits.

Trenches 2 and 3 were excavated 2–2.5 m deep, parallel to the fault scarp (NNE–SSW) from the mouth of the drainage southward across the alluvial fan. These fault-parallel trenches, located 4 and 7 m from the fault, were excavated in order to explore for indications of lateral displacement. Furthermore, the intersection of Trenches 1 and 2 provided possible stratigraphic ties within the excavation site.

The results presented below reflect all six trench logs. However, for the sake of simplicity, only two trench logs are shown: one wall of the trench crossing the fault (Trench 1; Figs 7 and 8), and one wall of the fault-parallel trench nearer the fault scarp (Trench 2; Figs 9 and 10).

2.3 Radiocarbon dating

The critical age control in this study relied upon radiocarbon dating of buried organic material (Table 2). Samples of detrital charcoal, buried wood and buried seeds were collected from the trench walls, as well as a sample of charcoal collected from the lacustrine sediments approximately 0.5 km to the south of the trench site (see Table 2). In addition, bulk sediment samples were collected from stratigraphic units more than 1 m below the surface. Small samples were dated using accelerator mass spectrometry (AMS), and bulk samples from buried soils were crushed, slurried and sieved prior to chemical pretreatment and dating by decay counting.

Some of the samples, particularly those from shallow levels in the trenches, show evidence of probable contamination. These samples are evident with ^{14}C concentrations greater than 100 per cent of the modern value in Table 1. These samples were typically very small and collected from the uppermost colluvial deposit. We interpret

Figure 4. An example of a small, displaced drainage crossing the Serghaya fault. The minimum offset is 2.3–2.5 m. The view is facing west; see Fig. 3 for location.

Table 1. Large historical earthquakes in western Syria and Lebanon (32.5°–35.5°N).

Year	*M*	Affected areas (in order of decreasing intensity)
198 BC	?	Lebanese coast, southern Syria
115 AD	?	Northwest Syria
303 AD	~7.0	Lebanese coast, southern Syria
551 AD	7.0–7.5	Lebanese coast
749 AD	7.0–7.5	Southern Bekaa Valley, southern Syria
859 AD	7.0–7.5	Northwest Syria
991 AD	7.0–7.5	Bekaa Valley, AntiLebanon
1063 AD	~7.0	Northern Lebanese coast, Syrian coast
1157 AD	7.0–7.5	Northwest Syria, Ghab Valley
1170 AD	>7.5	Northern Lebanon, Syrian coast
1202 AD	>7.5	Mt Lebanon, Bekaa Valley, Hula Basin, Lebanese–Syrian coast
1705 AD	~7.0	AntiLebanon, Zabadani and Bekaa Valleys, Damascus, northern Lebanese coast
1759 AD	~7.4	Bekaa Valley, AntiLebanon, Golan Heights, Mt Lebanon, Damascus
1837 AD	7.0–7.5	Western Lebanon, southern Bekaa Valley, Hula Basin

Data from Poirier & Taher (1980), Ambraseys & Barazangi (1989), Ambraseys & White (1997), Ambraseys & Jackson (1998) and Sbeinati *et al.* (2003).

these as probable contamination based on previous information concerning the uppermost colluvial deposit. Previous dating of relatively intact exposures of the uppermost colluvial wedge (which we correlate with the uppermost colluvial deposit in this study) was reported by Gomez *et al.* (2001) as radiocarbon 'modern'. Furthermore, in this study area, the uppermost colluvial wedge has been severely truncated by agricultural activity. These samples were collected just below the plow zone at depths of 0.2 m. Hence, there seems to be considerable potential for contamination of these small samples by post-bomb carbon.

The quality of the other reported charcoal samples (from deeper levels in the trenches) is generally good—these were typically larger samples (>120 μM of graphitized carbon). However, both of the bulk sediment samples yielded very small amounts of organic carbon (<0.5 g) and required extended counting.

We calibrated radiocarbon ages to calendar dates with the correction curve of Stuiver *et al.* (1998) using the OxCal program (Bronk Ramsey 1998), and these calibrated ages are reported as ranges of dates representing the probability density function at the 95 per cent (2σ) confidence limits (Table 2). In some cases, the calibrated age ranges were further constrained by applying rules of superposition and Bayesian analysis (e.g. Biasi & Weldon 1994; Bronk Ramsey 1998). This was particularly helpful in assigning probable ages to the base of the earthquake sequence where there is sufficient age control (i.e. relating Channel C3 incision and fill to Wedge 2, see below).

2.4 Trench 1: colluvial wedge stratigraphy

Across the fault zone, Trench 1 exposed a stratigraphy of Late Pleistocene lacustrine marl and sandy gravel in the up-thrown block and reddish brown to yellowish alluvium and colluvium on the down-thrown (western) side of the fault. The photomosaic of the northern trench wall in Fig. 7 and the associated trench log in Fig. 8 show the abrupt fault contact between the lacustrine sediments and the younger alluvium. The fault zone is 3–4 m wide, as revealed by shear fabrics in the silt and clay and by alignments of elongate clasts in the matrix-supported alluvium.

Undifferentiated reddish brown alluvium (unit a) characterizes much of the lower stratigraphy (Fig. 8). This deposit consists of gravel, sand, and occasional cobble supported by a clay matrix. This stratigraphic unit appears to correspond to the alluvial apron flanking the mountain front. Locally, it is buried beneath the younger alluvial fan deposit, and adjacent to the fault scarp, it has been buried beneath up to 1.5 m of scarp-derived colluvium. A bulk soil sample from the top of unit a (i.e. just below colluvial deposit W2) yielded an age of 5280 ± 230 BP. Applying Bayesian methods to the radiocarbon calibration (Biasi & Weldon 1994)—specifically, knowing that the undifferentiated alluvium predates buried channels

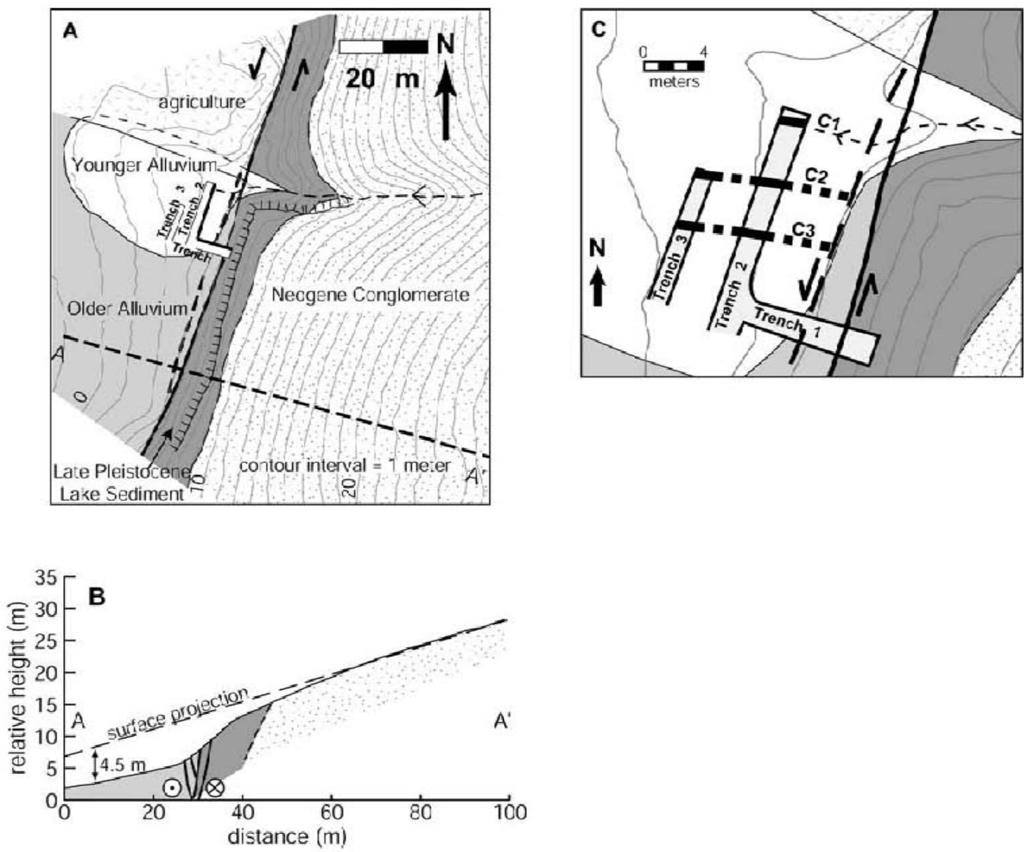

Figure 5. (a) Map of trench site. 1 m relative contours are based on mapping with a total station. *See* Fig. 3 for location. (b) Topographic profile and cross-section illustrating composite fault scarp approximately 4.5 m in height. (c) Enlarged map of the trench site depicting the positions of the present channel (C1) and the precise locations of the buried channels (C2 and C3). Solid black lines indicate where the buried channels were observed and dashed lines indicate where buried channels were inferred. The patterns are consistent with Fig. 5(a).

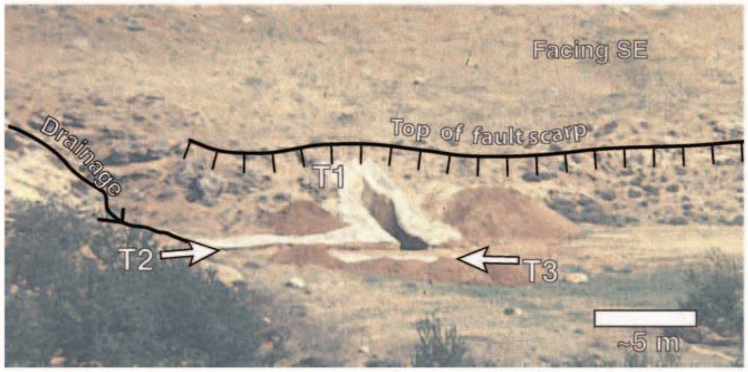

Figure 6. Photograph of the trench site facing SE. Note the position of the trench system relative to the fault scarp and the small drainage. See Fig. 3 for location.

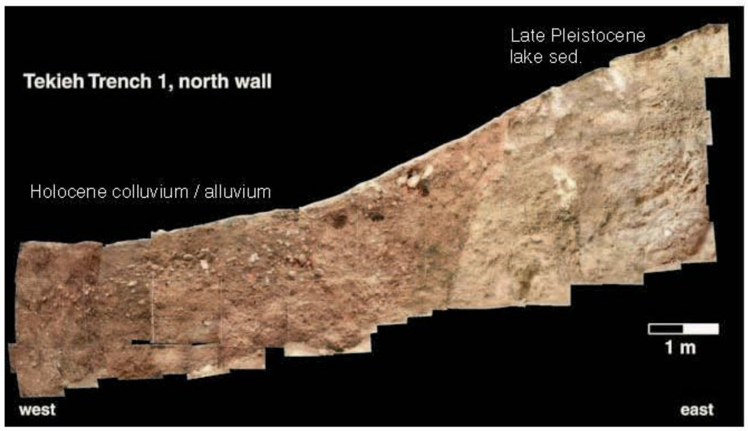

Figure 7. Photomosaic of the north wall of Trench 1.

incised into unit a (discussed below)—we calculate a calibrated age of 4720–4270 BC for the undifferentiated alluvium.

Colluvial 'wedge' deposits along fault scarps are important palaeoseismic indicators in cases where local fault movements involve repeated uplift (e.g. McCalpin 1996). In Trench 1, individual colluvial deposits are distinguished by pebbles and other larger clasts defining buried depositional surfaces. The colluvium consists of poorly sorted, matrix-supported clasts of Late Pliocene–Quaternary conglomerate and lacustrine marl, and the clasts are typically angular to subangular, suggesting proximal sources. The development of distinct soils in each colluvial wedge suggests long-term stability of the surface during the time between colluvial depositional events. These colluvial wedges are bounded on the up-thrown, eastern sides by buried scarps 20–40 cm in height. These scarps align with shear zones truncating the lower strata, implying that the buried scarps result from fault movements. Furthermore, some of these colluvial bodies are themselves truncated by subsequent faulting as indicated by shear fabrics and buried by younger colluvium.

In total, we distinguished five colluvial wedges above the undifferentiated alluvium (unit a), as well as one within. For this discussion, these are labelled in ascending order as Wedges 1 through 6 (Fig. 8). The colluvial wedges proved challenging for dating owing to a lack of sufficient organic material. Some of the samples show apparent contamination such as modern radiocarbon ages reported for samples from considerable depth. Dates from Wedges 6, 5 and 2 (corresponding to the uppermost, penultimate and earliest post-unit-a colluvium, respectively) were obtained.

At this site, the uppermost colluvial wedge (Wedge 6) was to be truncated by the plow zone—the thickness is minimal, and a plastic cigarette wrapper was found 25 cm below the surface, implying recent modification. The remnant of this wedge consisted of centimetre-size pebbles and gravel clasts of limestone and lake

Table 2. Radiocarbon dates of relevant samples from Trenches 1 and 2 and nearby areas.

Sample	Method	Material	Sampled layer	δ^{13}C per mil	Radiocarbon age years BP	2σ calibrated age range
LS-1	AMS	Charcoal	Quaternary lake sediment	−25.0	44 630 ± 1570	n/a
T1-02Nd	AMS	Charcoal	Colluvium, Wedge 5	−25.0	2060 ± 30	170 BC–20 AD
T1-09N	AMS	Seed	Colluvium, Wedge 6	−24.2	>Modern (122.8 ± 0.3 per cent)	Post 1950 AD
T1-04S	AMS	Seed	Colluvium, Wedge 6	−25.2	>Modern (111.4 ± 0.5 per cent)	Post 1950 AD
T1-15S	AMS	Seed	Silty sand below Wedge 6	−24.1	>Modern (125.8 ± 0.3 per cent)	Post 1950 AD
T2-05E	AMS	Charcoal	Sandy gravel, Channel 3	−26.0	5510 ± 80	4540BC–4160 BC
T1-03N	AMS	Charcoal	Silty sand below Wedge 6	(−25.0)	>Modern (103.9 ± 1.8 per cent)	Post 1650 AD
T2-10W	AMS	Charcoal	Sandy gravel, Channel 3	(−25.0)	5450 ± 140	4600 BC–3950 BC
T1-108S	AMS	Charcoal	Silty sand below Wedge 6	−27.3	>Modern (110.7 ± 0.5 per cent)	Post 1950 AD
T2-15E	AMS	Charcoal	Sandy gravel, Channel 1	−26.2	1354 ± 52	600 AD–780 AD
T2-101W	AMS	Charcoal	Sandy gravel, Channel 2	−25.4	3233 ± 57	1690 BC–1400 BC
T2-101 E	AMS	Charcoal	Sandy gravel, Channel 3	−25.6	5492 ± 57	4460 BC–4250 BC
T1-107S	AMS	Charcoal	Silty sand below Wedge 6	−27.7	>Modern (133.7 ± 0.5 per cent)	Post 1950 AD
T3-07E	AMS	Charcoal	Sandy gravel, Channel 3	−25.7	5540 ± 51	4500 BC–4250 BC
T1-110Nbk	CONV	Soil organics	Colluvium, Wedge 2	−25.7	4870 ± 160	4050 BC–3100 BC
T1-104Sbk	CONV	Soil organics	Undifferentiated alluvium	−24.7	5280 ± 230	4700 BC–3700 BC
T1-107Nbk	CONV	Soil organics	Soil below colluvium	−25.0	6590 ± 120	5730 BC–5320 BC

Dating methods are AMS (accelerator mass spectrometer) and conventional (i.e. decay counting). Samples have been calibrated with OxCal 3.5 by Bronk Ramsey using the data set of Stuiver *et al.* (1998). Radiocarbon ages of >modern are listed with the per cent Modern values. δ^{13}C values in parentheses indicate that the sample was too small for a δ^{13}C measurement and a value was assumed.

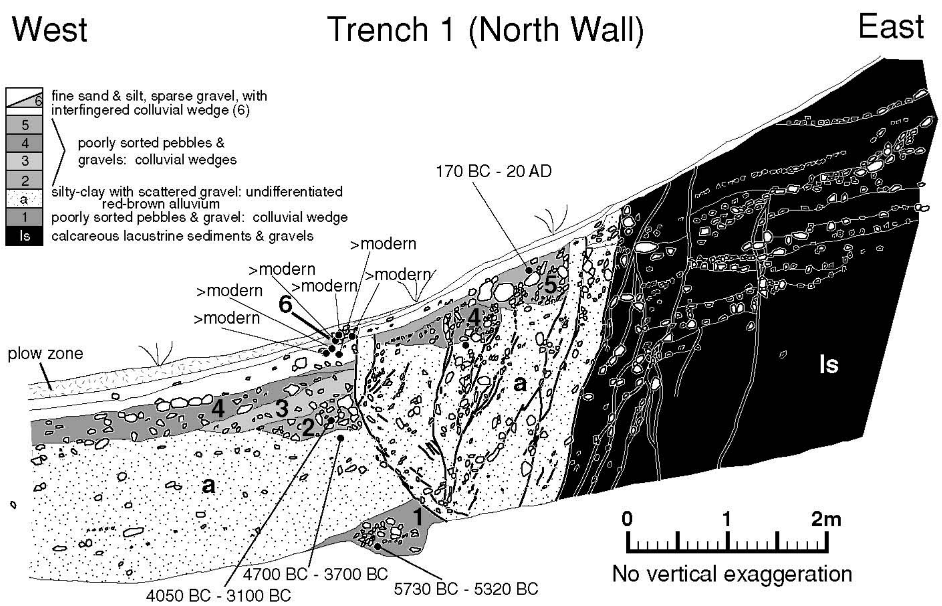

Figure 8. Trench log for the northern wall of Trench 1 (see Fig. 7), exposing colluvial wedges, undifferentiated alluvium and Late Pleistocene lake sediments. Calibrated radiocarbon ages are shown.

sediments. Dating of this wedge was difficult. From within Wedge 6, only small seeds were extracted yielding high concentrations of ^{14}C in excess of 100 per cent modern. These 'post-bomb' samples may, in fact, be very recently deposited, particularly since the top of Wedge 6 has been truncated by modern cultivation (Fig. 8). One charcoal fragment from the sand immediately below Wedge 6 (sample T1-03N with 103.9 ± 1.8 per cent modern) yielded a calendar age of 1650 AD to present. Owing to its small size (<27 μM of

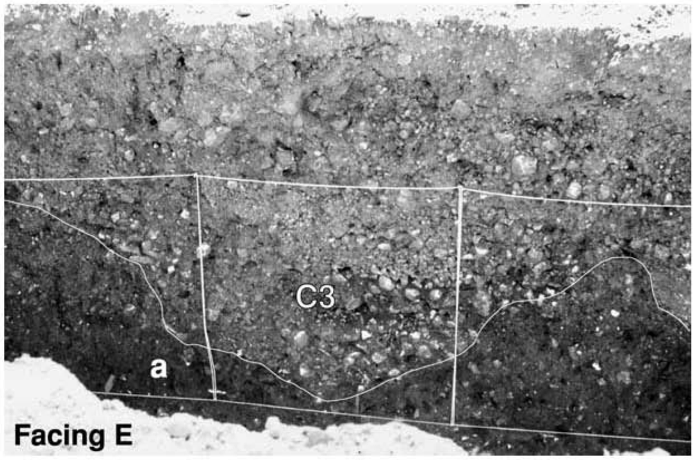

Figure 9. Photo of incised and filled channel exposed in Trench 2. Channel C3 is incised into the older alluvium (unit a) and filled with clast-supported cobble, gravel, and sand. White string grid has 1 m spacing.

graphitized carbon), a $\delta^{13}C$ measurement was not possible, hence an assumed value of 25 per cent was used. Other pre-Wedge 6 charcoal samples (also small) yielded high percentage modern values, and these probably reflect contamination. Radiocarbon dating of a complete (i.e. not truncated) exposure of this upper wedge in a small excavation to the north (see Fig. 3) demonstrated modern and >modern radiocarbon ages (Gomez *et al.* 2001). In summary, this uppermost colluvial wedge can be assigned a probable age 1650 AD to present.

Wedge 5 had a yellowish colour and consisted of large clasts with a white patina in a silty–sandy matrix. Charcoal from Wedge 5 yielded an age of 170 BC to 20 AD (2060 ± 30 BP). The down-slope stratigraphic equivalent is a fine sand/silt that can be traced across the shear zone abutting Wedge 6.

Wedge 4 rests directly beneath Wedge 5 and consists of small gravel and cobble-sized clasts in a silty-sandy matrix. Clasts of limestone and lacustrine sediment are present. Appropriate material for radiocarbon dating could not be found within this deposit. The sandy silt and gravel unit in the western end of the trench appears to be the down-slope stratigraphic equivalent of this unit.

Wedge 3 comprises limestone pebbles (centimetre size) and gravel in a sandy matrix. This unit is covered by the down-slope stratigraphic equivalent of Wedge 4 and truncates against the undifferentiated alluvium.

The oldest colluvium above the undifferentiated alluvium was Wedge 2. This deposit consisted of rounded pebbles and flat gravel in a stratified, reddish-brown matrix. Weakly developed soil structures were observed. Clasts consisted of limestone and lacustrine sediment. A bulk sediment sample from Wedge 2 yielded an age of 4050–3100 BC (4870 ± 160 BP).

Wedge 1 was identified in the base of the trench, within the undifferentiated alluvium. Well rounded pebbles and flat gravel of limestone and lacustrine sediment rest within a reddish-brown matrix. A bulk sample of the soil buried by this colluvial wedge was dated at 5730–5320 BC (6590 ± 120 BP).

In summary, the upper five distinct colluvial deposits post-date 5280 ± 230 BP. Stratigraphic relations demonstrate that all five post-alluvium colluvial wedges represent separate depositional episodes; i.e. there is a clear sequence of deposition and burial by successive colluvial deposits. The presence of weakly developed soil structures in the colluvial wedges suggests surface stability between distinct depositional events and argues against creation of the buried scarp by multiple events or fault creep. Hence, we interpret each colluvial wedge to post-date a separate palaeoseismic event that created each buried scarp.

2.5 Trench 2: abandoned channels

Trenches 2 and 3, parallel to the fault scarp, exposed the reddish-brown alluvium incised by channels (Fig. 9). Each channel was filled with moderately to well sorted, frequently clast supported gravel and occasional cobble, within a sandy matrix. This sedimentology indicates a moderately high-energy stream flow. Detrital charcoal collected from each of the channels provided age control of the filling sediments. In total, three channels, including the incision beneath the present-day drainage, were identified and correlated between the two trenches, with onlapping relationships demonstrating a consistent northward sense of younging (Fig. 10). For each channel, the magnitude of incision is greater in Trench 2 than in Trench 3, i.e. greater incision is found closer to the mouth of the drainage. In addition to stratigraphy, radiocarbon dating confirmed the correlation of channels between Trenches 2 and 3.

Channel C1 is filled by a fining upward sequence approximately 1 m thick. This is covered by about 1 m of recent alluvium that truncates and caps Channels C2 and C3. A charcoal fragment from the upper part of Channel C1 yields a calendar age of 600–780 AD (1354 ± 53 BP).

Channel C2 is very narrow and deeply incised (>2 m) into the older alluvium (unit a). During filling, small episodes of re-incision occurred, and the channel was capped by a thin veneer of alluvium

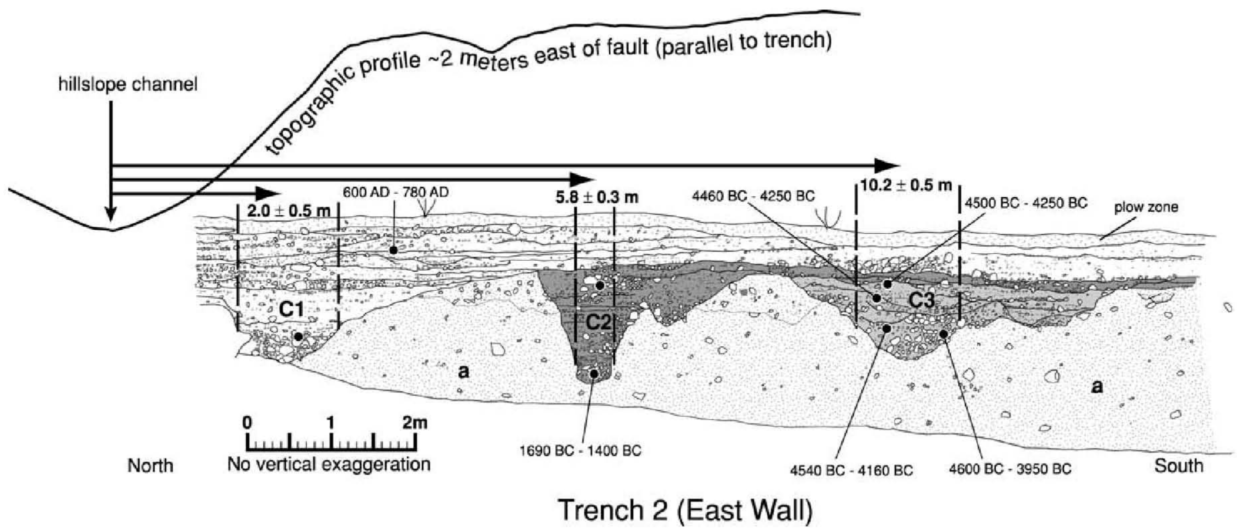

Figure 10. Trench log for the east wall of Trench 2. A sequence of three incised and filled channels is shown, with a northward sense of younging. Black discs denote the positions of samples for radiocarbon dating. The profile above the trench log depicts the hillslope channel morphology east of the fault zone. The relative positions of the channel mouth and the buried channels were mapped using a total station. Apparent offsets of the buried channels are shown.

that also caps Channel C3. The base of Channel C2 fill dates at 1690–1400 BC (3233 ± 57 BP).

Channel C3 depicts an initial incision followed by filling with minor episodes of entrenchment, meandering and widening of the original channel. Charcoal fragments from throughout the filling strata in Channel C3 yield statistically identical ages ($\chi^2 = 0.6 < 7.8$ (95 per cent), three degrees of freedom). Since these are from the same deposit, the ages and their Gaussian errors can be combined prior to calibration (Bronk Ramsey 1998) to yield a combined age of 5498 ± 46 BP for the fill. Recalling the 5280 ± 230 BP age from the top of the undifferentiated alluvium (unit a), which represents the incised surface, these ages are statistically very similar. This suggests that the cycle of incision and filling for Channel C3 was a relatively short-lived episode.

Channels 2 and 3 are exposed in both walls of trenches 2 and 3, and the positions of these channels depict linear traces approximately perpendicular to trenches 2 and 3 and to the fault trace (Fig. 5c). In addition, the active stream bed above incised Channel C1 also shows a very linear trace, aside from its abrupt deflection at the fault (Fig. 5c).

3 PALAEOSEISMIC INTERPRETATION: SLIP HISTORY OF THE SERGHAYA FAULT

3.1 Palaeoseismic chronology

Trench stratigraphy and associated chronological information allow the construction of a palaeoseismic record for the SFZ. The key palaeoseismic indicators in this study are the colluvial deposits exposed in Trench 1, along with the offsets of modern and buried stream channels. In Trench 1, Wedges 4–6 rest in depositional contact with the buried scarp located above shear zones. This suggests that each of these colluvial wedges corresponds to only one faulting event, i.e. that which produced the buried scarp. The sedimentary geometries of Wedges 1–3 suggest that they too each represent one depositional episode. Following the colluvial wedge model (McCalpin 1996), one colluvial wedge is deposited following each surface-rupturing earthquake. Stratigraphic relationships depict the colluvial wedges following a sequence, i.e. two wedges are not contemporaneous. Hence, we interpret six surface-rupturing earthquakes from this trench study (Fig. 11).

Combining the relative and absolute age control, a history of colluvial wedge deposition (each post-dating a palaeoseismic event) and channel scour-and-fill cycles can be assembled from the trench site. We interpret palaeoseismic events to pre-date colluvial wedges and to post-date channel incision/fill—if the fill post-dated an event, then it would be expected to comprise more chaotic colluvium derived from the channel wall, rather than the well-sorted sand and gravel that are observed. We also assume that the rapid incision/fill cycle of Channel C3 characterizes the incision and fill of Channels 1 and 2, although the geochronological data to test this assumption are lacking. We interpret these channel-scouring events to represent relatively short-lived climatic events within the increasing aridity during the Holocene.

Stratigraphic ties between Trenches 1 and 2 provide additional control on the relative timing of colluvial deposition and the scouring and filling of the buried channels. These stratigraphic ties are illustrated in the 3-D block diagram shown in Fig. 12. The upper fill of Channel C1 corresponds to the younger alluvial fan that locally buries the older alluvial apron. Stratigraphically, the remnant of Wedge 6 lies within this younger alluvial deposit. Another important stratigraphic tie is apparent between the upper part of the Channel C2 fill and the down-slope deposits interpreted to correspond to Wedge 4.

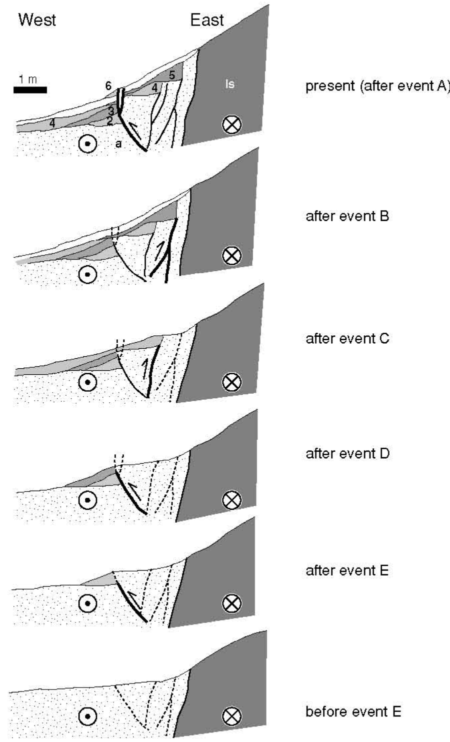

Figure 11. Cross-sections showing schematic reconstruction of the past five palaeoseismic events indicated in Trench 1. Numbers correspond to colluvial wedges 2–6. Bold lines depict the most recent fault splay in each stage; dashed lines denote restored faults. ls = lacustrine sediment; a = undifferentiated alluvium.

The channel incision/fill episodes and colluvial deposition events are summarized in Fig. 13, along with the interpreted palaeoseismic events, labelled A–F in order of increasing age. In total, five events are interpreted to post-date the older alluvium.

Remnants of Wedge 6 are within the younger alluvium and post-date the filling of Channel C1 (600–780 AD). Based on the remnants of Wedge 6, and the previous dating of the youngest colluvial wedge (Gomez *et al.* 2001), we interpret Wedge 6 as corresponding to an earthquake that occurred during the past two to three centuries (Event A), and this probably represents one of two well-documented, historical earthquakes that occurred in 1705 and 1759 (Table 1). Both earthquakes caused considerable damage in the AntiLebanon region. The 1705 earthquake caused considerable damage to Damascus (Poirier & Taher 1980). The earthquake of 1759 has been well documented (e.g. Ambraseys & Barazangi 1989) and most intensely affected towns in the western part of the AntiLebanon Mountains

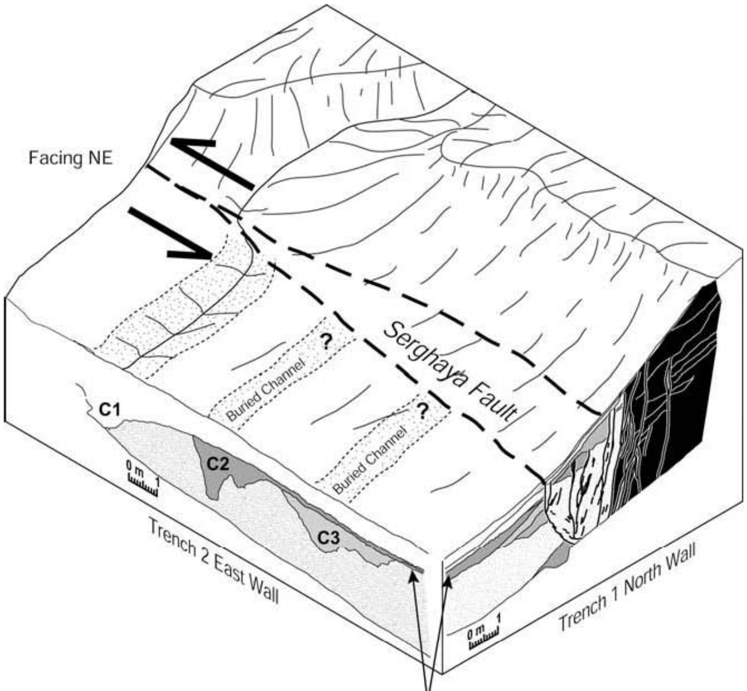

Figure 12. Schematic block diagram illustrating the 3-D relationships of the features exposed in the trenches. A stratigraphic tie between the filling deposit of Channel C2 with the down-slope equivalent of Wedge 4 can be observed.

and the Bekaa Valley. The macroseismic data suggest a magnitude of about 7.4 and up to 100 km of surface rupture. Reports of surface rupturing 'north of Baalbek' (Ambraseys & Barazangi 1989) are ambiguous concerning which side of the Bekaa Valley, and the surface rupture has not yet been identified in the field. From the dating in this trench alone, it is not possible to distinguish between these two events, as they occurred relatively close in time to one another during a time period for which radiocarbon age calibration is poorly controlled (e.g. Stuiver *et al.* 1998).

Wedges 5 is radiometrically constrained to pre-date the Channel C1 fill, and Wedge 4 is stratigraphically constrained to post-date the Channel C2 fill. Hence, two palaeoseismic events (events B and C) are interpreted as being between 170 BC–20 AD (Wedge 5) and 1690 BC–1400 BC (Channel C2). It may be possible that Wedge 5 (170 BC–20 AD) corresponds to a poorly documented earthquake that occurred in 198 BC. Although the reports for this earthquake come primarily from Sidon on the coast of present-day Lebanon, the onshore location of this earthquake is suggested by the report that a town inland was 'engulfed' by the earthquake (Ambraseys & White 1997). However, such an interpretation is speculative until the other possible fault branches (e.g. Yammouneh and Roum faults) have been studied and discounted as possible sources.

Wedge 2 is radiometrically constrained to post-date the Channel C3 fill, and we believe that Wedge 3 also pre-dates Channel C2. Consequently, two additional palaeoseismic events (events D and E) are interpreted between 1690–1400 BC (Channel C2) and 4460–4250 BC (radiocarbon dates combined before calibration) (Channel C3). Event E can be constrained to post-date the Channel C3 fill (4460–4250 BC) and pre-date Wedge 2 (4050–3250 BC).

The oldest palaeoseismic event in the trench, represented by Wedge 1, pre-dates the bulk sample from the upper part of the undifferentiated alluvium (unit a) and postdates the buried soil below Wedge 1 (5730– 5320 BC). Hence, this palaeoseismic event probably occurred some time between 5600 and 4400 BC (at the 2σ confidence limits).

3.2 Displacements

The buried channels exposed in Trenches 2 and 3 serve as piercing points of different ages and provide a means of determining a Holocene slip rate for the Serghaya fault. These channels depict quasi-linear traces and a northward sense of younging consistent with left-lateral transport of the downstream reaches from the mouth of the drainage. Although it is not possible to date the incision

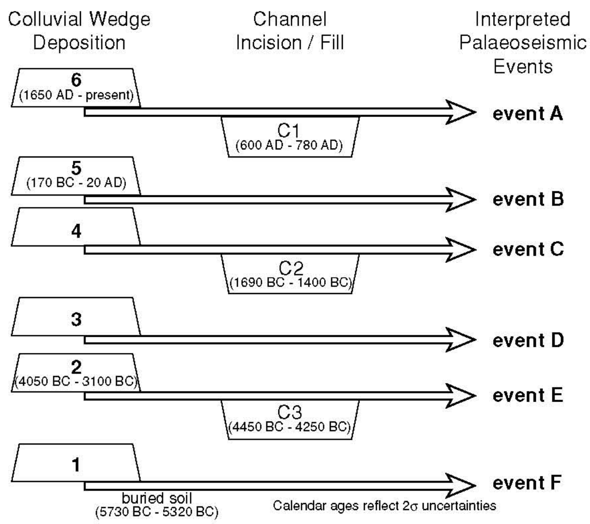

Figure 13. Summary of events observed in the trenches and the interpreted palaeoseismic history of the Serghaya fault. Colluvial wedge deposits post-date palaeoseismic events. Stratigraphic ties provide additional constraint on the relative timing of events. Ages represent calendar corrected radiocarbon ages for given features (2σ uncertainties provided).

directly, the rapid cycle of incision and fill in Channel C3 based on the radiocarbon dates may characterize Channels 1 and 2, as well.

The buried channels correspond to episodic entrenchment of the alluvial apron, probably resulting from infrequent major storms in this semi-arid environment. The fill, consisting of sorted sand and gravel, is consistent with water-lain transport. Short-lived cycles of channel incision and subsequent filling are typical in arroyo development in the semi-arid regions of western North America where incision results from increased stream power, probably due to a short-lived, but relatively intense flow in the channel (Bull 1997). A concentrated flow (required to erode the channel) exiting the mouth of the drainage would probably follow a linear flow path, and this interpretation is consistent with the quasi-linear channel traces observed in the trenches and the present-day drainage. Hence, it seems reasonable to project the linear traces of the channels uphill to the fault zone in order to estimate the amount of displacement for each channel. Linear channels are also suggested by the exposures of Channels C2 and C3 in both walls of trenches 2 and 3 (Fig. 5c). The channel mouth morphology and its position relative to the trench wall were mapped with a total station. The incised widths are estimated based on the bottom 50 cm of each channel, and displacements of 2.0 ± 0.5, 5.8 ± 0.3 and 10.2 ± 0.5 m are estimated from the channels (see Figs 10 and 5c).

A plot of displacement versus age of the channel fill depicts an average slip rate of 1.4 ± 0.2 mm yr^{-1} (Fig. 14). This slope was determined by linear regression of the displaced channel data with 2σ uncertainties. Although the sand and gravel in Channel C1 is dated to 680–780 AD, the timing of the displacement of this channel is constrained by historical records to post-date the channel by more than 1000 yr (following our interpretation of an 18th century earthquake on the Serghaya fault). Hence, the slope of the line in Fig. 14 was determined using the timing of displacement of C1 in the 18th century.

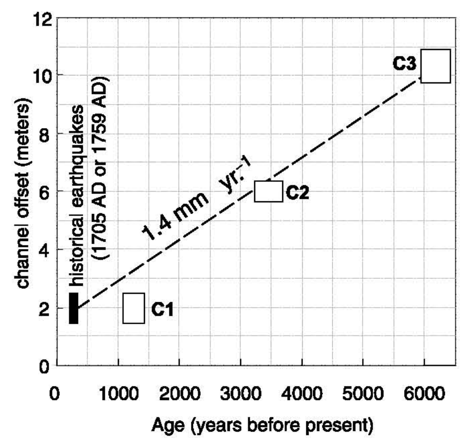

Figure 14. Plot of offset versus age for buried channels. The 2 m displacement of the youngest channel corresponds to a historically documented earthquake in the early or mid 18th century. The slope of the linear fit is the average Holocene slip rate for the Serghaya fault.

The displacements and event histories tie together as follows: (1) 2 m of displacement associated with event A (the historical event and the small stream deflection); (2) ~4 m of displacement associated with events B and C; and (3) ~4 m of displacement associated with events D and E. The displacement for the last event appears to be roughly constant over the 6–7 km spanning the southern Zebadani Valley, as suggested by the minimum drainage deflections (Fig. 3). The individual slip for events B, C, D and E cannot be estimated. However, each pair of events B/C (corresponding to the displacement of channel C2) and D/E (corresponding to the offset of channel C3) demonstrates an average left-lateral slip of ~2 m per event. Hence, this section of the Serghaya fault might be characterized by similar slip in each of the last five paleoseismic events. Similar slip per event is also suggested by the similar thickness of colluvial wedges 1–5 (30–50 cm), although, as discussed by McCalpin (1996), colluvial wedge thickness is not always and uniquely related to uplift.

Constant slip for repeated earthquakes is also inferred on the southern section of the DSFS by Klinger *et al.* (2000b), as well as on strike-slip faults in California (e.g. Lindvall *et al.* 1989; Sieh 1996; Rubin & Sieh 1997). This co-seismic slip behaviour is typical for both the uniform slip (Sieh 1981) and characteristic earthquake (Schwartz & Coppersmith 1984) models of earthquake repetition. However, in order to discriminate between these two types of earthquake behaviour, additional locations along the 125 km long Serghaya fault need to be studied. For example, the uniform slip model involves a constant slip rate along the fault and frequent moderate earthquakes to compensate for along-strike variations in slip per event at a given location; the characteristic earthquake model allows a variable slip rate along the fault and infrequent moderate earthquakes. It should also be noted that other sections of the DSFS demonstrate variable displacement for repeated earthquakes (e.g. Ellenblum *et al.* 1998).

Applying published scaling laws relating slip to moment magnitude (e.g. Wells & Coppersmith 1994), 2 m of slip corresponds to an earthquake of $M_w \sim 7$–7.2. On average, this portion of the Serghaya fault has experienced one such event every ~1300 yr. Although in many cases, the time brackets on the individual palaeoseismic events are not well resolved, the available timing constraints are consistent with this mean return period. However, the actual recurrence intervals may vary significantly. For example, Wedge 2, which post-dates the penultimate event, is dated as 170 BC–20 AD, whereas the last event occurred in the early to mid 18th century. This implies that at least 1700–1900 yr elapsed between these two events.

A time-predictable earthquake model uses the displacement of the last event and the slip rate to predict the time to the next earthquake, assuming that the fault fails at a critical stress level (Shimazaki & Nakata 1980). In the context of such an earthquake recurrence model, the slip rate and the palaeoseismic history (2.0–2.5 m of slip in the last earthquake with a slip rate of 1.4 mm yr^{-1}) suggest that there is probably not a slip deficit on this portion of the Serghaya fault. However, this is only a preliminary interpretation based on this one palaeoseismic investigation. Regardless of the lack of a slip deficit, consideration should be given to possible stress interactions between the Serghaya fault and the nearby Yammouneh or Roum faults.

4 TECTONIC IMPLICATIONS

Active strike-slip movement of the Serghaya fault contrasts with suggestions that strike-slip faulting within the restraining bend and northwards have been rendered inactive as a result of an evolving regional stress field in the eastern Mediterranean region (e.g. Butler *et al.* 1997). A recent plate model for the Arabian and African plates based on GPS measurements (McClusky *et al.* 2003) predicts the total motion of the Arabian plate relative to the African plate at this latitude to be ~6.8 mm yr^{-1} with an azimuth of about N25W, i.e. 45° to the azimuth of the restraining bend. Primarily left-lateral slip on the Serghaya fault, striking N20E, suggests a regional partitioning of strain.

One simple geometrical model of strain partitioning in the restraining bend along the Dead Sea fault system is illustrated schematically in Fig. 15(a). In this model, the plate motion is decomposed into 4.8 mm yr^{-1} of strike-slip along faults striking N20E in the restraining bend, as well as a similar magnitude of shortening perpendicular to the faults (Fig. 15a). In this case, the 1.4 ±

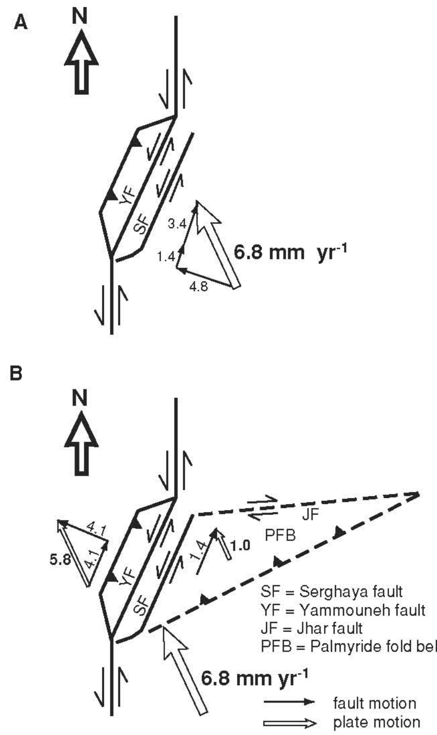

Figure 15. Two simplified geometrical models for the restraining bend of the Dead Sea fault system and the role of the Serghaya fault. Predicted plate motion is based on the GPS-derived regional plate model of McClusky *et al.* (2003, in press). (a) Decomposing the predicted plate motion into N20E strike-slip fault and orthogonal shortening, the 1.4 mm yr^{-1} of slip on the Serghaya fault accounts for ~30 per cent of the expected strike-slip movement on faults striking N20E. The orthogonal shortening would be accommodated in the Mt Lebanon and/or AntiLebanon Mountains. (b) An alternative model in which the Serghaya fault acts as an oblique back-stop behind the Palmyride fold belt and contributes to internal deformation of the Arabian plate. The remaining portion of Arabian–African plate motion may then be composed into strike-slip movement (N20E faults) and orthogonal shortening.

0.2 mm yr^{-1} of slip on the Serghaya fault only accounts for $\sim$30 per cent of total predicted strike-slip motion. Consequently, this implies that other strike-slip faults in the restraining bend, such as the Yammouneh fault, should be active in order to accommodate the remaining plate motion.

However, the Serghaya fault does not appear to reconnect with the transform (Figs 1 and 2), suggesting a slightly more complicated fault model. One possibility might involve the Serghaya fault acting as an oblique 'back-stop' for active shortening within the adjacent Palmyride fold belt, perhaps along with the right-lateral Jhar fault north of the Palmyrides (Fig. 15b). In this case, the 1.4 $\pm$ 0.2 mm yr^{-1} of slip on the Serghaya fault may be used to infer from the geometry that NNW shortening in the Palmyrides accommodates approximately 1 mm yr^{-1} of the relative plate motion. The remaining 5.8 mm yr^{-1} of plate motion could be decomposed into 4.1 mm yr^{-1} of strike-slip on N20E strike-slip faults (e.g. the Yammouneh fault), and a similar amount of shortening perpendicular to these faults.

Regardless of the general tectonic model for the restraining bend, the Serghaya fault seems insufficient to account for all predicted plate motion. Hence, multiple strike-slip faults imply more complicated scenarios for earthquake hazard assessments.

As noted by previous workers this structural configuration bears similarity to the 'Big Bend' of the San Andreas fault system in southern California (e.g. Chaimov *et al.* 1990), which comprises several active fault branches, including both reverse and strike-slip faults. In addition, internal deformation of the North American Plate is also significant—although the major component of plate motion is accommodated by the San Andreas fault, studies have demonstrated that the Eastern California Shear Zone and the Basin and Range (e.g. Dokka & Travis 1990; Dickinson & Wernicke 1997) accommodate significant components of the total plate motion.

5 CONCLUSIONS

This study provides an initial view of the earthquake behaviour and active fault kinematics for the Serghaya fault, and these results depict recent tectonic activity that is not readily apparent in the instrumentally recorded seismicity alone. The Serghaya fault is active, and the total fault length and 2–2.5 m displacements, combined with historical seismicity, suggest that the fault may be capable of generating large ($M \sim 7$) earthquakes. This study also provides a first view of the earthquake recurrence history along the Serghaya fault. The results suggest a slip rate of about 1.4 mm yr^{-1}, with an average of approximately 2 m of slip per event at this location and a mean repeat time of about 1300 yr. However, the age control from the colluvial deposits is relatively limited for placing tight limits on the timing of past events, although these can be identified with loose constraints. Additional studies are needed to illuminate any fault-wide behaviour, such as fault segmentation, to distinguish between models of fault behaviour such as the characteristic earthquake and uniform slip models. Understanding the extent and magnitude of past ruptures can also provide critical input for modelling static stress interactions on nearby faults that can increase or decrease the probabilities of subsequent earthquakes.

Although this study has documented the inferred effects of large, surface-rupturing earthquakes on the Serghaya fault, moderate earthquakes ($M \sim 5$–6) are also a concern for seismic hazard assessments. The recurrence of moderate earthquakes can be difficult to assess using palaeoseismic techniques—moderate earthquakes do not always produce a surface rupture, and when they do, slip is small and of limited spatial extent. However, moderate earthquakes, if relatively frequent, can also present a considerable hazard if the epicentres are located near cities such as Damascus or Beirut. Eventual distinction of different models for earthquake behaviour, such as the characteristic earthquake (infrequent moderate earthquakes) versus uniform slip (relatively frequent moderate earthquakes) models, will assist in assessing the level of hazard posed by moderate earthquakes.

The results of this study demonstrate that the Serghaya fault is a significant element of this portion of the Arabian–African plate boundary. When placed in the context of Arabian–African relative plate motions, the slip rate and fault kinematics suggest that other structures must also be active within the restraining bend in order to accommodate the expected plate motion. Ongoing GPS observations and future geological studies should help clarify the kinematics of the restraining bend and the means by which it connects the two simpler sections of the Dead Sea fault system. This will ultimately contribute to a better understanding of the structural behaviour and evolution of continental transform systems.

ACKNOWLEDGMENTS

The field investigation presented here benefited from significant logistical support provided by the Higher Institute of Applied Sciences and Technology (HIAST). G. Brew, Y. Radwan, I. Layous, H. Al-Najar, M. Daoud, C. Tabet and M. Khawlie contributed additional assistance to the trench study. D. Seber provided helpful comments in the development of this manuscript. The late Dr G. Bock provided constructive comments and support as the editor of GJI. We also thank S. Marco and A. Agnon as official reviewers of GJI for their helpful suggestions in revising the manuscript. Radiocarbon dating by PRIME Laboratory (Purdue University) was provided through seed project J019. This research was partially supported by NSF grants EAR-0106238 and NSF INT-9810510. MM was supported by CNRS-UMR 7516.

REFERENCES

Al Ghazzi, R., 1982. Les failles libano-syriennes; implications tectoniques et sismiques a l'aide des donnees Landsat, *Proc. of the International Symp. of Commission VII of the International Society of Photogrammetry and Remote Sensing*, pp. 562–565, Groupement Develop. Teledetection Aerospatiale. Toulouse, France.

Ambraseys, N.N. & Barazangi, M., 1989. The 1759 Earthquake in the Bekaa Valley: implications for earthquake hazard assessment in the Eastern Mediterranean region, *J. geophys. Res.*, **94**, 4007–4013.

Ambraseys, N.N. & Jackson, J.A., 1998. Faulting associated with historical and recent earthquakes in the Eastern Mediterranean region, *Geophys. J. Int.*, **133**, 390–406.

Ambraseys, N.N. & White, D., 1997. The seismicity of the eastern Mediterranean region 550–1 BC: a re-appraisal, *J. Earthquake Eng.*, **1**, 603–632.

Ambraseys, N.N., Melville, C.P. & Adams, R.D., 1994. *The Seismicity of Egypt, Arabia and the Red Sea; a Historical Review*, p. 181, Cambridge University Press, Cambridge.

Amiran, D.H.K., Arieh, E. & Turcotte, T., 1994. Earthquakes in Israel and adjacent areas: macroseismic observations since 100 B.C.E., *Israel expl. J.*, **44**, 260–305.

Ben Menahem, A., Nur, A. & Vered, M., 1976. Tectonics, seismicity and structure of the Afro-Eurasian Junction; the breaking of an incoherent plate, *Phys. Earth planet. Inter.*, **12**, 1–50.

Beydoun, Z.R., 1999. Evolution and development of the Levant (Dead Sea Rift) Transform System: a historical-chronological review of a structural controversy, in *Continental Tectonics*, pp. 239–255, eds MacNiocaill, C. & Ryan, P.D., Geological Society of London, London.

Biasi, G. & Weldon, R., 1994. Quantitative refinement of C-14 distributions, *Quat. Res.,* **41,** 1–18.

Brew, G., Barazangi, M., Al-Maleh, A.K. & Sawaf, T., 2001. Tectonic and geologic evolution of Syria, *GeoArabia,* **6,** 573–616.

Bronk Ramsey, C., 1998. Probability and dating, *Radiocarbon,* **40,** 461–474.

Bull, W., 1997. Discontinuous ephemeral streams, *Geomorphology,* **19,** 227–276.

Butler, R.W.H., Spencer, S. & Griffiths, H.M., 1997. Transcurrent fault activity on the Dead Sea Transform in Lebanon and its implications for plate tectonics and seismic hazard, *J. geol. Soc. Lond.,* **154,** 757–760.

Chaimov, T.A., Barazangi, M., Al-Saad, D., Sawaf, T. & Gebran, A., 1990. Crustal shortening in the Palmyride fold belt, Syria, and implications for movement along the Dead Sea fault system, *Tectonics,* **9,** 1369–1386.

Darawcheh, R., Sbeinati, M.R., Margottini, C. & Paolini, S., 2000. The 9 July 551 AD Beirut earthquake, eastern Mediterranean region, *J. Earthquake Eng.,* **4,** 403–414.

Dickinson, W.R. & Wernicke, B.P., 1997. Reconciliation of San Andreas slip discrepancy by a combination of interior Basin and Range extension and transrotation near the coast, *Geology,* **25,** 663–665.

Dokka, R.K. & Travis, C.J., 1990. Role of the Eastern California shear zone in accommodating Pacific–North American Plate motion, *Geophys. Res. Lett.,* **17,** 1323–1326.

Dubertret, L., 1955. Carte Geologique du Liban, Lebanese Ministry of Public Works, 1:200 000.

Dubertret, L., 1962. Carte Geologique du Liban, Syrie et bordure des pays voisins, Museum National D'Histoire Naturelle, Paris, 1:1,000 000.

El-Isa, Z.H. & Mustafa, H., 1986. Earthquake deformations in the Lisan deposits and seismotectonic implications, *Geophys. J. R. astr. Soc.,* **86,** 413–424.

Ellenblum, R., Marco, S., Agnon, A., Rockwell, T. & Boas, A., 1998. Crusader castle torn apart by earthquake at dawn, 20 May 1202, *Geology,* **26,** 303–306.

Freund, R., Zak, I., Goldberg, M., Weissbrod, T. & Derin, B., 1970. The shear along the Dead Sea Rift, *Phil. Trans. R. Soc. Lond.,* A., **267,** 107–310.

Garfunkel, Z., Zak, I. & Freund, R., 1981. Active faulting in the Dead Sea rift, *Tectonophysics,* **80,** 1–26.

Girdler, R.W., 1990. The Dead Sea transform fault system, *Tectonophysics,* **180,** 1–13.

Gomez, F. *et al.,* 2001. Coseismic displacements along the Serghaya fault: an active branch of the Dead Sea fault system in Syria and Lebanon, *J. geol. Soc. Lond.,* **158,** 405–408.

Heimann, A. & Ron, H., 1993. Geometric changes of plate boundaries along part of the northern Dead Sea Transform; geochronologic and paleomagnetic evidence, *Tectonics,* **12,** 477–491.

Hempton, M.R., 1987. Consrtaints on Arbaian plate motion and extensional history of the Red Sea, *Tectonics,* **6,** 687–705.

Jackson, J. & McKenzie, D., 1988. The relationship between plate motions and seismic moment tensors, and rates of active deformation in the Mediterranean and Middle East, *Geophys. J.,* **93,** 45–73.

Jestin, F., Huchon, P. & Gaulier, J.M., 1994. The Somalia plate and the Eastern Africa Rift System: present-day kinematics, *Geophys. J. Int.,* **116,** 637–654.

Joffe, S. & Garfunkel, Z., 1987. Plate kinematics of the circum Red Sea—a re-evaluation, *Tectonophysics,* **141,** 5–22.

Ken-Tor, R., Agnon, A., Enzel, Y., Stein, M., Marco, S. & Negendank, J.F.W., 2001. High-resolution geological record of historic earthquakes in the Dead Sea basin, *J. geophys. Res.,* **106,** 2221–2234.

Klinger, Y., Rivera, L., Haessler, H. & Maurin, J.-C., 1999. Active faulting in the Gulf of Aqaba: new knowledge from the M_w 7.3 earthquake of 22 November 1995, *Bull. seism. Soc. Am.,* **89,** 1025–1036.

Klinger, Y., Avouac, J.P., Abou Karaki, N., Dorbath, L., Bourles, L. & Reys, J., 2000a. Slip rate on the Dead Sea transform fault in the northern Araba Valley (Jordan), *Geophys. J. Int.,* **142,** 755–768.

Klinger, Y., Avouac, J.P., Dorbath, L., Abou Karaki, N. & Tisnerat, N., 2000b. Seismic behaviour of the Dead Sea fault along the Araba valley, Jordan, *Geophys. J. Int.,* **142,** 769–782.

Lindvall, S.C., Rockwell, T.K. & Hudnut, K.W., 1989. Evidence for prehistoric earthquakes on the Superstition Hills fault from offset geomorphic features, *Bull. seism. Soc. Am.,* **79,** 342–361.

Marco, S., Stein, M., Agnon, A. & Ron, H., 1996. Long-term earthquake clustering: A 50 000 year paleoseismic record in the Dead Sea Graben, *J. geophys. Res.,* **101,** 6179–6191.

McCalpin, J.P., 1996. *Paleoseismology,* p. 588, Academic Press, San Diego, CA.

McClusky, S. *et al.,* 2000. GPS constraints on plate motion and deformation in the eastern Mediterranean: Implications for plate dynamics, *J. geophys. Res.,* **105,** 5695–5719.

McClusky, S., Reilinger, R., Mahmoud, S., Ben Sari, D. & Tealeb, A., 2003. GPS Constraints on Africa (Nubia) and Arabia plate motions, *Geophys. J. Int.,* in press.

Meghraoui, M. *et al.,* 2003. Evidence for 830 years of seismic quiescence from paleoseismology, archeoseismology and historical seismicity along the Dead Sea Fault in Syria, *Earth planet. Sci. Lett.,* in press.

Mohamad, R., Darkal, A.N., Seber, D., Sandvol, E., Gomez, F. & Barazangi, M., 2000. Remote earthquake triggering along the Dead Sea fault system following the 1995 Gulf of Aqaba earthquake (M_s = 7.3), *Seism. Res. Lett.,* **71,** 47–52.

Pinar, A. & Turkelli, N., 1997. Source inversion of the 1993 and 1995 Gulf of Aqaba earthquakes, *Tectonophysics,* **283,** 279–288.

Poirier, J.P. & Taher, M.A., 1980. Historical seismicity in the Near and Middle East, North Africa, and Spain from Arabic documents (VIIth–XVIIIth century), *Bull. seism. Soc. Am.,* **70,** 2185–2201.

Quennell, A.M., 1984. The Western Arabia rift system, in *The Geological Evolution of the Eastern Mediterranean,* pp. 775–788, eds Dixon, J.E. & Robertson, A.H.F., Blackwell, Oxford.

Ron, H., 1987. Deformation along the Yammuneh, the restraining bend of the Dead Sea transform: paleomagnetic data and kinematic implications, *Tectonics,* **6,** 653–666.

Rubin, C.M. & Sieh, K., 1997. Long dormancy, low slip rate, and similar slip-per-event for the Emerson fault, eastern California shear zone, *J. geophys. Res.,* **102,** 15 319–15 333.

Sbeinati, M.R., Darawcheh, R. & Mouty, M., 2003. Seismic data for siting and site-revalidation of nuclear facility, Part 1: Catalog of historical earthquakes in and around Syria, *Ann. Geofis.,* in press.

Schwartz, D.P. & Coppersmith, K.J., 1984. Fault behavior and characteristic earthquakes: examples from the Wasatch and San Andreas Fault zones, *J. geophys. Res.,* **89,** 5681–5698.

Shimazaki, K. & Nakata, T., 1980. Time-predictable recurrence model for large earthquakes, *Geophys. Res. Lett.,* **7,** 279–282.

Sieh, K., 1981. A review of geological evidence for recurrence times of large earthquakes, in *Earthquake Prediction, an International Review,* pp. 181–207, eds Simpson, D.W. & Richards, P.G., Maurice Ewing Series, Volume 4, American Geophysical Union, Washington, DC.

Sieh, K., 1996. The repetition of large-earthquakes ruptures, *Proc. Natl Acad. Sci., USA,* **93,** 3764–3771.

Stein, R.S., Barka, A.A. & Dieterich, J.H., 1997. Progressive failure on the North Anatolian fault since 1939 by earthquake stress triggering, *Geophys. J. Int.,* **128,** 594–604.

Stuiver, M. *et al.,* 1998. INTCAL98 Radiocarbon Age Calibration, 24 000–0 cal BP, *Radiocarbon,* **40,** 1041–1083.

Walley, C.D., 1988. A braided strike-slip model for the northern continuation of the Dead Sea Fault and its implications for Levantine tectonics, *Tectonophysics,* **145,** 63–72.

Wells, D.L. & Coppersmith, K.J., 1994. New empirical relationships among magnitude, rupture length, rupture width, rupture area, and surface displacement, *Bull. seism. Soc. Am.,* **84,** 974–1002.

Westaway, R., 1994. Present-day kinematics of the Middle East and eastern Mediterranean, *J. geophys. Res.,* **99,** 12 071–12 090.

Zilberman, E., Amit, R., Heimann, A. & Porat, N., 2000. Changes in Holocene paleoseismic activity in the Hula pull-apart basin, Dead Sea Rift, northern Israel, *Tectonophysics,* **321,** 237–252.

Earth and Planetary Science Letters 210 (2003) 35–52

EPSL

www.elsevier.com/locate/epsl

Evidence for 830 years of seismic quiescence from palaeoseismology, archaeoseismology and historical seismicity along the Dead Sea fault in Syria

Mustapha Meghraoui[a,*], Francisco Gomez[b], Reda Sbeinati[c], Jerome Van der Woerd[a], Michel Mouty[d], Abdul Nasser Darkal[e], Youssef Radwan[c], Ihsan Layyous[c], Haithem Al Najjar[c], Ryad Darawcheh[c], Fouad Hijazi[d], Riad Al-Ghazzi[d], Muawia Barazangi[b]

[a] *EOST, Institut de Physique du Globe de Strasbourg (UMR 7516), 5 rue René Descartes, 67084 Strasbourg Cedex, France*
[b] *Institute for the Study of the Continents, Cornell University, Ithaca, NY 14853, USA*
[c] *Department of Geology, Atomic Energy Commission, Damascus, Syria*
[d] *Department of Remote Sensing, Higher Institute for Applied Sciences and Technology, Damascus, Syria*
[e] *Department of Geology, Damascus University, Damascus, Syria*

Received 10 September 2002; received in revised form 6 March 2003; accepted 14 March 2003

Abstract

The long historical record of earthquakes, the physical effects on ancient building structures and the palaeoseismology provide a unique opportunity for an interdisciplinary tectonic analysis along a major plate boundary and a realistic evaluation of the seismic hazard assessment in the Middle East. We demonstrate with micro-topographic surveys and trenching that the Dead Sea fault (DSF) offsets left-laterally by 13.6 ± 0.2 m a repeatedly fractured ancient Roman aqueduct (older than AD 70 and younger than AD 30). Carbon-14 dating of faulted young alluvial deposits documents the occurrence of three large earthquakes in the past 2000 years between AD 100 and 750, between AD 700 and 1030 and between AD 990 and 1210. Our study provides the timing of late Holocene earthquakes and constrains the 6.9 ± 0.1 mm/yr slip rate of the Dead Sea transform fault in northwestern Syria along the Missyaf segment. The antepenultimate and most recent faulting events may be correlated with the AD 115 and AD 1170 large earthquakes for which we estimate $M_w = 7.3$–7.5. The $\sim$830 yr of seismic quiescence along the Missyaf fault segment implies that a large earthquake is overdue and may result in a major catastrophe to the population centres of Syria and Lebanon.

Keywords: active faulting; palaeoseismology; archaeoseismology; Dead Sea fault

1. Introduction

The long and rich cultural history of the eastern Mediterranean provides a special opportunity to incorporate physical and written history with

* Corresponding author.
E-mail address: mustapha@eost.u-strasbg.fr (M. Meghraoui).

0012-821X/03/$ – see front matter © 2003 Elsevier Science B.V. All rights reserved.
doi:10.1016/S0012-821X(03)00144-4

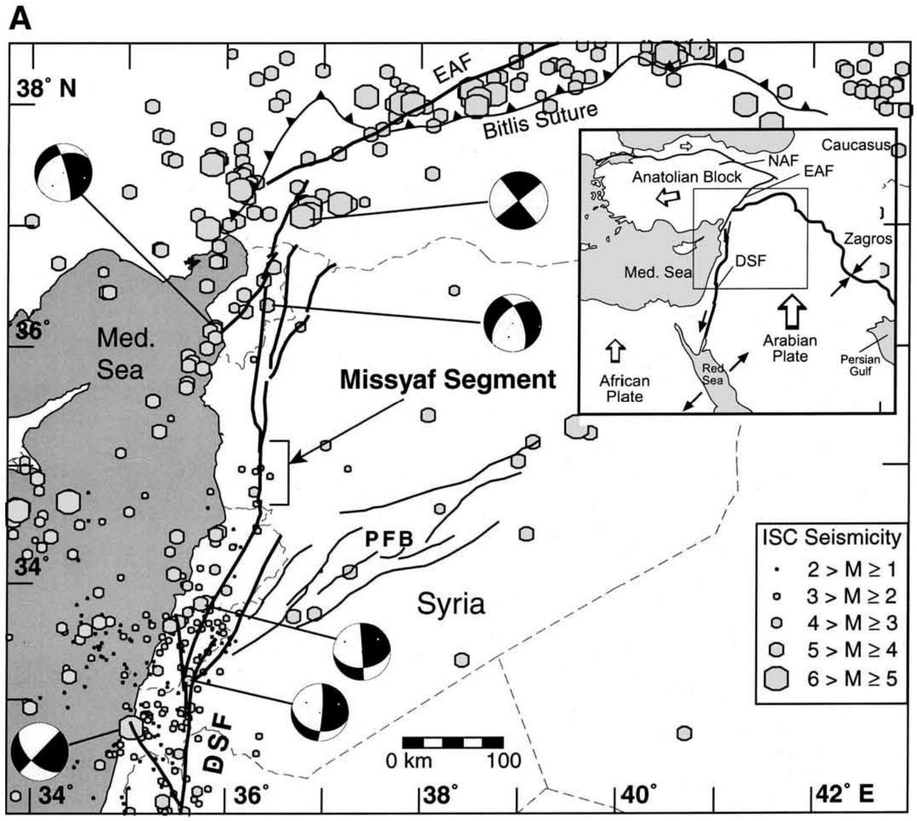

Fig. 1. (A) Map showing the tectonic setting and instrumental seismicity from 1963 to 1997 (International Seismological Centre data file, $M > 1$) of the study area along the Missyaf segment of the DSF. Focal mechanisms along the DSF are of moderate earthquakes ($5 < M_w < 6$; from CMT Harvard and MEDNET-INGV Rome). PFB, Palmyride fold belt; EAF, East Anatolian fault. (B) Map of fault segments interpreted from structural pattern along the northern section of the DSF and inferred ruptures of the main historical seismic events (see also Table 1) [1,4,6,17]; B is Beirut and D is Damascus. The historical seismicity that documents the sequence of AD 1157, 1170 and 1202 large events is based on original Arabic sources [4 6,24]; their spatial distribution suggests a structural control of coseismic ruptures associated with a fault segmentation along the DSF. (C) Shaded topographic image from radar interferometry of the northern DSF; arrows denote the Missyaf fault segment, which is limited by the Ghab pull-apart to the north and Qalaat Al Hosn pull-apart to the south; the square is the location of Fig. 2.

earthquake geology for a more refined assessment of the seismic hazard. This approach is particularly important along the Dead Sea fault (DSF) that corresponds to a major plate boundary (Fig. 1). However, the fault produced very few large continental earthquakes during the past 8 centuries and this low level of seismic activity contrasts with written accounts of large devastating historical earthquakes [1].

The identification of seismic gaps and sequences along major fault systems requires an accurate knowledge of the seismicity catalogue ideally covering several large earthquakes. A time-averaged slip rate and an understanding of the related seismic cycle also contribute to better constrain the long-term faulting behaviour and recurrence interval of large seismic events. Hence, for equal rates of fault slip, the fault zone with the longest period of seismic quiescence is therefore considered as an earthquake-prone area where the hazard is a func-

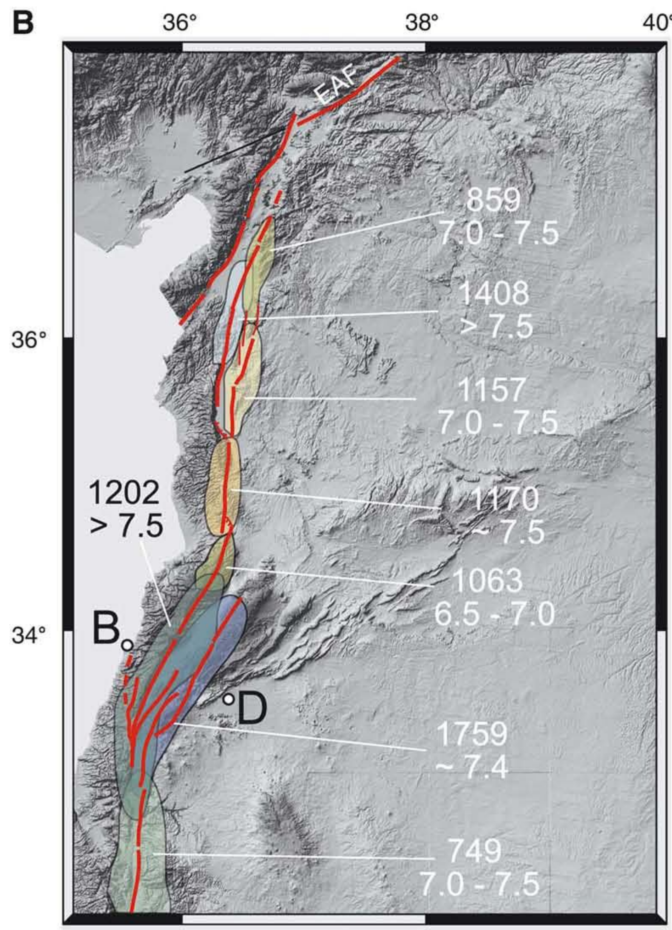

Fig. 1 (*Continued*).

tion of the elapsed time since the last seismic event and the physical dimensions of the related active fault segment.

The occurrence of large earthquakes and their associated damage in the Middle East are frequently reported during the Greek, Hebrew, Assyrian, Roman, Byzantine and Islamic times (Fig. 1A,B) [1–4]. In particular, Arab chroniclers describe with details main shocks, aftershocks, surface breaks and related damage distribution in the Middle East as early as the 7th–8th centuries [4–6]. Hence, the DSF provides a rare opportunity of correlating the historical descriptions of seismicity with field investigations in active tectonics, archaeoseismology and palaeoseismology.

Compared to other worldwide major strike-slip faults, the DSF is poorly understood as an active, seismogenic structure, and recent studies consider its northern section in Lebanon and Syria as inactive [7]. The late Quaternary tectonic activity along the DSF is characterised by: (i) faulted young alluvial, colluvial and lacustrine deposits, (ii) deflected streams with consistent left-lateral displacements of tens to hundred of metres, and

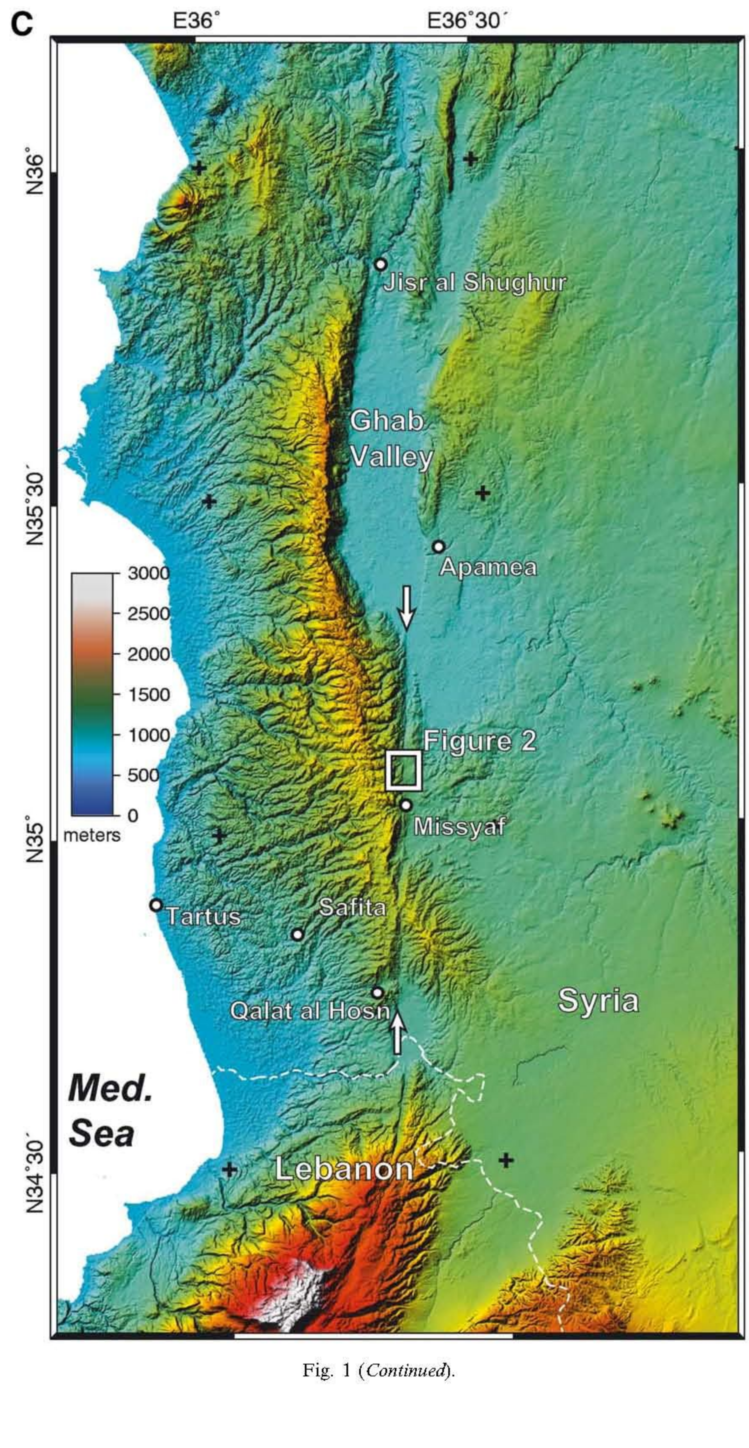

Fig. 1 (*Continued*).

(iii) evidence of large shutter ridges and small pull-apart basins along strike. Both geologic and geodetic studies along the fault poorly constrain its kinematics, as demonstrated by the wide range, 2–10 mm/yr slip rates [2,8–12].

Here, we present results from palaeoseismic and archaeoseismic investigations along the 70 km long Missyaf segment of the northern section of the DSF. Historical Arabic documents allow the identification of an ~830 yr seismic gap along the fault since medieval times and help in identifying damaged areas. Total station mapping, archaeoseismology and palaeoseismology provide new constraints on the seismic slip history during the past 2000 yr along the fault and related seismic slip deficit. Finally, we discuss the consistency of the results, the fault segmentation and the slip model along the northern DSF. The multidisciplinary approach is emphasised for a realistic assessment of the seismic hazard along the DSF in the Middle East.

2. Seismotectonic setting

The DSF is a large continental strike-slip fault corresponding to the boundary between the Arabia and Africa plates. It is a left-lateral transform fault system, striking north–south and extending for ~1000 km from the Gulf of Aqaba to join the East Anatolian fault zone in southern Turkey (Fig. 1A). The tectonic deformation associated with the DSF began in the early Pliocene with initiation of sea-floor spreading in the Red Sea

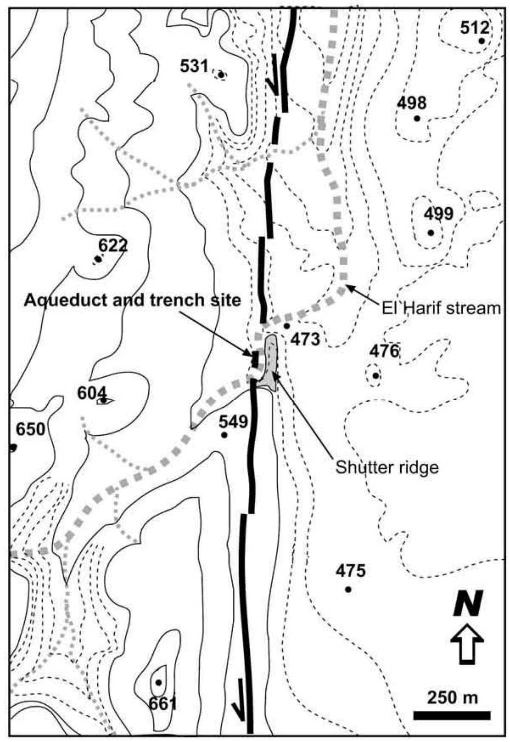

Fig. 2. Morphotectonic map showing the DSF and location of the ancient aqueduct and trench site west of the shutter ridge (in grey). Numbers denote elevation (in metres). Thick contour lines are for 50 m and dashed lines are for 10 m. The shutter ridge (shaded area) indicates the fault location and related cumulative left-lateral movement. The ~200 m deflection of the Al Harif stream is about 40 50 times the individual coseismic displacement inferred from the aqueduct (Fig. 3).

Table 1
Large historical earthquakes along the northern section of the DSF (see also Fig. 1B)

Date (AD)	*M* (estimated)	Areas with maximum damage and related fault segment
749	7.0 7.5	Southern Bekaa Hula basin, Yammouneh Ghab (two events)
859	7.0 7.5	Antioch, Lattakia, Homs, Sergilla segment
1063	6.5 7.0	Qalaat Hosn (Crak), Tripoli, northern Yammouneh segment
1157	7.0 7.5	Apamea, Hama, Aleppo, Apamea segment
1170	~7.5	Missyaf, Shaizar, Homs, Hama, Missyaf segment
1202	> 7.5	Mt. Lebanon, Bekaa Valley, Hula basin, Yemmouneh segment
1408	> 7.5	Qalaat Blatnes, west of Aleppo, Lattakia segment
1759	~7.4	Bekaa Valley, Anti-Lebanon, Golan Heights, Serghaya segment

Surface faulting reports and a rich description of damage exist in original Arabic sources [1,3 6,17]. Estimated magnitudes are from Ambraseys and Jackson [1]. We have interpreted the associated fault ruptures in terms of possible segmentation of the northern DSF.

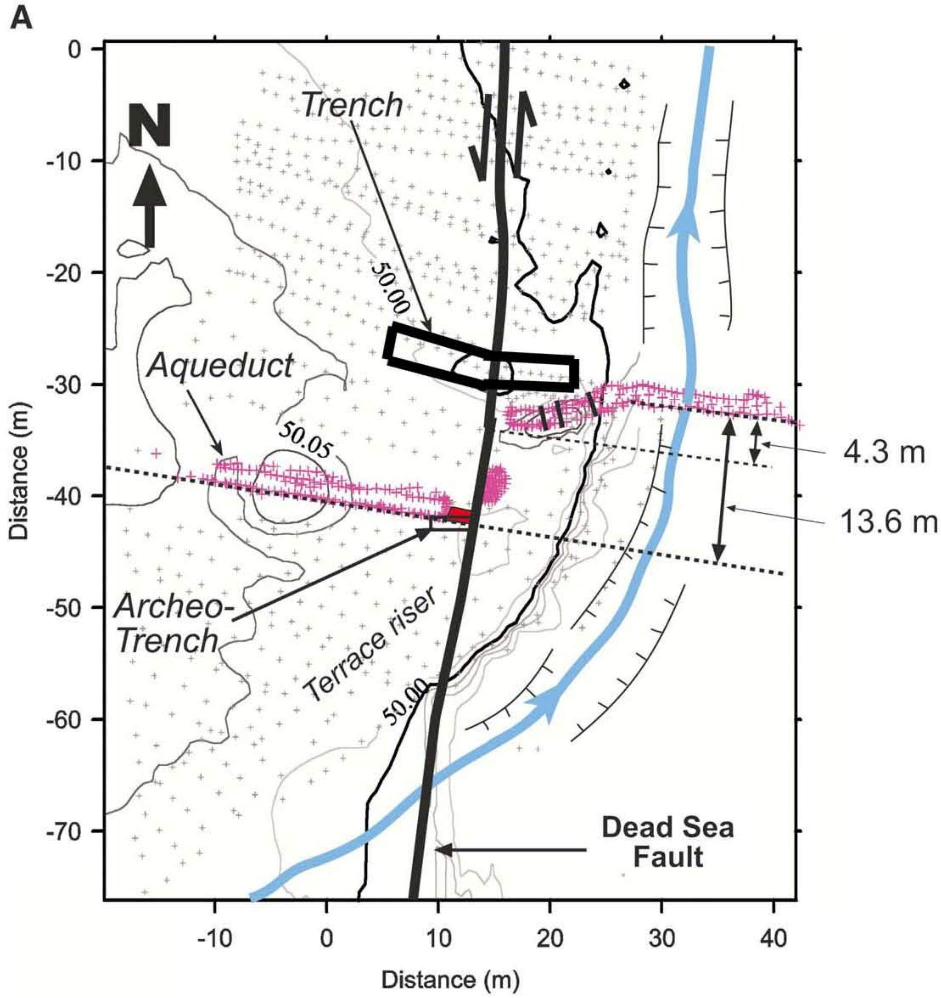

Fig. 3. (A) Detailed map of the aqueduct, trench site, and surrounding area based on precise mapping with a total station (red crosses are points levelled on the aqueduct, small crosses are the background levelling points for the alluvial terrace). A 13.6 m total left-lateral displacement is measured between straight sections of the aqueduct. The 4.3 m are interpreted as resulting from the first coseismic slip after building the aqueduct and after projecting the eastern wall on the fault. Additional breaks in the travertine wall (see also Fig. 4B) and rebuilt phases inferred from two different types of building stones, and the remaining fallen piece of wall near the fault attests to repeated coseismic movements (see text). The trench exposes the fault zone and the archeo-trench excavates the wall foundation (red area) orthogonal to the fault (Fig. 4A). (B) Photograph of the aqueduct looking west. The aqueduct used to bring fresh water from the wet western high mountains to wheat and olive oil mills and local cities and villages located in the eastern plains. In the foreground, the bridge allows the aqueduct to cross the El Harif River (see also Fig. 4B). It has been faulted three times and displays a total left-lateral offset of 13.6 ± 0.2 m (note the trench nearby and related log in Fig. 5A). Radiocarbon dating of travertine accumulation and unit e below its foundation indicate that the aqueduct may be younger than AD 30 and older than AD 70 (see text for explanation).

B

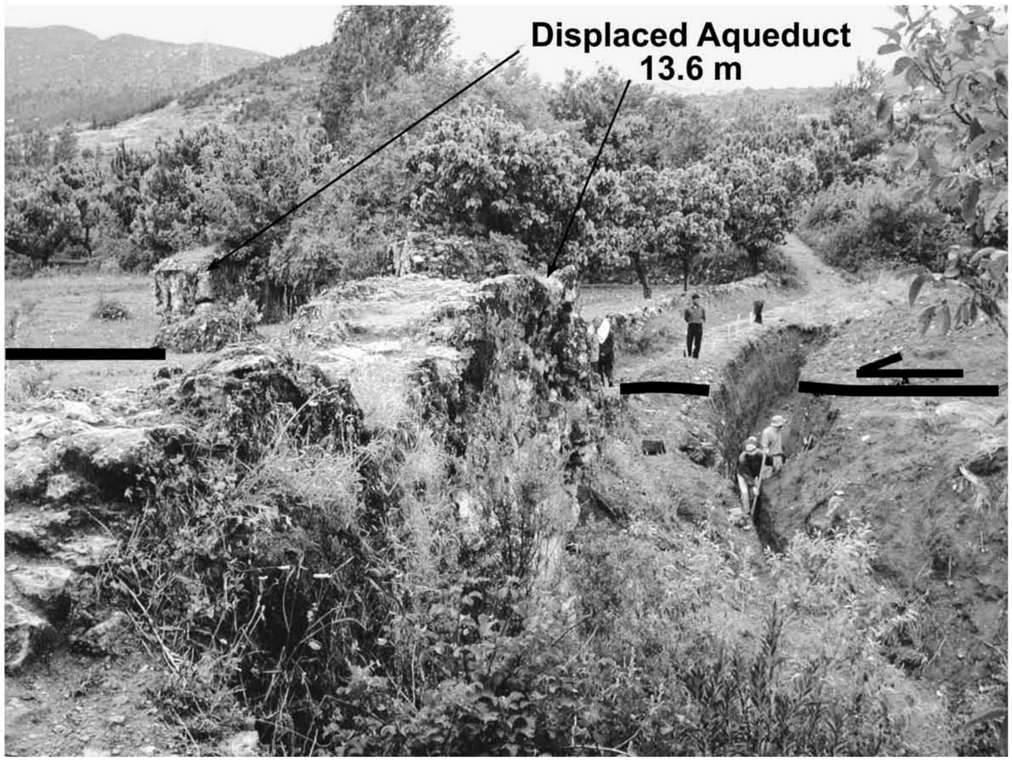

Fig. 3 (*Continued*).

[13,14]. The total left-lateral displacements along the DSF since the Pliocene and the initiation of sea-floor spreading of the Red Sea are estimated to be 45 km to the south and 20–25 km to the north [15]. This difference in displacements may be explained by up to 20 km of shortening in the NE–SW-trending Palmyride fold belt (Fig. 1A) [16].

The low level of instrumental seismicity as observed from 1900 to the present and the scarce focal mechanisms along the central and northern DSF may suggest the idea that the DSF is moderately active (Fig. 1A). However, this view is inconsistent with historical records of large, devastating earthquakes that attest to the activity and seismogenic potential (Fig. 1B and Table 1), and with field observations, as described below. One of the best-documented and most recent events occurred in 1759, affecting the Bekaa Valley of Lebanon ($M = 7.4$) with a rupture length of at least 100 km [3]. Other significant seismic events with probable surface faulting occurred in the past and ruptured different segments of the DSF [17]. Fault segments can be delimited according to the structural pattern of strike-slip faults (e.g. main pull-apart basins, steps, releasing and restraining bends). The northern DSF follows a relatively narrow trace between the Qalaat Al Hosn (Crak des Chevaliers) pull-apart basin at the Syrian/Lebanese border to the south and in the Ghab Valley to the north (Fig. 1C). Tectonic indicators include faulted alluvial fans, small and large stream deflections (tens to a few thousand metres), and the faulted Neogene and Quaternary

Homs basaltic flows [18]. The Ghab Valley is a large pull-apart basin with up to 3.5–4 km of Pliocene and Quaternary fill [19]. Between the Ghab Valley and the Qalaat Al Hosn plain to the south the DSF forms the ~70 km long Missyaf segment. Historical data suggest that this section of the DSF may presently exhibit seismic quiescence and has not experienced a large earthquake since the 12th–13th century (Fig. 1A,B).

3. Historical constraints of the seismic gap

The historical record of seismicity of Syria and surrounding regions is one of the richest because of the numerous archaeological and historical sources dating back at least to BC 1365 [1,4–6,20–22]. Among the most important seismic events, a southward-migrating sequence of large earthquakes took place in 1157, 1170 and 1202 along the Apamea, Missyaf, and Yammouneh segments of the DSF, respectively (Fig. 1B). Several contemporaneous accounts describe the successive land-shaking and related destructions of cities and villages. The 12 August 1157 (4 Rajab 552 Hegirian) earthquake is extensively described by Ibn El Qualansi (AD 1073–1160) who reported in detail a long period of seismic activity that affected Damascus and its surrounding regions between 28 September 1156 and 30 May 1159 [4]. In particular, El Qualansi mentions the different localities that were badly damaged by the main shock of 1157. This description allows the assessment of the area of maximum damage, which constrains the earthquake parameters, including the location of the epicentre area near Apamea (see Fig. 1B) and the size that may reach an intensity IX (MKS scale). Reported details reflect the severity of the damage in a north–south-elongated area that is consistent with El Qalansi's report in the region of Apamea [4]. According to the distribution of maximum intensity, this event corresponds with the Apamea segment of the DSF.

The 29 June 1170 (12 Shawwal 565 Hegirian) earthquake is reported primarily by Ibn El Athir (1160–1232), who describes in his book 'El Kamil fi El Tarikh' more than 56 felt earthquakes in the region [23]. Despite his young age at the time of the 1170 earthquake, he kept in his memory the 'terrible' feeling of the quake and later on, during his travelling, investigated the earthquake damage. Ibn El Athir provides numerous detailed descriptions of strongly damaged cities such as Homs and Hama, which define an area of maximum damage in the region named '*bilad el Firanj*', literally 'country of the Christians' or the crusaders' region located in Crak des Chevaliers, Missyaf Fortress and Borj Safita (Fig. 1B,C).

A

Fig. 4. (A) Excavation of the western section of the aqueduct (archeo-trench in Fig. 3A) and the prominent travertine accumulation on the wall. Although a section of the wall above the ground surface is missing (stones were probably removed to construct nearby fences), the aqueduct foundation indicates a straight line (white arrows) and reaches to the east the fault trace (black arrows). (B) Details of the warped section at the west side of the bridge showing travertine filling ruptures and cracks of building stones (see black arrows). The excavation below the rupture (white arrow) does not show any faulting. Ruptures in travertine filling previous cracks indicate at least two episodes of deformation since the building of the aqueduct.

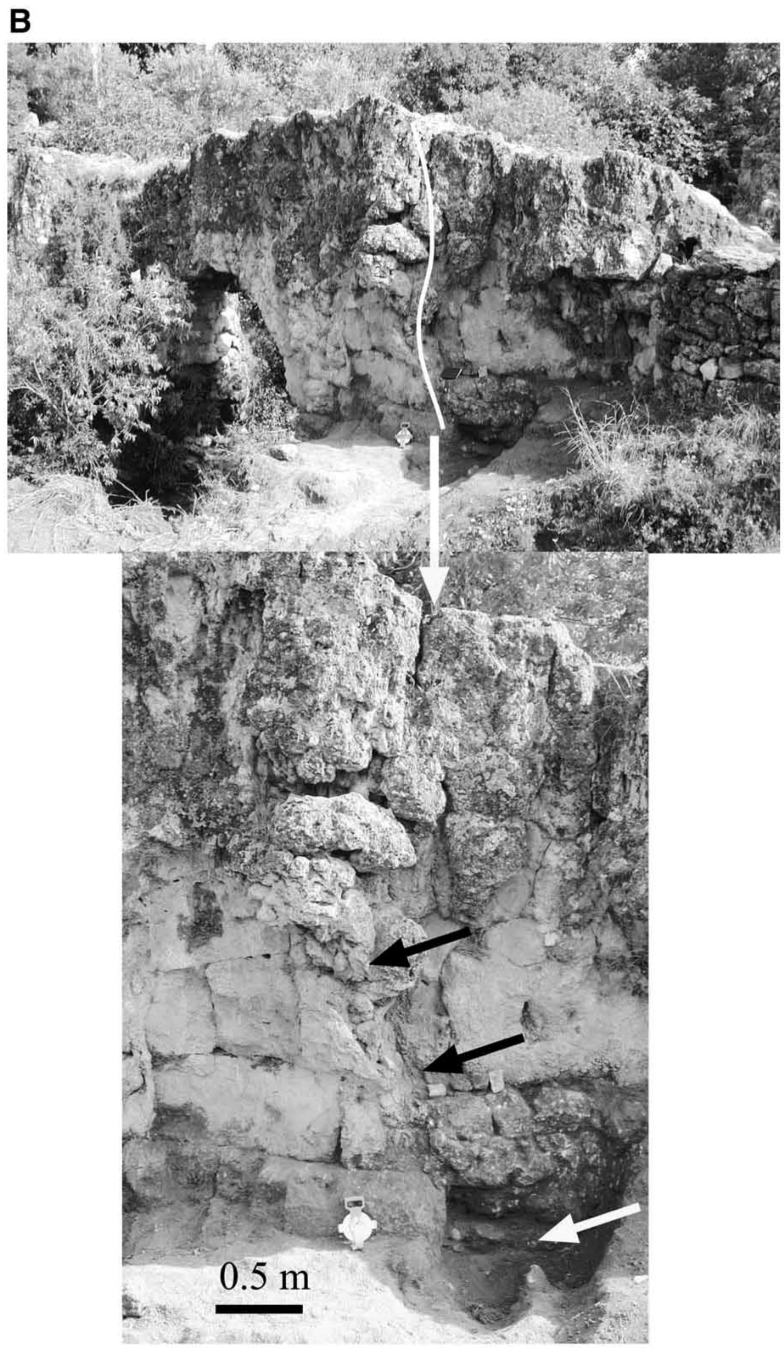

Fig. 4 (*Continued*).

A

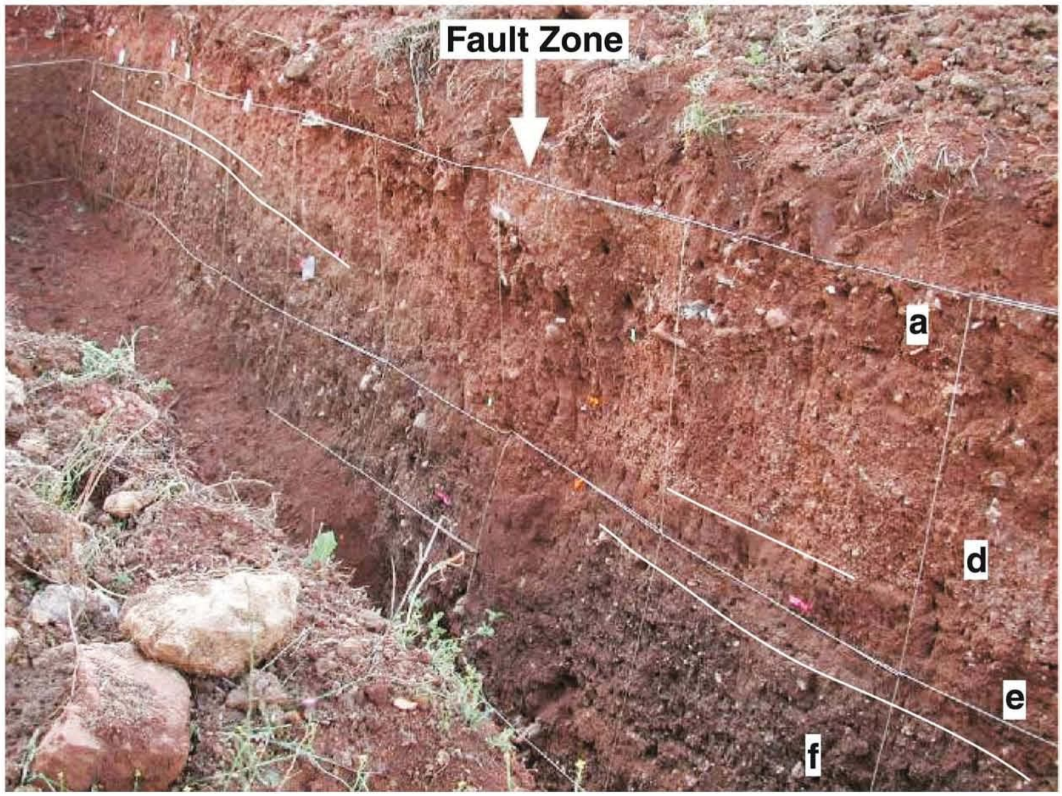

Fig. 5. (A) Photograph of the V-shaped structure of the fault zone visible in the trench walls. White string grid is spaced 1 m. The white lines delimit unit e interrupted and vertically displaced at the fault zone. (B) Trench log of the fault zone and related alluvial terrace deposits. Multiple ruptures with displacement of units b, c, d and e mark the three most recent faulting events at this site. Repeated small depressions (likely small pull-apart basins filled by units c and b) with coarse deposits mixed with debris flow probably from previous flood events and thickening of units d and b are visible in the shear zone. Squares depict the locations of dated charcoal samples. The vertical separation visible from unit e results from cumulative movement on the fault.

These rich descriptions allow us to define the epicentre area with an estimated maximum intensity IX (MKS) between the well-known historical sites of Crak des Chevaliers and Missyaf Fortress [4], and to associate the AD 1170 event with the Missyaf segment of the DSF.

The 20 May 1202 earthquake took place mostly in Lebanon along the Yammouneh fault and has been extensively studied by Ambraseys and Melville (Fig. 1B) [24]. The related surface rupture has been confirmed by palaeoseismic studies along the DSF near the Hula depression [9].

4. Faulted aqueduct and holocene palaeoseismic timing at Al Harif site

Faulting of late Pleistocene and Holocene deposits, prominent fault scarps and shutter ridges with stream deflections, and faulted archaeological sites provide the best location for palaeoseismic and archaeoseismic studies (Fig. 2). We conducted a combined study in archaeoseismology with excavation and detailed descriptions and mapping (with a total station) of the faulted aqueduct and the related evidence of deformation

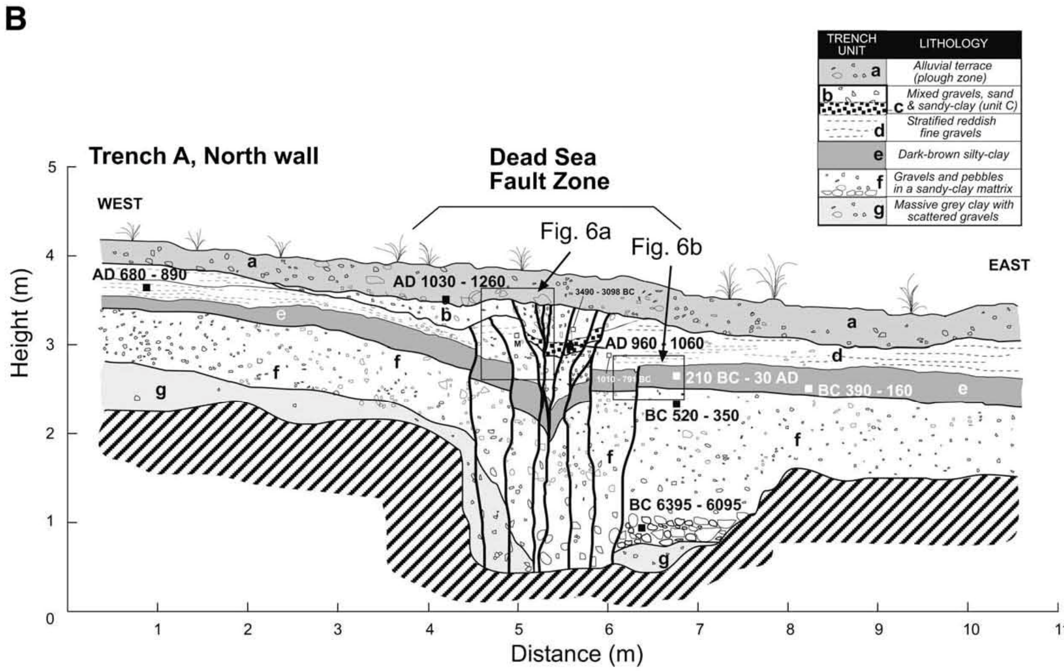

Fig. 5 (*Continued*).

(Figs. 3 and 4). In parallel, palaeoseismic investigations consisted of a 20 m long and 3.5 m deep trench near the aqueduct and across the fault (Fig. 5A,B). The faulted aqueduct and the trench provide an interesting opportunity for investigating both the vertical and lateral offsets along the fault.

4.1. Archaeoseismic evidence

Of particular interest is the Al Harif shutter-ridge site, which shows an ancient aqueduct cut and displaced left-laterally by the fault (Figs. 2 and 3). This latter observation is apparently mentioned by Trifonov [18] in his work along the DSF, but curiously with only 0.6 m of displacement. An excavation, 8 m long and 1 m deep, along the western wall and at the intersection with the fault constrains the rupture pattern and stratigraphic age of the ancient building. The aqueduct wall foundation was found to end to the east against the discrete fault rupture while about 2.5 m of aqueduct wall above the ground is missing west of the fault (Figs. 3A and 4A). At about 0.8–1 m depth, the wall is built into unit d and above unit e, which predate the aqueduct (see also trench log description below and in Fig. 5B). The large fallen piece of wall (made of small stone pieces) found in between the two prominent eastern and western aqueduct sections, has no foundation, and most likely corresponds to a piece from the rebuilt eastern section that was rotated and dragged along the fault. According to local witnesses many of the aqueduct stones are reutilised for nearby fences.

The maximum age for the aqueduct may be bracketed from the age of the sedimentary units below its foundation and from early travertine accumulation on its wall. The 1–2 m deep excavation at the base of the aqueduct wall clearly show that the foundation stones are within unit d and rest on the uppermost layers of unit e (BC 210–AD 30, 2σ calibrated age, Table 2). The maximum possible age of the aqueduct is best defined

Table 2
Characteristics of radiocarbon dating of samples of the aqueduct site

Sample name	Material	Amount of carbon (mg)	$\Delta^{13}C$ (%)	Radiocarbon age (BP)	Unit	Calibrated age AD (− = BC; 2σ age range)	
TA N31	Charcoal	2	−24.16	874 ± 34	a	1030	1260
TA N23	Charcoal	5.9	−27.90	1013 ± 36	c	960	1060
TA S33	Charcoal	4.3	−25.90	1237 ± 36	d	680	890
TA N25	Charcoal	2	−22.95	2091 ± 50	e	−210	30
TA S7	Charcoal		−25.5	2195 ± 40	e	−390	−160
TA N21	Charcoal	0.3	−33.06	2718 ± 73	d-R	−1010	−791
TA N27	Charcoal	4.1	−23.61	2337 ± 31	f	−520	−350
TA N47	Charcoal	1.7	−25.93	7409 ± 46	f	−6395	−6095
TA N61	Charcoal	1	−26.52	4553 ± 42	b-R	−3490	−3098
TrB13	Travertine	3.7	−28.57	1880 ± 25	Aqueduct	70	230
TrD5	Travertine	1.1	−27.97	1865 ± 30	Aqueduct	80	240

All dating methods are AMS. R is for reworked and units are illustrated in Fig. 5B. All samples have been calibrated using the Oxcal programme v3.5 [25] and calibration curve INTCAL98 [26]. Adopted age ranges are equivalent to calibrated 2σ ranges (94.5%), in AD and BC and without taking into account ranges with probability of 1% and less.

by the minimum age of uppermost deposits of unit e, AD 30. In addition, organic fractions extracted from two early sections of cores of the ~0.40 m thick travertine deposits on the aqueduct wall yield nearly identical radiocarbon calibrated ages of AD 80–240 and AD 70–230. These travertine ages indicate a building period younger than AD 70. Hence, the initial building of the aqueduct can be bracketed between AD 30 and AD 70 and may probably correspond to the early Roman period in the Middle East (post BC 64).

A detailed topographic survey of the area around the aqueduct accompanies the detailed mapping of the aqueduct itself (one point measured every 0.5 m at the base and on the top of each wall face). The straight original shape of the building is attested by: (i) the linear and orthogonal foundation of the aqueduct wall immediately west of the fault (Figs. 3 and 4A), (ii) the warped section east of the fault zone with rotated blocks and the dragged and fallen block, (iii) the ruptured travertine filling previous ruptures and cracks at the warped section (Fig. 4B), (iv) the two ~20 m long and linear parallel sections of the aqueduct and related bridge. Projecting the aqueduct walls into the N07°E-striking DSF displays a total left-lateral displacement of 13.6 ± 0.2 m between the two pieces of the faulted aqueduct (Fig. 3A,B). In addition, the eastern warped wall shows a deflection of 3.9 ± 0.2 m, reaching 4.3 ± 0.2 m when projected on the fault line (Fig. 3A). This observation suggests 4.0–4.5 m left-lateral coseismic slip for the successive faulting events. Furthermore, the aqueduct is built on a bridge across the river, which displays at least two kinds of building stones, suggesting rebuilding episodes. At the warped section, the numerous ruptured stones and cracks filled with brecciated and ruptured travertine indicate at least two episodes of deformation, indicating the abandonment of the aqueduct before the third event (Fig. 4B). Rebuilt phases and cracks in travertine help in documenting the two first successive faulting events. It is likely that no travertine accumulation and rebuilding phase were present any longer after the second event.

4.2. Palaeoseismic trenching

The trench was dug in an alluvial terrace made of 4–5 m thick young sediments likely deposited by the nearby stream (Figs. 2, 3 and 5A). The terrace rests approximately 5 m above the current streambed that flows across bedrock, forming a dogleg offset of about 200 m. The trench walls expose sediments with different units, illustrated by the log of Fig. 5B. The trench bottom shows unit g, which consists of a massive and plastic grey clay with some scattered breccia elements (mainly limestone). Unit f, which covers unit g, corresponds to a massive alluvial deposit with 1–2 m thick dark-brown sandy clay with breccias and rounded gravels and about 0.3 m thick stratified pebbles. Deposit f shows a dramatic increase of its thickness to the east and the coarse gravel and pebble at its base suggest the location of an old channel. Unit e is 0.10–0.25 m thick dark-brown silt-clay. Well-sorted reddish fine gravels with cross-bedding correspond to unit d, which shows a variable thickness of 0.10–0.50 m due to the above truncation surfaces. Unit c is a thin sandy clay deposit with a limited extension below unit b that corresponds to a chaotic deposit with mixed gravels and clastic (limestone) elements in a sandy clay matrix. Unit a, which shows clearly stratified gravels and pebbles at its base, truncates units b and d all along the wall. Unit a also forms a 0.20–0.40 m thick coarse gravel deposit on which de-

Table 3
Probability distribution of calibrated ^{14}C ages (in cal yr BC/AD) obtained from sequential radiocarbon dates (BP) using Oxcal v3.5 [24] and INTCAL98 calibration curve [25]

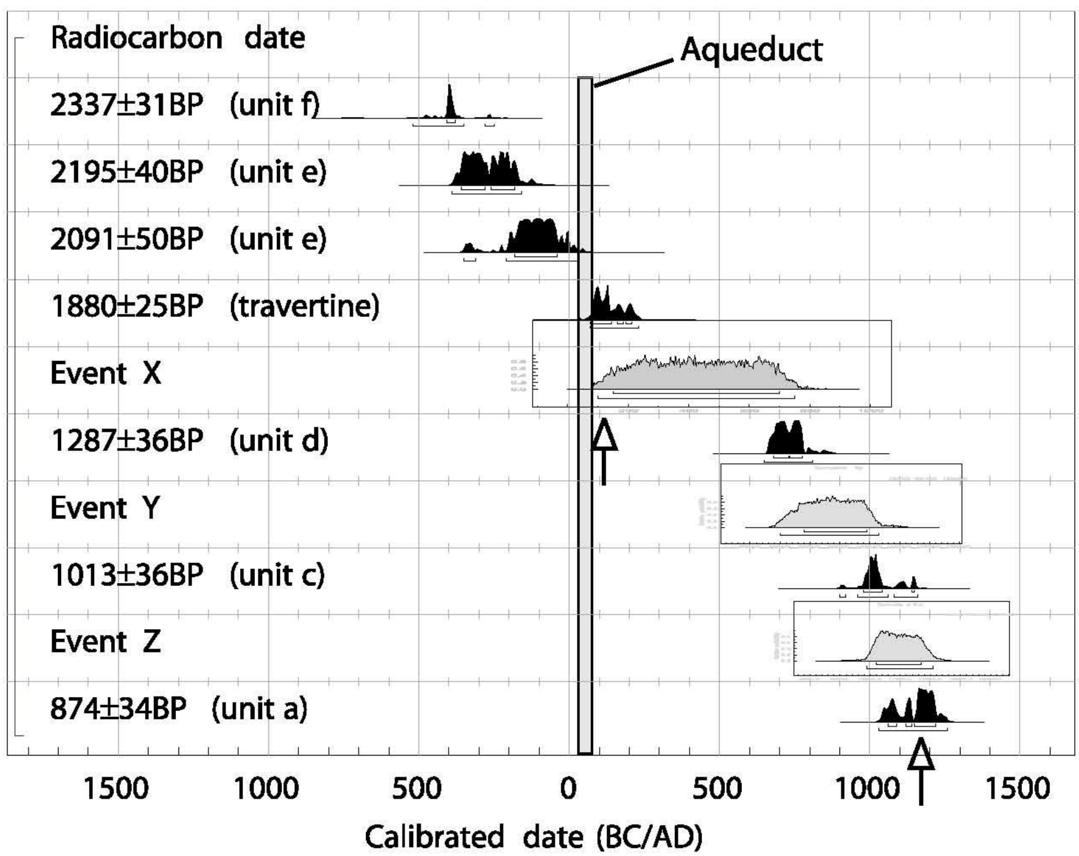

As indicated in Table 2, calibrated dates are presented with 2σ age range (95.4% density). The age of the aqueduct is estimated considering unit e, which pre-dates the building (see text for explanation), and the travertine age, which post-dates the building. Age ranges of seismic events X (AD 100 750), Y (AD 700 1030) and Z (AD 990 1210) are determined using Bayesian analysis (probability distribution of the ages). Arrows show our preferred ages associated with two historical large earthquakes in AD 115 and AD 1170.

A

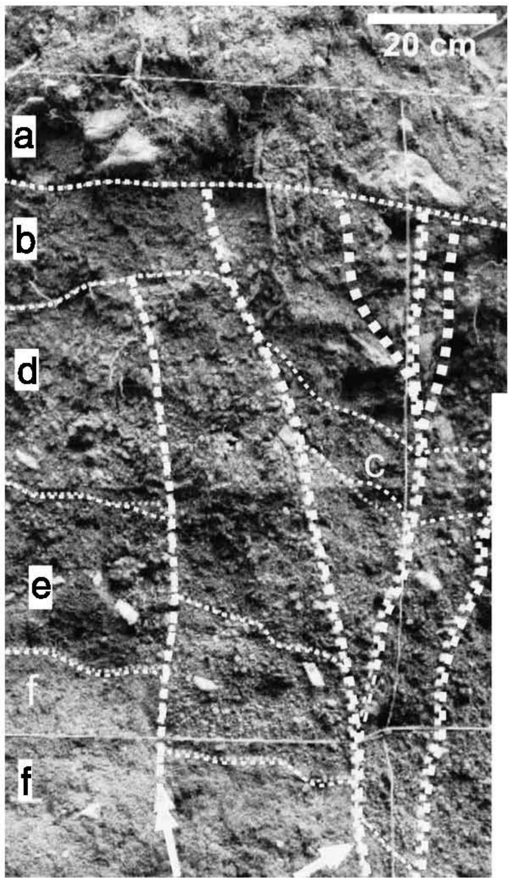

Fig. 6. (A) Central shear zone of the fault with vertical offset visible at the interface between units f and e (see also Fig. 5B). Note the flat-lying coarse gravel and pebbles of unit a, and the oriented clasts in unit b. (B) Event X shown by the fault displacement of unit e eroded (white arrows) and buried below unit d (black arrows show the easternmost fault branch in Fig. 5B).

velops the present soil. All interfaces of units above f are erosion surfaces except between b and c.

Pottery shards and detrital fragments of charcoal are well distributed through the trench walls and were collected for dating (Table 2). Eight samples of charcoal from the north wall were dated using the ^{14}C accelerator mass spectrometry (AMS) methods and calibrated with 2σ age range using Oxcal v3.5 [25]. Six of the collected charcoal fragments were of large size and angular shape (suggesting limited transport or initial deposition and no reworking) and revealed a fairly large amount of carbon fraction after laboratory treatment (Table 2). In Fig. 5B, samples of units a, c, d, e and f gave 2, 5.9, 4.3, 2 and 4.1 mg of carbon content, respectively, and the $\Delta^{13}C$ attests to the good quality of radiocarbon dating. Only two samples show out-of-sequence ages in units b and d, but they yielded 1 and 0.3 mg of carbon, respectively (see BC 3490–3098 and BC 1010–791 in Fig. 5B and Table 2) and are therefore interpreted as reworked detrital charcoal in mixed deposits. Additional constraints on the timing of individual palaeoseismic events is provided by considering the stratigraphic superposition and applying Bayesian analysis (conditional probability for the stratigraphic succession and datings) to the age ranges obtained from calibration of radiocarbon ages (Table 3) [27].

Both walls reveal a 2 m wide fault zone that consists on intensely sheared sedimentary deposits (Fig. 5A,B). No other shear zone or minor faulting exists in trench walls (the northern trench wall joins the edge of the river and exhibits a large stratigraphic section). While motion on the fault is mostly left-lateral, it bears a small but significant vertical component at this site, as pointed out by the vertical offset of ~1 m of units e and d in the trench. Some fault strands are clearly truncated by the successive deposits that register the faulting episodes (Fig. 6A,B). Furthermore, the intense deformational structures visible along the shear zone and the numerous rupture strands that affect the successive sedimentary units testify that the palaeoearthquakes were large faulting events. The successive truncated fault strands that can be recognised in Fig. 5B represent, therefore, past large earthquakes in the trench wall:

Event Z: Unit a caps the entire fault zone and post-dates all coseismic movements which appear to have occurred before AD 1030–1260; AD 1260 provides a minimum age for unit a and a maximum age for the most recent large earthquake along the fault. The most recent large seismic event can be defined within the large age bracket

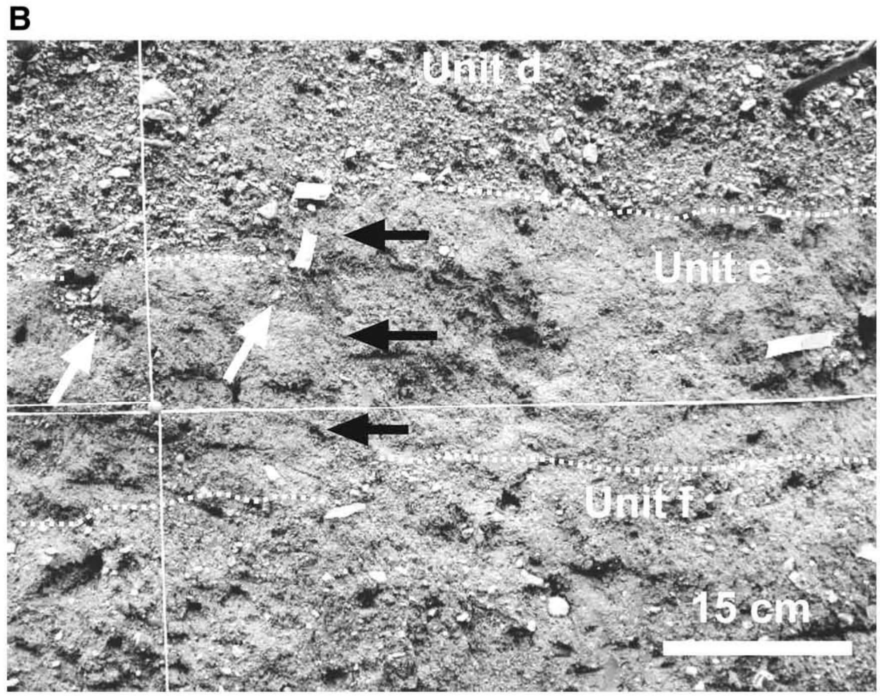

Fig. 6 (*Continued*).

between units a and c. After Bayesian analysis, this event is constrained at the 95% confidence limit by radiocarbon dating between AD 990 and 1210 (Table 3). This result is consistent with the occurrence of the historical earthquake of 29 June 1170 along the Missyaf fault segment.

Event Y: The penultimate event is visible immediately west of the shear zone, where unit b truncates two fault strands and related shear zone that affect unit d. Unit d is dated at AD 680–890. Applying Bayesian analysis determines the occurrence of a large event between AD 700 and 1030 (Table 3). This time range of about 340 yr is quite large. The historical seismicity, however, allows us to infer that the earthquake took place during the Byzantine time or at the very beginning of the Islamic time (>AD 680). Several candidate historical earthquakes (see [4–6]) can be associated with the faulting event, but further palaeoseismic and historical investigations with precise dating are needed for a reliable correlation.

Event X: The third faulting event visible in the trench occurred between units e and d, according to the easternmost rupture and associated shear zone buried below d. Although the step is eroded, the top stratigraphic line of unit e shows a clear displacement capped by unit d (Fig. 6B). This erosional truncation of the fault suggests a distinct palaeoseismic event and not simply a plunging tip line within the strike-slip shear zone. The larger offset of unit e within the shear zone and with respect to the offset bedding in unit d, immediately below unit b (west branch of the fault zone), also attests to the occurrence of event X. Radiocarbon dating of units e and d, along with Bayesian analysis, indicates that the seismic event occurred between AD 100 and 750 (Table 3). However, this event may also be correlated with the large earthquake that destroyed the ancient city of Apamea and damaged Beirut on 13 December 115 [4,6].

In summary, Table 3 shows that the antepenultimate event X probably took place during the Roman occupation after AD 70 and perhaps in AD 115, the penultimate event Y after the Byzantine period and perhaps during the early Islamic period (AD 690–1030), and the most recent event most likely in AD 1170.

The 13.6 m total horizontal offset of the aqueduct likely results from successive displacements during seismic events X, Y and Z that occurred in the last 2000 yr (Fig. 7). The age of the aqueduct, bracketed between AD 30 and 70, implies a late Holocene slip rate of 6.8–7.0 mm/yr along the Missyaf segment of the DSF. Furthermore, archaeoseismic and palaeoseismic data suggest a comparable coseismic slip of 4.0–4.5 m for the last three events (X, Y and Z), consistent with an $M \geq 7$ size of historical earthquakes as assigned by Ambraseys and Jackson [1]. The slip rate and mean coseismic displacement suggest an average recurrence interval for large earthquakes of 550 yr, and the 830 yr that have elapsed since the most recent earthquake suggest a short time left until the next large earthquake (Fig. 7).

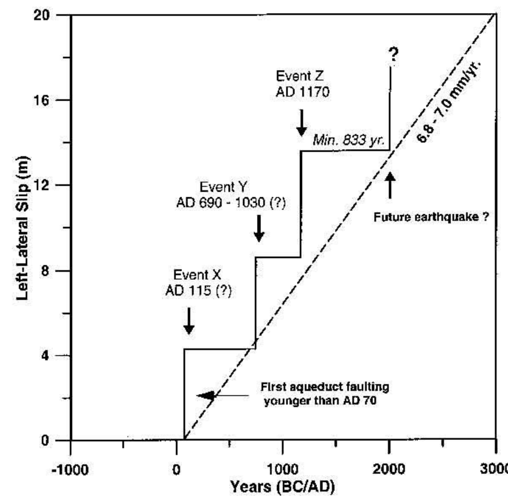

Fig. 7. Cumulative left-lateral offset over the last 2000 yr along the Missyaf segment of the DSF obtained from palaeoseismic and historical data. The succession of past earthquakes is deduced from radiocarbon dating of faulted units in trench (Fig. 5B). The first coseismic displacement (4.3 m) and the cumulative slip for the three events (13.6 m) were measured from the faulted aqueduct (Fig. 3A). The late Holocene slip rate of 6.8 7.0 mm/yr and mean coseismic displacement suggest an average recurrence time for large earthquakes of about 550 yr. 833 yr has elapsed since the last earthquake in AD 1170. Following a time-predictable earthquake recurrence model, the slip-rate line projects from the last event to suggest that failure of this segment of the DSF fault may perhaps be imminent, or possibly overdue.

5. Implications of the 830 yr seismic quiescence for the seismic hazard evaluation

Historical documents show that several large earthquakes have occurred along the northern strand of the DSF from AD 749 to 1408 (Fig. 1B). In particular, the sequence of historical earthquakes in AD 1157, 1170 and 1202 took place in continuity along three fault segments in Syria and Lebanon, with a migration toward the south in relatively short time intervals (13 and 32 yr). Several fault segments are defined and among them the Missyaf fault segment, which is identified as a 70 km long earthquake fault along the DSF.

The correlation between palaeoseismological and archaeological investigations offers an opportunity for a quasi-3D study along a seismogenic fault. Trench results and total and first displacements of the aqueduct imply a left-lateral slip per event at Al Harif site of about 4.0–4.5 m. A similar amount of coseismic slip has been observed along other major continental faults, e.g. the North Anatolian fault in Turkey and the related $M_w = 7.3$, 1999 Izmit earthquake [28]. Using scaling laws for large earthquakes [29] we obtain a range of M_w between 7.0 and 7.5 for the events along the Missyaf segment. The analysis of faulting episodes and dated units in the trench reveal that three large seismic events have occurred in the last 2000 yr (Table 3): (i) the antepenultimate event between AD 100 and 750 that may be correlated with the 13 December 115 earthquake, (ii) the penultimate event between AD 690 and 1030, and (iii) the most recent event, between AD 990 and 1210, that may be correlated with the large earthquake of 29 June 1170 along the DSF.

The slip rate deduced from the displaced aqueduct and trench dating ranges between 6.8 and 7.0 mm/yr for the past 2000 yr, and is consistent with predicted values along the northern DSF from plate motions between Arabia and Africa [12]. Recent geological investigations along the southern DSF (Wadi Araba fault zone) indicate various late Pleistocene and Holocene slip rates of 2–6 mm/yr [9], 3.9–6 mm/yr [30], 10 mm/yr [31] and 2.5 mm/yr [32]. They denote the complex fault zone and the difficulty in characterising and dating offset of alluvial fan and gullies. Owing to the short time period spanned by the aqueduct, it is clear that further palaeoseismic studies that cover the Holocene and late Pleistocene are needed for better constraining the slip rate along the DSF.

The seismic behaviour of the northern DSF appears to involve long periods of seismic quiescence punctuated by infrequent, large earthquakes. Three events are interpreted to have occurred between AD 70 and 1170 (1100 yr) followed by about 830 yr without a major earthquake along the Missyaf segment. The 6.8–7.0 mm/yr slip rate at depth would accumulate a slip deficit of 5.6–5.8 m on the locked upper part of the fault, which exceeds the average estimated past coseismic slip (Fig. 7). Due to our single observation concerning the amount of slip at the aqueduct site and complicated fault segmentation along strike, the rupture history of the DSF can be driven by either slip patches or characteristic slip behaviour [33]. However, a large earthquake with $M>7$ along the Missyaf and adjacent fault segments would induce severe damage to the region. We interpret the seismic quiescence during the past 830 yr to possibly represent a high level of seismic hazard in Syria and Lebanon.

Acknowledgements

This research benefited from the full field support of the Higher Institute of Applied Sciences and Technology (HIAST) in Damascus. Additionally, the Syrian Atomic Energy Commission and Damascus University provided logistical support to this project. We thank Professors Mikhail Mouty and Khaled Al-Maleh (Damascus University) for their constant support during the 3-year study of the Dead Sea fault in Syria. We also thank Mrs Ghada Suleiman (DGAM, Damascus) for assistance on the aqueduct archaeology and Mr Jean Vogt for fruitful discussions on the historical seismicity of Syria. We are grateful to Professor Pieter Grootes (Kiel University) for the radiocarbon dating results and detailed analysis of travertine. This research is partially supported by NSF Grant EAR-0106238 to Cornell University, by the UMR 7516 of CNRS in Strasbourg and the European Commission project APAME (ICA3-CT-2002–10024).*[BARD]*

References

[1] N.N. Ambraseys, J.A. Jackson, Faulting associated with historical and recent earthquakes in the Eastern Mediterranean region, Geophys. J. Int. 133 (1998) 390 406.

[2] Z. Garfunkel, I. Zak, R. Freund, Active faulting in the Dead Sea rift, Tectonophysics 80 (1981) 1 26.

[3] N.N. Ambraseys, M. Barazangi, The 1759 earthquake in the Bekaa Valley: Implications for earthquake hazard assessment in the Eastern Mediterranean Region, J. Geophys. Res. 94 (1989) 4007 4013.

[4] M.R. Sbeinati, R. Darawcheh, M. Mouty, The historical earthquake catalogue in Syria and its vicinity (BC 1365-AD 1900), submitted to Ann. Geofis., 152 pp.

[5] J.P. Poirier, M.A. Taher, Historical seismicity in the Near and Middle East, North Africa, and Spain from Arabic documents (VIIth-XVIIIth century), Bull. Seism. Soc. Am. 70 (1980) 2185 2201.

[6] E. Guidoboni, Catalogue of Ancient Earthquakes in the Mediterranean Area up to the 10th Century, Istituto Nazionale di Geofisica Rome, 1994, 503 pp.

[7] R.W.H. Butler, S. Spencer, H.M. Griffiths, Transcurrent fault activity on the Dead Sea Transform in Lebanon and its implications for plate tectonics and seismic hazard, J. Geol. Soc. London 154 (1997) 757 760.

[8] J. Jackson, D. McKenzie, The relationship between plate motions and seismic moment tensors, and rates of active deformation in the Mediterranean and Middle East, Geophys. J. 93 (1988) 45 73.

[9] R. Ellenblum, S. Marco, A. Agnon, T. Rockwell, A. Boas, Crusader castle torn apart by earthquake at dawn, 20 May 1202, Geology 26 (1998) 303 306.

[10] Y. Klinger et al., Slip rate on the Dead Sea transform fault in the northern Araba Valley (Jordan), Geophys. J. Int. 142 (2000) 755 768.

[11] F. Gomez et al., Coseismic displacements along the Serghaya fault: An active branch of the Dead Sea fault sys-

tem in Syria and Lebanon, J. Geol. Soc. London 158 (2000) 405 408.

[12] S. McClusky et al., GPS constraints on plate kinematics and dynamics in the eastern Mediterranean and Caucasus, J. Geophys. Res. 105 (2000) 5695 5719.

[13] R. Freund et al., The shear along the Dead Sea rift, Philos. Trans. R. Soc. London A 267 (1970) 107 130.

[14] A.M. Quennell, The Western Arabia rift system, in: J.E. Dixon, A.H.F. Robertson (Eds.), The Geological Evolution of the Eastern Mediterranean, Blackwell Scientific, Oxford, 1984, pp. 775 788.

[15] M.R. Hempton, Constraints on Arabian plate motion and extensional history of the Red Sea, Tectonics 6 (1987) 687 705.

[16] T.A. Chaimov, M. Barazangi, D. Al-Saad, T. Sawaf, A. Gebran, Crustal shortening in the Palmyride fold belt, Syria, and implications for movement along the Dead Sea fault system, Tectonics 9 (1990) 1369 1386.

[17] N. Ambraseys, C.P. Melville, Historical evidence of faulting in Eastern Anatolia and northern Syria, Ann. Geofis. 28 (1988) 337 343.

[18] V.G. Trifonov, Levant fault zone in northwest Syria, Geotectonics 25 (1991) 145 154.

[19] G. Brew, M. Barazangi, A.K. Al-Maleh, T. Sawaf, Tectonic and geologic evolution of Syria, GeoArabia 6 (2001) 573 616.

[20] S.J. Plassard, B. Kogoj, Sismicité du Liban: Catalogue des séismes ressentis, 3rd edn., in: Collection des Annales-Mémoires de l'Observatoire de Ksara, vol. IV (Sismologie) Cahier 1, Conseil National Libanais de la Recherche Scientifique, Beyrouth, 1981, 67 pp.

[21] A. Ben Menahem, Earthquake catalogue for the Middle East (BC 92 to AD 1980), Bol. Geof. Teor. Applic. 21, Trieste, 1979.

[22] A. Nur, E.H. Cline, Poseidon's Horses: Plate tectonics and earthquake storms in the late Bronze age Aegean and Eastern Mediterranean, J. Archaeol. Sci. 27 (2000) 43 63.

[23] E. Ibn Al-Athir, The Complete in History (Al-Kamil fi al-tarikh), vols. 8 12, Dar Sader, Beirut, 1982.

[24] N. Ambraseys, C.P. Melville, An analysis of the eastern Mediterranean earthquake of 20 May 1202, in: W. Lee (Ed.), Historical Seismograms and Earthquakes of the World, Academic Press, San Diego, CA, 1988, pp. 181 200.

[25] C. Bronk-Ramsey, Probability and dating, Radiocarbon 40 (1998) 461 474.

[26] M. Stuiver, P.J. Reimer, E. Bard, J.W. Beck, G.S. Burr, K.A. Hughen, B. Kromer, G. McCormac, J. van der Plicht, M. Spurk, 1998 INTCAL9 radiocarbon age calibration, 24000-0 cal BP, Radiocarbon 40 (1998) 1041 1083.

[27] G. Biasi, R.J. Weldon, Palaeoseismic date refinement and implications for seismic hazard estimation, Quat. Res. 41 (1994) 1 18.

[28] A. Barka, The August 1999 Izmit earthquake, Science 285 (1999) 1858 1859.

[29] D. Wells, K. Coppersmith, New empirical relationships among magnitude, rupture length, rupture width, rupture area, and surface displacement, Bull. Seism. Soc. Am. 84 (1994) 974 1002.

[30] T. Niemi et al., Late Pleistocene and Holocene slip rate of the Northern Wadi Araba fault, Dead Sea Transform, Jordan J. Seismol. 5 (2001) 449 474.

[31] P. Galli, Active tectonics along the Wadi Araba-Jordan Valley, J. Geophys. Res. 104 (1999) 2777 2796.

[32] S. Marco et al., 817 year-old-walls offset sinistrally 2.1 m by the Dead Sea Transform, Israel, J. Geodyn. 24 (1997) 11 20.

[33] K. Sieh, The repetition of large-earthquake ruptures, Proc. Natl. Acad. Sci. 93 (1996) 3764 3771.

Geophysical Journal International

Geophys. J. Int. (2009) doi: 10.1111/j.1365-246X.2009.04431.x

Crustal deformation in northwestern Arabia from GPS measurements in Syria: Slow slip rate along the northern Dead Sea Fault

Abdulmutaleb Alchalbi,[1] Mohamad Daoud,[1] Francisco Gomez,[2] Simon McClusky,[3] Robert Reilinger,[3] Mohamad Abu Romeyeh,[1] Adham Alsouod,[1] Rayan Yassminh,[1] Basel Ballani,[1] Ryad Darawcheh,[4] Reda Sbeinati,[4] Youssef Radwan,[4] Riad Al Masri,[5] Mazhar Bayerly,[6] Riad Al Ghazzi[7] and Muawia Barazangi[8]

[1]*Syrian National Earthquake Center, Damascus, Syria*
[2]*Department of Geological Sciences, University of Missouri, Columbia,* MO 65211, *USA. E-mail: fgomez@missouri.edu*
[3]*Department of Earth, Atmospheric, and Planetary Sciences, Massachusetts Institute of Technology, Cambridge,* MA 02142, *USA*
[4]*Department of Geology, Syrian Atomic Energy Commission, Damascus, Syria*
[5]*Department of Civil Engineering, Damascus University, Damascus, Syria*
[6]*Department of Geology, Tishreen University, Latakia, Syria*
[7]*Syrian Virtual University, Damascus, Syria*
[8]*Institute for the Study of the Continents,Cornell University, Snee Hall, Ithaca,* NY 14853, *USA*

GJI Geodynamics and tectonics

Accepted 2009 October 26. Received 2009 October 2; in original form 2009 February 23

SUMMARY

New Global Positioning System (GPS) measurements in NW Syria provide the first direct observations of near-field deformation associated with the northern Dead Sea fault system (DSFS) and demonstrate that the kinematics of the northern section of this transform plate boundary between the Arabian and Sinai plates deviate significantly from plate model predictions. Velocity estimates based on GPS survey campaigns in 2000, 2007 and 2008, demonstrate left-lateral shear along the northern DSFS with 1σ uncertainties less than 0.7 mm yr^{-1}. These velocities are consistent with an elastic dislocation model with a slip rate of 1.8–3.3 mm yr^{-1} and a locking depth of 5–16 km. This geodetically determined slip rate is about half of that reported farther south along the central section (Lebanese restraining bend) and the southern section (Jordan Valley and Wadi Araba) of the transform and consequently requires some deformation to occur away from the transform along other geological structures. The factor of two difference in slip rates along the transform is also consistent with differing estimates of total fault slip that have occurred since the mid Miocene: 20–25 km along the northern DSFS (in NW Syria) versus about 45 km along the southern DSFS segment. Some of the strain deficit may be accommodated by north–south shortening within the southwestern segment of the Palmyride fold belt of central Syria. Additionally, a distinct change in velocity occurs within the Sinai plate itself. These new GPS measurements, when viewed alongside the palaeoseismic record and the modest level of present-day seismicity, suggest that the reported estimates of recurrence time of large earthquakes ($M > 7$) along the northern section of the DSFS may be underestimated owing to temporal clustering of such large historical earthquakes. Hence, a revised estimate of the earthquake hazard may be needed for NW Syria.

Key words: Space geodetic surveys; Continental tectonics: strike-slip and transform; Neotectonics; Kinematics of crustal and mantle deformation; Asia.

1 INTRODUCTION

The Dead Sea fault system (DSFS) is the left-lateral transform boundary between the Arabian and Sinai plates as they converge with Eurasia. Despite a 2000+ year historical record of large and damaging earthquakes, the kinematics of the northern part of this transform have not been well documented. Although a palaeoseismic estimate of the slip rate has recently been reported (Meghraoui *et al.* 2003), measurements of short-term (i.e. 'geodetic') deformation and strain accumulation have not been available. Comparisons of slip rates estimated at various timescales are essential to characterize time-variable tectonic activity, including earthquake clustering and time-dependent slip rates. In addition to the slip along the northern Dead Sea fault, there have also been suggestions of active internal deformation within the northern Arabian Plate, most significantly along the Palmyride fold belt (Chaimov *et al.* 1990).

This study presents new GPS measurements from Syria that constrain crustal deformation in the northwestern part of the Arabian Plate and the northern part of DSFS (Fig. 1). The results provide a more complete picture of the active tectonic framework in this region and show unanticipated variations in the kinematics along the transform. In particular, the northern Dead Sea fault demonstrates slower GPS velocities (and a slower slip rate) than are observed along the sections of the transform farther south. Furthermore, the GPS velocities suggest possible ongoing shortening across the Palmyride fold belt. Overall, these results suggest that the kinematics of the northern DSFS deviate significantly from what is expected based on regional plate models that assume coherent Sinai and Arabia plates. Accordingly, the results presented here will have significant implications for revising plate models, as well as the regional earthquake hazard.

2 TECTONIC SETTING

The northwestern region of the Arabian Plate encompasses several active tectonic elements including the DSFS, the Arabian-Eurasian continental collision in southern Turkey (Bitlis-Zagros fold-thrust belt), the intracontinental Palmyride fold-thrust belt, and the Euphrates depression (Fig. 1). The left-lateral DSFS bounds northwestern Arabia for nearly 800 km, from the Gulf of Aqaba northward to the East Anatolian fault, and is generally subdivided into three sections: (1) A southern section from the Gulf of Aqaba (Red Sea) through the Jordan Valley; (2) A central, NE–SW striking restraining bend through Lebanon and SW Syria and (3) A N–S striking section adjacent to the Syrian Coast Range (Brew *et al.* 2001). Additionally, the Kara Su Valley fault (southern Turkey) has been considered part of the northern DSFS (e.g. Westaway 2004). A total of 105 km of slip since the Cretaceous is documented along the southern DSFS (Freund *et al.* 1970; Hatcher *et al.* 1981; Quennell 1984), and about 45 km since the Early Pliocene when the DSFS

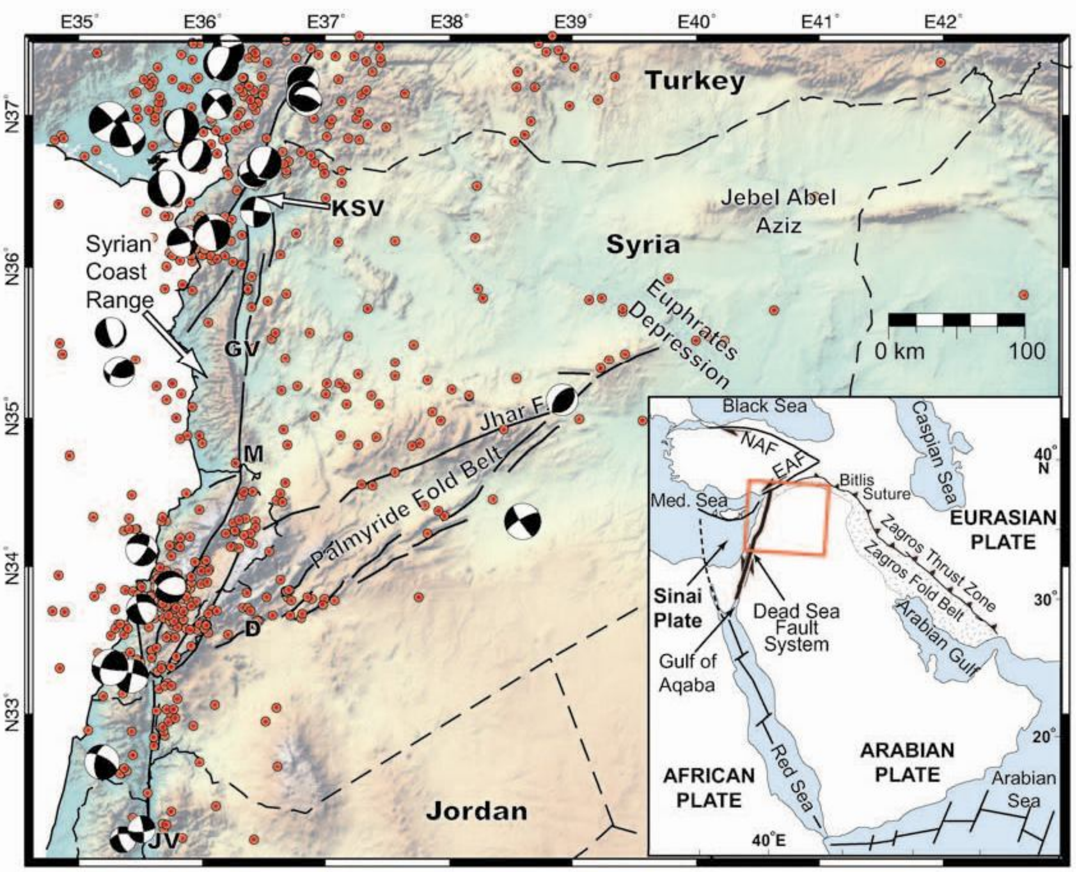

Figure 1. Seismicity and major neotectonic elements of Syria and the adjacent area. Heavy lines denote major faults. Red dots denote earthquake epicentres ($M > 2.5$) located by the Syrian National Earthquake Center (1994–2006). Focal mechanisms are from the compilation of Salamon *et al.* (2003). Abbreviations of geographic features cited in text: D, Damascus; M, Misyaf; JV, Jordan Valley; GV, Ghab Valley; KSV, Kara Su Valley. Inset: regional plate tectonic setting. EAF, East Anatolian fault; NAF, North Anatolian fault.

reactivated (Hempton 1987). Estimates of total slip along the northern DSFS are more disputed, ranging from ~25 km (Chaimov *et al.* 1990) to 70–80 km (Freund *et al.* 1970), and 20–25 km since the Early Pliocene (Hempton 1987). The shorter estimates of displacement on the northern DSFS are based on Neogene volcanic features, whereas the larger estimates are based on apparent displacement of the ophiolite in southern Turkey.

Published plate models describing motion between the Arabian and Sinai plates are based on geological criteria (Joffe & Garfunkel 1987) and, more recently, GPS measurements. We regard the GPS-based estimates of Reilinger *et al.* (2006) and Wdowinski *et al.* (2004) as particularly robust owing to their bases in the analysis of daily data from continuous GPS stations, which yield the most precise velocity estimates. Considering the uncertainties on the corresponding Euler poles, the plate models of Reilinger *et al.* (2006) and Wdowinski *et al.* (2004) are statistically compatible with one another.

In addition to the DSFS, central Syria comprises the intraplate, Palmyride fold belt (Chaimov *et al.* 1990). Crustal shortening across the ~120-km-wide Palmyride fold belt has been minor, about 20–25 per cent, and has taken place intermittently since Late Cretaceous time (Chaimov *et al.* 1990)—about 40 Myr, prior to the initiation of the main phase of left slip along the DSFS. However, historically documented earthquakes (Sbeinati *et al.* 2005), instrumental seismicity (Fig. 1), and geomorphology (e.g. Abou Romieh *et al.* 2009) suggest ongoing activity in the Palmyride region. In addition to the Palmyride fold belt, other late Cenozoic deformation in northern Arabia has occurred in the Euphrates depression (Litak *et al.* 1997) and the Jebel Abdel Aziz (Brew *et al.* 1999).

Historical records of seismicity attest to the tectonic activity of the region (e.g. Ambraseys & Barazangi 1989; Ambraseys & Jackson 1998; Sbeinati *et al.* 2005). For example, the catalogue of Sbeinati *et al.* (2005) represents a comprehensive databank on the historical earthquakes for Syria and surroundings, covering more than 2000 yr. While it is certain that many small earthquakes are missing from the record, the historical catalogue of large, earthquakes ($M > 7$) seems relatively complete for the past 2000 yr. The occurrence of large earthquakes in the historical records contrasts with the relative lack of instrumentally recorded seismicity (e.g. Ambraseys & Jackson 1998); hence, the instrumental seismicity represents an apparent quiescence that may not accurately reflect the earthquake potential of the northern DSFS.

Near-field geodetic analyses of present-day deformation along the central and southern DSFS suggest slip rates of 4–6 mm yr^{-1} (Wdowinski *et al.* 2004; Mahmoud *et al.* 2005; Gomez *et al.* 2007; Le Beon *et al.* 2008), and these generally agree with regional plate models (e.g. Joffe & Garfunkel 1987; Wdowinski *et al.* 2004; Reilinger *et al.* 2006). These fault slip rates are also consistent with 1000–1300 yr mean return periods for strike-slip earthquakes within the Lebanese restraining bend (Gomez *et al.* 2003; Daeron *et al.* 2007; Nemer *et al.* 2008) and along the southern DSFS (Klinger *et al.* 2000; Ferry *et al.* 2007).

Pertinent to this study, the only Holocene estimate of slip rate along the northern DSFS is reported near the village of Misyaf (Fig. 1), where the DSFS left-laterally offsets a Roman aqueduct (older than AD 70 and younger than AD 30) by 13.6 ± 0.2 m suggesting a slip rate of 6.9 ± 0.1 mm yr^{-1} (Meghraoui *et al.* 2003). This has led to the suggestion of an earthquake gap along the northern DSFS (Meghraoui *et al.* 2003). However, as shown by Meghraoui *et al.* (2003), this total displacement resulted from a cluster of earthquakes that occurred between 100 AD and 1170 AD. Hence, this estimate may reflect a bias, as it does not clearly span a complete 'earthquake cycle' for the northern DSFS, if this section of the fault is characterized by temporal clustering of earthquakes along the same fault segment. Palaeoseismic analyses along the northern DSFS north of the Ghab Valley (Akyuz *et al.* 2006) also document the repetition of three faulting events along that segment occurring over ~1000 yr (859–1872 AD); the trench stratigraphy in that study spans too short of a time to ascertain whether this earthquake recurrence is quasi-periodic or clusters in time. Additionally, evidence of temporal earthquake clustering along the southern DSFS has been reported by Marco *et al.* (1996). Essential to testing the possibility of an earthquake gap is an independent estimate of the slip rate along the northern DSFS. To that end, and to constrain active deformation of the northern Arabian Plate, we here report and analyse near-field Global Positioning System (GPS) velocity estimates for the northern DSFS and across the Palmyride Mountains in Syria, and use these velocities to estimate the fault slip rate using elastic dislocation models.

3 GPS MEASUREMENTS AND DATA PROCESSING

The regional GPS network used in this study consists of 36 survey monuments (surveyed three times; see Table 1) and one continuous GPS station (UDMC in Damascus; Fig. 2). Monumentation at the 36 survey sites consist of 15 cm steel pins cemented into bedrock. The campaign sites were installed and initially measured in late 2000 and early 2001. During the initial survey campaign, each site was observed for at least 48 hr using Trimble 4000 SSE and SSI receivers with Trimble L1/L2 with ground plane geodetic antennae. The sites were remeasured in the summer of 2007 and, again, in the summer of 2008 by the Syrian National Earthquake Center for at least 24 hr each, using Thales DSNP 6502MK receivers and Leica AT504 Choke ring Antennae. In all surveys, data were logged with a 30 s sampling rate.

GPS data were processed following a standard, two-step procedure using the GAMIT/GLOBK software (Herring *et al.* 1997; Dong *et al.* 1998; King & Bock 1998). In the first step, loosely constrained estimates of station coordinates, orbital and Earth orientation parameters, and atmospheric zenith delays were determined from raw GPS observables using GAMIT. Robust models for antenna phase centres were used to account for differences in field equipment between the surveys; uncertainties in those phase models were propagated into the loosely constrained solutions. Data from the Syrian GPS network were analysed along with raw GPS data from other continuously operating GPS (CGPS) stations in the region. Data from survey campaigns were subdivided into 8–10 hr epochs (typically at 2400 UTC), so that multiple, loosely constrained solutions were available for each site during each given campaign. In addition to the times of the three survey campaigns in Syria, CGPS data, when available, were also analysed at numerous epochs between 2002 and 2005, corresponding with survey campaigns in Lebanon (Gomez *et al.* 2007). A summary of the CGPS stations and their observations epochs is provided in Table 1.

Subsequently, a global Kalman filter (GLOBK) was applied to the loosely constrained solutions and their associated covariances in order to estimate a self-consistent set of station coordinates and velocities. As part of this second step, a six-parameter Helmert transformation was estimated by minimizing the horizontal velocities of 37 globally distributed IGS stations with respect to the IGS00 realization of the ITRF 2000 no-net-rotation reference (NNR) frame. The WRMS of the residual velocities for the IGS stations into ITRF

Table 1. Summary of GPS observation campaigns used in this study.

Date[a]	2000/12	2002/04	2002/10	2003/09	2004/09	2005/09	2007/07	2008/07
Survey-Mode GPS								
Syria	X						X	X
Lebanon[b]		X	X	X	X	X		
Continuous GPS								
UDMC		X	X	X			X	X
LAUG			X	X	X	X	X	X
HUGS					X	X	X	X
								X
Other CGPS[c]								
BAHR	X	X	X	X	X	X	X	X
BSHM	X	X	X	X	X	X	X	X
CSAR					X	X	X	X
ELRO	X	X	X	X	X	X	X	X
GILB	X	X	X	X	X	X	X	X
HALY			X		X	X	X	
KABR	X	X	X	X	X	X	X	X
NAMA			X		X	X	X	
SOLA			X		X	X	X	
YIBL					X	X	X	X

[a]Dates expressed as year and month (YYYY/MM).
[b]Details on Lebanon survey campaigns are found in Gomez *et al.* (2007).
[c]Data provided from Scripps Orbital and Permanent Array (SOPAC) archive.

2000 was 0.8 mm yr^{-1}. During this process, obvious outliers in the continuous and campaign time series were identified and removed; data from individual survey campaigns were then amalgamated into a single epoch corresponding with each survey campaign. Data for sites in Lebanon spanning 2002–2005 (Gomez *et al.* 2007) were also included in the velocity stabilization (including regional CGPS sites, as stated above).

Accurate characterization of the uncertainties in the velocities is critical to avoid over interpretation of the small tectonic signal associated with the DSFS. It is well regarded that the formal, standard error of the GPS solution underestimates the true uncertainty in the GPS velocities (e.g. Zhang *et al.* 1997; McClusky *et al.* 2000). Detailed studies of CGPS data indicate that the noise in GPS time-series may be characterized by colored noise that varies from fractal white noise to fractal random walk (Zhang *et al.* 1997; Mao *et al.* 1999). However, by estimating relative velocities (i.e. defining 'local' plate reference frames), we implicitly remove the common mode component of the noise within the region and, thus, within the noise (McClusky *et al.* 2000). White noise error in GPS observations accounts for factors such as monument stability and setup errors. In GPS processing with GLOBK, white noise is added as a time-dependent, random walk error in the velocity estimation. In our study, we applied a random walk noise of 1.3 mm yr^{-2}, which represents the average of random walk noise estimated for CGPS sites in the eastern Mediterranean region by Reilinger *et al.* (2006). We believe this is justified owing to the use of extremely stable, fixed-height antenna masts during the 2007 and 2008 survey campaigns.

After stabilizing the reference frame, the site velocities were resolved to an Arabia-fixed reference frame, which facilitates assessing the local deformation. The reference frame was defined by minimizing the motion of six GPS sites distributed around Arabia (Fig. 2, inset); the WRMS of the residual velocities used to define the Arabian Plate is 1.0 mm yr^{-1}. Similarly, the velocities were also translated into a Eurasia-fixed reference frame that was defined using 26 CGPS sites within Eurasia (WRMS of residuals = 1.1 mm yr^{-1}). GPS velocities (in ITRF2000-NNR, Arabia-fixed and Eurasia-fixed reference frames) for the sites around the northern DSFS are provided in Table 2. We estimate ITRF2000 euler pole for the Arabian Plate is 48.790 ± 0.9°N/5.133 ± 1.9°W/0.481 ± 0.019° Myr^{-1}. For comparison, the Eurasia–Arabia euler pole from this study, 26.843 ± 1.3°N/17.796 ± 1.5°W/0.385 ± 0.025° Myr^{-1}, is consistent with the pole reported by Reilinger *et al.* (2006). The error reported here is larger because Reilinger *et al.* analysed detailed time series for the regional CGPS sites, whereas our study only analysed data during the time periods of GPS survey campaigns in Syria and Lebanon.

4 RESULTS AND MODELLING

As shown in Fig. 2, the resulting velocity field depicts the general, left-lateral shear along the northern DSFS, although the magnitudes of the velocities crossing the northern segment in Syria appear to be smaller than for sites crossing the central DSFS. 1σ uncertainties for the survey sites in Syria are typically less than 0.7 mm yr^{-1} (Table 2). Additionally, GPS sites within the interior of Syria suggest possible contraction across the Palmyride fold belt. These are explored further below.

4.1 Slip rate and locking depth of the northern DSFS

In order to infer the slip rate for the northern DSFS, we examine profiles of the GPS velocities across the fault (see Fig. 2 for locations). The profile in NW Syria (Figs 3a and b) decomposes the velocities into motions parallel and perpendicular to the transform near Misyaf, located across the transform where it is a single fault trace. The velocities parallel to the transform (Fig. 3b) show a progressive increase in northward velocity from west to east—a pattern that is generally consistent with basic models of elastic strain accumulation (Savage & Burford 1973).

To infer possible slip rates, we apply a 1-D, elastic dislocation model across the northern DSFS. This standard analytical method follows the approach originally discussed by Savage & Burford (1973): This profile model assumes an infinitely long strike-slip

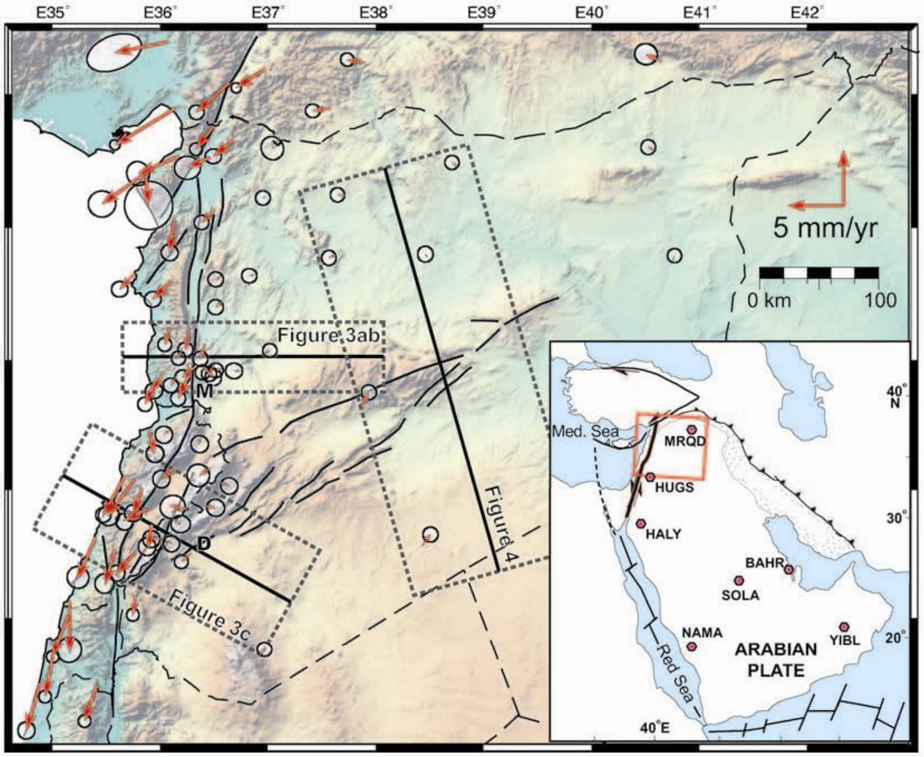

Figure 2. GPS velocities for the network used in this study (Arabia-fixed reference frame) with 1σ uncertainties. Abbreviations follow Fig. 1; GPS velocities in Turkey are from Reilinger *et al.* (2006); other velocities are from this study (see Table 2). Inset: map showing GPS sites used to estimate the Arabian Plate motion.

fault and expresses the station velocity, b, as a function of the long-term slip rate (V), fault locking depth (D) and distance from the fault (x)

$$b = (V/\pi)\tan-1(x/D). \qquad (1)$$

Despite its simplicity, this model continues to provide basic, first-order kinematic parameters when applied to large, strike-slip faults globally (e.g. Lisowski *et al.* 1991; Pearson *et al.* 2000; Wright *et al.* 2001; Segall 2002; Wdowinski *et al.* 2004). The assumptions behind the 1-D profile are appropriate to the Misyaf section of the northern DSFS, as the transform consists of a single fault that traces from the northern end of the Lebanese Restraining Bend to the southern end of the Ghab Valley.

This analytical model permits assessing a range of values of fault slip rates and locking depths consistent with the GPS data using a grid search that explores the misfit of the model for a given range of parameters (locking depth and slip rate). Our implementation of the model also solves for a third parameter that applies a constant offset to the velocity in order to minimize the velocity at the fault (ideally zero). This grid search provided the basis for a 'Monte Carlo' simulation of the assumed, Gaussian noise level in the data (Sandvol & Hearn 1994; Gomez *et al.* 2007). The 1σ contour for the profile is shown in Fig. 3(d). As demonstrated in Figs 3(a) and (d), the entire range of geological slip estimates (1.8–3.3 mm yr^{-1}) can be modeled to fit nearly all of the velocities, with locking depths of 5–16 km. As depicted in Fig. 3(d), the peak of the probability distribution corresponds with a slip rate of 2.5 mm yr^{-1} and a locking depth of 9 km. This locking depth is shallower than those reported from 1-D elastic dislocation profiles across the central and southern DSFS (e.g. Wdowinski *et al.* 2004; Gomez *et al.* 2007; Le Beon *et al.* 2008), and the profile across the central DSFS shown in Fig. 3(c) is provided for comparison. It should also be noted that the locking depths for dislocation models across the southern DSFS (Wdowinski *et al.* 2004; Le Beon *et al.* 2008), where the fault consists of a single segment, are also deeper than our result for the northern DSFS. As shown by the 1σ confidence ellipses in Fig. 3(d), the range of fault parameters that best fit the northern and central DSFS are statistically distinct.

The GPS-based slip rate along the northern DSFS is about half of the Holocene slip rate proposed by Meghraoui *et al.* (2003) based on the displaced Roman aqueduct near Misyaf. However, the palaeoseismically estimated slip rate in the study by Meghraoui

Table 2. Velocities of GPS sites shown in Fig. 2.

			ITRF 2000		Arabia-fixed		Eurasia-fixed				
Site	Long	Lat	Vel E	Vel N	Vel E	Vel N	Vel E	Vel N	σ E	σ N	corr
Syria											
AJSH	36.156	34.882	17.45	22.35	−0.55	−0.89	−5.17	10.82	0.45	0.45	−0.004
AKIL	37.634	35.800	16.99	23.63	−0.65	−0.29	−5.72	12.33	0.44	0.45	−0.006
ASAL	36.400	33.879	19.97	23.18	1.13	−0.18	−2.77	11.69	0.54	0.52	−0.04
BARN	36.404	34.948	17.91	22.85	−0.10	−0.51	−4.73	11.36	0.45	0.44	−0.002
BATH	36.091	35.247	17.24	21.69	−0.46	−1.52	−5.34	10.15	0.42	0.42	0.006
BLAN	36.754	34.914	17.46	23.55	−0.65	0.03	−5.23	12.11	0.52	0.47	−0.010
BMRA	36.343	34.957	16.67	22.29	−1.32	−1.04	−5.97	10.79	0.44	0.43	−0.003
BNAB	36.204	35.090	17.53	22.37	−0.32	−0.90	−5.08	10.85	0.43	0.43	0.003
DALY	36.270	35.215	17.44	21.68	−0.33	−1.62	−5.17	10.17	0.46	0.45	−0.004
DBSS	38.757	36.461	16.94	24.83	−0.46	0.41	−5.84	13.72	0.43	0.43	−0.001
DERS	36.419	35.118	17.44	22.08	−0.44	−1.28	−5.19	10.59	0.46	0.45	−0.006
DOHA	36.104	35.598	15.77	21.61	−1.66	−1.61	−6.78	10.07	0.50	0.47	0.012
HARM	36.508	36.146	15.9	22.19	−1.20	−1.21	−6.65	10.72	0.45	0.44	0.004
HASS	36.570	35.638	16.99	23.14	−0.52	−0.29	−5.61	11.68	0.47	0.45	−0.006
HBAB	36.033	34.915	17.08	21.41	−0.87	−1.78	−5.52	9.86	0.52	0.48	0.014
HMEH	40.596	36.584	17.13	25.54	−0.65	0.32	−5.85	14.73	0.45	0.45	−0.003
HMRY	36.503	34.965	17.55	22.56	−0.47	−0.84	−5.10	11.09	0.46	0.45	−0.018
HOOR	36.111	33.781	19.63	22.72	0.78	−0.51	−3.08	11.18	0.59	0.52	−0.006
HOWR	36.974	36.233	16.95	23.56	−0.19	−0.06	−5.64	12.16	0.46	0.45	0.001
JHAR	37.869	34.643	19.25	25.32	0.66	1.29	−3.59	14.06	0.46	0.45	−0.011
KATR	36.881	35.649	17.06	23.48	−0.51	−0.01	−5.58	12.06	0.46	0.44	−0.008
KBDD	38.437	33.571	20.24	25.27	0.70	0.99	−2.74	14.10	0.46	0.45	−0.010
KHAS	36.578	35.449	17.05	22.89	−0.61	−0.55	−5.57	11.43	0.47	0.46	−0.004
KHBZ	37.716	36.246	16.62	24.03	−0.69	0.08	−6.06	12.75	0.43	0.43	−0.011
KRIN	38.481	35.782	17.67	24.57	−0.19	0.27	−5.14	13.41	0.47	0.48	−0.018
MJDL	35.954	34.838	17.08	21.06	−0.91	−2.09	−5.52	9.50	0.44	0.43	−0.008
MRQD	40.761	35.754	18.57	25.76	0.12	0.47	−4.49	14.98	0.43	0.43	−0.006
MSHR	36.550	34.059	19.62	23.14	0.89	−0.29	−3.12	11.67	0.52	0.50	−0.028
MSHT	36.269	34.885	17.05	21.19	−0.97	−2.11	−5.59	9.68	0.45	0.44	−0.004
RAJO	36.681	36.664	14.92	22.01	−1.81	−1.47	−7.6	10.56	0.51	0.45	0.019
ROZA	36.010	33.625	18.07	23.14	−0.87	−0.04	−4.64	11.59	0.52	0.52	−0.011
RSHD	36.913	32.702	20.39	24.23	0.54	0.63	−2.49	12.82	0.44	0.43	−0.009
RSHM	35.769	35.659	15.91	21.63	−1.39	−1.43	−6.6	10.04	0.50	0.47	0.009
SALM	36.966	35.049	18.57	23.89	0.51	0.28	−4.13	12.49	0.43	0.42	0.000
SOBA	36.051	33.613	19.49	22.88	0.53	−0.32	−3.23	11.33	0.50	0.49	−0.012
TELF	36.573	34.934	17.51	23.29	−0.55	−0.15	−5.15	11.83	0.45	0.44	0.002
UDMC	36.285	33.510	18.31	22.61	−0.78	−0.70	−4.44	11.10	0.42	0.42	0.002
Lebanon											
ADAS	35.909	34.466	17.01	20.80	−1.25	−2.32	−5.62	9.23	0.75	0.71	0.011
ANJR	35.922	33.730	18.08	20.56	−0.75	−2.58	−4.61	8.99	0.74	0.76	−0.022
ARSL	36.467	34.164	17.39	22.37	−1.23	−1.02	−5.33	10.89	0.89	0.85	−0.011
BRKA	36.143	34.184	17.45	21.23	−1.08	−2.01	−5.23	9.70	0.76	0.74	−0.045
FRYA	35.829	34.005	17.23	20.08	−1.37	−3.02	−5.43	8.50	0.86	0.86	−0.008
HABT	36.084	34.451	17.24	20.90	−1.07	−2.31	−5.41	9.36	0.74	0.72	−0.007
HAYT	35.767	34.094	16.38	20.04	−2.15	−3.02	−6.27	8.45	0.75	0.75	0.016
HRML	36.379	34.412	17.79	22.21	−0.63	−1.13	−4.90	10.71	0.85	0.78	0.028
HZRT	35.880	33.869	17.41	21.43	−1.32	−1.69	−5.27	9.86	0.81	0.76	0.006
JIYE	35.411	33.651	17.18	19.19	−1.61	−3.70	−5.46	7.55	0.76	0.76	−0.022
JZIN	35.589	33.555	17.70	19.84	−1.21	−3.14	−4.97	8.22	0.76	0.75	−0.001
MCHK	35.771	33.526	17.05	20.80	−1.92	−2.26	−5.64	9.21	0.73	0.73	−0.051
RBDA	35.162	33.139	18.46	18.53	−0.66	−4.25	−4.19	6.85	0.81	0.79	0.025
TFEL	36.225	33.860	17.14	22.98	−1.68	−0.31	−5.58	11.46	0.90	0.92	−0.004
LAUG	35.674	34.115	17.17	19.86	−1.32	−3.16	−5.46	8.26	0.46	0.46	0.003
Other CGPS sites (data obtained from SOPAC archive)											
BAHR	50.608	26.209	28.09	28.26	0.66	−0.87	3.84	19.30	0.36	0.35	0.001
BSHM	35.023	32.779	18.50	18.25	−0.88	−4.47	−4.16	6.55	0.38	0.38	0.003
CSAR	34.89	32.488	18.67	18.42	−0.90	−4.23	−4.00	6.70	0.53	0.53	0.001
ELRO	35.771	33.182	18.95	21.32	−0.28	−1.75	−3.77	9.73	0.38	0.38	0.003
GILB	35.416	32.479	18.53	19.62	−1.17	−3.28	−4.2	7.98	0.38	0.38	0.003
HALY	36.100	29.139	23.37	21.87	1.01	−0.86	0.47	10.23	0.72	0.68	0.009

Table 2. (*Continued.*)

Site	Long	Lat	ITRF 2000 Vel E	ITRF 2000 Vel N	Arabia-fixed Vel E	Arabia-fixed Vel N	Eurasia-fixed Vel E	Eurasia-fixed Vel N	σ E	σ N	corr
KABR	35.145	33.023	17.78	19.05	−1.44	−3.72	−4.88	7.37	0.38	0.38	0.003
NAMA	42.045	19.211	30.85	27.58	0.64	1.02	7.34	17.01	1.10	0.84	0.051
SOLA	46.401	24.911	28.25	26.73	0.89	−0.87	4.31	16.95	0.58	−.58	−0.001
YIBL	56.112	21.186	33.08	29.89	1.14	−1.01	8.64	22.06	0.51	0.49	−0.004

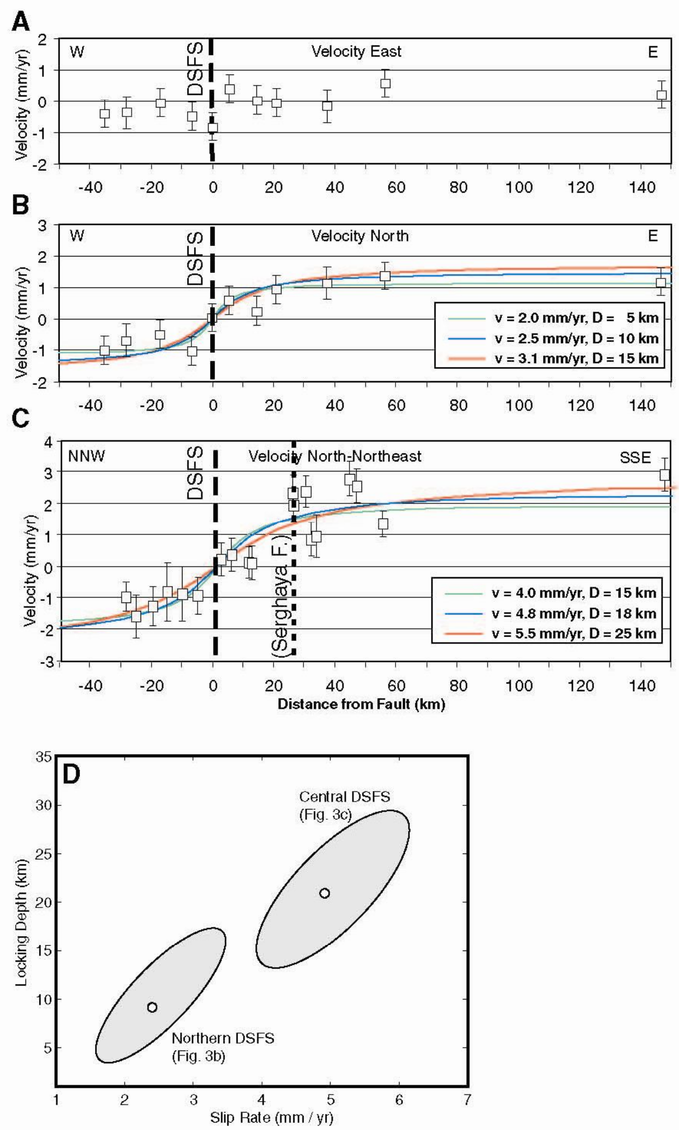

Figure 3. (a)–(b). Profile across the northern DSFS showing the GPS velocities perpendicular and parallel to the DSFS, respectively. (c) Profile depicting GPS velocities parallel to the Yammouneh fault (central DSFS) and corresponding elastic dislocation models (from Gomez *et al.* 2007). (d) A plot depicting the 1σ confidence limits on the slip rates and locking depths for profiles B and C based on a Monte Carlo simulation to estimate the noise level in the data. See Fig. 2 for locations of profiles. Heavy, dashed line shows where the DSFS crosses the profiles.

et al. (2003) is based on a ~3000 yr palaeoseismic record containing one earthquake cluster (three events during the first millennium: 115 AD, 700 AD–1030 AD and 1170 AD). Hence, without proper constraints on the repetition of the clusters, a large bias in the slip rate may be expected.

Although the kinematic modeling of GPS data reflects model-specific assumptions (e.g. the uniform elastic half-space used in this study), we believe the GPS analysis more accurately reflects the present-day slip rate for the northern DSFS. In general, elastic dislocation models have compared well with long-term slip rates along other major strike-slip faults in the region (e.g. Allen *et al.* 2004; Reilinger *et al.* 2006), as well as the central and southern DSFS (e.g. Mahmoud *et al.* 2005; Gomez *et al.* 2007; Le Beon *et al.* 2008). In any event, since the same basic model (1-D dislocation in a uniform elastic half-space) was applied to both the northern and the central DSFS, systematic errors owing to model-specific assumptions do not preclude the general result of a statistically distinct kinematic change along strike of the transform.

4.2 Internal deformation of Arabia

Aside from the motion of the DSFS, the new GPS results also permit a preliminary assessment of possible internal deformation within the northwestern Arabian Plate. Internal deformation of northern Arabia can be assessed from relative changes in GPS velocities. Hence it is independent of the sites selected for the definition of the Arabian Plate motion. Although the distribution of GPS sites and the velocity uncertainties are insufficient to analyse individual structures within northern Arabia, the current network provides a basis to assess large, regional patterns of crustal deformation by identifying differences in coherent, block-like motions. Internal deformation, particularly associated with the Palmyride fold belt, has been suggested based on recent seismicity (e.g. Chaimov *et al.* 1990; Salamon *et al.* 1996), historically documented seismicity (Sbeinati *et al.* 2005) and evidence of late Quaternary deformation in the Palmyrides (e.g. Abou Romieh *et al.* 2009).

Fig. 4 depicts the GPS velocities resolved along a NNW–SSE profile across central Syria (see Fig. 2 for location), and roughly perpendicular to the strike of the Palmyride fold belt. In general, the sites shown in these profiles are located sufficiently far from the major faults so that they likely are not affected by transient, elastic strains. The velocities in the NNW–SSE direction (Fig. 4a) demonstrate ~1 mm yr^{-1} of consistent motion between the southern two sites relative to the rest of the profile points in northern Syria. These two sites are located within and south of the Palmyride fold belt, and their motion is also consistent with the southernmost site in Syria. Although the uncertainties are relatively large and the station spacing is sparse, the motion of the southern vectors (also including the southernmost site in Syria, shown in Fig. 2) is coherent and distinct from the overall motion of the sites at the northern end of the profile. Additionally, this is consistent with one reverse-fault focal

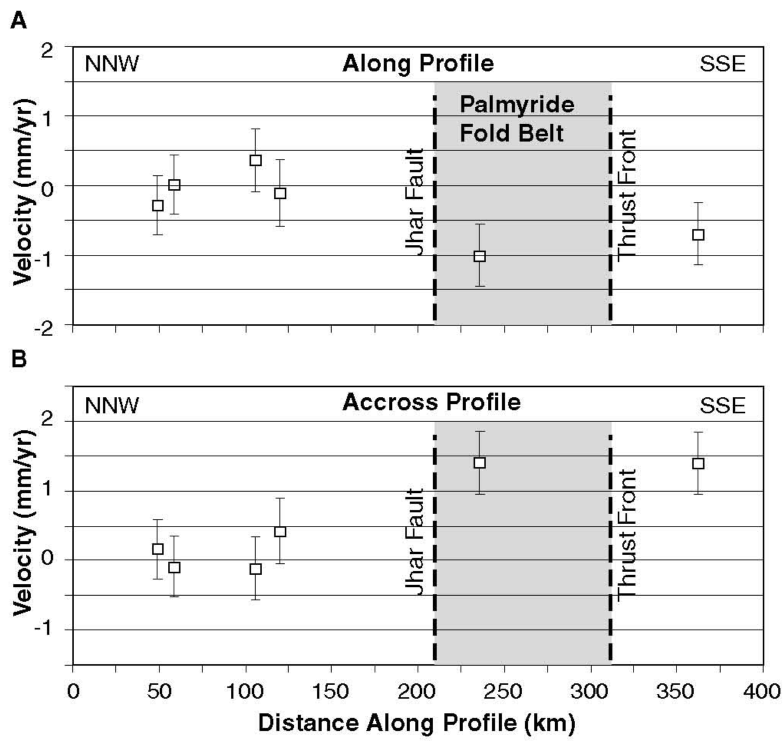

Figure 4. Plots showing GPS velocities (a) parallel and (b) perpendicular to the NNW–SSE profile across northwestern Arabia (oriented perpendicular to the main strike of the Palmyride fold belt; see Fig. 2 for profile location). A systematic offset between sites north and south of the Palmyride fold belt suggests up to 1 mm yr^{-1} of contraction and possible left-lateral shear along the Jhar fault.

mechanism shown in Fig. 1. Hence, we suggest the GPS data may reflect up to 1 mm yr^{-1} of active, regional shortening, although the level of uncertainty in these data precludes assessing the kinematics of specific structures within the Palmyride fold belt.

In the ENE–WSW direction (parallel to the strike of the Jhar fault and the structural trend of the Palmyride fold belt), the southern GPS sites also demonstrate consistent ENE motion relative to the sites located north of the Palmyride fold belt (Fig. 4b). Although the differential motion falls generally within the uncertainties of the velocities, we suggest that these velocities might be the results of up to 0.5–1.0 mm yr^{-1} of left-lateral slip along the Jhar fault. Such lateral shear is consistent with the earthquake focal mechanisms reported for recent earthquakes in the Palmyrides (e.g. Chaimov *et al.* 1990; Salamon *et al.* 2003; Fig. 1).

5 DISCUSSION

The GPS results demonstrate that the northern DSFS is actively shearing and accumulating strain, contrasting with previous suggestions, based in part on a paucity of seismicity, that the northern DSFS has become inactive (e.g. Girdler 1990; Butler *et al.* 1997, 1998). Furthermore, the present-day slip rates may reflect the longer-term (late Cenozoic) tectonism of the northern Dead Sea fault. The geodetic-derived slip rate reported here is similar to the long-term estimate of 3.3–4.0 mm yr^{-1} reported by Gomez *et al.* (2006) based on an apparent displacement of a large, Pliocene volcano in NW Syria. More significantly, the present-day contraction across the Palmyride fold belt and the slower slip rate along the northern DSFS appear to reflect the long-term deficit in total geological slip between the northern and southern DSFS (Chaimov *et al.* 1990). Hence, this regional partitioning of deformation has likely persisted through the Late Cenozoic.

Our geodetic slip rate is lower than (and statistically distinct from) predictions from well-constrained, plate tectonic models (e.g. Wdowinski *et al.* 2004; Reilinger *et al.* 2006)—hence, there appears to be a northward decrease, rather than the predicted increase, in the slip rate of the DSFS. Additionally, this northward decrease cannot be completely explained by shortening within northern Arabia (i.e. the Palmyride fold belt)—there is a distinct velocity gradient within the Sinai Plate between NW Syria and northern Lebanon. Furthermore, the predicted convergence across the northern DSFS is not apparent in the GPS velocities; within the uncertainties, the GPS data suggest neither contraction nor extension across the DSFS.

In summary, the GPS velocities demonstrate that the kinematics of the northern DSFS deviate significantly from plate tectonic predictions based on models that consider the Arabian and Sinai plates to be rigid. Both the Sinai and Arabian plates actively converge with Eurasia. However, whereas N–S GPS velocities on the Arabian Plate decrease northward across the Palmyride fold belt, N–S GPS velocities on the Sinai Plate increase at the latitude of northern Lebanon. In an Arabia-fixed reference frame, this is expressed as the northward decrease in velocity of sites on the Sinai Plate that is observed in northern Lebanon and NW Syria (Fig. 2)—that is, a spatially abrupt and statistically significant velocity gradient exists between the relatively coherent GPS velocities in central & southern Lebanon versus those in northern Lebanon and NW Syria (see profiles in Fig. 2). The nature of this velocity gradient requires N–S extension.

As one possible hypothesis, we suggest that the NE part of the Sinai Plate may be broken and partially decoupled from the southern part of the 'plate' (Fig. 5). In this case, the northern DSFS would reflect relative motion between Arabia and this smaller block, rather

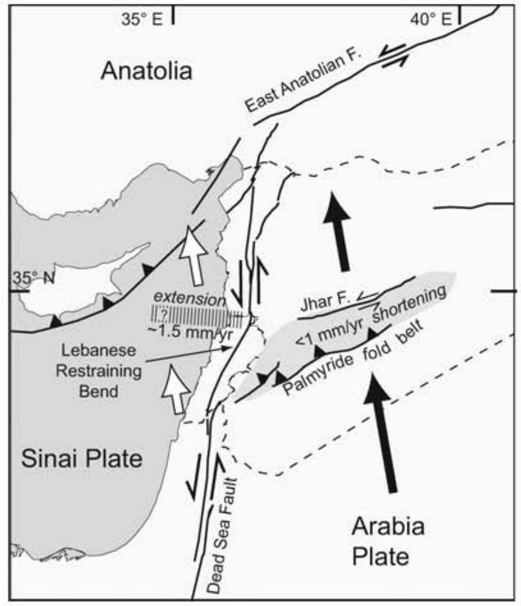

Figure 5. Conceptual model illustrating the motion of the northwestern Arabia Plate (large black arrow) and the northeastern Sinai Plate (large white arrow) relative to Eurasia. Total predicted plate motion of northwestern Arabia is decomposed into transpression across the Palmyride fold belt (PFB) and north–south strike-slip along the DSFS, resulting in a northward decrease in motion of Arabia relative to Eurasia. Based on the velocity gradient shown by the GPS data, we suggest ~N–S extension within the small, Sinai Plate, near the northern end of the Lebanese Restraining Bend to account for (1) the observed northward decrease in GPS velocities within the Sinai Plate and (2) the decrease in slip rate on the N segment of the DSFS. Although the GPS demonstrate N–S extension near the DSFS, the western limit of the extension is not constrained; hence it is denoted with a question mark. *Note:* Length of arrow schematically depicts the magnitude of motion, but arrows are not drawn to scale.

than the larger Sinai Plate. Such a hypothesis explains the observed extensional velocity gradient in northern Lebanon. Late Cenozoic, horizontal extension in this area would also be consistent with the Neogene and Quaternary alkali volcanic activity observed at the northern part of the restraining bend (Mouty *et al.* 1992). Alternatively, N–S extension may be localized to the vicinity of the DSFS. Furthermore, a single structure bounding such a block (and linking it to the Sinai–Anatolia plate boundary) is not clearly expressed in the topography, nor evident on existing geological maps, suggesting that this horizontal extension, if occurring over geological timescales, would be spatially distributed. Further geophysical and geological observations are needed to test this preliminary hypothesis.

In terms of the earthquake hazard, the lower slip rate also suggests that the 800-yr seismic quiescence along the Misyaf fault (Meghraoui *et al.* 2003) may not necessarily represent a seismic gap. Assuming an average coseismic slip of 4.5 m (one-third of the offset of the faulted Roman aqueduct reported by Meghraoui *et al.*), the 2.5 mm yr^{-1} slip rate would be consistent with an average recurrence period of 1800 yr. However, owing to the clearly non-periodic behaviour of the northern DSFS (Meghraoui *et al.* 2003), the appropriateness of such a calculation is questionable. In addition, the GPS velocities indicate present-day tectonism in the Palmyride fold belt, which should also be considered within the context of the regional earthquake hazard.

6 CONCLUSIONS

The GPS results presented herein provide direct geodetic measurement of present-day fault slip along the northern DSFS in Syria and within the northwestern part of the Arabian Plate. The deformation is reasonably well constrained by GPS measurements spanning 7.5 yr yielding velocities with 1σ uncertainties generally less than 0.6 mm yr^{-1}.

The GPS velocities in Syria demonstrate along-strike variations from the central and southern DSFS, which suggest that the DSFS may not behave as a 'simple' transform. Although inferring fault slip rates from geodetic data is inherently model dependent, the 1-D dislocation models shown here demonstrate that the northern DSFS is kinematically distinct from the central and southern parts of the transform—namely, the slip rate appears to be significantly slower than the central and southern sections of the transform. Shortening across the Palmyride fold belt may account for some of this slip deficiency, but there is also a distinct GPS velocity gradient within the Sinai Plate itself. We speculate that active, N–S extension of the Sinai micro plate near the northern end of the DSFS in Lebanon may account for the reduced slip on the northern fault segment in Syria. Hence, the tectonic configuration of the northeastern Mediterranean region is likely more complicated than previously thought.

ACKNOWLEDGMENTS

We are grateful to the Syrian National Earthquake Center for logistical support and for many of their personnel who assisted with the field observations, particularly the engineering assistance provided by Marwan Alkasser and Fadia Bazo. The Syrian Atomic Energy Commission also provided logistical support. This manuscript also benefited from the constructive suggestions provided by Oliver Ritter, Jorgen Klotz and an anonymous reviewer. This research has been partially supported by NSF grants EAR-0439021 to the University of Missouri, EAR-0439807 to MIT and EAR-0106238 to Cornell University. The 2000 field survey was made possible with equipment services provided by the UNAVCO Facility with support from the National Science Foundation and NASA. This study also acknowledges data services provided by the UNAVCO Facility and SOPAC.

REFERENCES

Abou Romeih, M. *et al.*, 2009. Active crustal shortening in NE Syria revealed by deformed terraces of the River Euphrates, *Terra Nova*, in press.

Akyuz, H.S., Altunel, E., Karabacak, V. & Yalciner, C.C., 2006. Historical earthquake activity of the northern part of the Dead Sea Fault Zone, southern Turkey, *Tectonophysics,* **426,** 281–293.

Allen, M., Jackson, J. & Walker, R., 2004. Late Cenozoic reorganization of the Arabia-Eurasia collision and the comparison of short-term and long-term deformation rates, tectonics, *Tectonics,* **23,** TC2008, doi:2010.1029/2003TC001530.

Ambraseys, N.N. & Barazangi, M., 1989. The 1759 earthquake in the Bekaa Valley: implications for earthquake hazard assessment in the Eastern Mediterranean region, *J. geophys. Res.,* **94,** 4007–4013.

Ambraseys, N.N. & Jackson, J.A., 1998. Faulting associatd with historical and recent earthquakes in the Eastern Mediterranean region, *Geophys. J. Int.,* **133,** 390–406.

Brew, G., Litak, R., Barazangi, M. & Sawaf, T., 1999. Tectonic evolution of Northeast Syria: regional implications and hydrocarbon prospects, *GeoArabia,* **4,** 289–318.

Brew, G., Lupa, J., Barazangi, M., Sawaf, T., Al-Imam, A. & Zaza, T., 2001. Structure and tectonic development of the Ghab basin and the Dead Sea fault system, Syria, *J. geol. Soc. Lond.,* **158,** 665–674.

Butler, R.W.H., Spencer, S. & Griffiths, H.M., 1997. Transcurrent fault activity on the Dead Sea Transform in Lebanon and its implications for plate tectonics and seismic hazard, *J. geol. Soc. Lond.,* **154,** 757–760.

Butler, R.W.H., Spencer, S. & Griffiths, H.M., 1998. The structural response to evolving plate kinematics during transpression: evolution of the Lebanese restraining bend of the Dead Sea Transform, in *Continental Transpressional and Transtensional Tectonics,* pp. 81–106, eds. Holdsworth, R.E., Strahan, R.A. & Dewey, J.F., Geological Soc. London, London.

Chaimov, T.A., Barazangi, M., Al-Saad, D., Sawaf, T. & Gebran, A., 1990. Crustal shortening in the Palmyride fold belt, Syria, and implications for movement along the Dead Sea fault system, *Tectonics,* **9,** 1369–1386.

Daeron, M., Klinger, Y., Tapponnier, P., Elias, A., Jacques, E. & Sursock, A., 2007. 12,000-year long Record of 10 to 13 Paleo-Earthquakes on the Yammouneh Fault (Levant Fault System, Lebanon), *Bull. seism. Soc. Am.,* **97,** 749–771.

Dong, D., Herring, T.A. & King, R.W., 1998. Estimating regional deformation from a combination of space and terrestrial geodetic data, *J. Geod.,* **71,** 200–211.

Ferry, M., Meghraoui, M., Karaki, N.A., Al-Taj, M., Amoush, H., Al-Dhaisat, S. & Barjous, M., 2007. A 48-kyr-long slip rate history for the Jordan Valley segment of the Dead Sea Fault, *Earth planet. Sci. Lett.,* **260,** 394–406.

Freund, R., Garfunkel, Z., Zak, I., Goldberg, M., Weissbrod, T. & Derin, B., 1970. The shear along the Dead Sea rift, *Phil. Trans. R. Soc. Lond.,* **267,** 107–130.

Girdler, R.W., 1990. The Dead Sea transform fault system, *Tectonophysics,* **180,** 1–13.

Gomez, F. *et al.*, 2007. Global Positioning System measurements of strain accumulation and slip transfer through the restraining bend along the Dead Sea fault system in Lebanon, *Geophys. J. Int.,* **168,** 1021–1028.

Gomez, F., Khawlie, M., Tabet, C., Darkal, A.N., Khair, K. & Barazangi, M., 2006. Late Cenozoic uplift along the northern Dead Sea transform in Lebanon and Syria, *Earth planet. Sci. Lett.,* **241,** 913–931.

Gomez, F. *et al.*, 2003. Holocene faulting and earthquake recurrence along the Serghaya branch of the Dead Sea fault system in Syria and Lebanon, *Geophys. J. Int.,* **153,** 658–674.

Hatcher, R.D., Jr., Zietz, I., Regan, R.D. & Abu-Ajamieh, M., 1981. Sinistral strike-slip motion on the Dead Sea Rift; confirmation from new magnetic data, *Geology,* **9,** 458–462.

Hempton, M.R., 1987. Constraints on Arabian plate motion and extensional history of the Red Sea, *Tectonics,* **6,** 687–705.

Herring, T.A., King, R.W. & McClusky, S.C., 1997. Geodetic constraints on interseismic, coseismic, and postseismic deformation in southern California, Annual Report to SCEC.

Joffe, S. & Garfunkel, Z., 1987. Plate kinematics of the circum Red Sea–a re-evaluation, *Tectonophysics,* **141,** 5–22.

King, R.W. & Bock, Y., 1998. Documentation of MIT GPS Analysis Software: GAMIT, Massachusetts Institute of Technology, Cambridge, MA.

Klinger, Y., Avouac, J.P., Abou Karaki, N., Dorbath, L., Bourles, L. & Reys, J., 2000. Slip rate on the Dead Sea transform fault in the northern Araba Valley (Jordan), *Geophys. J. Int.,* **142,** 755–768.

Le Beon, M. *et al.*, 2008. Slip rate and locking depth from GPS profiles across the southern Dead Sea Transform, *J. geophys. Res.,* **113,** B11403, doi:11410.11029/12007JB005280.

Lisowski, M., Savage, J.C. & Prescott, W.H., 1991. The velocity field along the San Andreas fault in central and southern California, *J. geophys. Res.,* **96,** 8369–8389.

Litak, R.K., Barazangi, M., Beauchamp, W., Seber, D., Brew, G., Sawaf, T. & Al-Youssef, W., 1997. Mesozoic-Cenozoic evolution of the intraplate Euphrates fault system, Syria: implication for regional tectonics, *J. geol. Soc. Lond.,* **154,** 653–666.

Mahmoud, S., Reilinger, R., McClusky, S., Vernant, P. & Tealeb, A., 2005. GPS evidence for northward motion of the Sinai block: implications for E. Mediterranean tectonics, *Earth planet. Sci. Lett.,* **238,** 217–227.
Mao, A., Harrison, C. & Dixon, T., 1999. Noise in GPS coordinate time series, *J. geophys. Res.,* **104,** 2797–2816.
Marco, S., Stein, M. & Agnon, A., 1996. Long-term earthquake clustering: a 50,000-year paleoseismic record in the Dead Sea Graben, *Geophys. J. Int.,* **101,** 6179–6191.
McClusky, S. *et al.*, 2000. Global Positioning System constraints on plate kinematics and dynamics in the easterm Mediterranean and Caucasus, *J. geophys. Res.,* **105,** 5695–5719.
Meghraoui, M. *et al.*, 2003. Evidence for 830 years of seismic quiescence from palaeoseismology, archaeosesimology, and historical seismicity along the Dead Sea fault in Syria, *Earth planet. Sci. Lett.,* **210,** 35–52.
Mouty, M., Delaloye, M., Fontignie, D., Piskin, O. & Wagner, J.-J., 1992. The volcanic activity in Syria and Lebanon between Jurassic and Actual, *Schweiz. Mineral. Petrogr. Mitt.,* **72,** 91–105.
Nemer, T., Gomez, F., Haddad, S. & Tabet, C., 2008. Coseismic growth of sedimentary basins along the Yammouneh strike-slip fault (Lebanon), *Geophys. J. Int.,* **175,** 1023–1039.
Pearson, C., Denys, P. & Hodgkinson, K., 2000. Geodetic constraints on the kinematics of the Alpine Fault in the southern South Island of New Zealand, using results from the Hawea-Haast GPS transect, *Geophys. Res. Lett.,* **27,** 1319–1322.
Quennell, A.M., 1984. The Western Arabia rift system, in *The Geological Evolution of the Eastern Mediterranean,* pp. 775–788, eds Dixon, J.E. & Robertson, A.H.F., Blackwell Scientific, Oxford.
Reilinger, R. *et al.*, 2006. GPS Constraints on Continental deformation in the Africa-Arabia-Eurasia continental collision zone and implications for the dynamics of plate interactions, *J. geophys. Res.,* **111,** doi:10.1029/2005JB004051.
Salamon, A., Hofstetter, A., Garfunkel, Z. & Ron, H., 1996. Seismicity of the eastern Mediterranean region: Perspective from the Sinai subplate, *Tectonophysics,* **263,** 293–305.
Salamon, A., Hofstetter, A., Garfunkel, Z. & Ron, H., 2003. Seismotectonics of the Sanai subplate–the eastern Mediterranean region, *Geophys. J. Int.,* **155,** 149–173.
Sandvol, E. & Hearn, T., 1994. Bootstrapping shear-wave splitting errors, *Bull. seism. Soc. Am.,* **84,** 1971–1977.
Savage, J.C. & Burford, R.O., 1973. Geodetic determination of relative plate motion in central California, *J. geophys. Res.,* **78,** 832–845.
Sbeinati, M.R., Darawcheh, R. & Mouty, M., 2005. Catalog of historical earthquakes in and around Syria, *Ann. Geofis.,* **48,** 347–435.
Segall, P., 2002. Integrating geologic and geodetic estimates of slip rate on the San Andreas fault system, *Int. Geol. Rev.,* **44,** 62–82.
Wdowinski, S. *et al.*, 2004. GPS measurements of current crustal movements along the Dead Sea Fault, *J. geophys. Res.,* **109,** doi:10.1029/2003JB002640.
Westaway, R., 2004. Kinematic consistency between the Dead Sea Fault Zone and the Neogene and Quaternary left-lateral faulting in SE Turkey, *Tectonophysics,* **391,** 203–237.
Wright, T., Parsons, B. & Fielding, E., 2001. Measurement of interseismic strain accumulation across the North Anatolian Fault by satellite radar interferometry, *Geophys. Res. Lett.,* **28,** 2117–2120.
Zhang, J., Bock, Y., Johnson, H., Fang, P., Williams, S., Genrich, J., Wdowinski, S. & Behr, J., 1997. Southern California Permanent GPS Geodetic Array: error analysis of daily position estimates and site velocities, *J. geophys. Res.,* **102,** 18 035–18 055.